ISSN 1007-9327 (print)
ISSN 2219-2840 (online)

World Journal of *Gastroenterology*

World J Gastroenterol 2015 September 7; 21(33): 9683-9832

Published by Baishideng Publishing Group Inc

World Journal of Gastroenterology

A peer-reviewed, online, open-access journal of gastroenterology and hepatology

Editorial Board

2014-2017

The *World Journal of Gastroenterology* Editorial Board consists of 1379 members, representing a team of worldwide experts in gastroenterology and hepatology. They are from 68 countries, including Algeria (2), Argentina (7), Australia (31), Austria (9), Belgium (11), Brazil (20), Brunei Darussalam (1), Bulgaria (2), Cambodia (1), Canada (26), Chile (4), China (164), Croatia (2), Cuba (1), Czech (6), Denmark (2), Egypt (9), Estonia (2), Finland (6), France (20), Germany (58), Greece (31), Guatemala (1), Hungary (15), Iceland (1), India (33), Indonesia (2), Iran (10), Ireland (9), Israel (18), Italy (194), Japan (151), Jordan (1), Kuwait (1), Lebanon (7), Lithuania (1), Malaysia (1), Mexico (11), Morocco (1), Netherlands (5), New Zealand (4), Nigeria (3), Norway (6), Pakistan (6), Poland (12), Portugal (8), Puerto Rico (1), Qatar (1), Romania (10), Russia (3), Saudi Arabia (2), Singapore (7), Slovenia (2), South Africa (1), South Korea (69), Spain (51), Sri Lanka (1), Sudan (1), Sweden (12), Switzerland (5), Thailand (7), Trinidad and Tobago (1), Tunisia (2), Turkey (55), United Kingdom (49), United States (181), Venezuela (1), and Vietnam (1).

Gordon Stanley Howarth, *Roseworthy*
Seungha Kang, *Brisbane*
Alfred King Lam, *Gold Coast*
Ian C Lawrance, *PerthFremantle*
Barbara Anne Leggett, *Brisbane*
Daniel A Lemberg, *Sydney*
Rupert W Leong, *Sydney*
Finlay A Macrae, *Victoria*
Vance Matthews, *Melbourne*
David L Morris, *Sydney*
Reme Mountifield, *Bedford Park*
Hans J Netter, *Melbourne*
Nam Q Nguyen, *Adelaide*
Liang Qiao, *Westmead*
Rajvinder Singh, *Adelaide*
Ross Cyril Smith, *StLeonards*
Kevin J Spring, *Sydney*
Debbie Trinder, *Fremantle*
Daniel R van Langenberg, *Box Hill*
David Ian Watson, *Adelaide*
Desmond Yip, *Garran*
Li Zhang, *Sydney*

Austria

Felix Aigner, *Innsbruck*
Gabriela A Berlakovich, *Vienna*
Herwig R Cerwenka, *Graz*
Peter Ferenci, *Wien*
Alfred Gangl, *Vienna*
Kurt Lenz, *Linz*
Markus Peck-Radosavljevic, *Vienna*
Markus Raderer, *Vienna*
Stefan Riss, *Vienna*

Belgium

Michael George Adler, *Brussels*
Benedicte Y De Winter, *Antwerp*
Mark De Ridder, *Jette*
Olivier Detry, *Liege*
Denis Dufrane Dufrane, *Brussels*
Sven M Francque, *Edegem*
Nikos Kotzampassakis, *Liège*
Geert KMM Robaeys, *Genk*
Xavier Sagaert, *Leuven*
Peter Starkel, *Brussels*
Eddie Wisse, *Keerbergen*

Brazil

SMP Balzan, *Santa Cruz do Sul*
JLF Caboclo, *Sao jose do rio preto*
Fábio Guilherme Campos, *Sao Paulo*
Claudia RL Cardoso, *Rio de Janeiro*
Roberto J Carvalho-Filho, *Sao Paulo*
Carla Daltro, *Salvador*
José Sebastiao dos Santos, *Ribeirao Preto*
Eduardo LR Mello, *Rio de Janeiro*
Sthela Maria Murad-Regadas, *Fortaleza*
Claudia PMS Oliveira, *Sao Paulo*
Júlio C Pereira-Lima, *Porto Alegre*
Marcos V Perini, *Sao Paulo*
Vietla Satyanarayana Rao, *Fortaleza*
Raquel Rocha, *Salvador*
AC Simoes e Silva, *Belo Horizonte*
Mauricio F Silva, *Porto Alefre*
Aytan Miranda Sipahi, *Sao Paulo*
Rosa Leonôra Salerno Soares, *Niterói*
Cristiane Valle Tovo, *Porto Alegre*
Eduardo Garcia Vilela, *Belo Horizonte*

Brunei Darussalam

Vui Heng Chong, *Bandar Seri Begawan*

Bulgaria

Tanya Kirilova Kadiyska, *Sofia*
Mihaela Petrova, *Sofia*

Cambodia

Francois Rouet, *Phnom Penh*

Canada

Brian Bressler, *Vancouver*
Frank J Burczynski, *Winnipeg*
Wangxue Chen, *Ottawa*
Francesco Crea, *Vancouver*
Mirko Diksic, *Montreal*
Jane A Foster, *Hamilton*
Hugh J Freeman, *Vancouver*
Shahrokh M Ghobadloo, *Ottawa*
Yuewen Gong, *Winnipeg*
Philip H Gordon, *Quebec*
Rakesh Kumar, *Edmonton*
Wolfgang A Kunze, *Hamilton*
Patrick Labonte, *Laval*
Zhikang Peng, *Winnipeg*
Jayadev Raju, *Ottawa*
Maitreyi Raman, *Calgary*
Giada Sebastiani, *Montreal*
Maida J Sewitch, *Montreal*
Eldon A Shaffer, *Alberta*
Christopher W Teshima, *Edmonton*
Jean Sévigny, *Québec*
Pingchang Yang, *Hamilton*
Pingchang Yang, *Hamilton*
Eric M Yoshida, *Vancouver*
Bin Zheng, *Edmonton*

Chile

Marcelo A Beltran, *La Serena*
Flavio Nervi, *Santiago*
Adolfo Parra-Blanco, *Santiago*
Alejandro Soza, *Santiago*

China

Zhao-Xiang Bian, *Hong Kong*
San-Jun Cai, *Shanghai*
Guang-Wen Cao, *Shanghai*
Long Chen, *Nanjing*
Ru-Fu Chen, *Guangzhou*
George G Chen, *Hong Kong*
Li-Bo Chen, *Wuhan*
Jia-Xu Chen, *Beijing*
Hong-Song Chen, *Beijing*
Lin Chen, *Beijing*
Yang-Chao Chen, *Hong Kong*
Zhen Chen, *Shanghai*
Ying-Sheng Cheng, *Shanghai*
Kent-Man Chu, *Hong Kong*
Zhi-Jun Dai, *Xi'an*
Jing-Yu Deng, *Tianjin*
Yi-Qi Du, *Shanghai*
Zhi Du, *Tianjin*
Hani El-Nezami, *Hong Kong*
Bao-Ying Fei, *Hangzhou*
Chang-Ming Gao, *Nanjing*
Jian-Ping Gong, *Chongqing*
Zuo-Jiong Gong, *Wuhan*
Jing-Shan Gong, *Shenzhen*
Guo-Li Gu, *Beijing*
Yong-Song Guan, *Chengdu*
Mao-Lin Guo, *Luoyang*
Jun-Ming Guo, *Ningbo*
Yan-Mei Guo, *Shanghai*
Xiao-Zhong Guo, *Shenyang*
Guo-Hong Han, *Xi'an*
Ming-Liang He, *Hong Kong*
Peng Hou, *Xi'an*
Zhao-Hui Huang, *Wuxi*
Feng Ji, *Hangzhou*
Simon Law, *Hong Kong*
Yu-Yuan Li, *Guangzhou*
Meng-Sen Li, *Haikou*
Shu-De Li, *Shanghai*
Zong-Fang Li, *Xi'an*
Qing-Quan Li, *Shanghai*
Kang Li, *Lasa*
Han Liang, *Tianjin*
Xing'e Liu, *Hangzhou*
Zheng-Wen Liu, *Xi'an*
Xiao-Fang Liu, *Yantai*
Bin Liu, *Tianjin*
Quan-Da Liu, *Beijing*
Hai-Feng Liu, *Beijing*
Fei Liu, *Shanghai*
Ai-Guo Lu, *Shanghai*
He-Sheng Luo, *Wuhan*
Xiao-Peng Ma, *Shanghai*
Yong Meng, *Shantou*
Ke-Jun Nan, *Xi'an*
Siew Chien Ng, *Hong Kong*
Simon SM Ng, *Hong Kong*
Zhao-Shan Niu, *Qingdao*
Di Qu, *Shanghai*
Ying-Mo Shen, *Beijing*
Rui-Hua Shi, *Nanjing*
Bao-Min Shi, *Shanghai*
Xiao-Dong Sun, *Hangzhou*
Si-Yu Sun, *Shenyang*
Guang-Hong Tan, *Haikou*
Wen-Fu Tang, *Chengdu*
Anthony YB Teoh, *Hong Kong*
Wei-Dong Tong, *Chongqing*
Eric Tse, *Hong Kong*
Hong Tu, *Shanghai*
Rong Tu, *Haikou*
Jian-She Wang, *Shanghai*
Kai Wang, *Jinan*
Xiao-Ping Wang, *Xianyang*
Xiu-Yan Wang, *Shanghai*

Dao-Rong Wang, *Yangzhou*
De-Sheng Wang, *Xi'an*
Chun-You Wang, *Wuhan*
Ge Wang, *Chongqing*
Xi-Shan Wang, *Harbin*
Wei-hong Wang, *Beijing*
Zhen-Ning Wang, *Shenyang*
Wai Man Raymond Wong, *Hong Kong*
Chun-Ming Wong, *Hong Kong*
Jian Wu, *Shanghai*
Sheng-Li Wu, *Xi'an*
Wu-Jun Wu, *Xi'an*
Qing Xia, *Chengdu*
Yan Xin, *Shenyang*
Dong-Ping Xu, *Beijing*
Jian-Min Xu, *Shanghai*
Wei Xu, *Changchun*
Ming Yan, *Jinan*
Xin-Min Yan, *Kunming*
Yi-Qun Yan, *Shanghai*
Feng Yang, *Shanghai*
Yong-Ping Yang, *Beijing*
He-Rui Yao, *Guangzhou*
Thomas Yau, *Hong Kong*
Winnie Yeo, *Hong Kong*
Jing You, *Kunming*
Jian-Qing Yu, *Wuhan*
Ying-Yan Yu, *Shanghai*
Wei-Zheng Zeng, *Chengdu*
Zong-Ming Zhang, *Beijing*
Dian-Liang Zhang, *Qingdao*
Ya-Ping Zhang, *Shijiazhuang*
You-Cheng Zhang, *Lanzhou*
Jian-Zhong Zhang, *Beijing*
Ji-Yuan Zhang, *Beijing*
Hai-Tao Zhao, *Beijing*
Jian Zhao, *Shanghai*
Jian-Hong Zhong, *Nanning*
Ying-Qiang Zhong, *Guangzhou*
Ping-Hong Zhou, *Shanghai*
Yan-Ming Zhou, *Xiamen*
Tong Zhou, *Nanchong*
Li-Ming Zhou, *Chengdu*
Guo-Xiong Zhou, *Nantong*
Feng-Shang Zhu, *Shanghai*
Jiang-Fan Zhu, *Shanghai*
Zhao-Hui Zhu, *Beijing*

Croatia

Tajana Filipec Kanizaj, *Zagreb*
Mario Tadic, *Zagreb*

Cuba

Damian Casadesus, *Havana*

Czech

Jan Bures, *Hradec Kralove*
Marcela Kopacova, *Hradec Kralove*
Otto Kucera, *Hradec Kralove*
Marek Minarik, *Prague*
Pavel Soucek, *Prague*
Miroslav Zavoral, *Prague*

Denmark

Vibeke Andersen, *Odense*
E Michael Danielsen, *Copenhagen*

Egypt

Mohamed MM Abdel-Latif, *Assiut*
Hussein Atta, *Cairo*
Ashraf Elbahrawy, *Cairo*
Mortada Hassan El-Shabrawi, *Cairo*
Mona El Said El-Raziky, *Cairo*
Elrashdy M Redwan, *New Borg Alrab*
Zeinab Nabil Ahmed Said, *Cairo*
Ragaa HM Salama, *Assiut*
Maha Maher Shehata, *Mansoura*

Estonia

Margus Lember, *Tartu*
Tamara Vorobjova, *Tartu*

Finland

Marko Kalliomäki, *Turku*
Thomas Kietzmann, *Oulu*
Kaija-Leena Kolho, *Helsinki*
Eija Korkeila, *Turku*
Heikki Makisalo, *Helsinki*
Tanja Pessi, *Tampere*

France

Armando Abergel Clermont, *Ferrand*
Elie K Chouillard, *Polssy*
Pierre Cordelier, *Toulouse*
Pascal P Crenn, *Garches*
Catherine Daniel, *Lille*
Fanny Daniel, *Paris*
Cedric Dray, *Toulouse*
Benoit Foligne, *Lille*
Jean-Noel Freund, *Strasbourg*
Hervé Guillou, *Toulouse*
Nathalie Janel, *Paris*
Majid Khatib, *Bordeaux*
Jacques Marescaux, *Strasbourg*
Jean-Claude Marie, *Paris*
Driffa Moussata, *Pierre Benite*
Hang Nguyen, *Clermont-Ferrand*
Hugo Perazzo, *Paris*
Alain L Servin, *Chatenay-Malabry*
Chang Xian Zhang, *Lyon*

Germany

Stavros A Antoniou, *Monchengladbach*
Erwin Biecker, *Siegburg*
Hubert E Blum, *Freiburg*
Thomas Bock, *Berlin*
Katja Breitkopf-Heinlein, *Mannheim*
Elke Cario, *Essen*
Güralp Onur Ceyhan, *Munich*
Angel Cid-Arregui, *Heidelberg*
Michael Clemens Roggendorf, *München*
Christoph F Dietrich, *Bad Mergentheim*
Valentin Fuhrmann, *Hamburg*
Nikolaus Gassler, *Aachen*
Andreas Geier, *Wuerzburg*
Markus Gerhard, *Munich*
Anton Gillessen, *Muenster*
Thorsten Oliver Goetze, *Offenbach*
Daniel Nils Gotthardt, *Heidelberg*
Robert Grützmann, *Dresden*
Thilo Hackert, *Heidelberg*
Claus Hellerbrand, *Regensburg*
Harald Peter Hoensch, *Darmstadt*
Jens Hoeppner, *Freiburg*
Richard Hummel, *Muenster*
Jakob Robert Izbicki, *Hamburg*
Gernot Maximilian Kaiser, *Essen*
Matthias Kapischke, *Hamburg*
Michael Keese, *Frankfurt*
Andrej Khandoga, *Munich*
Jorg Kleeff, *Munich*
Alfred Koenigsrainer, *Tuebingen*
Peter Christopher Konturek, *Saalfeld*
Michael Linnebacher, *Rostock*
Stefan Maier, *Kaufbeuren*
Oliver Mann, *Hamburg*
Marc E Martignoni, *Munic*
Thomas Minor, *Bonn*
Oliver Moeschler, *Osnabrueck*
Jonas Mudter, *Eutin*
Sebastian Mueller, *Heidelberg*
Matthias Ocker, *Berlin*
Andreas Ommer, *Essen*
Albrecht Piiper, *Frankfurt*
Esther Raskopf, *Bonn*
Christoph Reichel, *Bad Brückenau*
Elke Roeb, *Giessen*
Udo Rolle, *Frankfurt*
Karl-Herbert Schafer, *Zweibrücken*
Peter Schemmer, *Heidelberg*
Andreas G Schreyer, *Regensburg*
Manuel A Silva, *Penzberg*
Georgios C Sotiropoulos, *Essen*
Ulrike S Stein, *Berlin*
Dirk Uhlmann, *Leipzig*
Michael Weiss, *Halle*
Hong-Lei Weng, *Mannheim*
Karsten Wursthorn, *Hamburg*

Greece

Alexandra Alexopoulou, *Athens*
Nikolaos Antonakopoulos, *Athens*
Stelios F Assimakopoulos, *Patras*
Grigoris Chatzimavroudis, *Thessaloniki*
Evangelos Cholongitas, *Thessaloniki*
Gregory Christodoulidis, *Larisa*
George N Dalekos, *Larissa*
Urania Georgopoulou, *Athens*
Eleni Gigi, *Thessaloniki*
Stavros Gourgiotis, *Athens*
Leontios J Hadjileontiadis, *Thessaloniki*
Thomas Hyphantis, *Ioannina*
Ioannis Kanellos, *Thessaloniki*
Stylianos Karatapanis, *Rhodes*
Michael Koutsilieris, *Athens*
Spiros D Ladas, *Athens*

Theodoros K Liakakos, *Athens*
Emanuel K Manesis, *Athens*
Spilios Manolakopoulos, *Athens*
Gerassimos John Mantzaris, *Athens*
Athanasios D Marinis, *Piraeus*
Nikolaos Ioannis Nikiteas, *Athens*
Konstantinos X Papamichael, *Athens*
George Sgourakis, *Athens*
Konstantinos C Thomopoulos, *Patras*
Konstantinos Triantafyllou, *Athens*
Christos Triantos, *Patras*
Georgios Zacharakis, *Athens*
Petros Zezos, *Alexandroupolis*
Demosthenes E Ziogas, *Ioannina*

Guatemala

Carlos Maria Parellada, *Guatemala*

Hungary

Mihaly Boros, *Szeged*
Tamás Decsi, *Pécs*
Gyula Farkas, *Szeged*
Andrea Furka, *Debrecen*
Y vette Mandi, *Szeged*
Peter L Lakatos, *Budapest*
Pal Miheller, *Budapest*
Tamás Molnar, *Szeged*
Attila Olah, *Gyor*
Maria Papp, *Debrecen*
Zoltan Rakonczay, *Szeged*
Ferenc Sipos, *Budapest*
Miklós Tanyi, *Debrecen*
Tibor Wittmann, *Szeged*

Iceland

Tryggvi Bjorn Stefánsson, *Reykjavík*

India

Brij B Agarwal, *New Delhi*
Deepak N Amarapurkar, *Mumbai*
Shams ul Bari, *Srinagar*
Sriparna Basu, *Varanasi*
Runu Chakravarty, *Kolkata*
Devendra C Desai, *Mumbai*
Nutan D Desai, *Mumbai*
Suneela Sunil Dhaneshwar, *Pune*
Radha K Dhiman, *Chandigarh*
Pankaj Garg, *Mohali*
Uday C Ghoshal, *Lucknow*
Kalpesh Jani, *Vadodara*
Premashis Kar, *New Delhi*
Jyotdeep Kaur, *Chandigarh*
Rakesh Kochhar, *Chandigarh*
Pradyumna K Mishra, *Mumbai*
Asish K Mukhopadhyay, *Kolkata*
Imtiyaz Murtaza, *Srinagar*
P Nagarajan, *New Delhi*
Samiran Nundy, *Delhi*
Gopal Pande, *Hyderabad*
Benjamin Perakath, *Vellore*
Arun Prasad, *New Delhi*
D Nageshwar Reddy, *Hyderabad*
Lekha Saha, *Chandigarh*
Sundeep Singh Saluja, *New Delhi*
Mahesh Prakash Sharma, *New Delhi*
Sadiq Saleem Sikora, *Bangalore*
Sarman Singh, *New Delhi*
Rajeev Sinha, *Jhansi*
Rupjyoti Talukdar, *Hyderabad*
Rakesh Kumar Tandon, *New Delhi*
Narayanan Thirumoorthy, *Coimbatore*

Indonesia

David Handojo Muljono, *Jakarta*
Andi Utama, *Jakarta*

Iran

Arezoo Aghakhani, *Tehran*
Seyed Mohsen Dehghani, *Shiraz*
Ahad Eshraghian, *Shiraz*
Hossein Khedmat, *Tehran*
Sadegh Massarrat, *Tehran*
Marjan Mohammadi, *Tehran*
Roja Rahimi, *Tehran*
Farzaneh Sabahi, *Tehran*
Majid Sadeghizadeh, *Tehran*
Farideh Siavoshi, *Tehran*

Ireland

Gary Alan Bass, *Dublin*
David J Brayden, *Dublin*
Ronan A Cahill, *Dublin*
Glen A Doherty, *Dublin*
Liam J Fanning, *Cork*
Barry Philip McMahon, *Dublin*
RossMcManus, *Dublin*
Dervla O'Malley, *Cork*
Sinead M Smith, *Dublin*

Israel

Dan Carter, *Ramat Gan*
Jorge-Shmuel Delgado, *Metar*
Eli Magen, *Ashdod*
Nitsan Maharshak, *Tel Aviv*
Shaul Mordechai, *Beer Sheva*
Menachem Moshkowitz, *Tel Aviv*
William Bahij Nseir, *Nazareth*
Shimon Reif, *Jerusalem*
Ram Reifen, *Rehovot*
Ariella Bar-Gil Shitrit, *Jerusalem*
Noam Shussman, *Jerusalem*
Igor Sukhotnik, *Haifa*
Nir Wasserberg, *Petach Tiqwa*
Jacob Yahav, *Rehovot*
Doron Levi Zamir, *Gedera*
Shira Zelber-Sagi, *Haifa*
Romy Zemel, *Petach-Tikva*

Italy

Ludovico Abenavoli, *Catanzaro*
Luigi Elio Adinolfi, *Naples*
Carlo Virginio Agostoni, *Milan*
Anna Alisi, *Rome*
Piero Luigi Almasio, *Palermo*
Donato Francesco Altomare, *Bari*
Amedeo Amedei, *Florence*
Pietro Andreone, *Bologna*
Imerio Angriman, *Padova*
Vito Annese, *Florence*
Paolo Aurello, *Rome*
Salavtore Auricchio, *Naples*
Gian Luca Baiocchi, *Brescia*
Gianpaolo Balzano, *Milan*
Antonio Basoli, *Rome*
Gabrio Bassotti, *San Sisto*
Mauro Bernardi, *Bologna*
Alberto Biondi, *Rome*
Ennio Biscaldi, *Genova*
Massimo Bolognesi, *Padua*
Luigi Bonavina, *Milano*
Aldo Bove, *Chieti*
Raffaele Bruno, *Pavia*
Luigi Brusciano, *Napoli*
Giuseppe Cabibbo, *Palermo*
Carlo Calabrese, *Bologna*
Daniele Calistri, *Meldola*
Vincenza Calvaruso, *Palermo*
Lorenzo Camellini, *Reggio Emilia*
Marco Candela, *Bologna*
Raffaele Capasso, *Naples*
Lucia Carulli, *Modena*
Renato David Caviglia, *Rome*
Luigina Cellini, *Chieti*
Giuseppe Chiarioni, *Verona*
Claudio Chiesa, *Rome*
Michele Cicala, *Roma*
Rachele Ciccocioppo, *Pavia*
Sandro Contini, *Parma*
Gaetano Corso, *Foggia*
Renato Costi, *Parma*
Alessandro Cucchetti, *Bologna*
Rosario Cuomo, *Napoli*
Giuseppe Currò, *Messina*
Paola De Nardi, *Milano*
Giovanni D De Palma, *Naples*
Raffaele De Palma, *Napoli*
Giuseppina De Petro, *Brescia*
Valli De Re, *Aviano*
Paolo De Simone, *Pisa*
Giuliana Decorti, *Trieste*
Emanuele Miraglia del Giudice, *Napoli*
Isidoro Di Carlo, *Catania*
Matteo Nicola Dario Di Minno, *Naples*
Massimo Donadelli, *Verona*
Mirko D'Onofrio, *Verona*
Maria Pina Dore, *Sassari*
Luca Elli, *Milano*
Massimiliano Fabozzi, *Aosta*
Massimo Falconi, *Ancona*
Ezio Falletto, *Turin*
Silvia Fargion, *Milan*
Matteo Fassan, *Verona*
Gianfranco Delle Fave, *Roma*
Alessandro Federico, *Naples*
Francesco Feo, *Sassari*
Davide Festi, *Bologna*
Natale Figura, *Siena*
Vincenzo Formica, *Rome*
Mirella Fraquelli, *Milan*

Marzio Frazzoni, *Modena*
Walter Fries, *Messina*
Gennaro Galizia, *Naples*
Andrea Galli, *Florence*
Matteo Garcovich, *Rome*
Eugenio Gaudio, *Rome*
Paola Ghiorzo, *Genoa*
Edoardo G Giannini, *Genova*
Luca Gianotti, *Monza*
Maria Cecilia Giron, *Padova*
Alberto Grassi, *Rimini*
Gabriele Grassi, *Trieste*
Francesco Greco, *Bergamo*
Luigi Greco, *Naples*
Antonio Grieco, *Rome*
Fabio Grizzi, *Rozzano*
Laurino Grossi, *Pescara*
Simone Guglielmetti, *Milan*
Tiberiu Hershcovici, *Jerusalem*
Calogero Iacono, *Verona*
Enzo Ierardi, *Bari*
Amedeo Indriolo, *Bergamo*
Raffaele Iorio, *Naples*
Paola Iovino, *Salerno*
Angelo A Izzo, *Naples*
Loreta Kondili, *Rome*
Filippo La Torre, *Rome*
Giuseppe La Torre, *Rome*
Giovanni Latella, *L'Aquila*
Salvatore Leonardi, *Catania*
Massimo Libra, *Catania*
Anna Licata, *Palermo*
C armela Loguercio, *Naples*
Amedeo Lonardo, *Modena*
Carmelo Luigiano, *Catania*
Francesco Luzza, *Catanzaro*
Giovanni Maconi, *Milano*
Antonio Macrì, *Messina*
Mariano Malaguarnera, *Catania*
Francesco Manguso, *Napoli*
Tommaso Maria Manzia, *Rome*
Daniele Marrelli, *Siena*
Gabriele Masselli, *Rome*
Sara Massironi, *Milan*
Giuseppe Mazzarella, *Avellino*
Michele Milella, *Rome*
Giovanni Milito, *Rome*
Antonella d'Arminio Monforte, *Milan*
Fabrizio Montecucco, *Genoa*
Giovanni Monteleone, *Rome*
Mario Morino, *Torino*
Vincenzo La Mura, *Milan*
Gerardo Nardone, *Naples*
Riccardo Nascimbeni, *Brescia*
Gabriella Nesi, *Florence*
Giuseppe Nigri, *Rome*
Erica Novo, *Turin*
Veronica Ojetti, *Rome*
Michele Orditura, *Naples*
Fabio Pace, *Seriate*
Lucia Pacifico, *Rome*
Omero Alessandro Paoluzi, *Rome*
Valerio Pazienza, *San Giovanni Rotondo*
Rinaldo Pellicano, *Turin*
Adriano M Pellicelli, *Rome*
Nadia Peparini, *Ciampino*
Mario Pescatori, *Rome*
Antonio Picardi, *Rome*
Alberto Pilotto, *Padova*
Alberto Piperno, *Monza*
Anna Chiara Piscaglia, *Rome*
Maurizio Pompili, *Rome*
Francesca Romana Ponziani, *Rome*
Cosimo Prantera, *Rome*
Girolamo Ranieri, *Bari*
Carlo Ratto, *Tome*
Barbara Renga, *Perugia*
Alessandro Repici, *Rozzano*
Maria Elena Riccioni, *Rome*
Lucia Ricci-Vitiani, *Rome*
Luciana Rigoli, *Messina*
Mario Rizzetto, *Torino*
Ballarin Roberto, *Modena*
Roberto G Romanelli, *Florence*
Claudio Romano, *Messina*
Luca Roncucci, *Modena*
Cesare Ruffolo, *Treviso*
L ucia Sacchetti, *Napoli*
Rodolfo Sacco, *Pisa*
Lapo Sali, *Florence*
Romina Salpini, *Rome*
Giulio Aniello, *Santoro Treviso*
Armando Santoro, *Rozzano*
Edoardo Savarino, *Padua*
Marco Senzolo, *Padua*
Annalucia Serafino, *Rome*
Giuseppe S Sica, *Rome*
Pierpaolo Sileri, *Rome*
Cosimo Sperti, *Padua*
Vincenzo Stanghellini, *Bologna*
Cristina Stasi, *Florence*
Gabriele Stocco, *Trieste*
Roberto Tarquini, *Florence*
Mario Testini, *Bari*
Guido Torzilli, *Milan*
Guido Alberto Massimo, *Tiberio Brescia*
Giuseppe Toffoli, *Aviano*
Alberto Tommasini, *Trieste*
Francesco Tonelli, *Florence*
Cesare Tosetti Porretta, *Terme*
Lucio Trevisani, *Cona*
Guglielmo M Trovato, *Catania*
Mariapia Vairetti, *Pavia*
Luca Vittorio Valenti, *Milano*
Mariateresa T Ventura, *Bari*
Giuseppe Verlato, *Verona*
Marco Vivarelli, *Ancona*
Giovanni Li Volti, *Catania*
Giuseppe Zanotti, *Padua*
Vincenzo Zara, *Lecce*
Gianguglielmo Zehender, *Milan*
Anna Linda Zignego, *Florence*
Rocco Antonio Zoccali, *Messina*
Angelo Zullo, *Rome*

Japan

Yasushi Adachi, *Sapporo*
Takafumi Ando, *Nagoya*
Masahiro Arai, *Tokyo*
Makoto Arai, *Chiba*
Takaaki Arigami, *Kagoshima*
Itaru Endo,*Yokohama*
Munechika Enjoji, *Fukuoka*
Shunji Fujimori, *Tokyo*
Yasuhiro Fujino, *Akashi*
Toshiyoshi Fujiwara, *Okayama*
Yosuke Fukunaga, *Tokyo*
Toshio Fukusato, *Tokyo*
Takahisa Furuta, *Hamamatsu*
Osamu Handa, *Kyoto*
Naoki Hashimoto, *Osaka*
Yoichi Hiasa, *Toon*
Masatsugu Hiraki, *Saga*
Satoshi Hirano, *Sapporo*
Keiji Hirata, *Fukuoka*
Toru Hiyama, *Higashihiroshima*
Akira Hokama, *Nishihara*
Shu Hoteya, *Tokyo*
Masao Ichinose, *Wakayama*
Tatsuya Ide, *Kurume*
Masahiro Iizuka, *Akita*
Toshiro Iizuka, *Tokyo*
Kenichi Ikejima, *Tokyo*
Tetsuya Ikemoto, *Tokushima*
Hiroyuki Imaeda, *Saitama*
Atsushi Imagawa, *Kan-onji*
Hiroo Imazu, *Tokyo*
Shuji Isaji, *Tsu*
Toru Ishikawa, *Niigata*
Toshiyuki Ishiwata, *Tokyo*
Soichi Itaba, *Kitakyushu*
Yoshiaki Iwasaki, *Okayama*
Tatehiro Kagawa, *Isehara*
Satoru Kakizaki, *Maebashi*
Naomi Kakushima, *Shizuoka*
Terumi Kamisawa, *Tokyo*
Akihide Kamiya, *Isehara*
Osamu Kanauchi, *Tokyo*
Tatsuo Kanda, *Chiba*
Shin Kariya, *Okayama*
Shigeyuki Kawa, *Matsumoto*
Takumi Kawaguchi, *Kurume*
Takashi Kawai, *Tokyo*
Soo Ryang Kim, *Kobe*
Shinsuke Kiriyama, *Gunma*
Tsuneo Kitamura, *Urayasu*
Masayuki Kitano, *Osakasayama*
Hirotoshi Kobayashi, *Tokyo*
Hironori Koga, *Kurume*
Takashi Kojima, *Sapporo*
Satoshi Kokura, *Kyoto*
Shuhei Komatsu, *Kyoto*
Tadashi Kondo, *Tokyo*
Yasuteru Kondo, *Sendai*
Yasuhiro Kuramitsu, *Yamaguchi*
Yukinori Kurokawa, *Osaka*
Shin Maeda, *Yokohama*
Koutarou Maeda, *Toyoake*
Hitoshi Maruyama, *Chiba*
Atsushi Masamune, *Sendai*
Hiroyuki Matsubayashi, *Suntogun*
Akihisa Matsuda, *Inzai*
Hirofumi Matsui, *Tsukuba*
Akira Matsumori, *Kyoto*
Yoichi Matsuo, *Nagoya*
Y Matsuzaki, *Ami*
Toshihiro Mitaka, *Sapporo*
Kouichi Miura, *Akita*
Shinichi Miyagawa, *Matumoto*
Eiji Miyoshi, *Suita*
Toru Mizuguchi, *Sapporo*
Nobumasa Mizuno, *Nagoya*
Zenichi Morise, *Nagoya*

Tomohiko Moriyama, *Fukuoka*
Kunihiko Murase, *Tusima*
Michihiro Mutoh, *Tsukiji*
Akihito Nagahara, *Tokyo*
Hikaru Nagahara, *Tokyo*
Hidenari Nagai, *Tokyo*
Koichi Nagata, *Shimotsuke-shi*
Masaki Nagaya, *Kawasaki*
Hisato Nakajima, *Nishi-Shinbashi*
Toshifusa Nakajima, *Tokyo*
Hiroshi Nakano, *Kawasaki*
Hiroshi Nakase, *Kyoto*
Toshiyuki Nakayama, *Nagasaki*
Takahiro Nakazawa, *Nagoya*
Shoji Natsugoe, *Kagoshima City*
Tsutomu Nishida, *Suita*
Shuji Nomoto, *Naogya*
Sachiyo Nomura, *Tokyo*
Takeshi Ogura, *Takatsukishi*
Nobuhiro Ohkohchi, *Tsukuba*
Toshifumi Ohkusa, *Kashiwa*
Hirohide Ohnishi, *Akita*
Teruo Okano, *Tokyo*
Satoshi Osawa, *Hamamatsu*
Motoyuki Otsuka, *Tokyo*
Michitaka Ozaki, *Sapporo*
Satoru Saito, *Yokohama*
Chouhei Sakakura, *Kyoto*
Naoaki Sakata, *Sendai*
Ken Sato, *Maebashi*
Toshiro Sato, *Tokyo*
Tomoyuki Shibata, *Toyoake*
H Shimada, *Tokyo*
Tomohiko Shimatani, *Kure*
Yukihiro Shimizu, *Nanto*
Tadashi Shimoyama, *Hirosaki*
Masayuki Sho, *Nara*
Ikuo Shoji, *Kobe*
Atsushi Sofuni, *Tokyo*
Takeshi Suda, *Niigata*
M Sugimoto, *Hamamatsu*
Ken Sugimoto, *Hamamatsu*
Haruhiko Sugimura, *Hamamatsu*
Shoichiro Sumi, *Kyoto*
Hidekazu Suzuki, *Tokyo*
Masahiro Tajika, *Nagoya*
Hitoshi Takagi, *Takasaki*
Toru Takahashi, *Niigata*
Yoshihisa Takahashi, *Tokyo*
Shinsuke Takeno, *Fukuoka*
Akihiro Tamori, *Osaka*
Kyosuke Tanaka, *Tsu*
Shinji Tanaka, *Hiroshima*
Atsushi Tanaka, *Tokyo*
Yasuhito Tanaka, *Nagoya*
Shinji Tanaka, *Tokyo*
Minoru Tomizawa, *Yotsukaido City*
Kyoko Tsukiyama-Kohara, *Kagoshima*
Takuya Watanabe, *Niigata*
Kazuhiro Watanabe, *Sendai*
Satoshi Yamagiwa, *Niigata*
Takayuki Yamamoto, *Yokkaichi*
Hiroshi Yamamoto, *Otsu*
Kosho Yamanouchi, *Nagasaki*
Ichiro Yasuda, *Gifu*
Yutaka Yata, *Maebashi-city*
Shin-ichi Yokota, *Sapporo*
Norimasa Yoshida, *Kyoto*
Hiroshi Yoshida, *Tama-City*
Hitoshi Yoshiji, *Kashihara*
Kazuhiko Yoshimatsu, *Tokyo*
Kentaro Yoshioka, *Toyoake*
Nobuhiro Zaima, *Nara*

Jordan
Khaled Ali Jadallah, *Irbid*

Kuwait
Islam Khan, *Kuwait*

Lebanon
Bassam N Abboud, *Beirut*
Kassem A Barada, *Beirut*
Marwan Ghosn, *Beirut*
Iyad A Issa, *Beirut*
Fadi H Mourad, *Beirut*
AIa Sharara, *Beirut*
Rita Slim, *Beirut*

Lithuania
Antanas Mickevicius, *Kaunas*

Malaysia
Huck Joo Tan, *Petaling Jaya*

Mexico
Richard A Awad, *Mexico City*
Carlos R Camara-Lemarroy, *Monterrey*
Norberto C Chavez-Tapia, *Mexico City*
Wolfgang Gaertner, *Mexico City*
Diego Garcia-Compean, *Monterrey*
Arturo Panduro, *Guadalajara*
OT Teramoto-Matsubara, *Mexico City*
Felix Tellez-Avila, *Mexico City*
Omar Vergara-Fernandez, *Mexico City*
Saúl Villa-Trevino, *Cuidad de México*

Morocco
Samir Ahboucha, *Khouribga*

Netherlands
Robert J de Knegt, *Rotterdam*
Tom Johannes Gerardus Gevers, *Nijmegen*
Menno Hoekstra, *Leiden*
BW Marcel Spanier, *Arnhem*
Karel van Erpecum, *Utrecht*

New Zealand
Leo K Cheng, *Auckland*
Andrew Stewart Day, *Christchurch*
Jonathan Barnes Koea, *Auckland*
Max Petrov, *Auckland*

Nigeria
Olufunmilayo Adenike Lesi, *Lagos*
Jesse Abiodun Otegbayo, *Ibadan*
Stella Ifeanyi Smith, *Lagos*

Norway
Trond Berg, *Oslo*
Trond Arnulf Buanes, *Krokkleiva*
Thomas de Lange, *Rud*
Magdy El-Salhy, *Stord*
Rasmus Goll, *Tromso*
Dag Arne Lihaug Hoff, *Aalesund*

Pakistan
Zaigham Abbas, *Karachi*
Usman A Ashfaq, *Faisalabad*
Muhammad Adnan Bawany, *Hyderabad*
Muhammad Idrees, *Lahore*
Saeed Sadiq Hamid, *Karachi*
Yasir Waheed, *Islamabad*

Poland
Thomas Brzozowski, *Cracow*
Magdalena Chmiela, *Lodz*
Krzysztof Jonderko, *Sosnowiec*
Anna Kasicka-Jonderko, *Sosnowiec*
Michal Kukla, *Katowice*
Tomasz Hubert Mach, *Krakow*
Agata Mulak, *Wroclaw*
Danuta Owczarek, *Kraków*
Piotr Socha, *Warsaw*
Piotr Stalke, *Gdansk*
Julian Teodor Swierczynski, *Gdansk*
Anna M Zawilak-Pawlik, *Wroclaw*

Portugal
Marie Isabelle Cremers, *Setubal*
Ceu Figueiredo, *Porto*
Ana Isabel Lopes, *LIsbon*
M Paula Macedo, *Lisboa*
Ricardo Marcos, *Porto*
Rui T Marinho, *Lisboa*
Guida Portela-Gomes, *Estoril*
Filipa F Vale, *Lisbon*

Puerto Rico
Caroline B Appleyard, *Ponce*

Qatar
Abdulbari Bener, *Doha*

Romania
Mihai Ciocirlan, *Bucharest*
Dan LucianDumitrascu, *Cluj-Napoca*
Carmen Fierbinteanu-Braticevici, *Bucharest*

Romeo G Mihaila, *Sibiu*
Lucian Negreanu, *Bucharest*
Adrian Saftoiu, *Craiova*
Andrada Seicean, *Cluj-Napoca*
Ioan Sporea, *Timisoara*
Letiţia Adela Maria Streba, *Craiova*
Anca Trifan, *Iasi*

Russia

Victor Pasechnikov, *Stavropol*
Vasiliy Ivanovich Reshetnyak, *Moscow*
Vitaly Skoropad, *Obninsk*

Saudi Arabia

Abdul-Wahed N Meshikhes, *Dammam*
M Ezzedien Rabie, *Khamis Mushait*

Singapore

Brian KP Goh, *Singapore*
Richie Soong, *Singapore*
Ker-Kan Tan, *Singapore*
Kok-Yang Tan, *Singapore*
Yee-Joo Tan, *Singapore*
Mark Wong, *Singapore*
Hong Ping Xia, *Singapore*

Slovenia

Matjaz Homan, *Ljubljana*
Martina Perse, *Ljubljana*

South Korea

Sang Hoon Ahn, *Seoul*
Seung Hyuk Baik, *Seoul*
Soon Koo Baik, *Wonju*
Soo-Cheon Chae, *Iksan*
Byung-Ho Choe, *Daegu*
Suck Chei Choi, *Iksan*
Hoon Jai Chun, *Seoul*
Yeun-Jun Chung, *Seoul*
Young-Hwa Chung, *Seoul*
Ki-Baik Hahm, *Seongnam*
Sang Young Han, *Busan*
Seok Joo Han, *Seoul*
Seung-Heon Hong, *Iksan*
Jin-Hyeok Hwang, *Seoungnam*
Jeong Won Jang, *Seoul*
Jin-Young Jang, *Seoul*
Dae-Won Jun, *Seoul*
Young Do Jung, *Kwangju*
Gyeong Hoon Kang, *Seoul*
Sung-Bum Kang, *Seoul*
Koo Jeong Kang, *Daegu*
Ki Mun Kang, *Jinju*
Chang Moo Kang, *Seodaemun-gu*
Gwang Ha Kim, *Busan*
Sang Soo Kim, *Goyang-si*
Jin Cheon Kim, *Seoul*
Tae Il Kim, *Seoul*
Jin Hong Kim, *Suwon*
Kyung Mo Kim, *Seoul*
Kyongmin Kim, *Suwon*
Hyung-Ho Kim, *Seongnam*
Seoung Hoon Kim, *Goyang*
Sang Il Kim, *Seoul*
Hyun-Soo Kim, *Wonju*
Jung Mogg Kim, *Seoul*
Dong Yi Kim, *Gwangju*
Kyun-Hwan Kim, *Seoul*
Jong-Han Kim, *Ansan*
Sang Wun Kim, *Seoul*
Ja-Lok Ku, *Seoul*
Kyu Taek Lee, *Seoul*
Hae-Wan Lee, *Chuncheon*
Inchul Lee, *Seoul*
Jung Eun Lee, *Seoul*
Sang Chul Lee, *Daejeon*
Song Woo Lee, *Ansan-si*
Hyuk-Joon Lee, *Seoul*
Seong-Wook Lee, *Yongin*
Kil Yeon Lee, *Seoul*
Jong-Inn Lee, *Seoul*
Kyung A Lee, *Seoul*
Jong-Baeck Lim, *Seoul*
Eun-Yi Moon, *Seoul*
SH Noh, *Seoul*
Seung Woon Paik, *Seoul*
Won Sang Park, *Seoul*
Sung-Joo Park, *Iksan*
Kyung Sik Park, *Daegu*
Se Hoon Park, *Seoul*
Yoonkyung Park, *Gwangju*
Seung-Wan Ryu, *Daegu*
Il Han Song, *Cheonan*
Myeong Jun Song, *Daejeon*
Yun Kyoung Yim, *Daejeon*
Dae-Yeul Yu *Daejeon*

Spain

Mariam Aguas, *Valencia*
Raul J Andrade, *Málaga*
Antonio Arroyo, *Elche*
Josep M Bordas, *Barcelona*
Lisardo Boscá, *Madrid*
Ricardo Robles Campos, *Murcia*
Jordi Camps, *Reus*
Carlos Cervera *Barcelona*
Alfonso Clemente, *Granada*
Pilar Codoner-Franch, *Valencia*
Fernando J Corrales, *Pamplona*
Fermin Sánchez de Medina, *Granada*
Alberto Herreros de Tejada, *Majadahonda*
Enrique de-Madaria, *Alicante*
JE Dominguez-Munoz, *Santiago de Compostela*
Vicente Felipo, *Valencia*
CM Fernandez-Rodriguez, *Madrid*
Carmen Frontela-Saseta, *Murcia*
Julio Galvez, *Granada*
Maria Teresa García, *Vigo*
MI Garcia-Fernandez, *Málaga*
Emilio Gonzalez-Reimers, *La Laguna*
Marcel Jimenez, *Bellaterra*
Angel Lanas, *Zaragoza*
Juan Ramón Larrubia, *Guadalajara*
Antonio Lopez-Sanroman, *Madrid*
Vicente Lorenzo-Zuniga, *Badalona*
Alfredo J Lucendo, *Tomelloso*
Vicenta Soledad Martinez-Zorzano, *Vigo*
José Manuel Martin-Villa, *Madrid*
Julio Mayol, *Madrid*
Manuel Morales-Ruiz, *Barcelona*
Alfredo Moreno-Egea, *Murcia*
Albert Pares, *Barcelona*
Maria Pellise, *Barcelona*
José Perea, *Madrid*
Miguel Angel Plaza, *Zaragoza*
María J Pozo, *Cáceres*
Enrique Quintero, *La Laguna*
Jose M Ramia, *Madrid*
Francisco Rodriguez-Frias, *Barcelona*
Silvia Ruiz-Gaspa, *Barcelona*
Xavier Serra-Aracil, *Barcelona*
Vincent Soriano, *Madrid*
Javier Suarez, *Pamplona*
Carlos Taxonera, *Madrid*
M Isabel Torres, *Jaén*
Manuel Vazquez-Carrera, *Barcelona*
Benito Velayos, *Valladolid*
Silvia Vidal, *Barcelona*

Sri Lanka

Arjuna Priyadarsin De Silva, *Colombo*

Sudan

Ishag Adam, *Khartoum*

Sweden

Roland G Andersson, *Lund*
Bergthor Björnsson, *Linkoping*
Johan Christopher Bohr, *Örebro*
Mauro D'Amato, *Stockholm*
Thomas Franzen, *Norrkoping*
Evangelos Kalaitzakis, *Lund*
Riadh Sadik, *Gothenburg*
Per Anders Sandstrom, *Linkoping*
Ervin Toth, *Malmö*
Konstantinos Tsimogiannis, *Vasteras*
Apostolos V Tsolakis, *Uppsala*

Switzerland

Gieri Cathomas, *Liestal*
Jean Louis Frossard, *Geneve*
Christian Toso, *Geneva*
Stephan Robert Vavricka, *Zurich*
Dominique Velin, *Lausanne*

Thailand

Thawatchai Akaraviputh, *Bangkok*
P Yoysungnoen Chintana, *Pathumthani*
Veerapol Kukongviriyapan, *Muang*
Vijittra Leardkamolkarn, *Bangkok*
Varut Lohsiriwat, *Bangkok*
Somchai Pinlaor, *Khaon Kaen*
D Wattanasirichaigoon, *Bangkok*

Trinidad and Tobago

B Shivananda Nayak, *Mount Hope*

Tunisia

Ibtissem Ghedira, *Sousse*
Lilia Zouiten-Mekki, *Tunis*

Turkey

Inci Alican, *Istanbul*
Mustafa Altindis, *Sakarya*
Mutay Aslan, *Antalya*
Oktar Asoglu, *Istanbul*
Yasemin Hatice Balaban, *Istanbul*
Metin Basaranoglu, *Ankara*
Yusuf Bayraktar, *Ankara*
Süleyman Bayram, *Adiyaman*
Ahmet Bilici, *Istanbul*
Ahmet Sedat Boyacioglu, *Ankara*
Züleyha Akkan Cetinkaya, *Kocaeli*
Cavit Col, *Bolu*
Yasar Colak, *Istanbul*
Cagatay Erden Daphan, *Kirikkale*
Mehmet Demir, *Hatay*
Ahmet Merih Dobrucali, *Istanbul*
Gülsüm Ozlem Elpek, *Antalya*
Ayse Basak Engin, *Ankara*
Eren Ersoy, *Ankara*
Osman Ersoy, *Ankara*
Yusuf Ziya Erzin, *Istanbul*
Mukaddes Esrefoglu, *Istanbul*
Levent Filik, *Ankara*
Ozgur Harmanci, *Ankara*
Koray Hekimoglu, *Ankara*
Abdurrahman Kadayifci, *Gaziantep*
Cem Kalayci, *Istanbul*
Selin Kapan, *Istanbul*
Huseyin Kayadibi, *Adana*
Sabahattin Kaymakoglu, *Istanbul*
Metin Kement, *Istanbul*
Mevlut Kurt, *Bolu*
Resat Ozaras, *Istanbul*
Elvan Ozbek, *Adapazari*
Cengiz Ozcan, *Mersin*
Hasan Ozen, *Ankara*
Halil Ozguc, *Bursa*
Mehmet Ozturk, *Izmir*
Orhan V Ozkan, *Sakarya*
Semra Paydas, *Adana*
Ozlem Durmaz Suoglu, *Istanbul*
Ilker Tasci, *Ankara*
Müge Tecder-ünal, *Ankara*
Mesut Tez, *Ankara*
Serdar Topaloglu, *Trabzon*
Murat Toruner, *Ankara*
Gokhan Tumgor, *Adana*
Oguz Uskudar, *Adana*
Mehmet Yalniz, *Elazig*
Mehmet Yaman, *Elazig*
Veli Yazisiz, *Antalya*
Yusuf Yilmaz, *Istanbul*
Ozlem Yilmaz, *Izmir*
Oya Yucel, *Istanbul*
Ilhami Yuksel, *Ankara*

United Kingdom

Nadeem Ahmad Afzal, *Southampton*
Navneet K Ahluwalia, *Stockport*
Yeng S Ang, *Lancashire*
Ramesh P Arasaradnam, *Coventry*
Ian Leonard Phillip Beales, *Norwich*
John Beynon, *Swansea*
Barbara Braden, *Oxford*
Simon Bramhall, *Birmingham*
Geoffrey Burnstock, *London*
Ian Chau, *Sutton*
Thean Soon Chew, *London*
Helen G Coleman, *Belfast*
Anil Dhawan, *London*
Sunil Dolwani, *Cardiff*
Piers Gatenby, *London*
Anil T George, *London*
Pasquale Giordano, *London*
Paul Henderson, *Edinburgh*
Georgina Louise Hold, *Aberdeen*
Stefan Hubscher, *Birmingham*
Robin D Hughes, *London*
Nusrat Husain, *Manchester*
Matt W Johnson, *Luton*
Konrad Koss, *Macclesfield*
Anastasios Koulaouzidis, *Edinburgh*
Simon Lal, *Salford*
John S Leeds, *Aberdeen*
JK K Limdi, *Manchester*
Hongxiang Liu, *Cambridge*
Michael Joseph McGarvey, *London*
Michael Anthony Mendall, *London*
Alexander H Mirnezami, *Southampton*
J Bernadette Moore, *Guildford*
Claudio Nicoletti, *Norwich*
Savvas Papagrigoriadis, *London*
Sylvia LF Pender, *Southampton*
David Mark Pritchard, *Liverpool*
James A Ross, *Edinburgh*
Kamran Rostami, *Worcester*
Xiong Z Ruan, *London*
Frank I Tovey, *London*
Dhiraj Tripathi, *Birmingham*
Vamsi R Velchuru, *Great Yarmouth*
Nicholas T Ventham, *Edinburgh*
Diego Vergani, *London*
Jack Westwood Winter, *Glasgow*
Terence Wong, *London*
Ling Yang, *Oxford*

United States

Daniel E Abbott, *Cincinnati*
Ghassan K Abou-Alfa, *New York*
Julian Abrams, *New York*
David William Adelson, *Los Angeles*
Jonathan Steven Alexander, *Shreveport*
Tauseef Ali, *Oklahoma City*
Mohamed R Ali, *Sacramento*
Rajagopal N Aravalli, *Minneapolis*
Hassan Ashktorab, *Washington*
Shashi Bala, *Worcester*
Charles F Barish, *Raleigh*
P Patrick Basu, *New York*
Robert L Bell, *Berkeley Heights*
David Bentrem, *Chicago*
Henry J Binder, *New Haven*
Joshua Bleier, *Philadelphia*
Wojciech Blonski, *Johnson City*
Kenneth Boorom, *Corvallis*
Brian Boulay, *Chicago*
Carla W Brady, *Durham*
Kyle E Brown, *Iowa City*
Adeel A Butt, *Pittsburgh*
Weibiao Cao, *Providence*
Andrea Castillo, *Cheney*
Fernando J Castro, *Weston*
Adam S Cheifetz, *Boston*
Xiaoxin Luke Chen, *Durham*
Ramsey Cheung, *Palo Alto*
Parimal Chowdhury, *Little Rock*
Edward John Ciaccio, *New York*
Dahn L Clemens, *Omaha*
Yingzi Cong, *Galveston*
Laura Iris Cosen-Binker, *Boston*
Joseph John Cullen, *Lowa*
Mark J Czaja, *Bronx*
Mariana D Dabeva, *Bronx*
Christopher James Damman, *Seattle*
Isabelle G De Plaen, *Chicago*
Punita Dhawan, *Nashville*
Hui Dong, *La Jolla*
Wael El-Rifai, *Nashville*
Sukru H Emre, *New Haven*
Paul Feuerstadt, *Hamden*
Josef E Fischer, *Boston*
Laurie N Fishman, *Boston*
Joseph Che Forbi, *Atlanta*
Temitope Foster, *Atlanta*
Amy E Foxx-Orenstein, *Scottsdale*
Daniel E Freedberg, *New York*
Shai Friedland, *Palo Alto*
Virgilio George, *Indianapolis*
Ajay Goel, *Dallas*
Oliver Grundmann, *Gainesville*
Stefano Guandalini, *Chicago*
Chakshu Gupta, *St. Joseph*
Grigoriy E Gurvits, *New York*
Xiaonan Han, *Cincinnati*
Mohamed Hassan, *Jackson*
Martin Hauer-Jensen, *Little Rock*
Koichi Hayano, *Boston*
Yingli Hee, *Atlanta*
Samuel B Ho, *San Diego*
Jason Ken Hou, *Houston*
Lifang Hou, *Chicago*
K-Qin Hu, *Orange*
Jamal A Ibdah, *Columbia*
Robert Thomas Jensen, *Bethesda*
Huanguang "Charlie" Jia, *Gainesville*
Rome Jutabha, *Los Angeles*
Andreas M Kaiser, *Los Angeles*
Avinash Kambadakone, *Boston*
David Edward Kaplan, *Philadelphia*
Randeep Kashyap, *Rochester*
Rashmi Kaul, *Tulsa*
Ali Keshavarzian, *Chicago*
Amir Maqbul Khan, *Marshall*
Nabeel Hasan Khan, *New Orleans*
Sahil Khanna, *Rochester*
Kusum K Kharbanda, *Omaha*

World Journal of Gastroenterology

Contents

Weekly Volume 21 Number 33 September 7, 2015

EDITORIAL

TOPIC HIGHLIGHT

ORIGINAL ARTICLE

Basic Study

Retrospective Cohort Study

Retrospective Study

World Journal of Gastroenterology
Volume 21 Number 33 September 7, 2015

Contents

NAME OF JOURNAL
World Journal of Gastroenterology

ISSN
ISSN 1007-9327 (print)
ISSN 2219-2840 (online)

LAUNCH DATE
October 1, 1995

FREQUENCY
Weekly

EDITORIAL OFFICE
Jin-Lei Wang, Director
Xiu-Xia Song, Vice Director
World Journal of Gastroenterology
Room 903, Building D, Ocean International Center,
No. 62 Dongsihuan Zhonglu, Chaoyang District,
Beijing 100025, China
Telephone: +86-10-59080039
Fax: +86-10-85381893
E-mail: editorialoffice@wjgnet.com
Help Desk: http://www.wjgnet.com/esps/helpdesk.aspx
http://www.wjgnet.com

PUBLISHER
Baishideng Publishing Group Inc
8226 Regency Drive,
Pleasanton, CA 94588, USA
Telephone: +1-925-223-8242
Fax: +1-925-223-8243
E-mail: bpgoffice@wjgnet.com
Help Desk: http://www.wjgnet.com/esps/helpdesk.aspx
http://www.wjgnet.com

PUBLICATION DATE
September 7, 2015

INSTRUCTIONS TO AUTHORS
Full instructions are available online at http://www.wjgnet.com/1007-9327/g_info_20100315215714.htm

ONLINE SUBMISSION
http://www.wjgnet.com/esps/

World Journal of Gastroenterology

Submit a Manuscript: http://www.wjgnet.com/esps/
Help Desk: http://www.wjgnet.com/esps/helpdesk.aspx
DOI: 10.3748/wjg.v21.i33.9683

World J Gastroenterol 2015 September 7; 21(33): 9683-9687
ISSN 1007-9327 (print) ISSN 2219-2840 (online)

EDITORIAL

Pediatric intestinal motility disorders

Stefan Gfroerer, Udo Rolle

Stefan Gfroerer, Udo Rolle, Department of Pediatric Surgery and Pediatric Urology, Goethe-University Frankfurt/M., 60590 Frankfurt/M., Germany

Author contributions: Gfroerer S and Rolle U both contributed to the design, drafting and final approval of the manuscript.

Conflict-of-interest statement: No conflict of interest for Gfroerer S and Rolle U.

Correspondence to: Udo Rolle, MD, FEBPS, Professor, Head of the Department of Pediatric Surgery and Pediatric Urology, Goethe-University Frankfurt/M., 60590 Frankfurt/M., Germany. udo.rolle@kgu.de
Telephone: +49-69-63016659
Fax: +49-69-63017140

Received: January 29, 2015
Peer-review started: January 29, 2015
First decision: April 27, 2015
Revised: May 7, 2015
Accepted: July 3, 2015
Article in press: July 3, 2015
Published online: September 7, 2015

Abstract

Pediatric intestinal motility disorders affect many children and thus not only impose a significant impact on pediatric health care in general but also on the quality of life of the affected patient. Furthermore, some of these conditions might also have implications for adulthood. Pediatric intestinal motility disorders frequently present as chronic constipation in toddler age children. Most of these conditions are functional, meaning that constipation does not have an organic etiology, but in 5% of the cases, an underlying, clearly organic disorder can be identified. Patients with organic causes for intestinal motility disorders usually present in early infancy or even right after birth. The most striking clinical feature of children with severe intestinal motility disorders is the delayed passage of meconium in the newborn period. This sign is highly indicative of the presence of Hirschsprung disease (HD), which is the most frequent congenital disorder of intestinal motility. HD is a rare but important congenital disease and the most significant entity of pediatric intestinal motility disorders. The etiology and pathogenesis of HD have been extensively studied over the last several decades. A defect in neural crest derived cell migration has been proven as an underlying cause of HD, leading to an aganglionic distal end of the gut. Numerous basic science and clinical research related studies have been conducted to better diagnose and treat HD. Resection of the aganglionic bowel remains the gold standard for treatment of HD. Most recent studies show, at least experimentally, the possibility of a stem cell based therapy for HD. This editorial also includes rare causes of pediatric intestinal motility disorders such as hypoganglionosis, dysganglionosis, chronic intestinal pseudo-obstruction and ganglioneuromatosis in multiple endocrine metaplasia. Underlying organic pathologies are rare in pediatric intestinal motility disorders but must be recognized as early as possible.

Key words: Intestinal motility disorder; Children; Hirschsprung disease; Chronic constipation; Delayed passage of meconium; Rectal biopsy; Stem cell based treatment; Multiple endocrine metaplasia

Core tip: Intestinal motility disorders are frequent in early childhood. Despite the fact that most of these patients suffer from functional problems it is of major importance to recognize the cases with severe

underlying organic causes. Pediatric patients with intestinal motility disorders require a standardized diagnostic and if necessary therapeutic approach. Functional constipation is the most frequent condition in toddlers and preschool age, which requires demystification, diet and concomitant laxative treatment. Functional constipation carries a very good prognosis. Organic causes are rare in intestinal motility disorders and require therefore meticulous diagnostics and adequate surgical treatment. Hirschsprung disease is the most relevant organic cause for pediatric intestinal motility disorders.

Gfroerer S, Rolle U. Pediatric intestinal motility disorders. *World J Gastroenterol* 2015; 21(33): 9683-9687 Available from: URL: http://www.wjgnet.com/1007-9327/full/v21/i33/9683.htm DOI: http://dx.doi.org/10.3748/wjg.v21.i33.9683

EPIDEMIOLOGY

Defecation disorder is among the most common complaints in pediatric patients. Chronic constipation accounts for 3%-5% of consultations to pediatricians and for 10%-25% of referrals to pediatric gastroenterologists[1,2]. Nevertheless, less than 5% of the affected children have an underlying organic cause for this condition.

Possible congenital anomalies of the intestinal motor functions must be detected as early as possible.

The most common congenital disease presenting with intestinal motor dysfunction is Hirschsprung disease (HD). Its incidence varies between 1:5000 and 1:10000 live births. Hirschsprung disease is characterized by the congenital absence of ganglion cells starting distally from the inner circular muscle with a varying extent towards the proximal bowel. The most frequent localization of the congenital aganglionosis is confined to the rectosigmoid colon[3].

Hypoganglionosis is an abnormality that is usually observed in conjunction with HD in the transitional zone proximal to the aganglionosis. Isolated hypoganglionosis is extremely rare and has only been reported in approximately 100 cases[4,5].

Dysganglionosis of the enteric nervous system (ENS) has previously been described as intestinal neuronal dysplasia (IND). This entity may not really exist as a clinical condition because, despite the described histopathological changes, almost all affected patients improve with time and conservative treatment. Currently it is assumed that the so-called IND is a normal age-related variant[6].

Ganglioneuromatosis usually presents with an intestinal motility disorder and is an important and mostly primary feature of the multiple endocrine neoplasia (MEN) syndrome type 2B[7].

Chronic intestinal pseudo-obstruction is a rare but severe condition, which is characterized by repetitive episodes or continuous symptoms of intestinal obstruction without a fixed obstructive bowel lesion. This disease frequently presents with radiological signs of bowel obstruction[8].

CLINICAL PRESENTATION

Functional constipation has been discussed within several consensus conferences for functional gastrointestinal disorders (FGIDs) and was revised in 2006, leading to the ROME Ⅲ child and adolescent criteria. Functional constipation usually presents with a decreased frequency of bowel motions per week. At least two of the following criteria must be present for more than two months to be regarded as functional constipation: (1) two or fewer defecations per week; (2) at least one episode of fecal incontinence per week; (3) retentive posturing or excessive volitional stool retention; (4) painful or hard bowel movements; (5) presence of a large fecal mass in the rectum; and (6) large diameter stools that may obstruct the toilet[9].

The most striking symptom of severe intestinal motility disorder is the delayed passage of meconium. Healthy newborn babies usually evacuate meconium in the first hours after birth, at the latest 24-48 h postnatally. Delayed passage of meconium combined with defecation problems in infancy is clinically very suggestive of Hirschsprung disease[10].

Patients suffering from hypoganglionosis or ganglioneuromatosis usually present with severe chronic constipation and ongoing defecation problems or occasional bowel obstruction mimicking HD[11].

Patients with ganglioneuromatosis in MEN2b may reveal intestinal problems characterized by constipation, bowel obstruction or diarrhea up to 7 years before the final diagnosis is made (own unpublished data).

The clinical presentation of chronic intestinal pseudo-obstruction (CIPO) comprises symptoms and signs of severe bowel dysmotility that frequently lead to vomiting and repetitive bowel obstruction.

DIAGNOSIS

Pediatric intestinal motility disorders should be diagnosed by the standardized approach of taking the patient's history and conducting clinical investigations, imaging and biopsy[12,13].

Coordinated intestinal motility (peristalsis) is a result of the interaction of the ENS, interstitial cells of Cajal (ICCs) and intestinal smooth muscles[14,15].

Functional, radiological and histological investigations are applied in pediatric motility disorders to diagnose the potentially underlying disease[16,17].

First step is usually a radiographic investigation, *i.e.,* a contrast enema to reveal a suspected narrow rectosigmoid segment in Hirschsprung disease. Contrast enema has a sensitivity of 76% and a specificity of

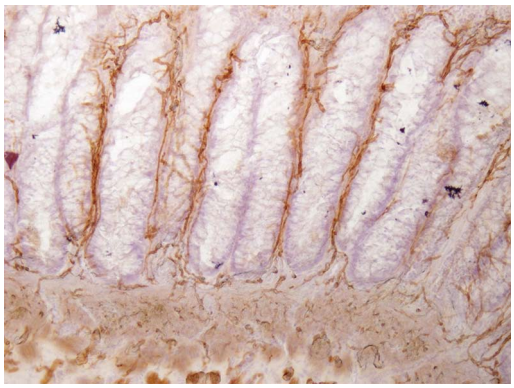

Figure 1 Acetylcholine-Esterase-Histochemistry-staining of a rectal biopsy in a patient with Hirschsprung disease. Note absence of ganglion cells and presence of hypertrophic cholinergic fibres within the mucosal layer (original magnification × 40).

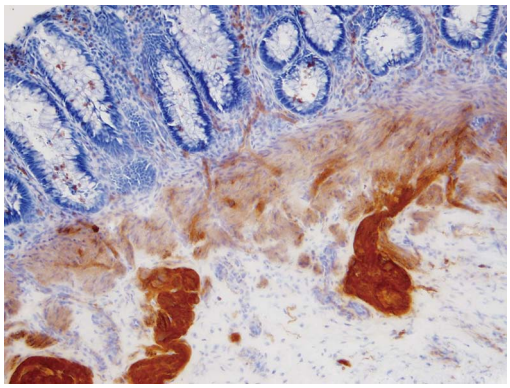

Figure 2 Acetylcholine-Esterase-Histochemistry-staining of a rectal biopsy in a patient with ganglioneuromatosis in MEN2b. Note presence of hyperplastic submucosal ganglions and hypertrophic cholinergic fibres (original magnification × 20).

97% to diagnose HD[18]. Furthermore contrast enema is usually not conclusive in the attempt to clearly estimate the length of the transition zone in HD[19].

Anorectal manometry (ARM) could be performed in each age group to assess the rectoanal inhibitory reflex. Absent rectoanal inhibitory reflex indicates HD. Sensitivity and specificity of ARM is 91% and 94%[18].

Rectal biopsies are the gold standard for the final diagnosis of severe motility disorders, especially Hirschsprung disease[20]. Routine staining methods are hematoxylin-eosin (HE) and Acetylcholine-Esterase-Histochemistry (AChE). Recent studies revealed that several new immunohistochemical markers, *i.e.*, calretinin, peripherin and S-100, are useful for the diagnostic of rectal biopsies[21,22] Especially calretinin allows the staining of formaldehyde fixed specimen which enables reference pathology on the respective specimen.

Typical and therefore pathognomonic findings at the specimen are the absence of ganglion cells and the presence of hypertrophic AChE-positive fibers within the submucosal and mucosal layers of rectal biopsies in patients with HD (Figure 1)[6]. Serial biopsies are required to define the length of the aganglionic bowel segment. Rectosigmoid disease is the most frequent form of HD (up to 90%). Rarely, patients suffer from total colonic or even total intestinal aganglionosis. At the present time, genetic investigations do not play an important role in the clinical management of HD but point towards further valuable research.

Hypoganglionosis is a disease that is not easily diagnosed, even in rectal biopsies. The use of full-thickness biopsies and the careful interpretation by an experienced pediatric pathologist are necessary[6]. Severe cases of hypoganglionosis that possibly require segmental resection must be evaluated using serial biopsies.

A histological finding of ganglioneuromatosis is a hyperplastic submucosal and myenteric plexus containing an increased number of ganglion cells, glial cells and nerve fibres (Figure 2)[23]. The diagnosis of MEN type 2b should to be evaluated by a genetic investigation, and the analysis should show the specific mutations of the codon 918 in RET exon 16 (95% of MEN2B patients)[24].

Clinical symptoms and typical radiological signs usually make the diagnosis of CIPO. Previous histological studies have revealed distinct abnormalities in the enteric nervous system, intestinal smooth muscles (visceral neuropathy) and ICCs, which might also be a secondary phenomenon[1].

MANAGEMENT

Management of chronic functional constipation is conservative and, in nearly all cases, successful. The major components of the treatment are demystification, toilet training, diet and the careful use of laxatives[9].

The treatment of choice in HD is resection of the aganglionic bowel segment with preservation of the anal sphincter muscles. Recently established less invasive transanal surgical procedures might lead to better postoperative results and improved long-term outcome[25].

Severe cases of hypoganglionosis also require surgical treatment comparable to that of HD.

The diagnosis of ganglioneuromatosis in rectal or other intestinal biopsies requires additional studies to rule out MEN2B. Proven cases of MEN2B require an intermediate thyroidectomy. The intestinal symptoms of MEN2B should be treated conservatively as long as possible. Bowel resection and/or stoma creation are very rarely indicated[24].

Treatment of CIPO is primarily conservative, but surgery might be required. The surgical procedures carried out might be the creation of a catheterizeable stoma for antegrade bowel irrigation or other enterostomata. Furthermore, parenteral nutrition or even small bowel transplantation is required in severe cases[26].

OUTCOME

Appropriately treated functional constipation has a good prognosis, but it has to be taken into account that up to 20% of patients with chronic constipation continue to have symptoms until adulthood[27].

The classical form of rectosigmoid HD is amenable to a straightforward surgical correction. Intra- and/or postoperative complications are rare. Nevertheless, the long-term outcome after surgical treatment of HD is compromised in 20%-25% of patients still suffering from chronic constipation and/or enterocolitis even after complete resection of the aganglionic bowel including the transitional zone. Several conditions might be responsible for that phenomenon such as reduced numbers of ICCs in the ganglionic bowel[28].

CIPO is a chronic disease that produces a severe impact on the quality of life. The underlying malignant disease mainly determines the outcome of MEN2b. The gastrointestinal symptoms usually improve with time.

CONCLUSION

Pediatric intestinal motility disorders require careful and meticulous diagnostic measures to rule out significant underlying organic disease. There have been numerous advances in diagnostic methods and surgical treatment options, leading to a better outcome for the affected children. Nevertheless, further research in needed in the field of genetics for long-term treatment and transition of these diseases.

REFERENCES

1 **van den Berg MM**, Di Lorenzo C, Mousa HM, Benninga MA, Boeckxstaens GE, Luquette M. Morphological changes of the enteric nervous system, interstitial cells of cajal, and smooth muscle in children with colonic motility disorders. *J Pediatr Gastroenterol Nutr* 2009; **48**: 22-29 [PMID: 19172119 DOI: 10.1097/MPG.0b013e318173293b]

2 **Peeters B**, Benninga MA, Hennekam RC. Childhood constipation; an overview of genetic studies and associated syndromes. *Best Pract Res Clin Gastroenterol* 2011; **25**: 73-88 [PMID: 21382580 DOI: 10.1016/j.bpg.2010.12.005]

3 **Wetherill C**, Sutcliffe J. Hirschsprung disease and anorectal malformation. *Early Hum Dev* 2014; **90**: 927-932 [PMID: 25448783 DOI: 10.1016/j.earlhumdev.2014.09.016]

4 **Puri P**, Rolle U. Variant Hirschsprung's disease. *Semin Pediatr Surg* 2004; **13**: 293-299 [PMID: 15660323]

5 **Dingemann J**, Puri P. Isolated hypoganglionosis: systematic review of a rare intestinal innervation defect. *Pediatr Surg Int* 2010; **26**: 1111-1115 [PMID: 20721562 DOI: 10.1007/s00383-010-2693-3]

6 **Schäppi MG**, Staiano A, Milla PJ, Smith VV, Dias JA, Heuschkel R, Husby S, Mearin ML, Papadopoulou A, Ruemmele FM, Vandenplas Y, Koletzko S. A practical guide for the diagnosis of primary enteric nervous system disorders. *J Pediatr Gastroenterol Nutr* 2013; **57**: 677-686 [PMID: 24177787 DOI: 10.1097/MPG.0b013e3182a8bb50]

7 **Lee NC**, Norton JA. Multiple endocrine neoplasia type 2B--genetic basis and clinical expression. *Surg Oncol* 2000; **9**: 111-118 [PMID: 11356339]

8 **Ambartsumyan L**, Rodriguez L. Gastrointestinal motility disorders in children. *Gastroenterol Hepatol* (N Y) 2014; **10**: 16-26 [PMID: 24799835]

9 **Rasquin A**, Di Lorenzo C, Forbes D, Guiraldes E, Hyams JS, Staiano A, Walker LS. Childhood functional gastrointestinal disorders: child/adolescent. *Gastroenterology* 2006; **130**: 1527-1537 [PMID: 16678566]

10 **Keckler SJ**, St Peter SD, Spilde TL, Tsao K, Ostlie DJ, Holcomb GW, Snyder CL. Current significance of meconium plug syndrome. *J Pediatr Surg* 2008; **43**: 896-898 [PMID: 18485962 DOI: 10.1016/j.jpedsurg.2007.12.035]

11 **Friedmacher F**, Puri P. Classification and diagnostic criteria of variants of Hirschsprung's disease. *Pediatr Surg Int* 2013; **29**: 855-872 [PMID: 23943250 DOI: 10.1007/s00383-013-3351-3]

12 **Rolle U**, Till H. [Therapeutic strategies for chronic constipation in childhood: pediatric gastroenterological and surgical aspects]. *Pathologe* 2007; **28**: 155-160 [PMID: 17277918]

13 **Di Lorenzo C**, Youssef NN. Diagnosis and management of intestinal motility disorders. *Semin Pediatr Surg* 2010; **19**: 50-58 [PMID: 20123274 DOI: 10.1053/j.sempedsurg.2009.11.006]

14 **Gfroerer S**, Rolle U. Interstitial cells of Cajal in the normal human gut and in Hirschsprung disease. *Pediatr Surg Int* 2013; **29**: 889-897 [PMID: 23917331 DOI: 10.1007/s00383-013-3364-y]

15 **Mazet B**. Gastrointestinal motility and its enteric actors in mechanosensitivity: past and present. *Pflugers Arch* 2015; **467**: 191-200 [PMID: 25366494 DOI: 10.1007/s00424-014-1635-7]

16 **Sutcliffe JR**, King S, Hutson JM, Southwell B. What is new in radiology and pathology of motility disorders in children? *Semin Pediatr Surg* 2010; **19**: 81-85 [PMID: 20307844 DOI: 10.1053/j.sempedsurg.2009.11.014]

17 **Raghunath N**, Glassman MS, Halata MS, Berezin SH, Stewart JM, Medow MS. Anorectal motility abnormalities in children with encopresis and chronic constipation. *J Pediatr* 2011; **158**: 293-296 [PMID: 20850765 DOI: 10.1016/j.jpeds.2010.07.063]

18 **de Lorijn F**, Kremer LC, Reitsma JB, Benninga MA. Diagnostic tests in Hirschsprung disease: a systematic review. *J Pediatr Gastroenterol Nutr* 2006; **42**: 496-505 [PMID: 16707970 DOI: 10.1097/01.mpg.0000214164.90939.92]

19 **Muller CO**, Mignot C, Belarbi N, Berrebi D, Bonnard A. Does the radiographic transition zone correlate with the level of aganglionosis on the specimen in Hirschsprung's disease? *Pediatr Surg Int* 2012; **28**: 597-601 [PMID: 22534881 DOI: 10.1007/s00383-012-3094-6]

20 **de Arruda Lourenção PL**, Takegawa BK, Ortolan EV, Terra SA, Rodrigues MA. A useful panel for the diagnosis of Hirschsprung disease in rectal biopsies: calretinin immunostaining and acetylcholinesterase histochesmistry. *Ann Diagn Pathol* 2013; **17**: 352-356 [PMID: 23683882]

21 **Holland SK**, Hessler RB, Reid-Nicholson MD, Ramalingam P, Lee JR. Utilization of peripherin and S-100 immunohistochemistry in the diagnosis of Hirschsprung disease. *Mod Pathol* 2010; **23**: 1173-1179 [PMID: 20495540]

22 **Montedonico S**, Piotrowska AP, Rolle U, Puri P. Histochemical staining of rectal suction biopsies as the first investigation in patients with chronic constipation. *Pediatr Surg Int* 2008; **24**: 785-792 [PMID: 18463882 DOI: 10.1007/s00383-008-2173-1]

23 **Feichter S**, Meier-Ruge WA, Bruder E. The histopathology of gastrointestinal motility disorders in children. *Semin Pediatr Surg* 2009; **18**: 206-211 [PMID: 19782302 DOI: 10.1053/j.sempedsurg.2009.07.002]

24 **Walls GV**. Multiple endocrine neoplasia (MEN) syndromes. *Semin Pediatr Surg* 2014; **23**: 96-101 [PMID: 24931355 DOI: 10.1053/j.sempedsurg.2014.03.008]

25 **Levitt MA**, Hamrick MC, Eradi B, Bischoff A, Hall J, Peña A. Transanal, full-thickness, Swenson-like approach for Hirschsprung disease. *J Pediatr Surg* 2013; **48**: 2289-2295 [PMID: 24210201 DOI: 10.1016/j.jpedsurg.2013.03.002]

26 **Chumpitazi B**, Nurko S. Pediatric gastrointestinal motility disorders: challenges and a clinical update. *Gastroenterol Hepatol* (N Y) 2008; **4**: 140-148 [PMID: 21904491]

27 **Nurko S**, Scott SM. Coexistence of constipation and incontinence in children and adults. *Best Pract Res Clin Gastroenterol* 2011; **25**: 29-41 [PMID: 21382577 DOI: 10.1016/j.bpg.2010.12.002]

28 **Rolle U**, Piotrowska AP, Nemeth L, Puri P. Altered distribution of interstitial cells of Cajal in Hirschsprung disease. *Arch Pathol Lab Med* 2002; **126**: 928-933 [PMID: 12171490]

P- Reviewer: Han-Geurts IJM, Kwon S, Lourencao PLTD, Ueno T
S- Editor: Yu J **L- Editor**: A **E- Editor**: Zhang DN

World Journal of Gastroenterology

Submit a Manuscript: http://www.wjgnet.com/esps/
Help Desk: http://www.wjgnet.com/esps/helpdesk.aspx
DOI: 10.3748/wjg.v21.i33.9688

World J Gastroenterol 2015 September 7; 21(33): 9688-9692
ISSN 1007-9327 (print) ISSN 2219-2840 (online)

EDITORIAL

Cardiovascular involvement in inflammatory bowel disease: Dangerous liaisons

Ana Maria Filimon, Lucian Negreanu, Michelle Doca, Andreea Ciobanu, Carmen Monica Preda, Dragos Vinereanu

Ana Maria Filimon, Andreea Ciobanu, Dragos Vinereanu, Internal Medicine and Cardiology Department, University Hospital Carol Davila University of Medicine Bucharest, 011465 Bucharest, Romania

Lucian Negreanu, Michelle Doca, Internal Medicine 2 Gastroenterology Department, University Hospital, Carol Davila University of Medicine Bucharest, 011465 Bucharest, Romania

Carmen Monica Preda, Gastroenterology Department, Fundeni Clinical Institute, Carol Davila Medicine University, 011465 Bucharest, Romania

Author contributions: All authors contributed equally to the article.

Supported by (in part) Sectorial Operational Program Human Resources Development; European social fund; and the Romanian government, No. POSDRU 141531.

Conflict-of-interest statement: The authors declare no conflicts of interest.

Correspondence to: Lucian Negreanu, MD, PhD, Internal Medicine 2 Gastroenterology Department, University Hospital, Carol Davila University of Medicine Bucharest, 169, splaiul Independentei Street, Sector 5, 011465 Bucharest, Romania. negreanu_99@yahoo.com
Telephone: +40-72-2546405
Fax: +40-21-3180505

Received: March 9, 2015
Peer-review started: March 10, 2015
First decision: March 26, 2015
Revised: April 14, 2015
Accepted: July 18, 2015

Article in press: July 18, 2015
Published online: September 7, 2015

Abstract

Increasing evidence of a link between inflammatory bowel disease (IBD) and adverse cardiovascular events has emerged during the last decade. In 2014, an important number of meta-analyses and cohort studies clarified the subtle *dangerous liaisons* between gut inflammation and cardiovascular pathology. The evidence suggests that patients with IBD have a significantly increased risk of myocardial infarction, stroke, and cardiovascular mortality, especially during periods of IBD activity. Some populations (*e.g.*, women, young patients) may have an even greater risk. Current effective treatment of IBD is aimed at disease remission and seems to reduce cardiovascular risk in these patients. A beneficial effect was demonstrated for salicylates, but not for steroids or azathioprine. tumor necrosis factor-α antagonists, which are highly effective in the reduction of inflammation and in the restoration of the digestive mucosa, lead to conflicting cardiovascular effects, as they seem to reduce the risk for ischemic heart disease but increase the rate of cerebrovascular events. Future supplemental treatment strategies that may reduce the atherothrombotic risk during periods of IBD activity should be explored.

Key words: Inflammatory bowel disease; Thrombotic events; Active disease; Cardiovascular risk; Anti-tumor necrosis factor-α

Core tip: New evidence from an important number of meta-analyses and cohort studies suggests that patients with inflammatory bowel disease (IBD) have a significantly increased risk of myocardial infarction,

stroke, and cardiovascular mortality especially during periods of active disease and particularly in some high-risk populations, such as women and younger patients. The current treatment paradigm, which is aimed at deep, sustained remission, might reduce cardiovascular risk in patients with IBD. Treatment strategies such as the supplemental administration of statins to reduce the atherothrombotic risk should be further explored.

Filimon AM, Negreanu L, Doca M, Ciobanu A, Preda CM, Vinereanu D. Cardiovascular involvement in inflammatory bowel disease: Dangerous liaisons. *World J Gastroenterol* 2015; 21(33): 9688-9692 Available from: URL: http://www.wjgnet.com/1007-9327/full/v21/i33/9688.htm DOI: http://dx.doi.org/10.3748/wjg.v21.i33.9688

Inflammatory bowel disease (IBD) comprises two types of chronic intestinal disorders: Crohn's disease (CD) and ulcerative colitis (UC).

Increasing evidence of a link between inflammatory bowel disease and adverse cardiovascular events has emerged during the last decade. The association of IBD with an increased risk of venous thromboembolic disease is now clearly recognized and has been confirmed by many studies[1].

However, considerable heterogeneity was observed in the current study in regards to how IBD modifies the risk of arterial thromboembolic events, including cerebrovascular accidents (CVA), ischemic heart disease (IHD), and myocardial infarction (MI). The relationship of inflammatory bowel disease to heart failure (HF) is also uncertain. Two registry-based studies of approximately 17000 and 25000 patients with IBD, respectively, reported that the risk of MI in IBD patients was comparable to matched control subjects without IBD[2,3]. In addition, in a meta-analysis of 11 studies with a total of almost 14000 patients, no increase in cardiovascular mortality was observed in the IBD group compared with the control group[4].

In 2014, an important number of meta-analyses and cohort studies clarified these subtle dangerous liaisons between gut inflammation and cardiovascular pathology.

A meta-analysis of publications in MEDLINE, the Cochrane Library, EMBASE as well as of international conference abstracts was conducted. It included all controlled observational studies that evaluated the incidence of venous and/or arterial thromboembolic events and cardiovascular mortality in adult patients with IBD. This analysis included 33 studies that enrolled 207814 IBD patients and 5774898 controls. The risk of thromboembolic events was increased in patients with IBD, which was mainly due to an increased risk of venous thromboembolism (VTE). No increased risk of arterial thromboembolism or cardiovascular mortality in patients with IBD was observed, but an increased risk for both ischemic heart disease and mesenteric ischemia was observed[5].

The exact etiology of the higher occurrence of thromboembolic events is not yet completely understood, although it seems that multiple acquired and inherited factors may be involved. In patients with IBD, a persistent latent activation of hemostasis exists in cases of both active and inactive disease and is implicated in thrombotic diathesis. The detailed mechanisms of this process were recently and extensively presented in a comprehensive review. The mechanisms include the following: elevated levels of coagulation factors and products of thrombin and fibrin formation, increased markers of acquired vascular endothelial deficiencies, dysfunction of natural anticoagulants, defects in the fibrinolytic system and an elevated number of circulating platelets with increased platelet activation and an increased tendency for platelet aggregation[1].

In a recent cohort study that included 1708 patients (648 with CD, 1060 with UC) who were followed for 35 years, the risk of venous thromboembolism was 1.03 per 1000 patients-year. The cumulative risk of VTE 15 years after the diagnosis was 1.5%, which was similar for both CD and UC, and was significantly higher in males. The risk of VTE in patients with UC was associated with extensive location of the disease (OR = 3.25, 95%CI: 1.13-9.35), the presence of a fulminant episode during the disease course (OR = 4.15, 95%CI: 1.28-13.5), smoking (OR = 3.46, 95%CI: 1.14-10.5) and the need for steroids (OR = 2.97, 95%CI: 0.99-8.92). Similarly, in regards to CD, all but one patient with VTE were smokers[6].

In a recent study on global assays of coagulation and factor assays (procoagulant factor Ⅷ, von Willebrand factor), the authors demonstrated that acute severe colitis is a hypercoagulable disease state. Although this hypercoagulable profile improves over time, it is still present up to 8-12 wk after hospital admission compared with control patients with quiescent, extensive UC[7].

Another systematic review and meta-analysis included cohort and case-control studies that reported incident cases of CVA and/or IHD in patients with IBD and compared them with a non-IBD control population (or they were compared with a standardized population). The presence of IBD was associated with a modest increase in the risk of CVA, especially among women and in young patients (< 40-50 years old). IBD was also associated with a 19% increase in the risk of IHD, also primarily in women. In this study, no association was observed between IBD and an increased risk of peripheral arterial thromboembolic events[8].

Very important data have resulted from a series of nationwide Danish population-based cohort studies that were recently published.

In a cohort of 20795 patients with new-onset

Table 1 Cardiovascular risk in inflammatory bowel disease-the liaisons

Study	Results
MEDLINE, Cochrane Library, EMBASE meta-analysis; 33 studies enrolling 207814 IBD patients and 5774898 controls[5]	Increased risk of venous thromboembolism Increased risk of both ischemic heart disease and mesenteric ischemia No increased risk of arterial thromboembolism No increased cardiovascular mortality
Cohort study, 1708 patients (648 Crohn's disease, 1060 ulcerative colitis), 35 yr follow-up[6]	A cumulative risk of venous thromboembolism after 15 yr after the diagnosis of 1.5% similar for both CD and UC
Systematic review and meta-analysis 9 studies 2424 CVA events in 5 studies and 6478 IHD events 6 studies[8]	Modest increase in the risk of CVA, especially among women and in young patients (< 40-50 yr old) 19% increase in the risk of IHD, primarily in women also No increased risk of peripheral arterial thromboembolic events
Cohort study, 20795 new onset IBD patients matched with 199978 controls[9]	Overall increased risk of MI, stroke, and cardiovascular death Increased risk during flares
Nation wide cohort study, 5436647 subjects without IBD or HF; follow up 11.8 yr 23681 IBD patients developed IBD follow up 6.4 yr	37% increased risk of hospitalization for HF in IBD Increased risk during flares
86790 Danish patients with first-time MI[11]	Increased risk of recurrent MI and for all-cause mortality especially during flares
Historical cohort study 2004-2010[12] Interventional catheterization database 131 IBD patients and 524 matched controls	IBD patients had CAD at a younger age as compared with non-IBD patients IBD patients less likely to be active smokers and had a lower body mass index. No difference in post-PCI outcome in patients with IBD *vs* non-IBD controls with CAD

CD: Crohn's disease; UC: Ulcerative colitis; IBD: Inflammatory bowel disease; CVA: Cerebrovascular accidents; IHD: Ischemic heart disease; HF: Heart failure; MI: Myocardial infarction; CAD: Coronary artery disease; PCI: Percutaneous intervention.

IBD and a mean age of 40 years who were matched according to age and sex with 199978 controls, patients with IBD had an overall increased risk of MI, stroke, and cardiovascular death. During flares and persistent IBD activity the rate ratios of MI, stroke, and cardiovascular death were significantly increased[9].

The same Danish team showed that IBD is associated with an increased risk of hospitalization for HF and that this risk was strongly correlated with periods of active disease[10].

The effect of active IBD on major adverse cardiovascular outcomes after MI was studied in 86790 Danish patients with a first-time MI between 2002 and 2011. IBD was associated with hazard ratios of 1.21 (95%CI: 0.99-1.49) for recurrent MI, 1.14 (95%CI: 1.01-1.28) for all-cause mortality, and 1.17 (95%CI: 1.03-1.34) for the composite end point. Compared with the non-IBD group, IBD flares in particular were associated with increased risks of recurrent MI and all-cause mortality, whereas no increased risk was identified during remission[11].

The correlation between IBD and coronary artery disease (CAD) was already confirmed in a smaller study, where IBD patients tended to have CAD at a younger age compared with patients without IBD; in addition, they were less likely to be active smokers and had a lower body mass index. However, in this study, the post-PCI outcome in patients with IBD and CAD was similar to that in controls with CAD but without concurrent IBD[12].

Only a few studies have addressed the impact of the use of anti-inflammatory drugs for the management of cardiovascular risk in patients with IBD (Table 1).

One small longitudinal study included 14 patients with IBD who were treated with salicylates alone, 11 subjects who were treated with steroids and azathioprine, 7 subjects who were treated with anti-tumor necrosis factor (TNF)-α, and 30 matched controls. The effect of therapy on pulse wave velocity (PWV) was measured at baseline and at 3.4 ± 0.5 years later. In an adjusted model, carotid-femoral PWV increased significantly at follow-up in subjects with IBD who were treated with salicylates, but not in those who were treated with steroids and azathioprine or with anti TNF-α[13].

TNF-α antagonists have increasingly been used in the treatment of IBD, and they are highly effective in the reduction of the inflammatory burden and in mucosal healing in some patients. However, data on the potential impact of this anti-inflammatory effect on the risk of cardiovascular diseases (CVD) in the setting of IBD remain limited. Important evidence in regards to the role of anti TNF-α also comes from Denmark. With the same design of a nationwide, population-based cohort study, the authors addressed the risk of CVD, which was subdivided into ischemic heart disease (IHD) and cerebrovascular accidents (CVA), among patients with IBD who were followed for up to 11 years after exposure to TNF-α antagonists. The cohort consisted of 50756 patients with IBD, of whom 3109 had been exposed to TNF-α antagonists during 1999-2010. Thirty-one patients who were treated with TNF-α antagonists and 2641 patients who were not treated with TNF-α antagonists developed IHD. This yielded an adjusted HR of 0.85 (95%CI: 0.59-1.24), whereas the risk of CVA associated with TNF-α antagonists was 1.42 (95%CI: 0.82-2.45). These suggest a protective effect of TNF-α antagonists on IHD, but at the same time, the use of TNF-α antagonists might be a risk factor for

Table 2 Cardiovascular risk and inflammatory bowel disease treatment

Study	Results
Longitudinal study[13] 14 IBD subjects treated only with salicylates, 11 subjects treated with steroids and azathioprine, 7 subjects treated with anti TNF-α, and 30 matched controls pulse wave velocity was measured at baseline and 3.4 ± 0.5 yr later	Carotid-femoral pulse wave velocity increased significantly at follow-up in IBD subjects treated with salicylates, No increase of PWV in patients treated with steroids and azathioprine or anti TNF-α
Nationwide, population-based, cohort study, patients with IBD followed for up to 11 years after exposure to TNF-α antagonists	Protective effect of TNF-α antagonist on IHD
Cohort of 50756 IBD patients of whom 3109 had been exposed to TNF-α antagonists during 1999-2010[14]	TNF-α antagonists use might be a risk factor for CVA (increased trend, none of the values reached statistical significance)
Large retrospective study[15] 1986 statin exposed and 9871 unexposed subjects with IBD	18% reduction in initiation of oral steroids Statistical significance for atorvastatin only Greater reduction in steroid use for UC patients and no reduction in Crohn's disease Reduce hazard of anti TNF-α use, surgery and hospitalization (no statistical significance)

UC: Ulcerative colitis; IBD: Inflammatory bowel disease; CVA: Cerebrovascular accidents; IHD: Ischemic heart disease.

CVA, although none of the values reached statistical significance. Therefore, further studies are necessary to clarify this issue[14].

The anti-inflammatory capacity of HMG-CoA-reductase inhibitors was evaluated in patients with IBD in a large retrospective study, which revealed an 18% reduction in the initiation of oral steroid use in patients with IBD (HR = 0.82; 95%CI: 0.71-0.94), and an even greater reduction in patients with UC (HR = 0.75; 95%CI: 0.62-0.91). The beneficial effect of statins in patients with IBD and whether this effect is linked to their potential to decrease the risk of atherosclerosis and inflammation requires clarification in further studies[15].

These studies add considerable evidence to the existing literature as they confirm the substantial negative impact that IBD may have on cardiovascular outcomes. However, some variables lack statistical significance in the three studies, and thus we need further evidence regarding the use of steroids, the risk of VTE, IBD, and recurrent MI as well as exposure to anti TNF-α and CVA[6,11,14].

However, have these recent studies changed our treatment paradigm or do they confirm that we are on the correct path? Currently, our goal is to progress beyond deep sustained remission.

The location, extension, activity, and severity of the inflammatory lesions and the potential existence of complications must be carefully evaluated in all patients at the time of diagnosis and throughout the course of the disease. This allows the selection of a targeted therapeutic strategy in a particular patient, and has important prognostic implications. An approach that uses endoscopic healing and tight control of inflammation based on the monitoring of symptoms and biomarkers is proposed. The observation of inflammatory activity is actively utilized throughout the disease course to optimize management. Certain high-risk populations (*e.g.*, those with active disease, women, and young patients) should be counseled routinely on the modification of aggressive risk factors and adherence to the treatment guidelines.

CONCLUSION

New evidence suggests that patients with IBD have a significantly increased risk of MI, stroke, and cardiovascular mortality especially during periods of IBD activity. Some populations (*e.g.*, women, young patients) may have an increased cardiovascular risk. Effective treatment of IBD that is aimed at disease remission may also reduce the cardiovascular risk in these patients. Treatment strategies, such as supplemental statin administration during periods of IBD activity, for the reduction of atherothrombotic risk should be further explored (Table 2).

REFERENCES

1 **Zezos P**, Kouklakis G, Saibil F. Inflammatory bowel disease and thromboembolism. *World J Gastroenterol* 2014; **20**: 13863-13878 [PMID: 25320522 DOI: 10.3748/wjg.v20.i38.13863]

2 **Ha C**, Magowan S, Accortt NA, Chen J, Stone CD. Risk of arterial thrombotic events in inflammatory bowel disease. *Am J Gastroenterol* 2009; **104**: 1445-1451 [PMID: 19491858 DOI: 10.1016/s0016-5085(08)62341-0]

3 **Osterman MT**, Yang YX, Brensinger C, Forde KA, Lichtenstein GR, Lewis JD. No increased risk of myocardial infarction among patients with ulcerative colitis or Crohn's disease. *Clin Gastroenterol Hepatol* 2011; **9**: 875-880 [PMID: 21749853 DOI: 10.1016/j.cgh.2011.06.032]

4 **Dorn SD**, Sandler RS. Inflammatory bowel disease is not a risk factor for cardiovascular disease mortality: results from a systematic review and meta-analysis. *Am J Gastroenterol* 2007; **102**: 662-667 [PMID: 17156143 DOI: 10.1111/j.1572-0241.2006.01018.x]

5 **Fumery M**, Xiaocang C, Dauchet L, Gower-Rousseau C, Peyrin-Biroulet L, Colombel JF. Thromboembolic events and cardiovascular mortality in inflammatory bowel diseases: a meta-analysis of observational studies. *J Crohns Colitis* 2014; **8**: 469-479 [PMID: 24183231 DOI: 10.1016/j.crohns.2013.09.021]

6 **Vegh Z**, Golovics PA, Lovasz BD, Kurti Z, Gecse KB, Szita I, Balogh M, Pandur T, Lakatos L, Lakatos PL. Low incidence of venous thromboembolism in inflammatory bowel diseases: prevalence and predictors from a population-based inception cohort. *Scand J Gastroenterol* 2015; **50**: 306-311 [PMID:

25471148 DOI: 10.3109/00365521.2014.985708]
7 **Griffiths B**, Curry N, Desborough M, Henton S, Bryant RV, Travis SP, Jairath V. Evaluation of global coagulation profiles in patients with acute severe colitis: Implications for thromboprophylaxis. *J Crohns Colitis* 2015; **9** Suppl 1: S32
8 **Singh S**, Singh H, Loftus EV, Pardi DS. Risk of cerebrovascular accidents and ischemic heart disease in patients with inflammatory bowel disease: a systematic review and meta-analysis. *Clin Gastroenterol Hepatol* 2014; **12**: 382-393.e1: quiz e22 [PMID: 23978350 DOI: 10.1016/j.cgh.2013.08.023]
9 **Kristensen SL**, Ahlehoff O, Lindhardsen J, Erichsen R, Jensen GV, Torp-Pedersen C, Nielsen OH, Gislason GH, Hansen PR. Disease activity in inflammatory bowel disease is associated with increased risk of myocardial infarction, stroke and cardiovascular death--a Danish nationwide cohort study. *PLoS One* 2013; **8**: e56944 [PMID: 23457642 DOI: 10.1371/journal.pone.0056944]
10 **Kristensen SL**, Ahlehoff O, Lindhardsen J, Erichsen R, Lamberts M, Khalid U, Nielsen OH, Torp-Pedersen C, Gislason GH, Hansen PR. Inflammatory bowel disease is associated with an increased risk of hospitalization for heart failure: a Danish Nationwide Cohort study. *Circ Heart Fail* 2014; **7**: 717-722 [PMID: 25052190 DOI: 10.1161/CIRCHEARTFAILURE.114.001152]
11 **Kristensen SL**, Ahlehoff O, Lindhardsen J, Erichsen R, Lamberts M, Khalid U, Nielsen OH, Torp-Pedersen C, Gislason GH, Hansen PR. Prognosis after first-time myocardial infarction in patients with inflammatory bowel disease according to disease activity: nationwide cohort study. *Circ Cardiovasc Qual Outcomes* 2014; **7**: 857-862 [PMID: 25316773]
12 **Aggarwal A**, Atreja A, Kapadia S, Lopez R, Achkar JP. Conventional risk factors and cardiovascular outcomes of patients with inflammatory bowel disease with confirmed coronary artery disease. *Inflamm Bowel Dis* 2014; **20**: 1593-1601 [PMID: 25105946 DOI: 10.1097/MIB.0000000000000109]
13 **Zanoli L**, Rastelli S, Inserra G, Lentini P, Valvo E, Calcagno E, Boutouyrie P, Laurent S, Castellino P. Increased arterial stiffness in inflammatory bowel diseases is dependent upon inflammation and reduced by immunomodulatory drugs. *Atherosclerosis* 2014; **234**: 346-351 [PMID: 24732573 DOI: 10.1016/j.atherosclerosis.2014.03.023]
14 **Andersen NN**, Rungoe C, Andersson M, Munkholm P, Pasternak B, Jess T. Tumor Necrosis Factor-Alpha Antagonists And Cardiovascular Disease In Inflammatory Bowel Disease. European Crohn Colitis Organisation Congress, Vienna, Austria, February 14-16. 2013. Available from: URL: https://www.ecco-ibd.eu/publications/congress-abstract-s/abstracts-2013/item/19-tumor-necrosis-factor-alpha-antagonists-and-cardiovascular-disease-in-inflammatory-bowel-disease.html
15 **Crockett SD**, Hansen RA, Stürmer T, Schectman R, Darter J, Sandler RS, Kappelman MD. Statins are associated with reduced use of steroids in inflammatory bowel disease: a retrospective cohort study. *Inflamm Bowel Dis* 2012; **18**: 1048-1056 [PMID: 21826766 DOI: 10.1002/ibd.21822]

P- Reviewer: Ahluwalia NK, Iizuka M, Kuo SM, Manguso F
S- Editor: Ma YJ **L- Editor**: A **E- Editor**: Liu XM

World Journal of Gastroenterology

Submit a Manuscript: http://www.wjgnet.com/esps/
Help Desk: http://www.wjgnet.com/esps/helpdesk.aspx
DOI: 10.3748/wjg.v21.i33.9693

World J Gastroenterol 2015 September 7; 21(33): 9693-9706
ISSN 1007-9327 (print) ISSN 2219-2840 (online)

TOPIC HIGHLIGHT

2015 Advances in Gastrointestinal Endoscopy

Value of screening endoscopy in evaluation of esophageal, gastric and colon cancers

Tae H Ro, Michelle A Mathew, Subhasis Misra

Tae H Ro, Michelle A Mathew, Subhasis Misra, Division of Surgical Oncology, Texas Tech University Health Science Center School of Medicine, Amarillo, TX 79106, United States

Author contributions: Ro TH and Mathew MA contributed equally to the writing of this paper and should be deemed both first authors; Misra S was the senior author and guide for this paper.

Conflict-of-interest statement: Subhasis Misra has received a research grant from the Cancer Prevention Research, Institute of Texas for colorectal cancer screening. No other contributing authors from this manuscript has received fees for serving as a speaker, owns stocks and/or shares in any affiliated organization, or owns a patent related to this research.

Correspondence to: Subhasis Misra, MD, MS, FACCWS, FACS, Associate Professor, Chief of GastroIntestinal and Hepato-Pancreato-Biliary Surgery, Division of Surgical Oncology, Texas Tech University Health Science Center School of Medicine, 1400 S Coulter St.Amarillo, Amarillo, TX 79106, United States. subhasis.misra@ttuhsc.edu
Telephone: +1-806-3545563
Fax: +1-806-3545561

Received: April 13, 2015
Peer-review started: April 15, 2015
First decision: May 18, 2015
Revised: May 27, 2015
Accepted: July 3, 2015
Article in press: July 3, 2015
Published online: September 7, 2015

Abstract

Esophageal, gastric, and colorectal cancers are deadly diseases that continue to plague our world today. The value of screening endoscopy in evaluating these types of cancers is a critical area of discussion due to a potential reduction in morbidity and mortality. This article describes how to identify a good screening test and explains what are important criteria in the field of screening endoscopy. Furthermore, the current status and progress of screening endoscopy for esophageal, gastric, and colorectal cancer will be evaluated and discussed. Mass screening programs have not been implemented for esophageal and gastric carcinomas in those with average or low risk populations. However, studies of high-risk populations have found value and a cost-benefit in conducting screening endoscopy. Colorectal cancer, on the other hand, has had mass screening programs in place for many years due to the clear evidence of improved outcomes. As the role of endoscopy as a screening tool has continued to develop, newer technology and techniques have emerged to improve its utility. Many new image enhancement techniques and computer processing programs have shown promise and may have a significant role in the future of endoscopic screening. These developments are paving the way for improving the diagnostic and therapeutic capability of endoscopy in the field of gastroenterology.

Key words: Endoscopic screening; Esophageal cancer; Gastric cancer; Esophagogastroduodenoscopy; Colon cancer

Core tip: The value of screening endoscopy in evaluating esophageal, gastric, and colon cancers is a critical area

of discussion due to a potential reduction in morbidity and mortality. Studies have found value and cost-benefit in conducting screening endoscopy in esophageal and gastric cancer in high-risk populations. Colorectal cancer has had mass screening programs implemented for many years due to the clear evidence of improved outcomes. New innovations in technology have emerged and shown promise in playing a significant role in the future of endoscopic screening. These developments are paving the way for improving the diagnostic capability of endoscopy in the field of gastroenterology.

Ro TH, Mathew MA, Misra S. Value of screening endoscopy in evaluation of esophageal, gastric and colon cancers. *World J Gastroenterol* 2015; 21(33): 9693-9706 Available from: URL: http://www.wjgnet.com/1007-9327/full/v21/i33/9693.htm DOI: http://dx.doi.org/10.3748/wjg.v21.i33.9693

INTRODUCTION

Screening tests are important tools for health maintenance that have been around for the past half-century. Since its development, the number of screening tests has increased exponentially and it has sparked the creation of many innovative technologies. The purpose of screening is to catch early stages of disease and to delay or prevent further development of the disease course. In contrast to diagnostic tests, screening tests evaluate individuals that have a low pretest probability of a particular disease. These individuals are either asymptomatic or are at preclinical stages of their disease[1].

While evaluating the utility of a screening tool, several aspects need to be examined in order to support its validity and practical use. For a screening test to be effective, there needs to be a change in patient outcome with early detection of a disease. Standard measures of patient outcome include morbidity, mortality, and quality of life. Once a value for the test is established, a risk-benefit analysis is typically assessed, and then accuracy of the test is evaluated. Screening test accuracy is measured by sensitivity, specificity, and predictive value. Sensitivity is the ability of a test to detect positive results in patients with disease, while specificity is the ability of a test to detect negative results in patients without disease, and predictive value is the probability of a condition given by the result of a test. A good screening test will have high percentages in these categories. Cost analysis is one of the last measures to determine practicality and implementation on a larger scale. Implementation of a screening program must find a balance between the reduction in cancer mortality and the costs associated with screening and subsequent diagnostic evaluations due to false-positive results[2]. While there are many screening modalities used today, we will be discussing the efficacy of the screening endoscopy.

In 1853, the French surgeon Desormeaux, coined the term "endoscope" to describe the instrument he created to inspect cavities of the body. Through this illumination device, Kusmaul performed the first esophagoscopies in 1867-1868[3]. Hollow tubes and spatulas connected to illumination sources were the main way esophagoscopies were first performed. Years later the light source was incorporated into the endoscopes, which was followed by the creation of the semi-flexible gastroscope by Wolf and Schindler in 1930. Due to the development of very transparent optical quality glass, Basil Hirschowitz and Larry Curtiss were able to build the flexible fiber optic endoscope in 1958[4]. The flexible endoscope depends on delivering light and transmitting the image along bundles of chemically treated glass fibers. Initially, the endoscopist viewed the image through an eyepiece on the instrument, but eventually a video system was incorporated into the scope, which led to the videoscopes used today[5]. While the basic structure has remained the same, there have been advances in technology that have led to the development of new endoscopic techniques. These developments are paving the way for improving the diagnostic and therapeutic capability of endoscopes in the field of gastroenterology. We will be discussing the value of screening endoscopies in the evaluation of esophageal, gastric, and colon carcinomas.

ESOPHAGEAL CANCER ENDOSCOPIC SCREENING

Epidemiology

In 2012, there was an estimated 455800 new cases of esophageal carcinoma and 400200 deaths worldwide[6]. Esophageal carcinoma is the eighth most common cancer and sixth leading cause of cancer related deaths[7]. While other types of cancer are expected to decrease in incidence over the next 10 years, the prevalence of esophageal cancer is expected to increase by 140% by the year 2025[7]. The predominant esophageal cancer in North America and Europe is esophageal adenocarcinoma (EA), while esophageal squamous-cell carcinoma (ESCC) is the predominant type in Asia, Africa, and South America[8]. The highest risk area is referred to as the "esophageal cancer belt" and runs from Northern Iran to North-Central China[6].

Risk factors

Obesity and gastroesophageal reflux disease are the key risk factors for EA, with Barrett's esophagus as the precursor lesion in the majority of cases. Alcohol and tobacco are the leading risk factors for ESCC in Western countries, with esophageal squamous dysplasia as the precursor lesion. The risk factors in high-risk areas of Iran and China are not fully established, but are associated with poor nutritional status, low intake of fruits and vegetables, and drinking beverages at high

Table 1 Accuracy of endoscopic modalities in esophageal carcinoma, which reveal the efficacy of endoscopic screening

Type of study	BE/ESCC	Patient group	Disease prevalence (%)	Accuracy of screen (%)
Endoscopic screening				
Prospective	ESCC	Asymptomatic; Linxian, China	ESCC: 9.5	Relative risk of ESCC: 2.9/9.8/28.3 (mild/moderate/sever dysplasia); 34.4 (carcinoma in situ)
Prospective	ESCC	Asymptomatic; Linxian, China	Not determined	Sensitivity/specificity for high-grade dysplasia or ESCC: 62/79 (visible lesions); 96/63 (unstained lesions)
Ultrathin endoscopes				
Randomized crossover	BE	GERD; United States	Not determined	Sensitivity: 26/30 (standard/small caliber endoscopy)
Randomized crossover	BE	BE and controls; United Kingdom	Not determined	Sensitivity/specificity small vs standard caliber: 100/100
Capsule endoscopy				
Prospective single screen	BE	GERD and under surveillance BE; United States	Not determined	Sensitivity/specificity for BE: 67/84
Prospective single screen	BE	GERD; United States	Not determined	Sensitivity/specificity for BE: 60/100
Prospective single screen	BE	GERD; United States	Not determined	Sensitivity/specificity for BE: 78/82 (visual lesions); 93/78 (biopsy)

Adapted from Lao-Sirieix *et al*[11]. BE: Barrett's esophagus; ESCC: Esophageal squamous cell cancer; GERD: Gastro-esophageal reflux disease.

temperatures[6]. There is a higher risk of both types of esophageal cancer with high intake of fats, red meats, and processed foods. Adenocarcinoma is three to four times more common in men, and the incidence of both types of esophageal carcinoma increases with age[8].

Current screening methods

Early detection of esophageal carcinoma through cytological and endoscopic screening methods has been primarily concentrated in countries where there is a high incidence[9]. Endoscopy is the gold standard for diagnosing esophageal cancer and precancerous lesions. The standard esophagogastroduodenoscopy (EGD) uses a small chip camera and a non-coaxial optic fiber system to carry white light down the oropharynx to examine different levels of the gastrointestinal mucosa. Other screening methods such as cytological examination and molecular markers have been studied, but endoscopy with biopsy and iodine staining remains as the diagnostic choice to detect esophageal squamous dysplasia[10]. Endoscopy with iodine staining (Lugol's solution) is known as chromoendoscopy. The normal squamous epithelium of the esophagus contains abundant glycogen, which the iodine stains brown. Abnormal mucosal lesions such as squamous dysplasia and carcinoma in situ remain unstained due to the low glycogen content[10]. Lao-Sirieix *et al*[11] discuss the accuracy of endoscopic modalities in esophageal carcinoma, which reveal the efficacy of endoscopic screening (Table 1).

Utility of endoscopic screening

Chromoendoscopy has been studied in various countries with high-risk populations. In a high-risk population of ESCC in Linxian, China, standard white light imaging (WLI) was used to detect severe dysplasia or cancer with a sensitivity of 62% and specificity of 79%, while chromoendoscopy had a sensitivity of 96% and specificity of 63%[12]. In Japan, a study stratified Japanese men into high risk and low risk groups based on diet, drinking, and smoking. Chromoendoscopy resulted in a diagnosis of esophageal carcinoma in 0.86% of the subjects. The detection rate was 4.27% in the high-risk group, as opposed to 0.67% in the lower risk groups[13]. A study of a high-risk population in the Henan Province of China detected precancerous lesions in 46.6% of the subjects through chromoendoscopy, and 2.42% were cancerous. Among those diagnosed with cancer, 84.5% were in the early stage[14]. These studies convey that in high-risk populations for esophageal carcinoma, there is value in implementing endoscopic screening for early detection and treatment of esophageal carcinoma. The effect of screening endoscopy on morbidity and mortality in esophageal carcinoma is an area that needs to be further studied.

Cost analysis

Evaluating the cost effectiveness of screening endoscopy is difficult due to the variability in costs and services in different countries. There is not enough evidence to implement a mass-screening program in the United States due to the low incidence of disease. However, in areas with high-risk populations, there may be value in implementing such screening measures. Yang *et al*[15] found that screening in high risk areas of China, and subsequent early diagnosis and treatment, provide great cost savings due to the much lower cost of screening compared to the cost of multimodality treatment of invasive esophageal carcinoma with endoscopic mucosal resection, esophagectomy, radiotherapy, or chemotherapy. In another study in high-risk areas of China, chromoendoscopy screening resulted in substantial net price values and high benefit-cost ratios[16]. Other factors must still be considered,

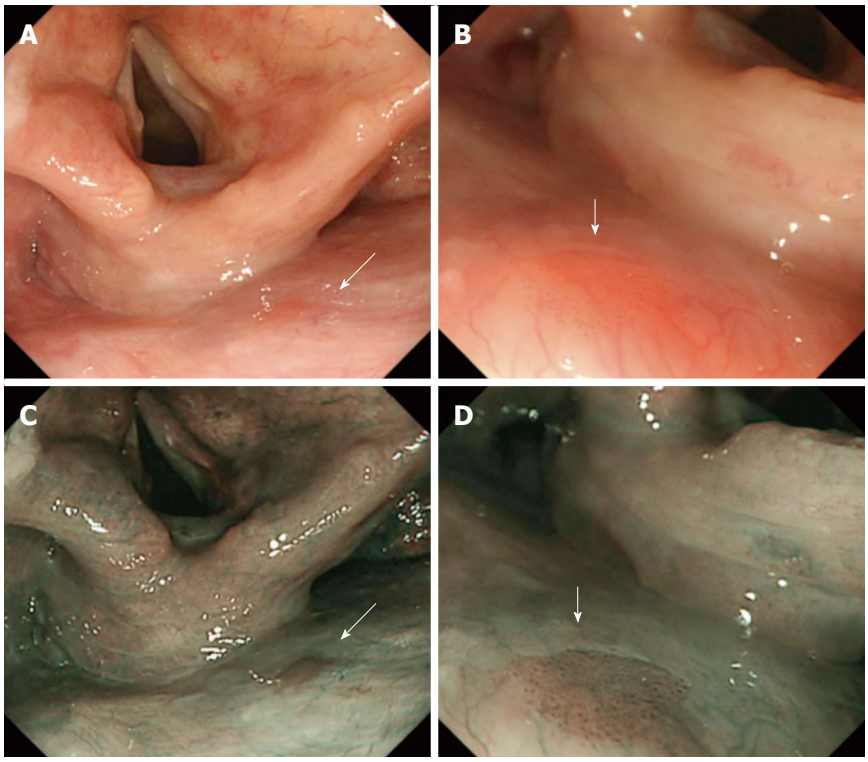

Figure 1 Differences in white light imaging from narrow-band imaging. A: White light imaging (WLI) displays an erythematous area in the posterior wall of the hypopharynx (white arrow); B: Magnifying WLI reveals a minimally erythematous patch with tiny microdots (white arrow): C: Narrow-band imaging (NBI) locates a distinct brown lesion in the posterior wall of the hypopharynx (white arrow); D: Magnifying NBI also demonstrates a distinct brown lesion with microdots that can be distinguished from the healthy mucosa surrounding it (white arrow)[20].

such as the frequency of screening, the invasive nature of endoscopy with its accompanying complications, and health resource status.

Novel techniques and technology

Early diagnosis of esophageal cancers are difficult to make due to minimal morphological changes noted on visualization. Therefore, targeted biopsies for precise histological diagnosis requires better endoscopic sensitivity rates. Novel techniques and technology in this field have shown significant potential to improve screening utility for esophageal cancers[17].

Narrow band imaging

Narrow-band imaging (NBI) is an endoscopic imaging technique that displays microstructures and capillaries in the superficial mucosal layer by using optical filters that narrow the respective red-green-blue bands, while simultaneously increasing the relative intensity of the blue band. In theory, this allows the physician to distinguish tissue surfaces much easier and optimizes the ability to diagnose a cancerous lesion[18]. Kara *et al*[19] found that the sensitivity for detecting high-grade dysplasia or early cancerous lesions was 93% and 86% for indigo carmine chromoendoscopy and narrow band imaging, respectively. Muto *et al*[20] compared NBI with conventional WLI to detect superficial ESCC lesions in patients with head and neck cancer. They found that NBI detected cancer more frequently than WLI (97% *vs* 55%, $P < 0.001$, respectively) with a sensitivity of 97.2%, specificity of 42.1%, and accuracy of 88.9% compared to 55.2%, 63.2%, and 56.5% with WLI, respectively. Yokoyama *et al*[21] found that the sensitivity of NBI was superior to WLI and equivocal to chromoendoscopy (92% *vs* 42%, $P < 0.05$, 92% *vs* 100%, NS) and specificity of NBI was equivalent to WLI (89% *vs* 94%, NS). Images adapted from Muto *et al*[20], above, illustrate the differences in WLI from NBI (Figure 1).

Video capsule endoscopy

The videocapsule endoscopy system includes a wireless capsule that contains a video camera, a sensing system, and a personal computer workstation. Studies have shown that the Pillcam esophageal video capsule has good sensitivity and specificity in detecting abnormalities in the esophagus, including Barrett's esophagus[22]. Domingos *et al*[23] assessed the use of esophageal capsule endoscopy (ECE) with methylene blue chromoendoscopy and found that the sensitivity, negative predictive value, and accuracy were 100%, 100%, and 79%, respectively for detecting esophageal lesions suspicious of cancer. ECE is still not as widely used as the standard chromoendoscopy with biopsy, but it is an acceptable and sensitive method to detect esophageal abnormalities.

Table 2 Different screening modalities

Modality	Sensitivity (95%CI)	Specificity (95%CI)	PPV (95%CI)	NPV (95%CI)	Accuracy (95%CI)
WL	47.3%	97.4%	79.4%	89.8%	88.7%
NBI	84.2%	95.6%	80.0%	96.6%	93.6%
Lugol[1]	93.0%	90.7%	67.9%	98.4%	91.1%
NBI or Lugol	94.7%	90.4%	67.5%	98.8%	91.1%
NBI or Lugol	82.6%	95.9%	81.0%	93.6%	93.6%

[1]Lugol is iodine staining solution used in chromoendoscopy. Adapted from Wang *et al*[26].

Autofluorescence endoscopy

This method provides real-time fluorescent images provided by adding a fluorescent agent to the standard endoscope using an image-processing module. This provides cellular and histological details of the tissue, aiding in detection of mucosal lesion[24]. Uedo *et al*[17] studied the use of videoendoscopy system with autofluorescence and reflectance imaging, which had a 100% detection rate of superficial esophageal cancers. The autofluorescence imaging (AFI) revealed flat or isochromatic extensions that were not detected by WLI. Lopes and Fagundes[25] discussed how AFI had a higher sensitivity than WLI in detecting superficial esophageal lesions (79% *vs* 51%, respectively), but its accuracy was worse than chromoendoscopy or NBI.

Ultrathin transnasal endoscopy

Another advance in technology is the use of transnasal endoscopy (TNE), which has the advantages of a small caliber device, ability for insufflation and biopsy, no need for sedation, and use with NBI and chromoendoscopy. Wang *et al*[26] compared the different screening modalities (Table 2) and found that unsedated TNE is a safe and reasonable option for esophageal screening. They found that TNE had a detection rate of ESCC and high-grade intraepithelial neoplasms of 10.1% and 7.3%, respectively, with mean procedure duration of 14.6 min. Arantes *et al*[27] studied the feasibility and tolerance of TNE in Brazilian patients undergoing esophageal screening. TNE was feasible in 99.1%, with an ESCC detection rate of 12.7%, and 92% of patients rated the discomfort as absent or minimal. They found no difference between WLI (sensitivity 92.3%, specificity 98.9%, accuracy 98.1%, area under curve 0.995) and digital chromoendoscopy [flexible spectral imaging color enhancement (FICE)] (sensitivity 100%, specificity 98.9%, accuracy 99%, area under curve 0.956) for detection of esophageal neoplasms. The ability to avoid sedation could be a significant advantage of TNE by decreasing complications.

GASTRIC CANCER ENDOSCOPIC SCREENING

Epidemiology

With the aging population, the burden of cancer continues to grow and remains one of the most difficult disease groups to cure. Gastric cancer is the third leading cause of cancer death worldwide, following lung and liver cancer. There was an estimated 951600 new gastric cancer cases and 723100 deaths that occurred in 2012[6]. However, gastric cancer rates have substantially declined in recent years. Studies have shown that this decline is due to refrigeration, less processed foods, and the availability of fresh produce[28]. In addition, the dramatic reduction of Helicobacter Pylori infections and the implementation of endoscopic screening in high-risk populations have also played a critical role in this decline[29].

Risk factors

Gastric cancer has distinct geographical and socioeconomic differences in distribution. Much of these differences are due to specific ethnic diets that result in continuous inflammation of the gastric lining. Diets high in salt, processed foods, nitroso compounds, and low in fruits, vegetables, and fiber are at increased risk of epithelial cell damage and pre-cancerous lesions[30-32]. Another major contributor to gastric cancer is H. pylori infections. They are the most common cause of gastritis and evidence suggests an approximate six-fold increase in the risk of gastric adenocarcinomas[33]. Other major risk factors include atrophic gastritis, gastric surgery, obesity, smoking, and genetic predisposition[34].

Current screening methods

The implementation of endoscopic gastric cancer screening has been limited to high-risk populations. Several countries including Venezuela, Chile, and East Asian countries such as China and Japan have implemented a variety of screening programs. In 2001 the Korean Gastric Cancer Association and National Cancer Center established nationwide endoscopic screening guidelines to the general populous in the Republic of Korea. The guidelines recommended biennial endoscopy or upper gastrointestinal series (UGIS) in men and women aged 40 years or older[35]. Several other screening methods for the early detection of gastric cancer include serum pepsinogen, serum gastrin-17, and *Helicobacter pylori* antibody testing. Endoscopic studies have shown the highest detection rates amongst the screening tests and have universally been used as the gold standard for diagnosis. Upper GI series has continuously been

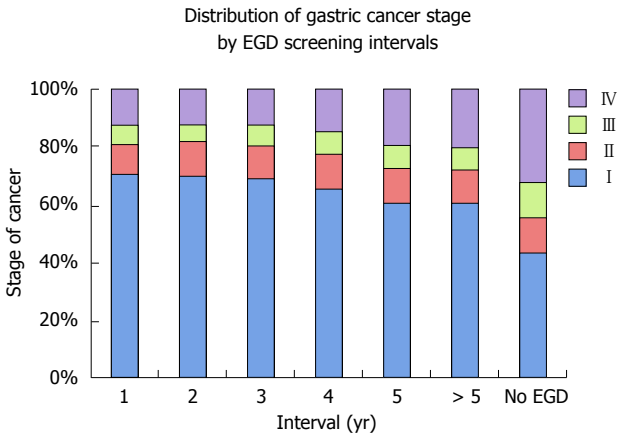

Figure 2 Diagnosis of stage Ⅳ gastric cancer increased substantially when the screening intervals extended beyond 3 yr. Adapted from Nam *et al*[41]. EGD: Esophagogastroduodenscopy.

analyzed as a rivaling modality for cancer detection but has not shown clear benefits over endoscopy[36].

UTILITY OF ENDOSCOPIC SCREENING

Mortality rate evaluation

There has been considerable evidence that those with early gastric cancer who undergo surgical treatment have an excellent prognosis[37,38]. However, there is a dramatic drop off in prognosis with the advanced stages of gastric cancer[39]. In Table 3[40], the 5-year survival rates, by stage, for stomach cancer treated with surgery are provided by the National Cancer Institute's SEER database.

A large cohort study done at the Korean National Cancer Center in Goyang, Korea discussed the relationship of gastric cancer stage and endoscopic screening intervals. Based on their findings, a significant benefit was observed in all screened subjects compared to those who were never screened, and they found that it was optimal to screen at intervals of 2 or 3 years. From Figure 2, it is evident that the diagnosis of stage IV gastric cancer increased substantially when the screening intervals extended beyond 3 years[41].

There are very few studies on the mortality reduction rates with the use of endoscopic screening programs. However, Hamashima *et al*[42] conducted a case-control study evaluating mortality rates of those screened and not screened for gastric cancer. Case subjects were defined as those who had died of gastric cancer in a certain time period. Control subjects were required to be disease-free at the time when the corresponding case subjects were diagnosed with gastric cancer. Compared with those who had never been screened before the date of diagnosis of gastric cancer in the case subjects, the odds ratios within 36 mo from the date of diagnosis were 0.695 for endoscopic screening. Although the study admits bias limitations, the results suggested a 30% reduction in gastric cancer mortality by endoscopic screening compared to no screening at all.

Table 3 Five-year survival rates by stage for stomach cancer treated with surgery

Stage	5-year observed survival rate
Stage ⅠA	71%
Stage ⅠB	57%
Stage ⅡA	46%
Stage ⅡB	33%
Stage ⅢA	20%
Stage ⅢB	14%
Stage ⅢC	9%
Stage Ⅳ	4%

Adapted from National Cancer Institute's SEER database[40].

Table 4 Endoscopy used in cancer screening

Ref.	Number of Subjects	Sensitivity	Specificity	PPV
Hamashima *et al*[44], 2013	EGD: 7388	88.60% (69.8-97.6)[1]	85.10% (84.3-85.9)[1]	5.50% (4.3-7.0)[1]
	Upper GI series: 5410	83.10% (58.6-96.4)[1]	85.60% (84.6-86.5)[1]	4.30% (3.4-5.2)[1]
Choi *et al*[43,45], 2011	EGD: 924822	66.90% (59.8-74.0)[1]	96.20% (95.7-96.7)[1]	5.30% (4.8-5.9)[1]
	Upper GI series: 1765909	27.30% (22.6-32.0)[1]	96.60% (96.3-97.0)[1]	1.30% (1.1-1.6)[1]

[1]The 95% confidential intervals are given in parentheses[35]. Adapted from Choi *et al*[43].

Test accuracy

Esophagogastroduodenscopy (EGD) and UGIS have been the main screening tools for gastric cancer. However, there has historically been some debate as to which test is more effective. Two newer studies by Hamashima *et al*[42] and Choi *et al*[43] show a comparison of sensitivity, specificity, and positive predictive value (PPV) of these two modalities. Although there were some differences in sensitivity and specificity between the two studies, the conclusions were similar. The studies suggest that endoscopy is the better test for gastric cancer screening due to its superior performance and high detection rate. Table 4 displays the comparative values[35,43-45].

Cost analysis

Again, the analysis of cost effectiveness is a difficult evaluation to make due to the lack of consistency and prices in different world markets. However, in most high-risk populations, such as Singapore, Japan, and Korea, endoscopy was found to be the most cost-effective screening method using incremental cost-effective ratio (ICER) analysis[35]. Additionally, in several other Korean studies, screening endoscopy was also found to be more cost-effective than no screening done at all[35]. In low-incidence rate populations, such as the United States, there is not convincing evidence for a nationwide screening program. Gupta *et al*[46] concluded

Table 5 Risk factors and proposed screening recommendations for gastric cancer

Risk factors	Risk for developing gastric cancer	Recommendation	First author
Helicobacter pylori infection	Odds ratio (OR): 2.3	High risk area - mass screening possible benefit Low risk area - mass screening not cost-effective	Huang, 1998
Pernicious anemia	Standardized incidence ratio: 5	Screening by upper endoscopy (UE) recommended	Kokkola, 1998
Partial gastrectomy	15-24 yr, RR = 9.4 25-46 yr, RR = 55.6	Screening by UE recommended	Lundegardh, 1988 Tersmette, 1991
Familial adenomatous polyposis	Not available	Screening by UE recommended	Alexander, 1989
Hereditary nonpolyposis colorectal cancer	Not available	Screening by UE recommended	Aarnio, 1997
Positive family history of gastric cancer	OR: 2.5-5.1	HP eradication +/- UE screening	Yatsuya, 2004 Chen, 2004

Adapted from Chan *et al*[48].

that ICER remains high for upper GI screening and would not be a cost effective program in the United States. A separate study by Yeh *et al*[47] also concluded that endoscopic surveillance would not be cost-effective. However, the study suggested that immigrants from high-risk countries for gastric cancer might have a cost benefit. Although ethnic implications are not included, Table 5 constructed by Chan *et al*[48] displays recommendations of endoscopic screening according to different risk factors.

Novel techniques and technology

In recent years there have been new techniques and technology that have showed significant promise in improving early gastric cancer diagnosis. Autofluorescence endoscopy and narrow-band imaging are some of the leading areas of technological development.

Autofluorescence endoscopy

Much like its use in esophageal cancer screening, autofluorescence imaging (AFI) is a newer concept that uses the natural tissue fluorescence emitted by endogenous molecules (fluorophores) after excitation by light to produce real-time images. Therefore, using the differences of fluorophore concentration, metabolic state, and spatial distribution allows the physician to identify irregular lesions[49]. A pilot study from Japan compared the results of detecting gastric cancer lesions with AFI *vs* conventional EGD in experienced and less experienced endoscopists. While there wasn't significant change in efficacy for the experienced endoscopists, for the less experienced endoscopists AFI substantially improved sensitivity of detecting neoplastic lesions. However, there was insignificant improvement in specificity and accuracy. A major reason for a lack of specificity was because the AFI was unable to distinguish cancerous lesions from inflammatory and hyperplastic changes. Nonetheless, the study argues that the primary objective in early gastric cancer screening should be higher sensitivity rather than diagnostic accuracy. Though there hasn't been definitive evidence of significant benefit, especially in experienced endoscopists, high-risk populations that already follow screening guidelines might consider implementing AFI over white light endoscopy to improve sensitivities[50]. Images adapted by the pilot study from Tada *et al*[50], demonstrate AFI's limited role in certain lesions and benefit in others (Figure 3).

Ultrathin transnasal endoscopy with narrow-band imaging

Ultrathin transnasal endoscopy, as the name implies, is a much thinner scope that has fallen into favor over the conventional white-light imaging EGD due to decreased procedural discomfort and minimal effects on the circulatory system. However, since the endoscope is much thinner, there has historically been a sacrifice to the optical resolution, resulting in decreased detection rates. The development of a new ultrathin non-magnifying transnasal endoscope, the GIF-XP290N (Olympus Medical System, Tokyo, Japan), has been documented to provide better details and improved diagnostic utility. Many studies have determined that the use of narrow band imaging with this scope has demonstrated significant diagnostic usefulness. However, it has not shown reliability in predicting depth of invasion[51]. Therefore, the use of these scopes have been considered limited in its role for gastric cancer T staging. The Kawai *et al*[52] study showed that NBI examination using the new ultrathin endoscope yielded a sensitivity of 87.5%, specificity of 93.2%, and accuracy of 92.3%. Whereas WLI examination yielded a sensitivity of 50.0%, specificity of 63.6%, and accuracy 61.5%. Although it may have poor staging utility, the benefits of ultrathin transnasal endoscopy with narrow-band imaging are improving and can soon become the standard technique for diagnosing gastric cancer.

COLORECTAL CANCER ENDOSCOPIC SCREENING

Epidemiology

Colorectal cancer (CRC) is the third leading cause of cancer death in the United States and is a prevalent disease that accounted for an estimated 1.4 million cases and 693900 deaths worldwide in 2012. The most recent cancer data suggests that the mortality

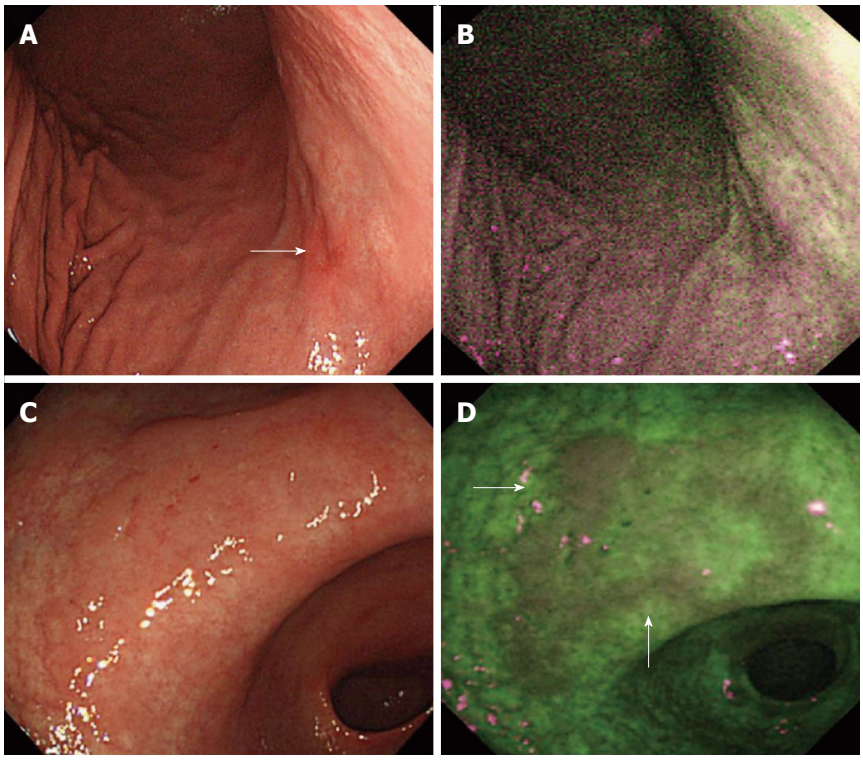

Figure 3 Autofluorescence imaging's limited role in certain lesions and benefit in others. A: White light imaging (WLI) displays a red lesion with a slightly depressed area on the bottom right corner (white arrow); B: Autofluorescence imaging (AFI) does not demonstrate a distinct lesion that can be ruled neoplastic; C: WLI made it difficult for the endoscopists to identify the isochromatic flat lesion: D: AFI displays a well-marked lesion with slightly raised borders (white arrows)[50].

rates for colorectal cancer are trending down and are likely due to colorectal cancer screening, diminished risk factors, and improved treatment options[6,53].

Risk factors

Environmental influences and hereditary conditions are the primary risk factors for CRC. Inflammation of the large bowel result in the most substantial increases in risk for CRC and many of these diseases are inherited. To name a few, familial adenomatous polyposis, lynch syndrome (hereditary nonpolyposis colorectal cancer), or a family history of these diseases have shown to have very high risk of CRC[54]. Other conditions that also increase risk include ulcerative colitis, Crohn's disease, diabetes, and patients who received abdominal radiation in the past. After inflammatory bowel conditions, there has been substantial evidence that sedentary lifestyles and poor food choices have led to increased risk. Many describe these attributes as the "western lifestyle", and have studied its detrimental effects in the body. Studies show that an active lifestyle with a diet high in nutrients, fruits, and vegetables are protective to the large bowel mucosa[55,56].

Current screening methods

The 1970s to 1990s marked an era of some of the greatest advancements in GI endoscopy. In those 20 years, the medical world saw the first utilizations of ERCP, endoscopic sphincterotomy, endoscopic ultrasound, and colonoscopies[57]. Eventually, researches began to observe the benefits of colonoscopy as a screening tool and started to seriously consider implementation of its use globally. In the United States, the American College of Gastroenterology was the first organization to recommend colonoscopy as the preferred standard for CRC screening, which was subsequently endorsed by the American Society for Gastrointestinal Endoscopy and the National Comprehensive Cancer Network. These recommendations were quickly followed by the American Cancer Society in 1997 and the US Multi-Society Task Force in 2003 with a "menu of options" approach. This approach offered several options for screening and left it to the patients and physicians discretion to choose which method was preferred[58].

Today, screening for colorectal cancer is still offered in a "menu of options" approach and is largely influenced by two major United States guidelines: the Multi-Society Task Force and the US Preventative Services Task Force (USPSTF). The latest guidelines were released in 2008 and the two organizations have agreeing recommendations. These guidelines recommend the following options as acceptable choices for endoscopic colorectal cancer screening in average-risk adults between the age of 50 to 75: colonoscopy every 10 years, flexible sigmoidoscopy every 5 years, annual fecal occult blood test, computed tomography colonography every 5 years, annual fecal immunochemical test, and stool DNA testing (cologuard). Other than colonoscopy the remaining

Table 6 Colorectal cancer screening guidelines for the United States

Guidelines for screening for the early detection of colorectal cancer and adenomas for average-risk women and men aged 50 yr and older	
Test	**Interval**
Tests that detect adenomatous polyps and cancer	
FSIG with insertion up to 40 cm from anal verge or to splenic flexure	Every 5 yr
Colonoscopy	Every 10 yr
DCBE	Every 5 yr
CTC	Every 5 yr
Tests that primarily detect cancer	
gFOBT	Annual
FIT	Annual
sDNA	Interval uncertain

Adapted from Levin *et al*[59]. FSIG: Flexible sigmoidoscopy; DCBE: Double-contrast barium enema; CTC: Computed tomography colonography; gFOBT: Guaiac-based fecal occult blood test; FIT: Fecal immunochemical test; sDNA: Stool DNA test.

screening modalities will not be further discussed in this review article. Table 6 provides the colorectal cancer screening guidelines for the United States[59,60].

Utility of endoscopic screening

Since most colorectal cancers develop from pre-cancerous polyps, it is important to detect these polyps early with colonoscopy. With early detection and removal of these polyps, it reduces the risk of developing colorectal cancer by up to 90 percent. In addition, early detection of cancer that is already present in the colon or rectum lead to better treatment outcomes and reduced chance of metastasis. There are several risks involved with the procedure, including severe bleeding or a tear in the intestinal wall. However, these risks are minimal and are usually avoided by sound clinical judgment[58,61,62].

Novel techniques and technology

Early detection and management is crucial for good prognosis in colorectal cancer. Unfortunately, several studies have shown close to 20% of adenomas are missed during colonoscopies[63,64]. In order to improve visualization and increase the adenoma detection rates, there have been many advancements in endoscopic techniques and technology. Like all other endoscopy screens, the results of these new techniques are operator-dependent and vary according to the skills and experience of the physician performing the endoscopy.

High definition colonoscopy

One of many attempts to improve functionality was to have better quality images with high definition (HD) colonoscopy. This was a simple enhancement of resolution with refined images displayed by the scope. There has been mixed results with the use of HD colonoscopies. However, a meta-analysis of HD colonoscopy compared to standard colonoscopy showed a slight increase of 3.5% (95%CI: 0.9%-6.1%) for adenomatous polyp detection[65]. Therefore the use of HD endoscopies combined with other image enhancement techniques have been in favor compared to HD enhancements alone.

Wide angle colonoscopies

In addition to quality images, another idea to improve detection rates was to widen the view of the camera in order to reduce blind spots. Wide angle and full spectrum colonoscopy are several techniques that were developed to accomplish this. The standard colonoscope allows 140 degrees of viewing angle. In comparison, the wide angle (WA) colonoscope reveals 170 degrees of forward viewing angle and the newer full spectrum endoscopy (FUSE; EndoChoice, Alpharetta, GA, United States) uses 3 different cameras to expose 330 degrees of viewing. Based on several studies, the WA colonoscopy showed no benefits for polyp detection rates but had marginally reduced withdrawal times (4.9 min *vs* 5.4 min, $P = 0.0001$). The FUSE technology, on the other hand, has a more promising outlook based on recent studies. In a 185 participant prospective, non-randomized study, there was significant decrease in adenoma miss rates compared to the standard forward-viewing colonoscope. Based on per-lesion analysis, the adenoma miss rate was 7% for the FUSE colonoscope and 41% for forward-viewing colonoscope ($P < 0.0001$). However, there was a median withdrawal time delay of about 30 s compared to the traditional method[66]. This, we believe, is not too much of a delay for the benefit it may provide.

Third-Eye retroscope

Another new development of extended angle colonoscopes is the Third-Eye Retroscope (TER; Avantis Medical Systems, Sunnyval, CA, United States, Figure 4). This disposable device is an add-on instrument that is passed through the channel of a standard colonoscope that will allow the physician to have an accessory retrograde view that complements the forward view of the colonoscope. Several studies have shown evidence of significant increases in polyp and adenoma detection rates. Polyps are defined as projections of tissue from the inner lining of the colon into the lumen of the colon. An adenoma is a type of polyp that has a different growth pattern, only distinguished by pathology, which usually has higher risk for cancer. Initial pilot studies showed that there was an 11.8% increased diagnostic yield for these lesions with TER. Furthermore, DeMarco *et al*[67] used a prospective, multicenter study to show a polyp detection rate (PDR) increase of about 14.8% ($P < 0.001$) and adenoma detection rate (ADR) increase by 16% ($P < 0.001$) compared to the traditional forward-facing scope. There was no evidence of significant increase in procedure time or complications. The most recent TERRACE study also concluded that

Figure 4 Third Eye Retroscope® attachment, extends out in its retroflexed position[69].

the TER increases adenoma detection rate by visualizing areas behind folds[68] (Figure 4[69]). Thus far, the data suggests this instrument may be a safe and effective addition to screening endoscopies (Figure 5).

Colon capsule endoscopy

Colon Capsule Endoscopy (CCE, PillCam; Given Imaging; Yoqneam, Israel) is a ingestible double-sided camera to access nearly 360 degrees of viewing that was first used for large bowel imaging in 2006. There seemed to be a significant draw to the technology early in its development because it didn't require sedation or gas insufflation. Unfortunately, the CCE lost favor and had many negative opinions due to high procedural costs, the need for extensive bowel cleansing, and poor accuracy. Since then, CCE technology has been constantly refined as new indications and new capsule functions have been developed in order to improve the diagnostic and possible therapeutic utility[22]. The second generation of CCE (CCE-2) was developed to improve effectiveness and proved to be an accurate tool to detect colonic neoplastic lesions when used in average-risk individuals[70]. However, many studies have concluded that CCE is not a first-line screening device due to the inability to take tissue samples and no significant improvement of accuracy compared to conventional colonoscopy. Current recommendations state that patients who have contraindications or do not wish to perform conventional colonoscopy, the CCE-2 remains a good second option for screening[71] (Figure 6).

Image-enhanced endoscopy

A recent area of much interest is the use of image-enhanced endoscopies (IEEs). These are imaging techniques that may use topical dyes, optical filtering, or ultramagnification that allows more contrast and tissue differentiation during the endoscopic procedure. Chromoendoscopy with indigo carmine (IC), for example, has been a relatively classic procedure for diagnosis of colorectal cancer and remains one of the most effective techniques for evaluating lesions[72]. The newer equipment-based IEEs include NBI, the Fujinon spectral estimation technology, and the Pentax surface enhancement endoscopy. Table 7 further explains each IEE and how they differ.

Table 7 Different image-enhanced endoscopy

Type	Mode (solution/instrument)	Mechanism of contrast
Dye-based IEE (chromoscopy)		
Dye enhancement		
Contrast dye indigo carmine	0.1%-0.4% solution For 0.2% dilution, mix 5 mL 0.8% solution) with 15 mL sterile water	Dye pools in mucosal crevices; no cellular staining
Equipment-based IEE		
Optical enhancement		
Narrow band imaging	Olympus	Modification of light source with narrowed wavelengths to enhance capillary patterns
Electronic enhancement		
Spectral estimation technology	Fujinon	Processing of image to enhance capillary patterns
Surface enhancement	Pentax	Processing of image to enhance color pattern or structure (I-Scan Technology)

Adapted from Ko[72]. IEE: Image-enhanced endoscopy.

Narrow band imaging

Narrow band imaging trials have shown minimal benefits in decreasing lesion miss rates for colorectal cancer. According to a study by Pasha *et al*[73], HD-NBI compared with HD-WLI, did not increase the yield of colon polyps, adenomas, or flat adenomas, nor does it decrease the miss rate of colon polyps or adenomas for colorectal cancer screening or surveillance.

Fujinon spectral estimation technology

The Fujinon intelligent chromoendoscopy (FICE) uses different filters to visualize the mucosal tissue and reconstructs the image to display what the mucosa would look like if illuminated using certain wavelengths. The FICE allows a total of 10 different digital filters and does not need any dye spraying techniques, which gives its name "virtual chromoendoscopy". Based on a recent Spanish study, indigo carmine dye (the classic chromoendoscopy) was better than any FICE filter setting. However, IC and FICE filter 4 were both found to be better than WLI alone. Therefore, FICE filter 4 was suggested a feasible option over the traditional WLI[74].

Pentax surface enhancement technology

The Pentax technology uses a similar image refining process to enhance the display of endoscopy. There has been mixed reports on the benefit of the Pentax HiLine colonscopy (PHL). One study concluded that

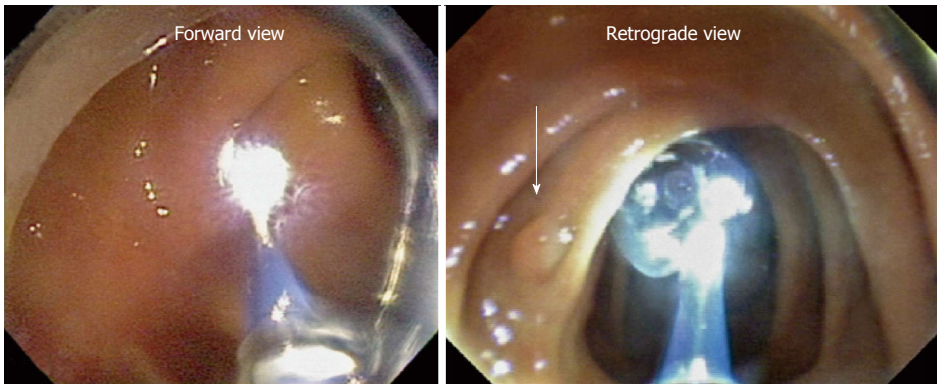

Figure 5 Advantage of retrograde visibility. The retrograde view (right) clearly sights a polyp (arrow) that the forward view (left) would not have spotted[67].

Figure 6 First and second generation Colon Capsule Endoscopy by Given Imaging[71].

PHL compared to NBI-White Light Endoscopy, which they refer to as Olympus Lucera (OL), showed no significant difference. According to the results the polyp detection rates were 58% in OL and 67% in PHL, with the adenoma detection rates of 49% in OL and 56% in PHL. The study concluded there was no advantage of using the PHL over NBI endoscopy[75]. Image processing improvements with the Fujinon and Pentax still remain to show clear benefit and more investigation may be required to demonstrate utility in a theoretically promising field of technology.

CONCLUSION

Esophageal, gastric, and colorectal cancers are deadly diseases that continue to plague our world today. The value of screening endoscopy in evaluating these types of cancers is a critical area of discussion due to a potential reduction in morbidity and mortality. Esophageal and gastric cancers have yet to have mass screening programs in average-risk populations. However, in high-risk populations screening endoscopy has shown significant benefit and a decrease in mortality. Many researchers agree that cost analysis and risk-benefit show no practical implementation of esophageal and gastric endoscopic screening in average or low-risk populations. On the contrary, however, colorectal cancer screening programs have been implemented for many years. The use of colonoscopy has shown drastic improvements in morbidity and mortality, and is the reason it is recommended as the primary screening tool in colon cancer screening guidelines. As the role of endoscopy as a screening tool has continued to develop, newer technology and techniques have emerged to improve its utility. Many new image enhancement techniques and computer processing programs have shown promise and may have a significant role in the future of endoscopic screening.

REFERENCES

1 **Black WC**, Welch HG. Screening for disease. *AJR Am J Roentgenol* 1997; **168**: 3-11 [PMID: 8976910 DOI: 10.2214/ajr.168.1.8976910]
2 **Misra S**, Solomon NL, Moffat FL, Koniaris LG. Screening criteria for breast cancer. *Adv Surg* 2010; **44**: 87-100 [PMID: 20919516 DOI: 10.1016/j.yasu.2010.05.008]
3 **Becker H**. Introduction to Bronchoscopy. Cambridge: Cambridge University Press, 2009
4 **Mancino MG**, Bianchi M, Festa V, Koch M, Dezi A. Recent advances in endoscopic management of gastrointestinal cancers. *Transl Gastrointest Cancer* 2014 [DOI: 10.3978/j.issn.2224-4778.2013.10.05]
5 **Marks J**, Ponsky J. Upper Gastrointestinal Endoscopy. Decker: Intellectual Properties Inc, 2010
6 **Torre LA**, Bray F, Siegel RL, Ferlay J, Lortet-Tieulent J, Jemal A. Global cancer statistics, 2012. *CA Cancer J Clin* 2015; **65**: 87-108 [PMID: 25651787 DOI: 10.3322/caac.21262]
7 **Napier KJ**, Scheerer M, Misra S. Esophageal cancer: A Review of epidemiology, pathogenesis, staging workup and treatment modalities. *World J Gastrointest Oncol* 2014; **6**: 112-120 [PMID: 24834141 DOI: 10.4251/wjgo.v6.i5.112]
8 **Rustgi AK**, El-Serag HB. Esophageal carcinoma. *N Engl J Med* 2014; **371**: 2499-2509 [PMID: 25539106 DOI: 10.1056/NEJMra1314530]
9 **Roshandel G**, Nourouzi A, Pourshams A, Semnani S, Merat S, Khoshnia M. Endoscopic screening for esophageal squamous cell carcinoma. *Arch Iran Med* 2013; **16**: 351-357 [PMID: 23725069]
10 **Roshandel G**, Semnani S, Malekzadeh R. None-endoscopic Screening for Esophageal Squamous Cell Carcinoma- A Review. *Middle East J Dig Dis* 2012; **4**: 111-124 [PMID: 24829644]
11 **Lao-Sirieix P**, Fitzgerald RC. Screening for oesophageal cancer. *Nat Rev Clin Oncol* 2012; **9**: 278-287 [PMID: 22430857 DOI: 10.1038/nrclinonc.2012.35]
12 **Dawsey SM**, Fleischer DE, Wang GQ, Zhou B, Kidwell JA, Lu N, Lewin KJ, Roth MJ, Tio TL, Taylor PR. Mucosal iodine staining

improves endoscopic visualization of squamous dysplasia and squamous cell carcinoma of the esophagus in Linxian, China. *Cancer* 1998; **83**: 220-231 [PMID: 9669803]

13 **Yokoyama A**, Oda J, Iriguchi Y, Kumagai Y, Okamura Y, Matsuoka M, Mizukami T, Yokoyama T. A health-risk appraisal model and endoscopic mass screening for esophageal cancer in Japanese men. *Dis Esophagus* 2013; **26**: 148-153 [PMID: 22458712 DOI: 10.1111/j.1442-2050.2012.01343.x]

14 **Lu YF**, Liu ZC, Li ZH, Ma WH, Wang FR, Zhang YB, Lu JB. Esophageal/gastric cancer screening in high-risk populations in Henan Province, China. *Asian Pac J Cancer Prev* 2014; **15**: 1419-1422 [PMID: 24606476 DOI: 10.7314/APJCP.2014.15.3.1419]

15 **Yang J**, Wei WQ, Niu J, He YT, Liu ZC, Song GH, Zhao de L, Qiao YL, Yang CX. Estimating the costs of esophageal cancer screening, early diagnosis and treatment in three high risk areas in China. *Asian Pac J Cancer Prev* 2011; **12**: 1245-1250 [PMID: 21875275]

16 **Yang J**, Wei WQ, Niu J, Liu ZC, Yang CX, Qiao YL. Cost-benefit analysis of esophageal cancer endoscopic screening in high-risk areas of China. *World J Gastroenterol* 2012; **18**: 2493-2501 [PMID: 22654446 DOI: 10.3748/wjg.v18.i20.2493]

17 **Uedo N**, Iishi H, Tatsuta M, Yamada T, Ogiyama H, Imanaka K, Sugimoto N, Higashino K, Ishihara R, Narahara H, Ishiguro S. A novel videoendoscopy system by using autofluorescence and reflectance imaging for diagnosis of esophagogastric cancers. *Gastrointest Endosc* 2005; **62**: 521-528 [PMID: 16185965 DOI: 10.1016/j.gie.2005.06.031]

18 **Matsuo K**, Takedatsu H, Mukasa M, Sumie H, Yoshida H, Watanabe Y, Akiba J, Nakahara K, Tsuruta O, Torimura T. Diagnosis of early gastric cancer using narrow band imaging and acetic acid. *World J Gastroenterol* 2015; **21**: 1268-1274 [PMID: 25632201 DOI: 10.3748/wjg.v21.i4.1268]

19 **Kara MA**, Peters FP, Rosmolen WD, Krishnadath KK, ten Kate FJ, Fockens P, Bergman JJ. High-resolution endoscopy plus chromoendoscopy or narrow-band imaging in Barrett's esophagus: a prospective randomized crossover study. *Endoscopy* 2005; **37**: 929-936 [PMID: 16189764 DOI: 10.1055/s-2005-870433]

20 **Muto M**, Minashi K, Yano T, Saito Y, Oda I, Nonaka S, Omori T, Sugiura H, Goda K, Kaise M, Inoue H, Ishikawa H, Ochiai A, Shimoda T, Watanabe H, Tajiri H, Saito D. Early detection of superficial squamous cell carcinoma in the head and neck region and esophagus by narrow band imaging: a multicenter randomized controlled trial. *J Clin Oncol* 2010; **28**: 1566-1572 [PMID: 20177025 DOI: 10.1200/JCO.2009.25.4680]

21 **Yokoyama A**, Ichimasa K, Ishiguro T, Mori Y, Ikeda H, Hayashi T, Minami H, Hayashi S, Watanabe G, Inoue H, Kudo SE , Minami H, Hayashi S, Watanabe G, Inoue H, Kudo SE. Is it proper to use non-magnified narrow-band imaging for esophageal neoplasia screening? Japanese single-center, prospective study. *Dig Endosc* 2012; **24**: 412-418 [PMID: 23078432 DOI: 10.1111/j.1443-1661.2012.01309.x]

22 **Bouchard S**, Ibrahim M, Van Gossum A. Video capsule endoscopy: perspectives of a revolutionary technique. *World J Gastroenterol* 2014; **20**: 17330-17344 [PMID: 25516644 DOI: 10.3748/wjg.v20.i46.17330]

23 **Domingos TA**, Moura EG, Mendes DC, Martins BC, Sallum RA, Nasi A, Sakai P, Cecconello I. Comparative evaluation of esophageal Barrett's epithelium through esophageal capsule endoscopy and methylene blue chromoendoscopy. *Rev Gastroenterol Mex* 2013; **78**: 57-63 [PMID: 23680052 DOI: 10.1016/j.rgmx.2012.11.003]

24 **Kwon RS**, Sahani DV, Brugge WR. Gastrointestinal cancer imaging: deeper than the eye can see. *Gastroenterology* 2005; **128**: 1538-1553 [PMID: 15887150 DOI: 10.1053/j.gastro.2005.03.034]

25 **Lopes AB**, Fagundes RB. Esophageal squamous cell carcinoma - precursor lesions and early diagnosis. *World J Gastrointest Endosc* 2012; **4**: 9-16 [PMID: 22267978 DOI: 10.4253/wjge.v4.i1.9]

26 **Wang CH**, Lee YC, Wang CP, Chen CC, Ko JY, Han ML, Chen TC, Lou PJ, Yang TL, Hsiao TY, Wu MS, Wang HP, Tseng PH. Use of transnasal endoscopy for screening of esophageal squamous cell carcinoma in high-risk patients: yield rate, completion rate, and safety. *Dig Endosc* 2014; **26**: 24-31 [PMID: 23551305 DOI: 10.1111/den.12053]

27 **Arantes V**, Albuquerque W, Salles JM, Freitas Dias CA, Alberti LR, Kahaleh M, Ferrari TC, Coelho LG. Effectiveness of unsedated transnasal endoscopy with white-light, flexible spectral imaging color enhancement, and lugol staining for esophageal cancer screening in high-risk patients. *J Clin Gastroenterol* 2013; **47**: 314-321 [PMID: 23059405 DOI: 10.1097/MCG.0b013e3182617fc1]

28 **Lee SA**, Kang D, Shim KN, Choe JW, Hong WS, Choi H. Effect of diet and Helicobacter pylori infection to the risk of early gastric cancer. *J Epidemiol* 2003; **13**: 162-168 [PMID: 12749604 DOI: 10.2188/jea.13.162]

29 **Bertuccio P**, Chatenoud L, Levi F, Praud D, Ferlay J, Negri E, Malvezzi M, La Vecchia C. Recent patterns in gastric cancer: a global overview. *Int J Cancer* 2009; **125**: 666-673 [PMID: 19382179 DOI: 10.1002/ijc.24290]

30 **Tsugane S**, Sasazuki S. Diet and the risk of gastric cancer: review of epidemiological evidence. *Gastric Cancer* 2007; **10**: 75-83 [PMID: 17577615 DOI: 10.1007/s10120-007-0420-0]

31 **You WC**, Zhang L, Yang CS, Chang YS, Issaq H, Fox SD, Utermahlen WE, Zhao L, Keefer L, Liu WD, Chow WH, Ma JL, Kneller R, Ho MY, Fraumeni JF, Xu GW, Blot WJ. Nitrite, N-nitroso compounds, and other analytes in physiological fluids in relation to precancerous gastric lesions. *Cancer Epidemiol Biomarkers Prev* 1996; **5**: 47-52 [PMID: 8770466]

32 **Peleteiro B**, Lopes C, Figueiredo C, Lunet N. Salt intake and gastric cancer risk according to Helicobacter pylori infection, smoking, tumour site and histological type. *Br J Cancer* 2011; **104**: 198-207 [PMID: 21081930 DOI: 10.1038/sj.bjc.6605993]

33 **Hung IF**, Wong BC. Assessing the risks and benefits of treating Helicobacter pylori infection. *Therap Adv Gastroenterol* 2009; **2**: 141-147 [PMID: 21180540 DOI: 10.1177/1756283X08100279]

34 **Compare D**, Rocco A, Nardone G. Risk factors in gastric cancer. *Eur Rev Med Pharmacol Sci* 2010; **14**: 302-308 [PMID: 20496539]

35 **Choi KS**, Suh M. Screening for gastric cancer: the usefulness of endoscopy. *Clin Endosc* 2014; **47**: 490-496 [PMID: 25505713 DOI: 10.5946/ce.2014.47.6.490]

36 **Tashiro A**, Sano M, Kinameri K, Fujita K, Takeuchi Y. Comparing mass screening techniques for gastric cancer in Japan. *World J Gastroenterol* 2006; **12**: 4873-4874 [PMID: 16937471]

37 **Okada K**, Fujisaki J, Yoshida T, Ishikawa H, Suganuma T, Kasuga A, Omae M, Kubota M, Ishiyama A, Hirasawa T, Chino A, Inamori M, Yamamoto Y, Yamamoto N, Tsuchida T, Tamegai Y, Nakajima A, Hoshino E, Igarashi M. Long-term outcomes of endoscopic submucosal dissection for undifferentiated-type early gastric cancer. *Endoscopy* 2012; **44**: 122-127 [PMID: 22271022 DOI: 10.1055/s-0031-1291486]

38 **Misra S**, Pedroso FE, DiPasco PJ, Solomon NL, Gennis E, Franceschi D, Ardalan B, Koniaris LG. Does neoadjuvant chemotherapy improve outcomes for patients with gastric cancer? *J Surg Res* 2012; **178**: 623-631 [PMID: 22682528 DOI: 10.1016/j.jss.2012.04.062]

39 **Hundahl SA**, Phillips JL, Menck HR. The National Cancer Data Base Report on poor survival of U.S. gastric carcinoma patients treated with gastrectomy: Fifth Edition American Joint Committee on Cancer staging, proximal disease, and the "different disease" hypothesis. *Cancer* 2000; **88**: 921-932 [PMID: 10679663]

40 **Howlader N**, Noone AM, Krapcho M, Garshell J, Miller D, Altekruse SF, Kosary CL, Yu M, Ruhl J, Tatalovich Z, Mariotto A, Lewis DR, Chen HS, Feuer EJ, Cronin KA. SEER Cancer Statistics Review, 1975-2011, National Cancer Institute. Bethesda, MD. SEER data submission, posted to the SEER web site, April 2014. (Accessed November 2013). Available from: URL: http://seer.cancer.gov/csr/1975_2011/

41 **Nam JH**, Choi IJ, Cho SJ, Kim CG, Jun JK, Choi KS, Nam BH, Lee JH, Ryu KW, Kim YW. Association of the interval between endoscopies with gastric cancer stage at diagnosis in a region of high prevalence. *Cancer* 2012; **118**: 4953-4960 [PMID: 22806878 DOI: 10.1002/cncr.27495]

42 **Hamashima C**, Ogoshi K, Okamoto M, Shabana M, Kishimoto T, Fukao A. A community-based, case-control study evaluating

mortality reduction from gastric cancer by endoscopic screening in Japan. *PLoS One* 2013; **8**: e79088 [PMID: 24236091 DOI: 10.1371/journal.pone.0079088]

43 **Choi KS**, Jun JK, Park EC, Park S, Jung KW, Han MA, Choi IJ, Lee HY. Performance of different gastric cancer screening methods in Korea: a population-based study. *PLoS One* 2012; **7**: e50041 [PMID: 23209638 DOI: 10.1371/journal.pone.0050041]

44 **Hamashima C**, Okamoto M, Shabana M, Osaki Y, Kishimoto T. Sensitivity of endoscopic screening for gastric cancer by the incidence method. *Int J Cancer* 2013; **133**: 653-659 [PMID: 23364866 DOI: 10.1002/ijc.28065]

45 **Choi KS**, Jun JK, Lee HY, Park S, Jung KW, Han MA, Choi IJ, Park EC. Performance of gastric cancer screening by endoscopy testing through the National Cancer Screening Program of Korea. *Cancer Sci* 2011; **102**: 1559-1564 [PMID: 21564421 DOI: 10.1111/j.1349-7006.2011.01982.x]

46 **Gupta N**, Bansal A, Wani SB, Gaddam S, Rastogi A, Sharma P. Endoscopy for upper GI cancer screening in the general population: a cost-utility analysis. *Gastrointest Endosc* 2011; **74**: 610-624.e2 [PMID: 21741639 DOI: 10.1016/j.gie.2011.05.001]

47 **Yeh JM**, Hur C, Kuntz KM, Ezzati M, Goldie SJ. Cost-effectiveness of treatment and endoscopic surveillance of precancerous lesions to prevent gastric cancer. *Cancer* 2010; **116**: 2941-2953 [PMID: 20564399 DOI: 10.1002/cncr.25030]

48 **Chan A**, Wong B. Risk factors and proposed screening recommendations for gastric cancer. (Accessed February 25, 2015). Available from: URL: http://www.uptodate.com/contents/screening-and-prevention-of-gastric-cancer?source=search_result&search=screening and prevention of gastric cancer&selectedTitle=1~150

49 **Song LM**, Banerjee S, Desilets D, Diehl DL, Farraye FA, Kaul V, Kethu SR, Kwon RS, Mamula P, Pedrosa MC, Rodriguez SA, Tierney WM. Autofluorescence imaging. *Gastrointest Endosc* 2011; **73**: 647-650 [PMID: 21296349 DOI: 10.1016/j.gie.2010.11.006]

50 **Tada K**, Oda I, Yokoi C, Taniguchi T, Sakamoto T, Suzuki H, Nonaka S, Yoshinaga S, Saito Y, Gotoda T. Pilot study on clinical effectiveness of autofluorescence imaging for early gastric cancer diagnosis by less experienced endoscopists. *Diagn Ther Endosc* 2011; **2011**: 419136 [PMID: 21804754 DOI: 10.1155/2011/419136]

51 **Yoon H**, Lee DH. New approaches to gastric cancer staging: beyond endoscopic ultrasound, computed tomography and positron emission tomography. *World J Gastroenterol* 2014; **20**: 13783-13790 [PMID: 25320516 DOI: 10.3748/wjg.v20.i38.13783]

52 **Kawai T**, Yanagizawa K, Naito S, Sugimoto H, Fukuzawa M, Gotoda T, Matsubayashi J, Nagao T, Hoshino S, Tsuchida A, Moriyasu F. Evaluation of gastric cancer diagnosis using new ultrathin transnasal endoscopy with narrow-band imaging: preliminary study. *J Gastroenterol Hepatol* 2014; **29** Suppl 4: 33-36 [PMID: 25521731 DOI: 10.1111/jgh.12797]

53 **Siegel RL**, Miller KD, Jemal A. Cancer statistics, 2015. *CA Cancer J Clin* 2015; **65**: 5-29 [PMID: 25559415 DOI: 10.3322/caac.21254]

54 **Rustgi AK**. The genetics of hereditary colon cancer. *Genes Dev* 2007; **21**: 2525-2538 [PMID: 17938238 DOI: 10.1101/gad.1593107]

55 **Terry P**, Giovannucci E, Michels KB, Bergkvist L, Hansen H, Holmberg L, Wolk A. Fruit, vegetables, dietary fiber, and risk of colorectal cancer. *J Natl Cancer Inst* 2001; **93**: 525-533 [PMID: 11287446 DOI: 10.1093/jnci/93.7.525]

56 **Chan AT**, Giovannucci EL. Primary prevention of colorectal cancer. *Gastroenterology* 2010; **138**: 2029-2043.e10 [PMID: 20420944 DOI: 10.1053/j.gastro.2010.01.057]

57 **Sivak MV**. Polypectomy: looking back. *Gastrointest Endosc* 2004; **60**: 977-982 [PMID: 15605015 DOI: 10.1016/S0016-5107(04)02380-6]

58 **Whitlock EP**, Lin JS, Liles E, Beil TL, Fu R. Screening for colorectal cancer: a targeted, updated systematic review for the U.S. Preventive Services Task Force. *Ann Intern Med* 2008; **149**: 638-658 [PMID: 18838718 DOI: 10.7326/0003-4819-149-9-200811040-00245]

59 **Levin B**, Lieberman DA, McFarland B, Smith RA, Brooks D, Andrews KS, Dash C, Giardiello FM, Glick S, Levin TR, Pickhardt P, Rex DK, Thorson A, Winawer SJ. Screening and surveillance for the early detection of colorectal cancer and adenomatous polyps, 2008: a joint guideline from the American Cancer Society, the US Multi-Society Task Force on Colorectal Cancer, and the American College of Radiology. *CA Cancer J Clin* 2008; **58**: 130-160 [PMID: 18322143 DOI: 10.3322/CA.2007.0018]

60 **U.S. Preventive Services Task Force**. Screening for colorectal cancer: U.S. Preventive Services Task Force recommendation statement. *Ann Intern Med* 2008; **149**: 627-637 [PMID: 18838716 DOI: 10.7326/0003-4819-149-9-200811040-00243]

61 **Vijan S**, Hwang EW, Hofer TP, Hayward RA. Which colon cancer screening test? A comparison of costs, effectiveness, and compliance. *Am J Med* 2001; **111**: 593-601 [PMID: 11755501 DOI: 10.1016/S0002-9343(01)00977-9]

62 **Rex DK**. Rationale for colonoscopy screening and estimated effectiveness in clinical practice. *Gastrointest Endosc Clin N Am* 2002; **12**: 65-75 [PMID: 11916162 DOI: 10.1016/S1052-5157(03)00058-8]

63 **van Rijn JC**, Reitsma JB, Stoker J, Bossuyt PM, van Deventer SJ, Dekker E. Polyp miss rate determined by tandem colonoscopy: a systematic review. *Am J Gastroenterol* 2006; **101**: 343-350 [PMID: 16454841 DOI: 10.1111/j.1572-0241.2006.00390.x]

64 **Moriyama T**, Uraoka T, Esaki M, Matsumoto T. Advanced technology for the improvement of adenoma and polyp detection during colonoscopy. *Dig Endosc* 2015; **27** Suppl 1: 40-44 [PMID: 25556542 DOI: 10.1111/den.12428]

65 **Subramanian V**, Mannath J, Hawkey CJ, Ragunath K. High definition colonoscopy vs. standard video endoscopy for the detection of colonic polyps: a meta-analysis. *Endoscopy* 2011; **43**: 499-505 [PMID: 21360420 DOI: 10.1055/s-0030-1256207]

66 **Gralnek IM**, Siersema PD, Halpern Z, Segol O, Melhem A, Suissa A, Santo E, Sloyer A, Fenster J, Moons LM, Dik VK, D'Agostino RB, Rex DK. Standard forward-viewing colonoscopy versus full-spectrum endoscopy: an international, multicentre, randomised, tandem colonoscopy trial. *Lancet Oncol* 2014; **15**: 353-360 [PMID: 24560453 DOI: 10.1016/S1470-2045(14)70020-8]

67 **DeMarco DC**, Odstrcil E, Lara LF, Bass D, Herdman C, Kinney T, Gupta K, Wolf L, Dewar T, Deas TM, Mehta MK, Anwer MB, Pellish R, Hamilton JK, Polter D, Reddy KG, Hanan I. Impact of experience with a retrograde-viewing device on adenoma detection rates and withdrawal times during colonoscopy: the Third Eye Retroscope study group. *Gastrointest Endosc* 2010; **71**: 542-550 [PMID: 20189513 DOI: 10.1016/j.gie.2009.12.021]

68 **Leufkens AM**, DeMarco DC, Rastogi A, Akerman PA, Azzouzi K, Rothstein RI, Vleggaar FP, Repici A, Rando G, Okolo PI, Dewit O, Ignjatovic A, Odstrcil E, East J, Deprez PH, Saunders BP, Kalloo AN, Creel B, Singh V, Lennon AM, Siersema PD. Effect of a retrograde-viewing device on adenoma detection rate during colonoscopy: the TERRACE study. *Gastrointest Endosc* 2011; **73**: 480-489 [PMID: 21067735 DOI: 10.1016/j.gie.2010.09.004]

69 **Gralnek IM**. Emerging technological advancements in colonoscopy: Third Eye® Retroscope® and Third Eye® Panoramic(TM) , Fuse ® Full Spectrum Endoscopy® colonoscopy platform, Extra-Wide-Angle-View colonoscope, and NaviAid(TM) G-EYE(TM) balloon colonoscope. *Dig Endosc* 2015; **27**: 223-231 [PMID: 25251748 DOI: 10.1111/den.12382]

70 **Spada C**, Barbaro F, Andrisani G, Minelli Grazioli L, Hassan C, Costamagna I, Campanale M, Costamagna G. Colon capsule endoscopy: What we know and what we would like to know. *World J Gastroenterol* 2014; **20**: 16948-16955 [PMID: 25493007 DOI: 10.3748/wjg.v20.i45.16948]

71 **Tal AO**, Vermehren J, Albert JG. Colon capsule endoscopy: current status and future directions. *World J Gastroenterol* 2014; **20**: 16596-16602 [PMID: 25469027 DOI: 10.3748/wjg.v20.i44.16596]

72 **Ko BM**. Colon cancer screening with image-enhanced endoscopy. *Clin Endosc* 2014; **47**: 504-508 [PMID: 25505715 DOI: 10.5946/ce.2014.47.6.504]

73 **Pasha SF**, Leighton JA, Das A, Harrison ME, Gurudu SR, Ramirez FC, Fleischer DE, Sharma VK. Comparison of the yield and miss rate of narrow band imaging and white light endoscopy in patients undergoing screening or surveillance colonoscopy: a meta-analysis. *Am J Gastroenterol* 2012; **107**: 363-70; quiz 371 [PMID: 22186978

DOI: 10.1038/ajg.2011.436]

74 **Parra-Blanco A**, Jiménez A, Rembacken B, González N, Nicolás-Pérez D, Gimeno-García AZ, Carrillo-Palau M, Matsuda T, Quintero E. Validation of Fujinon intelligent chromoendoscopy with high definition endoscopes in colonoscopy. *World J Gastroenterol* 2009; **15**: 5266-5273 [PMID: 19908333 DOI: 10.3748/wjg.15.5266]

75 **Chernolesskiy A**, Swain D, Lee JC, Corbett GD, Cameron EA. Comparison of Pentax HiLine and Olympus Lucera systems at screening colonoscopy. *World J Gastrointest Endosc* 2013; **5**: 62-66 [PMID: 23424182 DOI: 10.4253/wjge.v5.i2.62]

P- Reviewer: Pan WS **S- Editor**: Yu J **L- Editor**: A
E- Editor: Wang CH

World Journal of Gastroenterology

Submit a Manuscript: http://www.wjgnet.com/esps/
Help Desk: http://www.wjgnet.com/esps/helpdesk.aspx
DOI: 10.3748/wjg.v21.i33.9707

World J Gastroenterol 2015 September 7; 21(33): 9707-9716
ISSN 1007-9327 (print) ISSN 2219-2840 (online)

TOPIC HIGHLIGHT

2015 Advances in Gastric Cancer

Contactin 1: A potential therapeutic target and biomarker in gastric cancer

De-Hu Chen, Ji-Wei Yu, Bo-Jian Jiang

De-Hu Chen, Ji-Wei Yu, Bo-Jian Jiang, Department of General Surgery, Shanghai Ninth People's Hospital, Shanghai Jiao Tong University School of Medicine, Shanghai 201900, China

Author contributions: Chen DH and Jiang BJ initiated the study; Chen DH performed the literature search and wrote the paper; and Yu JW and Jiang BJ evaluated and edited the paper.

Supported by National Natural Science Foundation of China, No. 81101850; the Shanghai Municipal Health Bureau Foundation of China, No. 20134393; and the Science Research Foundation of Shanghai Jiao Tong University School of Medicine, No. 13XJ10028.

Conflict-of-interest statement: The authors declare no conflicts of interest.

Correspondence to: Bo-Jian Jiang, MD, PhD, Professor of Surgery, Department of General Surgery, Shanghai Ninth People's Hospital, Shanghai Jiao Tong University School of Medicine, Shanghai 201900, China. jiang-bj2102@hotmail.com
Telephone: +86-21-56691101

Received: March 18, 2015
Peer-review started: March 19, 2015
First decision: May 18, 2015
Revised: June 2, 2015
Accepted: July 15, 2015
Article in press: July 15, 2015
Published online: September 7, 2015

Abstract

Despite advances in diagnosis and treatment, gastric cancer remains one of the most common malignant tumors worldwide, and early diagnosis remains a challenge. The lack of effective methods to detect these tumors early is a major factor contributing to the high mortality in patients with gastric cancer, who are typically diagnosed at an advanced stage. Additionally, the early detection of metastases and the curative treatment of gastric cancer are difficult to achieve, and the detailed mechanisms remain to be fully elucidated. Thus, the identification of valuable predictive biomarkers and therapeutic targets to improve the prognosis of patients with gastric cancer is becoming increasingly important. Contactin 1 (CNTN1), a cell adhesion molecule, is a glycosylphosphatidylinositol-anchored neuronal membrane protein that plays an important role in cancer progression. The expression of CNTN1 is upregulated in primary lesions, and its expression level correlates with tumor metastasis in cancer patients. The current evidence reveals that the functions of CNTN1 in the development and progression of cancer likely promote the invasion and metastasis of cancer cells *via* the VEGFC/FLT4 axis, the RHOA-dependent pathway, the Notch signaling pathway and the epithelial-mesenchymal transition progression. Therefore, CNTN1 may be a novel biomarker and a possible therapeutic target in cancer treatment in the near future.

Key words: Cancer/neoplasms; Stomach; Contactin 1; Metastasis; Molecular target

Core tip: Gastric cancer remains a major public health

issue, and the investigation of therapeutic targets and biomarkers is of great importance. The accumulated evidence demonstrates that contactin 1 (CNTN1) plays a crucial role in cancer progression. In this manuscript, the role of CNTN1 in cancer is discussed and the mechanisms through which CNTN1 mediates the invasion and metastasis of cancer cells are summarized.

Chen DH, Yu JW, Jiang BJ. Contactin 1: A potential therapeutic target and biomarker in gastric cancer. *World J Gastroenterol* 2015; 21(33): 9707-9716 Available from: URL: http://www.wjgnet.com/1007-9327/full/v21/i33/9707.htm DOI: http://dx.doi.org/10.3748/wjg.v21.i33.9707

INTRODUCTION

Gastric cancer (GC) remains a global cancer burden, with a total of 9896000 new GC cases and 738000 deaths in 2008, accounting for 8% of the total cancer cases and 10% of the total cancer-related deaths[1], which makes GC the fifth most common malignancy and the third leading cause of death in the world[1,2]. More than 70% of GC cases occur in developing countries, and half of the total number of GC cases around the world occur in East Asia (mainly China)[3]. Although various factors, including early detection strategies[4,5] and improvements in living standards[6,7], have contributed to the observed decrease in the incidence of GC, it remains one of the most frequently occurring cancers, and the early diagnosis and effective treatment of GC remain challenging. Early in the disease course, patients with GC experience nonspecific symptoms, and most GC patients are diagnosed with advanced GC due to a lack of early-stage symptoms; late-stage diagnoses are generally too late for effective treatment, resulting in a five-year survival rate of only approximately 20%[8].

At present, the effects of conventional chemotherapy, radiotherapy and immunotherapy are generally not satisfactory, and surgery remains the main choice for the treatment of patients with GC if R_0, or at least R_1, resection can be achieved. Despite developments in oncology theory, surgical technique, operative skill and chemotherapy in recent decades, metastasis and post-surgery recurrence are critical obstacles to the curative treatment of GC in patients with metastatic cancer[9]. Thus, a comprehensive investigation of the mechanisms of initiation and progression of GC is crucial for the identification of novel, sensitive and specific biomarkers for early diagnosis and for the detection of potential therapeutic targets. In recent years, several novel targets and biomarkers for GC such as long noncoding RNAs[10], promoter methylated microRNAs[11], circulating microRNAs[12], and the EZH2[13], SPARC[14], EPHA2[15,16] and CNTN1 genes[17,18] that are involved in signaling pathways have been identified, and these may have potential prognostic value and application as novel therapeutic targets.

BIOLOGY-BIOCHEMISTRY OF CNTN1 IN NON-CANCER DISEASE

CNTNs are a subpopulation of molecules belonging to the immunoglobulin (Ig) superfamily, which contains six members: CNTN1, TAG-1/CNTN2, BIG-1/CNTN3, BIG-2/CNTN4, NB-2/CNTN5 and NB-3/CNTN6[19,20]. CNTN1, as the first identified member of the CNTN family of CAMs[21], was mapped to the chromosome 12q11-q12 region and exhibits a common structure of six C2 Ig-like repeats, four fibronectin type Ⅲ (FNIII) domains, and a glycosylphosphatidylinositol (GPI)-linkage at the carboxy-terminus that anchors the protein to the extracellular plasma membrane[22] (Figure 1).

Previous investigations involving limited organs and diseases have revealed that CNTN1 is highly expressed in the human brain and neuronal tissues and is of vital importance for nervous system development. The gene plays a critical role in neuronal and glial development and differentiation, in myelination and synaptogenesis, and in fasciculation[19,23-27]. Indeed, CNTN1 mediates neuron-glial interactions mainly through binding with elements [tenascin-C, tenascin-R, and receptor protein tyrosine phosphatase β (RPTPβ)/phosphagen] in the extracellular matrix, leading to axonal growth and fasciculation[21]. Interestingly, since the discovery of specific interactions between CNTN1 and PTPRZ[20,28], it is widely accepted that the transmembrane form of PTPRZ expressed on glial cells interacts in trans with CNTN1 expressed on the surface of axons, leading to neurite outgrowth and glial adhesion[29,30]. Unlike the general conception, the most recent study concluded that CNTN1 expressed on the surface of oligodendrocyte precursor cells (OPCs) interacts with a soluble form of PTPRZ to modulate the proliferation of OPCs[31]. Other major functions of CNTN1 include serving as a ligand to the Notch receptor, thereby influencing oligodendrocyte maturation[27], and interacting in cis with receptor protein tyrosine phosphatase α to transduce extracellular signals to tyrosine kinase FYN[32], thereby regulating cell mobility[33]. Furthermore, the CNTN1 expression level has been found to decrease as patients exhibit age-related declines in memory[34], to progressively increase during postnatal life[35] and to enhance neurogenesis, synaptic plasticity and memory[36], suggesting that it may be involved in memory processes, consistent with the results of studies investigating its participation in some forms of synaptic plasticity and in neurotransmitter release[37]. In addition to the roles described above, CNTN1 has been correlated with devastating brain disorders such as autism and schizophrenia[38].

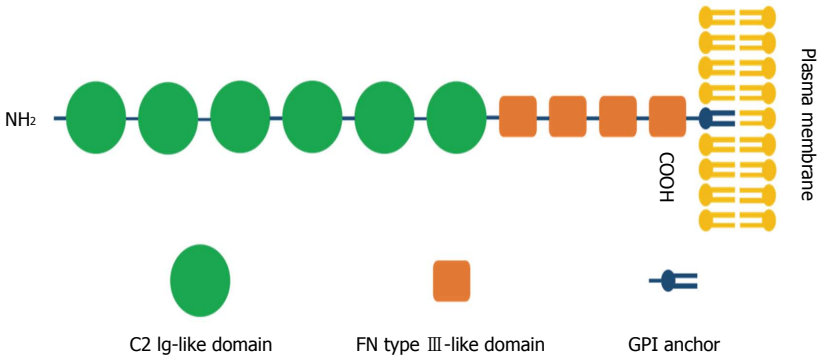

Figure 1 Schematic representation of the structure of contactin 1. Contactin 1 (CNTN1) is composed of an N-terminal signal peptide, six C2 immunoglobulin (Ig)-like repeats, four fibronectin type III-like domains and a glycosylphosphatidylinositol (GPI)-anchor at the carboxy-terminus linked to the plasma membrane.

RELEVANCE OF CNTN1 IN CANCER PROGRESSION

Despite the increasing number of studies focusing on the regulatory roles of CNTN1 in the nervous system, little attention has been paid to its function outside of the nervous system. Strikingly, several recent studies have demonstrated that CNTN1 also plays a key role in diseases not related to the nervous system, and its most notable function is its participation in cancer progression in cancers such as esophageal squamous cell carcinoma (ESCC)[39], GC[40], lung adenocarcinoma[17,41], oral squamous cell carcinoma (OSCC)[42], hepatocellular carcinoma[43] and prostate cancer[44], which is in agreement with accumulating evidence supporting the finding that certain members of the Ig superfamily promote the invasion and metastasis of cancer[45,46]. Moreover, the 12q11-q12 chromosomal region, the location of CNTN1, is a breakpoint region in certain types of cancer, further demonstrating that CNTN1 plays a potential role in tumor formation and/or advancement. Su *et al*[17,41] first described CNTN1 as a metastasis-promoting oncogenic gene.

In a study of the crucial regulatory genes responsible for the invasion and metastasis of cancer cells, Su *et al*[17] unexpectedly discovered, through genome-wide cDNA microarray analysis, that CNTN1, which is detected in primary lung cancer, plays an essential role in lung cancer metastasis. These researchers demonstrated that the expression level of CNTN1, which is differentially expressed in tumor tissues, is positively correlated with the tumor stage and lymph node metastasis and negatively correlated with the prognosis of patients with lung adenocarcinoma. Similarly, reduced CNTN1 expression has been found to result in impairments in the ability of lung adenocarcinoma cells to invade Matrigel *in vitro*, the polymerization of filamentous-actin and the formation of focal adhesion structures. Additionally, the knockdown of CNTN1 in lung cancer cells specifically inhibits their ability to metastasize, but not their proliferation *in vitro,* and abolishes their metastatic capacity to increase survival but not the formation of subcutaneously transplanted tumors in an animal model, suggesting that CNTN1 plays a crucial role in the invasion and metastasis of lung cancer cells[17]. In support of this finding, Su *et al*[41] also demonstrated that the upregulation of CNTN1, induced by the VEGFC/FLT4 axis through the activation of the SRC/p38 MAPK-mediated CEBPA-dependent signaling pathway, may enhance the invasive capacity of different types of cancer cells (*e.g.*, lung, cervical and breast cancers). Consistent with these reports, the tobacco carcinogen 4-(methylnitrosamino)-1-(3-pyridyl)-1-butanone (NNK) has been reported to enhance the invasiveness of lung cancer cells by elevating the expression level of CNTN1, which is regarded as a downstream effector of NNK *via* the α7 nicotinic acetylcholine receptor (α7 nAChR) downstream of the AKT and extracellular signal-regulated kinase (ERK) signaling pathway[47].

Since the discovery of the CNTN1-mediated invasion and metastasis of lung cancer cells, it has become increasingly evident that CNTN1 is also of critical importance in the induction of the invasion and metastasis of other cancer cells. Recent studies have revealed that the knockdown of FLT4 in human GC MKN45 cells using a short hairpin RNA lentiviral vector contributes to the downregulation of the downstream molecule CNTN1, indicating the possible involvement of CNTN1 in the invasion and metastasis of human GC cells[40]. Furthermore, CNTN1 is considered a recurrently mutated cell adhesion gene. Moreover, cell adhesion is the most highly enriched biological process among the mutated genes in the GC exomes[48]. More importantly, the mRNA and protein expression levels of CNTN1 are increased in primary lesions compared with adjacent normal gastric mucosal tissue[18,49]. The expression level of CNTN1 in primary lesions is significantly related to VEGFC or FLT4 expression; positively correlated with lymphatic invasion, lymph node metastasis and the TNM stage of patients with GC; and inversely associated with the prognosis of these patients. Moreover, patients with CNTN1-positive expression show a higher lymphatic vessel density (LVD)[18]. Taken together, the results show that CNTN1

may facilitate the invasion and metastasis of GC cells and may be a valuable indicator of poor prognosis in patients with GC.

In addition to these observations associated with GC, previous studies have demonstrated CNTN1 expression in upper gastrointestinal cancers and have noted its involvement in esophageal cancer[50] and ESCC[39] and OSCC[42]. As previously reported, the expression of CNTN1 is closely correlated with that of VEGFC because VEGFC can induce the recruitment of CEBPA to bind with the CNTN1 promoter[41]. Interestingly, the enhancement of the migration of esophageal cancer cells, which is attributable to a corresponding increase in VEGFC expression, is significantly reversed through a reduction in CNTN1 expression[50], suggesting that CNTN1 may play a key role in the VEGFC-induced migration of esophageal cancer cells. Moreover, the mRNA and protein expression levels of CNTN1 have been found to be elevated in ESCC tissues by real-time PCR and immunohistochemistry and to be significantly correlated with the ESCC stage, lymph node metastasis and lymphatic invasion, indicating the participation of CNTN1 in esophageal cancer progression[39]. Therefore, inhibitors against CNTN1 may be a promising therapy for ESCC. Similarly, CNTN1 is overexpressed in patients with OSCC. High expression of CNTN1 is markedly correlated with regional lymph node metastasis in patients with OSCC. CNTN1 expression is markedly associated with the survival time of patients with OSCC. The knockdown of CNTN1 expression decreases the invasion potential of OSCC cells, but CNTN1 ablation exerts no effect on the proliferation of OSCC cells, confirming that CNTN1 promotes the malignant progression of OSCC through an exclusive activation of the metastatic potential. Thus, CNTN1 may be a useful predictor of prognostic outcome in patients with OSCC[42].

Studies on the identification of new genes associated with melanoma have suggested that CNTN1, as an activator of Notch signaling, has been overlooked as a key factor in the progression of melanoma and should be investigated in greater depth[51]. The deregulation of CNTN1 mRNA expression has also been demonstrated in endometrial adenocarcinoma (EAC). The expression level of CNTN1 is higher in late-stage than early-stage EAC[52]. Additionally, CNTN1 has been reported to be involved in human astrocytic gliomas[53], glioblastoma[54], hepatocellular carcinoma[43] and prostate cancer[44].

Recent data have indicated that several genetic and epigenetic changes have an influence on patient prognosis and survival[55-57]. The field of "molecular pathological epidemiology (MPE)", addressing the basic heterogeneity of disease processes, has emerged as an interdisciplinary integration of "molecular pathology" and "epidemiology" that aims to understand the interplay among etiological factors, cellular molecular characteristics and disease evolution. The holistic MPE approach can be performed to assess the interactive effects of environmental influences and disease molecular signatures on disease progression and enables us to obtain novel pathogenic insights regarding causality[58]. In conclusion, the gene encoding CNTN1, a factor that potentially accelerates cancer progression, should be further investigated with the ultimate aim of developing an effective cancer treatment.

MECHANISM THROUGH WHICH CNTN1 PROMOTES CANCER METASTASIS

Despite mounting evidence supporting the influence of CNTN1 on cancer metastasis, insights into the underlying mechanisms responsible for this process remain to be discovered for the development of targeted therapy. At present, several studies have shown that a variety of signaling pathways are involved in CNTN1-mediated cell functions. CNTN1 is a GPI-anchored neuronal membrane protein that functions as a neural cell adhesion molecule (NCAM) and has been observed to interact with other cell-surface proteins that are thought to participate in a variety of signaling pathways and cell functions in the nervous system[20,25,31]. As previously reported, CNTN1 interacts in trans with RPTPβ to facilitate neurite outgrowth[29] and in cis with RPTPα to transduce extracellular signals to FYN kinase[32], a member of the SRC kinase family that modulates cell mobility[33,59]. In addition, the involvement of Notch signaling pathways in CNTN1-mediated cell function has been demonstrated. Nonetheless, the mechanism through which CNTN1 promotes the metastasis of cancer cells remains unclear.

Recently, the VEGFC/FLT4 axis, which stimulates the upregulation of CNTN1 expression, has emerged as a central feature of CNTN1-induced cancer cell metastasis[41]. Su *et al*[41] concluded that the expression of VEGFC/FLT4 correlates with the stage and lymph node metastasis of cancer and the survival of cancer patients and that the VEGFC/FLT4 axis promotes the migration and invasion of cancer cells. Investigations into the functional linkages between CNTN1 and VEGFC/FLT4-induced cell invasion revealed that CNTN1 is involved in cancer cell invasiveness and acts as a downstream effector of the VEGFC/FLT4 signaling pathway, in which SRC/p38 MAPK-mediated CEBPA signaling is required for VEGFC/FLT4-mediated CNTN1 expression. Furthermore, rearrangements of F-actin-containing microfilament bundles have been found in VEGFC/FLT4-mediated CNTN1 expression, indicating that the VEGFC/FLT4 axis regulates cancer cell invasion *via* CNTN1-dependent F-actin (a member of the actin cytoskeleton) rearrangement in cancer cells[41]. Indeed, F-actin is regularly polymerized and depolymerized in migratory cells and is required for cell motility[60]. Furthermore, RHO genes, including CDC42, RAC1, and RHOA, are best characterized by their effects on

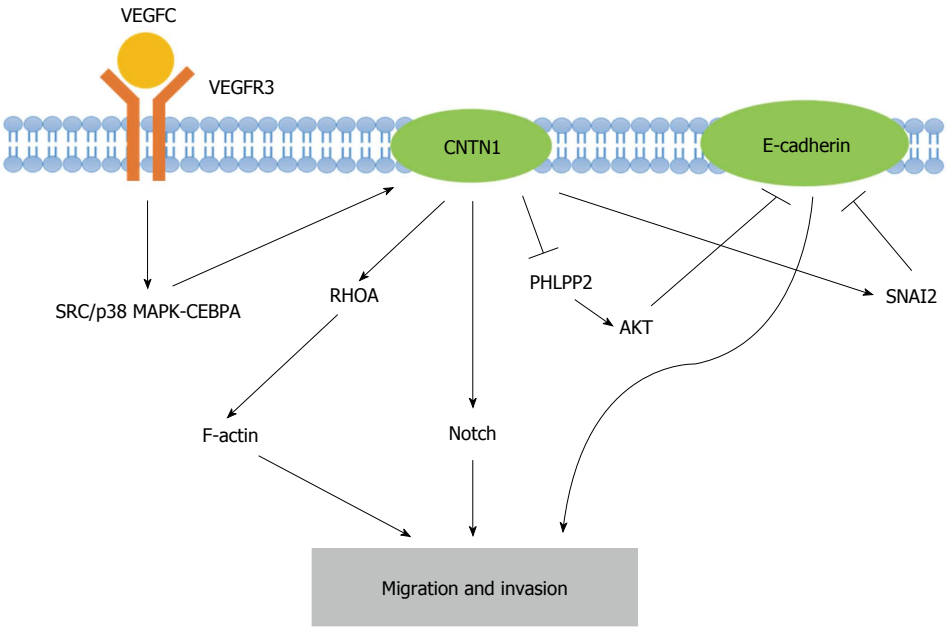

Figure 2 Graphic representation of the molecular mechanisms underlying the contactin 1-induced migration and invasion of cancer cells. Contactin 1 (CNTN1) serves as a downstream effector of the vascular endothelial growth factor C (VEGFC)/FLT4 axis, which activates SRC/p38 mitogen-activated protein kinase (MAPK)-CEBPA signaling. CNTN1 regulates F-actin rearrangement with the aid of RhoA and activates Notch signaling. Furthermore, CNTN1 inhibits E-cadherin through the activation of SNAI2 as well as the upregulation of AKT, which result from the CNTN1-induced inhibition of PHLPP2. These mechanisms of CNTN1 contribute to the migration and invasion of cancer cells. PHLPP2: PH domain and leucine rich repeat protein phosphatase 2.

the cytoskeleton and cell adhesion. Interestingly, the activity of the small GTP-binding protein RHOA has also been demonstrated to be involved in CNTN1-induced F-actin polymerization and cell invasion[17]. In addition to the VEGFC/FLT4 axis and the RHOA-dependent pathway, Notch signaling may play a partial role in CNTN1-mediated cancer cell invasion. In melanoma, the activation of Notch signaling appears to be of vital importance throughout tumor progression. For example, the activation of Notch1 in primary melanoma cells leads to a more metastatic phenotype[61]. Indeed, CNTN1, an activator of Notch, has been identified as a novel melanoma-associated biomarker[51]. Hence, the interaction between CNTN1 and Notch signaling may be a crucial factor in melanoma progression.

In addition to signaling, other factors play important roles in CNTN1-mediated cancer cell metastasis. It has been revealed that CNTN1 promotes cancer cell invasion through the inhibition of CDH1 (E-cadherin) expression[49]. The downregulation of E-cadherin is largely achieved through transcriptional regulatory mechanisms, including SNAIL, SNAI2, TWIST, ZEB1 and SIP1[62]. CNTN1 may indirectly inhibit E-cadherin through the upregulation of transcriptional factor SNAI2 rather than SNAIL. In addition, CNTN1 may decrease E-cadherin at the gene level as well as the transcriptional level. The mechanism through which the inhibition of the PH domain and leucine-rich repeat protein phosphatase 2 (PHLPP2), instead of phosphatase and tensin homolog (PTEN), results in AKT activation explains how CNTN1 reduces E-cadherin expression[63]. Furthermore, as previously demonstrated, the loss of E-cadherin is a major contributor to the invasion and metastasis of cancers[64]. The epithelial-mesenchymal transition (EMT) of cancer cells may provide a novel perspective for the theory of cancer stem cells (CSCs) and stem cell research in the relevant field of cancer progression. Thus, CNTN1 represses E-cadherin expression in cancer cells through the acquisition of a more invasive phenotype. Overall, CNTN1 induces the migration and invasion of cancer cells through a combination of the above-described mechanisms (Figure 2).

CHALLENGES AND ADVANCES IN THE PREVENTION OF CANCER METASTASIS AND RECURRENCE, PARTICULARLY IN GC

Recent advances in understanding the mechanism of cancer metastasis

The origin of cancer has long been debated. The concept of clonal evolution, which explains how a set of clone cells accumulate mutations over a period of time to result in damage to normal cells and ultimately cancer, remains widely accepted as explaining the origin of cancer[65]. The theory of CSCs, so-called "tumor-initiating cells", was first proposed in 1994[66], explaining how a small subpopulation of cells with self-renewal and pluripotency capabilities can explain why some cancer patients will likely relapse with metastatic and/or recurrent cancer even

though the primary neoplasm has been completely resected. Mounting lines of evidence have indicated that CSCs play a crucial role in cancer recurrence and metastasis and exhibit resistance to chemotherapy and radiotherapy[67]. The presence of human CSCs has been confirmed in solid tumors, including breast, colon, pancreas, prostate[68] and stomach cancers[69,70]. However, the maintenance of CSCs can largely depend on their microenvironment (the stem cell niche), which can protect CSCs from extrinsic stimuli. Overall, the CSC niche is composed of proteins, cellular elements (*e.g.*, macrophages, fibroblasts, and endothelial cells), and structural moieties (*e.g.*, E-cadherin) that interact with each other to protect CSCs. In addition, several signaling pathways [*e.g.*, WNT, Notch, TAB2 (TGF-β) and NF-κB] participate in the maintenance of the undifferentiated state of CSCs[65,71]. Therefore, in the current theory, the CSC niche is a prerequisite for carcinogenesis[71]; thus, the therapeutic targeting of this niche is of great interest.

Similarly, it has been widely acknowledged that CAMs play an important role in cancer progression as well as cancer cell invasion and metastasis[72]. Consistent with the identification of several signaling pathways that trigger EMT involved in CSC development[73], researchers have demonstrated that the EMT of cancer cells can result in the properties of migration, invasion and CSCs[74,75]. Loss of E-cadherin expression is regarded as the hallmark of the invasive phase of cancer. Moreover, the reversible switch of the EMT, which is termed the mesenchymal-to-epithelial transition (MET), is considered to participate in the establishment and stabilization of distant metastases in the target organ by allowing cancerous cells to regain an epithelial identity and thereby regain their proliferating ability[76].

Similarly, the EMT participates in the progression of GC and endows GC cells with the properties of migration and invasion, thus promoting cancer metastasis. This multi-step process includes the loss of cellular adhesion molecules, promoting cell adhesion to the extracellular matrix (ECM), the degradation of the ECM and the motility of tumor cells. Additionally, the CSC characteristics acquired by the EMT endow GC cells with the abilities to self-renew and to develop drug resistance and apoptotic resistance[62].

In recent years, circulating tumor cells (CTCs), which are defined as tumor cells originating from either the primary tumor or metastatic tissues, have been discovered in most epithelial tumors and increase the risk of regional recurrence as well as distant metastasis. Stem cell properties and the EMT are commonly observed in CTCs, and the phenotype of CTCs is regarded as a more attractive predictor of prognosis than solely the number of CTCs in the blood[77]. Indeed, only a small population of CTCs with some properties of stem cells, which are called circulating tumor stem cells (CTSCs), can migrate to other targeted organs/tissues for the development of secondary tumors[78]. Strikingly, in addition to their clinical importance as an independent predictive biomarker of poor prognosis in patients with GC[79], evaluating the number of CTCs in therapy may greatly improve the management of patients, and recent developments of novel technology have enabled the detection of CTCs in cancer patients[80]. Moreover, a recent study revealed that CTSCs provide a more important and specific value for the prognosis of in patients with GC[81]. Nevertheless, further investigations of the molecular mechanisms of CTCs and CTSCs are urgently required to discover potential therapeutic targets for the prevention of micrometastasis and affecting the migration and TNM classification in GC[82], thereby improving the prognosis of cancer patients.

Necessity of identifying predictive biomarkers and therapeutic targets to improve the prognosis of patients with GC

In recent decades, improvements in strategies for the detection, treatment and care of patients have contributed to a marked decrease in the mortality of GC worldwide. It is clear that upper gastrointestinal endoscopy is beneficial for improvements in the earlier diagnosis of GC. Magnifying endoscopy with narrow-band imaging (NBI), which is the result of technological innovations, has been reported to be more reliable for the early diagnosis of GC[83,84], and endoscopic submucosal dissection (ESD) is a preferred option compared with endoscopic mucosal resection (EMR)[85]. For advanced GC, surgery is usually regarded as the only curative treatment, whereas perioperatively adjuvant chemotherapy can to some extent improve the prognosis of resectable GC[86,87]. Advancements in surgical techniques, such as laparoscopic surgery and robot-assisted gastrectomy[88,89], are beneficial to the outcome of patients. Despite these findings, limited success has been achieved in the prevention of advanced GC, and most patients with GC are diagnosed at an advanced stage worldwide due mainly to the absence of adequate and appropriate screening that would identify gastric cancer in early stages, causing the optimal window for curative surgery to be missed. However, tumor biomarkers, such as the auxiliary analysis of disease-related indicators, have drawn increased attention over the years. Investigations of the mechanisms of invasion and metastasis of GC, which may provide key targets for new drug development, are of vital importance. Additionally, the identification of predictive and prognostic biomarkers can better provide targeted therapy for ideal patients.

Notable achievements have been made in molecularly targeted therapy. The use of the anti-ERBB2 (HER2) antibody trastuzumab and the anti-KDR (VEGFR2) antibody ramucirumab as supplementary chemotherapy for patients overexpressing HER2 or VEGFR2 receptor has led to significant gains in overall

survival compared with chemotherapy alone[86,90]. In recent years, the potential molecular target CNTN1 has been the focus of investigations on its role in cancer metastasis. To the best of our knowledge, elevated CNTN1 expression levels in primary lesions are correlated with lymph node metastasis and the prognosis of patients with GC[18]. Thus, CNTN1 may be considered a potentially promising prognostic indicator and therapeutic target.

POTENTIAL OF CNTN1 AS A THERAPEUTIC TARGET AND PROGNOSTIC BIOMARKER IN GC

With regard to VEGF-C expression, previous studies have revealed a significant difference between positive and negative lymph node metastasis in patients with GC. VEGFC/FLT4 plays an important role in the development of GC, and GC patients overexpressing VEGFC/FLT4 in the primary lesion are more likely to present with lymph node metastasis[91]. Recent investigations have demonstrated that CNTN1 not only correlates with VEGFC, FLT4, lymph node metastasis and prognosis in patients with GC[18] but also acts as a downstream effector of the VEGFC/FLT4 axis to mediate GC cell invasion[40]. In addition to these findings, CNTN1 seems to promote the migration and invasion of GC cells *via* EMT alteration probably induced by inhibition of SNAI2[49]. As a consequence, CNTN1 may be a novel prognostic biomarker and potential therapeutic target in patients with GC. Despite this finding, the mechanism through which CNTN1 modulates GC cell invasion and metastasis remains incompletely explained. Further investigations are therefore required to obtain an in-depth characterization of its role and the mechanisms underlying the invasion and metastasis of GC.

CONCLUSION

CNTN1, a GPI-anchored adhesion molecule, was recently found to be overexpressed in various cancer tissues, including lung cancer, melanoma, OSCC, esophageal cancer, and GC. CNTN1 has been shown to not only promote the invasion and metastasis of cancer cells but also correlate with tumor metastasis in cancer patients. The VEGFC/FLT4 axis, Notch signaling and loss of E-cadherin *via* the inhibition of SNAI2 or the activation of AKT may contribute to the CNTN1-facilitated invasion and metastasis of cancer cells. Similarly, the expression level of CNTN1 is correlated with lymph node metastasis and the prognosis of patients with GC and positively associated with the invasion of GC cells. An in-depth understanding of the functional aspects of CNTN1 and the full mechanisms underlying CNTN1-induced invasion that result in a potentially applicable treatment for patients with GC is urgently needed. In conclusion, CNTN1 may be useful as a potential therapeutic target and biomarker in cancer in the future.

REFERENCES

1 **Jemal A**, Bray F, Center MM, Ferlay J, Ward E, Forman D. Global cancer statistics. *CA Cancer J Clin* 2011; **61**: 69-90 [PMID: 21296855 DOI: 10.3322/caac.20107]

2 **Ferlay J**, Soerjomataram I, Dikshit R, Eser S, Mathers C, Rebelo M, Parkin DM, Forman D, Bray F. Cancer incidence and mortality worldwide: sources, methods and major patterns in GLOBOCAN 2012. *Int J Cancer* 2015; **136**: E359-E386 [PMID: 25220842 DOI: 10.1002/ijc.29210]

3 **Ferlay J**, Shin HR, Bray F, Forman D, Mathers C, Parkin DM. Estimates of worldwide burden of cancer in 2008: GLOBOCAN 2008. *Int J Cancer* 2010; **127**: 2893-2917 [PMID: 21351269 DOI: 10.1002/ijc.25516]

4 **Kaltenbach T**, Sano Y, Friedland S, Soetikno R. American Gastroenterological Association (AGA) Institute technology assessment on image-enhanced endoscopy. *Gastroenterology* 2008; **134**: 327-340 [PMID: 18061178 DOI: 10.1053/j.gastro.2007.10.062]

5 **Lee KJ**, Inoue M, Otani T, Iwasaki M, Sasazuki S, Tsugane S. Gastric cancer screening and subsequent risk of gastric cancer: a large-scale population-based cohort study, with a 13-year follow-up in Japan. *Int J Cancer* 2006; **118**: 2315-2321 [PMID: 16331632 DOI: 10.1002/ijc.21664]

6 **Tkachenko MA**, Zhannat NZ, Erman LV, Blashenkova EL, Isachenko SV, Isachenko OB, Graham DY, Malaty HM. Dramatic changes in the prevalence of Helicobacter pylori infection during childhood: a 10-year follow-up study in Russia. *J Pediatr Gastroenterol Nutr* 2007; **45**: 428-432 [PMID: 18030208 DOI: 10.1097/MPG.0b013e318064589f]

7 **Bertuccio P**, Chatenoud L, Levi F, Praud D, Ferlay J, Negri E, Malvezzi M, La Vecchia C. Recent patterns in gastric cancer: a global overview. *Int J Cancer* 2009; **125**: 666-673 [PMID: 19382179 DOI: 10.1002/ijc.24290]

8 **Jemal A**, Tiwari RC, Murray T, Ghafoor A, Samuels A, Ward E, Feuer EJ, Thun MJ; American Cancer Society. Cancer statistics, 2004. *CA Cancer J Clin* 2004; **54**: 8-29 [PMID: 14974761]

9 **Catalano V**, Labianca R, Beretta GD, Gatta G, de Braud F, Van Cutsem E. Gastric cancer. *Crit Rev Oncol Hematol* 2009; **71**: 127-164 [PMID: 19230702 DOI: 10.1016/j.critrevonc.2009.01.004]

10 **Fang XY**, Pan HF, Leng RX, Ye DQ. Long noncoding RNAs: novel insights into gastric cancer. *Cancer Lett* 2015; **356**: 357-366 [PMID: 25444905 DOI: 10.1016/j.canlet.2014.11.005]

11 **Guo X**, Xia J, Yan J. Promoter methylated microRNAs: potential therapeutic targets in gastric cancer. *Mol Med Rep* 2015; **11**: 759-765 [PMID: 25351138 DOI: 10.3892/mmr.2014.2780]

12 **Tsujiura M**, Ichikawa D, Komatsu S, Shiozaki A, Takeshita H, Kosuga T, Konishi H, Morimura R, Deguchi K, Fujiwara H, Okamoto K, Otsuji E. Circulating microRNAs in plasma of patients with gastric cancers. *Br J Cancer* 2010; **102**: 1174-1179 [PMID: 20234369 DOI: 10.1038/sj.bjc.6605608]

13 **Matsukawa Y**, Semba S, Kato H, Ito A, Yanagihara K, Yokozaki H. Expression of the enhancer of zeste homolog 2 is correlated with poor prognosis in human gastric cancer. *Cancer Sci* 2006; **97**: 484-491 [PMID: 16734726 DOI: 10.1111/j.1349-7006.2006.00203.x]

14 **Zhao ZS**, Wang YY, Chu YQ, Ye ZY, Tao HQ. SPARC is associated with gastric cancer progression and poor survival of patients. *Clin Cancer Res* 2010; **16**: 260-268 [PMID: 20028745 DOI: 10.1158/1078-0432.CCR-09-1247]

15 **Hou F**, Yuan W, Huang J, Qian L, Chen Z, Ge J, Wu S, Chen J, Wang J, Chen Z. Overexpression of EphA2 correlates with epithelial-mesenchymal transition-related proteins in gastric cancer and their prognostic importance for postoperative patients. *Med Oncol* 2012; **29**: 2691-2700 [PMID: 22189617 DOI: 10.1007/s12032-011-0127-2]

16 **Huang J**, Xiao D, Li G, Ma J, Chen P, Yuan W, Hou F, Ge J,

Zhong M, Tang Y, Xia X, Chen Z. EphA2 promotes epithelial-mesenchymal transition through the Wnt/β-catenin pathway in gastric cancer cells. *Oncogene* 2014; **33**: 2737-2747 [PMID: 23752181 DOI: 10.1038/onc.2013.238]

17 **Su JL**, Yang CY, Shih JY, Wei LH, Hsieh CY, Jeng YM, Wang MY, Yang PC, Kuo ML. Knockdown of contactin-1 expression suppresses invasion and metastasis of lung adenocarcinoma. *Cancer Res* 2006; **66**: 2553-2561 [PMID: 16510572 DOI: 10.1158/0008-5472.CAN-05-2645]

18 **Yu JW**, Wu SH, Lu RQ, Wu JG, Ni XC, Zhou GC, Jiang HG, Zheng LH, Li XQ, Du GY, Jiang BJ. Expression and significances of contactin-1 in human gastric cancer. *Gastroenterol Res Pract* 2013; **2013**: 210205 [PMID: 23606831 DOI: 10.1155/2013/210205]

19 **Bizzoca A**, Corsi P, Gennarini G. The mouse F3/contactin glycoprotein: structural features, functional properties and developmental significance of its regulated expression. *Cell Adh Migr* 2009; **3**: 53-63 [PMID: 19372728 DOI: 10.4161/cam.3.1.7462]

20 **Bouyain S**, Watkins DJ. The protein tyrosine phosphatases PTPRZ and PTPRG bind to distinct members of the contactin family of neural recognition molecules. *Proc Natl Acad Sci USA* 2010; **107**: 2443-2448 [PMID: 20133774 DOI: 10.1073/pnas.0911235107]

21 **Shimoda Y**, Watanabe K. Contactins: emerging key roles in the development and function of the nervous system. *Cell Adh Migr* 2009; **3**: 64-70 [PMID: 19262165 DOI: 10.4161/cam.3.1.7764]

22 **Berglund EO**, Ranscht B. Molecular cloning and in situ localization of the human contactin gene (CNTN1) on chromosome 12q11-q12. *Genomics* 1994; **21**: 571-582 [PMID: 7959734 DOI: 10.1006/geno.1994.1316]

23 **Bizzoca A**, Corsi P, Polizzi A, Pinto MF, Xenaki D, Furley AJ, Gennarini G. F3/Contactin acts as a modulator of neurogenesis during cerebral cortex development. *Dev Biol* 2012; **365**: 133-151 [PMID: 22360968 DOI: 10.1016/j.ydbio.2012.02.011]

24 **Bizzoca A**, Virgintino D, Lorusso L, Buttiglione M, Yoshida L, Polizzi A, Tattoli M, Cagiano R, Rossi F, Kozlov S, Furley A, Gennarini G. Transgenic mice expressing F3/contactin from the TAG-1 promoter exhibit developmentally regulated changes in the differentiation of cerebellar neurons. *Development* 2003; **130**: 29-43 [PMID: 12441289 DOI: 10.1242/dev.00183]

25 **Çolakoğlu G**, Bergstrom-Tyrberg U, Berglund EO, Ranscht B. Contactin-1 regulates myelination and nodal/paranodal domain organization in the central nervous system. *Proc Natl Acad Sci USA* 2014; **111**: E394-E403 [PMID: 24385581 DOI: 10.1073/pnas.1313769110]

26 **Dityatev A**, Bukalo O, Schachner M. Modulation of synaptic transmission and plasticity by cell adhesion and repulsion molecules. *Neuron Glia Biol* 2008; **4**: 197-209 [PMID: 19674506 DOI: 10.1017/S1740925X09990111]

27 **Hu QD**, Ang BT, Karsak M, Hu WP, Cui XY, Duka T, Takeda Y, Chia W, Sankar N, Ng YK, Ling EA, Maciag T, Small D, Trifonova R, Kopan R, Okano H, Nakafuku M, Chiba S, Hirai H, Aster JC, Schachner M, Pallen CJ, Watanabe K, Xiao ZC. F3/contactin acts as a functional ligand for Notch during oligodendrocyte maturation. *Cell* 2003; **115**: 163-175 [PMID: 14567914 DOI: 10.1016/S0092-8674(03)00810-9]

28 **Peles E**, Nativ M, Campbell PL, Sakurai T, Martinez R, Lev S, Clary DO, Schilling J, Barnea G, Plowman GD, Grumet M, Schlessinger J. The carbonic anhydrase domain of receptor tyrosine phosphatase beta is a functional ligand for the axonal cell recognition molecule contactin. *Cell* 1995; **82**: 251-260 [PMID: 7628014 DOI: 10.1016/0092-8674(95)90312-7]

29 **Sakurai T**, Lustig M, Nativ M, Hemperly JJ, Schlessinger J, Peles E, Grumet M. Induction of neurite outgrowth through contactin and Nr-CAM by extracellular regions of glial receptor tyrosine phosphatase beta. *J Cell Biol* 1997; **136**: 907-918 [PMID: 9049255 DOI: 10.1083/jcb.136.4.907]

30 **Parent AS**, Mungenast AE, Lomniczi A, Sandau US, Peles E, Bosch MA, Rønnekleiv OK, Ojeda SR. A contactin-receptor-like protein tyrosine phosphatase beta complex mediates adhesive communication between astroglial cells and gonadotrophin-releasing hormone neurones. *J Neuroendocrinol* 2007; **19**: 847-859 [PMID: 17927663 DOI: 10.1111/j.1365-2826.2007.01597.x]

31 **Lamprianou S**, Chatzopoulou E, Thomas JL, Bouyain S, Harroch S. A complex between contactin-1 and the protein tyrosine phosphatase PTPRZ controls the development of oligodendrocyte precursor cells. *Proc Natl Acad Sci USA* 2011; **108**: 17498-17503 [PMID: 21969550 DOI: 10.1073/pnas.1108774108]

32 **Zeng L**, D'Alessandri L, Kalousek MB, Vaughan L, Pallen CJ. Protein tyrosine phosphatase alpha (PTPalpha) and contactin form a novel neuronal receptor complex linked to the intracellular tyrosine kinase fyn. *J Cell Biol* 1999; **147**: 707-714 [PMID: 10562275 DOI: 10.1083/jcb.147.4.707]

33 **Umemori H**, Sato S, Yagi T, Aizawa S, Yamamoto T. Initial events of myelination involve Fyn tyrosine kinase signalling. *Nature* 1994; **367**: 572-576 [PMID: 7509042 DOI: 10.1038/367572a0]

34 **Shimazaki K**, Hosoya H, Takeda Y, Kobayashi S, Watanabe K. Age-related decline of F3/contactin in rat hippocampus. *Neurosci Lett* 1998; **245**: 117-120 [PMID: 9605499 DOI: 10.1016/S0304-3940(98)00179-7]

35 **Hosoya H**, Shimazaki K, Kobayashi S, Takahashi H, Shirasawa T, Takenawa T, Watanabe K. Developmental expression of the neural adhesion molecule F3 in the rat brain. *Neurosci Lett* 1995; **186**: 83-86 [PMID: 7777204]

36 **Puzzo D**, Bizzoca A, Privitera L, Furnari D, Giunta S, Girolamo F, Pinto M, Gennarini G, Palmeri A. F3/Contactin promotes hippocampal neurogenesis, synaptic plasticity, and memory in adult mice. *Hippocampus* 2013; **23**: 1367-1382 [PMID: 23939883 DOI: 10.1002/hipo.22186]

37 **Milanese C**, Fiumara F, Bizzoca A, Giachello C, Leitinger G, Gennarini G, Montarolo PG, Ghirardi M. F3/contactin-related proteins in Helix pomatia nervous tissue (HCRPs): distribution and function in neurite growth and neurotransmitter release. *J Neurosci Res* 2008; **86**: 821-831 [PMID: 17941055 DOI: 10.1002/jnr.21539]

38 **Burbach JP**, van der Zwaag B. Contact in the genetics of autism and schizophrenia. *Trends Neurosci* 2009; **32**: 69-72 [PMID: 19135727 DOI: 10.1016/j.tins.2008.11.002]

39 **Liu P**, Chen S, Wu W, Liu B, Shen W, Wang F, He X, Zhang S. Contactin-1 (CNTN-1) overexpression is correlated with advanced clinical stage and lymph node metastasis in oesophageal squamous cell carcinomas. *Jpn J Clin Oncol* 2012; **42**: 612-618 [PMID: 22581910 DOI: 10.1093/jjco/hys066]

40 **Qin XJ**, Dai DJ, Gao ZG, Huan JL, Zhu L. Effect of lentivirus-mediated shRNA targeting VEGFR-3 on proliferation, apoptosis and invasion of gastric cancer cells. *Int J Mol Med* 2011; **28**: 761-768 [PMID: 21805024 DOI: 10.3892/ijmm.2011.758]

41 **Su JL**, Yang PC, Shih JY, Yang CY, Wei LH, Hsieh CY, Chou CH, Jeng YM, Wang MY, Chang KJ, Hung MC, Kuo ML. The VEGF-C/Flt-4 axis promotes invasion and metastasis of cancer cells. *Cancer Cell* 2006; **9**: 209-223 [PMID: 16530705 DOI: 10.1016/j.ccr.2006.02.018]

42 **Wu HM**, Cao W, Ye D, Ren GX, Wu YN, Guo W. Contactin 1 (CNTN1) expression associates with regional lymph node metastasis and is a novel predictor of prognosis in patients with oral squamous cell carcinoma. *Mol Med Rep* 2012; **6**: 265-270 [PMID: 22580838 DOI: 10.3892/mmr.2012.910]

43 **Tsai KH**, Hsien HH, Chen LM, Ting WJ, Yang YS, Kuo CH, Tsai CH, Tsai FJ, Tsai HJ, Huang CY. Rhubarb inhibits hepatocellular carcinoma cell metastasis via GSK-3-β activation to enhance protein degradation and attenuate nuclear translocation of β-catenin. *Food Chem* 2013; **138**: 278-285 [PMID: 23265488 DOI: 10.1016/j.foodchem.2012.10.038]

44 **Vinarskaja A**, Yamanaka M, Ingenwerth M, Schulz WA. DNA Methylation and the HOXC6 Paradox in Prostate Cancer. *Cancers* (Basel) 2011; **3**: 3714-3725 [PMID: 24213107 DOI: 10.3390/cancers3043714]

45 **Prag S**, Lepekhin EA, Kolkova K, Hartmann-Petersen R, Kawa A, Walmod PS, Belman V, Gallagher HC, Berezin V, Bock E, Pedersen N. NCAM regulates cell motility. *J Cell Sci* 2002; **115**: 283-292 [PMID: 11839780]

46 **Lehembre F**, Yilmaz M, Wicki A, Schomber T, Strittmatter K, Ziegler D, Kren A, Went P, Derksen PW, Berns A, Jonkers

J, Christofori G. NCAM-induced focal adhesion assembly: a functional switch upon loss of E-cadherin. *EMBO J* 2008; **27**: 2603-2615 [PMID: 18772882 DOI: 10.1038/emboj.2008.178]
47 **Hung YH**, Hung WC. 4-(Methylnitrosamino)-1-(3-pyridyl)-1-butanone (NNK) enhances invasiveness of lung cancer cells by up-regulating contactin-1 via the alpha7 nicotinic acetylcholine receptor/ERK signaling pathway. *Chem Biol Interact* 2009; **179**: 154-159 [PMID: 19027725 DOI: 10.1016/j.cbi.2008.10.042]
48 **Zang ZJ**, Cutcutache I, Poon SL, Zhang SL, McPherson JR, Tao J, Rajasegaran V, Heng HL, Deng N, Gan A, Lim KH, Ong CK, Huang D, Chin SY, Tan IB, Ng CC, Yu W, Wu Y, Lee M, Wu J, Poh D, Wan WK, Rha SY, So J, Salto-Tellez M, Yeoh KG, Wong WK, Zhu YJ, Futreal PA, Pang B, Ruan Y, Hillmer AM, Bertrand D, Nagarajan N, Rozen S, Teh BT, Tan P. Exome sequencing of gastric adenocarcinoma identifies recurrent somatic mutations in cell adhesion and chromatin remodeling genes. *Nat Genet* 2012; **44**: 570-574 [PMID: 22484628 DOI: 10.1038/ng.2246]
49 **Chen H**, Yu JW, Wu JG, Wang SL, Jiang BJ. Significances of contactin-1 expression in human gastric cancer and knockdown of contactin-1 expression inhibits invasion and metastasis of MKN45 gastric cancer cells. *J Cancer Res Clin Oncol* 2015; Epub ahead of print [PMID: 25952582]
50 **Liu P**, Zhou J, Zhu H, Xie L, Wang F, Liu B, Shen W, Ye W, Xiang B, Zhu X, Shi R, Zhang S. VEGF-C promotes the development of esophageal cancer via regulating CNTN-1 expression. *Cytokine* 2011; **55**: 8-17 [PMID: 21482472 DOI: 10.1016/j.cyto.2011.03.008]
51 **Mauerer A**, Roesch A, Hafner C, Stempfl T, Wild P, Meyer S, Landthaler M, Vogt T. Identification of new genes associated with melanoma. *Exp Dermatol* 2011; **20**: 502-507 [PMID: 21410771 DOI: 10.1111/j.1600-0625.2011.01254.x]
52 **Mhawech-Fauceglia P**, Wang D, Kesterson J, Clark K, Monhollen L, Odunsi K, Lele S, Liu S. Microarray analysis reveals distinct gene expression profiles among different tumor histology, stage and disease outcomes in endometrial adenocarcinoma. *PLoS One* 2010; **5**: e15415 [PMID: 21079744 DOI: 10.1371/journal.pone.0015415.s001]
53 **Eckerich C**, Zapf S, Ulbricht U, Müller S, Fillbrandt R, Westphal M, Lamszus K. Contactin is expressed in human astrocytic gliomas and mediates repulsive effects. *Glia* 2006; **53**: 1-12 [PMID: 16078236 DOI: 10.1002/glia.20254]
54 **Nord H**, Hartmann C, Andersson R, Menzel U, Pfeifer S, Piotrowski A, Bogdan A, Kloc W, Sandgren J, Olofsson T, Hesselager G, Blomquist E, Komorowski J, von Deimling A, Bruder CE, Dumanski JP, Díaz de Ståhl T. Characterization of novel and complex genomic aberrations in glioblastoma using a 32K BAC array. *Neuro Oncol* 2009; **11**: 803-818 [PMID: 19304958 DOI: 10.1215/15228517-2009-013]
55 **Colussi D**, Brandi G, Bazzoli F, Ricciardiello L. Molecular pathways involved in colorectal cancer: implications for disease behavior and prevention. *Int J Mol Sci* 2013; **14**: 16365-16385 [PMID: 23965959 DOI: 10.3390/ijms140816365]
56 **Bardhan K**, Liu K. Epigenetics and colorectal cancer pathogenesis. *Cancers* (Basel) 2013; **5**: 676-713 [PMID: 24216997 DOI: 10.3390/cancers5020676]
57 **Zoratto F**, Rossi L, Verrico M, Papa A, Basso E, Zullo A, Tomao L, Romiti A, Lo Russo G, Tomao S. Focus on genetic and epigenetic events of colorectal cancer pathogenesis: implications for molecular diagnosis. *Tumour Biol* 2014; **35**: 6195-6206 [PMID: 25051912 DOI: 10.1007/s13277-014-1845-9]
58 **Ogino S**, Lochhead P, Chan AT, Nishihara R, Cho E, Wolpin BM, Meyerhardt JA, Meissner A, Schernhammer ES, Fuchs CS, Giovannucci E. Molecular pathological epidemiology of epigenetics: emerging integrative science to analyze environment, host, and disease. *Mod Pathol* 2013; **26**: 465-484 [PMID: 23307060 DOI: 10.1038/modpathol.2012.214]
59 **Huang J**, Asawa T, Takato T, Sakai R. Cooperative roles of Fyn and cortactin in cell migration of metastatic murine melanoma. *J Biol Chem* 2003; **278**: 48367-48376 [PMID: 13129922 DOI: 10.1074/jbc.M308213200]
60 **Cooper JA**. The role of actin polymerization in cell motility. *Annu Rev Physiol* 1991; **53**: 585-605 [PMID: 2042972 DOI: 10.1146/annurev.ph.53.030191.003101]
61 **Pinnix CC**, Lee JT, Liu ZJ, McDaid R, Balint K, Beverly LJ, Brafford PA, Xiao M, Himes B, Zabierowski SE, Yashiro-Ohtani Y, Nathanson KL, Bengston A, Pollock PM, Weeraratna AT, Nickoloff BJ, Pear WS, Capobianco AJ, Herlyn M. Active Notch1 confers a transformed phenotype to primary human melanocytes. *Cancer Res* 2009; **69**: 5312-5320 [PMID: 19549918 DOI: 10.1158/0008-5472.CAN-08-3767]
62 **Peng Z**, Wang CX, Fang EH, Wang GB, Tong Q. Role of epithelial-mesenchymal transition in gastric cancer initiation and progression. *World J Gastroenterol* 2014; **20**: 5403-5410 [PMID: 24833870 DOI: 10.3748/wjg.v20.i18.5403]
63 **Yan J**, Wong N, Hung C, Chen WX, Tang D. Contactin-1 reduces E-cadherin expression via activating AKT in lung cancer. *PLoS One* 2013; **8**: e65463 [PMID: 23724143 DOI: 10.1371/journal.pone.0065463]
64 **Onder TT**, Gupta PB, Mani SA, Yang J, Lander ES, Weinberg RA. Loss of E-cadherin promotes metastasis via multiple downstream transcriptional pathways. *Cancer Res* 2008; **68**: 3645-3654 [PMID: 18483246 DOI: 10.1158/0008-5472.CAN-07-2938]
65 **Boral D**, Nie D. Cancer stem cells and niche mircoenvironments. *Front Biosci* (Elite Ed) 2012; **4**: 2502-2514 [PMID: 22652656]
66 **Lapidot T**, Sirard C, Vormoor J, Murdoch B, Hoang T, Caceres-Cortes J, Minden M, Paterson B, Caligiuri MA, Dick JE. A cell initiating human acute myeloid leukaemia after transplantation into SCID mice. *Nature* 1994; **367**: 645-648 [PMID: 7509044 DOI: 10.1038/367645a0]
67 **Yu Z**, Pestell TG, Lisanti MP, Pestell RG. Cancer stem cells. *Int J Biochem Cell Biol* 2012; **44**: 2144-2151 [PMID: 22981632 DOI: 10.1016/j.biocel.2012.08.022]
68 **Ailles LE**, Weissman IL. Cancer stem cells in solid tumors. *Curr Opin Biotechnol* 2007; **18**: 460-466 [PMID: 18023337 DOI: 10.1016/j.copbio.2007.10.007]
69 **Takaishi S**, Okumura T, Tu S, Wang SS, Shibata W, Vigneshwaran R, Gordon SA, Shimada Y, Wang TC. Identification of gastric cancer stem cells using the cell surface marker CD44. *Stem Cells* 2009; **27**: 1006-1020 [PMID: 19415765 DOI: 10.1002/stem.30]
70 **Zhang C**, Li C, He F, Cai Y, Yang H. Identification of CD44+CD24+ gastric cancer stem cells. *J Cancer Res Clin Oncol* 2011; **137**: 1679-1686 [PMID: 21882047 DOI: 10.1007/s00432-011-1038-5]
71 **Barcellos-Hoff MH**, Lyden D, Wang TC. The evolution of the cancer niche during multistage carcinogenesis. *Nat Rev Cancer* 2013; **13**: 511-518 [PMID: 23760023 DOI: 10.1038/nrc3536]
72 **Bendas G**, Borsig L. Cancer cell adhesion and metastasis: selectins, integrins, and the inhibitory potential of heparins. *Int J Cell Biol* 2012; **2012**: 676731 [PMID: 22505933 DOI: 10.1155/2012/676731]
73 **Gradilone A**, Raimondi C, Nicolazzo C, Petracca A, Gandini O, Vincenzi B, Naso G, Aglianò AM, Cortesi E, Gazzaniga P. Circulating tumour cells lacking cytokeratin in breast cancer: the importance of being mesenchymal. *J Cell Mol Med* 2011; **15**: 1066-1070 [PMID: 21352474 DOI: 10.1111/j.1582-4934.2011.01285.x]
74 **Floor S**, van Staveren WC, Larsimont D, Dumont JE, Maenhaut C. Cancer cells in epithelial-to-mesenchymal transition and tumor-propagating-cancer stem cells: distinct, overlapping or same populations. *Oncogene* 2011; **30**: 4609-4621 [PMID: 21643013 DOI: 10.1038/onc.2011.184]
75 **Scheel C**, Weinberg RA. Phenotypic plasticity and epithelial-mesenchymal transitions in cancer and normal stem cells? *Int J Cancer* 2011; **129**: 2310-2314 [PMID: 21792896 DOI: 10.1002/ijc.26311]
76 **Yang J**, Weinberg RA. Epithelial-mesenchymal transition: at the crossroads of development and tumor metastasis. *Dev Cell* 2008; **14**: 818-829 [PMID: 18539112 DOI: 10.1016/j.devcel.2008.05.009]
77 **Tinhofer I**, Saki M, Niehr F, Keilholz U, Budach V. Cancer stem cell characteristics of circulating tumor cells. *Int J Radiat Biol* 2014; **90**: 622-627 [PMID: 24460132 DOI: 10.3109/09553002.2014.886798]
78 **Książkiewicz M**, Markiewicz A, Zaczek AJ. Epithelial-mesenchymal transition: a hallmark in metastasis formation linking circulating tumor cells and cancer stem cells. *Pathobiology* 2012;

79: 195-208 [PMID: 22488297 DOI: 10.1159/000337106]
79 **Illert B**, Fein M, Otto C, Cording F, Stehle D, Thiede A, Timmermann W. Disseminated tumor cells in the blood of patients with gastric cancer are an independent predictive marker of poor prognosis. *Scand J Gastroenterol* 2005; **40**: 843-849 [PMID: 16109661 DOI: 10.1080/00365520510015557]
80 **Zhang Y**, Li J, Cao L, Xu W, Yin Z. Circulating tumor cells in hepatocellular carcinoma: detection techniques, clinical implications, and future perspectives. *Semin Oncol* 2012; **39**: 449-460 [PMID: 22846862 DOI: 10.1053/j.seminoncol.2012.05.012]
81 **Li M**, Zhang B, Zhang Z, Liu X, Qi X, Zhao J, Jiang Y, Zhai H, Ji Y, Luo D. Stem cell-like circulating tumor cells indicate poor prognosis in gastric cancer. *Biomed Res Int* 2014; **2014**: 981261 [PMID: 24963492 DOI: 10.1155/2014/981261]
82 **Yu JW**, Wu JG, Tajima Y, Li XQ, Du GY, Zheng LH, Zhang B, Ni XC, Jiang BJ. Study on lymph node metastasis correlated to lymphangiogenesis, lymphatic vessel invasion, and lymph node micrometastasis in gastric cancer. *J Surg Res* 2011; **168**: 188-196 [PMID: 20189585 DOI: 10.1016/j.jss.2009.10.030]
83 **Ezoe Y**, Muto M, Uedo N, Doyama H, Yao K, Oda I, Kaneko K, Kawahara Y, Yokoi C, Sugiura Y, Ishikawa H, Takeuchi Y, Kaneko Y, Saito Y. Magnifying narrowband imaging is more accurate than conventional white-light imaging in diagnosis of gastric mucosal cancer. *Gastroenterology* 2011; **141**: 2017-2025.e3 [PMID: 21856268 DOI: 10.1053/j.gastro.2011.08.007]
84 **Nagahama T**, Yao K, Maki S, Yasaka M, Takaki Y, Matsui T, Tanabe H, Iwashita A, Ota A. Usefulness of magnifying endoscopy with narrow-band imaging for determining the horizontal extent of early gastric cancer when there is an unclear margin by chromoendoscopy (with video). *Gastrointest Endosc* 2011; **74**: 1259-1267 [PMID: 22136775 DOI: 10.1016/j.gie.2011.09.005]
85 **Oka S**, Tanaka S, Kaneko I, Mouri R, Hirata M, Kawamura T, Yoshihara M, Chayama K. Advantage of endoscopic submucosal dissection compared with EMR for early gastric cancer. *Gastrointest Endosc* 2006; **64**: 877-883 [PMID: 17140890 DOI: 10.1016/j.gie.2006.03.932]
86 **Orditura M**, Galizia G, Sforza V, Gambardella V, Fabozzi A, Laterza MM, Andreozzi F, Ventriglia J, Savastano B, Mabilia A, Lieto E, Ciardiello F, De Vita F. Treatment of gastric cancer. *World J Gastroenterol* 2014; **20**: 1635-1649 [PMID: 24587643 DOI: 10.3748/wjg.v20.i7.1635]
87 **Pasini F**, Fraccon AP, DE Manzoni G. The role of chemotherapy in metastatic gastric cancer. *Anticancer Res* 2011; **31**: 3543-3554 [PMID: 21965776]
88 **Coratti A**, Annecchiarico M, Di Marino M, Gentile E, Coratti F, Giulianotti PC. Robot-assisted gastrectomy for gastric cancer: current status and technical considerations. *World J Surg* 2013; **37**: 2771-2781 [PMID: 23674257 DOI: 10.1007/s00268-013-2100-z]
89 **Uyama I**, Suda K, Satoh S. Laparoscopic surgery for advanced gastric cancer: current status and future perspectives. *J Gastric Cancer* 2013; **13**: 19-25 [PMID: 23610715 DOI: 10.5230/jgc.2013.13.1.19]
90 **Smyth EC**, Cunningham D. Targeted therapy for gastric cancer. *Curr Treat Options Oncol* 2012; **13**: 377-389 [PMID: 22552927 DOI: 10.1007/s11864-012-0192-6]
91 **Liu XE**, Sun XD, Wu JM. Expression and significance of VEGF-C and FLT-4 in gastric cancer. *World J Gastroenterol* 2004; **10**: 352-355 [PMID: 14760756]

P- Reviewer: Georgoulias V, Goral V, Ogino S **S- Editor**: Yu J
L- Editor: Wang TQ **E- Editor**: Ma S

World Journal of Gastroenterology

Submit a Manuscript: http://www.wjgnet.com/esps/
Help Desk: http://www.wjgnet.com/esps/helpdesk.aspx
DOI: 10.3748/wjg.v21.i33.9717

World J Gastroenterol 2015 September 7; 21(33): 9717-9726
ISSN 1007-9327 (print) ISSN 2219-2840 (online)

TOPIC HIGHLIGHT

2015 Advances in Gastric Cancer

Role of cancer-associated fibroblasts in invasion and metastasis of gastric cancer

Yu Yan, Li-Feng Wang, Rui-Fen Wang

Yu Yan, Li-Feng Wang, Rui-Fen Wang, Department of Pathology, Xin Hua Hospital Affiliated to Shanghai Jiao Tong University School of Medicine, Shanghai 200092, China

Author contributions: Wang LF designed this review; Yan Y and Wang RF wrote the manuscript; Yan Y and Wang RF edited the manuscript.

Conflict-of-interest statement: We declare that there are no conflicts of interest related to this work.

Correspondence to: Li-Feng Wang, MD, PhD, Professor, Department of Pathology, Xin Hua Hospital Affiliated to Shanghai Jiao Tong University School of Medicine, 1665 Kongjiang Road, Shanghai 200092, China. wlf6009@163.com
Telephone: +86-21-25077215
Fax: +86-21-25077215

Received: April 24, 2015
Peer-review started: April 26, 2015
First decision: May 18, 2015
Revised: June 5, 2015
Accepted: July 18, 2015
Article in press: July 18, 2015
Published online: September 7, 2015

Abstract

Cancer-associated fibroblasts (CAFs) are important components of various types of tumors, including gastric cancer (GC). During tumorigenesis and progression, CAFs play critical roles in tumor invasion and metastasis *via* a series of functions including extracellular matrix deposition, angiogenesis, metabolism reprogramming and chemoresistance. However, the mechanism of the interaction between gastric cancer cells and CAFs remains largely unknown. MicroRNAs (miRNAs) are a class of non-coding small RNA molecules, and their expression in CAFs not only regulates the expression of a number of target genes but also plays an essential role in the communication between tumor cells and CAFs. In this review, we provide an overview of recent studies on CAF miRNAs in GC and the relevant signaling pathways in gastrointestinal tumors. Focusing the attention on these signaling pathways may help us better understand their role in tumor invasion and metastasis and identify new molecular targets for therapeutic strategies.

Key words: Cancer-associated fibroblasts; MicroRNA; Signaling pathway; Invasion; Gastric cancer; Metastasis

Core tip: Gastric cancer (GC) is one of the most common cancers worldwide. GC usually metastasizes to distant organs in advanced stages. Cancer-associated fibroblasts (CAFs) play an important role in GC invasion and metastasis. Therefore, a better understanding of the special interaction between GC cells and CAFs may be useful for identifying the underlying mechanisms of tumor progression.

Yan Y, Wang LF, Wang RF. Role of cancer-associated fibroblasts in invasion and metastasis of gastric cancer. *World J Gastroenterol* 2015; 21(33): 9717-9726 Available from: URL: http://www.wjgnet.com/1007-9327/full/v21/i33/9717.htm DOI: http://dx.doi.org/10.3748/wjg.v21.i33.9717

INTRODUCTION

Gastric cancer (GC) is the fourth most common cancer and the second leading cause of cancer deaths worldwide[1]. More than 70% of GC cases occur in Asia, of which half are in China[2]. Although a recent study has reported that the death and adverse event rates for GC patients under surgical care have decreased[3], the morbidity of GC remains high in Asia, and it is the third most common cancer after breast and lung cancers[4].

Patients with precancerous lesions and early GC typically have no obvious symptoms. Many GC individuals are diagnosed at an advanced stage. Due to a lack of appropriate diagnostic biomarkers and personalized anti-cancer treatment, the survival rate of GC patients is poor[2]. In advanced stages of GC, tumor cells have invaded into the blood or lymphatic vessels and metastasized to distant organs. Multiple steps and factors are involved in the progression towards advanced stages of GC. One of the most crucial factors is the bidirectional interaction between tumor cells and their microenvironment[5].

It is well recognized that the tumor microenvironment (TME) plays an important role in tumor progression. The TME is a complex tissue environment, composed of the extracellular matrix (ECM) and various types of stromal cells, such as cancer-associated fibroblasts (CAFs), macrophages, inflammatory cells, and mesenchymal stem cells[6]. All of these factors, but especially CAFs, make tremendous contributions to tumor growth and metastasis. In this review, we elaborate some novel and valuable results of recent studies regarding CAFs in GC and also highlight possible research directions for future studies.

ORIGIN AND PHENOTYPE OF CAFS

CAFs, which are characterized by multiple specific markers, are most frequently reported to overexpress α-smooth muscle actin (α-SMA) and fibroblast-activated protein (FAP), whereas caveolin-1 (Cav-1) typically shows reduced expression[7-9]. CAFs have been extracted from different types of human carcinomas, including pancreatic and gastric[9,10]. CAFs are the most prominent components of the TME in tumor tissue and play an essential role in tumor-stromal interactions[5].

CAFs are spindle-shaped, blast-like cells, and a number of reports have stated that they originate from cells through a variety of different mechanisms[11]. Several experimental studies have reported that mesenchymal stem cells (MSCs) are a significant source of CAFs. Zhu *et al*[12] found that GC-MSCs-primed neutrophils could induce MSCs to gradually differentiate into CAFs *in vitro*. Gu also discovered that GC cells activate human umbilical cord-derived MSCs (hucMSCs) and induce them to differentiate into CAFs by stimulating TGF-β/Smad signaling[9]. Recent studies also have demonstrated that CAFs are generated during the epithelial mesenchymal transition (EMT) *via* tumor-associated endothelial cells, which delaminate from blood vessels to generate mesenchymal cells with multiple-differentiation potential[6]. Moreover, increased levels of TGF-β in the microenvironment can induce resident tissue fibroblasts to acquire a CAF phenotype, which is associated with the up-regulation of α-SMA and the down-regulation of CD34[7,13]. Our previous study demonstrated that fibroblasts from the gastric cancer invasive front (interface zone fibroblasts, INFs) have a strongly positive FAP expression[14].

In general, the CAF phenotype is distinct from normal fibroblasts (NFs). CAFs can overexpress a wide range of factors, such as cytokines, growth factors and chemokines (MMPs, TGF-β, MCT4, VEGF, HGF, IL-22) that are critical to induce the deposition of ECM, promote angiogenesis and EMT, regulate metabolic reprogramming, and enhance proliferation and chemotherapy resistance[11,15,16]. These CAF functions play important roles in cancer progression and promote tumor cell invasion and metastasis.

RECENT STUDIES OF CAFS INVOLVED IN GC INVASION AND METASTASIS

MicroRNAs (miRNAs) are a class of non-coding small RNA molecules that play a key role in regulating the expression of target genes at the post-transcriptional level[17]. In recent decades, miRNAs have become a topic of interest in oncology. Many studies have suggested that miRNAs affect tumor growth, invasion and metastasis. Some miRNAs have been reported as novel diagnostic biomarkers and as new therapeutic targets for tumors such as gastric cancer, breast cancer and others[18,19]. Many studies have demonstrated that miRNAs, such as miR-20b, miR-20a, miR-17, and miR-382, are expressed by tumor cells in various types of tumors[20,21]. Recently, miRNAs related to CAFs have aroused increased attention. Several reports have shown that miRNAs also play critical roles in the CAFs of various human cancers. miRNAs can not only orchestrate the expression of target genes, but also promote tumor invasion and migration. Next, we summarize the recent research on the miRNAs in CAFs that are involved in GC invasion and metastasis (Figure 1) and discuss future prospects.

miRNA-106b

miRNA-106b is a member of the miRNA-106b~25 cluster that plays oncogenic roles in tumors *via* impacting tumor cell proliferation, apoptosis, and the cell cycle *in vitro* and tumorigenesis *in vivo*[22-24]. Prasad *et al*[24] showed that in melanoma cells, miRNA-106b is markedly up-regulated and acts as an oncogene to enhance cell proliferation. Exposure of melanoma cells to grape seed proanthocyanidins (GSPs), an inhibitor of miRNA-106b, can down-regulate miRNA-106b levels and inhibit cell proliferation by blocking the cell cycle.

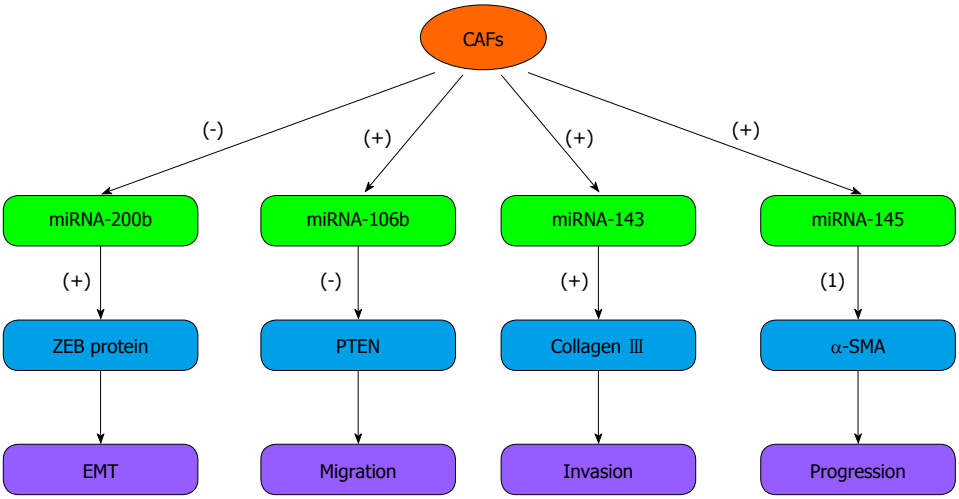

Figure 1 Roles of miRNAs associated with cancer-associated fibroblasts in gastric cancer. Cancer-associated fibroblasts (CAFs) not only express miRNA-106b, 143 and 145 themselves, they also down-regulate the expression of miRNA-200b in gastric cancer cells. All of these miRNAs can induce gastric cancer (GC) invasion and metastasis through various cascades. (+): Promoting effects; (-): Inhibiting effects; (1) Enhancing the expression of α-SMA in both normal gastric fibroblasts and CAFs. ZEB: Zinc finger E-box-binding homeobox; PTEN: Phosphatase and tensin homolog deleted on chromosome ten.

In a large-scale analysis, plasma concentration of miRNA-106b was notably higher in GC patients than in controls and dramatically decreased in post-operative samples compared with pre-operative samples[25].

In addition, miRNA-106b can also be overexpressed in CAFs. Yang *et al*[19] showed that miRNA-106b levels are increased in CAFs compared with NFs established from patients with GC. A decrease in miRNA-106b expression in CAFs notably inhibited gastric tumor cell migration and invasion by increasing the expression of PTEN.PTEN is regarded as a tumor suppressor gene that influences the pathogenesis, invasion and metastasis of carcinomas possibly through modulating the balance between apoptosis and proliferation[26]. Lost or decreased expression of PTEN protein occurs commonly in GC tumorigenesis and progression[27].

Twist is a helix-loop-helix transcription factor that includes two twist-like proteins, Twist-1 and Twist-2[28]. Accumulating evidence indicates that Twist-1 is a key regulator in the process of tumor cell invasion and metastasis by inducing EMT[29]. In gastric CAFs, Twist-1 expression is up-regulated, and its expression facilitates GC progression and poor clinical outcomes[30]. Woo *et al*[31] demonstrated that Twist-1 expression is induced by the IL6/STAT3 axis. Furthermore, the authors also revealed that Twist-1 is an important regulator in suppressing the senescence of CAFs and NFs. Knockdown of Twist-1 gene expression in the rat choroid plexus epithelial cell line Z310 markedly reduced tumor cell proliferation and invasion[32].

However, it has been reported that miRNA-106b could down-regulate Twist-1 expression *via* its direct interaction with Twist-1 mRNA at the 3′-untranslated region (3′-UTR) to suppress EMT-associated endometrial tumor cell invasion[33]. This result is in accordance with miRNA-106b expression in renal cell carcinoma, where it is over-expressed in tumor tissue but significantly lower in the tumors of patients with metastasis[34]. Therefore, these results suggest that miRNA-106b may be a more complex miRNA and have multiple effects in different types of tumor cells.

miRNA-143 and miRNA-145

It is well known that miRNA-143 serve as a tumor suppressor. In GC cell lines, miRNA-143 expression is significantly decreased. Increasing miRNA-143 expression can suppress cancer cell growth and induce apoptosis by targeting cycloxygenase-2 (COX-2)[35]. COX-2 and VEGF interact together to induce local angiogenesis and promote tumorigenesis and metastasis[36]. Down-regulation of COX-2 expression can significantly promote apoptosis and inhibit proliferation, migration and invasion of human gastric cancer cells[37]. Naito *et al*[38] also discovered that DNA methylation might cause the transcriptional inactivation of miRNA-143 to suppress its expression in GC cells. Using 5-aza-2-deoxycytidine to treat GC cell lines can restore miRNA-143 expression and inhibit cancer cell invasion.

Nevertheless, several studies have suggested that miRNA-143 plays a dual role in cancer, and its expression in tumor stromal cells may support tumor progression. Naito discovered that miRNA-143 is overexpressed in CAFs derived from diffuse type GC compared with NFs. The authors found that miRNA-143 promoted gastric cancer cell invasion by regulating the expression of collagen type Ⅲ in CAFs[38]. Collagen type Ⅲ is an extracellular matrix protein in the soft tissue tumor that significantly increases tumor cell migration and invasion in a dose-dependent manner[39]. Collagen Ⅲ and fibronectin are up-regulated by the TGF-β/Smad pathway in mesothelial cells. This effect can increase GC cell adhesion to mesothelial cells and promote GC cell

peritoneal metastasis[40]. Transfection of an miRNA-143 inhibitor can down-regulate miRNA-143 expression significantly, and the induction of collagen type Ⅲ in fibroblasts is suppressed[38].

miRNA-145, another well-known non-coding small RNA located on chromosome 5, is suggested to be co-transcribed with miRNA-143[41]. These molecules can work together to target a group of transcription factors, such as Kruppel-like factor 4(KLF4), myocardin and ELK-1, to induce differentiation and repress proliferation of smooth muscle cells[42]. Similar to miRNA-143, a low level of miRNA-145 in cancer cells induces cell proliferation through interacting with SENPI[43]. However, miRNA-145 is up-regulated by TGF-β and mainly localized in stromal fibroblasts but not in cancer cells. In addition, high expression of miRNA-145 in activated fibroblasts is viewed as a potential prognostic factor of diffuse type GC and is associated with a more advanced tumor stage and histological classification[44].

miRNA-200b

CAF, a type of complex stroma cell in TME, not only contributes to cancer cell malignant progression and metastatic dissemination by expressing miRNAs themselves, but they can also modulate the expression of miRNAs in the surrounding tumor cells.

miRNA-200b is a member of microRNA-200 family that plays a critical role in suppressing tumor invasion and regulating EMT in some types of human cancer, such as lung adenocarcinoma and breast cancer[45-47]. Its expression decreased docetaxel chemoresistance of lung adenocarcinoma cells *via* directly targeting E2F3. Attenuated miRNA-200b levels were demonstrated to be associated with high chemoresistance and poor prognosis[45]. Current research suggests that CAFs can down-regulate the expression of miRNA-200b, which can up-regulate *ZEB* expression and down-regulate *CDH1* expression in epithelial cells to induce tumor cell invasion and peritoneal dissemination in GC[48]. ZEB could lead to EMT and tumor metastasis through the TGF-β-miRNA-200-ZEB network. In hepatocellular carcinoma (HCC), the lncRNA activated by TGF-β could increase ZEB1 and ZEB2 expression by binding the miRNA-200 family, including miRNA-200b. Therefore, the overexpression of ZEB1/2 induces EMT and promotes tumor invasion and metastasis[49].

Because miRNA-200b has been suggested to play a pivotal role in tumor progression, most researchers have focused on miRNA-200b in tumor cell metastasis. However, there is no information regarding its role in CAFs. At present, the effect of miRNA-200b in CAFs is still unclear. It has been reported that miRNA-143 and miRNA-145 have different expression patterns in tumor cells and CAFs. The expression of miRNA-143 and miRNA-145 is up-regulated in CAFs but down-regulated in tumor cells. Whether the miRNA-200b has a similar behavior is unclear. Further studies are needed to clarify this question.

SIGNALING PATHWAYS INVOLVED IN INVASION AND METASTASIS OF GASTROINTESTINAL TUMORS

There are various factors and steps involved in cancer progression. Multiple cytokines and intracellular signaling pathways are involved in each step of tumor progression[5]. Extracellular or intracellular factors induce target gene mutation and abnormal expression through signaling transduction pathways to influence tumor initiation and progression. Elucidating these complicated signaling pathways is essential to understanding various biological tumor behaviors[50].

TGF-β/Smad signaling pathway

It is common knowledge that TGF-β/Smad signaling is a major signaling pathway in various types of tumor cells. This signaling pathway is closely related to the malignant progression of tumors. TGF-β, as the main regulator of TGF-β/Smad signaling, can induce nuclear localization and the transcriptional activity of Smads when activated[51]. Smad, a complex protein, plays essential roles in tumor progression. Liu *et al*[52] demonstrated that miRNA-130a/301a/454 share the same 3'-UTR binding seed sequence, and these molecules reduce the expression level of Smad4 protein, which directly correlates to the development of colon cancer.

When TGF-β/Smad signaling is activated, the downstream factors, such as MMPs, plasminogen activator inhibitor (PAI)-1 and TGF-β1 itself, are largely overexpressed[53]. TGF-β1 is closely related to tumor invasion and metastasis and can modulate its downstream transcription factor KLF8 to induce EMT in gastric cancer cells[54]. Moreover, KLF8 increases anti-apoptotic Bcl-2 and decreases pro-apoptotic Bax and caspase-3 expression in the SEC7901 cell line[55]. Treatment of tumor cells with the Chinese herbs *Scutellariabaicalensis* and *Fritillariacirrhosa* markedly block cancer cell proliferation and invasion through inhibiting the TGF-β/Smad pathway, which is accompanied by the down-regulation of the expression of Snail, Slug, and MMPs[56].

RAS/RAF/MEK/ERK signaling pathway

The Ras signaling pathway plays an important role in human cancers and is now considered a potential target for tumor treatment[57]. The activated Ras stimulates downstream signaling cascades to complete the link between the cell surface and the nucleus[58]. Some experimental data have indicated that K-Ras, the most frequently mutated Ras isoform, is a key factor in cell growth, angiogenesis, tumorigenesis and progression[59]. A recent study found that YAP1 and K-Ras converged specifically on the transcription

factor FOS and then coordinately activated the EMT program[60]. Moreover, ZNF312b could promote the transcriptional activation of the *K-Ras* gene and accelerate GC cell proliferation by binding ZNF312b in the ZNF-binding region of *K-Ras* promoter[61]. Therefore, inhibition of *K-Ras* activation is considered a significant approach in anticancer research. In colon cancer, the p38γ inhibitor pirfenidone preferentially reduced mutated K-Ras protein expression in tumor tissues and restrained the xenograft growth of K-Ras-dependent colon cancers in nude mice[62].

JAK/STAT signaling pathway

The JAK/STAT signaling pathway conveys information from the membrane to the nucleus to orchestrate target gene expression[63]. Cytokines bind to a specific receptor on the cell surface and recruit JAKs. The JAK molecules are recruited and activated by cytokine receptors, leading to the phosphorylation of the downstream STAT proteins. Once STAT proteins are activated, they dissociate from the receptor and rapidly translocate from the cytoplasm into the nucleus. Then, phosphorylated STAT proteins increase or decrease the expression of target genes through recognizing and binding to specific DNA sequences[64,65].

Accumulating evidence has indicated that numerous cytokines are involved in the JAK/STAT signaling pathway, such as IL-3, IL-6, IL-21, and IL-22[12,64,66]. Their receptors are divided into four primary families: the IL-2R family; the IL-3R family; the IL-6R family; and the INF-R family[64]. IL-6 and IL-22 activate STAT3 and contribute to colorectal cancer cell (CRC) proliferation and growth. Anti-IL-6 reduces p-STAT3 Y705 expression and leads to the growth inhibition of CRC cells[67]. Furthermore, IL-6 might promote tumor cell genetic alteration through interfering hMSH3 nuclear localization and DNA repair[68].

NF-κB signaling pathway

The NF-κB transcription factor is a heterodimeric protein, which was first identified based on its interaction with the immunoglobulin light-chain enhancer in B cells[69]. In recent years, NF-κB has been considered a key link between inflammation and cancer. NF-κB activation is mainly driven by inflammatory cytokines within the TME, such as IL-6 and TNF-α, or survival genes, such as *Bcl-X* (*L*)[70]. Moreover, NF-κB cooperates with the JAK/STAT pathway to promote tumor proliferation and progression *via* controlling distinct or overlapping groups of downstream genes[69,71].

NF-κB is a significant transcription factor in the regulation of MMP expression. In HCC, IL-17A induced MMP2 and MMP9 expression to promote tumor invasion and metastasis *via* NF-κB activation[72]. NF-κB also induces EMT in mammary epithelium *via* ROS activation[73]. Inhibiting the NF-κB pathway can restrain tumor growth and the expression of relevant inflammatory cytokines. miRNA-181c negatively regulates the inflammatory response *via* inhibiting NF-κB pathway activation and down-regulating the production of proinflammatory mediators, such as IL-1β and iNOS[74]. Gallotannin suppresses the activity of the NF-κB pathway through the inhibition of IκBα phosphorylation and degradation, which is accompanied with the low expression of NF-κB-regulated inflammatory cytokines (IL-8, TNF-α, IL-1α) and cell cycle arrest in HT-29 and HCT-166 cell lines[75].

MOST IMPORTANT SIGNALING PATHWAY INVOLVED IN CAFS IN CANCER

The critical signaling pathways in gastrointestinal tumors have been reported. However, what is the most important signaling pathway involved in CAFs in GC? Recently, hypoxia signaling has been extensively reported.

Hypoxia is a universal phenomenon in solid tumors compared with normal tissues, as well as gastrointestinal cancers[76]. Hypoxia not only leads to the expression of multiple target genes but also participates in various signaling pathways. Under hypoxic conditions, HIF-1α activates the EGFR/STAT and TGF-β/Smad signaling pathways and increases the levels of their downstream targets, and this effect enhances cell proliferation and promotes EMT[77]. Therefore, hypoxia signaling has been universally acknowledged as a noteworthy pathway in tumorigenesis and progression. The foremost hypoxia-responsive protein is hypoxia-inducible factor (HIF)[76,78]. HIF is a heterodimer consisting of an oxygen-sensitive α-subunit (HIF-1α, HIF-2α or HIF-3α) and a constitutively expressed β-subunit[78,79]. In normoxia, HIF-1α is ubiquitylated and degraded by interaction with prolyl hydroxylases (PHDs) and the tumor suppressor von Hippel-Lindau (VHL) protein. However, this process is suppressed in hypoxia, resulting in HIF-1α accumulation[80]. In most tumor types, such as pancreatic cancer and nasopharyngeal cancer, HIF-1α overexpression reduces overall survival and results in a poor patient prognosis[81,82]. In addition, HIF-1α-positive expression could be a useful prognostic marker for GC[83].

A growing body of evidence has suggested that the hypoxia signaling pathway plays a critical role in tumorigenesis through inducing EMT, angiogenesis, energy metabolism and chemotherapy resistance. Survivin is an inhibitor of apoptosis protein family that is scarcely expressed in normal tissues but is overexpressed in most human cancers. HIF-1α can up-regulate survivin levels, which will cause cisplatin resistance in GC cells[84]. In addition, HIF-1α induces chemoresistance by activating the MDR1 gene. MDR1 is a tumor promoter gene that encodes for P-gp, which can reduce the intracellular concentration of chemotherapeutic drugs[55,85].

With tumor progression, the tumor gradually exhibits a hypoxic and under-nourished niche. To sustain growth, the formation of a large number of new blood vessels plays a pivotal role in providing sufficient nutrients and oxygen concentration for tumor cells. However, a high density of blood vessel is related to tumor metastasis[86].

Under hypoxic conditions, CAFs increase the expression levels of genes related to angiogenesis, such as VEGF and angiopoietin[87,88]. VEGF is the most important factor to induce tumor vessel formation, and VEGF overexpression promotes tumor growth[89]. Down-regulated expression of HIF-1α and VEGF can suppress tumor angiogenesis. A member of p53 family, Tap73, is a tumor suppressor that decreases HIF-1 activity *via* promoting HIF-1α polyubiquitination and consequent proteasomal degradation in an oxygen-independent manner. Consequently, the expression of HIF-1α downstream factors, such as VAGF-A and VAGF-R2, is decreased[90]. In contrast, human rhomboid family-1 (RHBDF1) can protect HIF-1α protein stability and activity by diminishing RACK1-HIF-1α interaction, thus decreasing HIF-1α proteasomal degradation and shifting HIF-1α protein binding to HSP90[91].

Furthermore, recent evidence has also suggested that hypoxia is a key regulatory factor of energy metabolic reprogramming of CAFs[16]. HIF-1α induces CAFs to up-regulate the expression of monocarboxylate transporter-4 (MCT4) and reduces Cav-1 expression, releasing a mass of energy metabolites (such as L-lactate and ketones) to "feed" the tumor cells[16,92]. Subsequently, the tumor cells use the energy metabolites *via* mitochondrial tricarboxylic acid (TCA) cycle and oxidative phosphorylation (OXPHOS), thereby producing efficient adenosine triphosphate (ATP) production and facilitating tumor growth, invasion and metastasis[16,93].

From the above, we can observe that hypoxia signaling is a fatal pathway both in tumor cells and CAFs. It appears reasonable that the relevant genes of the hypoxia signaling pathway, such as HIF-1α, may be therapeutic targets for cancer. Therefore, it is strongly suggested that hypoxia signaling may serve as the most important pathway in CAFs and will be a potential cancer therapeutic target.

NEW THERAPEUTIC VIEW OF GC

Previous studies have shown that adriamycin induces chemoresistance and increases tumor cell invasion[94]. Pantoprazole, a proton pump inhibitor, suppresses adriamycin-resistant GC cell invasion *via* inhibiting the induction of EMT and the activation of the canonical Wnt/β-catenin signaling pathway in SGC7901/ADR cells[95].

Tumor vascularization indicates that nutrition has been reestablished. Therefore, inhibiting the formation of tumor blood vessels is an effective method to treat tumors. In recent years, VEGF has become a research topic of interest and an important therapeutic target in GC. Certain VEGF pathway target agents are used in preclinical and clinical treatment of GC[96]. For example, ramucirumab, a new monoclonal antibody VEGFR-2 antagonist, was shown to prolong survival in patients with advanced GC in a phase Ⅲ clinicaltrial. In a phase 3 study, 355 patients were assigned to receive ramucirumab (n = 238) or placebo (n = 117).The median overall survival was 5.2 mo (IQR: 2.3-9.9) in patients in the ramucirumab group and higher than 3.8 mo (1.7-7.1) in those in the placebo group. However, the rate of hypertension in the ramucirumab group was higher than in the placebo group [38 (16%) *vs* 9 (8%)][97].

Recent clinical trials with conventional chemotherapeutic agents have shown encouraging results in GC. However, chemoresistance is a main obstacle for GC treatment with the wide application of chemotherapy agents. 5-Fluorouracil (5-Fu) is one of the most common antineoplastic agents for GC. This drug can lead to cell damage and death by influencing mRNA translation and DNA synthesis[98]. Current research has found that 5-Fu induces residual cells to differentiate into $CD133^+$, $CD326^+$ and $CD44^+CD24^-$ subpopulation, which is associated with properties of cancer stem cells and chemoresistance. Furthermore, 5-Fu-resistant cells have enhanced BMI1 expression, which correlates with decreased recurrence-free survival compared with BMI1-negative GC patients[99].

The interaction between tumor cells and their microenvironment is regarded as a key factor in tumor invasion and metastasis. CAFs, one of the foremost components of TME, exist in all types of human cancer. Compared with tumor cells, the genotypes of CAFs are stabilized. This characteristic of CAFs may make them effective treatment targets in antitumor therapy.

For example, several FAP-related drugs have been discovered in tumor therapy by targeting CAFs, such as FAP activity inhibitors and anti-FAP antibodies[15]. In tumor-bearing mice that were vaccinated against FAP, tumor growth is significantly retarded[100]. Furthermore, Ohshio *et al*[101] demonstrated that inhibition of CAF function improved the antitumor immune responses in tumor tissues of tumor-bearing mouse models. The populations of the suppressor immune cells $CD4^+CD25^+Foxp3^+$Tregs and $CD11b^+Gr\text{-}1^+$MDSCs are decreased in the anti-CAF therapy group compared with those in controls. Furthermore, the levels of SDF-1, PEG2 and TGF-β1 expression in tumor tissues were also dramatically reduced. However, tumor growth suppression was not observed. This result implies that the antitumor effects are complicated in CAF-targeted techniques.

CONCLUSION

In this review, we describe the role of CAFs and the relevant signaling pathways in gastric carcinoma. Various cytokines, growth factors and chemokines

secreted by CAFs constitute a favorable environment that can induce tumor growth, invasion and metastasis. At present, miRNA- and signaling pathway-related studies are becoming hotspots in the oncology field. However, our current understanding of these factors in CAFs is limited. The function of miRNAs is still controversial. Therefore, it is necessary to develop several specific animal models focusing on the mechanisms of miRNAs and signaling pathways in CAFs in further research. Looking forward, perhaps some specific targets will be identified in our future studies by the accumulating successful research. Inhibition of these targets in CAFs will provide a new therapeutic direction for tumor treatment.

REFERENCES

1 **Montori G**, Coccolini F, Ceresoli M, Catena F, Colaianni N, Poletti E, Ansaloni L. The treatment of peritoneal carcinomatosis in advanced gastric cancer: state of the art. *Int J Surg Oncol* 2014; **2014**: 912418 [PMID: 24693422 DOI: 10.1155/2014/912418]

2 **Shen L**, Shan YS, Hu HM, Price TJ, Sirohi B, Yeh KH, Yang YH, Sano T, Yang HK, Zhang X, Park SR, Fujii M, Kang YK, Chen LT. Management of gastric cancer in Asia: resource-stratified guidelines. *Lancet Oncol* 2013; **14**: e535-e547 [PMID: 24176572 DOI: 10.1016/S1470-2045(13)70436-4]

3 **Young JA**, Shimi SM, Kerr L, McPhillips G, Thompson AM. Reduction in gastric cancer surgical mortality over 10 years: An adverse events analysis. *Ann Med Surg* (Lond) 2014; **3**: 26-30 [PMID: 25568781 DOI: 10.1016/j.amsu.2014.03.003]

4 **Rahman R**, Asombang AW, Ibdah JA. Characteristics of gastric cancer in Asia. *World J Gastroenterol* 2014; **20**: 4483-4490 [PMID: 24782601 DOI: 10.3748/wjg.v.i16.4483]

5 **Chung HW**, Lim JB. Role of the tumor microenvironment in the pathogenesis of gastric carcinoma. *World J Gastroenterol* 2014; **20**: 1667-1680 [PMID: 24587646 DOI: 10.3748/wjg.v20.i7.1667]

6 **Quail DF**, Joyce JA. Microenvironmental regulation of tumor progression and metastasis. *Nat Med* 2013; **19**: 1423-1437 [PMID: 24202395 DOI: 10.1038/nm.3394]

7 **Calon A**, Tauriello DV, Batlle E. TGF-beta in CAF-mediated tumor growth and metastasis. *Semin Cancer Biol* 2014; **25**: 15-22 [PMID: 24412104 DOI: 10.1016/j.semcancer.2013.12.008]

8 **Wang RF**, Zhang LH, Shan LH, Sun WG, Chai CC, Wu HM, Ibla JC, Wang LF, Liu JR. Effects of the fibroblast activation protein on the invasion and migration of gastric cancer. *Exp Mol Pathol* 2013; **95**: 350-356 [PMID: 24422232]

9 **Zhao X**, He Y, Gao J, Fan L, Li Z, Yang G, Chen H. Caveolin-1 expression level in cancer associated fibroblasts predicts outcome in gastric cancer. *PLoS One* 2013; **8**: e59102 [PMID: 23527097 DOI: 10.1371/journal.pone.0059102]

10 **Özdemir BC**, Pentcheva-Hoang T, Carstens JL, Zheng X, Wu CC, Simpson TR, Laklai H, Sugimoto H, Kahlert C, Novitskiy SV, De Jesus-Acosta A, Sharma P, Heidari P, Mahmood U, Chin L, Moses HL, Weaver VM, Maitra A, Allison JP, LeBleu VS, Kalluri R. Depletion of carcinoma-associated fibroblasts and fibrosis induces immunosuppression and accelerates pancreas cancer with reduced survival. *Cancer Cell* 2014; **25**: 719-734 [PMID: 24856586 DOI: 10.1016/j.ccr.2014.04.005]

11 **Valcz G**, Sipos F, Tulassay Z, Molnar B, Yagi Y. Importance of carcinoma-associated fibroblast-derived proteins in clinical oncology. *J Clin Pathol* 2014; **67**: 1026-1031 [PMID: 25135950 DOI: 10.1136/jclinpath-2014-202561]

12 **Zhu Q**, Zhang X, Zhang L, Li W, Wu H, Yuan X, Mao F, Wang M, Zhu W, Qian H, Xu W. The IL-6-STAT3 axis mediates a reciprocal crosstalk between cancer-derived mesenchymal stem cells and neutrophils to synergistically prompt gastric cancer progression. *Cell Death Dis* 2014; **5**: e1295 [PMID: 24946088 DOI: 10.1038/cddis.2014.263]

13 **Terai S**, Fushida S, Tsukada T, Kinoshita J, Oyama K, Okamoto K, Makino I, Tajima H, Ninomiya I, Fujimura T, Harada S, Ohta T. Bone marrow derived "fibrocytes" contribute to tumor proliferation and fibrosis in gastric cancer. *Gastric Cancer* 2015; **18**: 306-313 [PMID: 24792410]

14 **Shan LH**, Sun WG, Han W, Qi L, Yang C, Chai CC, Yao K, Zhou QF, Wu HM, Wang LF, Liu JR. Roles of fibroblasts from the interface zone in invasion, migration, proliferation and apoptosis of gastric adenocarcinoma. *J Clin Pathol* 2012; **65**: 888-895 [PMID: 22844068]

15 **Madar S**, Goldstein I, Rotter V. 'Cancer associated fibroblasts' --more than meets the eye. *Trends Mol Med* 2013; **19**: 447-453 [PMID: 23769623 DOI: 10.1016/j.molmed.2013.05.004]

16 **Martinez-Outschoorn UE**, Lisanti MP, Sotgia F. Catabolic cancer-associated fibroblasts transfer energy and biomass to anabolic cancer cells, fueling tumor growth. *Semin Cancer Biol* 2014; **25**: 47-60 [PMID: 24486645 DOI: 10.1016/j.semcancer.2014.01.005]

17 **Zhang B**, Wang Q, Pan X. MicroRNAs and their regulatory roles in animals and plants. *J Cell Physiol* 2007; **210**: 279-289 [PMID: 17096367]

18 **Gyparaki MT**, Basdra EK, Papavassiliou AG. MicroRNAs as regulatory elements in triple negative breast cancer. *Cancer Lett* 2014; **354**: 1-4 [PMID: 25107641 DOI: 10.1016/j.canlet.2014.07.036]

19 **Yang TS**, Yang XH, Chen X, Wang XD, Hua J, Zhou DL, Zhou B, Song ZS. MicroRNA-106b in cancer-associated fibroblasts from gastric cancer promotes cell migration and invasion by targeting PTEN. *FEBS Lett* 2014; **588**: 2162-2169 [PMID: 24842611 DOI: 10.1016/j.febslet.2014.04.050]

20 **Guo J**, Miao Y, Xiao B, Huan R, Jiang Z, Meng D, Wang Y. Differential expression of microRNA species in human gastric cancer versus non-tumorous tissues. *J Gastroenterol Hepatol* 2009; **24**: 652-657 [PMID: 19175831 DOI: 10.1111/j.1440-1746.2008.05666.x]

21 **Seok JK**, Lee SH, Kim MJ, Lee YM. MicroRNA-382 induced by HIF-1α is an angiogenic miR targeting the tumor suppressor phosphatase and tensin homolog. *Nucleic Acids Res* 2014; **42**: 8062-8072 [PMID: 24914051 DOI: 10.1093/nar/gku515]

22 **Li F**, Liu J, Li S. MicorRNA 106b~25 cluster and gastric cancer. *Surg Oncol* 2013; **22**: e7-10 [PMID: 23510949 DOI: 10.1016/j.suronc.2013.01.003]

23 **Li B**, Shi XB, Nori D, Chao CK, Chen AM, Valicenti R, White Rde V. Down-regulation of microRNA 106b is involved in p21-mediated cell cycle arrest in response to radiation in prostate cancer cells. *Prostate* 2011; **71**: 567-574 [PMID: 20878953 DOI: 10.1002/pros.21272]

24 **Prasad R**, Katiyar SK. Down-regulation of miRNA-106b inhibits growth of melanoma cells by promoting G1-phase cell cycle arrest and reactivation of p21/WAF1/Cip1 protein. *Oncotarget* 2014; **5**: 10636-10649 [PMID: 25361006]

25 **Tsujiura M**, Ichikawa D, Komatsu S, Shiozaki A, Takeshita H, Kosuga T, Konishi H, Morimura R, Deguchi K, Fujiwara H, Okamoto K, Otsuji E. Circulating microRNAs in plasma of patients with gastric cancers. *Br J Cancer* 2010; **102**: 1174-1179 [PMID: 20234369 DOI: 10.1038/sj.bjc.6605608]

26 **Li XH**, Zheng HC, Takahashi H, Masuda S, Yang XH, Takano Y. PTEN expression and mutation in colorectal carcinomas. *Oncol Rep* 2009; **22**: 757-764 [PMID: 19724853]

27 **Yang L**, Kuang LG, Zheng HC, Li JY, Wu DY, Zhang SM, Xin Y. PTEN encoding product: a marker for tumorigenesis and progression of gastric carcinoma. *World J Gastroenterol* 2003; **9**: 35-39 [PMID: 12508347]

28 **Wushou A**, Hou J, Zhao YJ, Shao ZM. Twist-1 up-regulation in carcinoma correlates to poor survival. *Int J Mol Sci* 2014; **15**: 21621-21630 [PMID: 25429425 DOI: 10.3390/ijms151221621]

29 **Nuti SV**, Mor G, Li P, Yin G. TWIST and ovarian cancer stem cells: implications for chemoresistance and metastasis. *Oncotarget* 2014; **5**: 7260-7271 [PMID: 25238494]

30 **Sung CO**, Lee KW, Han S, Kim SH. Twist1 is up-regulated in gastric cancer-associated fibroblasts with poor clinical outcomes. *Am J Pathol* 2011; **179**: 1827-1838 [PMID: 21854747 DOI:

10.1016/j.ajpath.2011.06.032]
31 **Lee KW**, Yeo SY, Sung CO, Kim SH. Twist1 is a key regulator of cancer-associated fibroblasts. *Cancer Res* 2015; **75**: 73-85 [PMID: 25368021 DOI: 10.1158/0008-5472.CAN-14-0350]
32 **Hasselblatt M**, Mertsch S, Koos B, Riesmeier B, Stegemann H, Jeibmann A, Tomm M, Schmitz N, Wrede B, Wolff JE, Zheng W, Paulus W. TWIST-1 is overexpressed in neoplastic choroid plexus epithelial cells and promotes proliferation and invasion. *Cancer Res* 2009; **69**: 2219-2223 [PMID: 19276370 DOI: 10.1158/0008-5472.CAN-08-3176]
33 **Dong P**, Kaneuchi M, Watari H, Sudo S, Sakuragi N. MicroRNA-106b modulates epithelial-mesenchymal transition by targeting TWIST1 in invasive endometrial cancer cell lines. *Mol Carcinog* 2014; **53**: 349-359 [PMID: 24002805 DOI: 10.1002/mc.21983]
34 **Slaby O**, Jancovicova J, Lakomy R, Svoboda M, Poprach A, Fabian P, Kren L, Michalek J, Vyzula R. Expression of miRNA-106b in conventional renal cell carcinoma is a potential marker for prediction of early metastasis after nephrectomy. *J Exp Clin Cancer Res* 2010; **29**: 90 [PMID: 20609231 DOI: 10.1186/1756-9966-29-90]
35 **Wu XL**, Cheng B, Li PY, Huang HJ, Zhao Q, Dan ZL, Tian DA, Zhang P. MicroRNA-143 suppresses gastric cancer cell growth and induces apoptosis by targeting COX-2. *World J Gastroenterol* 2013; **19**: 7758-7765 [PMID: 24616567 DOI: 10.3748/wjg.v19.i43.7758]
36 **Han X**, Li H, Su L, Zhu W, Xu W, Li K, Zhao Q, Yang H, Liu H. Effect of celecoxib plus standard chemotherapy on serum levels of vascular endothelial growth factor and cyclooxygenase-2 in patients with gastric cancer. *Biomed Rep* 2014; **2**: 183-187 [PMID: 24649093]
37 **Zhang H**, Sun K, Ding J, Xu H, Zhu L, Zhang K, Li X, Sun W. Harmine induces apoptosis and inhibits tumor cell proliferation, migration and invasion through down-regulation of cyclooxygenase-2 expression in gastric cancer. *Phytomedicine* 2014; **21**: 348-355 [PMID: 24176842 DOI: 10.1016/j.phymed.2013.09.007]
38 **Naito Y**, Sakamoto N, Oue N, Yashiro M, Sentani K, Yanagihara K, Hirakawa K, Yasui W. MicroRNA-143 regulates collagen type III expression in stromal fibroblasts of scirrhous type gastric cancer. *Cancer Sci* 2014; **105**: 228-235 [PMID: 24283360 DOI: 10.1111/cas.12329]
39 **Chintala SK**, Sawaya R, Gokaslan ZL, Rao JS. The effect of type III collagen on migration and invasion of human glioblastoma cell lines in vitro. *Cancer Lett* 1996; **102**: 57-63 [PMID: 8603379]
40 **Lv ZD**, Na D, Liu FN, Du ZM, Sun Z, Li Z, Ma XY, Wang ZN, Xu HM. Induction of gastric cancer cell adhesion through transforming growth factor-beta1-mediated peritoneal fibrosis. *J Exp Clin Cancer Res* 2010; **29**: 139 [PMID: 21034459 DOI: 10.1186/1756-9966-29-139]
41 **Cui SY**, Wang R, Chen LB. MicroRNA-145: a potent tumour suppressor that regulates multiple cellular pathways. *J Cell Mol Med* 2014; **18**: 1913-1926 [PMID: 25124875 DOI: 10.1111/jcmm.12358]
42 **Cordes KR**, Sheehy NT, White MP, Berry EC, Morton SU, Muth AN, Lee TH, Miano JM, Ivey KN, Srivastava D. miR-145 and miR-143 regulate smooth muscle cell fate and plasticity. *Nature* 2009; **460**: 705-710 [PMID: 19578358 DOI: 10.1038/nature08195]
43 **Wang C**, Tao W, Ni S, Chen Q, Zhao Z, Ma L, Fu Y, Jiao Z. Tumor-suppressive microRNA-145 induces growth arrest by targeting SENP1 in human prostate cancer cells. *Cancer Sci* 2015; **106**: 375-382 [PMID: 25645686 DOI: 10.1111/cas.12626]
44 **Naito Y**, Yasuno K, Tagawa H, Sakamoto N, Oue N, Yashiro M, Sentani K, Goto K, Shinmei S, Oo HZ, Yanagihara K, Hirakawa K, Yasui W. MicroRNA-145 is a potential prognostic factor of scirrhous type gastric cancer. *Oncol Rep* 2014; **32**: 1720-1726 [PMID: 25051317 DOI: 10.3892/or.2014.3333]
45 **Feng B**, Wang R, Song HZ, Chen LB. MicroRNA-200b reverses chemoresistance of docetaxel-resistant human lung adenocarcinoma cells by targeting E2F3. *Cancer* 2012; **118**: 3365-3376 [PMID: 22139708 DOI: 10.1002/cncr.26560]
46 **Zhang X**, Zhang B, Gao J, Wang X, Liu Z. Regulation of the microRNA 200b (miRNA-200b) by transcriptional regulators PEA3 and ELK-1 protein affects expression of Pin1 protein to control anoikis. *J Biol Chem* 2013; **288**: 32742-32752 [PMID: 24072701 DOI: 10.1074/jbc.M113.478016]
47 **Li X**, Roslan S, Johnstone CN, Wright JA, Bracken CP, Anderson M, Bert AG, Selth LA, Anderson RL, Goodall GJ, Gregory PA, Khew-Goodall Y. MiR-200 can repress breast cancer metastasis through ZEB1-independent but moesin-dependent pathways. *Oncogene* 2014; **33**: 4077-4088 [PMID: 24037528 DOI: 10.1038/onc.2013.370]
48 **Kurashige J**, Mima K, Sawada G, Takahashi Y, Eguchi H, Sugimachi K, Mori M, Yanagihara K, Yashiro M, Hirakawa K, Baba H, Mimori K. Epigenetic modulation and repression of miR-200b by cancer-associated fibroblasts contribute to cancer invasion and peritoneal dissemination in gastric cancer. *Carcinogenesis* 2015; **36**: 133-141 [PMID: 25411357 DOI: 10.1093/carcin/bgu232]
49 **Yuan JH**, Yang F, Wang F, Ma JZ, Guo YJ, Tao QF, Liu F, Pan W, Wang TT, Zhou CC, Wang SB, Wang YZ, Yang Y, Yang N, Zhou WP, Yang GS, Sun SH. A long noncoding RNA activated by TGF-β promotes the invasion-metastasis cascade in hepatocellular carcinoma. *Cancer Cell* 2014; **25**: 666-681 [PMID: 24768205 DOI: 10.1016/j.ccr.2014.03.010]
50 **Chowdhury S**, Sarkar RR. Comparison of human cell signaling pathway databases--evolution, drawbacks and challenges. *Database* (Oxford) 2015; 2015 [PMID: 25632107 DOI: 10.1093/database/bau126]
51 **Pickup M**, Novitskiy S, Moses HL. The roles of TGFβ in the tumour microenvironment. *Nat Rev Cancer* 2013; **13**: 788-799 [PMID: 24132110 DOI: 10.1038/nrc3603]
52 **Liu L**, Nie J, Chen L, Dong G, Du X, Wu X, Tang Y, Han W. The oncogenic role of microRNA-130a/301a/454 in human colorectal cancer via targeting Smad4 expression. *PLoS One* 2013; **8**: e55532 [PMID: 23393589 DOI: 10.1371/journal.pone.0055532]
53 **Hawinkels LJ**, Paauwe M, Verspaget HW, Wiercinska E, van der Zon JM, van der Ploeg K, Koelink PJ, Lindeman JH, Mesker W, ten Dijke P, Sier CF. Interaction with colon cancer cells hyperactivates TGF-β signaling in cancer-associated fibroblasts. *Oncogene* 2014; **33**: 97-107 [PMID: 23208491 DOI: 10.1038/onc.2012.536]
54 **Zhang H**, Liu L, Wang Y, Zhao G, Xie R, Liu C, Xiao X, Wu K, Nie Y, Zhang H, Fan D. KLF8 involves in TGF-beta-induced EMT and promotes invasion and migration in gastric cancer cells. *J Cancer Res Clin Oncol* 2013; **139**: 1033-1042 [PMID: 23504025 DOI: 10.1007/s00432-012-1363-3]
55 **Zhang H**, Sun L, Xiao X, Xie R, Liu C, Wang Y, Wei Y, Zhang H, Liu L. Krüppel-like factor 8 contributes to hypoxia-induced MDR in gastric cancer cells. *Cancer Sci* 2014; **105**: 1109-1115 [PMID: 25040744 DOI: 10.1111/cas.12483]
56 **Bokhari AA**, Syed V. Inhibition of Transforming Growth Factor-β (TGF-β) Signaling by Scutellaria baicalensis and Fritillaria cirrhosa Extracts in Endometrial Cancer. *J Cell Biochem* 2015; **116**: 1797-1805 [PMID: 25683036 DOI: 10.1002/jcb.25138]
57 **Ward AF**, Braun BS, Shannon KM. Targeting oncogenic Ras signaling in hematologic malignancies. *Blood* 2012; **120**: 3397-3406 [PMID: 22898602 DOI: 10.1182/blood-2012-05-378596]
58 **Shields JM**, Pruitt K, McFall A, Shaub A, Der CJ. Understanding Ras: 'it ain't over 'til it's over'. *Trends Cell Biol* 2000; **10**: 147-154 [PMID: 10740269]
59 **Friday BB**, Adjei AA. K-ras as a target for cancer therapy. *Biochim Biophys Acta* 2005; **1756**: 127-144 [PMID: 16139957]
60 **Shao DD**, Xue W, Krall EB, Bhutkar A, Piccioni F, Wang X, Schinzel AC, Sood S, Rosenbluh J, Kim JW, Zwang Y, Roberts TM, Root DE, Jacks T, Hahn WC. KRAS and YAP1 converge to regulate EMT and tumor survival. *Cell* 2014; **158**: 171-184 [PMID: 24954536 DOI: 10.1016/j.cell.2014.06.004]
61 **Song IS**, Oh NS, Kim HT, Ha GH, Jeong SY, Kim JM, Kim DI, Yoo HS, Kim CH, Kim NS. Human ZNF312b promotes the progression of gastric cancer by transcriptional activation of the K-ras gene. *Cancer Res* 2009; **69**: 3131-3139 [PMID: 19318583 DOI: 10.1158/0008-5472.CAN-08-2240]

62 **Qi X**, Xie C, Hou S, Li G, Yin N, Dong L, Lepp A, Chesnik MA, Mirza SP, Szabo A, Tsai S, Basir Z, Wu S, Chen G. Identification of a ternary protein-complex as a therapeutic target for K-Ras-dependent colon cancer. *Oncotarget* 2014; **5**: 4269-4282 [PMID: 24962213]

63 **O'Shea JJ**, Plenge R. JAK and STAT signaling molecules in immunoregulation and immune-mediated disease. *Immunity* 2012; **36**: 542-550 [PMID: 22520847 DOI: 10.1016/j.immuni.2012.03.014]

64 **Coskun M**, Salem M, Pedersen J, Nielsen OH. Involvement of JAK/STAT signaling in the pathogenesis of inflammatory bowel disease. *Pharmacol Res* 2013; **76**: 1-8 [PMID: 23827161 DOI: 10.1016/j.phrs.2013.06.007]

65 **Quintás-Cardama A**, Verstovsek S. Molecular pathways: Jak/STAT pathway: mutations, inhibitors, and resistance. *Clin Cancer Res* 2013; **19**: 1933-1940 [PMID: 23406773 DOI: 10.1158/1078-0432.CCR-12-0284]

66 **Ma J**, Ma D, Ji C. The role of IL-21 in hematological malignancies. *Cytokine* 2011; **56**: 133-139 [PMID: 21824785 DOI: 10.1016/j.cyto.2011.07.011]

67 **De Simone V**, Franzè E, Ronchetti G, Colantoni A, Fantini MC, Di Fusco D, Sica GS, Sileri P, MacDonald TT, Pallone F, Monteleone G, Stolfi C. Th17-type cytokines, IL-6 and TNF-α synergistically activate STAT3 and NF-kB to promote colorectal cancer cell growth. *Oncogene* 2015; **34**: 3493-3503 [PMID: 25174402 DOI: 10.1038/onc.2014.286]

68 **Tseng-Rogenski SS**, Hamaya Y, Choi DY, Carethers JM. Interleukin 6 alters localization of hMSH3, leading to DNA mismatch repair defects in colorectal cancer cells. *Gastroenterology* 2015; **148**: 579-589 [PMID: 25461668 DOI: 10.1053/j.gastro.2014.11.027]

69 **He G**, Karin M. NF-κB and STAT3 - key players in liver inflammation and cancer. *Cell Res* 2011; **21**: 159-168 [PMID: 21187858 DOI: 10.1038/cr.2010.183]

70 **Karin M**. NF-kappaB as a critical link between inflammation and cancer. *Cold Spring Harb Perspect Biol* 2009; **1**: a000141 [PMID: 20066113 DOI: 10.1101/cshperspect.a000141]

71 **Grivennikov SI**, Karin M. Dangerous liaisons: STAT3 and NF-kappaB collaboration and crosstalk in cancer. *Cytokine Growth Factor Rev* 2010; **21**: 11-19 [PMID: 20018552 DOI: 10.1016/j.cytogfr.2009.11.005]

72 **Li J**, Lau GK, Chen L, Dong SS, Lan HY, Huang XR, Li Y, Luk JM, Yuan YF, Guan XY. Interleukin 17A promotes hepatocellular carcinoma metastasis via NF-kB induced matrix metalloproteinases 2 and 9 expression. *PLoS One* 2011; **6**: e21816 [PMID: 21760911 DOI: 10.1371/journal.pone.0021816]

73 **Cichon MA**, Radisky DC. ROS-induced epithelial-mesenchymal transition in mammary epithelial cells is mediated by NF-kB-dependent activation of Snail. *Oncotarget* 2014; **5**: 2827-2838 [PMID: 24811539]

74 **Zhang L**, Li YJ, Wu XY, Hong Z, Wei WS. MicroRNA-181c negatively regulates the inflammatory response in oxygen-glucose-deprived microglia by targeting Toll-like receptor 4. *J Neurochem* 2015; **132**: 713-723 [PMID: 25545945 DOI: 10.1111/jnc.13021]

75 **Al-Halabi R**, Bou Chedid M, Abou Merhi R, El-Hajj H, Zahr H, Schneider-Stock R, Bazarbachi A, Gali-Muhtasib H. Gallotannin inhibits NFκB signaling and growth of human colon cancer xenografts. *Cancer Biol Ther* 2011; **12**: 59-68 [PMID: 21532339 DOI: 10.4161/cbt.12.1.15715]

76 **Griffiths EA**, Pritchard SA, Welch IM, Price PM, West CM. Is the hypoxia-inducible factor pathway important in gastric cancer? *Eur J Cancer* 2005; **41**: 2792-2805 [PMID: 16290133]

77 **Kannan A**, Krishnan A, Ali M, Subramaniam S, Halagowder D, Sivasithamparam ND. Caveolin-1 promotes gastric cancer progression by up-regulating epithelial to mesenchymal transition by crosstalk of signalling mechanisms under hypoxic condition. *Eur J Cancer* 2014; **50**: 204-215 [PMID: 24070739 DOI: 10.1016/j.ejca.2013.08.016]

78 **Pouysségur J**, Dayan F, Mazure NM. Hypoxia signalling in cancer and approaches to enforce tumour regression. *Nature* 2006; **441**: 437-443 [PMID: 16724055]

79 **Nauta TD**, van Hinsbergh VW, Koolwijk P. Hypoxic signaling during tissue repair and regenerative medicine. *Int J Mol Sci* 2014; **15**: 19791-19815 [PMID: 25365172 DOI: 10.3390/ijms151119791]

80 **Koh MY**, Powis G. HAF : the new player in oxygen-independent HIF-1alpha degradation. *Cell Cycle* 2009; **8**: 1359-1366 [PMID: 19377289]

81 **Ye LY**, Zhang Q, Bai XL, Pankaj P, Hu QD, Liang TB. Hypoxia-inducible factor 1α expression and its clinical significance in pancreatic cancer: a meta-analysis. *Pancreatology* 2014; **14**: 391-397 [PMID: 25278309 DOI: 10.1016/j.pan.2014.06.008]

82 **Chen Y**, Li X, Wu S, Xu G, Zhou Y, Gong L, Li Z, Yang D. Expression of HIF-1α and CAIX in nasopharyngeal carcinoma and their correlation with patients' prognosis. *Med Oncol* 2014; **31**: 304 [PMID: 25377659 DOI: 10.1007/s12032-014-0304-1]

83 **Lin S**, Ma R, Zheng XY, Yu H, Liang X, Lin H, Cai XJ. Meta-analysis of immunohistochemical expression of hypoxia inducible factor-1α as a prognostic role in gastric cancer. *World J Gastroenterol* 2014; **20**: 1107-1113 [PMID: 24574785 DOI: 10.3748/wjg.v20.i4.1107]

84 **Sun XP**, Dong X, Lin L, Jiang X, Wei Z, Zhai B, Sun B, Zhang Q, Wang X, Jiang H, Krissansen GW, Qiao H, Sun X. Up-regulation of survivin by AKT and hypoxia-inducible factor 1α contributes to cisplatin resistance in gastric cancer. *FEBS J* 2014; **281**: 115-128 [PMID: 24165223 DOI: 10.1111/febs.12577]

85 **Liang Y**, Zheng T, Song R, Wang J, Yin D, Wang L, Liu H, Tian L, Fang X, Meng X, Jiang H, Liu J, Liu L. Hypoxia-mediated sorafenib resistance can be overcome by EF24 through Von Hippel-Lindau tumor suppressor-dependent HIF-1α inhibition in hepatocellular carcinoma. *Hepatology* 2013; **57**: 1847-1857 [PMID: 23299930 DOI: 10.1002/hep.26224]

86 **Takahashi Y**, Cleary KR, Mai M, Kitadai Y, Bucana CD, Ellis LM. Significance of vessel count and vascular endothelial growth factor and its receptor (KDR) in intestinal-type gastric cancer. *Clin Cancer Res* 1996; **2**: 1679-1684 [PMID: 9816116]

87 **Rupp C**, Scherzer M, Rudisch A, Unger C, Haslinger C, Schweifer N, Artaker M, Nivarthi H, Moriggl R, Hengstschläger M, Kerjaschki D, Sommergruber W, Dolznig H, Garin-Chesa P. IGFBP7, a novel tumor stroma marker, with growth-promoting effects in colon cancer through a paracrine tumor-stroma interaction. *Oncogene* 2015; **34**: 815-825 [PMID: 24632618]

88 **De Francesco EM**, Lappano R, Santolla MF, Marsico S, Caruso A, Maggiolini M. HIF-1α/GPER signaling mediates the expression of VEGF induced by hypoxia in breast cancer associated fibroblasts (CAFs). *Breast Cancer Res* 2013; **15**: R64 [PMID: 23947803 DOI: 10.1186/bcr3458]

89 **Nagasaki T**, Hara M, Nakanishi H, Takahashi H, Sato M, Takeyama H. Interleukin-6 released by colon cancer-associated fibroblasts is critical for tumour angiogenesis: anti-interleukin-6 receptor antibody suppressed angiogenesis and inhibited tumour-stroma interaction. *Br J Cancer* 2014; **110**: 469-478 [PMID: 24346288 DOI: 10.1038/bjc.2013.748]

90 **Amelio I**, Inoue S, Markert EK, Levine AJ, Knight RA, Mak TW, Melino G. TAp73 opposes tumor angiogenesis by promoting hypoxia-inducible factor 1α degradation. *Proc Natl Acad Sci USA* 2015; **112**: 226-231 [PMID: 25535359 DOI: 10.1073/pnas.1410609111]

91 **Zhou Z**, Liu F, Zhang ZS, Shu F, Zheng Y, Fu L, Li LY. Human rhomboid family-1 suppresses oxygen-independent degradation of hypoxia-inducible factor-1α in breast cancer. *Cancer Res* 2014; **74**: 2719-2730 [PMID: 24648344 DOI: 10.1158/0008-5472.CAN-13-1027]

92 **Chiavarina B**, Whitaker-Menezes D, Migneco G, Martinez-Outschoorn UE, Pavlides S, Howell A, Tanowitz HB, Casimiro MC, Wang C, Pestell RG, Grieshaber P, Caro J, Sotgia F, Lisanti MP. HIF1-alpha functions as a tumor promoter in cancer associated fibroblasts, and as a tumor suppressor in breast cancer cells: Autophagy drives compartment-specific oncogenesis. *Cell Cycle* 2010; **9**: 3534-3551 [PMID: 20864819 DOI: 10.4161/cc.9.17.12908]

93 **Suh DH**, Kim HS, Kim B, Song YS. Metabolic orchestration between cancer cells and tumor microenvironment as a co-evolutionary source of chemoresistance in ovarian cancer: a

therapeutic implication. *Biochem Pharmacol* 2014; **92**: 43-54 [PMID: 25168677 DOI: 10.1016/j.bcp.2014.08.011]

94 **Shi Y**, Zhang Y, Zhao Y, Hong L, Liu N, Jin X, Pan Y, Fan D. Overexpression of ZNRD1 promotes multidrug-resistant phenotype of gastric cancer cells through upregulation of P-glycoprotein. *Cancer Biol Ther* 2004; **3**: 377-381 [PMID: 14726695]

95 **Zhang B**, Yang Y, Shi X, Liao W, Chen M, Cheng AS, Yan H, Fang C, Zhang S, Xu G, Shen S, Huang S, Chen G, Lv Y, Ling T, Zhang X, Wang L, Zhuge Y, Zou X. Proton pump inhibitor pantoprazole abrogates adriamycin-resistant gastric cancer cell invasiveness via suppression of Akt/GSK-β/β-catenin signaling and epithelial-mesenchymal transition. *Cancer Lett* 2015; **356**: 704-712 [PMID: 25449432 DOI: 10.1016/j.canlet.2014.10.016]

96 **Abdel-Rahman O**. Targeting vascular endothelial growth factor (VEGF) pathway in gastric cancer: preclinical and clinical aspects. *Crit Rev Oncol Hematol* 2015; **93**: 18-27 [PMID: 24970311 DOI: 10.1016/j.critrevonc.2014.05.012]

97 **Fuchs CS**, Tomasek J, Yong CJ, Dumitru F, Passalacqua R, Goswami C, Safran H, dos Santos LV, Aprile G, Ferry DR, Melichar B, Tehfe M, Topuzov E, Zalcberg JR, Chau I, Campbell W, Sivanandan C, Pikiel J, Koshiji M, Hsu Y, Liepa AM, Gao L, Schwartz JD, Tabernero J. Ramucirumab monotherapy for previously treated advanced gastric or gastro-oesophageal junction adenocarcinoma (REGARD): an international, randomised, multicentre, placebo-controlled, phase 3 trial. *Lancet* 2014; **383**: 31-39 [PMID: 24094768 DOI: 10.1016/S0140-6736(13)61719-5]

98 **Álvarez P**, Marchal JA, Boulaiz H, Carrillo E, Vélez C, Rodríguez-Serrano F, Melguizo C, Prados J, Madeddu R, Aranega A. 5-Fluorouracil derivatives: a patent review. *Expert Opin Ther Pat* 2012; **22**: 107-123 [PMID: 22329541 DOI: 10.1517/13543776.2012.661413]

99 **Xu ZY**, Tang JN, Xie HX, Du YA, Huang L, Yu PF, Cheng XD. 5-Fluorouracil chemotherapy of gastric cancer generates residual cells with properties of cancer stem cells. *Int J Biol Sci* 2015; **11**: 284-294 [PMID: 25678847 DOI: 10.7150/ijbs.10248]

100 **Lee J**, Fassnacht M, Nair S, Boczkowski D, Gilboa E. Tumor immunotherapy targeting fibroblast activation protein, a product expressed in tumor-associated fibroblasts. *Cancer Res* 2005; **65**: 11156-11163 [PMID: 16322266]

101 **Ohshio Y**, Teramoto K, Hanaoka J, Tezuka N, Itoh Y, Asai T, Daigo Y, Ogasawara K. Cancer-associated fibroblast-targeted strategy enhances antitumor immune responses in dendritic cell-based vaccine. *Cancer Sci* 2015; **106**: 134-142 [PMID: 25483888 DOI: 10.1111/cas.12584]

P- Reviewer: Fujiwara T, Shi C **S- Editor**: Ma YJ
L- Editor: Wang TQ **E- Editor**: Ma S

World Journal of Gastroenterology

Submit a Manuscript: http://www.wjgnet.com/esps/
Help Desk: http://www.wjgnet.com/esps/helpdesk.aspx
DOI: 10.3748/wjg.v21.i33.9727

World J Gastroenterol 2015 September 7; 21(33): 9727-9735
ISSN 1007-9327 (print) ISSN 2219-2840 (online)

ORIGINAL ARTICLE

Basic Study

Notch1 downregulation combined with interleukin-24 inhibits invasion and migration of hepatocellular carcinoma cells

Bing Han, Shi-Hai Liu, Wei-Dong Guo, Bin Zhang, Jian-Ping Wang, Yu-Kun Cao, Jun Liu

Bing Han, Jian-Ping Wang, Yu-Kun Cao, Jun Liu, Department of Liver Transplantation and Hepatobiliary Surgery, Shandong Provincial Hospital Affiliated to Shandong University, Jinan 250021, Shandong Province, China

Shi-Hai Liu, Central Laboratory, The Affiliated Hospital of Qingdao University, Qingdao 266003, Shandong Province, China

Bing Han, Wei-Dong Guo, Bin Zhang, Department of Hepatobilliary and Pancreatic Surgery, The Affiliated Hospital of Qingdao University, Qingdao 266003, Shandong Province, China

Author contributions: Han B and Liu SH contributed equally to this work; Han B, Liu SH, Guo WD, Zhang B, Wang JP, Cao YK and Liu J designed the research; Han B, Liu SH, Wang JP and Cao YK performed the research; Han B, Liu SH, Guo WD and Zhang B analyzed the data; Han B and Liu SH wrote the paper; all authors read and approved the final manuscript.

Supported by Shandong Provincial Natural Science Foundation, China, No. ZR2012HQ039 and No. ZR2014HP065; National Natural Science Foundation of China, No. 81373172 and No.81402579.

Conflict-of-interest statement: There is no conflict of interest in this study.

Data sharing statement: No additional unpublished data are available.

Correspondence to: Jun Liu, MD, PhD, Professor, Department of Liver Transplantation and Hepatobiliary Surgery, Shandong Provincial Hospital Affiliated to Shandong University, No. 324 Jingwu Road, Jinan 250021, Shandong Province, China. dr_junliu@163.com
Telephone: +86-531-68776905
Fax: +86-531-68776905

Received: March 15, 2015
Peer-review started: March 15, 2015
First decision: April 13, 2015
Revised: June 6, 2015
Accepted: June 26, 2015
Article in press: June 26, 2015
Published online: September 7, 2015

Abstract

AIM: To confirm the anti-invasion and anti-migration effects of down-regulation of Notch1 combined with interleukin (IL)-24 in hepatocellular carcinoma (HCC) cells.

METHODS: γ-secretase inhibitors (GSIs) were used to down-regulate Notch1. HepG2 and SMMC7721 cells were seeded in 96-well plates and treated with GSI-I or/and IL-24 for 48 h. Cell viability was measured by MTT assay. The cellular and nuclear morphology was observed under a fluorescence microscope. To further verify the apoptotic phenotype, cell cultures were also analyzed by flow cytometry with Annexin V-FITC/propidium iodide staining. The expression of Notch1, SNAIL1, SNAIL2, E-cadherin, IL-24, XIAP and VEGF was detected by Western blot. The invasion and migration capacities of HCC cells were detected by wound healing assays. Notch1 and Snail were down-regulated by RNA interference, and the target proteins were analyzed by Western blot. To investigate the mechanism of apoptosis, we analyzed HepG2 cells treated with siNotch1 or siCON plus IL-24 or not for 48

h by caspase-3/7 activity luminescent assay.

RESULTS: GSI-I at a dose of 2.5 μmol/L for 24 h caused a reduction in cell viability of about 38% in HepG2 cells. The addition of 50 ng/mL IL-24 in combination with 1 or 2.5 μmol/L GSI-I reduced cell viability of about 30% and 15%, respectively. Treatment with IL-24 alone did not induce any cytotoxic effect. In SMMC7721 cells with the addition of IL-24 to GSI-I (2.5 μmol/L), the reduction of cell viability was only about 25%. Following GSI-I/IL-24 combined treatment for 6 h, the apoptotic rate of HepG2 cells was 47.2%, while no significant effect was observed in cells treated with the compounds employed separately. Decreased expression of Notch1 and its associated proteins SNAIL1 and SNAIL2 was detected in HepG2 cells. Increased E-cadherin protein expression was noted in the presence of IL-24 and GSI-I. Furthermore, the increased GSI-I and IL-24 in HepG2 cell was associated with downregulation of MMP-2, XIAP and VEGF. In the absence of treatment, HepG2 cells could migrate into the scratched space in 24 h. With IL-24 or GSI-I treatment, the wound was still open after 24 h. And the distance of the wound closure strongly correlated with the concentrations of IL-24 and GSI-I. Treatment of Notch-1 silenced HepG2 cells with 50 ng/mL IL-24 alone for 48 h induced cytotoxic effects very similar to those observed in non-silenced cells treated with GSI-I/IL-24 combination. Caspase-3/7 activity was increased in the presence of siNotch1 plus IL-24 treatment.

CONCLUSION: Down-regulation of Notch1 by GSI-I or siRNA combined with IL-24 can sensitize apoptosis and decrease the invasion and migration capabilities of HepG2 cells.

Key words: Notch signaling pathway; Interleukin-24; γ-secretase inhibitor; Invasion; Migration; Hepatocellular carcinoma

Core tip: The down-regulation of Notch1 by γ-secretase inhibitor (GSI-I) or siRNA combined with interleukin (IL)-24, could sensitize apoptosis, increase expression of E-cadherin and decrease the invasion and migration capabilities of HepG2 cells. These results indicate for the first time that GSI-I/IL-24 combination might represent a novel and potentially effective tool for hepatocellular carcinoma treatment.

Han B, Liu SH, Guo WD, Zhang B, Wang JP, Cao YK, Liu J. Notch1 downregulation combined with interleukin-24 inhibits invasion and migration of hepatocellular carcinoma cells. *World J Gastroenterol* 2015; 21(33): 9727-9735 Available from: URL: http://www.wjgnet.com/1007-9327/full/v21/i33/9727.htm DOI: http://dx.doi.org/10.3748/wjg.v21.i33.9727

INTRODUCTION

Hepatocellular carcinoma (HCC) is one of the most common cancers worldwide[1] and approximately half of these cases occurred in China[2]. Despite the development of various therapies, the outcome for HCC patients is still poor. The major reason is that HCC often relapses due to intrahepatic and distant metastases after curative surgical resection or transplantation[3]. Thus, the discovery and research of new molecular targets of blocking metastasis are the primary goal for HCC therapy.

Notch signaling is not only involved in the regulation of cell proliferation and differentiation but also plays an important role in cancer[4]. The Notch signaling pathway includes Notch ligands, negative and positive regulators, and transcription factors. The mRNA and protein expression of Notch1, which is one of the Notch signaling pathway receptors, is significantly higher in HCC than in adjacent non-tumor liver tissue in the previous report. Deregulated Notch receptor expression in human HCC was reported by Gao *et al*[5]. Snail, which is one of the zinc-finger transcription factors, has the function of repressing the transcription of the E-cadherin gene through binding to the E-boxes of the CDH1 promoter[6]. The up-regulation of Snail is also correlated with metastasis and poor prognosis, whereas decrease of Snail is critical for reducing growth and invasiveness of cancer[7,8]. Many studies have shown that E-cadherin is a cell-cell adhesion protein fulfilling a prominent role in epithelial differentiation, which is relevant to metastasis, tumor invasion, motility, and unfavorable prognosis[9-11]. E-cadherin expression is beneficial for intraepithelial expansion and invasiveness in a variety of solid tumors, as well as for the intrahepatic metastasis of HCC[12-15]. In the MHCC97L (HCC cell lines), abnormal Notch1 expression has been shown to be strongly associated with HCC metastasis, which may be regulated through the Notch1/Snail1/E-cadherin pathway[16].

Melanoma differentiation associated gene-7 (MDA-7)/interleukin-24 (IL-24) is a member of the IL-10 family, and previous reports have showed that overexpression of MDA-7/IL-24 causes tumor growth suppression and tumor cell apoptosis in lung cancer, mesotheliomas, melanoma, breast cancer, osteosarcoma, pancreatic cancer, glioblastoma, prostate cancer and so on[17-19], indicating that MDA-7/IL-24 may prove to be a potential drug for cancer therapy. MDA-7/IL-24 inhibits HepG2 and BEL-7402 cell adhesion and invasion by increasing the expression of E-cadherin and p-ERK[20].

Since Notch receptors are activated by γ-secretase, γ-secretase inhibitors (GSIs) have attracted increasing interest[21]. GSIs have been used for the treatment of Alzheimer's disease to prevent amyloid precursor protein cleavage and the consequent release of amyloid β-peptide[22]. Recently, it has been reported

that GSIs also have the ability to induce growth arrest and/or apoptosis in some tumor cell lines, while other tumor cells were resistant to the molecules[23].

In this study, we found that the IL-24 mediated apoptosis of HCC cells was sensitized by GSI-I. The down-regulation of Notch1 by siRNA or GSI-I could increase the expression of E-cadherin and decrease the invasion and migration capabilities of HepG2 cells. These *in vitro* results indicate, for the first time, that GSI-I/IL-24 combination might be used as a novel and potentially effective tool for HCC treatment.

MATERIALS AND METHODS

Cell culture and reagents

The human HCC cell lines (HepG2 and SMMC-7721 were obtained from the Cell Bank of Type Culture Collection of Chinese Academy of Sciences) were cultivated in DMEM medium supplemented with 10% FCS (fetal calf serum, Hyclone laboratories, Logan, UT, United States). All experiments were carried out using a confluent monolayer of HCC cell cultures. Cells were maintained at 37 ℃ in a humidified atmosphere containing 5% CO_2. The primary antibodies for Notch1 (120 kDa), E-cadherin (120 kDa), SNAIL1 (29 kDa), SNAIL2 (29 kDa), MMP-2 (74 kDa), XIAP (55 kDa), VEGF (31 kDa) and GAPDH (37 kDa) were purchased from Santa Cruz Biotechnology (SantaCruz, CA, United States). All secondary antibodies were obtained from Pierce (Rockford, IL, United States). Small interfering RNA (siRNA) targeting Notch1 and control siRNA (siCON) were obtained from Santa Cruz Biotechnology. Lipofectin™2000 was purchased from Life Technologies (Carlsbad, CA, United States). All other chemicals and solutions were purchased from Sigma-Aldrich unless otherwise indicated.

Cell viability assay

HepG2 and SMMC7721 cells were seeded in 96-well plates and treated with GSI-I or/and IL-24 for 48 h, separately. Then, 10 μL of 3-(4,5-dimethylthiazolyl-2) 2,5-diphenyltetrazolium bromide (MTT, 5 mg/mL, Sigma-Aldrich) was added to each well and incubated for 4 h at 37 ℃. The formazan granules were dissolved in 150 μL dimethyl sulfoxide (DMSO) for 10 min. Optical density (OD) was then measured at a wavelength of 490 nm. Each MTT assay was performed in quadruplicate and repeated three times.

Cellular and nuclear morphology analysis

In order to observe the presence of condensed chromatin and apoptotic bodies, cells were stained with Hoechst 33258 dye. Cells seeded in 96-well plates were fixed in 3:1 methanol/acetic acid for 10 min at room temperature, washed in PBS (phosphate buffered saline) and stained for 30 min in PBS with 40% paraformaldehyde and 10 μg/mL Hoechst 33258. After washing in PBS for several times, nuclear morphology was observed under a fluorescence microscope (Zeiss, Germany).

Flow cytometry analysis

To further verify the apoptotic phenotype, cell cultures were also analyzed with an Annexin V-FITC/propidium iodide (PI) kit (Roche, Manheim, Germany), according to the manufacturer's instructions. Annexin-V immunocytofluorescence was detected by flow cytometry. After various treatments, cells were collected and centrifuged. The cell pellet was washed in PBS and centrifuged again. The pellet was resuspended in Annexin-V and PI according to the manufacturer's protocol. Cells were analyzed on a Beckman flow cytometer (Beckman Coulter, Brea, CA, United States).

Protein extraction and Western blot analysis

Cells were plated in 100-mm^2 tissue culture dishes at 60% confluence and incubated overnight. After treatment, cell lysates were obtained using cold radioimmunoprecipitation assay buffer [RIPA buffer contain: 20 mmol/L Tris-HCl (pH 8.0), 100 mmol/L NaCl, 10% glycerol, 1% NP-40, and 0.5% sodium deoxycholate]. Proteins (20 mg) were separated on precasted Bis-Tris NuPAGE gels (Bio-Rad, Hercules, CA, United States), electroblotted to polyvinylidene difluoride membranes (Millipore) and then blocked for 1 h at room temperature in TBS-T [50 mmol/L Tris-HCl (pH 7.5), 150 mmol/L NaCl, and 0.1% Tween 20] containing 5% nonfat milk. Membranes were then incubated overnight at 4 ℃ or for 1 h at room temperature with the indicated primary antibodies: Notch1 (1:1000), SNAIL1 (1:500), SNAIL2 (1:1,000), E-cadherin (1:1000), IL-24 (1:1000), XIAP (1:500), VEGF (1:1000) and GAPDH (1:5000). Anti-mouse or anti-rabbit secondary antibody conjugated to horseradish peroxidase (HRP) was used to visualize the stained bands with an ECL (enhanced chemiluminescence, Santa Cruz, CA, United States) kit.

Wound healing assay

HepG2 cells were seeded in 6-well plates and cultured until confluence. A wound was then created by manually scraping the cell monolayer with a 200-microliter pipette tip. The cultures were washed twice with serum free medium to remove floating cells. The cells were then incubated in DMEM supplemented with 1% FBS. Cell migration into the wound was observed at 12 h in eight randomly selected microscopic fields for each condition and time point. Images were acquired with a Nikon DS-5M Camera System mounted on a phase-contrast Leitz microscope.

Transient protein downregulation by short interfering RNA

Scrambled (siCON) and specific siRNAs targeting Notch1 were obtained from Santa Cruz Biotechnology. Transfection of HepG2 cells was performed using the Amaxa system (Amaxa, Cologne, Germany) following their specifications. Firstly, 10^6 cells in 100 μL of medium was mixed with 3 μg siRNA and then transferred to an Amaxa-certified cuvette. For transfection, we used the

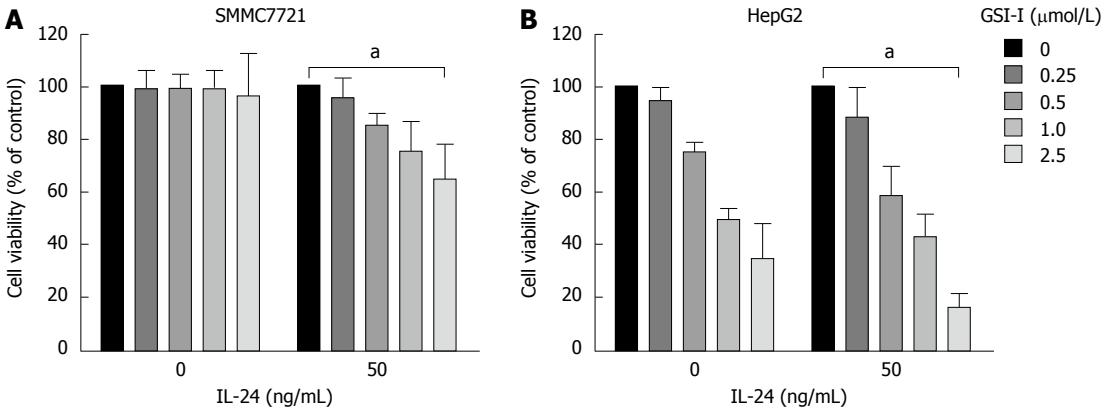

Figure 1 γ-secretase inhibitor-I/interleukin-24 combined treatment induces apoptotic cell death in hepatocellular carcinoma cells. A: Cytotoxic effects exerted on SMMC7721 cells by γ-secretase inhibitor-I (GSI-I) employed alone or in combination with recombinant interleukin (IL)-24. After treatment for 24 h cell viability was evaluated by MTT assay as reported in Materials and Methods; B: Cytotoxic effects exerted on HepG2 cells by GSI-I employed alone or in combination with recombinant IL-24. After treatment for 24 h cell viability was evaluated by MTT assay as reported in Materials and Methods. The data represent mean ± SD; $^{a}P < 0.05$ *vs* control cells.

program V-01. Transfection efficiency was between 75% and 85% (data not shown), as checked by flow cytometry, using a fluorescein-labeled non-targeted siRNA control (Cell Signaling). After 4 h cells were treated with IL-24 as indicated. Cells were examined for gene downregulation and other properties 48 h after transfection.

Viability and caspase-3/7 assays

The caspase-3/7 activity was detected with the Apo-One Homogeneous caspase-3/7 assay kit (Promega Corporation, Madison, WI). Briefly, cells were seeded into 96-well plates at a density of 2 x 10^4 cells/well, incubated overnight and subsequently treated with siCON, siNotch1 with or without IL-24. For the caspase assay, the substrate was added after treatment for 48 h (as indicated in the text) and plates were read 2 h later using a Tecan Plate Reader (Tecan, Group. Ltd., Switzerland). All treatments were done in triplicate. Background absorbance was determined by the incubating media with substrate alone or subtracting the values from wells containing cells.

Statistical analysis

Each experiment was repeated at least three times. All the experimental data are presented as mean ± SD. The differences among means were statistically analyzed by a *t*-test. All statistical analyses were performed using SPSS13.0 software (Chicago, IL, United States). $P < 0.05$ was considered statistically significant.

RESULTS

Effects of GSI-I/IL-24 combined treatment in SMMC7721 and HepG2 cells

The antiproliferative effects of GSI-I in combination with IL-24 were first examined in two hepatocellular carcinoma cell lines. Using as a single agent or in combination, the dose-response curves of the effects exerted by the compounds on cell viability are showed in Figure 1A. GSI-I at doses of 0-1 μmol/L for 24 h was almost ineffective in the cell lines. GSI-I at a dose of 2.5 μmol/L caused a remarkable reduction in cell viability of about 38% in HepG2 cells. The addition of IL-24 (at a concentration of 50 ng/mL) clearly potentiated the effects of GSI-I on HepG2 cells. IL-24 in combination with GSI-I (1 or 2.5 μmol/L) reduced cell viability of about 30% and 15%, respectively. However, treatment of cells with IL-24 alone did not induce any cytotoxic effect in the HCC cell lines. The addition of IL-24 to GSI-I treated SMMC7721 cells induced modest effects and the reduction of cell viability was only about 25%.

We next examined the effects of the two compounds IL-24 and GSI-I on cell morphology by means of light microscopy. As shown in Figure 2A (top panel), after treatment with the GSI-I/IL-24 combination for 24 h cells appeared rounded, fragmented and floated in the culture medium, while the two drugs, employed separately, did not induce any significant remarkable effect (Figure 2A). In the same experimental conditions, the nuclei stained with Hoechst 33258 and the fluorescence microscopy analysis of nuclei stained with Hoechst 33258 evidenced a significant increase in the number of cells with condensed and fragmented nuclei, which is a typical apoptotic feature (Figure 2A).

We analyzed the externalisation of phosphatidylserine on cell plasma membranes by Annexin V/PI staining to quantify early apoptotic effects. Following GSI-I/IL-24 combined treatment for 6 h, 47.2% of HepG2 cells were Annexin V positive/PI negative, while no significant effect was detected in cells treated with the compounds employed separately (Figure 2B).

GSI-I sensitizes HepG2 cells to IL-24-induced apoptosis by inhibition of Notch1-mediated epithelial-mesenchymal transition phenotype

Since Notch1 expression was associated with HCC

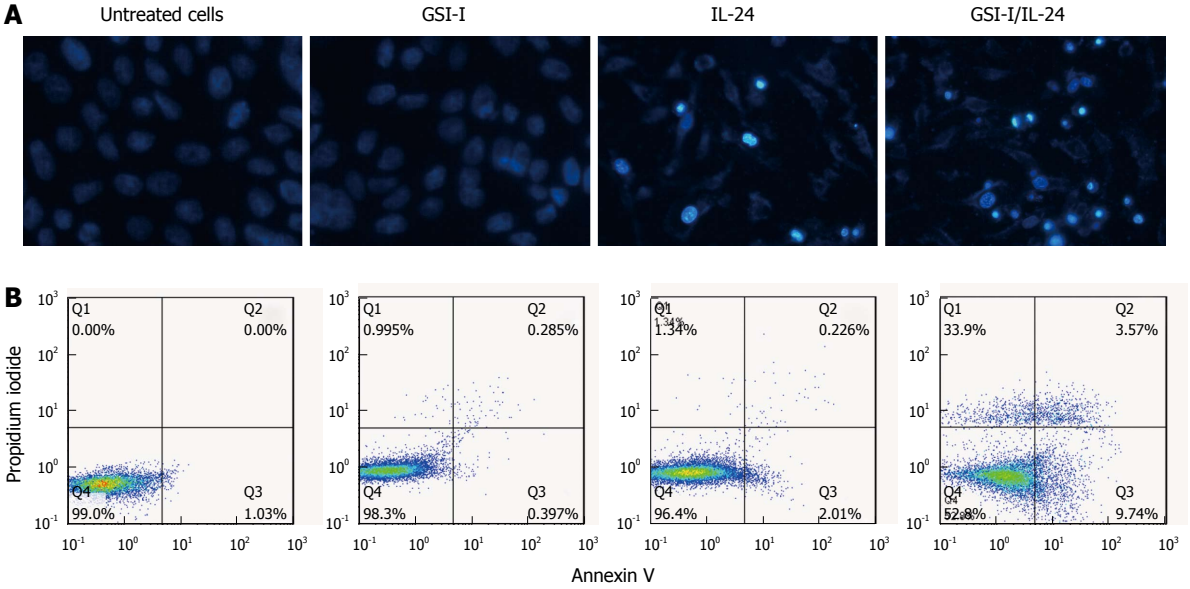

Figure 2 γ-secretase inhibitor-I/interleukin-24 combined treatment induces apoptotic cell death in hepatocellular carcinoma cells. A: Apoptotic effects induced by treatment of HepG2 cells with GSI-I and/or IL-24 for 24 h. Apoptotic morphology was evaluated by staining of the cells with Hoechst 33258 (magnification × 200); B: Annexin V positive cells were quantified by flow cytometric analysis after double staining of cells with Annexin V and propidium iodide at 6 h of treatment. Results are representative of three independent experiments. GSI-I: γ-secretase inhibitor-I; IL: Interleukin.

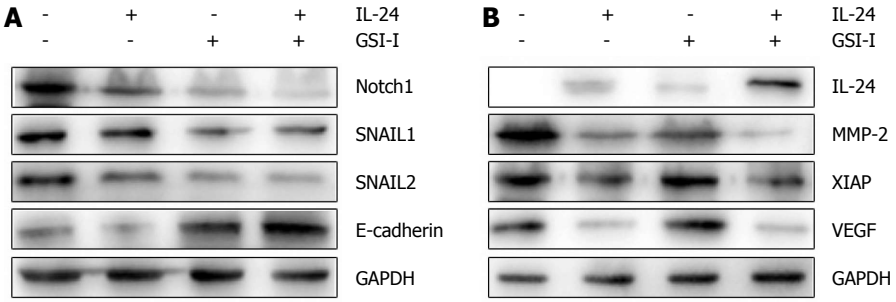

Figure 3 Cytotoxic effects of interleukin-24 and γ-secretase inhibitor-I assessed by Western blot analysis. A, B: HepG2 cells were treated for 48 h in the presence of GSI-I and/or IL-24. The levels of the proteins were determined by Western blot analysis using specific antibodies as indicated. GAPDH blots were included to show equal protein loading for all of the samples. Results are representative of three independent experiments. GSI-I: γ-secretase inhibitor-I; IL: Interleukin.

metastasis as previously reported, we further investigated the link between Notch1 expression and the epithelial-mesenchymal transition (EMT) in HCC cells. HepG2 cell line was used for a comparison of the target protein expression profile of Notch1- and EMT-related genes. Decreased expression of Notch1 and its associated proteins SNAIL1 and SNAIL2 was detected in metastatic HCC cells. Increased E-cadherin protein expression was noted in the presence of IL-24 and GSI-I (Figure 3A). Loss of E-cadherin expression is a remarkable feature of EMT. As we all know, the level of E-cadherin is inversely associated with the tumor stage. Programmed cell death can be regulated by certain factors with either pro- or anti-apoptotic action in human cells. The upregulation of the former and/or the downregulation of the latter can be considered as important events to induce cell apoptosis[24]. To this purpose, we examined the expression levels of MMP-2 and IAP family members in HepG2 cells treated with GSI-I and/or IL-24. Furthermore, we proved that increased GSI-I and IL-24 in HepG2 cancer cells were associated with downregulation of MMP-2, XIAP and VEGF (Figure 3B).

Inhibition of HCC cell invasion by GSI-I/IL-24

Wound healing assay is widely used to analyze cell proliferations and cell migration. As previously reported, for HepG2 cells, the cell invasion has a great corresponding relationship with cell migration and wound healing assay. The invasion properties of cancer cells were detected by the wound closure in these assays. In our study HepG2 cells were treated with IL-24 and/or GSI-I, and the wound closure was analyzed by microscopy. In the absence of treatment, HepG2 cells could migrate into the scratched space in 24 h (Figure 4A). With the treatment of IL-24 or GSI-I, the wound was still open after 24 h, indicating that IL-24 or GSI-I has the ability of inhibiting the HepG2 cell migration or invasion (Figure 4B and C). To further confirm the inhibition effectiveness, we loaded the cells

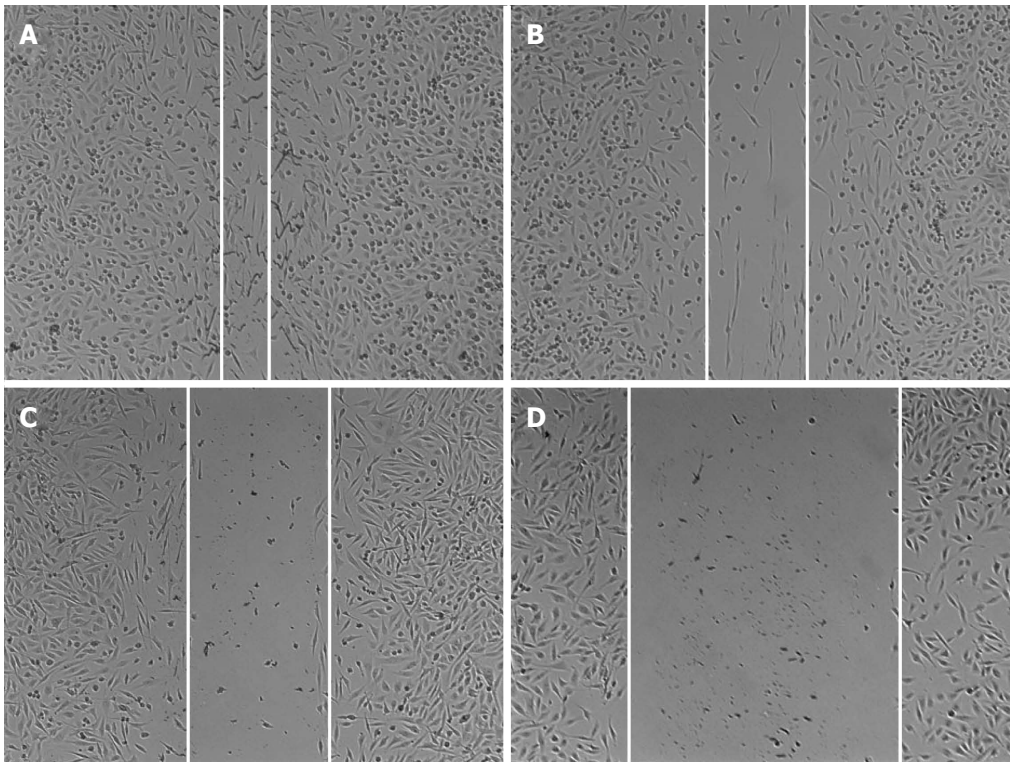

Figure 4 Wound healing in HepG2 cells treated with γ-secretase inhibitor-I and/or interleukin-24. Representative wounds after scratch wounding and after healing were recorded with a microscope (A-D). A: Control HepG2 cells; B: HepG2 cells treated with GSI-I; C: HepG2 cells treated with IL-24; D: HepG2 cells treated with GSI-I and IL-24. GSI-I: γ-secretase inhibitor-I; IL: Interleukin.

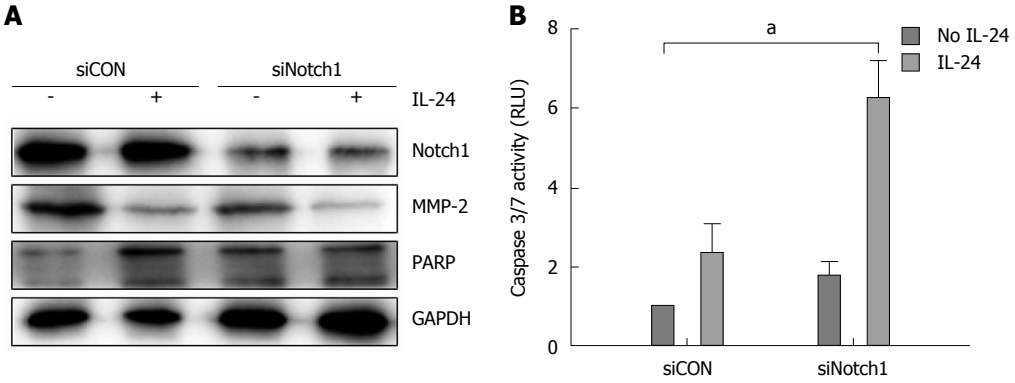

Figure 5 RNA interfering against Notch-1 in combination with interleukin-24 treatment in HepG2 cells. HepG2 cells were transfected for 48 h with siNotch-1 or siScr. Cells were treated with IL-24 for 48 h. A: Western blot analysis of the levels of Notch-1, MMP-2 and PARP was performed after siCON or siNotch1 treatment as reported in Materials and Methods; B: Caspase 3/7 activity was estimated by luminescent assay. $^{a}P < 0.05$ *vs* siCON in HepG2 cells.

with IL-24 and GSI-I. The distance of the wound closure significantly correlated with the concentrations of IL-24 and GSI-I (Figure 4).

Notch signaling knockdown promotes IL-24-induced apoptosis

It has been showed that GSIs can act through different biochemical pathways, and we next investigated whether the effects induced by GSI-I/IL-24 combination were related to the specific inhibition of Notch signaling caused by GSI-I. We downregulated the Notch gene and evaluated the biological effects of IL-24 addition. Notch-1, as demonstrated by the authors, is upstream of Notch-4. After confirming the downregulation of Notch-1 level (Figure 5A, upper panel), we analyzed the biological effect of IL-24 addition on HepG2 cell viability. MMP-2 and poly (ADP)-ribose polymerase (PARP) proteins are the key proteins in detecting cell apoptosis. Figure 5A demonstrated that treatment of Notch-1 silenced HepG2 cells with 50 ng/mL IL-24 alone for 48 h induced cytotoxic effects quite similar to those observed in non-silenced cells treated with GSI-I/IL-24 combination.

To investigate the mechanism of apoptosis, we analyzed HepG2 cells treated with siNotch1 or siCON plus IL-24 or not for 48 h by caspase-3/7 activity

analysis. Caspase-3/7 activity was increased in the addition of siNotch1 plus IL-24 treatment, indicating that siNotch1 plus IL-24 could sensitize HCC cells to the cytotoxic agents (Figure 5B)

DISCUSSION

We previously reported that LIGHT protein inhibited the proliferation and induced the apoptosis of HepG2 cells significantly[25]. However, little is known about the mechanism of HCC cell apoptosis. A large number of studies have showed that Notch signaling plays an important role in many kinds of malignant tumors[26-28]. Expression and localization of Notch receptors and their ligands have been observed in the normal human liver tissue in the previous report, while the deregulated Notch signaling has been found in malignant liver tumors[29-31].

This study was to investigate the biological effect of GSI-I, which is one of the most frequently employed GSIs. The association of IL-24 and GSIs arose by the observation that many tumor cells develop IL-24 sensitivity which can be overcome in the presence of different compounds. Although displaying anticancer potential, GSIs often show toxic side effects in some cells. Our data presented in this paper demonstrate a strong synergistic interaction between GSI-I and IL-24 which effectively reduced HCC cell viability for the first time. Noteworthy, GSI-I/IL-24 combined treatment was particularly effective in SMMC7721 and HepG2 cells (Figure 1).

Morphological observations demonstrated that HepG2 cell death was correlated with the induction of cell apoptosis; cells were positive for Annexin V/PI staining and the nuclei presented chromatin condensation (Figure 2A and B). After combined treatment, the activation of apoptotic pathway was also confirmed by Western blot.

Many studies indicated that GSI-I could be responsible for sensitization of cells to IL-24-mediated apoptosis and some of these are related to the activity of GSI-I, which is the inhibitor of γ-secretase, the main enzyme responsible for the cleavage and activation of Notch receptor and the following target proteins[32]. Data reported in this paper demonstrated that GSI-I/IL-24 combined treatment was able to modulate the expression level of related proteins in HepG2 cells (Figure 3).

Which GSI-I may sensitize HepG2 cells to apoptosis induced by IL-24 seems to be related to the modulation of pro- and anti-apoptotic factors through? In many experimental studies, the decreased survival factors and the concomitantly increased pro-apoptotic ones trigger a pathway that leads to cell death. Furthermore, a cross-talk has been showed between Notch signaling and the expression of some of these related signal pathway factors.

Sahlgren *et al*[33] reported that Notch signaling deploys a mechanism that acts in synergy to control the expression of SNAIL1 and SNAIL2, two critical regulators of EMT. Data of our study indicate that in HepG2 cells, besides the effects on SNAIL1 and SNAIL2, treatment with GSI-I/IL-24 combination also induced a clear upregulation of E-cadherin expression, which can be considered a key factor in cell growth and survival, together with that of MMP-2 factor. Moreover, some members of the tumor blood vessels related factors, such as XIAP and VEGF, are also downregulated following combined treatment with the two compounds (Figure 3).

The core role of Notch in HepG2 death pathway induced by GSI-I/IL-24 combination was also confirmed by Notch silencing experiments. In siNotch treated cells, we observed a decrease in the levels of both MMP-2 and PARP similar to that observed after GSI-I/IL-24 treatment (Figure 5A). Moreover, in siNotch silenced cells treated with IL-24 alone we also detected the Caspase 3/7 activity which is similar to that obtained after GSI-I/IL-24 combined treatment (Figure 5B). Overall, data reported seem to indicate that the synergistic effects induced by siNotch1/IL-24 combination are a specific consequence of GSI-I action on γ-secretase activity.

In conclusion, we found that the down-regulation of Notch1 by GSI-I or siRNA combined with IL-24 can sensitize apoptosis and increase expression of E-cadherin and decrease the invasion and migration capabilities of HepG2 cells. Taken together, these results demonstrated that GSI-I/IL-24 combination might represent a novel and potentially effective tool for HCC treatment for the first time.

COMMENTS

Background

Hepatocellular carcinoma (HCC) is one of the most common malignancies worldwide and half of these cases were estimated to occur in China. The major reason for the poor prognosis is that HCC often relapses due to intrahepatic and distant metastases. Thus, the discovery and research of new molecular targets of blocking metastasis are the primary goal for HCC therapy.

Research frontiers

Notch signaling pathway plays an important role in HCC metastasis. Notch1, one of the Notch pathway receptors, is significantly higher in HCC than in adjacent non-tumor liver tissue. Abnormal Notch1 expression has been shown to be strongly associated with HCC metastasis, which may be mediated through the Notch1/Snail1/E-cadherin pathway. Interleukin (IL)-24 mediates the inhibition of adhesion and invasion of HepG2 and BEL-7402 cells by increasing the expression of E-cadherin and p-ERK.

Innovations and breakthroughs

To date, there is no study regarding synergistic effect of Notch1 down-regulation and IL-24 on apoptosis, invasion and migration of HCC cells. In this study, the authors found that the down-regulation of Notch1 by γ-secretase inhibitor-I (GSI-I) or siRNA combined with IL-24 can sensitize apoptosis and decrease the invasion and migration capabilities of HepG2 cells. Furthermore, the authors researched the mechanism and found that besides the inhibiting effects on SNAIL1 and SNAIL2, treatment with GSI-I/IL-24 combination also induced a clear up-regulation of E-cadherin and down-regulation of MMP-2.

Applications

In understanding the role and mechanism of Notch1/Snail1/E-cadherin pathways in inhibiting invasion and migration of HCC cell lines, this study indicate, for the first time, that GSI-I/IL-24 combination might represent a novel and potentially effective tool for HCC treatment.

Terminology

All Notch receptors are activated by γ-secretase, and the inhibitors of this enzyme (GSIs) have attracted increasing interest. GSIs were firstly employed in the treatment of Alzheimer's disease to prevent amyloid precursor protein cleavage and the consequent release of amyloid β-peptide. More recently, it has been observed that GSIs also possess the ability to induce growth arrest and/or apoptosis in some tumor cell lines while other tumor cells were resistant to the molecules.

Peer-review

In this paper the role of Notch 1 deregulation in HCC has been evaluated. It was observed a decrease in HCC cell invasion and migration by Notch1 down-regulation. Notch 1 inhibition by GSI-I increased HCC cell apoptosis induced by IL-24. The down-regulation of Notch1 by specific siRNA or GSI-I increased E-cadherin expression and inhibited HCC cell invasion and migration. It is concluded that a combination therapy of GSI-I/IL-24 may be a novel and potentially effective treatment for HCC.

REFERENCES

1 **Yu MC**, Yuan JM, Govindarajan S, Ross RK. Epidemiology of hepatocellular carcinoma. *Can J Gastroenterol* 2000; **14**: 703-709 [PMID: 11185536]

2 **Singh SD**, Ajani UA, Johnson CJ, Roland KB, Eide M, Jemal A, Negoita S, Bayakly RA, Ekwueme DU. Association of cutaneous melanoma incidence with area-based socioeconomic indicators-United States, 2004-2006. *J Am Acad Dermatol* 2011; **65**: S58-S68 [PMID: 22018068 DOI: 10.1016/j.jaad.2011.05.035]

3 **Tung-Ping Poon R**, Fan ST, Wong J. Risk factors, prevention, and management of postoperative recurrence after resection of hepatocellular carcinoma. *Ann Surg* 2000; **232**: 10-24 [PMID: 10862190]

4 **Artavanis-Tsakonas S**, Rand MD, Lake RJ. Notch signaling: cell fate control and signal integration in development. *Science* 1999; **284**: 770-776 [PMID: 10221902]

5 **Gao J**, Song Z, Chen Y, Xia L, Wang J, Fan R, Du R, Zhang F, Hong L, Song J, Zou X, Xu H, Zheng G, Liu J, Fan D. Deregulated expression of Notch receptors in human hepatocellular carcinoma. *Dig Liver Dis* 2008; **40**: 114-121 [PMID: 17920003]

6 **Giroldi LA**, Bringuier PP, de Weijert M, Jansen C, van Bokhoven A, Schalken JA. Role of E boxes in the repression of E-cadherin expression. *Biochem Biophys Res Commun* 1997; **241**: 453-458 [PMID: 9425291 DOI: 10.1006/bbrc.1997.7831]

7 **Perl AK**, Wilgenbus P, Dahl U, Semb H, Christofori G. A causal role for E-cadherin in the transition from adenoma to carcinoma. *Nature* 1998; **392**: 190-193 [PMID: 9515965 DOI: 10.1038/32433]

8 **Moody SE**, Perez D, Pan TC, Sarkisian CJ, Portocarrero CP, Sterner CJ, Notorfrancesco KL, Cardiff RD, Chodosh LA. The transcriptional repressor Snail promotes mammary tumor recurrence. *Cancer Cell* 2005; **8**: 197-209 [PMID: 16169465 DOI: 10.1016/j.ccr.2005.07.009]

9 **Bremnes RM**, Veve R, Gabrielson E, Hirsch FR, Baron A, Bemis L, Gemmill RM, Drabkin HA, Franklin WA. High-throughput tissue microarray analysis used to evaluate biology and prognostic significance of the E-cadherin pathway in non-small-cell lung cancer. *J Clin Oncol* 2002; **20**: 2417-2428 [PMID: 12011119]

10 **Tsujii M**, DuBois RN. Alterations in cellular adhesion and apoptosis in epithelial cells overexpressing prostaglandin endoperoxide synthase 2. *Cell* 1995; **83**: 493-501 [PMID: 8521479]

11 **Liu D**, Huang C, Kameyama K, Hayashi E, Yamauchi A, Kobayashi S, Yokomise H. E-cadherin expression associated with differentiation and prognosis in patients with non-small cell lung cancer. *Ann Thorac Surg* 2001; **71**: 949-954; discussion 954-955 [PMID: 11269479]

12 **Wei Y**, Van Nhieu JT, Prigent S, Srivatanakul P, Tiollais P, Buendia MA. Altered expression of E-cadherin in hepatocellular carcinoma: correlations with genetic alterations, beta-catenin expression, and clinical features. *Hepatology* 2002; **36**: 692-701 [PMID: 12198663 DOI: 10.1053/jhep.2002.35342]

13 **Bignell GR**, Warren W, Seal S, Takahashi M, Rapley E, Barfoot R, Green H, Brown C, Biggs PJ, Lakhani SR, Jones C, Hansen J, Blair E, Hofmann B, Siebert R, Turner G, Evans DG, Schrander-Stumpel C, Beemer FA, van Den Ouweland A, Halley D, Delpech B, Cleveland MG, Leigh I, Leisti J, Rasmussen S. Identification of the familial cylindromatosis tumour-suppressor gene. *Nat Genet* 2000; **25**: 160-165 [PMID: 10835629 DOI: 10.1038/76006]

14 **Osada T**, Sakamoto M, Ino Y, Iwamatsu A, Matsuno Y, Muto T, Hirohashi S. E-cadherin is involved in the intrahepatic metastasis of hepatocellular carcinoma. *Hepatology* 1996; **24**: 1460-1467 [PMID: 8938181 DOI: 10.1053/jhep.1996.v24.pm0008938181]

15 **Tomlinson JS**, Alpaugh ML, Barsky SH. An intact overexpressed E-cadherin/alpha,beta-catenin axis characterizes the lymphovascular emboli of inflammatory breast carcinoma. *Cancer Res* 2001; **61**: 5231-5241 [PMID: 11431364]

16 **Wang XQ**, Zhang W, Lui EL, Zhu Y, Lu P, Yu X, Sun J, Yang S, Poon RT, Fan ST. Notch1-Snail1-E-cadherin pathway in metastatic hepatocellular carcinoma. *Int J Cancer* 2012; **131**: E163-E172 [PMID: 22052196 DOI: 10.1002/ijc.27336]

17 **Jiang H**, Lin JJ, Su ZZ, Goldstein NI, Fisher PB. Subtraction hybridization identifies a novel melanoma differentiation associated gene, mda-7, modulated during human melanoma differentiation, growth and progression. *Oncogene* 1995; **11**: 2477-2486 [PMID: 8545104]

18 **Allen M**, Pratscher B, Roka F, Krepler C, Wacheck V, Schöfer C, Pehamberger H, Müller M, Lucas T. Loss of novel mda-7 splice variant (mda-7s) expression is associated with metastatic melanoma. *J Invest Dermatol* 2004; **123**: 583-588 [PMID: 15304100 DOI: 10.1111/j.0022-202X.2004.23321.x]

19 **Yacoub A**, Mitchell C, Hong Y, Gopalkrishnan RV, Su ZZ, Gupta P, Sauane M, Lebedeva IV, Curiel DT, Mahasreshti PJ, Rosenfeld MR, Broaddus WC, James CD, Grant S, Fisher PB, Dent P. MDA-7 regulates cell growth and radiosensitivity in vitro of primary (non-established) human glioma cells. *Cancer Biol Ther* 2004; **3**: 739-751 [PMID: 15197348]

20 **Huo W**, Li ZM, Zhu XM, Bao YM, An LJ. MDA-7/IL-24 suppresses tumor adhesion and invasive potential in hepatocellular carcinoma cell lines. *Oncol Rep* 2013; **30**: 986-992 [PMID: 23722307 DOI: 10.3892/or.2013.2507]

21 **Bergmans BA**, De Strooper B. gamma-secretases: from cell biology to therapeutic strategies. *Lancet Neurol* 2010; **9**: 215-226 [PMID: 20129170 DOI: 10.1016/S1474-4422(09)70332-1]

22 **Panza F**, Frisardi V, Imbimbo BP, Capurso C, Logroscino G, Sancarlo D, Seripa D, Vendemiale G, Pilotto A, Solfrizzi V. REVIEW: γ-Secretase inhibitors for the treatment of Alzheimer's disease: The current state. *CNS Neurosci Ther* 2010; **16**: 272-284 [PMID: 20560993 DOI: 10.1111/j.1755-5949.2010.00164.x]

23 **Lin J**, Zhang XM, Yang JC, Ye YB, Luo SQ. γ-secretase inhibitor-I enhances radiosensitivity of glioblastoma cell lines by depleting CD133+ tumor cells. *Arch Med Res* 2010; **41**: 519-529 [PMID: 21167391 DOI: 10.1016/j.arcmed.2010.10.006]

24 **Youle RJ**, Strasser A. The BCL-2 protein family: opposing activities that mediate cell death. *Nat Rev Mol Cell Biol* 2008; **9**: 47-59 [PMID: 18097445 DOI: 10.1038/nrm2308]

25 **Han B**, Wu LQ, Ma X, Wang ZH, Li JP, Bi CY, Yong S. Synergistic effect of IFN-γ gene on LIGHT-induced apoptosis in HepG2 cells via down regulation of Bcl-2. *Artif Cells Blood Substit Immobil Biotechnol* 2011; **39**: 228-238 [PMID: 21117871 DOI: 10.3109/10731199.2010.538403]

26 **Sjölund J**, Manetopoulos C, Stockhausen MT, Axelson H. The Notch pathway in cancer: differentiation gone awry. *Eur J Cancer* 2005; **41**: 2620-2629 [PMID: 16239105 DOI: 10.1016/j.ejca.2005.06.025]

27 **Espinoza I**, Pochampally R, Xing F, Watabe K, Miele L. Notch signaling: targeting cancer stem cells and epithelial-to-mesenchymal

transition. *Onco Targets Ther* 2013; **6**: 1249-1259 [PMID: 24043949 DOI: 10.2147/OTT.S36162]

28 **Takebe N**, Nguyen D, Yang SX. Targeting notch signaling pathway in cancer: clinical development advances and challenges. *Pharmacol Ther* 2014; **141**: 140-149 [PMID: 24076266 DOI: 10.1016/j.pharmthera.2013.09.005]

29 **Nijjar SS**, Crosby HA, Wallace L, Hubscher SG, Strain AJ. Notch receptor expression in adult human liver: a possible role in bile duct formation and hepatic neovascularization. *Hepatology* 2001; **34**: 1184-1192 [PMID: 11732008 DOI: 10.1053/jhep.2001.29399]

30 **Zhou L**, Wang DS, Li QJ, Sun W, Zhang Y, Dou KF. Downregulation of the Notch signaling pathway inhibits hepatocellular carcinoma cell invasion by inactivation of matrix metalloproteinase-2 and -9 and vascular endothelial growth factor. *Oncol Rep* 2012; **28**: 874-882 [PMID: 22736202 DOI: 10.3892/or.2012.1880]

31 **Viatour P**, Ehmer U, Saddic LA, Dorrell C, Andersen JB, Lin C, Zmoos AF, Mazur PK, Schaffer BE, Ostermeier A, Vogel H, Sylvester KG, Thorgeirsson SS, Grompe M, Sage J. Notch signaling inhibits hepatocellular carcinoma following inactivation of the RB pathway. *J Exp Med* 2011; **208**: 1963-1976 [PMID: 21875955 DOI: 10.1084/jem.20110198]

32 **Benedito R**, Rocha SF, Woeste M, Zamykal M, Radtke F, Casanovas O, Duarte A, Pytowski B, Adams RH. Notch-dependent VEGFR3 upregulation allows angiogenesis without VEGF-VEGFR2 signalling. *Nature* 2012; **484**: 110-114 [PMID: 22426001 DOI: 10.1038/nature10908]

33 **Sahlgren C**, Gustafsson MV, Jin S, Poellinger L, Lendahl U. Notch signaling mediates hypoxia-induced tumor cell migration and invasion. *Proc Natl Acad Sci USA* 2008; **105**: 6392-6397 [PMID: 18427106 DOI: 10.1073/pnas.0802047105]

P- Reviewer: Tsegmed U **S- Editor**: Ma YJ
L- Editor: Wang TQ **E- Editor**: Wang CH

World Journal of Gastroenterology

Submit a Manuscript: http://www.wjgnet.com/esps/
Help Desk: http://www.wjgnet.com/esps/helpdesk.aspx
DOI: 10.3748/wjg.v21.i33.9736

World J Gastroenterol 2015 September 7; 21(33): 9736-9740
ISSN 1007-9327 (print) ISSN 2219-2840 (online)

ORIGINAL ARTICLE

Retrospective Cohort Study

Comparison of two types of colectomy in treating slow transit constipation with or without melanosis coli

Ji-Wei Sun, Jia-Ni Gu, Peng Du, Wei Chen

Ji-Wei Sun, Jia-Ni Gu, Peng Du, Wei Chen, Department of Anal and Rectal Surgery, Xin Hua Hospital Affiliated to Shanghai Jiao Tong University School of Medicine, Shanghai 200092, China

Author contributions: Sun JW and Chen W designed the research; Sun JW, Gu JN and Du P performed the research; Du P analyzed the data; Sun JW wrote the paper; and Chen W critically revised the manuscript for important intellectual content.

Institutional review board statement: The study was reviewed and approved by the Xin Hua Hospital Institutional Review Board.

Informed consent statement: All study participants, or their legal guardian, provided informed written consent prior to study enrollment.

Conflict-of-interest statement: We declare that we have no financial or personal relationships with other people or organizations that can inappropriately influence our work, and there is no professional or other personal interest of any nature or kind in any product, service and/or company that could be construed as influencing the position presented in, or the review of, the manuscript.

Data sharing statement: Technical appendix, statistical code, and dataset available from the corresponding author at xinhuawmz1@126.com. Participants gave informed consent for data sharing. No additional data are available.

Correspondence to: Wei Chen, MD, Professor, Department of Anal and Rectal Surgery, Xin Hua Hospital Affiliated to Shanghai Jiao Tong University School of Medicine, No. 1665 Kongjiang Street, Shanghai 200092, China. xinhuawmz1@126.com

Telephone: +86-21-25078999
Fax: +86-21-25078999

Received: December 13, 2014
Peer-review started: December 16, 2014
First decision: January 22, 2015
Revised: February 27, 2015
Accepted: June 10, 2015
Article in press: June 10, 2015
Published online: September 7, 2015

Abstract

AIM: To compare the follow-up outcomes of ileosigmoidal anastomosis (ISA) and caecorectal anastomosis (CRA) in patients with slow transit constipation (STC) with or without melanosis coli (MC).

METHODS: We collected the clinical data of 48 STC patients with or without MC from May 2002 to May 2007. Twenty-six patients underwent CRA (14 with MC) and 22 cases received ISA (14 with MC). A 3-year postoperative follow-up was conducted.

RESULTS: CRA improved the quality of life [evaluated by the gastrointestinal quality of life index (GIQLI)] in patients without MC, but was inferior to ISA in stool frequency and Wexner and GIQLI scores for MC patients. In the CRA group, patients with MC suffered worse outcomes than those without MC.

CONCLUSION: CRA is more suitable for STC patients without MC; however, for STC patients with MC, ISA is a better choice.

Key words: Constipation; Melanosis coli; Caecorectal anastomosis; Ileosigmoidal anastomosis; Prognosis

Core tip: The optimal surgical treatment for slow transit constipation (STC) is controversial. Based on our study, caecorectal anastomosis is more suitable for STC without melanosis coli (MC). However, for STC with MC, ileosigmoidal anastomosis, with a lower postoperative recurrence rate, is a better choice.

Sun JW, Gu JN, Du P, Chen W. Comparison of two types of colectomy in treating slow transit constipation with or without melanosis coli. *World J Gastroenterol* 2015; 21(33): 9736-9740 Available from: URL: http://www.wjgnet.com/1007-9327/full/v21/i33/9736.htm DOI: http://dx.doi.org/10.3748/wjg.v21.i33.9736

INTRODUCTION

Slow transit constipation (STC) is characterized by delay in the transit of stool in the presence of a morphologically normal colon and rectum[1,2]. Most patients experience long-term use of anthraquinone laxatives such as senna, aloe capsules, and maren pills, which may damage colonic epithelial cells and cause irreversible injury to organelles, finally resulting in colonic melanosis coli (MC)[3,4].

When medical treatment fails, surgery becomes the final effective choice[5,6]. Since Lane first reported that colectomy was an effective treatment in 1908, many different types of colectomy have been developed[7]. For example, ileosigmoidal anastomosis (ISA), caecorectal anastomosis (CRA) and colonic exclusion, a modified Duhamel procedure, have been developed. Currently, IRA and CRA are the most frequently adopted procedures, although there is still debate about which procedure is best[8-10]. In addition, whether MC is an important factor in choosing a surgical procedure has not been explored previously.

For this retrospective study we analyzed 3 years of follow-up data, investigated the post-operative outcomes regarding stool frequency per day, Wexner scores and gastrointestinal quality of life index (GIQLI) scores following colectomy for 48 STC patients with or without MC, with the aim of comparing the two procedures.

MATERIALS AND METHODS

Patients

We performed a retrospective study on 48 patients with STC diagnosed in the Department of Colorectal Surgery, Xinhua Hospital affiliated with the Shanghai University School of Medicine from May 2002 to May 2007 (Table 1).

All patients underwent pre-operative tests including: (1) repeated colonic transit time (CTT) study; (2) colonoscopy and multi-mucosa biopsy; (3) defecography; (4) anorectal manometry; and (5) radiopaque marker studies. Slow transit was defined as retention of more than 12 of 20 radiopaque markers.

Patients were enrolled in this study after satisfying the following criteria: (1) diagnosed as having chronic constipation according to Rome Ⅲ diagnosing criteria and preoperative tests[11]; (2) chronic constipation lasting for more than 3 years; and (3) failed conservative treatment for at least 2 years, such as oral laxatives, bowel cleansing solutions, and enemas or suppositories.

The exclusion criteria were as follows: (1) suspicion of organic colon diseases such as tumor, ankylenteron or congenital megacolon; and (2) patients with absolute surgical contraindication, for example, acute myocardial infarction within 6 mo, cardiac and respiratory failure, severe pulmonary infection and arrhythmia, diabetic ketoacidosis with blood glucose exceeding 11.1 mol/L, and mental disorder.

MC was diagnosed according to colonoscopic and histopathologic appearance, *i.e.*, brown or black pigmentation located in the colon mucosa and lamina propria.

All operations were performed by the same colorectal surgical team. Each patient who was accepted for colectomy signed an informed consent form and the study was approved by the Ethics Committee of Xinhua Hospital.

Data collection and follow-up

Clinical data regarding the Wexner constipation score (WCS)[12] and GIQLI score[13] were obtained by telephone interviews 3 years postoperatively. The Wexner constipation scale is a validated and internationally adopted questionnaire used to quantify the severity of constipation. It consists of questions examining the various clinical expressions of constipation, with scores ranging from 0 (best) to 30 (worst). The GIQLI is a validated quality-of-life questionnaire designed to evaluate specific gastrointestinal symptoms and the impact of the disease on the physical, psychological, and social spheres of the patient.

Statistical analysis

Statistical analyses were performed using SPSS 19.0 (SPSS, Inc., Chicago, IL, United States). Non-parametric analysis was performed by using a Wilcoxon signed rank test. A χ^2 criterion and a Fisher exact test were utilized to analyze contingency data. $P < 0.05$ was considered statistically significant. Values are expressed as mean ± SD.

RESULTS

Patient characteristics

A total of 48 patients were enrolled in the study, of whom 27 (56.2%) were female. The average age was 54.2 years. Constipation was the primary

Table 1 Patient characteristics

Variable	*n*	Gender (M/F)	Age (yr)	Duration of constipation (yr)	Number of stools per week (preoperative)
ISA	22				
With MC	14	6/8	54.8 ± 12.3	12 ± 3	1.1 ± 0.3
Without MC	8	4/4	52.6 ± 11.3	10 ± 2	1.2 ± 0.4
CRA	26				
With MC	14	7/7	53.1 ± 10.5	9 ± 2	1.0 ± 0.3
Without MC	12	4/8	55.8 ± 13.0	8 ± 2	1.1 ± 0.4

ISA: Ileosigmoidal anastomosis; MC: Melanosis coli; CRA: Caecorectal anastomosis.

Table 2 Three-year postoperative follow-up of ileosigmoidal anastomosis and caecorectal anastomosis

Variable	ISA			CRA		
	With MC (*n* = 14)	Without MC (*n* = 8)	Total (*n* = 22)	With MC (*n* = 14)	Without MC (*n* = 12)	Total (*n* = 26)
Number of stools (per day)	4.5 ± 1.8	5.5 ± 2.4	4.9 ± 2.0	1.7 ± 1.3[a]	3.0 ± 1.4[a,c]	2.3 ± 1.5[a]
Wexner scores	5.0 ± 1.5	4.9 ± 1.2	5.0 ± 1.4	3.1 ± 1.4[a]	3.3 ± 1.5[a]	3.2 ± 1.4[a]
GIQLI	106 ± 9	103 ± 12	105 ± 10	100 ± 6[a]	116 ± 6[a,c]	107 ± 10

[a]$P < 0.05$, ISA group *vs* CRA group; [c]$P < 0.05$, MC group *vs* no-MC group in respective subgroups. ISA: Ileosigmoidal anastomosis; MC: Melanosis coli; CRA: Caecorectal anastomosis; GIQLI: Gastrointestinal quality of life index.

symptom of all patients with an average duration of 9.8 years before the operation. The mean preoperative frequency of stools was 1.1 times per week and all patients had enema and laxative use history. No significant differences were detected between the two groups regarding gender, age, duration of constipation and number of stools per week (Table 1). Finally, 26 patients underwent CRA and 22 patients underwent ISA.

The mean follow-up was 3 years. No mortality was found. According to interviews, patients who underwent ISA had higher postoperative defecation frequencies (4.9 ± 2.0 *vs* 2.3 ± 1.5, $P < 0.01$), higher Wexner scores (5.0 ± 1.4 *vs* 3.2 ± 1.4, $P < 0.01$) and equal GIQLI scores ($P > 0.05$; Table 2). Focusing on STC with MC patients, the ISA group was superior to the CRA group based on the three criteria. However, in STC patients without MC, the ISA group had a higher stool frequency per day (5.5 ± 2.4 *vs* 3.0 ± 1.4, $P < 0.01$), higher Wexner scores (4.9 ± 1.2 *vs* 3.3 ± 1.5, $P < 0.01$), but lower GIQLI scores (103 ± 12 *vs* 116 ± 6, $P < 0.05$). In patients who underwent ISA, no significant difference was found between the MC and no-MC groups. Oppositely, a statistical difference was detected regarding defecation frequency (1.7 ± 1.3 *vs* 3.0 ± 1.4, $P < 0.05$) and GIQLI score (100 ± 6 *vs* 116 ± 6, $P < 0.01$) between the MC and no-MC groups.

DISCUSSION

The surgical treatment for constipation has long been a subject for debate. In China, the most frequently practiced procedure for STC is subtotal colectomy with CRA but not ISA, because former procedure preserves the ileocecal valve and reduces the possibility of postoperative diarrhea and malnutrition[14-17]. However, some surgeons have reported a higher recurrence rate with CRA[18-20]. In this study, we compared the 3-year follow-up outcomes of CRA with ISA and found that CRA improved the quality of life (evaluated by GIQLI scores) in patients without MC compared with ISA, but was inferior to ISA for patients with MC evaluated by stool frequency, Wexner and GIQLI scores. Two of MC patients undergoing CRA suffered from constipation recurrence. Further analysis showed that there were significant differences between MC and no-MC patients who underwent CRA regarding defecation frequency and GIQLI score. According to our results, it is recommended that CRA is suitable for STC without MC, and ISA is a better choice for STC with MC. It is hoped that this conclusion will provide a helpful suggestion when making clinical choice between CRA and ISA.

Feng *et al*[21] have compared CRA and ISA by functional outcomes, and they draw the conclusion that ISA is the superior method because it generates increased patient satisfaction, while the CRA procedure can be performed for selected patients with distal colonic inertia. Certainly, differences in the specific criteria (with or without MC) used to define subgroup could contribute to the differences between the present study and that of Knowles *et al*[22]. What's more, the standard evaluation system such as Wexner and GIQLI scores was more objective and accurate than counting single symptom[23,24].

Since first reported by Freeman *et al*[25] in 1829, MC has been found to be associated with constipation and use of laxatives. The incidence of MC was 44.4% in STC patients[26], which was in accord with our colonoscopic findings. The abnormal brown or black pigmentation was most intense and most readily

detected in the cecum and ascending colon[27-29], which appear to be the remaining part of colon after CRA. This may be the reason for unfavorable clinical outcomes and constipation recurrence. In addition, MC may contribute to colonic vegetative nerve dysfunction, especially at the ileocecum[30]. CRA is not a good choice to solve this problem.

This study preliminarily probed the choice of surgical procedures in treating STC with or without MC and had some limitations. First, the precise mechanism to determine which STC patients with MC were prone to recur remains unknown. Second, a larger sample size and further research are necessary to validate our conclusions. Lastly, this research was a retrospective study with limited clinical credibility and randomized clinical trials are necessary to confirm the conclusion.

COMMENTS

Background

Slow transit constipation (STC) is characterized by delay in the transit of stool in the presence of a morphologically normal colon and rectum. Currently, ileosigmoidal anastomosis (ISA) and caecorectal anastomosis (CRA) are the most frequently adopted procedures, although there is still debate about which procedure is best. Establishing the respective indication of the two procedures (ISA and CRA) is of clinical need.

Research frontiers

The surgical treatment for constipation has long been a subject for debate. In China, the most frequently practiced procedure for STC is subtotal colectomy with CRA but not ISA, because the former procedure preserves the ileocecal valve and reduces the possibility of postoperative diarrhea and malnutrition. However, some surgeons have reported a higher recurrence rate of STC with CRA. An important research hotspot in this area is to establish the respective indication of each procedure to reach better clinical outcome.

Innovations and breakthroughs

Studies have been conducted to compare CRA and ISA by functional outcomes. Some believed that ISA is the superior method because it generates increased patient satisfaction, however, some demonstrated that CRA would be more suite for selected patients with distal colonic inertia. This study is the first to utilize the diagnosis of melanosis coli (MC) as the crucial role when choosing CRA or ISA. In this study, the standard evaluation system instead of functional or subjective symptom was used as the evaluation criterion, and it was found that CRA improved the quality of life [evaluated by gastrointestinal quality of life index (GIQLI) scores] in patients without MC compared with ISA, but was inferior to ISA for patients with MC evaluated by stool frequency, Wexner and GIQLI scores. We first recommend that STC with MC is the indication for ISA while CRA is the better choice for STC without MC.

Applications

It is recommended that STC with MC is the indication for ISA while CRA is the better choice for STC without MC. This conclusion will provide a helpful suggestion when making clinical choice between CRA and ISA in treating STC.

Terminology

Slow transit constipation is characterized by delay in the transit of stool in the presence of a morphologically normal colon and rectum. Melanosis coli is a disorder of pigmentation of the wall of the colon, often identified at the time of colonoscopy and it is benign, and may have no significant correlation with disease.

Peer-review

The authors retrospectively assessed the clinical outcomes of 48 patients diagnosed with STC over a 5 year timeframe to determine a better clinical choice in treating STC. After comparing the 3-year follow-up outcomes of CRA with ISA, it was found that CRA improved the quality of life (evaluated by GIQLI scores) in patients without MC compared with ISA, but was inferior to ISA for patients with MC evaluated by stool frequency, Wexner and GIQLI scores. So it is recommended that CRA is suitable for STC without MC, and ISA is a better choice for STC with MC. This paper addressed the question thoroughly. All methods were sound. Authors did not overreach with the data analysis. A very sound paper with valid conclusions.

REFERENCES

1 **Jamshed N**, Lee ZE, Olden KW. Diagnostic approach to chronic constipation in adults. *Am Fam Physician* 2011; **84**: 299-306 [PMID: 21842777]

2 **Bassotti G**, de Roberto G, Castellani D, Sediari L, Morelli A. Normal aspects of colorectal motility and abnormalities in slow transit constipation. *World J Gastroenterol* 2005; **11**: 2691-2696 [PMID: 15884105 DOI: 10.3748/wjg.v11.i18.2691]

3 **Abendroth A**, Klein R, Schlaak J, Metz KA, Dobos GJ, Langhorst J. [Impressive picture of a melanosis coli after chronic anthraquinone laxative use--is there an increased risk for colorectal cancer?]. *Z Gastroenterol* 2009; **47**: 579-582 [PMID: 19533548 DOI: 10.1055/s-0028-1109056]

4 **El-Tawil AM**. Persistence of abdominal symptoms after successful surgery for idiopathic slow transit constipation. *South Med J* 2002; **95**: 1042-1046 [PMID: 12356105]

5 **Andromanakos N**, Skandalakis P, Troupis T, Filippou D. Constipation of anorectal outlet obstruction: pathophysiology, evaluation and management. *J Gastroenterol Hepatol* 2006; **21**: 638-646 [PMID: 16677147 DOI: 10.1111/j.1440-1746.2006.04333.x]

6 **Rao SS**, Ozturk R, Laine L. Clinical utility of diagnostic tests for constipation in adults: a systematic review. *Am J Gastroenterol* 2005; **100**: 1605-1615 [PMID: 15984989]

7 **MacDonald A**, Baxter JN, Finlay IG. Idiopathic slow-transit constipation. *Br J Surg* 1993; **80**: 1107-1111 [PMID: 8402105 DOI: 10.1002/bjs.1800800909]

8 **Knowles CH**, Scott M, Lunniss PJ. Outcome of colectomy for slow transit constipation. *Ann Surg* 1999; **230**: 627-638 [PMID: 10561086 DOI: 10.1097/00000658-199911000-00004]

9 **Bassotti G**, Blandizzi C. Understanding and treating refractory constipation. *World J Gastrointest Pharmacol Ther* 2014; **5**: 77-85 [PMID: 24868488 DOI: 10.4292/wjgpt.v5.i2.77]

10 **Hedrick TL**, Friel CM. Constipation and pelvic outlet obstruction. *Gastroenterol Clin North Am* 2013; **42**: 863-876 [PMID: 24280404 DOI: 10.1016/j.gtc.2013.09.004]

11 **Nessi N**, Iucci A, Cazalilla MA. Quantum quench and prethermalization dynamics in a two-dimensional fermi gas with long-range interactions. *Phys Rev Lett* 2014; **113**: 210402 [PMID: 25479478 DOI: 10.1103/PhysRevLett.113.210402]

12 **Govaert B**, Maeda Y, Alberga J, Buntzen S, Laurberg S, Baeten CG. Medium-term outcome of sacral nerve modulation for constipation. *Dis Colon Rectum* 2012; **55**: 26-31 [PMID: 22156864 DOI: 10.1097/DCR.0b013e31823898a5]

13 **Damon H**, Dumas P, Mion F. Impact of anal incontinence and chronic constipation on quality of life. *Gastroenterol Clin Biol* 2004; **28**: 16-20 [PMID: 15041805 DOI: 10.1016/S0399-8320(04)94835-X]

14 **Qian Q**, Jiang CQ, Liu ZS, Ai ZL, He YM, Zheng KY, Wu YH, Tang SL, Tao Q. [Efficacy comparison of subtotal colectomy with antiperistaltic cecoproctostomy and total colectomy with ileorectal anastomosis for patients with slow transit constipation]. *Zhonghua Weichang Waike Zazhi* 2008; **11**: 548-550 [PMID: 19031132]

15 **Costilla VC**, Foxx-Orenstein AE. Constipation: understanding mechanisms and management. *Clin Geriatr Med* 2014; **30**: 107-115 [PMID: 24267606 DOI: 10.1016/j.cger.2013.10.001]

16 **Bove A**, Pucciani F, Bellini M, Battaglia E, Bocchini R, Altomare DF, Dodi G, Sciaudone G, Falletto E, Piloni V, Gambaccini D, Bove V. Consensus statement AIGO/SICCR: diagnosis and treatment of chronic constipation and obstructed defecation (part

I: diagnosis). *World J Gastroenterol* 2012; **18**: 1555-1564 [PMID: 22529683 DOI: 10.3748/wjg.v18.i14.1555]

17 **Bove A**, Bellini M, Battaglia E, Bocchini R, Gambaccini D, Bove V, Pucciani F, Altomare DF, Dodi G, Sciaudone G, Falletto E, Piloni V. Consensus statement AIGO/SICCR diagnosis and treatment of chronic constipation and obstructed defecation (part II: treatment). *World J Gastroenterol* 2012; **18**: 4994-5013 [PMID: 23049207 DOI: 10.3748/wjg.v18.i36.4994]

18 **Leung L**, Riutta T, Kotecha J, Rosser W. Chronic constipation: an evidence-based review. *J Am Board Fam Med* 2011; **24**: 436-451 [PMID: 21737769 DOI: 10.3122/jabfm.2011.04.100272]

19 **Bharucha AE**. Difficult defecation: difficult problem assessment and management; what really helps? *Gastroenterol Clin North Am* 2011; **40**: 837-844 [PMID: 22100121 DOI: 10.1016/j.gtc.2011.09.001]

20 **van Wunnik BP**, Baeten CG, Southwell BR. Neuromodulation for constipation: sacral and transcutaneous stimulation. *Best Pract Res Clin Gastroenterol* 2011; **25**: 181-191 [PMID: 21382589 DOI: 10.1016/j.bpg.2010.12.008]

21 **Feng Y**, Jianjiang L. Functional outcomes of two types of subtotal colectomy for slow-transit constipation: ileosigmoidal anastomosis and cecorectal anastomosis. *Am J Surg* 2008; **195**: 73-77 [PMID: 18082545 DOI: 10.1016/j.amjsurg.2007.02.015]

22 **Knowles CH**, Farrugia G. Gastrointestinal neuromuscular pathology in chronic constipation. *Best Pract Res Clin Gastroenterol* 2011; **25**: 43-57 [PMID: 21382578 DOI: 10.1016/j.bpg.2010.12.001]

23 **Marchesi F**, Percalli L, Pinna F, Cecchini S, Ricco' M, Roncoroni L. Laparoscopic subtotal colectomy with antiperistaltic cecorectal anastomosis: a new step in the treatment of slow-transit constipation. *Surg Endosc* 2012; **26**: 1528-1533 [PMID: 22179477 DOI: 10.1007/s00464-011-2092-4]

24 **Collins B**, Norton C, Maeda Y. Percutaneous tibial nerve stimulation for slow transit constipation: a pilot study. *Colorectal Dis* 2012; **14**: e165-e170 [PMID: 21910815 DOI: 10.1111/j.1463-1318.2011.02820.x]

25 **Freeman HJ**. "Melanosis" in the small and large intestine. *World J Gastroenterol* 2008; **14**: 4296-4299 [PMID: 18666316 DOI: 10.3748/wjg.14.4296]

26 **Byers RJ**, Marsh P, Parkinson D, Haboubi NY. Melanosis coli is associated with an increase in colonic epithelial apoptosis and not with laxative use. *Histopathology* 1997; **30**: 160-164 [PMID: 9067741 DOI: 10.1046/j.1365-2559.1997.d01-574.x]

27 **Park HJ**, Kamm MA, Abbasi AM, Talbot IC. Immunohistochemical study of the colonic muscle and innervation in idiopathic chronic constipation. *Dis Colon Rectum* 1995; **38**: 509-513 [PMID: 7736882 DOI: 10.1007/BF02148851]

28 **López-Vicente J**, Lumbreras M. [Melanosis coli secondary to chronic ingest of chitticum bark]. *Med Clin* (Barc) 2011; **137**: 430 [PMID: 20416898 DOI: 10.1016/j.medcli.2010.02.021]

29 **Villanacci V**, Bassotti G, Cathomas G, Maurer CA, Di Fabio F, Fisogni S, Cadei M, Mazzocchi A, Salerni B. Is pseudomelanosis coli a marker of colonic neuropathy in severely constipated patients? *Histopathology* 2006; **49**: 132-137 [PMID: 16879390 DOI: 10.1111/j.1365-2559.2006.02481.x]

30 **Pearce CB**, Martin H, Duncan HD, Goggin PM, Poller DN. Colonic lymphoid hyperplasia in melanosis coli. *Arch Pathol Lab Med* 2001; **125**: 1110-1112 [PMID: 11473472]

P- Reviewer: Desiderio J, Esmat S, Stanciu C
S- Editor: Ma YJ **L- Editor**: Wang TQ **E- Editor**: Liu XM

World Journal of Gastroenterology

Submit a Manuscript: http://www.wjgnet.com/esps/
Help Desk: http://www.wjgnet.com/esps/helpdesk.aspx
DOI: 10.3748/wjg.v21.i33.9741

World J Gastroenterol 2015 September 7; 21(33): 9741-9748
ISSN 1007-9327 (print) ISSN 2219-2840 (online)

ORIGINAL ARTICLE

Retrospective Study

Hepatic fat quantification magnetic resonance for monitoring treatment response in pediatric nonalcoholic steatohepatitis

Hong Koh, Seung Kim, Myung-Joon Kim, Hyun Gi Kim, Hyun Joo Shin, Mi-Jung Lee

Hong Koh, Seung Kim, Department of Pediatrics, Severance Pediatric Liver Disease Research Group, Severance Children's Hospital, Yonsei University College of Medicine, Seoul 120-752, South Korea

Myung-Joon Kim, Hyun Gi Kim, Hyun Joo Shin, Mi-Jung Lee, Department of Radiology and Research Institute of Radiological Science, Severance Pediatric Liver Disease Research Group, Severance Children's Hospital, Yonsei University College of Medicine, Seoul 120-752, South Korea

Author contributions: Koh H and Lee MJ designed the research; Koh H, Kim MJ and Lee MJ performed the research; Kim S, Kim HG and Shin HJ contributed analytic tools; Koh H, Kim S and Lee MJ analyzed the data; Koh H and Lee MJ wrote the manuscript; Kim S, Kim MJ, Kim HG, Shin HJ and Lee MJ revised and approved the final version.

Supported by A new faculty research seed money grant of Yonsei University College of Medicine for 2013 (8-2013-0028).

Institutional review board statement: This study was reviewed and approved by the local ethics committee of the Severance Hospital, Yonsei University (register no. 1-2014-0007).

Informed consent statement: Because of the retrospective and anonymous character of this study, the need for informed consent was waived by the institutional review board.

Conflict-of-interest statement: The authors declare that there are no conflicts of interest.

Data sharing statement: No additional data are available.

Correspondence to: Mi-Jung Lee, MD, PhD, Department of Radiology and Research Institute of Radiological Science, Severance Pediatric Liver Disease Research Group, Severance Children's Hospital, Yonsei University College of Medicine, 50-1 Yonsei-ro, Seodaemun-gu, Seoul 120-752, South Korea. mjl1213@yuhs.ac
Telephone: +82-2-22287400
Fax: +82-2-3933035

Received: February 27, 2015
Peer-review started: February 27, 2015
First decision: March 26, 2015
Revised: April 23, 2015
Accepted: July 8, 2015
Article in press: July 8, 2015
Published online: September 7, 2015

Abstract

AIM: To evaluate the possibility of treatment effect monitoring using hepatic fat quantification magnetic resonance (MR) in pediatric nonalcoholic steatohepatitis (NASH).

METHODS: We retrospectively reviewed the medical records of patients who received educational recommendations and vitamin E for NASH and underwent hepatic fat quantification MR from 2011 to 2013. Hepatic fat fraction (%) was measured using dual- and triple-echo gradient-recalled-echo sequences at 3T. The compliant and non-compliant groups were compared clinically, biochemically, and radiologically.

RESULTS: Twenty seven patients (M:F = 24:3; mean age: 12 ± 2.3 years) were included (compliant group = 22, non-compliant = 5). None of the baseline findings differed between the 2 groups, except for triglyceride level (compliant *vs* non-compliant, 167.7 mg/dL *vs* 74.2 mg/dL, P = 0.001). In the compliant group, high-

density lipoprotein increased and all other parameters decreased after 1-year follow-up. However, there were various changes in the non-compliant group. Dual-echo fat fraction (-19.2% *vs* 4.6, $P < 0.001$), triple-echo fat fraction (-13.4% *vs* 3.5, $P < 0.001$), alanine aminotransferase (-110.7 IU/L *vs* -10.6 IU/L, $P = 0.047$), total cholesterol (-18.1 mg/dL *vs* 3.8 mg/dL, $P = 0.016$), and triglyceride levels (-61.3 mg/dL *vs* 11.2 mg/dL, $P = 0.013$) were significantly decreased only in the compliant group. The change in body mass index and dual-echo fat fraction showed a positive correlation ($\rho = 0.418$, $P = 0.030$).

CONCLUSION: Hepatic fat quantification MR can be a non-invasive, quantitative and useful tool for monitoring treatment effects in pediatric NASH.

Key words: Nonalcoholic fatty liver disease; Steatohepatitis; Hepatic fat quantification magnetic resonance; Child; Monitoring

Core tip: Few noninvasive methods have been evaluated to accurately assess and monitor the progression of nonalcoholic steatohepatitis (NASH) in children. In this study, we used hepatic fat quantification magnetic resonance (MR) and compared the compliant and non-compliant groups for treatment of pediatric NASH. The compliant group showed not only laboratory improvement but also a decrease in the fat fraction in both dual- and triple-echo sequences after follow-up. Therefore, hepatic fat quantification MR can be a non-invasive, quantitative and useful tool for monitoring treatment effects in pediatric NASH.

Koh H, Kim S, Kim MJ, Kim HG, Shin HJ, Lee MJ. Hepatic fat quantification magnetic resonance for monitoring treatment response in pediatric nonalcoholic steatohepatitis. *World J Gastroenterol* 2015; 21(33): 9741-9748 Available from: URL: http://www.wjgnet.com/1007-9327/full/v21/i33/9741.htm DOI: http://dx.doi.org/10.3748/wjg.v21.i33.9741

INTRODUCTION

Nonalcoholic fatty liver disease (NAFLD) is the most common cause of chronic liver disease in children and adolescents[1-3]. It varies in severity from simple fatty liver to nonalcoholic steatohepatitis (NASH), which may induce hepatic fibrosis, cirrhosis, and hepatocellular carcinoma[4,5]. Cirrhosis due to NAFLD has already been reported in 2 boys aged 10 and 14 years[6]. Therefore, prompt diagnosis and suitable treatment are mandatory. Proper diet, exercise, and vitamin E may help improve steatosis in liver histology[7-10].

Liver biopsy is the modality of choice to accurately diagnose NAFLD and to monitor disease progression during treatment, even in children and adolescents. However, this procedure is invasive and may result in life-threatening complications[11,12]. In addition, it has many drawbacks, including sampling error and inter- and intra-observer variability in interpretation. Liver biopsy can also be associated with complications such as abdominal pain, hypotension, hemobilia, and intraperitoneal hemorrhage, the last of which has an associated mortality rate of up to 0.5%. Furthermore, liver biopsy is not generally accepted by patients and especially not by children and adolescents[13-15]. Therefore, there is a need to develop noninvasive methods to accurately assess and monitor the progression of NAFLD in children.

Various imaging studies can be used for the noninvasive assessment of hepatic fat including ultrasonography, computed tomography (CT), and magnetic resonance (MR) imaging. Ultrasonography can detect fatty liver as increased liver parenchymal echogenicity. There is no risk of radiation exposure using this method. However, its ability to grade the fatty liver in children is limited[5], despite an attempt to quantitatively analyze hepatic fat with ultrasonography[16]. Moreover, positive ultrasonographic results in severely obese adolescents cannot be used to accurately predict the presence and severity of hepatic steatosis[17].

CT can also detect hepatic fat infiltration by analyzing hepatic parenchymal attenuation[18]. However, hepatic attenuation can also be affected by other conditions such as hemosiderin deposition[19]. Moreover, the risk of radiation exposure is a major disadvantage, especially in children. No studies have yet compared the CT assessment of hepatic steatosis with histologic grades of fatty infiltration in children[5].

Both MR imaging and MR spectroscopy can detect hepatic fat infiltration simply and accurately without radiation exposure[20], even though MR spectroscopy needs a long examination time for a small volume of the liver. When using MR imaging, quantitative measurement of the fat fraction using a chemical shift technique, which distinguishes resonant frequencies between fat and water, can easily evaluate fat in the liver. In addition, it can be obtained using the dual- or triple-echo gradient recalled-echo sequences, which can be used easily and quickly in children[21]. However, there is limited information regarding the utility of hepatic fat quantification MR in children with NASH, and no studies have used this technique to monitor treatment effects in these patients. Therefore, the purpose of this study was to evaluate the possibility of treatment monitoring with hepatic fat quantification MR as a non-invasive and quantitative method in pediatric NASH.

MATERIALS AND METHODS

Patients

This retrospective study was approved by the Insti-

tutional Review Board of our hospital (1-2014-0007) and the acquisition of informed consent for review of patients' images and medical records was waived. We declare that none of the authors of the present study has any competing commercial, personal, political, intellectual or religious interest with respect to the present study. We reviewed the medical records of 27 pediatric patients referred for NASH between January 2011 and December 2013. Diet and a physical exercise education program for the reduction of body weight were provided carefully and continuously to all patients. A low-calorie diet (25-30 kcal/kg per day) composed of specified quantities of fat (25%-30%), carbohydrate (50%-60%) and protein (15%-20%) was recommended. Clinical nutritionists in our hospital guided the diet planning and a moderate exercise program (1 h/d at least 5 d a week). Vitamin E (daily dose 800 IU) was also recommended to all patients to improve liver histology[22]. Compliance with the diet and exercise treatment regime was checked at every clinic visit from daily records about feeding, exercise, and medication history written by parents and caregivers. Treatments other than diet, physical exercise education, and vitamin E were not provided. Sex, age at the time of diagnosis, body weight, body mass index (BMI), and laboratory data were collected. Hepatic fat quantification MR was performed at the initial referral and 1 year later for follow-up. We reviewed body weight, BMI, and laboratory results at the time of MR acquisition. Laboratory results included aspartate aminotransferase (AST), alanine aminotransferase (ALT), total bilirubin, albumin, alkaline phosphatase (ALP), cholesterol, triglycerides, high density lipoprotein (HDL), and low density lipoprotein (LDL) levels.

Hepatic fat quantification MR

We retrospectively reviewed hepatic fat quantification MR of NASH patients. The hepatic fat fraction (%) was measured using dual- and triple-echo gradient-recalled-echo sequences on a 3T MR system (Tim Trio; Siemens Medical Solutions, Erlangen, Germany) with a phased body array coil. For dual-echo chemical-shift gradient-echo MR, we obtained axial images of the liver using gradient echo T1-weighted, dual-echo, in-phase, and opposed-phase sequences [TR 226 ms; TE 1.23 (opposed-phase) and 2.46 (in-phase) ms; flip angle 65°; section thickness 6 mm; matrix size 192 × 256; and field of view 300 cm × 400 cm]. For triple-echo MR, the imaging protocol included a breath-hold low-flip-angle T1-weighted, triple-echo, spoiled gradient-echo sequence [TR 226 ms; TE 2.46 (in-phase 1), 3.69 (opposed-phase), and 4.92 (in-phase 2) ms; flip angle 20°; section thickness 6 mm; matrix size 256 × 192; and field of view 315 cm × 420 cm].

One radiologist (Lee MJ), who had 10 years' experience in pediatric radiology, randomly drew 2 regions of interest (ROIs) that avoided hepatic vessels in the homogenous parenchyma of the right hepatic lobe on a picture archiving and communication system (Centricity, General Electric Corporation, Milwaukee, WI, United States). The reviewer obtained signal intensity at the same level of in-phase (IP) and opposed-phase (OP) images. The hepatic fat fraction in dual-echo MR was calculated from the following equation: Dual-echo fat fraction (%) = [(IP-OP)/(2 × IP)] × 100[23].

Theoretically, three ROIs should be obtained with the same method used to measure the triple-echo fat fraction. The signal intensities can be obtained at the same level IP1, OP, and IP2 images. The hepatic fat fraction in triple-echo MR can be calculated from the equation as follows: Triple-echo fat fraction (%) $\leqslant$ [(IP1 + IP2)/2 - OP]/(IP1 + IP2) > × 100[24].

In our workstation, the triple-echo fat fraction was automatically calculated and we obtained a triple-echo fat map for direct fat fraction measurement in a single ROI.

Statistical analysis

Patients who followed the educational recommendations and showed marked changes in BMI, AST, and ALT over 1 year under observation were defined as the compliant group. Patients who did not follow the recommendations well were defined as the non-compliant group. Statistical analysis was performed using SPSS version 20.0.0 (IBM Corp., Armonk, NY, United States). We compared clinical, biochemical, and radiological parameters between the compliant group and the non-compliant group. Continuous variables, including age, body weight, BMI, laboratory results, and hepatic fat fractions on MR, were analyzed with the Mann-Whitney *U* test. The difference in sex between the 2 groups was analyzed using Fisher's exact test. To compare the results of the initial study with 1 year follow-up, the Wilcoxon signed-rank test was used. Spearman correlation analysis between body weight or BMI change and fat fraction change measured on MR was also performed. *P* values < 0.05 were considered statistically significant. The statistical methods of this study were reviewed by Ha Yan Kim from Biostatistics Collaboration Unit, Yonsei University College of Medicine.

RESULTS

Baseline findings

Twenty seven children with NASH underwent fat quantification MR during the study period. All children underwent both a pre-treatment and a follow-up MR and were included in this study. There were 24 boys and 3 girls, with a mean age of 12.0 ± 2.3 years (range, 9-19 years). There were 22 patients (81.5%) in the compliant group and 5 (18.5%) in the non-compliant group. Table 1 demonstrates the baseline findings in all children. There were no significant differences between the groups except for the triglyceride level, which was

Table 1 Baseline characteristics of all patients, and comparison between the compliant and non-compliant groups

		All children (n = 27)	Compliant group (n = 22)	Non-compliant group (n = 5)	P value[1]
Demographics	Male, n (%)	24 (88.9)	20 (90.9)	4 (80.0)	NS
	Age (yr)	12.0 ± 2.3	11.8 ± 1.9	12.8 ± 3.7	NS
	B.wt (kg)	66.2 ± 16.0	65.4 ± 16.5	70.0 ± 14.5	NS
	BMI (kg/m^2)	26.6 ± 3.4	28.8 ± 3.6	25.9 ± 2.5	NS
Laboratory findings	AST (IU/L)	79.9 ± 79.4	83.0 ± 85.8	66.0 ± 44.0	NS
	ALT (IU/L)	138.7 ± 112.0	148.6 ± 119.2	95.2 ± 63.7	NS
	T.Bil (mg/dL)	0.6 ± 0.3	0.6 ± 0.3	0.6 ± 0.3	NS
	Albumin (g/dL)	4.6 ± 0.2	4.6 ± 0.2	4.5 ± 0.2	NS
	ALP (IU/L)	208.6 ± 77.3	210.5 ± 73.8	200.4 ± 100.8	NS
	Cholesterol (mg/dL)	187.9 ± 30.0	192.6 ± 30.0	167.0 ± 21.0	NS
	TG (mg/dL)	150.4 ± 74.1	167.7 ± 71.1	74.2 ± 16.4	0.001
	HDL (mg/dL)	45.0 ± 8.3	44.9 ± 9.0	45.2 ± 4.7	NS
	LDL (mg/dL)	120.5 ± 30.3	123.3 ± 32.0	108.0 ± 18.5	NS
Hepatic fat fraction on MR	Dual-echo sequence (%)	34.2 ± 8.5	34.9 ± 8.2	31.3 ± 9.8	NS
	Triple-echo sequence (%)	22.8 ± 7.3	23.6 ± 7.2	19.5 ± 7.4	NS

[1]Comparison between the compliant and non-compliant groups using the Mann-Whitney U test, except for gender, which was compared using Fisher's exact test. All data show mean ± standard deviation. B.wt: Body weight; BMI: Body mass index; AST: Aspartate aminotransferase; ALT: Alanine aminotransferase; T.Bil: Total bilirubin; ALP: Alkaline phosphatase; TG: Triglyceride; HDL: High density lipoprotein; LDL: Low density lipoprotein; NS: Not significant.

Table 2 Comparison of clinical outcomes between initial diagnosis and 1 year after referral

	Compliant group (n = 22)			Non-compliant group (n = 5)		
	Initial	After 1 yr	P-value[1]	Initial	After 1 yr	P value[1]
Male, n (%)	20 (90.9)			4 (80.0)		
Age (yr)	11.8 ± 1.9			12.8 ± 3.7		
B.wt (kg)	65.4 ± 16.5	67.3 ± 14.7	NS	70.0 ± 14.5	72.3 ± 15.0	NS
BMI (kg/m^2)	28.8 ± 3.6	26.3 ± 3.4	0.016	25.9 ± 2.5	26.4 ± 2.7	NS
AST (IU/L)	83.0 ± 85.8	29.2 ± 20.0	0.002	66.0 ± 44.0	50.0 ± 37.5	NS
ALT (IU/L)	148.6 ± 119.2	37.9 ± 41.8	< 0.001	95.2 ± 63.7	84.6 ± 63.5	NS
T.Bil (mg/dL)	0.6 ± 0.3	0.7 ± 0.4	0.015	0.6 ± 0.3	0.70 ± 0.37	NS
Albumin (g/dL)	4.6 ± 0.2	4.6 ± 0.3	NS	4.5 ± 0.2	4.70 ± 0.30	NS
ALP (IU/L)	210.5 ± 73.8	202.1 ± 93.5	NS	200.4 ± 100.8	153.6 ± 71.6	NS
Cholesterol (mg/dL)	192.6 ± 30.0	174.5 ± 28.2	0.001	167.0 ± 21.0	170.8 ± 22.5	NS
TG (mg/dL)	167.7 ± 71.1	106.4 ± 39.8	< 0.001	74.2 ± 16.4	85.4 ± 20.1	NS
HDL (mg/dL)	44.9 ± 9.0	48.4 ± 9.6	< 0.001	45.2 ± 4.7	46.0 ± 4.5	NS
LDL (mg/dL)	123.3 ± 32.0	100.3 ± 26.3	< 0.001	108.0 ± 18.5	105.0 ± 30.8	NS
Dual-echo sequence (%)	34.9 ± 8.2	15.8 ± 8.2	< 0.001	31.3 ± 9.8	35.9 ± 8.9	NS
Triple-echo sequence (%)	23.6 ± 7.2	10.1 ± 4.6	< 0.001	19.5 ± 7.4	22.9 ± 5.6	NS

[1]Comparison between initial and 1-year follow-up in the 2 groups using the Wilcoxon signed-rank test. All data show mean ± standard deviation.

higher in the compliant group (167.7 mg/dL) than in the non-compliant group (74.2 mg/dL) (P = 0.001).

Comparison of changes in the 2 groups at 1-year follow-up

Table 2 shows the results of the initial and follow-up findings in the 2 groups. Body weight did not change significantly in either group. However, BMI decreased only in the compliant group (from 28.8 kg/m^2 to 26.3 kg/m^2, P = 0.016). Almost all laboratory results except albumin and ALP changed significantly during follow-up in the compliant group. AST, ALT, cholesterol, triglycerides, and LDL decreased, and HDL increased in the compliant group, which reflected the treatment effect. However, no laboratory results changed during follow-up in the non-compliant group.

On hepatic fat quantification MR, both dual- and triple-echo fat fractions were decreased in the compliant group (P < 0.001) (Figure 1). The mean initial hepatic fat fraction was 34.9% on dual-echo MR and 23.6% on triple-echo MR, and it decreased to 15.8% on dual-echo MR and to 10.1% on triple-echo MR in the compliant group. The follow-up MR showed increased mean fat fraction in the non-compliant group on both dual-echo MR (from 31.3% to 35.9%, P > 0.05) and triple-echo MR (from 19.5% to 22.9%, P > 0.05) (Figure 2).

The 2 groups differed in both dual-echo fat fraction (-19.2% *vs* 4.6%, P < 0.001) and triple-echo fat fraction (-13.4% *vs* 3.5%, P < 0.001), with a decreased fat fraction observed only in the compliant group. Among the laboratory results, ALT (-110.7 IU/L *vs* -10.6 IU/L, P = 0.047), cholesterol (-18.1 mg/dL *vs* 3.8 mg/dL, P = 0.016), and triglycerides (-61.3 mg/dL *vs* 11.2

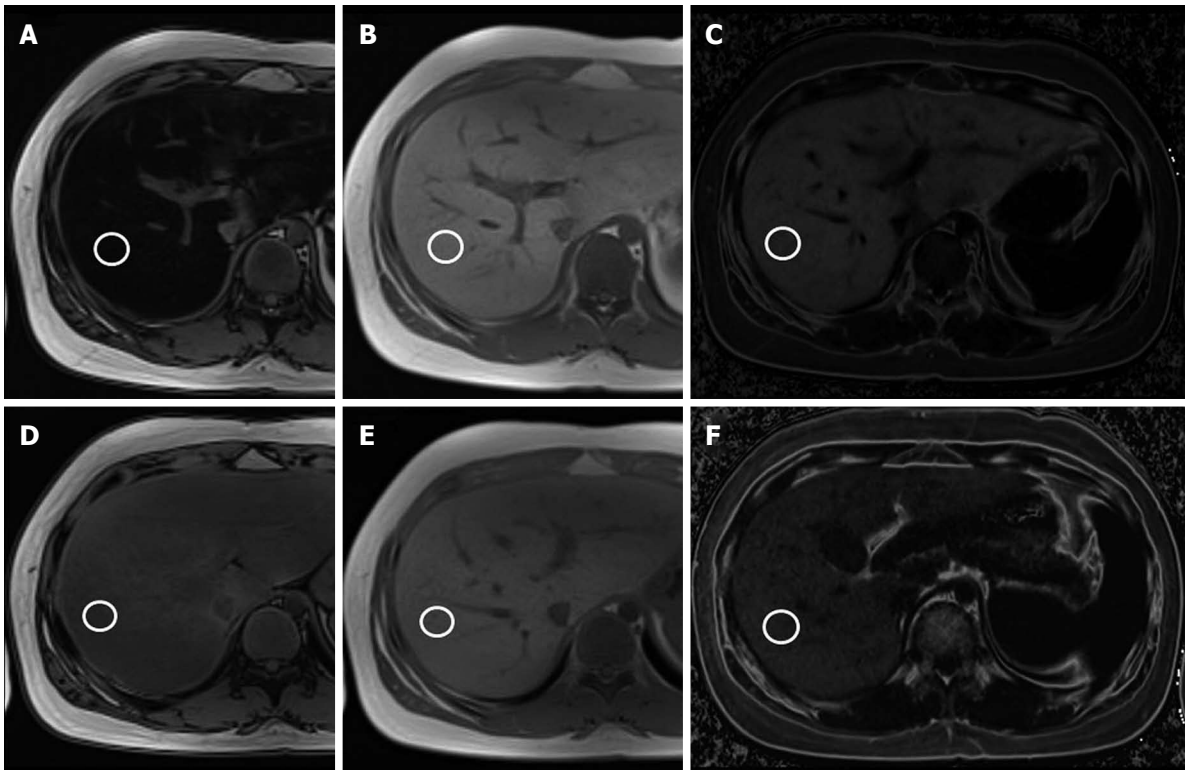

Figure 1 Liver fat quantification magnetic resonance in an 11-year-old boy in the compliant group. The same circular regions of interest (white circles) are drawn to measure signal intensity in the liver parenchyma. On initial magnetic resonance (MR) images (A-C), signal intensity of the liver is 56.6 on the opposed-phase image (A) and 725.4 on the in-phase image (B). Therefore, the calculated fat signal percentage in the liver on the dual-echo sequence is 46% [(725.4-56.6) × 100/2 × 725.4]. The fat signal percentage in the liver is 34.4% on the fat map image (C) of the triple-echo sequence. On follow-up liver MR after treatment (D-F), hepatic signal intensity is 331.1 on the opposed-phase image (D) and 617.8 on the in-phase image (E), with a calculated fat signal percentage of 23% [(617.8-331.1) × 100/2 × 617.8] on the dual-echo sequence. The triple-echo sequence image also demonstrates a decreased hepatic fat signal percentage of 15% on the fat map image (F).

mg/dL, $P = 0.013$) differed between the 2 groups.

In the correlation analysis which included all patients, the BMI change and the dual-echo fat fraction change showed a positive correlation ($\rho = 0.418$, $P = 0.030$). However, the BMI change and triple-echo fat fraction change was not correlated ($\rho = 0.316$, $P = 0.109$). The body weight change and fat fraction change also did not show a significant correlation in both dual-echo ($\rho = 0.213$, $P = 0.285$) and triple-echo ($\rho = 0.135$, $P = 0.501$) sequences.

DISCUSSION

Dual- and triple-echo gradient recalled-echo sequences can easily perform noninvasive assessment and quantitative measurement of hepatic fat, even in children. Our study demonstrated that not only clinical and laboratory results but also fat fraction on MR improved in children with good treatment compliance. These results suggest the possible usefulness of fat quantification MR as a noninvasive and quantitative tool for monitoring treatment effects in children with NASH.

Ultrasonography is the favored method for evaluating hepatic disease in children because results are easily obtainable and it is noninvasive. Disturbed propagation of ultrasound waves can occur when there are lipid droplets within hepatocytes[5]. This causes the scattering of the waves, which creates more returning echoes to the transducer. Therefore, we can qualitatively determine fatty infiltration in the liver when the liver parenchymal echogenicity is increased when compared with the kidney. Shannon *et al*[16] performed a cohort study of pediatric patients with biopsy-proven NAFLD and demonstrated excellent correlation between the ultrasonographic steatosis score and the histologic grade of steatosis. However, Bohte *et al*[17] showed the limitations of ultrasonography in severely obese adolescents when evaluating the severity of hepatic steatosis. In addition, a recent systemic review for imaging liver fat in children concluded that ultrasonography had a low positive predictive value of 47%-62% for the diagnosis of fatty liver[5].

MR imaging is one of the most sensitive tools used to evaluate fat infiltration in the liver. Both MR imaging and MR spectroscopy can accurately and reproducibly measure hepatic fat[25]. However, MR spectroscopy evaluates only a small portion of the liver and requires a long examination time and expertise for data acquisition and analysis[23,25]. When using MR imaging, the degree of fat infiltration can be estimated by using chemical shift imaging[20]. The term chemical shift refers to the difference in precessional (or resonance)

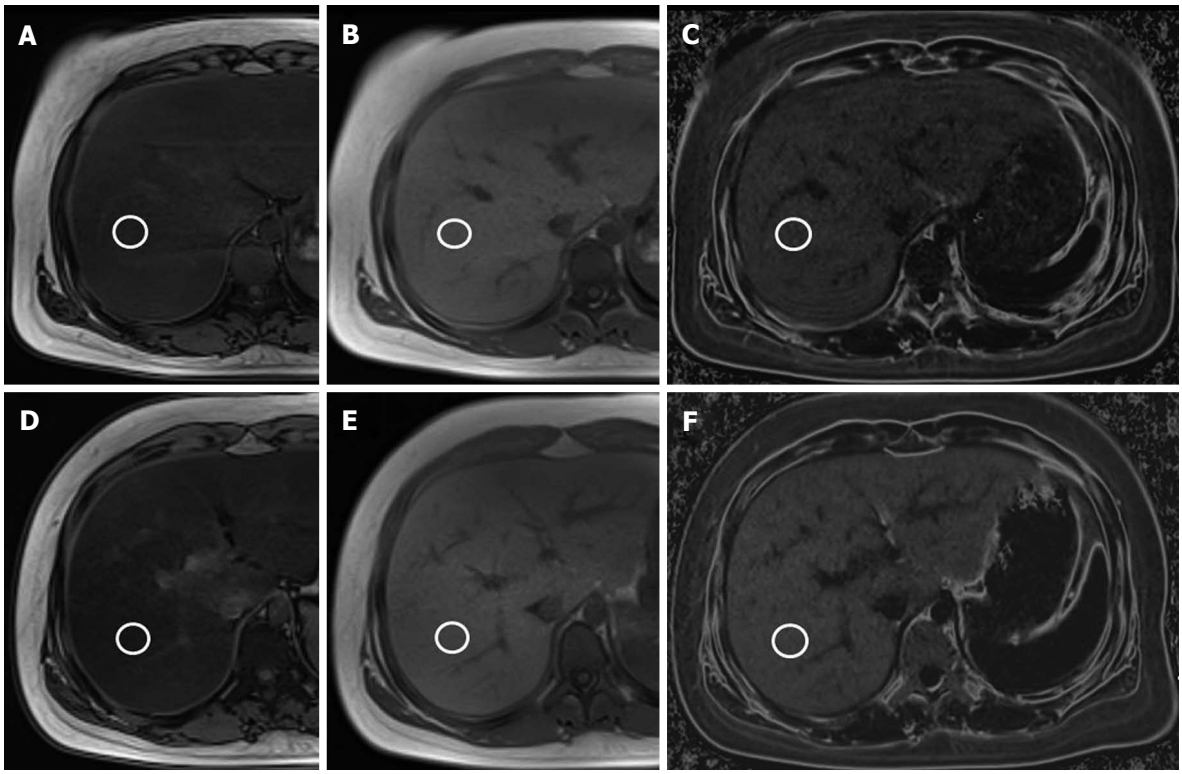

Figure 2 Liver fat quantification magnetic resonance in a 12-year-old girl in the non-compliant group. The same circular regions of interest (white circles) are drawn to measure signal intensity in the liver parenchyma. On initial MR images (A-C), signal intensity of the liver is 299.1 on the opposed-phase image (A) and 644.6 on the in-phase image (B). Therefore, the calculated fat signal percentage in the liver on the dual-echo sequence is 26.8% [(644.6-299.1) × 100/2 × 644.6]. The fat signal percentage in the liver is 16.6% on the fat map image (C) of the triple-echo sequence. On follow-up liver MR after treatment (D-F), the fat signal is 238.6 on the opposed-phase image (D) and 750.6 on the in-phase image (E), with a calculated fat signal percentage of 34.1% [(750.6-238.6) × 100/2 × 750.6] on the dual-echo sequence. The triple-echo sequence image also demonstrates an increased hepatic fat signal percentage of 20.4% on the fat map image (F).

frequency between 2 proton MR signals, expressed in parts per million of the resonance frequency of the static magnetic field B0. This technique uses differences in the resonance frequencies of water and lipids to differentiate tissues containing only water from those containing both water and lipids[5]. The characteristic resonance frequencies of fat and water and the detection of a fat-specific frequency allows for quantitative measurement of hepatic steatosis. Therefore, while normal liver parenchyma exhibits similar signal intensity on IP and OP images, the fatty liver shows diminished signal intensity on OP images, as seen in our study.

The dual-echo technique is available on most clinical imagers with a field strength of 1.0T or higher. We can obtain both IP and OP images after a single radiofrequency excitation using this technique, allowing rapid acquisition of images during a single breath hold[23]. There are many reports about the utility of this technique in evaluating hepatic steatosis in adults[26]. However, there is only one report of the dual-echo technique being performed in children. In 2011, Pacifico *et al*[21] demonstrated a strong correlation between the dual-echo MR fat fraction and the histologic grade of hepatic steatosis among 25 children with NAFLD. No studies have yet evaluated the utility of this technique for monitoring treatment effects in children with NASH. This is the first study detecting longitudinal changes in hepatic fat in pediatric NASH, even though we did not perform histologic correlation as biopsy is not considered a proper method for treatment monitoring, especially in children. We demonstrated that not only clinical and laboratory results but also fat fraction on MR improved in children with good treatment compliance. We also showed that the BMI change and the dual-echo fat fraction change had a positive correlation. Therefore, the dual-echo technique can be a useful monitoring tool in children with fatty liver disease.

Triple-echo MR imaging is somewhat similar to dual-echo MR imaging. However, the triple-echo technique acquires a second IP image in addition to the first OP and IP images. The signal intensities of the first OP and IP images are corrected for the T2* effect using the T2* time estimated from the signal decay between the first and second IP images[25]. The dual-echo technique cannot correct for potentially confounding T2* relaxation effects, which should considered in cases with elevated liver iron content, such as cirrhosis and hemochromatosis[23,27]. Qayyum *et al*[28] demonstrated that fat quantification determined with chemical shift imaging correlated better with the histopathologically determined percentage of fat in non-cirrhotic patients compared with cirrhotic patients.

Several recent reports evaluated the triple-echo technique for quantification of hepatic steatosis in

adults[29,30]. Hwang *et al*[29] demonstrated a correlation between both triple-echo MR imaging and MR spectroscopy with macrovesicular steatosis. They suggested cutoff values of 4.93% and 5.79% for the detection of substantial macrovesicular steatosis for both techniques, respectively, without a significant difference. Wu *et al*[30] compared dual-echo MR, triple-echo MR, and MR spectroscopy for the evaluation of hepatic steatosis and found that triple-echo MR imaging had the highest correlation. However, no studies evaluated triple-echo MR imaging in children with NASH. Our study demonstrated that both the dual-echo and triple-echo techniques showed a significant decrease in hepatic fat fraction after treatment. The mean fat fraction decreased from 34.9% to 15.8% with the dual-echo sequence and from 23.6% to 10.1% with the triple-echo sequence in the compliant group. However, we could not evaluate the effect of hepatic iron content or fibrosis between the 2 sequences in these patients. Further study is required to compare the accuracy of these sequences in children with NAFLD.

Our study has several limitations. First, diagnosis and improvement during NASH follow-up were not proven pathologically. We could not directly correlate or compare the MR fat fraction with histologic grades of fatty infiltration. We also could not evaluate or consider hepatic fibrosis in our patients. However, liver biopsy is not a routine examination in children with NASH and is not appropriate for treatment monitoring. The second limitation was the small number of patients with a short-term follow-up period. We included only children with NASH who underwent both a pre-treatment and a 1-year follow-up MR for hepatic fat quantification during the study period. Even though all children in the compliant group showed decreased hepatic fat fraction on both sequences in this short period of follow-up, long-term monitoring is mandatory in these patients. Additional prospective studies with a large number of children and long-term follow-up are needed to validate our results. The third limitation was that chemical shift MR imaging cannot differentiate the water dominant and fat dominant liver[23]. In fact, this technique cannot evaluate a fatty liver with more than a 50% fat component. However, a hepatic fat fraction of more than 50% is rare; in a study of over 2000 patients by Szczepaniak *et al*[31], no patients had a fat fraction exceeding 50%. Therefore, this may be only a theoretical concern.

In conclusion, hepatic fat quantification MR can be a useful tool to non-invasively and quantitatively monitor treatment effects in pediatric NASH. Furthermore, it can also help reduce the number of unnecessary biopsies in these patients.

COMMENTS

Background

Nonalcoholic fatty liver disease (NAFLD) is the most common cause of chronic liver disease in children. Prompt diagnosis and suitable treatment are necessary to prevent hepatic fibrosis and cirrhosis. In this study, we evaluated the possibility of treatment monitoring with hepatic fat quantification magnetic resonance (MR) as a non-invasive and quantitative method in pediatric nonalcoholic steatohepatitis (NASH).

Research frontiers

Even though liver biopsy is the modality of choice for NAFLD diagnosis, it is invasive and not favored especially in children. Therefore, there is a need to develop noninvasive methods to accurately assess and monitor the progression of NAFLD for children.

Innovations and breakthroughs

There is debate about the modality of choice for the diagnosis and monitoring of the NAFLD in pediatric patients. Non-invasive imaging studies such as hepatic fat quantification MR could be used to quantitatively monitor treatment effects in pediatric NAFLD. However, there is limited information regarding the utility of hepatic fat quantification MR in children with NAFLD.

Applications

Quantitative measurement of the fat fraction using a chemical shift technique on MR can be an accurate and easy method to evaluate hepatic fat, even in children. We need to validate the use of this technique not only for NAFLD diagnosis but also for treatment monitoring.

Terminology

Fat quantification MR using a chemical shift technique can evaluate fat in the liver by distinguishing resonant frequencies between fat and water. Both dual- and triple-echo gradient recalled-echo sequences can be used for this purpose. The dual-echo sequence can be obtained with a single radiofrequency excitation, allowing rapid acquisition of images during a single breath hold. The triple-echo sequence can correct for potentially confounding T2* relaxation effects, which should considered in cases with elevated liver iron content, such as cirrhosis and hemochromatosis.

Peer-review

This is an interesting research study which evaluated the utility of hepatic fat quantification MR as a non-invasive and quantitative method for treatment monitoring in pediatric NASH. This study compared the compliant and non-compliant groups and demonstrated fat fraction and laboratory findings change only in the compliant group. These results suggest that hepatic fat quantification MR can be used in the treatment monitoring in pediatric NASH.

REFERENCES

1 **Lavine JE**, Schwimmer JB, Van Natta ML, Molleston JP, Murray KF, Rosenthal P, Abrams SH, Scheimann AO, Sanyal AJ, Chalasani N, Tonascia J, Ünalp A, Clark JM, Brunt EM, Kleiner DE, Hoofnagle JH, Robuck PR. Effect of vitamin E or metformin for treatment of nonalcoholic fatty liver disease in children and adolescents: the TONIC randomized controlled trial. *JAMA* 2011; **305**: 1659-1668 [PMID: 21521847 DOI: 10.1001/jama.2011.520]

2 **Loomba R**, Sirlin CB, Schwimmer JB, Lavine JE. Advances in pediatric nonalcoholic fatty liver disease. *Hepatology* 2009; **50**: 1282-1293 [PMID: 19637286 DOI: 10.1002/hep.23119]

3 **Schwimmer JB**, Deutsch R, Kahen T, Lavine JE, Stanley C, Behling C. Prevalence of fatty liver in children and adolescents. *Pediatrics* 2006; **118**: 1388-1393 [PMID: 17015527 DOI: 10.1542/peds.2006-1212]

4 **Adams LA**, Sanderson S, Lindor KD, Angulo P. The histological course of nonalcoholic fatty liver disease: a longitudinal study of 103 patients with sequential liver biopsies. *J Hepatol* 2005; **42**: 132-138 [PMID: 15629518 DOI: 10.1016/j.jhep.2004.09.012]

5 **Awai HI**, Newton KP, Sirlin CB, Behling C, Schwimmer JB. Evidence and recommendations for imaging liver fat in children, based on systematic review. *Clin Gastroenterol Hepatol* 2014; **12**: 765-773 [PMID: 24090729 DOI: 10.1016/j.cgh.2013.09.050]

6 **Molleston JP**, White F, Teckman J, Fitzgerald JF. Obese children

with steatohepatitis can develop cirrhosis in childhood. *Am J Gastroenterol* 2002; **97**: 2460-2462 [PMID: 12358273 DOI: 10.1111/j.1572-0241.2002.06003.x]
7 **Pacana T**, Sanyal AJ. Vitamin E and nonalcoholic fatty liver disease. *Curr Opin Clin Nutr Metab Care* 2012; **15**: 641-648 [PMID: 23075940 DOI: 10.1097/MCO.0b013e328357f747]
8 **Musso G**, Cassader M, Rosina F, Gambino R. Impact of current treatments on liver disease, glucose metabolism and cardiovascular risk in non-alcoholic fatty liver disease (NAFLD): a systematic review and meta-analysis of randomised trials. *Diabetologia* 2012; **55**: 885-904 [PMID: 22278337 DOI: 10.1007/s00125-011-2446-4]
9 **Kawanaka M**, Nishino K, Nakamura J, Suehiro M, Goto D, Urata N, Oka T, Kawamoto H, Nakamura H, Yodoi J, Hino K, Yamada G. Treatment of nonalcoholic steatohepatitis with vitamins E and C: a pilot study. *Hepat Med* 2013; **5**: 11-16 [PMID: 24695939 DOI: 10.2147/hmer.s41258]
10 **Bell LN**, Wang J, Muralidharan S, Chalasani S, Fullenkamp AM, Wilson LA, Sanyal AJ, Kowdley KV, Neuschwander-Tetri BA, Brunt EM, McCullough AJ, Bass NM, Diehl AM, Unalp-Arida A, Chalasani N. Relationship between adipose tissue insulin resistance and liver histology in nonalcoholic steatohepatitis: a pioglitazone versus vitamin E versus placebo for the treatment of nondiabetic patients with nonalcoholic steatohepatitis trial follow-up study. *Hepatology* 2012; **56**: 1311-1318 [PMID: 22532269 DOI: 10.1002/hep.25805]
11 **Castéra L**, Nègre I, Samii K, Buffet C. Pain experienced during percutaneous liver biopsy. *Hepatology* 1999; **30**: 1529-1530 [PMID: 10610352 DOI: 10.1002/hep.510300624]
12 **Cadranel JF**, Rufat P, Degos F. Practices of liver biopsy in France: results of a prospective nationwide survey. For the Group of Epidemiology of the French Association for the Study of the Liver (AFEF). *Hepatology* 2000; **32**: 477-481 [PMID: 10960438 DOI: 10.1053/jhep.2000.16602]
13 **Kim SY**, Seok JY, Han SJ, Koh H. Assessment of liver fibrosis and cirrhosis by aspartate aminotransferase-to-platelet ratio index in children with biliary atresia. *J Pediatr Gastroenterol Nutr* 2010; **51**: 198-202 [PMID: 20531020 DOI: 10.1097/MPG.0b013e3181da1d98]
14 **Bravo AA**, Sheth SG, Chopra S. Liver biopsy. *N Engl J Med* 2001; **344**: 495-500 [PMID: 11172192 DOI: 10.1056/nejm200102153440706]
15 **Bonny C**, Rayssiguier R, Ughetto S, Aublet-Cuvelier B, Baranger J, Blanchet G, Delteil J, Hautefeuille P, Lapalus F, Montanier P, Bommelaer G, Abergel A. [Medical practices and expectations of general practitioners in relation to hepatitis C virus infection in the Auvergne region]. *Gastroenterol Clin Biol* 2003; **27**: 1021-1025 [PMID: 14732848]
16 **Shannon A**, Alkhouri N, Carter-Kent C, Monti L, Devito R, Lopez R, Feldstein AE, Nobili V. Ultrasonographic quantitative estimation of hepatic steatosis in children With NAFLD. *J Pediatr Gastroenterol Nutr* 2011; **53**: 190-195 [PMID: 21788761 DOI: 10.1097/MPG.0b013e31821b4b61]
17 **Bohte AE**, Koot BG, van der Baan-Slootweg OH, van Werven JR, Bipat S, Nederveen AJ, Jansen PL, Benninga MA, Stoker J. US cannot be used to predict the presence or severity of hepatic steatosis in severely obese adolescents. *Radiology* 2012; **262**: 327-334 [PMID: 22106358 DOI: 10.1148/radiol.11111094]
18 **Lee SW**, Park SH, Kim KW, Choi EK, Shin YM, Kim PN, Lee KH, Yu ES, Hwang S, Lee SG. Unenhanced CT for assessment of macrovesicular hepatic steatosis in living liver donors: comparison of visual grading with liver attenuation index. *Radiology* 2007; **244**: 479-485 [PMID: 17641368 DOI: 10.1148/radiol.2442061177]
19 **Limanond P**, Raman SS, Lassman C, Sayre J, Ghobrial RM, Busuttil RW, Saab S, Lu DS. Macrovesicular hepatic steatosis in living related liver donors: correlation between CT and histologic findings. *Radiology* 2004; **230**: 276-280 [PMID: 14695401 DOI: 10.1148/radiol.2301021176]
20 **Ma X**, Holalkere NS, Kambadakone R A, Mino-Kenudson M, Hahn PF, Sahani DV. Imaging-based quantification of hepatic fat: methods and clinical applications. *Radiographics* 2009; **29**: 1253-1277 [PMID: 19755595]
21 **Pacifico L**, Martino MD, Catalano C, Panebianco V, Bezzi M, Anania C, Chiesa C. T1-weighted dual-echo MRI for fat quantification in pediatric nonalcoholic fatty liver disease. *World J Gastroenterol* 2011; **17**: 3012-3019 [PMID: 21799647 DOI: 10.3748/wjg.v17.i25.3012]
22 **Pearlman M**, Loomba R. State of the art: treatment of nonalcoholic steatohepatitis. *Curr Opin Gastroenterol* 2014; **30**: 223-237 [PMID: 24717764 DOI: 10.1097/mog.0000000000000060]
23 **Cassidy FH**, Yokoo T, Aganovic L, Hanna RF, Bydder M, Middleton MS, Hamilton G, Chavez AD, Schwimmer JB, Sirlin CB. Fatty liver disease: MR imaging techniques for the detection and quantification of liver steatosis. *Radiographics* 2009; **29**: 231-260 [PMID: 19168847]
24 **Guiu B**, Loffroy R, Petit JM, Aho S, Ben Salem D, Masson D, Hillon P, Cercueil JP, Krause D. Mapping of liver fat with triple-echo gradient echo imaging: validation against 3.0-T proton MR spectroscopy. *Eur Radiol* 2009; **19**: 1786-1793 [PMID: 19247667 DOI: 10.1007/s00330-009-1330-9]
25 **Lee SS**, Park SH. Radiologic evaluation of nonalcoholic fatty liver disease. *World J Gastroenterol* 2014; **20**: 7392-7402 [PMID: 24966609 DOI: 10.3748/wjg.v20.i23.7392]
26 **Le TA**, Chen J, Changchien C, Peterson MR, Kono Y, Patton H, Cohen BL, Brenner D, Sirlin C, Loomba R. Effect of colesevelam on liver fat quantified by magnetic resonance in nonalcoholic steatohepatitis: a randomized controlled trial. *Hepatology* 2012; **56**: 922-932 [PMID: 22431131 DOI: 10.1002/hep.25731]
27 **Westphalen AC**, Qayyum A, Yeh BM, Merriman RB, Lee JA, Lamba A, Lu Y, Coakley FV. Liver fat: effect of hepatic iron deposition on evaluation with opposed-phase MR imaging. *Radiology* 2007; **242**: 450-455 [PMID: 17255416 DOI: 10.1148/radiol.2422052024]
28 **Qayyum A**, Goh JS, Kakar S, Yeh BM, Merriman RB, Coakley FV. Accuracy of liver fat quantification at MR imaging: comparison of out-of-phase gradient-echo and fat-saturated fast spin-echo techniques--initial experience. *Radiology* 2005; **237**: 507-511 [PMID: 16244259 DOI: 10.1148/radiol.2372040539]
29 **Hwang I**, Lee JM, Lee KB, Yoon JH, Kiefer B, Han JK, Choi BI. Hepatic steatosis in living liver donor candidates: preoperative assessment by using breath-hold triple-echo MR imaging and 1H MR spectroscopy. *Radiology* 2014; **271**: 730-738 [PMID: 24533869 DOI: 10.1148/radiol.14130863]
30 **Wu CH**, Ho MC, Jeng YM, Hsu CY, Liang PC, Hu RH, Lai HS, Shih TT. Quantification of hepatic steatosis: a comparison of the accuracy among multiple magnetic resonance techniques. *J Gastroenterol Hepatol* 2014; **29**: 807-813 [PMID: 24224538 DOI: 10.1111/jgh.12451]
31 **Szczepaniak LS**, Nurenberg P, Leonard D, Browning JD, Reingold JS, Grundy S, Hobbs HH, Dobbins RL. Magnetic resonance spectroscopy to measure hepatic triglyceride content: prevalence of hepatic steatosis in the general population. *Am J Physiol Endocrinol Metab* 2005; **288**: E462-E468 [PMID: 15339742 DOI: 10.1152/ajpendo.00064.2004]

P- Reviewer: Akarsu M, Chuang WL, Savopoulos CG
S- Editor: Wang JL **L- Editor**: Cant MR **E- Editor**: Zhang DN

World Journal of Gastroenterology

Submit a Manuscript: http://www.wjgnet.com/esps/
Help Desk: http://www.wjgnet.com/esps/helpdesk.aspx
DOI: 10.3748/wjg.v21.i33.9749

World J Gastroenterol 2015 September 7; 21(33): 9749-9757
ISSN 1007-9327 (print) ISSN 2219-2840 (online)

ORIGINAL ARTICLE

Retrospective Study

Annexin A10 expression in colorectal cancers with emphasis on the serrated neoplasia pathway

Jeong Mo Bae, Jung Ho Kim, Ye-Young Rhee, Nam-Yun Cho, Tae-You Kim, Gyeong Hoon Kang

Jeong Mo Bae, Jung Ho Kim, Ye-Young Rhee, Nam-Yun Cho, Gyeong Hoon Kang, Laboratory of Epigenetics, Cancer Research Institute, Seoul National University College of Medicine, Seoul 110-799, South Korea

Jeong Mo Bae, Jung Ho Kim, Ye-Young Rhee, Gyeong Hoon Kang, Department of Pathology, Seoul National University College of Medicine, Seoul 110-799, South Korea

Tae-You Kim, Department of Internal Medicine, Seoul National University College of Medicine, Seoul 110-799, South Korea

Author contributions: Bae JM, Kim TY and Kang GH designed the research; Bae JM, Kim JH, Rhee YY and Cho NY performed the research; Bae JM analyzed the data and wrote the paper.

Supported by Grant from Basic Science Research Program through the National Research Foundation (NRF) funded by the Ministry of Education, No. 2013R1A1A2059080; a grant from the Korean Health Technology R&D Project, Ministry of Health & Welfare, No. HI13C1804; Priority Research Centers Program through the NRF funded by the Ministry of Education, Science and Technology, No. 2009-0093820; and the NRF grant funded by the Ministry of Science, ICT, and Future planning, No. 2011-0030049; a grant of the Korea Health Technology R&D Project, Ministry of Health & Welfare, Republic of Korea, No. HI14C1277."

Institutional review board statement: This study was reviewed and approved by Institutional Review Board ofSeoul National University College of Medicine/Seoul National University Hospital (IRB No: H. 1502-029-647).

Informed consent statement: Because this study is a retrospective study with a minimal risk to patients, it was exempted from obtaining informed consent by the IRB.

Conflict-of-interest statement: The authors declare no conflict-of-interest.

Data sharing statement: No additional data are available.

Correspondence to: Gyeong Hoon Kang, MD, Professor, Department of Pathology, Seoul National University College of Medicine, 28 Yongon-dong, Chongno-gu, Seoul 110-799, South Korea. ghkang@snu.ac.kr
Telephone: + 82-2-20723312
Fax: +82-2-7435530

Received: March 1, 2015
Peer-review started: March 2, 2015
First decision: March 26, 2015
Revised: April 11, 2015
Accepted: June 16, 2015
Article in press: June 16, 2015
Published online: September 7, 2015

Abstract

AIM: To validate the utility of Annexin A10 as a surrogate marker of the serrated neoplasia pathway in invasive colorectal cancers (CRCs).

METHODS: A total of 1133 primary CRC patients who underwent surgical resection at Seoul National University Hospital between January 2004 and December 2007 were enrolled. Expression of Annexin A10 was evaluated by immunohistochemistry using tissue microarray and paired to our findings on clinicopathologic and molecular characteristics of each individual. CpG island methylator phenotype was determined by MethyLight assay and microsatellite instability was determined by high performance liquid chromatography. *KRAS* and *BRAF* mutation status was

evaluated by direct sequencing and allele-specific PCR. Univariate and stage-specific survival analyses were performed to reveal the prognostic value of Annexin A10 expression.

RESULTS: Annexin A10 expression was observed in 66 (5.8%) of the 1133 patients. Annexin A10 expression was more commonly found in females and was associated with proximal location, ulcerative gross type, advanced T category, N category and TNM stage. CRCs with Annexin A10 expression showed an absence of luminal necrosis, luminal serration and mucin production. CRCs with Annexin A10 expression were associated with CpG island methylator phenotype, microsatellite instability and *BRAF* mutation. In survival analysis, Annexin A10 expression was associated with poor overall survival and progression-free survival, especially in stage Ⅳ CRCs.

CONCLUSION: Annexin A10 expression is associated with poor clinical behavior and can be used a supportive surrogate marker of the serrated neoplasia pathway in invasive CRCs.

Key words: Annexin A10; Serrated neoplasia pathway; CpG island methylator phenotype; Colorectal cancer; *BRAF* mutation

Core tip: Annexin A10 is considered a surrogate immunohistochemical marker for sessile serrated adenomas/polyps. We validated the utility of Annexin A10 as a surrogate marker of the serrated neoplasia pathway in invasive colorectal cancers (CRCs). Annexin A10 expression was associated with female sex, proximal location, ulcerative gross type, advanced TNM stage, serration and mucin production. CRCs with Annexin A10 expression were associated with CpG island methylator phenotype, microsatellite instability and *BRAF* mutation. In stage-specific survival analysis, Annexin A10 expression was associated with poor clinical outcome in stage Ⅳ CRCs. Annexin A10 can be used a supportive surrogate marker of the serrated neoplasia pathway.

Bae JM, Kim JH, Rhee YY, Cho NY, Kim TY, Kang GH. Annexin A10 expression in colorectal cancers with emphasis on the serrated neoplasia pathway. *World J Gastroenterol* 2015; 21(33): 9749-9757 Available from: URL: http://www.wjgnet.com/1007-9327/full/v21/i33/9749.htm DOI: http://dx.doi.org/10.3748/wjg.v21.i33.9749

INTRODUCTION

Colorectal cancer (CRC) shows heterogeneity in terms of its molecular carcinogenesis, and this heterogeneity contributes to clinical and histomorphological variation[1]. Currently, there are three widely accepted colorectal carcinogenic pathways, the chromosomal instability (CIN) pathway, the microsatellite instability (MSI) pathway, and the epigenetic instability pathway, which corresponds to the CpG island methylator phenotype (CIMP). The CIN pathway is characterized by alterations in the number and structure of chromosomes, as well as by the accumulation of somatic mutations in genes including proto-oncogenes and tumor suppressor genes[2]. MSI is caused by a defective mismatch repair system and is characterized by alterations in the number of repeat nucleotide(s), leading to frame-shift mutations in the corresponding genes[3]. CIMP is characterized by widespread cancer-specific hypermethylation of numerous promoter CpG island loci[4]. Initially, these pathways were considered to be mutually exclusive, but recent comparative studies have reported that molecular alterations in these pathways can partially overlap[5].

CRC is one of the best models for studying multistep carcinogenesis. Virtually all CRCs originate from premalignant polyps, which can be detected by colonoscopy. Colorectal premalignant polyps are divided into two groups: adenomatous polyps (conventional adenomas), which are precursor lesions of CRCs with CIN, and serrated polyps, which are now considered to be precursor lesions of CRCs with CIMP and sporadic MSI[6]. Serrated polyps are series of polyps that share sawtooth-like glandular morphology. Serrated polyps are divided into hyperplastic polyps, sessile serrated adenomas/polyps (SSA/P) and traditional serrated adenomas (TSA). Serrated polyps are highly associated with CIMP, sporadic MSI and the *BRAF* mutation.

Annexin A10 is a member of the annexin family, a large multigene family of calcium- and phospholipid-binding proteins. It plays important roles in physiologic processes including differentiation and proliferation[7-9]. Annexin A10 is expressed in the foveolar cells and glandular cells of the normal antral or body-type gastric mucosa. In addition, Annexin A10 is expressed in Brunner gland cells of the duodenum and urothelial cells of the renal pelvis and urinary bladder[10]. However, aberrant expression of Annexin A10 was found in malignant tumors of other tissue types, including oral cancer, pancreatic cancer, and lung cancer[10,11]. Recently, Gonzalo *et al*[12] proposed Annexin A10 as a marker for the colorectal serrated neoplasia pathway. They observed increased expression of Annexin A10 in SSA/P compared with normal colonic epithelia and microvesicular hyperplastic polyps. However, little is known about Annexin A10 expression in invasive CRCs.

Previously, we reported the correlation of Annexin A10 expression with the serrated neoplasia pathway using 168 microsatellite-unstable CRCs[13]. However, the evaluation of Annexin A10 expression in a large

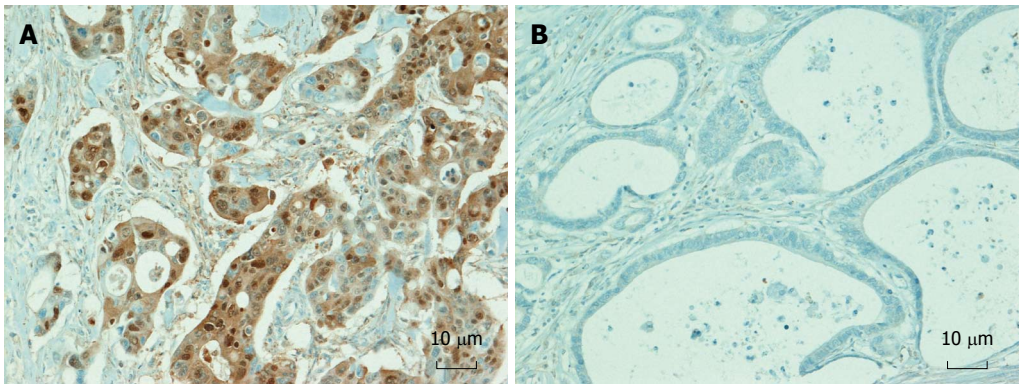

Figure 1 Representative images of immunohistochemical staining for Annexin A10. A: Colorectal cancers (CRCs) with Annexin A10 expression (magnification × 200); B: CRCs without Annexin A10 expression (magnification × 200).

population is required to characterize the clinicopathological and molecular characteristics of Annexin A10, because of its low prevalence in CRCs[10,14]. In this study, we evaluated the clinicopathological characteristics and prognostic value of Annexin A10 expression in 1133 primary CRCs and compared them with molecular profiles including CIMP, MSI, *KRAS* and *BRAF* mutation status. Finally, we evaluated whether Annexin A10 can be used as a surrogate marker for CRCs with CIMP.

MATERIALS AND METHODS

Tissue samples

A total of 1527 patients with CRC underwent curative surgery at Seoul National University Hospital, Seoul, South Korea, from January 2004 to December 2007. After the exclusion of 394 patients with CRC [refusal of molecular study (n = 136), non-invasive cancers (n = 50), familial adenomatous polyposis (n = 13), multiple occurrence (n = 78), neoadjuvant chemo- and/or radiotherapy (n = 89), recurrent tumors (n = 28)], formalin-fixed paraffin-embedded tissue samples from 1133 patients with CRC were selected for this study. This study was approved by the Institutional Review Board.

Clinicopathological analysis

Clinicopathological characteristics including age, sex, tumor location, and TNM stage were obtained from electronic medical records. Through microscopic examination of representative sections of the tumors, we evaluated the following parameters without knowledge of the CIMP, MSI, *KRAS* and *BRAF* mutation status of the specimen: tumor differentiation, luminal necrosis, tumor budding, Crohn-like lymphoid reaction, number of tumor-infiltrating lymphocytes, luminal serration and extraglandular mucin production. Overall survival and progression-free survival data were extracted from the patient's medical records, direct interviews with surviving patients or members of patients' families or death registry offices.

Evaluation of Annexin A10 expression

Tissue microarray (TMA) construction using formalin-fixed, paraffin-embedded (FFPE) tissues from 1133 CRCs was performed. Three different tumor areas in the FFPE tissue of individual CRCs were extracted as three tissue cores (2mm in diameter) for each case and were transferred to TMA blocks. Immunohistochemical analysis was performed with commercially available antibodies against Annexin A10 (1:300, NBP1-90156, Novus Biologicals). Expression of Annexin A10 was assessed independently by two pathologists (Bae JM and Kang GH). The presence of Annexin A10 nuclear staining in more than 5% of the tumor area in any TMA core was classified as expression of Annexin A10[13]. Tumors showing less than 5% nuclear staining of the tumor area or cytoplasmic staining without nuclear staining were classified as exhibiting no-expression of Annexin A10 (Figure 1).

KRAS, BRAF mutation and MSI analyses

Through histological examination, representative tumor portions were marked and then subjected to manual microdissection. Dissected tissues were collected into microtubes containing lysis buffer and proteinase K and were incubated at 55 ℃ for 2 d. DNA from paraffin-embedded tissue was extracted, and polymerase chain reaction (PCR) was performed. Direct sequencing of *KRAS* codons 12 and 13, and allele-specific PCR for *BRAF* codon 600 were performed as previously described[15]. MSI status was determined by 5 NCI markers including BAT25, BAT26, D2S123, D5S346 and D17S250. MSI was defined when two or more markers were unstable, and microsatellite stable (MSS) was defined when only one marker was unstable or when all five markers were stable.

Analysis of CpG island methylator phenotype

Bisulfite DNA modification and real-time methylation specific PCR (MethyLight) assays were performed as described previously[16]. We quantified methylation of eight CIMP-specific markers (*CACNA1G*, *CDKN2A*,

Table 1 Clinicopathologic and histologic features of Annexin A10 expression in colorectal cancers *n* (%)

Parameter	Annexin A10 no-expression (*n* = 1067, 94.2%)	Annexin A10 expression (*n* = 66, 5.8%)	*P* value
Age (mean ± SD)	61.0 ± 11.1	58.1 ± 12.6	0.038[1]
Sex			< 0.001
Male	650 (60.9)	27 (40.9)	
Female	417 (39.1)	39 (59.1)	
Location			< 0.001
Proximal colon	237 (22.2)	42 (63.6)	
Distal colon	430 (40.3)	11 (16.7)	
Rectum	400 (37.5)	13 (19.7)	
Gross type			0.027
Fungating	708 (66.3)	35 (53.0)	
Ulcerative	359 (33.7)	31 (47.0)	
T category			< 0.001[2]
1	47 (4.4)	1 (1.5)	
2	164 (15.4)	0 (0.0)	
3	756 (70.8)	52 (78.8)	
4	100 (9.4)	13 (19.7)	
N category			< 0.001[2]
0	558 (52.3)	16 (24.2)	
1	290 (27.2)	23 (34.9)	
2	219 (20.5)	27 (40.9)	
M category			0.049
0	892 (83.6)	49 (74.2)	
1	175 (16.4)	17 (25.8)	
Stage			< 0.001[2]
Ⅰ	173 (16.2)	0 (0.0)	
Ⅱ	351 (32.9)	15 (22.7)	
Ⅲ	368 (34.5)	34 (51.5)	
Ⅳ	175 (16.4)	17 (25.7)	
Differentiation			0.002
Well	64 (6.0)	2 (3.0)	
Differentiated Moderately	970 (90.9)	56 (84.9)	
Differentiated Poorly	33 (3.1)	8 (12.1)	
Differentiated Luminal necrosis			< 0.001
Absent	83 (7.8)	18 (27.3)	
Present	984 (92.2)	48 (72.7)	
Tumor budding			0.264[3]
Absent	36 (3.4)	0 (0.0)	
Present	1031 (96.6)	66 (100.0)	
Tumor-infiltrating Lymphocytes			0.316
Low TILs (< 8/HPF)	802 (75.2)	39 (59.1)	
High TILs (≥ 8/HPF)	265 (24.8)	27 (40.9)	
Crohn's-like Lymphoid reaction			0.470
Absent	908 (85.1)	54 (81.8)	
Present	159 (14.9)	12 (18.2)	
Luminal serration			< 0.001[3]
Absent	1039 (97.4)	50 (75.8)	
Present	28 (2.6)	16 (24.2)	
Mucin production			
Absent	958 (89.8)	43 (65.1)	< 0.001
Present	109 (10.2)	23 (34.9)	

1Student's *t*-test; [2]Wilcoxon rank-sum test; [3]Fisher's exact test. S.D: Standard deviation; HPF: High power field.

CRABP1, *IGF2*, *MLH1*, *NEUROG1*, *RUNX3* and *SOCS1*). CIMP-positive (CIMP-P) was defined by a tumor showing methylation in ≥ five markers of the 8-marker CIMP panel and CIMP-negative (CIMP-N) as tumors showing methylation in ≤ 4 markers (0 to 4 of 8 promoters).

Statistical analysis

SAS system (version 9.3, SAS Institute, Cary, NC, United States) and R software were used for statistical analyses. The age of each group was compared using Student's *t*-test. The other clinicopathological characteristics between groups were compared using χ^2 test or Fisher's exact test for categorical variables and Wilcoxon's rank-sum test for ordinal variables. The survival curves after surgery were estimated by Kaplan-Meier method and the differences in the survival curves were tested by log-rank test. Cox proportional hazards models were used to estimate hazard ratios and corresponding 95% confidence intervals (CIs) for the overall survival. The assumption of proportional hazards was checked by plotting the log[-log[S(t)]] against time on study. All statistical tests were two-sided, and statistical significance was defined as $P < 0.05$.

The statistical methods of this study were reviewed by Myoung Jin Jang from Medical Research Collaborating Center, Seoul National University Hospital.

RESULTS

Clinicopathological characteristics of Annexin A10 expression

Detailed clinicopathological features and histological features according to Annexin A10 expression are summarized in Table 1. A total of 1133 patients with CRC (mean age ± SD, 60.8 ± 11.2) were included in the immunohistochemical analysis. The male to female ratio was 1.48:1 (677 males and 456 females). Tumor location was proximal colon (proximal to the splenic flexure) in 279 patients, distal colon in 441 patients and rectum in 413 patients. Median follow-up duration was 58.1 mo (0.3-89.8 mo). 785 patients received 5-fluorouracil based adjuvant chemotherapy.

Annexin A10 expression was observed in 66 (5.8%) patients. Annexin A10 expression was associated with lower age at diagnosis ($P = 0.038$), female sex ($P < 0.001$), proximal tumor location ($P < 0.001$), advanced T category ($P < 0.001$), N category ($P < 0.001$), M category ($P = 0.049$) and more advanced TNM stage ($P < 0.001$). As shown with microscopic examination, Annexin A10 expression was associated with absence of luminal necrosis ($P < 0.001$), increased number of tumor-infiltrating lymphocytes ($P = 0.003$), luminal

Table 2 Comparison of Annexin A10 expression with other molecular characteristics in colorectal cancers *n* (%)

Parameter	Annexin A10 no-expression (*n* = 1067, 94.2%)	Annexin A10 expression (*n* = 66, 5.8%)	*P* value
CIMP			< 0.001[1]
CIMP-N	1029 (96.4)	41 (62.1)	
CIMP-P	38 (3.6)	25 (37.9)	
MSI			< 0.001[1]
MSS	995 (93.2)	49 (74.2)	
MSI	72 (6.8)	17 (25.8)	
KRAS mutation (*n* = 1071)			0.399
Wild type	745 (73.8)	42 (68.8)	
Mutant type	265 (26.2)	19 (31.2)	
BRAF mutation (*n* = 1005)			< 0.001[1]
Wild type	912 (96.4)	50 (84.7)	
Mutant type	34 (3.6)	9 (15.3)	

[1]Fisher's exact test. CIMP: CpG island methylator phenotype; MSI: Microsatellite instability.

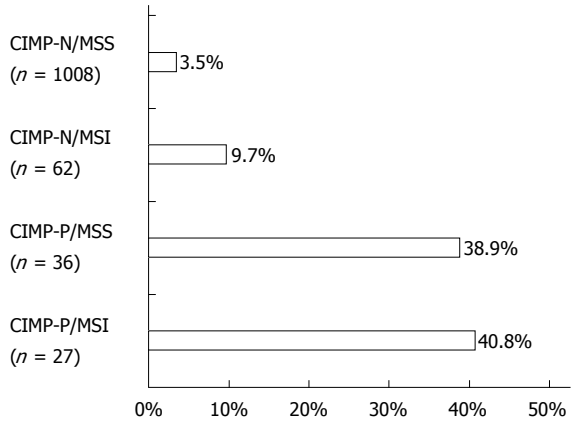

Figure 2 Frequency of Annexin A10 expression according to four molecular subtypes. CIMP-N: CpG island methylator phenotype-negative; CIMP-P: CpG island methylator phenotype-positive; MSS: Microsatellite stable; MSI: Microsatellite instability.

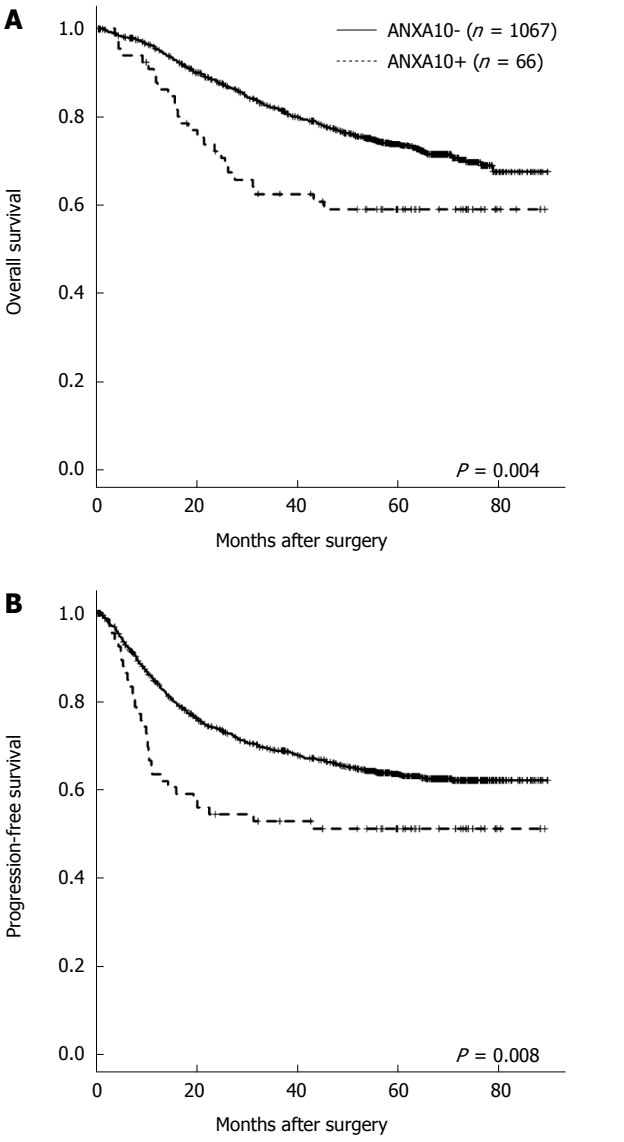

Figure 3 Univariate survival analysis in colorectal cancers according to Annexin A10 expression status. A: Overall survival; B: Progression-free survival. ANXA10-; Annexin A10 no-expression, ANXA10+: Annexin A10 expression.

serration ($P < 0.001$) and mucin production ($P < 0.001$).

Molecular characteristics of Annexin A10 expression

Table 2 shows molecular characteristics of CRCs according to Annexin A10 expression. Among the 1133 CRCs, CIMP-P CRCs were detected in 63 (5.6%) patients and MSI CRCs were found in 88 (7.8%) patients. Annexin A10 expression was associated with CIMP-P CRCs ($P < 0.001$) and MSI CRCs ($P < 0.001$). Sensitivity and specificity of Annexin A10 expression for detection of CIMP-P CRCs were 39.7% and 96.2%, respectively. Positive predictive value (PPV) and negative predictive value (NPV) of Annexin A10 expression for detection of CIMP-P CRCs were 0.38 and 0.96, respectively. In four molecular subtypes which were generated by the combined status of CIMP and MSI, Annexin A10 expression was observed in 3.5% of CIMP-N/MSS CRCs, 9.7% of CIMP-N/MSI CRCs, 38.9% of CIMP-P/MSS CRCs and 40.8% of CIMP-P/MSI CRCs (Figure 2). In the mutation studies, CRCs with Annexin A10 expression showed a higher frequency of the *BRAF* mutation than did CRCs with Annexin A10 no-expression ($P < 0.001$).

Survival analysis

As shown using univariate survival analysis with Kaplan-Meier survival curves, patients with Annexin A10 expression showed worse overall survival ($P = 0.004$) and progression-free survival ($P = 0.008$) than patients with Annexin A10 no-expression (Figure 3). Although sample size did not get enough power to predict clinical outcome, in stage Ⅳ CRCs, the Annexin A10 expression group showed shorter median overall survival (OS) (17.0 mo *vs* 25.3 mo, $P < 0.001$) and shorter progression-free survival (PFS) (7.5 mo *vs*

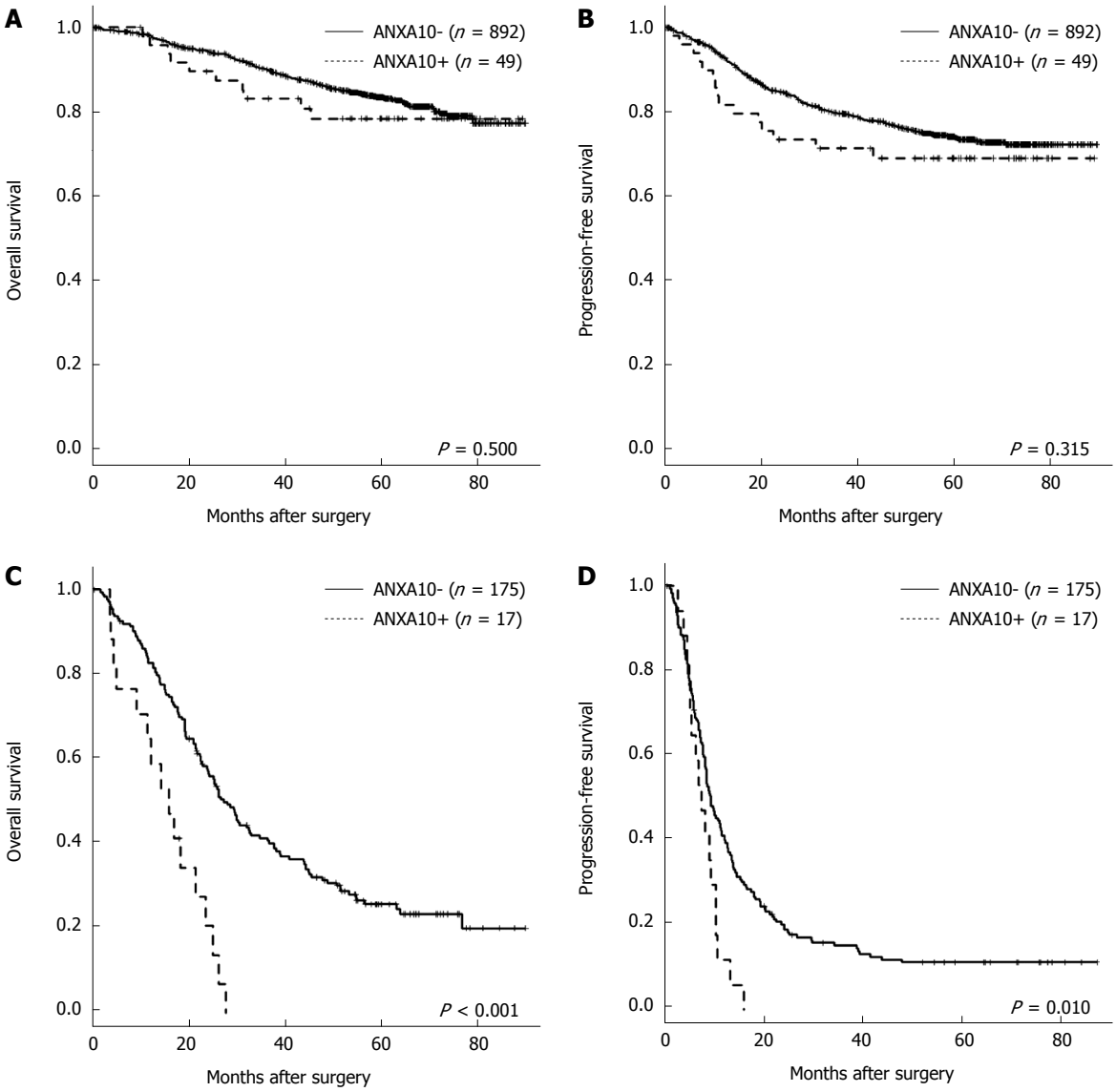

Figure 4 Stage-specific survival analysis according to Annexin A10 expression status. A: Overall survival for Stages Ⅰ-Ⅲ colorectal cancers (CRCs); B: Progression-free survival of Stages Ⅰ-Ⅲ CRCs; C: Overall survival of Stage Ⅳ CRCs; D: Progression-free survival of Stage Ⅳ CRCs. ANXA10-; Annexin A10 no-expression, ANXA10+: Annexin A10 expression.

9.2 mo, p=0.010) compared with the Annexin A10 no-expression group (Figure 4). However, stages Ⅰ-Ⅲ CRCs did not show a significant difference in clinical outcome according to Annexin A10 expression status (P = 0.500 for OS and P = 0.315 for PFS, median survival: not reached) (Figure 4). Multivariate survival analysis using Cox proportional hazard model in stage Ⅳ CRCs suggested that Annexin A10 expression could be an independent prognostic marker for overall survival in stage Ⅳ CRCs, despite limitation of insufficient sample size (Table 3).

DISCUSSION

CIMP is one of the molecular subtypes of CRC and is characterized by concurrent hypermethylation of promoter CpG islands in tumor-suppressor genes and tumor-associated genes. To characterize CIMP, we must measure the methylation status of several panels of multiple genes using methylation-specific PCR or the MethyLight assay[17-19]. However, these assays are not easily used in daily clinical practice because these assays require complicated work and show low cost-effectiveness and inconsistent results[20]. Therefore, an easily applicable strong surrogate marker is required to characterize CIMP clinically. Clear association of the *BRAF* mutation and CIMP led us to consider a recently developed BRAF V600E-specific antibody (clone VE1)[21]. Some studies showed excellent concordance of immunohistochemical staining results of clone VE1 and the *BRAF* mutation determined by sequence analysis[22-24]. However, other studies reported poor sensitivity of clone VE1 immunostaining owing to its vulnerability to pretreatment conditions[25,26].

In a recent study, Annexin A10 was proposed as a surrogate marker for SSA/P[12] and found to be

Table 3 Univariate and multivariate Cox proportional hazards models for overall survival of stage Ⅳ colorectal cancers

Variable	Univariate analysis		Multivariate analysis	
	HR (95%CI)	*P* value	HR (95%CI)	*P* value
Differentiation (undifferentiated/differentiated)	2.20 (1.31-3.72)	0.003	1.95 (1.07-3.56)	0.030
Tumor location (proximal colon/distal colon, rectum)	1.66 (1.16-2.38)	0.005	1.60 (1.06-2.42)	0.025
Adjuvant chemotherapy (treatment/no-treatment)	0.42 (0.27-0.66)	< 0.001	0.47 (0.27-0.81)	0.006
Annexin A10 (expression/no-expression)	3.13 (1.83-5.38)	< 0.001	2.38 (1.18-4.83)	0.016
Age (yr) (≥ 65/< 65)	1.54 (1.10-2.15)	0.012	1.37 (0.92-2.03)	0.123
Gross pattern (ulcerative/fungating)	1.41 (1.01-1.96)	0.042	1.18 (0.81-1.71)	0.387
CIMP (CIMP-P/CIMP-N)	2.24 (1.24-4.06)	0.008	1.13 (0.44-2.89)	0.801
MSI (MSI/MSS)	2.46 (1.08-5.63)	0.033	1.46 (0.44-4.86)	0.540
BRAF mutation (Mt/Wt)	2.42 (1.12-5.19)	0.024	1.67 (0.71-3.91)	0.239
Sex (male/female)	1.03 (0.74-1.45)	0.858	-	-
KRAS mutation (Mt/Wt)	1.09 (0.75-1.58)	0.653	-	-

HR: Hazard ratio; CI: Confidence interval; CIMP-P: CpG island methylator phenotype-positive; CIMP-N: CpG island methylator phenotype-negative; MSI: Microsatellite instability; MSS: Microsatellite stable; Mt: Mutant type; Wt: Wild type.

expressed even in traditional serrated adenomas[27]. Because SSA/P or traditional serrated adenomas are considered to be precursor lesions of CIMP-P CRCs, Annexin A10 expression could be another surrogate marker for CIMP-P CRCs. In a study by Tsai *et al*[28], Annexin A10 was found to be expressed in 28% of CIMP-P/MSI CRCs and 67% of CIMP-P/MSS CRCs. Our present study showed that Annexin A10 was expressed in 40.8% of CIMP-P/MSI CRCs and 38.9% of CIMP-P/MSS CRCs. These results imply that nuclear expression of Annexin A10 might be lost or reduced during multistep carcinogenesis of some SSA/P or another carcinogenic pathway can contribute to the development of CIMP-P CRCs.

The clinicopathological characteristics of CRCs in which Annexin A10 is expressed are not well known. In this study, Annexin A10 expression was observed in 5.8% of 1133 primary surgically resected CRCs. This result is similar to a previous study which reported that Annexin A10 was expressed in 6% of CRCs[10]. Tsai *et al*[28] reported that Annexin A10 expression is associated with right-side tumor location, moderate to poor differentiation, Crohn-like lymphoid reaction and lack of dirty necrosis, but there was no correlation with mucinous differentiation, medullary histology or tumor-infiltrating lymphocytes. Sajanti *et al*[29] reported that Annexin A10 expression was associated with proximal tumor location, mucin production and serrated histology, but there was no correlation with stage and grade. In our present study, CRCs with Annexin A10 expression were associated with lower age at diagnosis, female sex, proximal tumor location, advanced T, N, M category, advanced TNM stage, absence of luminal necrosis, increased number of tumor-infiltrating lymphocytes, luminal serration and mucin production. Ethnic difference and different proportion of molecular subtypes such as CIMP and MSI might contribute to discrepancies in clinicopathologic characteristics of Annexin A10 expression between studies. However, previous studies had several limitations. The study of Tsai *et al*[28] might have selection bias because they included entire CRCs which had CIMP, MSI and *BRAF* mutation as a case group, however CRCs with conventional pathway were randomly selected as a control group. The study of Sajanti *et al*[29] analyzed only 42.4% (146/344) of patients who underwent surgical resection in the enrollment period. Our present study showed clinicopathologic characteristics of Annexin A10 expression in a large and consecutively collected CRC patient population.

The prognostic value of Annexin A10 expression in CRCs has not yet been reported. However, association of Annexin A10 with poor prognostic molecular features such as CIMP and the *BRAF* mutation led us to assume that Annexin A10 was a poor prognostic indicator[30-32]. In this study, stage-specific survival analysis results showed that Annexin A10 expression is associated with poor OS and PFS in stage Ⅳ CRCs. Multivariate survival analysis confined to stage Ⅳ CRCs suggested that Annexin A10 expression could be an independent prognostic marker in advanced stage CRCs.

This study has several limitations. First, Annexin A10 expression was measured using TMA. Regional heterogeneity of Annexin A10 expression was reported, so we could not exclude the possibility of false-negativity in Annexin A10 expression[28]. Second, exclusivity of Annexin A10 for sporadic MSI CRCs is inconclusive, but we could not evaluate germline mutation status of MMR genes (*hMLH1*, *hMSH2*, *hMSH6* and *hPMS2*)[28,33,34]. Third, the proportion of CIMP-P, MSI and *BRAF* mutations in this study was low compared to Western population[31,35] .

In conclusion, Annexin A10 expression has a supportive but inconclusive role as a surrogate marker of CIMP-P CRCs. Further studies focusing on the molecular mechanisms of Annexin A10 expression and its oncogenic functions in CRCs are required.

COMMENTS

Background

The serrated neoplasia pathway is an explanatory model of multistep

carcinogenesis in CRC displaying the CpG island methylator phenotype (CIMP). Recently, Annexin A10, a eukaryotic calcium- and phospholipid-binding protein, was proposed to be a surrogate marker for sessile serrated adenomas/polyps.

Research frontiers

In this study, the authors attempted to validate the utility of Annexin A10 as a surrogate marker of the serrated neoplasia pathway in invasive CRCs.

Innovations and breakthroughs

Annexin A10 expression was observed in 66 (5.8%) patients. CRCs with Annexin A10 expression were associated with CIMP, microsatellite instability and *BRAF* mutation. Annexin A10 expression was associated with poor overall survival and progression-free survival in stage Ⅳ CRCs.

Applications

The study results suggest that Annexin A10 expression has a supportive but inconclusive role as a surrogate marker of CIMP-P CRCs

Terminology

Annexin A10 is a member of the annexin family, a large multigene family of calcium- and phospholipid-binding proteins and plays important roles in physiologic processes including differentiation and proliferation. Serrated neoplasia pathway is a model of multistep carcinogenesis for CRCs which share serrated morphology, CIMP and *BRAF* mutation.

Peer-review

This is an interesting study investigating the association between Annexin A10 expression and clinical behavior in CRC.

REFERENCES

1 **Jass JR**. Classification of colorectal cancer based on correlation of clinical, morphological and molecular features. *Histopathology* 2007; **50**: 113-130 [PMID: 17204026 DOI: 10.1111/j.1365-2559.2006.02549.x]

2 **Fearon ER**, Vogelstein B. A genetic model for colorectal tumorigenesis. *Cell* 1990; **61**: 759-767 [PMID: 2188735]

3 **Boland CR**, Goel A. Microsatellite instability in colorectal cancer. *Gastroenterology* 2010; **138**: 2073-2087.e3 [PMID: 20420947 DOI: 10.1053/j.gastro.2009.12.064]

4 **Hinoue T**, Weisenberger DJ, Lange CP, Shen H, Byun HM, Van Den Berg D, Malik S, Pan F, Noushmehr H, van Dijk CM, Tollenaar RA, Laird PW. Genome-scale analysis of aberrant DNA methylation in colorectal cancer. *Genome Res* 2012; **22**: 271-282 [PMID: 21659424 DOI: 10.1101/gr.117523.110]

5 **Cancer Genome Atlas Network**. Comprehensive molecular characterization of human colon and rectal cancer. *Nature* 2012; **487**: 330-337 [PMID: 22810696 DOI: 10.1038/nature11252]

6 **Rex DK**, Ahnen DJ, Baron JA, Batts KP, Burke CA, Burt RW, Goldblum JR, Guillem JG, Kahi CJ, Kalady MF, O'Brien MJ, Odze RD, Ogino S, Parry S, Snover DC, Torlakovic EE, Wise PE, Young J, Church J. Serrated lesions of the colorectum: review and recommendations from an expert panel. *Am J Gastroenterol* 2012; **107**: 1315-1329; quiz 1314, 1330 [PMID: 22710576 DOI: 10.1038/ajg.2012.161]

7 **Mussunoor S**, Murray GI. The role of annexins in tumour development and progression. *J Pathol* 2008; **216**: 131-140 [PMID: 18698663 DOI: 10.1002/path.2400]

8 **Rescher U**, Gerke V. Annexins--unique membrane binding proteins with diverse functions. *J Cell Sci* 2004; **117**: 2631-2639 [PMID: 15169834 DOI: 10.1242/jcs.01245]

9 **Gerke V**, Creutz CE, Moss SE. Annexins: linking Ca2+ signalling to membrane dynamics. *Nat Rev Mol Cell Biol* 2005; **6**: 449-461 [PMID: 15928709 DOI: 10.1038/nrm1661]

10 **Lu SH**, Yuan RH, Chen YL, Hsu HC, Jeng YM. Annexin A10 is an immunohistochemical marker for adenocarcinoma of the upper gastrointestinal tract and pancreatobiliary system. *Histopathology* 2013; **63**: 640-648 [PMID: 24024557 DOI: 10.1111/his.12229]

11 **Shimizu T**, Kasamatsu A, Yamamoto A, Koike K, Ishige S, Takatori H, Sakamoto Y, Ogawara K, Shiiba M, Tanzawa H, Uzawa K. Annexin A10 in human oral cancer: biomarker for tumoral growth via G1/S transition by targeting MAPK signaling pathways. *PLoS One* 2012; **7**: e45510 [PMID: 23029062 DOI: 10.1371/journal.pone.0045510]

12 **Gonzalo DH**, Lai KK, Shadrach B, Goldblum JR, Bennett AE, Downs-Kelly E, Liu X, Henricks W, Patil DT, Carver P, Na J, Gopalan B, Rybicki L, Pai RK. Gene expression profiling of serrated polyps identifies annexin A10 as a marker of a sessile serrated adenoma/polyp. *J Pathol* 2013; **230**: 420-429 [PMID: 23595865 DOI: 10.1002/path.4200]

13 **Kim JH**, Rhee YY, Kim KJ, Cho NY, Lee HS, Kang GH. Annexin A10 expression correlates with serrated pathway features in colorectal carcinoma with microsatellite instability. *APMIS* 2014; **122**: 1187-1195 [PMID: 24909058 DOI: 10.1111/apm.12284]

14 **Ogino S**, Chan AT, Fuchs CS, Giovannucci E. Molecular pathological epidemiology of colorectal neoplasia: an emerging transdisciplinary and interdisciplinary field. *Gut* 2011; **60**: 397-411 [PMID: 21036793 DOI: 10.1136/gut.2010.217182]

15 **Kim JH**, Shin SH, Kwon HJ, Cho NY, Kang GH. Prognostic implications of CpG island hypermethylator phenotype in colorectal cancers. *Virchows Arch* 2009; **455**: 485-494 [PMID: 19911194 DOI: 10.1007/s00428-009-0857-0]

16 **Yoo EJ**, Park SY, Cho NY, Kim N, Lee HS, Kang GH. Helicobacter pylori-infection-associated CpG island hypermethylation in the stomach and its possible association with polycomb repressive marks. *Virchows Arch* 2008; **452**: 515-524 [PMID: 18335237 DOI: 10.1007/s00428-008-0596-7]

17 **Toyota M**, Ahuja N, Ohe-Toyota M, Herman JG, Baylin SB, Issa JP. CpG island methylator phenotype in colorectal cancer. *Proc Natl Acad Sci USA* 1999; **96**: 8681-8686 [PMID: 10411935]

18 **Ogino S**, Cantor M, Kawasaki T, Brahmandam M, Kirkner GJ, Weisenberger DJ, Campan M, Laird PW, Loda M, Fuchs CS. CpG island methylator phenotype (CIMP) of colorectal cancer is best characterised by quantitative DNA methylation analysis and prospective cohort studies. *Gut* 2006; **55**: 1000-1006 [PMID: 16407376 DOI: 10.1136/gut.2005.082933]

19 **Weisenberger DJ**, Siegmund KD, Campan M, Young J, Long TI, Faasse MA, Kang GH, Widschwendter M, Weener D, Buchanan D, Koh H, Simms L, Barker M, Leggett B, Levine J, Kim M, French AJ, Thibodeau SN, Jass J, Haile R, Laird PW. CpG island methylator phenotype underlies sporadic microsatellite instability and is tightly associated with BRAF mutation in colorectal cancer. *Nat Genet* 2006; **38**: 787-793 [PMID: 16804544]

20 **Balic M**, Pichler M, Strutz J, Heitzer E, Ausch C, Samonigg H, Cote RJ, Dandachi N. High quality assessment of DNA methylation in archival tissues from colorectal cancer patients using quantitative high-resolution melting analysis. *J Mol Diagn* 2009; **11**: 102-108 [PMID: 19179456 DOI: 10.2353/jmoldx.2009.080109]

21 **Capper D**, Preusser M, Habel A, Sahm F, Ackermann U, Schindler G, Pusch S, Mechtersheimer G, Zentgraf H, von Deimling A. Assessment of BRAF V600E mutation status by immunohistochemistry with a mutation-specific monoclonal antibody. *Acta Neuropathol* 2011; **122**: 11-19 [PMID: 21638088 DOI: 10.1007/s00401-011-0841-z]

22 **Affolter K**, Samowitz W, Tripp S, Bronner MP. BRAF V600E mutation detection by immunohistochemistry in colorectal carcinoma. *Genes Chromosomes Cancer* 2013; **52**: 748-752 [PMID: 23650027 DOI: 10.1002/gcc.22070]

23 **Sinicrope FA**, Smyrk TC, Tougeron D, Thibodeau SN, Singh S, Muranyi A, Shanmugam K, Grogan TM, Alberts SR, Shi Q. Mutation-specific antibody detects mutant BRAFV600E protein expression in human colon carcinomas. *Cancer* 2013; **119**: 2765-2770 [PMID: 23657789 DOI: 10.1002/cncr.28133]

24 **Toon CW**, Walsh MD, Chou A, Capper D, Clarkson A, Sioson L, Clarke S, Mead S, Walters RJ, Clendenning M, Rosty C, Young JP, Win AK, Hopper JL, Crook A, von Deimling A, Jenkins MA, Buchanan DD, Gill AJ. BRAFV600E immunohistochemistry

facilitates universal screening of colorectal cancers for Lynch syndrome. *Am J Surg Pathol* 2013; **37**: 1592-1602 [PMID: 23797718 DOI: 10.1097/PAS.0b013e31828f233d]

25 **Adackapara CA**, Sholl LM, Barletta JA, Hornick JL. Immunohistochemistry using the BRAF V600E mutation-specific monoclonal antibody VE1 is not a useful surrogate for genotyping in colorectal adenocarcinoma. *Histopathology* 2013; **63**: 187-193 [PMID: 23763264 DOI: 10.1111/his.12154]

26 **Kuan SF**, Navina S, Cressman KL, Pai RK. Immunohistochemical detection of BRAF V600E mutant protein using the VE1 antibody in colorectal carcinoma is highly concordant with molecular testing but requires rigorous antibody optimization. *Hum Pathol* 2014; **45**: 464-472 [PMID: 24529329 DOI: 10.1016/j.humpath.2013.10.026]

27 **Wiland HO**, Shadrach B, Allende D, Carver P, Goldblum JR, Liu X, Patil DT, Rybicki LA, Pai RK. Morphologic and molecular characterization of traditional serrated adenomas of the distal colon and rectum. *Am J Surg Pathol* 2014; **38**: 1290-1297 [PMID: 25127095 DOI: 10.1097/pas.0000000000000253]

28 **Tsai JH**, Lin YL, Cheng YC, Chen CC, Lin LI, Tseng LH, Cheng ML, Liau JY, Jeng YM. Aberrant expression of annexin A10 is closely related to gastric phenotype in serrated pathway to colorectal carcinoma. *Mod Pathol* 2015; **28**: 268-278 [PMID: 25081749 DOI: 10.1038/modpathol.2014.96]

29 **Sajanti SA**, Väyrynen JP, Sirniö P, Klintrup K, Mäkelä J, Tuomisto A, Mäkinen MJ. Annexin A10 is a marker for the serrated pathway of colorectal carcinoma. *Virchows Arch* 2015; **466**: 5-12 [PMID: 25395067 DOI: 10.1007/s00428-014-1683-6014-1683-6]

30 **Kalady MF**, Dejulius KL, Sanchez JA, Jarrar A, Liu X, Manilich E, Skacel M, Church JM. BRAF mutations in colorectal cancer are associated with distinct clinical characteristics and worse prognosis. *Dis Colon Rectum* 2012; **55**: 128-133 [PMID: 22228154 DOI: 10.1097/DCR.0b013e31823c08b3]

31 **Ogino S**, Nosho K, Kirkner GJ, Kawasaki T, Meyerhardt JA, Loda M, Giovannucci EL, Fuchs CS. CpG island methylator phenotype, microsatellite instability, BRAF mutation and clinical outcome in colon cancer. *Gut* 2009; **58**: 90-96 [PMID: 18832519 DOI: 10.1136/gut.2008.155473]

32 **Juo YY**, Johnston FM, Zhang DY, Juo HH, Wang H, Pappou EP, Yu T, Easwaran H, Baylin S, van Engeland M, Ahuja N. Prognostic value of CpG island methylator phenotype among colorectal cancer patients: a systematic review and meta-analysis. *Ann Oncol* 2014; **25**: 2314-2327 [PMID: 24718889 DOI: 10.1093/annonc/mdu149]

33 **Pai RK**, Shadrach BL, Carver P, Heald B, Moline J, Church J, Kalady MF, Burke CA, Plesec TP, Lai KK, Gonzalo DH, Pai RK. Immunohistochemistry for annexin A10 can distinguish sporadic from Lynch syndrome-associated microsatellite-unstable colorectal carcinoma. *Am J Surg Pathol* 2014; **38**: 518-525 [PMID: 24625416 DOI: 10.1097/pas.0000000000000148]

34 **Kim JH**, Kang GH. Annexin A10 expression in microsatellite-unstable colorectal cancers: is it specific to sporadic tumors? *Am J Surg Pathol* 2014; **38**: 1577-1579 [PMID: 25118814 DOI: 10.1097/pas.0000000000000306]

35 **Dahlin AM**, Palmqvist R, Henriksson ML, Jacobsson M, Eklöf V, Rutegård J, Oberg A, Van Guelpen BR. The role of the CpG island methylator phenotype in colorectal cancer prognosis depends on microsatellite instability screening status. *Clin Cancer Res* 2010; **16**: 1845-1855 [PMID: 20197478 DOI: 10.1158/1078-0432.ccr-09-2594]

P- Reviewer: Hsu LS, Sakata Y **S- Editor**: Wang JL
L- Editor: Wang TQ **E- Editor**: Liu XM

World Journal of Gastroenterology

Submit a Manuscript: http://www.wjgnet.com/esps/
Help Desk: http://www.wjgnet.com/esps/helpdesk.aspx
DOI: 10.3748/wjg.v21.i33.9758

World J Gastroenterol 2015 September 7; 21(33): 9758-9764
ISSN 1007-9327 (print) ISSN 2219-2840 (online)

ORIGINAL ARTICLE

Retrospective Study

Changes in the spectrum of gastric polyps in the Chinese population

Nan-Nan Fan, Jing Yang, Gang Sun, Zhong-Sheng Lu, En-Qiang Ling Hu, Xiang-Dong Wang, Yun-Sheng Yang

Nan-Nan Fan, Jing Yang, Gang Sun, Zhong-Sheng Lu, En-Qiang Ling Hu, Xiang-Dong Wang, Yun-Sheng Yang, Institute of Digestive Diseases, Chinese PLA General Hospital, Beijing 100853, China

Nan-Nan Fan, Nankai University School of Medicine, Tianjin 300071, China

Author contributions: Yang YS designed the research; Fan NN, Yang J, Sun G, Lu ZS, Ling Hu EQ and Wang XD performed the research; Fan NN and Sun G contributed new reagents or analytic tools; Fan NN analyzed the data; Fan NN wrote the paper.

Informed consent statement: All patients gave signed informed consent for EGD before the procedure.

Conflict-of-interest statement: The authors have no conflicts of interest to disclose.

Data sharing statement: No additional data are available.

Correspondence to: Yun-Sheng Yang, MD, PhD, Institute of Digestive Diseases, Chinese PLA General Hospital, No. 28 Fuxing Road, Haidian District, Beijing 100853, China. sunny301ddc@126.com
Telephone: +86-10-55499007
Fax: +86-10-68212267

Received: January 15, 2015
Peer-review started: January 17, 2015
First decision: March 26, 2015
Revised: April 4, 2015
Accepted: April 28, 2015
Article in press: April 28, 2015

Published online: September 7, 2015

Abstract

AIM: To evaluate the change in spectrum of gastric polyps in the Chinese population in the past ten years.

METHODS: A total of 157902 consecutive patients undergoing esophagogastroduodenoscopy (EGD) from 2004 to 2013 in a tertiary hospital were retrospectively reviewed using an EGD database. Endoscopic records of 4043 patients diagnosed with gastric polyps were recalled for analysis. Data including demographics, information on polyps such as location, pathological diagnosis, reflux esophagitis and *Helicobacter pylori* infection were obtained. We focused on epithelial polyps, especially hyperplastic polyps, fundic gland polyps and adenomas, and histological classification of specimens from biopsy and endoscopic polypectomy was performed by professional pathologists, based on the updated guidelines. To explore the age distribution of gastric polyps over time, we divided patients with polyps into four groups: A (aged < 30 years), B (aged 30-44 years), C (aged 45-59 years) and D (aged > 60 years). Differences in localization, age, and sex distribution of gastric polyps were analyzed by statistical software.

RESULTS: A total of 157902 EGD procedures were performed in ten years at our digestive endoscopy center, of which 4043 cases were diagnosed with gastric polyps confirmed by pathology. There were 2574 (63%) female and 1469 (37%) male patients with an average age of 54.7 years. The overall prevalence of gastric polyps was 2.6% (4043/157902). Our database demonstrated a rising prevalence of gastric polyps over the decade, increasing from 1.0% (80/8025) to 4.70% (828/17787) between 2004 and 2013. There has been a change in the spectrum of gastric polyps with the

frequencies of FGPs increasing from 19% (15/80) to 77% (638/828) and hyperplastic polyps decreasing from 65% (52/80) to 15% (123/828). Moreover, data on 1921 polyps in 828 patients diagnosed with gastric polyps in 2013 showed that FGP was the most common type in the current polyp spectrum, making up 81.3% (1562/1921). Location and age distribution of gastric polyps have also altered. The prevalence of polyps located in the antrum decreased from 37.5% (30/80) to 9.30% (77/828), with an increasing prevalence of polyps in the corpus, from 45% (36/80) to 64.25% (532/828). The constituent ratio of older patients (aged > 60 years) in the polyp population decreased from 62.5% (50/80) to 32.13% (266/828), while that of patients aged 45-60 years showed an increased trend.

CONCLUSION: There was a shift change in the spectrum of gastric polyps in the Chinese population with altered location and age distribution in the past ten years.

Key words: Gastric polyps; Hyperplastic polyps; Fundic gland polyps; Adenomas; *Helicobacter pylori*

Core tip: Recent studies have suggested that fundic gland polyps (FGPs) are the dominant type of gastric polyps rather than hyperplasic polyps. In the Chinese population, data on the spectrum of gastric polyps are limited, and the dynamic change in polyp spectrum has never been evaluated on a large scale. Hence, we retrospectively reviewed 4043 cases with gastric polyps from 157902 patients who underwent esophagogastroduodenoscopy in a tertiary hospital over a 10-year period. We observed a dynamic change in the spectrum of gastric polyps, which presented as a shift in which FGPs rather than hyperplastic polyps were the most common type, and the age, location and sex distribution of gastric polyps were also altered.

Fan NN, Yang J, Sun G, Lu ZS, Ling Hu EQ, Wang XD, Yang YS. Changes in the spectrum of gastric polyps in the Chinese population. *World J Gastroenterol* 2015; 21(33): 9758-9764 Available from: URL: http://www.wjgnet.com/1007-9327/full/v21/i33/9758.htm DOI: http://dx.doi.org/10.3748/wjg.v21.i33.9758

INTRODUCTION

Polyps are defined as protuberant lesions into the lumen originating in the epithelium or submucosa, which are characterized as sessile or pedunculated, sporadic, or part of a syndrome[1]. Gastric polyps are usual finding under endoscopic exam and most patients are asymptomatic. However, larger gastric polyps may result in some symptoms, such as bleeding, anemia, abdominal pain, and even gastric outlet obstruction[2-4]. Widespread use of endoscopic examinations contributes to improving the detected rate of gastric polyps. Endoscopic features of some polyps may be useful for diagnosis, yet not every polypoid lesion can be defined as a polyp unless histopathologically confirmed[5]. Based on histological features, gastric polyps are classified into two groups: neoplastic and non-neoplastic polyps with several subtypes[6]. Most gastric polyps are non-neoplastic, which is different to colorectal polyps.

Hyperplastic polyps (HPPs) used to be the most common polyps[7,8], with a relative prevalence of approximately 70%[1]. However, results from recent studies indicate that the prevalence of fundic gland polyps (FGPs) has increased greatly in recent decades. The reasons for this change remain unclear. Some previous studies have suggested several circumstances that may result in a spectrum change of gastric polyps[5], which include expanded indications for esophagogastroduodenoscopy (EGD), long-term use of proton pump inhibitors (PPIs), decreasing *Helicobacter pylori* (*H. pylori*) infection, and enhanced health consciousness in the general population. FGPs are reported as the most common type of polyps detected at EGD in the United States[9]. Although a similar spectrum of gastric polyps is also reported in the Northern Chinese population[10], few Chinese population-based data exist. Data on the spectrum and distribution patterns of gastric polyps in the Chinese patient population are limited, particularly for the dynamic observation of the spectrum of gastric polyps.

In view of this, we evaluated the spectrum of gastric polyps in the Chinese population by reviewing a 10-year consecutive EGD database. We also hypothesized that location, age and sex distribution of gastric polyps may have changed with the altered spectrum of polyps over the past 10 years.

MATERIALS AND METHODS

This study was conducted at the Digestive Endoscopy Center of Chinese PLA General Hospital, which is a large hospital integrating medical services, education and research. All patients undergoing EGD in our center from January 1, 2004 to December 31, 2013 were analyzed retrospectively. All patients gave signed informed consent for EGD before the procedure. Specimens from biopsy and endoscopic polypectomy were interpreted by a professional group of pathologists. Gastric polyps of epithelial origin were included, while hamartomatous polyps, polyposis syndromes and non-mucosal intramural polyps were excluded. In particular, the study population excluded patients with esophageal, gastric or esophagogastric varices who underwent EGD, intended mainly for treatment with endoscopic cyanoacrylate injection, sclerotherapy or endoscopic variceal ligation, which is a characteristic endoscopy technique

Table 1 Overall demographics of gastric polyps, fundic gland polyps, hyperplastic polyps and adenomas *n* (%)

	GP	FGP	HPP	Adenomas
Age (yr) (mean ± SD)	54.7 ± 12.9	53.9 ± 12.6	55.2 ± 13.3	66.4 ± 10.1
Gender (F/M)	2574:1469 (1.75:1)	1190:857 (1.39:1)	580:439 (1.32:1)	16:59 (1:3.69)
Helicobacter pylori infection rate	186/4043 (4.60)	82/2047 (4.0)	59/1019 (5.79)	1/75 (1.33)
Reflux esophagitis incidence	356/4043 (8.81)	219/2047 (10.70)	39/1019 (3.83)	-
Dysplasia	68/4043 (1.68)	3/2047 (0.15)	14/2047 (0.68)	45/75 (60)
HIN	25/4043 (0.62)	-	-	23/75 (31)

GP: Gastric polyp; FGP: Fundic gland polyp; HPP: Hyperplastic polyp.

Table 2 Demographics, prevalence and sex distribution of gastric polyps in the past 10 years *n* (%)

Year	Cases	Age (yr) (mean ± SD)	Gender (M/F)	Prevalence
2004	80	59.6 ± 14.7	48:32 (1.5:1)	80/8025 (1.0)
2005	74	57.5 ± 11.4	34:40 (1:1.18)	74/10739 (0.7)
2006	140	55.6 ± 10.7	57:83 (1:1.46)	140/13814 (0.8)
2007	218	52.7 ± 11.3	93:125 (1:1.34)	218/17372 (1.3)
2008	275	53.3 ± 10.7	105:160 (1:1.52)	275/17941 (1.5)
2009	462	54.8 ± 13.1	171:291 (1:1.70)	462/18364 (2.5)
2010	496	54.7 ± 12.8	183:313 (1:1.71)	496/17125 (2.9)
2011	664	54.5 ± 12.5	223:441 (1:1.98)	664/17893 (3.7)
2012	806	54.8 ± 12.9	284:522 (1:1.83)	806/18842 (4.7)
2013	828	54.6 ± 12.1	271:575 (1:2.12)	828/17787 (4.7)
Total	4043	54.7 ± 12.9	1469:2574 (1:1.75)	4043/157902 (2.6)

performed in our department.

Information on patients and polyps were obtained from endoscopy reports, which included age, sex, and location of gastric polyps, and histological diagnosis. Histological classification was carried out according to an updated classification suggested in the 2010 guidelines of the British Society of Gastroenterology (BSG)[11]. Gastric polyps of epithelial origin mainly include HPPs, FGPs, and adenomas. We focused on epithelial polyps, especially HPPs, FGPs and adenomas, which are classic gastric polyps. Infection with *H. pylori* was diagnosed by histology.

Statistical analysis

All statistical calculations were performed with SPSS version 15.0. Mean and standard deviation (SD) were used to describe continuous variables, while percentages were used for discrete variables. The significance of possible associations between discrete variables was assessed by the Pearson χ^2 test.

RESULTS

Demographic characteristics of gastric polyps

We performed a total of 157902 EGD procedures over the 10-year review period. The study population comprised patients referred for various indications. Among these, 4043 (2.60%) cases were diagnosed with gastric polyps by pathology. The average age and sex distribution of patients with gastric polyps are shown in Table 1. There were 2574 (63%) female and 1469 (37%) male patients, with a mean age of 54.7 years (range: 8-92 years). Either FGP or HPP was significantly more frequent in women with a sex ratio of 1.39:1 and 1.32:1, respectively. However, only adenomas were predominant in men, with a male-to-female ratio of 3.69:1.0.

The incidence of *H. pylori* infection in patients with gastric polyps diagnosed by pathology was 4.60% (186/4043). Among 1019 patients with HPPs, 59 (5.79%) patients were pathologically confirmed to have *H. pylori* infection, which was significantly more common than that in the FGP (4.0%) and adenoma (1.33%) groups (P = 0.005). 293 (10.70%) patients with FGPs were diagnosed with reflux esophagitis (RE), which was higher than those without FGPs, yet there was no difference in the various types of gastric polyps. Information on dysplasia in FGPs, HPPs and adenomas was recorded, in terms of the malignant potential of different types of polyps causing differing consequences for patients. Dysplasia occurred in various types of gastric polyps. Notably, dyspepsia was detected in 45 of 75 patients with adenomas, and high-grade intraepithelial neoplasia was confirmed in 23 cases, which was significantly higher than for other types of gastric polyps (60% *vs* 8.81%, P < 0.001; 60% *vs* 0.15%, P = 0.0000; 60% *vs* 0.68%, P = 0.0000).

To explore the dynamic changes in age and sex distribution of gastric polyps, we also analyzed data on gastric polyp yield from EGD from 2004 to 2013 (Table 2). The average age of patients with polyps (54.7 years) was higher than the entire patient population (51.4 years). The average age of patients with gastric polyps showed a decreasing trend, from 59.6 years in 2004 to 54.7 years in 2013. A female predominance in the polyp population was present, with the highest sex ratio of 2.12:1.0. Moreover, the incidence of *H. pylori* in the polyp population decreased significantly from 8.75% (7/80) to 4.23% (35/828) (P = 0.2057), while the prevalence of reflux esophagitis rose from 1.25% (1/80) to 11.35% (94/828) (P = 0.0048).

Prevalence and distribution of various types of gastric polyps

Among the 4043 cases with documented true polyps (both endoscopically and histologically identified), 2647 cases were diagnosed with FGPs, followed by HPPs (1019 cases), with adenomas detected only in 75 cases, and the remaining 302 cases were diagnosed with other types of gastric epithelial polyps, including polyps that could not be classified into definite types. The relative prevalence of FGPs, HPs and adenomas

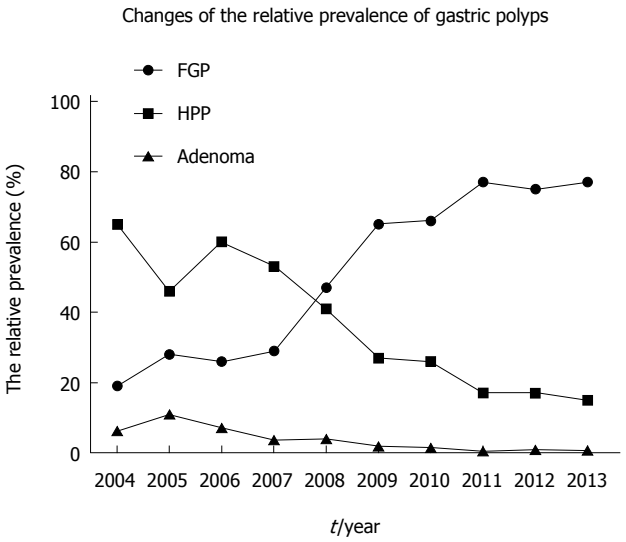

Figure 1 Changes in the relative prevalence of gastric polyps. The relative prevalence of FGPs increased with a decrease in HPPs, and no significant change in the prevalence of adenoma in the past ten years. FGP: Fundic gland polyp; HPP: Hyperplastic polyp.

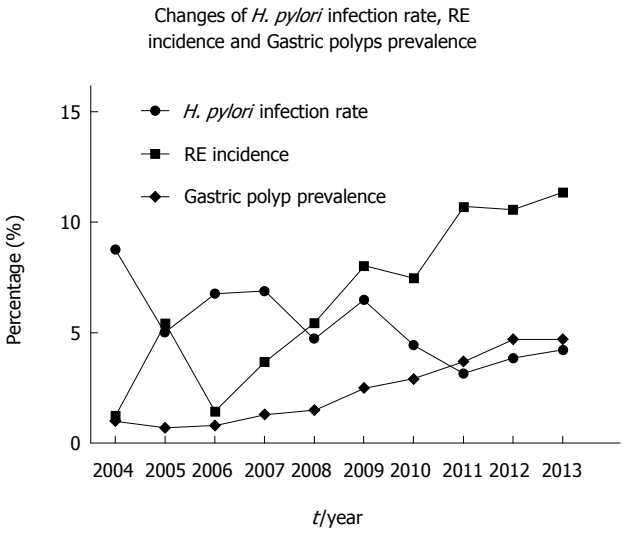

Figure 2 Changes in *Helicobacter pylori* infection rate, reflux esophagitis (RE) incidence and gastric polyp prevalence. There was a gradual increase in the prevalence of gastric polyps from 2004 (1.0%, 80/8025) to 2013 (4.7%, 828/17787), with an increased incidence of reflux esophagitis and a decrease in *Helicobacter pylori* infection rate in the overall patient population. RE: Reflux esophagitis.

in this decade are described in Figure 1. The overall prevalence of FGPs, HPs and adenomas was 65% (2647/4043), 25% (1019/4043) and 1.9% (75/4043), respectively. There was an increase in the prevalence of gastric polyps on EGD in the past 10 years, which rose from 1.0% (80/8025) to 77% (638/828) (P = 0.0000) (Figure 2). FGP has become the most common type of gastric polyp rather than HPP. Figure 1 indicates that the relative frequencies of FGPs and HPs have also altered, increasing from 19% (15/80) to 77% (638/828) (P = 0.0000) for FGPs, and decreasing from 65% (52/80) to 15% (123/828) for HPPs (P =

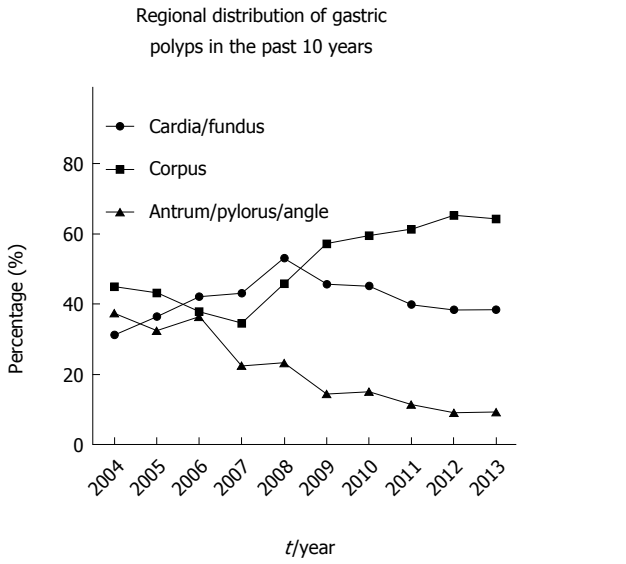

Figure 3 Regional distribution of gastric polyps in the past ten years. There was a progressive shift toward the corpus in the regional distribution of gastric polyps over the past 10 years. The detection rate of gastric polyps located in the corpus increased from 45% (36/80) to 64.25% (532/828), and polyps in the antrum, pylorus and angle deceased from 37.5% (30/80) to 9.30% (77/828).

0.0000). In order to re-evaluate the current spectrum of gastric polyps, we analyzed 1921 gastric polyps from 828 patients in 2013, of which 1561 were FGPs, 213 HPs, and 6 adenomas. FGP was confirmed as the most common type in the current polyp spectrum, comprising up to 81.30% (1562/1921).

Location and age distribution of gastric polyps

Moreover, we analyzed the regional distribution of gastric polyps over the past ten years. In our patient population, most gastric polyps were detected in the corpus and fundus (Figure 3). There was a progressive shift toward the corpus in the regional distribution of gastric polyps (45% *vs* 64.25%, P = 0.0007).

We divided patients with gastric polyps into four groups according to their age: Group A (aged < 30 years), Group B (aged 30-44 years), Group C (aged 45-59 years), and Group D (aged > 60 years). Overall, of 4043 cases, 1395 (34.5%) were aged > 60 years, with 17.29% and 44.99% in the younger age Groups B and C, respectively. Altered age distribution of gastric polyps was observed (Table 3). Patients aged 45-59 years comprised nearly half (44.99%) of the entire polyp population in 2013, while patients aged > 60 years were predominant in the polyp population before 2006 (41.43% *vs* 32.13%, P = 0.031). Gastric polyps were rarely detected in patients aged < 30 years, comprising only 3.22 % of patients with gastric polyps.

DISCUSSION

We reviewed some of the characteristics of gastric polyps in 4043 patients recorded in an EGD database

Table 3 Age distribution of gastric polyps in the past 10 years *n* (%)

Year	Group A	Group B	Group C	Group D
2004	3/80 (3.8)	10/80 (12.5)	17/80 (21.25)	50/80 (62.5)
2005	1/74 (1.35)	13/74 (17.57)	24/74 (32.43)	36/74 (48.65)
2006	5/140 (3.57)	22/140 (15.71)	55/140 (39.29)	58/140 (41.43)
2007	12/218 (5.5)	51/218 (23.4)	88/218 (40.37)	67/218 (30.73)
2008	14/275 (5.09)	54/275 (19.26)	121/275 (44)	86/275 (31.27)
2009	13/462 (2.81)	89/462 (18.75)	195/462 (42.21)	165/462 (35.71)
2010	10/496 (2.02)	93/496 (19.64)	229/496 (46.17)	164/496 (33.06)
2011	22/664 (3.31)	97/664 (14.61)	329/664 (49.55)	216/664 (32.53)
2012	28/806 (3.47)	131/806 (16.25)	360/806 (44.67)	287/806 (35.61)
2013	22/828 (2.66)	139/828 (16.69)	401/828 (48.43)	266/828 (32.13)
Total	130/4043 (3.22)	699/4043 (17.29)	1819/4043(44.99)	1395/4043 (34.5)

in a tertiary hospital over a 10-year period, which provided the first large-scale consecutive data on gastric polyps in the Chinese population in the past ten years. This is also the first report on the prevalence, location and sex distribution of gastric polyps in the Chinese population. The prevalence of gastric polyps on EGD ranges between 3.00% and 6.35%[5,12], which varies widely among published series, and correlates closely with the patient population[13]. In the present population, there was a gradual increase in the prevalence of gastric polyps in this decade, with the overall prevalence of 2.60% and 4.7% in 2013, respectively. Our data demonstrate the change in the spectrum of gastric polyps in China, with altered location and sex distribution. FGPs rather than HPPs are now the most common type of gastric polyps. Furthermore, there was an increasing age-specific prevalence of polyps in patients aged 45-59 years in this decade. We also confirmed a progressive shift towards the corpus in the regional distribution of gastric polyps. Gastric polyps occurred most frequently in the corpus of female patients aged 45-60 years, while adenomas were more frequent in the antrum of male patients aged > 60 years.

We compared our data with those from previous studies in China and other countries[1,5,10,14-17] (Table 4). The most significant difference in these studies of different populations was the relative proportion of FGPs. These differences may have been due to different populations, study design and methods, and time of study. Our data show a similar spectrum of polyps to that seen in a previous study in the Northern Chinese population[10] and in the USA[5]. In particular, the relative proportion of FGPs in the present study was consistent with that in the US study, which was up to 77% of gastric polyps. Our ten-year consecutive data on the relative proportion of FGPs suggest that FGPs have become the most predominant type since 2008. Moreover, the studies from the USA and China conducted after 2008 showed a similar spectrum of polyps. This phenomenon is believed not to be coincidental, and supports the notion that there has been a change in the spectrum of gastric polyps in western countries and China, and needs to be confirmed by more data from other countries.

In the present study, the polyp spectrum changed, with an increasing prevalence of FGPs. Several factors may explain this change. Although the relationship between PPI intake and FGP development remains controversial[18-22], a series of studies support the role of long-term PPI intake in the genesis of FGPs[21,23,24]. The increased incidence of gastroesophageal reflux disease and socioeconomic development in China has resulted in more individuals taking PPIs, and an increase in PPI-related FGPs. Our data indicated that there were significant differences in the incidence of reflux esophagitis under endoscopy in patients with FGPs compared with gastric polyps overall and those with HPPs. It is notable that the incidence of reflux esophagitis in patients with gastric polyps overall showed an increasing annual trend, which coincided with the increased detection rate of FGPs. This finding suggests a positive association between FGPs and reflux esophagitis, given that patients with reflux esophagitis tend to use PPIs for prolonged periods, while the latter (PPIs) has been associated with FGPs in a series of studies[24,25]. In the latest study performed in the USA, reflux disease was also reported to be significantly more common in patients with fundic gland polyps[17]. Thus, our data may indirectly support a possible correlation between PPIs and FGPs. However, we could not obtain information on the use of PPIs in this retrospective study, and our observations could not demonstrate a clear correlation between PPIs or reflux esophagitis and FGPs. Hence, further investigations are needed to determine the role of PPIs in the genesis of sporadic FGPs. The decrease in *H. pylori* infection may be another important factor, which is reported to be negatively associated with HPPs[26-29]. Most gastric HPPs disappear after eradication of *H. pylori*, therefore the decrease in infection may have led to a decrease in the prevalence of HPPs, which was confirmed in our study.

Few previous studies have addressed the prevalence of gastric polyps in different age groups. We demonstrated altered location and age distribution of gastric polyps over the past decade in the present study. Advances in digestive endoscopy techniques and enhanced health awareness have extended the indications for EGD. As a result, EGD has been performed in younger individuals, and gastric polyps have been detected at an early age. HPPs were most common in the antrum[30], while FGPs were most common in the fundus and upper corpus[31], thus the regional distribution of gastric polyps has changed with the spectrum. Our data demonstrate that adenomas are most common in elderly male patients, and have a high malignant potential with dysplasia occurring in 60% of cases, indicating that endoscopists should be aware of the presence of adenomas with high malignant potential in that population.

The present study was conducted in a tertiary hospital center over a long period of time, with large

Table 4 Spectra of gastric polyps in previous and current studies

Ref.	Country	Pub. year	Years	Prevalence of polyps	No. of polyps	Median age (yr)	Gender (F/M)	FGP	HPP	Adenoma
Deppisch *et al*[7]	United States	1989	10	-	121	-	-	17%	75%	8.6%
Stolte *et al*[12]	Germany	1994	20	-	5515	NR	NR	47%	28.3%	9%
Sivelli *et al*[13]	Italy	2002	6		164	61.4	01:01.5	NR	44.5%	16.4%
Gencosmanoglu *et al*[14]	Turkey	2003	5	-	150	53	1.4:1	14%	64%	3%
Morais *et al*[1]	Brazil	2007	5	153/26000 (0.59%)	153	64	01:01.4	16.3%	71.3%	12.4%
Carmack *et al*[5]	United States	2009	1	7877/121564 (6.35%)	7877	56	1.4:1	77%	17%	0.7%
Cao *et al*[10]	China	2000	1	68/6784 (1.0%)	68	56.8	1.7:1	8.8%	48.5%	14.7%
Cao *et al*[10]	China	2010	1	183/17337 (1.0%)	183	55.9	2.0:1	66.1%	20.8%	4.9%
The present study	China	2004-2013	10	183/157902 (2.60%)	4043	54.7	1.75: 1	65%	25%	1.9%
The present study	China	2013	1	828/17787 (4.7%)	828	54.6	2.12:1	75%	17%	0.5%
Sonnenberg *et al*[17]	United States	2015	1	71575 /927137 (7.72%)	71575	-	2.03:1	79.9%	18.6%	0.92%

NR: Not reported; GP: Gastric polyp; FGP: Fundic gland polyp; HPP: Hyperplastic polyp.

numbers of patients from different geographic areas in China, ensuring satisfactory representation of the entire nation in the results. However, this was a retrospective study and not a population-based screening study, therefore, when interpreting these data some factors should be taken into consideration. First, it was not a screening study based on an asymptomatic population undergoing EGD, and the study population comprised patients referred for various indications, and not all patients diagnosed with polyps or polypoid lesions by endoscopy accepted biopsy, thus the prevalence of polyps addressed in our study does not represent the true incidence in the entire population. Second, during the 10-year period, the guidelines for EGD and therapeutic trends have been updated. The biases of the population studied including socioeconomic, demographic and genetic characteristics should also be considered when comparing data from this study with previous studies. Lastly, *H. pylori* infection was diagnosed by pathology, which has a low sensitivity, resulting in a lower incidence of infection than the true situation.

In summary, the detection rate of gastric polyps in the Chinese population has gradually increased with widespread use of EGD in the recent decade. The spectrum of gastric polyps has changed, with FGPs rather than HPPs as the most common type of polyp. Widespread use of PPIs and decreased *H. pylori* infection may explain this change. Location and age distribution of gastric polyps have also been altered with the changed spectrum, where an increased number of polyps were detected in the corpus and a decreased proportion of patients aged > 60 years had polyps. These findings may allow us to explore the underlying factors associated with gastric polyps, and provide better endoscopic surveillance for the general population, especially in patients with gastric polyps.

COMMENTS

Background

Gastric polyps are the most common positive finding in gastroendoscopic procedures. The prevalence of gastric polyps varies widely among published studies, and correlates closely with the patient population. An altered spectrum of gastric polyps in the Western population has been reported, yet data from the Chinese population are limited.

Research frontiers

Hyperplasic polyps were the most common type of gastric polyps. However, recent studies suggest a shift towards fundic gland polyps, which may be associated with several circumstances such as widespread use and expanded indications for endoscopic examinations, increased incidence of gastroesophageal reflux disease, and frequent intake of proton pump inhibitors.

Innovations and breakthroughs

The present study provides the first large-scale consecutive data on gastric polyps in the Chinese population over a 10-year period. It also provides information on the prevalence, location and sex distribution of gastric polyps in the Chinese population.

Applications

Evaluation of the dynamic change in the spectrum, location and age distribution of gastric polyps can help determine the underlying factors associated with gastric polyps, and provide better endoscopic surveillance for the general population, especially patients with gastric polyps.

Terminology

Polyps are defined as protuberant lesions into the lumen originating in the epithelium or submucosa, which are characterized as sessile or pedunculated, sporadic, or part of a syndrome. Gastric polyps can be classified into various types, and hyperplastic polyps, fundic gland polyps and adenomas are common.

Peer-review

This is one of the largest series of the last years, providing a clear picture of epidemiology of gastric polyps in China, and underlines the correlation between type of polyps, location, age and associated pathologies. Moreover, a dynamic change in spectrum of gastric polyps is described. However, an obvious limitation is the retrospectivity of the present study, and further prospective studies should be encouraged.

REFERENCES

1 **Morais DJ**, Yamanaka A, Zeitune JM, Andreollo NA. Gastric polyps: a retrospective analysis of 26,000 digestive endoscopies. *Arq Gastroenterol* 2007; **44**: 14-17 [PMID: 17639176]

2 **Nayudu SK**, Niazi M, Balar B, Kumbum K. A rare complication of hyperplastic gastric polyp. *Case Rep Gastrointest Med* 2013; **2013**: 631975 [PMID: 23401808 DOI: 10.1155/2013/631975]

3 **He HY**, Shen ZB, Fang Y, Sun YH, Qin XY. Bleeding and hyperpyrexia in an adult with gastric inflammatory fibroid polyp. *Chin Med J* (Engl) 2013; **126**: 2594 [PMID: 23823846]
4 **Vlacancich R**, Sultan M, Al-Kawas F. Gastric outlet obstruction caused by prolapsed gastric polyp into the pyloric channel. *Clin Gastroenterol Hepatol* 2014; **12**: A27-A28 [PMID: 24362052 DOI: 10.1016/j.cgh.2013.12.015]
5 **Carmack SW**, Genta RM, Schuler CM, Saboorian MH. The current spectrum of gastric polyps: a 1-year national study of over 120,000 patients. *Am J Gastroenterol* 2009; **104**: 1524-1532 [PMID: 19491866 DOI: 10.1038/ajg.2009.139]
6 **Fock KM**, Ang TL. Epidemiology of Helicobacter pylori infection and gastric cancer in Asia. *J Gastroenterol Hepatol* 2010; **25**: 479-486 [PMID: 20370726 DOI: 10.1111/j.1440-1746.2009.06188.x]
7 **Deppisch LM**, Rona VT. Gastric epithelial polyps. A 10-year study. *J Clin Gastroenterol* 1989; **11**: 110-115 [PMID: 2921485]
8 **Roseau G**, Ducreux M, Molas G, Ponsot P, Amouyal P, Palazzo L, Amouyal G, Paolaggi JA. [Epithelial gastric polyps in a series of 13000 gastroscopies]. *Presse Med* 1990; **19**: 650-654 [PMID: 2139948]
9 **Shaib YH**, Rugge M, Graham DY, Genta RM. Management of gastric polyps: an endoscopy-based approach. *Clin Gastroenterol Hepatol* 2013; **11**: 1374-1384 [PMID: 23583466 DOI: 10.1016/j.cgh.2013.03.019]
10 **Cao H**, Wang B, Zhang Z, Zhang H, Qu R. Distribution trends of gastric polyps: an endoscopy database analysis of 24 121 northern Chinese patients. *J Gastroenterol Hepatol* 2012; **27**: 1175-1180 [PMID: 22414211 DOI: 10.1111/j.1440-1746.2012.07116.x]
11 **Goddard AF**, Badreldin R, Pritchard DM, Walker MM, Warren B. The management of gastric polyps. *Gut* 2010; **59**: 1270-1276 [PMID: 20675692 DOI: 10.1136/gut.2009.182089]
12 **Stolte M**, Sticht T, Eidt S, Ebert D, Finkenzeller G. Frequency, location, and age and sex distribution of various types of gastric polyp. *Endoscopy* 1994; **26**: 659-665 [PMID: 7859674]
13 **Sivelli R**, Del Rio P, Bonati L, Sianesi M. [Gastric polyps: a clinical contribution]. *Chir Ital* 2002; **54**: 37-40 [PMID: 11942007]
14 **Gencosmanoglu R**, Sen-Oran E, Kurtkaya-Yapicier O, Avsar E, Sav A, Tozun N. Gastric polypoid lesions: analysis of 150 endoscopic polypectomy specimens from 91 patients. *World J Gastroenterol* 2003; **9**: 2236-2239 [PMID: 14562385]
15 **Kelly PJ**, Lauwers GY. Clinical guidelines: Consensus for the management of patients with gastric polyps. *Nat Rev Gastroenterol Hepatol* 2011; **8**: 7-8 [PMID: 21119611 DOI: 10.1038/nrgastro.2010.187]
16 **Islam RS**, Patel NC, Lam-Himlin D, Nguyen CC. Gastric polyps: a review of clinical, endoscopic, and histopathologic features and management decisions. *Gastroenterol Hepatol* (N Y) 2013; **9**: 640-651 [PMID: 24764778]
17 **Sonnenberg A**, Genta RM. Prevalence of benign gastric polyps in a large pathology database. *Dig Liver Dis* 2015; **47**: 164-169 [PMID: 25458775 DOI: 10.1016/j.dld.2014.10.004]
18 **Matsuzaki J**, Suzuki H, Minegishi Y, Sugai E, Tsugawa H, Yasui M, Hibi T. Acid suppression by proton pump inhibitors enhances aquaporin-4 and KCNQ1 expression in gastric fundic parietal cells in mouse. *Dig Dis Sci* 2010; **55**: 3339-3348 [PMID: 20437101 DOI: 10.1007/s10620-010-1167-8]
19 **Thomson AB**, Sauve MD, Kassam N, Kamitakahara H. Safety of the long-term use of proton pump inhibitors. *World J Gastroenterol* 2010; **16**: 2323-2330 [PMID: 20480516]
20 **Fernández JL**, Viola LA. Reply: Is there any association between proton pump inhibitors and fundic gland polyps? *Rev Esp Enferm Dig* 2012; **104**: 45-47; author reply 48 [PMID: 22300123]
21 **Declich P**, Belloni J, Tavani E, Omazzi B, Bortoli A, Devani M, Arena I, Bellone S, Saibeni S, Prada A. Fundic gland polyps and proton pump inhibitors: an obvious link, or an open question? *Hum Pathol* 2014; **45**: 1122-1123 [PMID: 24560019 DOI: 10.1016/j.humpath.2013.11.020]
22 **Cao H**, Qu R, Zhang Z, Kong X, Wang S, Jiang K, Wang B. Sporadic fundic gland polyps are not associated with proton pump inhibitors therapy but negatively correlate with Helicobacter pylori infection in China. *Chin Med J* (Engl) 2014; **127**: 1239-1243 [PMID: 24709173]
23 **el-Zimaity HM**, Jackson FW, Graham DY. Fundic gland polyps developing during omeprazole therapy. *Am J Gastroenterol* 1997; **92**: 1858-1860 [PMID: 9382052]
24 **Jalving M**, Koornstra JJ, Wesseling J, Boezen HM, DE Jong S, Kleibeuker JH. Increased risk of fundic gland polyps during long-term proton pump inhibitor therapy. *Aliment Pharmacol Ther* 2006; **24**: 1341-1348 [PMID: 17059515]
25 **Freeman HJ**. Proton pump inhibitors and an emerging epidemic of gastric fundic gland polyposis. *World J Gastroenterol* 2008; **14**: 1318-1320 [PMID: 18322941]
26 **Dirschmid K**, Platz-Baudin C, Stolte M. Why is the hyperplastic polyp a marker for the precancerous condition of the gastric mucosa? *Virchows Arch* 2006; **448**: 80-84 [PMID: 16189701]
27 **Ljubicić N**, Banić M, Kujundzić M, Antić Z, Vrkljan M, Kovacević I, Hrabar D, Doko M, Zovak M, Mihatov S. The effect of eradicating Helicobacter pylori infection on the course of adenomatous and hyperplastic gastric polyps. *Eur J Gastroenterol Hepatol* 1999; **11**: 727-730 [PMID: 10445791]
28 **Ohkusa T**, Takashimizu I, Fujiki K, Suzuki S, Shimoi K, Horiuchi T, Sakurazawa T, Ariake K, Ishii K, Kumagai J, Tanizawa T. Disappearance of hyperplastic polyps in the stomach after eradication of Helicobacter pylori. A randomized, clinical trial. *Ann Intern Med* 1998; **129**: 712-715 [PMID: 9841603]
29 **Tokunaga K**, Tanaka A, Takahashi S. [Gastric hyperplastic polyps and H. pylori infection, their relationship and effects of eradication therapy]. *Nihon Rinsho* 2013; **71**: 1449-1452 [PMID: 23967678]
30 **Stolte M**. Hyperplastic polyps of the stomach: associations with histologic patterns of gastritis and gastric atrophy. *Am J Surg Pathol* 2001; **25**: 1342-1344 [PMID: 11688474]
31 **Carmack SW**, Genta RM, Graham DY, Lauwers GY. Management of gastric polyps: a pathology-based guide for gastroenterologists. *Nat Rev Gastroenterol Hepatol* 2009; **6**: 331-341 [PMID: 19421245 DOI: 10.1038/nrgastro.2009.70]

P- Reviewer: Arolfo S, De Lisi S **S- Editor**: Yu J
L- Editor: Webster JR **E- Editor**: Liu XM

World Journal of Gastroenterology

Submit a Manuscript: http://www.wjgnet.com/esps/
Help Desk: http://www.wjgnet.com/esps/helpdesk.aspx
DOI: 10.3748/wjg.v21.i33.9765

World J Gastroenterol 2015 September 7; 21(33): 9765-9773
ISSN 1007-9327 (print) ISSN 2219-2840 (online)

ORIGINAL ARTICLE

Retrospective Study

Thyroid dysfunction in Chinese hepatitis C patients: Prevalence and correlation with TPOAb and CXCL10

Ren-Wen Zhang, Cui-Ping Shao, Na Huo, Min-Ran Li, Hong-Li Xi, Min Yu, Xiao-Yuan Xu

Ren-Wen Zhang, Cui-Ping Shao, Na Huo, Min-Ran Li, Hong-Li Xi, Min Yu, Xiao-Yuan Xu, Department of Infectious Diseases, Peking University First Hospital, Beijing 100034, China

Author contributions: Xu XY designed the research; Zhang RW, Shao CP, Huo N, Li MR, Xi HL and Yu M performed the research; Zhang RW and Shao CP contributed new reagents/analytic tools; Zhang RW analyzed the data; Zhang RW and Xu XY wrote the paper.

Supported by National Major Project for Infectious Diseases Control, No. 2012ZX10002003-004-003; National Natural Science Foundation of China, No. 81373056; PhD Program Foundation of Ministry of Education of China, No. 20090001110081.

Institutional review board statement: The study was reviewed and approved by Peking University People Hospital Institutional Review Board.

Informed consent statement: All study participants provided informed written consent prior to study enrollment.

Conflict-of-interest statement: The authors declare that they have no conflict of interest.

Data sharing statement: No additional data are available.

Correspondence to: Xiao-Yuan Xu, Professor, Department of Infectious Diseases, Peking University First Hospital, No. 8, Xishiku Street, Xicheng District, Beijing 100034, China. xiaoyuanxu6@163.com
Telephone: +86-10-83575787

Received: April 9, 2015
Peer-review started: April 9, 2015
First decision: May 18, 2015
Revised: June 2, 2015
Accepted: July 8, 2015
Article in press: July 8, 2015
Published online: September 7, 2015

Abstract

AIM: To investigate the relationship among pretreatment serum CXC chemokine ligand 10 (CXCL10), thyroid peroxidase antibody (TPOAb) levels and thyroid dysfunction (TD) in Chinese hepatitis C patients.

METHODS: One hundred and thirty-nine treatment-naive genotype 1 chronic hepatitis C patients with no history of TD or treatment with thyroid hormones were enrolled in this study. Patients underwent peginterferon alfa-2a/ribavirin (PegIFNα-2a/RBV) treatment for 48 wk, followed by detection of clinical factors at each follow-up point. Hepatitis C virus (HCV) antibodies were analyzed using microsomal chemiluminescence, and serum HCV RNA was measured by real-time PCR assay at 0, 4, 12, 24 and 48 wk after the initiation of therapy and 24 wk after the end of therapy. To assess thyroid function, serum thyroid stimulating hormone (TSH), free thyroxine (FT4), free triodothyronine (FT3) and TPOAb/thyroglobulin antibody (TGAb) levels were determined using chemiluminescent immunoassays every 3 mo. Serum CXCL10 levels were determined at baseline.

RESULTS: The prevalence of TD was 18.0%. Twenty-one (84.0%) out of twenty-five patients exhibited normal thyroid function at week 24 after therapy. The rate of sustained virological response to PegIFNα-2a/RBV in our study was 59.0% (82/139), independent of thyroid function. Pretreatment serum CXCL10 levels were significantly increased in patients with euthyroid

status compared with patients with TD (495.2 ± 244.2 pg/mL *vs* 310.0 ± 163.4 pg/mL, *P* = 0.012). Patients with TD were more frequently TPOAb-positive than non-TD (NTD) patients (24.2% *vs* 12.3%, *P* = 0.047) at baseline. Three of the one hundred and fifteen patients without TPOAb at baseline developed TD at the end of treatment (37.5% *vs* 2.6%, *P* = 0.000). Female patients exhibited an increased risk for developing TD compared with male patients (*P* = 0.014).

CONCLUSION: Lower pretreatment serum CXCL10 levels are associated with TD, and TD prevalence increases in female patients and patients who are positive for TPOAb at baseline.

Key words: Thyroid dysfunction; Thyroid peroxidase antibody; CXC chemokine ligand 10; Peginterferon alfa-2a/ribavirin; China

Core tip: We present novel data on the influence of peginterferon alfa-2a/ribavirin (PegIFNα-2a/RBV) on thyroid function in Chinese genotype 1 hepatitis C virus (HCV)-infected patients over a 48-wk treatment period. The results demonstrate that the prevalence of thyroid dysfunction (TD) was 18.0%. Lower pretreatment serum CXCL10 levels were associated with PegIFNα-2a/RBV induced TD in genotype 1 HCV-infected patients, and female patients exhibited an increased risk for developing TD compared with male patients. Baseline TPOAb positivity may also be a risk factor for TD development. However, most (84%) of the TD cases were reversible. To our knowledge, this is the first study to investigate the association of CXCL10 levels with PegIFNα-2a/RBV induced TD in genotype 1 HCV-infected patients in China.

Zhang RW, Shao CP, Huo N, Li MR, Xi HL, Yu M, Xu XY. Thyroid dysfunction in Chinese hepatitis C patients: Prevalence and correlation with TPOAb and CXCL10. *World J Gastroenterol* 2015; 21(33): 9765-9773 Available from: URL: http://www.wjgnet.com/1007-9327/full/v21/i33/9765.htm DOI: http://dx.doi.org/10.3748/wjg.v21.i33.9765

INTRODUCTION

Of the estimated 185 million people infected with hepatitis C virus (HCV) worldwide, 350000 die each year[1,2]. Currently, the standard treatment for chronic hepatitis C (CHC) patients in China is peginterferon and ribavirin in combination (PegIFNα-2a/RBV), with sustained virological response (SVR) rates of 54% to 80%[3,4].

Despite its success, interferon-alpha (IFN-α) has a well-documented side effect profile, including influenza-like symptoms, and hematologic abnormalities lead to dose reductions in up to 40% of patients and drug discontinuation in 14% of patients[5]. Thyroid diseases, such as the emergence of thyroid autoantibodies (TAs) and thyroid dysfunction (TD), are common in CHC patients and represent extrahepatic manifestations of HCV infection[6,7]. Subclinical thyroiditis occurs in 20% to 40% of CHC patients, and clinical thyroiditis occurs in 5% to 10% of CHC patients[8]. TD may result from IFN-based therapy. In some cases, IFN-induced TD may lead to the discontinuation of IFN therapy, thus representing a major clinical problem in hepatitis C patients receiving IFN-α therapy[8]. IFN-α-related TD has been widely investigated, and preliminary studies have suggested that there are at least two different models by which IFN-α may induce TD: immune-mediated effects or direct toxicity to the thyroid. IFN-α exerts various effects on the immune system, many of which may lead to the development of autoimmunity. Upon culture with human thyroid follicular cells, type Ⅰ IFNs inhibit thyroid-stimulating hormone (TSH) -induced gene expression of thyroglobulin (TG), thyroperoxidase (TPO), and sodium iodide symporter (NIS). This study assessed TSH receptor, TG, and TPO gene expression levels in a rat thyroid cell line, and the results demonstrated that IFN-α has a direct toxic effect on the thyroid. Chronic HCV infection appears to play a significant role in triggering thyroiditis among IFN α-treated patients[8,9].

CXC chemokine ligand 10 (CXCL10 or IP-10), a member of the CXC chemokine family, is expressed in the liver of CHC patients and selectively recruits activated T cells to inflammatory sites[10]. Evidence also indicates that circulating CXCL10 levels increase in HCV-infected patients with autoimmune thyroiditis[11], potentially because CXCL10 recruits T-helper (Th) 1 lymphocytes. These cells secrete IFN-γ and tumor necrosis factor (TNF), promoting further CXCL10 secretion and perpetuating the autoimmune process[12,13].

Although most thyroid autoimmunity cases exhibit no clinical symptoms, they are often characterized by the expression of thyroid antibodies (TAs), including thyroperoxidase antibody (TPOAb) and thyroglobulin antibody (TGAb). Data from pooled studies revealed that the risk of developing TD in CHC patients with baseline TAs positivity was 46.1%; whereas this risk was only 5.4% in TAs-negative CHC patients[14]. Our preliminary results indicate that the positive TPOAb IgG2 subclass was a risk factor for TD in untreated HCV patients, and may play an important role in TD development in CHC patients[15]. The appearance of TPOAb before treatment was a strong indicator of subsequent TD for CHC patients receiving PegIFNα-2a/RBV combination therapy. Female and TAs-positive patients were also more likely to develop TD during IFNα/RBV therapy[9].

Previous investigations showed that the addition of RBV to IFN-α therapy in HCV patients could increase

the risk of developing hypothyroidism[16]. However, it is not clear whether the addition of RBV affects the emergence of other TDs. Most studies have focused on the effects of combination therapy with standard IFN-α and RBV on the thyroid gland and demonstrated that the risk for developing TD during IFN-α therapy is closely correlated with mixed HCV genotype infection and lower HCV RNA levels, female gender, and pretreatment positivity for TAs (particularly TPOAb)[9]. Corresponding data on PegIFNα-2a/RBV induced TD in genotype 1 HCV-infected patients in China are rare and the related factors have not yet been fully elucidated.

In the present study, we investigated the relationship among TPOAb, pretreatment serum CXCL10 levels and the occurrence of PegIFNα-2a/RBV induced TD in patients with genotype 1 HCV infection in China.

MATERIALS AND METHODS

Ethics statement

This study protocol conformed to the ethical guidelines of the 1975 Declaration of Helsinki and was approved by the ethics committee of Peking University People Hospital. Written informed consent was obtained from all participant subjects. Biological and behavioral information was linked anonymously to protect the participants' privacy. This procedure was approved by the ethics committee.

Patients

Two hundred and sixty CHC patients who visited the Department of Infectious Diseases, Peking University First Hospital from September 2009 to June 2011 were included in this study. These patients came from five different regions of China (Beijing, Hebei province, Henan province, Heilongjiang province and Shanxi province), and the criteria for CHC diagnosis followed the Guideline of Prevention and Treatment of Hepatitis C[17]. All patients had compensated liver disease without cirrhosis, but never received hepatitis C treatment. Patients with hepatitis B virus (HBV) infection, or human immunodeficiency virus (HIV) infection and those who were pregnant or using amiodarone or lithium were excluded. HCV patients with other autoimmune disorders or treated with immuno-modulant drugs were also excluded. Further screening excluded 25 patients with a history of thyroid gland dysfunction, 80 patients who previously received IFN-α treatment and 26 patients who were not infected with genotype 1 HCV. A total of 139 HCV genotype 1 treatment-naïve patients were enrolled in the final study. All participants included had euthyroid status and never received thyroid hormone treatment.

All enrolled CHC genotype-1 patients received a weekly 180 μg subcutaneous dose of PegIFNα-2a and a daily 600-1000 mg (according to body weight) dose of RBV for 48 wk.

Laboratory assessment

All patients fasted for 12 h prior to blood tests. Alanine aminotransferase (ALT), aspartate aminotransferase (AST), total and direct bilirubin (TBIL and DBIL), and albumin (ALB) were determined using an automatic biochemical analyzer[18]. HCV antibodies were analyzed using microsomal chemiluminescence (Abbott Diagnostics Division)[19], and serum HCV RNA was measured by real-time PCR assay (COBAS Taqman HCV Test; Roche Molecular Systems, Pleasanton, CA) at 0, 4, 12, 24 and 48 wk after the initiation of therapy and 24 wk after the end of therapy.

To assess thyroid function, serum TSH, TPOAb/TGAb, free thyroxine (FT4) and free triodothyronine (FT3) levels were determined using chemiluminescent immunoassays every 3 mo. Briefly, assay kits for TSH, FT3, and FT4 were purchased from ADVIA Centaur (Bayer Healthcare Diagnostics) and the kit for TPOAb/TGAb was from IMMULITE 1000 (Diagnostic Products Corporation, Los Angeles, CA, United States). The normal range of each assay was as follows: TSH, 0.35-5.5 μIU/mL; FT3, 3.50-6.50 pmol/L; and FT4, 11.48-22.70 pmol/L.

Clinical hypothyroidism was defined as a serum TSH level greater than 5.5 μIU/mL and a FT4 level less than 11.48 pmol/L. Clinical hyperthyroidism was diagnosed when TSH was less than 0.35 μIU/mL and FT4 was greater than 22.7 pmol/L and/or FT3 was greater than 6.5 pmol/L. Subclinical hypothyroidism or hyperthyroidism was diagnosed when serum TSH levels were greater than 5.5 μIU/mL or less than 0.35 μIU/mL, respectively, with normal FT3 and FT4 levels. TAs were considered positive when TPOAb $\geqslant$ 35 IU/mL or TGAb $\geqslant$ 40 IU/mL[15].

Serum CXCL10 measurements

Serum CXCL10 levels were measured prior to treatment using the Quantikine human CXCL10 immunoassay (RD Systems, Minneapolis, MN, United States). All blood samples were stored at -80 ℃ until use in assays. These samples were diluted 1:2 with Calibrator Diluent RD6Q solution and analyzed in duplicate. The linear dynamic range for CXCL10 measurement in this assay was 7.8 to 500 pg/mL.

Statistical analysis

Categorical variables were compared between the groups using the χ^2 test or the Fisher's exact test. Continuous variables were assessed using Student's *t*-test or the Mann-Whitney *U* test. Differences with a two-tailed *P*-value < 0.05 were considered statistically significant. Statistical analyses were conducted using SPSS version 16.0 (SPSS Inc, Chicago, IL, United States).

RESULTS

General information about the patients

The demographic characteristics of the 139 CHC

Table 1 Demographic characteristics of the enrolled population at baseline

	n = 139
Gender (%, male/female)	50.4/49.6
Age (yr)[1]	46.8 ± 14.0
HCV RNA (log_{10}, IU/mL)[2]	6.3 (3.0, 7.74)
ALT (IU/L)[2]	60.0 (10, 527)
AST (IU/L)[2]	46.0 (16.0, 264)
TBIL (μmol/L)[2]	16.1 (5.0, 150)
DBIL (μmol/L)[2]	4.51 (0.48, 108)
ALB (g/L)[1]	42.57 ± 4.16
Positive antibodies (%, TPOAb/TGAb)	15.8%/8.6%

[1]mean ± SD; [2]median (minimum, maximum). TBIL: Total bilirubin; DBIL: Direct bilirubin; TP: Total protein; ALT: Alanine aminotransferase; AST: Aspartate aminotransferase; ALB: Albumin; TPOAb: Thyroid peroxidase antibody; TGAb: Thyroglobulin antibody.

patients enrolled in the study are presented in Table 1. In total, 70 male and 69 female CHC patients, with a mean age of 46.8 ± 14.0 years, participated in this study. Twenty-four (17.3%) patients were TPOAb and/or TGAb positive (TPOAb: 15.8%; TGAb: 8.6%). Nine out of twenty-five patients with TD were TAs positive, and the ratio of TPOAb to TGAb was 8:3.

Prevalence of TD

The overall prevalence of thyroid abnormities was 18.0% (5.0% in men and 13.0% in women) during the therapy. Following 48 wk of exposure to PegIFNα-2a/RBV, 25 out of 139 patients developed TD, including 7 (6 females and 1 male) with subclinical hyperthyroidism, 16 (10 females and 6 males) with subclinical hypothyroidism and 2 female patients with hypothyroidism. Table 2 summarizes the findings from the patients who had chronic hepatitis C and developed PegIFNα-2a/RBV-induced TD. Clinical hypothyroidism (1.4%) and subclinical hypothyroidism (11.5%) were more frequent than clinical hyperthyroidism and subclinical hyperthyroidism (5.0%). Of these 25 patients, 15 developed TD at 24 wk of the therapy, including 9 with subclinical hypothyroidism, 5 with subclinical hyperthyroidism and 1 with hypothyroidism. An additional 2 patients developed subclinical hyperthyroidism at week 36 of the therapy. At 48 wk of the therapy, 3 patients with subclinical hypothyroidism and 1 patient with overt hypothyroidism were observed. In patients with overt hypothyroidism, we began L-thyroxine treatment, which halted TD progression. In 21 (84.0%) out of 25 patients, normal thyroid function was restored at 24 wk after the end of therapy. PegIFNα-2a/RBV SVR rate was 59.0% (82/139), independent of thyroid function.

Relationships among TPOAb, TD and CXCL10

Table 3 presents the baseline characteristics of the CHC patients with TD and NTD. Female patients exhibited an increases risk for TD development compared with male patients. Serum AST levels and the frequency of TPOAb positivity in TD patients were significantly increased compared with NTD patients (AST levels: $P = 0.018$; TPOAb positivity: 24.2% *vs* 12.3%, $P = 0.047$). However, no significant differences in ALT, TBIL, DBIL, ALB, HCV RNA levels, or the percentage of TGAb-positive patients were noted between the TD and NTD groups ($P > 0.05$).

In our study, pretreatment serum CXCL10 levels were significantly increased in patients with euthyroid status compared with TD patients (495.2 ± 244.2 pg/mL *vs* 310.0 ± 163.4 pg/mL, $P = 0.012$) (Figure 1A). Although pretreatment serum CXCL10 levels were increased in TPOAb-positive *vs* TPOAb-negative patients, no significant differences were detected. (TPOAb positive/negative: 542.5 ± 107.2 pg/mL *vs* 442.3 ± 249.8 pg/mL, $P = 0.433$) (Figure 1B).

The percentages of patients positive for TPOAb and/or TGAb were 17.3% (24/139) at baseline and 22.3% (31/139) at the end of treatment (Table 4). Nine of twenty-four patients with TPOAb/TGAb at baseline developed TD. By contrast, three (one male and two females) of one hundred and fifteen patients without TPOAb/TGAb at baseline developed TD at the end of the treatment (37.5% *vs* 2.6%, $P = 0.000$).

DISCUSSION

We present novel data regarding the influence of PegIFNα-2a combined with RBV on thyroid function in Chinese adult genotype 1 HCV-infected patients over a 48-wk treatment period. The results demonstrate that the prevalence of thyroid abnormities was 18.0%, and lower pretreatment serum CXCL10 levels were associated with PegIFNα-2a/RBV induced TD. The prevalence of TD was increased in female patients and those who were TPOAb-positive at baseline. However, most (84%) of the TD cases were reversible. To our knowledge, this is the first study to investigate the association of CXCL10 levels with PegIFNα-2a/RBV-induced TD in genotype 1 HCV-infected patients in China.

In our study, the PegIFNα-2a/RBV SVR rate was 59.0% (82/139), independent of thyroid function. After 48 wk of PegIFNα-2a/RBV treatment, 25 out of 139 patients developed TD, including 16 patients with subclinical hypothyroidism, 7 with subclinical hyperthyroidism and 2 with hypothyroidism. Although a previous study reported that hypothyroidism was the most common type of TD induced by IFN[20,21], subclinical hypothyroidism was most prevalent in our study. This discrepancy may be explained by differences in patient ethnicities, genetic backgrounds and the type of IFN used.

IFN-associated thyroid disease was first reported in 1985 when three cases of hypothyroidism were observed in breast cancer patients who received IFN α treatment[22]. Studies report an incidence of TD during IFN-α plus RBV combination therapy of 4.7% to 27.8%[23], which may result from immune activation

Table 2 Summary of thyroid dysfunction induced by pegylated interferon-α2a and ribavirin

No.	Gender	Age (yr)	Diagnosis time	FT3 (3.50-6.50 pmol/L)	FT4 (11.48-22.70 pmol/L)	TSH (0.35-5.50 μIU/mL)	Diagnosis	Outcome
1	Female	53	12th wk	4.81	11.66	6.62	Sub hypo	Normal
2	Female	61	48th wk	4.67	12.19	19.61	Sub hypo	Normal
3	Female	42	24th wk	6.02	11.56	7.13	Sub hypo	Normal
4	Female	40	24th wk	5.88	11.71	8.95	Sub hypo	Normal
5	Female	46	24th wk	4.13	14.13	6.25	Sub hypo	Normal
6	Female	56	24th wk	5.46	24.55	11.01	Sub hypo	Normal
7	Female	56	48th wk	5.12	12.89	8.45	Sub hypo	Normal
8	Female	44	48th wk	4.00	24.36	6.31	Sub hypo	Normal
9	Female	41	12th wk	6.19	13.48	5.58	Sub hypo	Sub hyper
10	Female	45	12th wk	5.27	19.24	6.15	Sub hypo	Normal
11	Male	39	24th wk	5.36	13.45	23.19	Sub hypo	Normal
12	Male	28	24th wk	5.44	15.27	6.66	Sub hypo	Normal
13	Male	53	24th wk	3.79	14.67	8.71	Sub hypo	Normal
14	Male	50	12th wk	6.20	11.85	37.42	Sub hypo	Normal
15	Male	51	24th wk	5.15	12.47	6.46	Sub hypo	Normal
16	Male	18	24th wk	4.95	13.99	6.16	Sub hypo	Normal
17	Female	43	24th wk	6.34	13.89	0.32	Sub hyper	Sub hyper
18	Female	21	36th wk	4.37	21.24	0.29	Sub hyper	Normal
19	Female	38	36th wk	5.72	12.97	0.24	Sub hyper	Normal
20	Female	28	24th wk	4.19	21.24	0.32	Sub hyper	Normal
21	Female	42	24th wk	4.67	16.47	0.01	Sub hyper	Normal
22	Female	33	24th wk	5.31	11.58	0.12	Sub hyper	Normal
23	Male	70	24th wk	5.77	16.70	0.02	Sub hyper	Normal
24	Female	21	24th wk	5.90	5.97	6.16	Hypo	Therapy
25	Female	66	48th wk	6.03	0.97	6.58	Hypo	Therapy

Sub hypo: Subclinical hypothyroidism; Sub hyper: Subclinical hyperthyroidism; Hypo: Hypothyroidism.

Table 3 Baseline characteristics of the thyroid dysfunction *vs* non-thyroid dysfunction chronic hepatitis C patients

	TD_{IFN}	NTD_{IFN}	*P* value
Gender (%, male/female)	28.0/72.0	55.3/45.7	0.014
Age (yr)[1]	43.40 ± 13.60	47.50 ± 14.0	0.183
HCV RNA (log_{10}, IU/mL)[2]	6.23 (3.54, 7.52)	6.36 (3.0, 7.74)	0.919
ALT (IU/L)[2]	81.0 (26, 416)	55.0 (10, 527)	0.162
AST (IU/L)[2]	67.0 (26, 248)	41.5 (16, 264)	0.018
TBIL(μmol/L)[2]	17.20 (8.9, 36.4)	16.0 (5.0, 150.0)	0.732
DBIL(μmol/L)[2]	4.57 (0.69, 13.80)	4.5 (0.48, 108)	0.447
ALB (g/L)[1]	42.30 ± 4.24	42.62 ± 4.15	0.764
TPOAb positivity	24.2%	12.3%	0.047
TGAb positivity	12.0%	7.9%	0.469
CXCL10 level (pg/mL)[1]	310.0 ± 163.4	495.20 ± 244.2	0.012

[1]mean ± SD; [2]median (minimum, maximum). TBIL: Total bilirubin; DBIL: Direct bilirubin; ALT: Alanine aminotransferase; AST: Aspartate aminotransferase; ALB: Albumin; TPOAb: Thyroid peroxidase antibody; TGAb: Thyroglobulin antibody.

mediated by IFN. Jami *et al*[24] demonstrated that patients who used pegylated IFN had a higher risk of TD than those using conventional IFN (14% *vs* 7%, *P* = 0.038). However, in a meta-analysis, Tran *et al*[25] found that pegylated IFN in combination with RBV did not cause more thyroid diseases in HCV-infected patients than classical IFN plus RBV. This variation may be explained by the differences in the race of the patients. In our study, 18.0% (25/139) of Chinese HCV-infected patients developed TD during PegIFNα-2a/RBV therapy. The incidence of TD in our subjects was increased compared with a large Australian cohort,

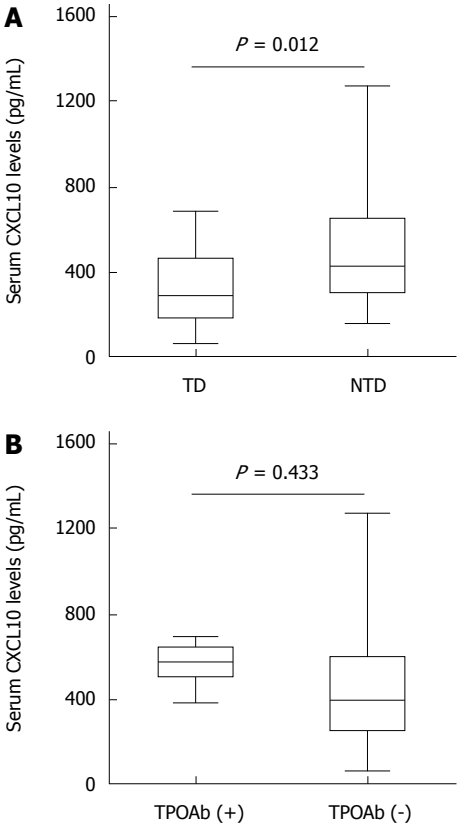

Figure 1 Pretreatment serum CXCL 10 levels according to patient characteristics. A: Serum CXCL 10 levels between PegIFNα-2a/RBV induced TD *vs* NTD; B: Serum CXCL 10 levels between TPOAb (+) and TPOAb (-). TD: Thyroid dysfunction; NTD: Non-thyroid dysfunction; PegIFNα-2a/RBV: Peginterferon alfa-2a/ribavirin.

Table 4 Numbers of patients treated with combination therapy positive for thyroid autoantibodies at enrollment and at the end of treatment

	TPOAb (+) only	TGAb (+) only	Both (+)	Both (-)
At baseline	12	7	5	115
At the end of treatment	13	10	8	108

TPOAb: Thyroid peroxidase antibody; TGAb: Thyroglobulin antibody.

in which approximately 14% of patients developed TD during PegIFN/RBV therapy[24]. The difference between these two studies may result from differences in the race of the included patient populations and the virus genotypes.

RBV can modulate the Th1 and Th2 subset balance by activating type 1 cytokines in the HCV-specific immune response. Furthermore, RBV could also enhance the non-virus-induced immune response, suggesting that RBV, as a type 1-inducing agent, can trigger autoimmune phenomena in predisposed patients[26]. In previous studies, the incidence of TD induced by IFN monotherapy in CHC patients was 4% to 18%, with a mean incidence of approximately 6% in a meta-analysis study[27]. Earlier studies reveal that the mean incidence of TD in patients treated with combination therapy is increased compared with those treated with IFN alone[16].

In the present study, the enrolled genotype-1 patients received PegIFNα-2a/RBV treatment for 48 wk, and the prevalence of thyroid abnormities was 18.0%. Some studies have suggested that higher doses of IFN-α and longer durations of therapy are risk factors for the development of IFN induced TD[14]. It is therefore possible that the longer time period of 48 wk of therapy in our study increased the likelihood that patients developed TD. Fifteen patients developed TD at 24 wk of therapy, including 9 with subclinical hypothyroidism, 5 with subclinical hyperthyroidism and 1 with hypothyroidism. An additional 2 patients developed subclinical hyperthyroidism at 36 wk of therapy. At 48 wk of therapy, 3 patients with subclinical hypothyroidism and 1 patient with overt hypothyroidism were noted. L-thyroxine treatment was initiated in patients with overt hypothyroidism. It is worth noting that, by the end of the therapy, TD did not further progress among these patients.

Whether the long-term evolution of TD is induced by IFN-α therapy remains controversial. Some studies indicate that TD is reversible in all patients, whereas others report that TD is only reversible in a proportion of the patients[28,29]. In our study, at week 24 post-treatment, normal thyroid function was restored in 21 (84.0%) out of 25 patients. Such a discrepancy may result from the short time period of the follow-up study and a subsequently incomplete evaluation of TD status. There also may have been additional factors, such as differences in study designs, the time period of the follow-up, the population races, and individual variations.

Our data revealed that 17.3% of patients were TAs-positive, whereas previous studies reported TAs incidence rates in HCV-infected patients ranging from 10% to 45%; this discrepancy may be related to differences in the population race, genetic variations, geographical distribution, and environmental factors[16]. Data from the pooled studies indicate that the risk of TD in patients who were positive for TAs at baseline was increased compared with those without TAs at baseline[14]. Female gender and TAs positivity were shown to be the predictive factors of TD development during IFN-α/RBV therapy[24,30]. In our study, female patients had a higher risk for the development of TD than male patients. The baseline TPOAb-positivity have been suggested to be a risk factor for TD development secondarily to PegIFNα-2a/RBV treatment. We also demonstrated that the percentage of patients with elevated autoantibody levels developing TD was significantly higher than that of patients with normal autoantibody levels before treatment.

A previous large-scale study in patients receiving combination therapy demonstrated that TGAb was present in 91.7% of patients, whereas TPOAb was present in 83.3% of those with overt hypothyroidism[31]. Thus, in combination therapy, TAs play an important role in predicting the emergence of TD. Analyzing TAs levels before combination therapy may therefore identify patients at risk for developing PegIFNα-2a/RBV-associated TD.

Many studies have noted the Th1 immune response and changes in CXCL10 chemokine level during HCV infection. It was recently reported that HCV-infected patients who developed IFN-induced dysfunction exhibited Th1 polarization in their innate immune responses. The Th1 immune response is characterized by increased IFN-γ and TNF-α production by Th1 lymphocytes. These chemokines subsequently stimulate CXCL10 secretion from the hepatocytes in chronic HCV infection, thus perpetuating the immune cascade[32]. Elevated serum CXCL10 levels are not only associated with the development of autoimmunity, but also lead to thyroid follicular destruction and hypothyroidism. Antonelli *et al*[33] demonstrated that the development of TD during the IFN-α therapy correlated with significantly reduced CXCL10 serum levels, both before and during the treatment. A prospective study found that CXCL10 increased in HCV-infected patients, with no associated TD development, even after matching for sex and age[34]. We demonstrated that pretreatment serum CXCL10 levels were significantly increased in patients with euthyroid status compared with patients with TD. Although pretreatment serum CXCL10 levels were higher in TPOAb-positive than in TPOAb-negative patients, no significant difference was detected. However, the prevalence of TD was increased

in patients who were TPOAb-positive at baseline than patients who were not TPOAb-positive at baseline.

Evidence also indicates that circulating CXCL10 levels increase in HCV-infected patients with autoimmune thyroiditis[11], potentially because CXCL10 recruits T-helper (Th) 1 lymphocytes. Indeed, it is reasonable to hypothesize that the changes in serum CXCL10 may be more evident in patients developing overt TD, who show a microenvironment much more enriched in Th1 molecules[33]. In our study, although high standard deviation was observed for both categories of patients, there was an important variation of the CXCL10 levels in HCV patients with or without TD. At least in the studied population, the values of CXCL10 were significantly lower in patients who developed TD. Maybe the reason is that the number of patients with overt TD was too small (only two) in our studied populations. Therefore, our results should be confirmed by studies with a much larger sample size.

We studied the occurrence of TD in genotype 1 HCV-infected patients, without examining other genotypes. Our findings must be confirmed by studies using a larger sample size with a longer follow-up period.

In conclusion, low pretreatment serum CXCL10 levels were associated with PegIFNα-2a/RBV induced TD in genotype 1 HCV-infected patients in China. The prevalence of TD was increased in female patients and patients who were TPOAb-positive at baseline. The appearance of TPOAb before treatment is predictive of subsequent TD for CHC patients receiving PegIFNα-2a/RBV combination therapy. Screening for TPOAb and CXCL10 before combination therapy may identify high-risk patients who are more likely to develop PegIFNα-2a/RBV-associated TD. Further studies are needed to elucidate the characteristics and mechanisms involved in PegIFNα-2a/RBV-induced TD in HCV-infected patients.

COMMENTS

Background

Currently, the standard treatment for chronic hepatitis C (CHC) in China is combination peginterferon and ribavirin (RBV) therapy, and the sustained virological response rates are 54% to 80%. Despite its success, interferon (IFN)-α has a well-documented side effect profile, including thyroid diseases. The emergence of thyroid dysfunction (TD) may result from IFN-based therapy. In some cases, IFN-induced TD may cause the discontinuation of IFN therapy. Most studies have focused on the effects of combination therapy with standard IFN-α and ribavirin (RBV) on the thyroid gland and demonstrated that the risk for developing TD during IFN-α therapy is closely correlated with female gender and pretreatment TAs positivity (particularly TPOAb). Evidence indicates that circulating CXCL10 levels are increased in HCV-infected patients with autoimmune thyroiditis. The relationship among the pretreatment serum CXCL10 levels, TPOAb levels and the occurrence of peginterferon alfa-2a (PegIFNα-2a)/RBV-induced TD in patients with genotype 1 HCV infection in China is unclear.

Research frontiers

CXCL10 recruits Th1 lymphocytes, which secrete IFN-γ and tumor necrosis factor, leading to further CXCL10 secretion and potentially the development of the autoimmunity. Data from pooled studies revealed that the risk of developing TD in CHC patients who were TAs-positive (TPOAb and TGAb) at baseline was 46.1%. By contrast, this risk was only 5.4% in CHC patients who were TAs-negative at baseline. The preliminary results indicate that the TPOAb IgG2 subclass was a risk factor for TD in untreated HCV patients, and may play an important role in TD development in CHC patients. The appearance of TPOAb before treatment is predictive of subsequent thyroid dysfunction for CHC patients receiving PegIFNα-2a/RBV combination therapy.

Innovations and breakthroughs

Lower pretreatment serum CXCL10 levels are associated with PegIFNα-2a/RBV- induced TD in genotype 1 HCV-infected patients in China. The frequency of TD is increased in female patients and patients who are TPOAb-positive at baseline. However, most (84%) of the TD cases were reversible. This is the first study to investigate the association of CXCL10 levels with PegIFNα-2a/RBV-induced TD in genotype 1 HCV-infected patients in China.

Applications

The study results indicate that screening for TPOAb and CXCL10 before combination therapy may identify the patients who are at high risk for developing PegIFNα-2a/RBV-associated thyroid dysfunction.

Terminology

Clinical hypothyroidism was defined by serum TSH levels greater than 5.5 μIU/mL and FT4 less than 11.48 pmol/L; whereas clinical hyperthyroidism was diagnosed when TSH levels were less than 0.35 μIU/mL and FT4 was greater than 22.7 pmol/L and/or FT3 was greater than 6.5 pmol/L. Subclinical hypothyroidism or hyperthyroidism were defined by serum TSH levels higher than 5.5 μIU/mL or lower than 0.35 μIU/mL, respectively, with normal levels of FT3 and FT4. The patients was considered to be positive for TAs when TPOAb was greater than or equal to 35 IU/mL or TGAb was greater than or equal to 40 IU/mL.

Peer-review

Well-written and with valuable data, this manuscript reinforces the recommendation that HCV-infected patients should be screened for the presence of thyroid dysfunction markers before undergoing IFN-a/ribavirin treatment, because such treatment may increase the prevalence of TD. The value of TPOAb positivity as a marker for treatment-induced TD in HCV infected patients is also suggested by several studies. There is variation in CXCL10 levels in HCV patients with or without TD, as demonstrated by a high standard deviation observed for both categories of patients.

REFERENCES

1 **Mohd Hanafiah K**, Groeger J, Flaxman AD, Wiersma ST. Global epidemiology of hepatitis C virus infection: new estimates of age-specific antibody to HCV seroprevalence. *Hepatology* 2013; **57**: 1333-1342 [PMID: 23172780 DOI: 10.1002/hep.26141]

2 **Lavanchy D**. The global burden of hepatitis C. *Liver Int* 2009; **29** Suppl 1: 74-81 [PMID: 19207969 DOI: 10.1111/j.1478-3231.2008.01934.x]

3 **McHutchison JG**, Gordon SC, Schiff ER, Shiffman ML, Lee WM, Rustgi VK, Goodman ZD, Ling MH, Cort S, Albrecht JK. Interferon alfa-2b alone or in combination with ribavirin as initial treatment for chronic hepatitis C. Hepatitis Interventional Therapy Group. *N Engl J Med* 1998; **339**: 1485-1492 [PMID: 9819446]

4 **Yu ML**, Dai CY, Huang JF, Hou NJ, Lee LP, Hsieh MY, Chiu CF, Lin ZY, Chen SC, Hsieh MY, Wang LY, Chang WY, Chuang WL. A randomised study of peginterferon and ribavirin for 16 versus 24 weeks in patients with genotype 2 chronic hepatitis C. *Gut* 2007; **56**: 553-559 [PMID: 16956917 DOI: 10.1136/gut.2006.102558]

5 **Russo MW**, Fried MW. Side effects of therapy for chronic hepatitis C. *Gastroenterology* 2003; **124**: 1711-1719 [PMID: 12761728 DOI: 10.1016/S0016-5085(03)00394-9]

6 **Hsieh MY**, Dai CY, Lee LP, Huang JF, Tsai WC, Hou NJ, Lin ZY, Chen SC, Wang LY, Chang WY, Chuang WL, Yu ML. Antinuclear

antibody is associated with a more advanced fibrosis and lower RNA levels of hepatitis C virus in patients with chronic hepatitis C. *J Clin Pathol* 2008; **61**: 333-337 [PMID: 17545561 DOI: 10.1136/jcp.2006.046276]

7 **Huang JF**, Chuang WL, Yu ML, Yu SH, Huang CF, Huang CI, Yeh ML, Hsieh MH, Yang JF, Lin ZY, Chen SC, Dai CY, Chang WY. Hepatitis C virus infection and metabolic syndrome---a community-based study in an endemic area of Taiwan. *Kaohsiung J Med Sci* 2009; **25**: 299-305 [PMID: 19560994 DOI: 10.1016/S1607-551X(09)70520-0]

8 **Tomer Y**, Blackard JT, Akeno N. Interferon alpha treatment and thyroid dysfunction. *Endocrinol Metab Clin North Am* 2007; **36**: 1051-1066; x-xi [PMID: 17983936 DOI: 10.1016/j.ecl.2007.07.001]

9 **Carella C**, Mazziotti G, Amato G, Braverman LE, Roti E. Clinical review 169: Interferon-alpha-related thyroid disease: pathophysiological, epidemiological, and clinical aspects. *J Clin Endocrinol Metab* 2004; **89**: 3656-3661 [PMID: 15292282 DOI: 10.1210/jc.2004-0627]

10 **Abe T**, Fukuhara T, Wen X, Ninomiya A, Moriishi K, Maehara Y, Takeuchi O, Kawai T, Akira S, Matsuura Y. CD44 participates in IP-10 induction in cells in which hepatitis C virus RNA is replicating, through an interaction with Toll-like receptor 2 and hyaluronan. *J Virol* 2012; **86**: 6159-6170 [PMID: 22491449 DOI: 10.1128/JVI.06872-11]

11 **Antonelli A**, Fallahi P, Ferrari SM, Sebastiani M, Manfredi A, Mazzi V, Fabiani S, Centanni M, Marchi S, Ferri C. Circulating CXCL11 and CXCL10 are increased in hepatitis C-associated cryoglobulinemia in the presence of autoimmune thyroiditis. *Mod Rheumatol* 2012; **22**: 659-667 [PMID: 22160826 DOI: 10.1007/s10165-011-0565-x]

12 **Antonelli A**, Fallahi P, Rotondi M, Ferrari SM, Romagnani P, Grosso M, Ferrannini E, Serio M. Increased serum CXCL10 in Graves' disease or autoimmune thyroiditis is not associated with hyper- or hypothyroidism per se, but is specifically sustained by the autoimmune, inflammatory process. *Eur J Endocrinol* 2006; **154**: 651-658 [PMID: 16645011 DOI: 10.1530/eje.1.02137]

13 **Antonelli A**, Ferri C, Ferrari SM, Colaci M, Sansonno D, Fallahi P. Endocrine manifestations of hepatitis C virus infection. *Nat Clin Pract Endocrinol Metab* 2009; **5**: 26-34 [PMID: 19079271 DOI: 10.1038/ncpendmet1027]

14 **Mandac JC**, Chaudhry S, Sherman KE, Tomer Y. The clinical and physiological spectrum of interferon-alpha induced thyroiditis: toward a new classification. *Hepatology* 2006; **43**: 661-672 [PMID: 16557537 DOI: 10.1002/hep.21146]

15 **Shao C**, Huo N, Zhao L, Gao Y, Fan X, Zheng Y, Wang L, Lu H, Xu X, Guo X. The presence of thyroid peroxidase antibody of IgG2 subclass is a risk factor for thyroid dysfunction in chronic hepatitis C patients. *Eur J Endocrinol* 2013; **168**: 717-722 [PMID: 23419250 DOI: 10.1530/EJE-12-0775]

16 **Carella C**, Mazziotti G, Morisco F, Rotondi M, Cioffi M, Tuccillo C, Sorvillo F, Caporaso N, Amato G. The addition of ribavirin to interferon-alpha therapy in patients with hepatitis C virus-related chronic hepatitis does not modify the thyroid autoantibody pattern but increases the risk of developing hypothyroidism. *Eur J Endocrinol* 2002; **146**: 743-749 [PMID: 12039693 DOI: 10.1530/eje.0.1460743]

17 **Asian Pacific Association for the Study of the Liver (APASL) Hepatitis C Working Party**; McCaughan GW, Omata M, Amarapurkar D, Bowden S, Chow WC, Chutaputti A, Dore G, Gane E, Guan R, Hamid SS, Hardikar W, Hui CK, Jafri W, Jia JD, Lai MY, Wei L, Leung N, Piratvisuth T, Sarin S, Sollano J, Tateishi R. Asian Pacific Association for the Study of the Liver consensus statements on the diagnosis, management and treatment of hepatitis C virus infection. *J Gastroenterol Hepatol* 2007; **22**: 615-633 [PMID: 17444847 DOI: 10.1111/j.1440-1746.2007.04883.x]

18 **Wang LF**, Wu CH, Shan Y, Fan XH, Huo N, Lu HY, Xu XY. Prevalence of abnormal glycometabolism in patients with chronic hepatitis C and related risk factors in China. *Chin Med J* (Engl) 2011; **124**: 183-188 [PMID: 21362362 DOI: 10.3760/cma.j.issn.0366-6999.2011.02.005]

19 **Bai L**, Feng ZR, Lu HY, Li WG, Yu M, Xu XY. Prevalence of antinuclear and anti-liver-kidney-microsome type-1 antibodies in patients with chronic hepatitis C in China. *Chin Med J* (Engl) 2009; **122**: 5-9 [PMID: 19187609 DOI: 10.3760/cma.j.issn.0366-6999.2009.01.002]

20 **Schultz M**, Müller R, von zur Mühlen A, Brabant G. Induction of hyperthyroidism by interferon-alpha-2b. *Lancet* 1989; **1**: 1452 [PMID: 2567459 DOI: 10.1016/S0140-6736(89)90157-8]

21 **Gisslinger H**, Gilly B, Woloszczuk W, Mayr WR, Havelec L, Linkesch W, Weissel M. Thyroid autoimmunity and hypothyroidism during long-term treatment with recombinant interferon-alpha. *Clin Exp Immunol* 1992; **90**: 363-367 [PMID: 1458673 DOI: 10.1111/j.1365-2249.1992.tb05852.x]

22 **Fentiman IS**, Thomas BS, Balkwill FR, Rubens RD, Hayward JL. Primary hypothyroidism associated with interferon therapy of breast cancer. *Lancet* 1985; **1**: 1166 [PMID: 2860373 DOI: 10.1016/S0140-6736(85)92475-4]

23 **Costelloe SJ**, Wassef N, Schulz J, Vaghijiani T, Morris C, Whiting S, Thomas M, Dusheiko G, Jacobs M, Vanderpump MP. Thyroid dysfunction in a UK hepatitis C population treated with interferon-alpha and ribavirin combination therapy. *Clin Endocrinol* (Oxf) 2010; **73**: 249-256 [PMID: 20148905 DOI: 10.1111/j.1365-2265.2010.03785.x]

24 **Jamil KM**, Leedman PJ, Kontorinis N, Tarquinio L, Nazareth S, McInerney M, Connelly C, Flexman J, Burke V, Metcalf C, Cheng W. Interferon-induced thyroid dysfunction in chronic hepatitis C. *J Gastroenterol Hepatol* 2009; **24**: 1017-1023 [PMID: 19054259 DOI: 10.1111/j.1440-1746.2008.05690.x]

25 **Tran HA**, Attia JR, Jones TL, Batey RG. Pegylated interferon-alpha2beta in combination with ribavirin does not aggravate thyroid dysfunction in comparison to regular interferon-alpha2beta in a hepatitis C population: meta-analysis. *J Gastroenterol Hepatol* 2007; **22**: 472-476 [PMID: 17376035 DOI: 10.1111/j.1440-1746.2006.04771.x]

26 **Tam RC**, Pai B, Bard J, Lim C, Averett DR, Phan UT, Milovanovic T. Ribavirin polarizes human T cell responses towards a Type 1 cytokine profile. *J Hepatol* 1999; **30**: 376-382 [PMID: 10190717 DOI: 10.1016/S0168-8278(99)80093-2]

27 **Hsieh MC**, Yu ML, Chuang WL, Shin SJ, Dai CY, Chen SC, Lin ZY, Hsieh MY, Liu JF, Wang LY, Chang WY. Virologic factors related to interferon-alpha-induced thyroid dysfunction in patients with chronic hepatitis C. *Eur J Endocrinol* 2000; **142**: 431-437 [PMID: 10802518 DOI: 10.1530/eje.0.1420431]

28 **Huang JF**, Chuang WL, Dai CY, Chen SC, Lin ZY, Lee LP, Lee PL, Wang LY, Hsieh MY, Chang WY, Yu ML. The role of thyroid autoantibodies in the development of thyroid dysfunction in Taiwanese chronic hepatitis C patients with interferon-alpha and ribavirin combination therapy. *J Viral Hepat* 2006; **13**: 396-401 [PMID: 16842442 DOI: 10.1111/j.1365-2893.2005.00705.x]

29 **Baudin E**, Marcellin P, Pouteau M, Colas-Linhart N, Le Floch JP, Lemmonier C, Benhamou JP, Bok B. Reversibility of thyroid dysfunction induced by recombinant alpha interferon in chronic hepatitis C. *Clin Endocrinol* (Oxf) 1993; **39**: 657-661 [PMID: 8287583 DOI: 10.1111/j.1365-2265.1993.tb02423.x]

30 **Gelu-Simeon M**, Burlaud A, Young J, Pelletier G, Buffet C. Evolution and predictive factors of thyroid disorder due to interferon alpha in the treatment of hepatitis C. *World J Gastroenterol* 2009; **15**: 328-333 [PMID: 19140232 DOI: 10.3748/wjg.15.328]

31 **Bini EJ**, Mehandru S. Incidence of thyroid dysfunction during interferon alfa-2b and ribavirin therapy in men with chronic hepatitis C: a prospective cohort study. *Arch Intern Med* 2004; **164**: 2371-2376 [PMID: 15557418 DOI: 10.1001/archinte.164.21.2371]

32 **Mazziotti G**, Sorvillo F, Piscopo M, Morisco F, Cioffi M, Stornaiuolo G, Gaeta GB, Molinari AM, Lazarus JH, Amato G, Carella C. Innate and acquired immune system in patients developing interferon-alpha-related autoimmune thyroiditis: a prospective study. *J Clin Endocrinol Metab* 2005; **90**: 4138-4144 [PMID: 15855253 DOI: 10.1210/jc.2005-0093]

33 **Antonelli A**, Rotondi M, Fallahi P, Romagnani P, Ferrari SM,

Buonamano A, Ferrannini E, Serio M. High levels of circulating CXC chemokine ligand 10 are associated with chronic autoimmune thyroiditis and hypothyroidism. *J Clin Endocrinol Metab* 2004; **89**: 5496-5499 [PMID: 15531503 DOI: 10.1210/jc.2004-0977]

34 **Rotondi M**, Minelli R, Magri F, Leporati P, Romagnani P, Baroni MC, Delsignore R, Serio M, Chiovato L. Serum CXCL10 levels and occurrence of thyroid dysfunction in patients treated with interferon-alpha therapy for hepatitis C virus-related hepatitis. *Eur J Endocrinol* 2007; **156**: 409-414 [PMID: 17389454 DOI: 10.1530/EJE-06-0735]

P- Reviewer: Florea D, Hughes E, Keppeke GD **S- Editor**: Ma YJ
L- Editor: Wang TQ **E- Editor**: Ma S

World Journal of Gastroenterology

Submit a Manuscript: http://www.wjgnet.com/esps/
Help Desk: http://www.wjgnet.com/esps/helpdesk.aspx
DOI: 10.3748/wjg.v21.i33.9774

World J Gastroenterol 2015 September 7; 21(33): 9774-9784
ISSN 1007-9327 (print) ISSN 2219-2840 (online)

ORIGINAL ARTICLE

Retrospective Study

Bezoar-induced small bowel obstruction: Clinical characteristics and diagnostic value of multi-slice spiral computed tomography

Pei-Yuan Wang, Xia Wang, Lin Zhang, Hai-Fei Li, Liang Chen, Xu Wang, Bin Wang

Pei-Yuan Wang, Lin Zhang, Liang Chen, Xu Wang, Department of Radiology, Affiliated Hospital of Binzhou Medical University, Binzhou 256603, Shandong Province, China

Pei-Yuan Wang, Hai-Fei Li, Department of Radiology, Yantai Affiliated Hospital of Binzhou Medical University, Yantai 264100, Shandong Province, China

Pei-Yuan Wang, Bin Wang, Medical Imaging Research Institute, Binzhou Medical University, Yantai 264003, Shandong Province, China

Xia Wang, Department of Pathology, Binzhou Medical University, Yantai 264003, Shandong Province, China

Author contributions: Wang PY and Wang Xia contributed equally to this work; Wang PY and Wang B designed the research; Wang PY, Wang Xia, Zhang L and Li HF performed the research; Li HF contributed new analytic tools; Chen L and Wang Xu analyzed the data; Wang PY and Wang Xia drafted the manuscript; all authors have read and approved the final version to be published.

Institutional review board statement: The study was reviewed and approved by the Ethics Committee of Binzhou Medical University.

Informed consent statement: All study participants, or their legal guardian, provided informed written consent prior to study enrollment.

Conflict-of-interest statement: The authors declare that there is no conflict of interest to disclose.

Data sharing statement: No additional data are available.

Correspondence to: Bin Wang, PhD, Medical Imaging Research Institute, Binzhou Medical University, No. 346 Guanhai Road, Yantai 264003, Shandong Province, China. binwang001@aliyun.com
Telephone: +86-535-6913002
Fax: +86-535-6913002

Received: January 10, 2015
Peer-review started: January 10, 2015
First decision: March 10, 2015
Revised: April 25, 2015
Accepted: June 16, 2015
Article in press: June 16, 2015
Published online: September 7, 2015

Abstract

AIM: To determine the possible predisposing factors of bezoar-induced small bowel obstruction (BI-SBO) and to discuss the diagnostic value of multi-slice spiral computed tomography, particularly contrast-enhanced scanning, in this condition.

METHODS: A total of 35 BI-SBO cases treated at our hospital from January 2007 to December 2013 were retrospectively analysed. Complete clinical and computed tomography (CT) data of the patients were available and confirmed by surgery. SBO was clinically diagnosed on the basis of clinical manifestations. Of the 35 patients, 18 underwent abdominal and pelvic CT planar scanning with GE 64-slice spiral CT and 17 underwent abdominal and pelvic CT planar scanning with GE 64-slice spiral CT combined with contrast-enhanced examination. Original images were processed

DOI: http://dx.doi.org/10.3748/wjg.v21.i33.9774

using a GE ADW4.3 workstation to obtain MPR, CPR, MIP and CTA images. The images of all patients were evaluated by two abdominal imaging experts. The main analytical contents of planar scanning included intestinal bezoar conditions, changes in the intestinal wall and changes in peri-intestinal conditions. Vascular hyperaemia and arterial blood supply conditions at a specific obstruction site and the distal end of the obstruction site were evaluated through contrast-enhanced examination.

RESULTS: The proportion of males to females among the 35 cases was 1:1.69 (13:22); median age was 63.3 years. The following cases were observed: 29 (82.8%) cases occurred in autumn and winter and showed a history of consuming high amounts of persimmon and hawthorn; 19 (54.3%) cases revealed a history of gastrointestinal surgery; 19 exhibited incomplete dentition, with missing partial or whole posterior teeth; 26 suffered from obstruction at the ileum. A total of 51 bezoars were found in these patients, of whom 16 (45.7%) had multiple bezoars. CT planar scanning of bezoars showed lumps with mottled gas inside the intestinal cavity. Furthermore, 9 cases of bezoars had envelopes and 11 cases were accompanied with thickening of the distal wall of the obstructed bowel. Scanning of 17 cases was enhanced; the results revealed that the mesenteric blood vessels at the obstruction site and the proximal site were dilated, and a total of 7 cases were accompanied with distal vascular dilation and intestinal wall thickening.

CONCLUSION: BI-SBO exhibits regional and seasonal characteristics. CT planar and contrast-enhanced scanning can be applied to diagnose and observe vascular conditions in obstructed zones.

Key words: Small bowel obstruction; Bezoar; Multi-slice computed tomography

Core tip: Bezoar-induced small bowel obstruction (BI-SBO) is a relatively rare clinical condition. BI-SBO exhibits regional and seasonal characteristics. This condition is associated with various predisposing factors. Multi-slice spiral computed tomography planar scanning can reveal intestinal bezoar conditions and changes in the intestinal wall and peri-intestinal conditions. Contrast-enhanced examination can further reveal vascular conditions, such as vascular hyperaemia and arterial blood supply conditions, in obstructed zones.

Wang PY, Wang X, Zhang L, Li HF, Chen L, Wang X, Wang B. Bezoar-induced small bowel obstruction: Clinical characteristics and diagnostic value of multi-slice spiral computed tomography. *World J Gastroenterol* 2015; 21(33): 9774-9784 Available from: URL: http://www.wjgnet.com/1007-9327/full/v21/i33/9774.htm

INTRODUCTION

Small bowel obstruction (SBO) is a common clinical disorder caused by various conditions. Common causes include postoperative adhesions (60%-80%), volvulus, intussusceptions, hernia, and tumours; bezoar-induced SBO (BI-SBO) is clinically rare, accounting for approximately 4% of all SBO cases[1-3]. Bezoars are solidified substances formed by mixing indigestible exogenous substances with other substances in the gastrointestinal tract; bezoars are commonly found inside the stomach but can enter the small intestine *via* the pylorus. Bezoar impaction in the small intestine likely causes SBO. BI-SBO cases are caused by small intestine-originated bezoars; in general, the small intestine of patients manifests common conditions, such as stenosis, diverticulum or tumorigenesis[4,5]. Bezoar formation is related to various factors, such as gastric motility disorders and gastrointestinal surgery. However, clinical manifestations of BI-SBO are not easily distinguished from intestinal obstruction caused by other factors[2]. As such, early surgical treatment is an essential and feasible treatment option; delayed treatment may significantly increase the incidence of complications and mortality[6].

Imaging examination plays an important role in the diagnosis of BI-SBO; for instance, multi-slice spiral computed tomography (MSCT) can be applied not only to accurately reveal causes, obstruction sites and obstruction degree but also to determine co-existing intestinal ischaemia or potential intestinal diseases[5,6]. Computed tomography (CT) images can also be used by clinicians as reference to develop rational treatment programs. With awareness of clinicians on BI-SBO and timely MSCT examination, this condition can be diagnosed in early stages and effectively treated. However, contrast-enhanced MSCT scanning has been rarely applied to diagnose BI-SBO. This study aimed to identify the predisposing factors affecting bezoar formation and to evaluate the diagnostic value of MSCT scanning, particularly contrast-enhanced examination, in BI-SBO; thus, clinical imaging and understanding of this disease can be enhanced.

MATERIALS AND METHODS

Clinical data

A total of 35 BI-SBO cases treated at our hospital (Affiliated Hospital of Binzhou Medical College) from January 2007 to December 2013 were retrospectively analysed. Complete clinical and CT data of patients were available. Of the 35 patients, 13 were male and 22 were female; the age of these patients ranged from 45 to 83 years, with a mean age of 63.3 ± 10.4 years. SBO was clinically diagnosed on the basis of clinical

Table 1 Predisposing factors of bezoar-induced small bowel obstruction *n* (%)

Predisposing factor	Case
Sex	
Male	13 (37.1)
Female	22 (62.9)
Age (yr)	
< 63	15 (42.9)
⩾ 63	20 (57.1)
Symptom	
Abdominal pain	23 (65.7)
Abdominal distension	35 (100)
Vomiting	15 (42.9)
Defecation and exhaust stopping	12 (34.3)
Physical sign	
Fever	7 (20)
Abdominal protuberance	29 (82.9)
Abdominal tenderness	9 (25.7)
Tenderness and rebound Tenderness	9 (25.7)
Cords	7 (20)
Food intake before the onset	
Persimmon, hawthorn, jujube	29 (82.9)
Uncertainty	6 (17.1)
Previous history	
Stomach stone or bezoar treatment history	3 (8.6)
Gastroduodenal operation history	19 (54.3)
Other history of abdominal operation	6 (8.6)
Dental status	
Teeth sound (partial denture)	9 (25.7)
Partial or total loss of posterior teeth	26 (74.3)

manifestations (vomiting, abdominal pain, bloating, blocked defecation and exsufflation). All of the patients were diagnosed with BI-SBO through CT examination and confirmed through surgical procedures, including laparotomy and gastric or small intestinal endoscopy-broken suction operations.

CT examination and image analysis

CT examination was performed using a GE 64-slice spiral CT scanner (GE Lightspeed 64 VCT, United States). Of the 35 patients, 18 underwent abdominal and pelvic CT planar scanning and 17 patients underwent abdominal and pelvic CT planar scanning combined with contrast-enhanced examination. None of the patients underwent intestinal CT visual examination. In enhanced examination, a high pressure syringe was used to inject 100 mL of a non-ionic contrast agent (300 mg I Omnipaque; GE Healthcare, Shanghai, China) *via* the cubital vein at an injection rate of 3.5 mL/s. After the contrast agent was injected, scanning was performed at 26 and 60 s; afterwards, arterial and portal venous phase images were obtained, respectively. The following CT scan parameters were set: collimation, 5 mm; thickness, 5 mm; layer interval, 2.5 mm; reconstructed layer thickness, 0.625 mm; 120 kVp; and 250 mAs. Clinical data, original images and images processed in a GE ADW4.3 workstation (MPR, CPR, MIP and CTA) were recorded.

The images of all patients were evaluated by two abdominal imaging experts; the following main analytical contents were considered: (1) intestinal bezoar conditions, such as location, number, shape, presence of an envelope and co-existence of a bezoar; (2) changes in the intestinal wall based on intestinal wall thickening, intestinal dilation and intestinal ischaemia or infarction, among others; (3) changes in peri-intestinal conditions, including mesenteric fuzzy (*i.e.*, mesenteric fat density increased) and ascites; (4) contrast-enhanced examination mainly evaluated vascular hyperaemia (*i.e.*, whether the number of mesenteric vessels increased or decreased and whether or not lumen expansion occurred) and arterial blood supply conditions at a particular obstruction site and the distal end of the obstruction site. If the two experts disagreed with a diagnostic opinion, a consensus was obtained after further consultations were performed.

RESULTS

Possible predisposing factors of BI-SBO

The patients' clinical data are shown in Table 1. The proportion of males to females among the 35 patients was 1:1.69 (13:22); median age was 63.3 years (with a range of 45 years to 83 years). Clinical manifestations included all of the symptoms of acute intestinal obstruction, particularly abdominal distension (100%) and abdominal pain (65.7%); the most common sign was the presence of an abdominal bulge (82.9%). Three patients with acute obstruction suffered from fever, tenderness at specific abdominal site and rebound tenderness during physical examination. The patients were subjected to emergent surgery after they underwent abdominal and pelvic CT planar scanning. Thirty-two patients received conservative treatments, such as gastrointestinal decompression for 1 d to 7 d. After the corresponding examinations were completed, 28 patients underwent open surgery, and 4 patients underwent gastrointestinal endoscopic bezoar-broken suction operations. The patients were followed for three months; no recurrence was found.

A total of 25 patients exhibited a history of abdominal surgery. Of these 25 patients, 19 underwent gastroduodenal surgery (3 cases of vagotomy and pyloroplasty; 16 cases of gastrectomy and gastrointestinal anastomosis, including 5 cases of gastroduodenal anastomosis and 11 cases of gastrojejunostomy), 3 underwent appendectomy, 2 underwent subtotal hysterectomy, and 1 underwent post-traumatic splenectomy. Other medical histories included 9 cases of diabetes (6 cases were subjected to abdominal surgery and 3 other cases did not undergo surgery) and 1 case of secondary hypothyroidism after this patient was subjected to hyperthyroid surgery.

The following patients manifested dental conditions. A total of 9 cases showed complete dentition (25.7%); of these cases, 2 retained all of their teeth, 4 had whole dentures and 3 exhibited partial dentures. A

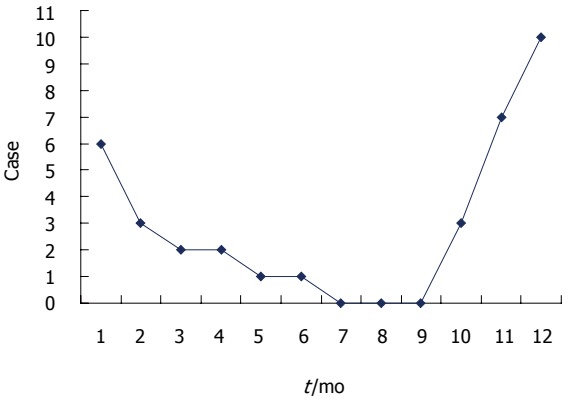

Figure 1 Monthly incidence of bezoar-induced small bowel obstruction.

Table 2 Impaction sites, concomitant bezoars and computed tomography diagnosis

Impaction site (n = 35)	Concomitant site	Case, n	CT confirmed, n	
			Impaction bezoars	Concomitant bezoars
Duodenum	No	1	1	0
Jejunum	No	6	6	0
	Stomach	2	2	2
	Ileum	1	1	1
Ileum	No	12	12	0
	Stomach	3	3	1
	Jejunum	3	3	3
	Ileum	7	7	7
Total		35	35	14

CT: Computed tomography.

total of 19 cases exhibited incomplete dentition with missing partial or whole posterior teeth.

BI-SBO may occur throughout a year, but this condition is common from October to February, which coincides with Chinese autumn and winter (29/35, 82.9%). Figure 1 shows the incidence of BI-SBO in each month. Before the onset of BI-SBO, 29 patients exhibited a history of consuming high amounts of persimmon (15 cases), hawthorn (13 cases) and jujube (1 case) under fasting conditions. Of these patients, 3 revealed a history of gastrolith treatment on 3 d to 9 d before the condition was manifested (gastroscopic broken suction operation) and 6 did not experience food intake-related conditions.

A total of 51 bezoars were found in the 35 BI-SBO patients, of whom 19 contained only one bezoar and 16 revealed multiple bezoars (45.7%, Table 2). The obstruction sites were the duodenum (1 case), jejunum (8 cases) and ileum (26 cases). Co-existing bezoars were located in the stomach (5 bezoars), jejunum (3 bezoars) and ileum (8 cases). A total of 35 bezoars (100%) were accurately diagnosed through CT examination, whereas 2 co-existing gastroliths among the 16 co-existing bezoars were misdiagnosed.

Table 3 Computed tomography findings of impaction bezoars

Signs		Case	Percentage
Impaction bezoars		35	
Well delineated mass in the intestinal lumen, with a mixed density and containing air	With encapsulating wall	6	17.1
	Without encapsulating wall	29	82.9
Bowel and perienteric changes			
Bowel wall thickening	Obstruction and proximal	34	97.1
	With distal to the obstruction	11	31.4
Lumen dilatation proximal to the obstruction		34	97.1
Intestinal infarction		0	0
Mesenteric haziness		32	91.4
Ascites		13	37.1
CTA changes		17	
Mesenteric vascular engorgement	Obstruction and proximal	17	100
	With distal to the obstruction	7	41.2

CT findings of BI-SBO

CT planar scanning revealed that the obstructed bezoars appeared as lumps with clear edges inside the intestinal cavity. The density of these bezoars revealed varied results with mottled gas shadow inside the cavity. In 3 cases of hawthorn bezoar, scattered high-density seeds were obtained. In terms of morphological characteristics, 26 were oval, 5 were tubular and 4 were round. The performance of coexisting bezoars was similar to the obstructed bezoars. Only 6 (17.1%) cases of single obstructed bezoars and 3 cases of co-existing gastroliths contained an envelope (Table 3). CT images revealed that the 2 misdiagnosed gastrolith cases were also covered by an envelope, whereas the remaining bezoars were not covered by an envelope. In terms of obstruction sites, 34 cases exhibited proximal bowel dilation and 1 case occurred at the bottom of the site subjected to surgical anastomosis without evident proximal bowel dilation. All of the patients showed a gas-liquid surface in the obstructed proximal dilated intestine or stomach. A total of 34 cases manifested thickening in the obstructed zone and proximal intestinal wall (97.1%) and 11 cases showed thickening of the obstructed distal intestinal wall. A total of 32 cases exhibited mesenteric fuzzy (91.4%) and 13 cases contained a small amount of ascites (37.1%).

Enhanced scanning revealed 17 cases of mesenteric vascular congestion and dilation in the obstructed zone and obstructed proximal end; of these 17 patients, 7 were accompanied with hyperaemia and thickening of the obstructed distal vessel wall. The obstruction

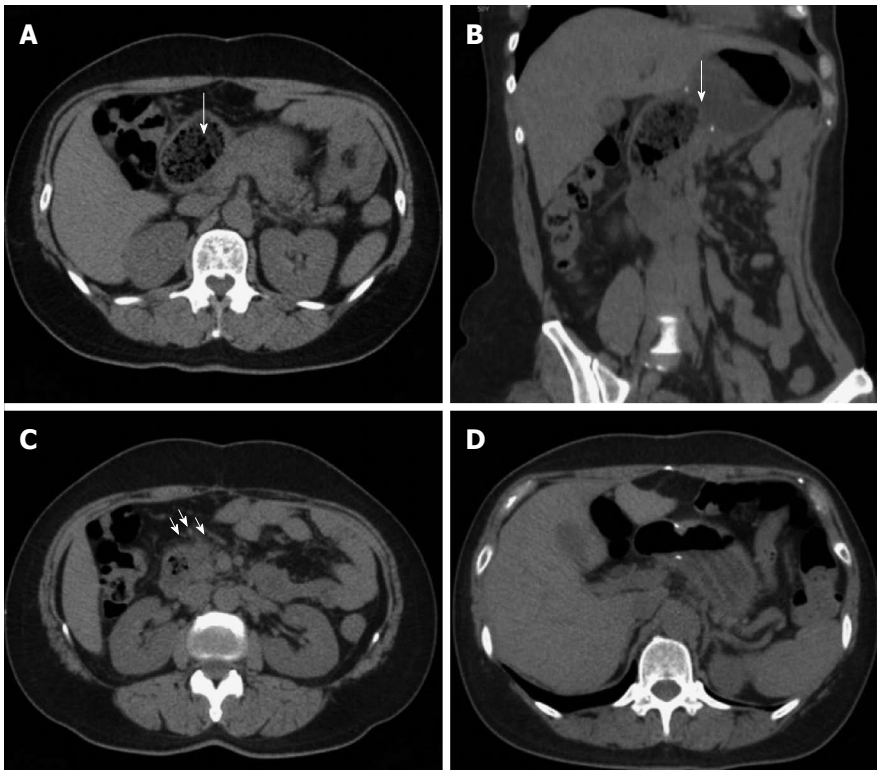

Figure 2 Representative case of a 50-year-old female with hawthorn small bowel obstruction. A: Computed tomography (CT) planar scan image showing that the duodenum expanded and contained an oval bezoar with gas (arrow); B: MPR image revealing the shape of bezoars and gastroduodenal anastomosis; anastomotic diameter was 4 cm (arrow); C: Peri-intestinal exudation and mesenteric vascular dilation of the distal end of SBO (arrows); D: Image displaying changes after bezoar-broken suction operation is performed.

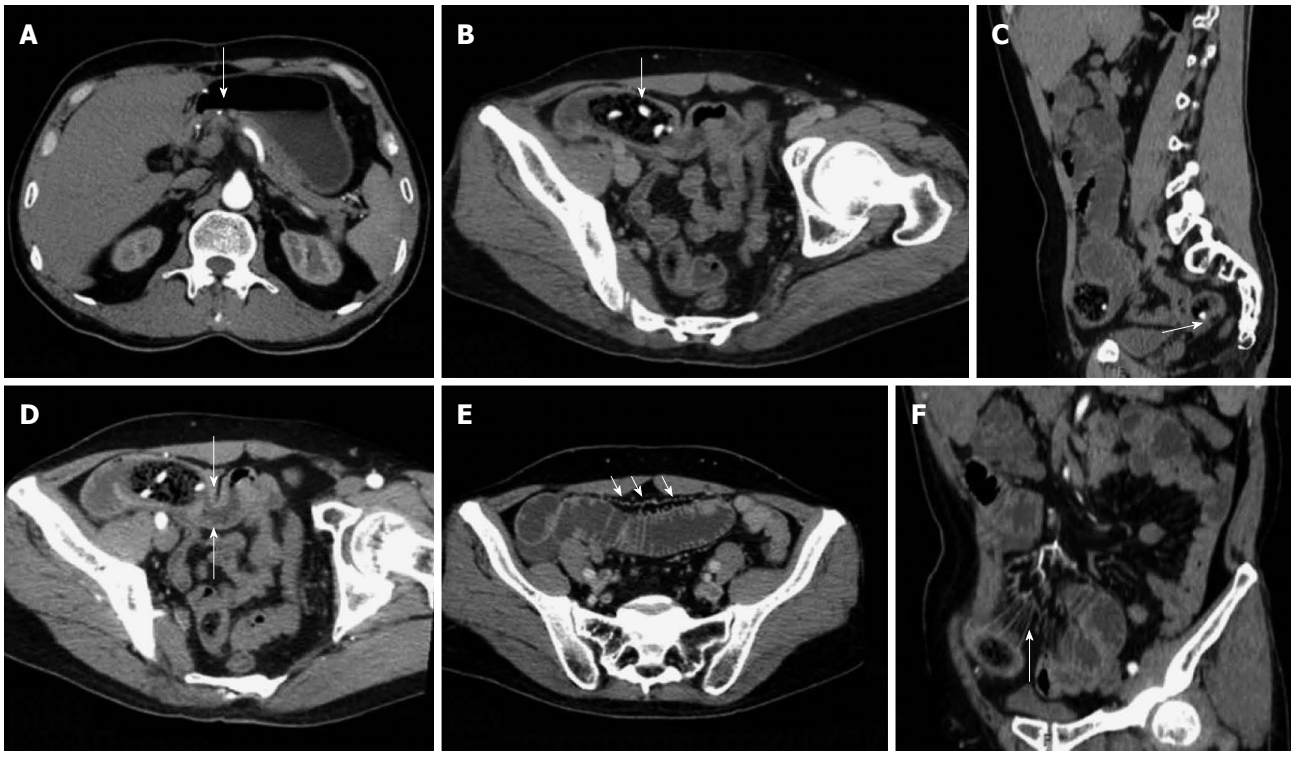

Figure 3 Representative case of a 58-year-old male with hawthorn small bowel obstruction. A: Contrast-enhanced examination result displaying the gastroduodenal anastomotic stoma of the artery; B: Oblique MPR revealing an oval bezoar in the distal end of the jejunum with shadows of high-density seeds (arrow); C: Sagittal reconstruction showing co-existing bezoar inside the ileum (arrow); D: Arterial phase image exhibiting the thickened and strengthened intestinal wall in the distal end of the obstruction site (arrow); E: Portal venous phase image showing a significantly enlarged vascular shadow and blurred mesentery of the proximal end of the dilated SBO intestine (arrow); F: CTA image revealing the thickening of the mesenteric blood vessel and peripheral exudation in the obstruction site (arrow).

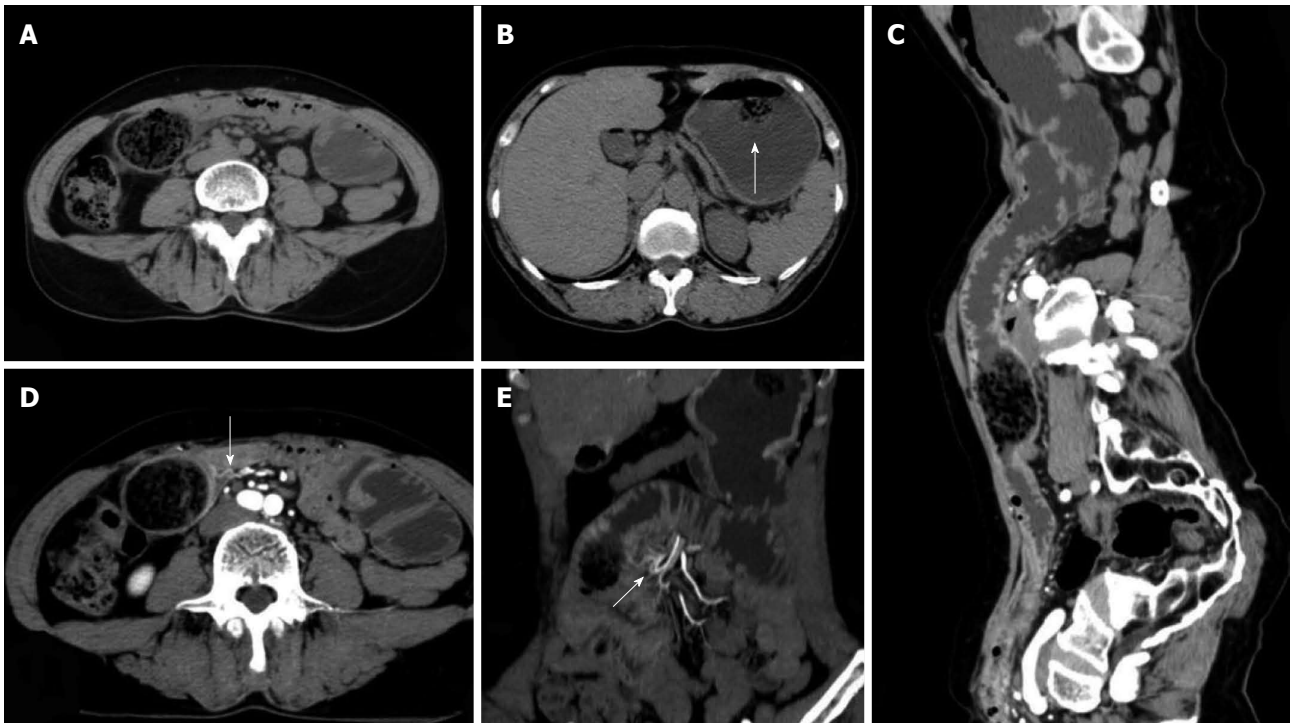

Figure 4 Representative case of a 60-year-old female with diospyrobezoar-induced small bowel obstruction previously subjected to gastrectomy and gastrojejunostomy. A: Computed tomography (CT) planar scan image displaying the bezoar without an envelope inside the proximal end of the ileum; B: co-existing gastric bezoar with an envelope (arrow); C: CPR image showing the dilation of the proximal end of the obstructed intestine, bezoar and distal wall thickening at the obstruction site; D: Contrast-enhanced CT scan with an arterial phase image revealing a significant enhancement and thickening of obstruction regions and the distal end of the obstructed intestine; blood-supplying arteries exhibited hyperaemia (arrow); E: CTA image showing the same mesenteric artery (arrow) that provides blood supply for the transitional zone and the distal end of the obstruction site.

sites and distal end of the obstruction sites of these 7 patients were supplied with blood *via* one mesenteric arterial branch (Table 3, Figures 2-5).

DISCUSSION

A bezoar refers to the coagulum formed inside the digestive tract when indigestible exogenous substances are mixed with other substances; this condition is affected by several factors. Bezoars can be classified into different groups according to component sources: phytobezoar, trichobezoar, drug bezoar and lactic acid bacterium bezoar. Among these groups, phytobezoar is the most common type[7]. Phytobezoar is commonly found inside the stomach; partial phytobezoars may enter the small intestine, thereby causing impaction and complete SBO. BI-SBO is clinically rare, accounting for approximately 4% of all SBO cases[1-3,8]. Bezoar formation is not directly correlated with gender and age[1,9-11]; furthermore, bezoar formation may be affected by several factors, such as diet, anatomical features, organic composition of the gastrointestinal tract and functional disorders[7,8,12-16].

In terms of diet, phytobezoar is mainly caused by consuming high amounts of vegetables or fruits, such as persimmon, hawthorn, date, prune, grape skin, celery, mango, banana, cactus fruit, fig and mushroom, which contain indigestible plant fibres[12,17,18]. These fruits and vegetables are rich in fibres, tannic acid and lignins. When consumed at high amounts, tannic acid is transformed from a monomeric form into a tannin-cellulose-protein complex *via* the actions of gastric acid. This complex exhibits a concrete-like viscosity and easily adhered to the gastrointestinal wall; a viscous mass is formed and may be incarcerated inside the gastrointestinal lumen, thereby causing obstruction[12,19,20]. Furthermore, seeds of multi-seed fruits, such as cactus fruit and fig, are prone to accumulate inside the small intestine and form obstructive lumps inside the intestinal cavity; as a result, intestinal obstruction occurs[12,13]. BI-SBO can affect individuals worldwide, although regional and seasonal characteristics can be observed. Conditions, such as persimmon and hawthorn stones, are more common in subtropical and temperate regions than in other regions; the onset of these conditions usually occurs in autumn and winter. In this study, all of the patients were located in the temperate zone; of these patients, 82.9% were detected in autumn and winter (31/35), and this finding is consistent with that described in previous studies[12,17,21].

In addition to the intake of large amounts of cellulose materials, other possible risk factors include history of gastrointestinal surgeries (such as vagotomy and pyloroplasty, gastrectomy and gastrojejunostomy or gastroduodenal anastomosis, and gastrointestinal

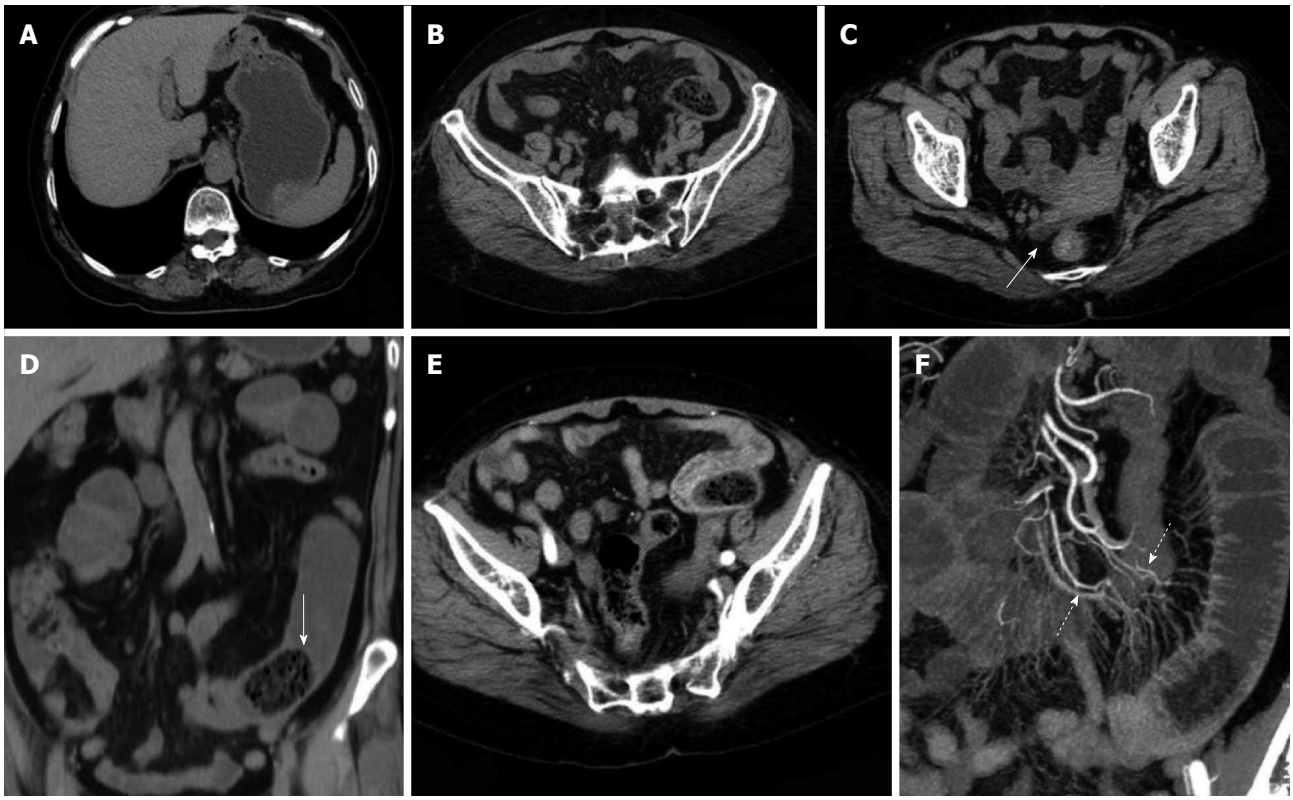

Figure 5 Representative case of a 71-year-old female with diospyrobezoar-induced small bowel obstruction. A and B: Computed tomography (CT) planar scan image revealing oval bezoars inside the gastrointestinal anastomotic stoma and the distal end of the jejunal cavity; adjacent mesentery was slightly blurred; C: The right rear end of the uterine bottom with a small amount of seroperitoneum (white arrow); D: MPR image showing the shape of a bezoar and a linear envelope (solid arrow); E: Artery phase image displaying no thickening of the distal intestinal wall at the obstruction site but with significant enhancement; F: CTA image showing different mesenteric arteries (dotted arrow) that provide blood supply for the transitional zone and the distal end of the obstruction site.

stoma anastomosis), gastric motility disorders caused by various factors and poor dentition[2,5,22,23].

Vagotomy and partial gastrectomy can reduce gastric acid secretion, resulting in a weakly acidic environment and decrease in gastric motility; thus, removal of undigested solids from the stomach is likely delayed, thereby causing high amounts of viscous contents to form inside the stomach, which is prone to bezoar formation[12]. Gastroenterostomy, gastrojejunostomy or pyloroplasty can expand the outlet of the stomach; as such, undigested vegetable or fruit fibre lumps inside the stomach easily enter and form obstructive lumps in the small intestine, thereby causing incarceration and obstruction[12,16,19,24,25]. After gastroenterostomia occurs, the stricture of anastomotic stoma is a possible cause of bezoar formation[12,16,25]. In this study, 19 patients, including 11 cases of major gastrectomy plus gastrojejunostomy and 5 cases of major gastrectomy plus gastroduodenal anastomosis, revealed a history of gastrointestinal surgery. This high incidence of gastroenterostomia is similar to that recorded by Bedioui *et al*[12]. Ho *et al*[19] and Ulusan *et al*[24] also summarised the surgical histories of patients with BI-SBO, but relationships between different surgical methods and BI-SBO have not been reported.

The hypodontia of posterior dentition or dentural malocclusion likely affects chewing functions; as a result, chewing and digestion disorders related to fibrous food occur; thus, lumps in the gastrointestinal tract can be easily formed and the probability of SBO occurrence possibly increases[15,22]. In this study, patients with partial or complete hypodontia of posterior dentition exhibited a significantly higher incidence of SBO than those with complete dentition; this result indicated that dentition status affects the incidence of BI-SBO. Similar to other studies, our study showed that diabetes, hypothyroidism, pernicious anaemia, kidney failure, postoperative bowel adhesions and other diseases can indirectly affect gastrointestinal motility and emptying; thus, BI-SBO occurs[17,25,26].

BI-SBO usually occurs at the narrow part of the small intestine, in particular, the distal end of the ileum is the most common site, especially at 50 cm to 70 cm away from the ileocaecal valve. This condition commonly occurs at this site because the lumen of this small intestinal segment is narrow. Thus, bowel movements are slowed down, and a large amount of water inside bezoars is absorbed and motility is reduced. The jejunum is the second most common site[27,28]. In this study, 9 cases of BI-SBO were found in the jejunum and 26 cases were detected in the ileum; this finding is consistent with that described in previous studies. Considering patients' histories of gastrointestinal surgery, we found that

the obstructive sites of BI-SBO may be related to the size of gastrointestinal anastomosis. On one hand, a large anastomotic size (diameter ⩾ 30 mm) may easily cause a high incidence of SBO. This condition is possible because a large gastrolith mat easily enter the small intestine *via* the anastomotic stoma and cause incarceration in the corresponding luminal stenotic site; in particular, a bezoar with a diameter greater than that of the small intestine may easily form incarceration at a region closer to the anastomotic site. On the other hand, a small anastomotic stoma likely results in a low incidence of SBO. This condition is possible because a gastrolith larger than anastomotic stoma cannot easily enter the small intestine *via* the anastomotic stoma; thus, gastrolith enlarges in the stomach. By contrast, a small gastrolith easily enters the small intestine and gradually forms a large bezoar with slow intestinal movements; for instance, patients with reduced gastrointestinal motor functions exhibit reduced bezoar movement. Thus, obstruction sites are often found away from anastomotic sites. In this study, the patient with gastroduodenal anastomosis exhibited the largest SBO site. This patient revealed a wide anastomotic stoma (diameter = 40 mm). The obstruction site was located beneath the anastomotic stoma and above the duodenal papilla. Patients with BI-SBO exhibited co-existing bezoars in other parts, in addition to the obstructive bezoar; co-existing bezoars could be found in any part of the stomach and the small intestine. Approximately one-third of the patients also have gastroliths; these residual co-existing bezoars may be the main reason for recurrence after patients undergo surgery to remove bezoars from the small intestine[5,10]. In this study, 16 (45.7%) patients showed co-existing bezoars, of whom 5 manifested co-existing gastroliths. This ratio was lower than that documented in a previous study. Only 3 patients underwent gastroscopic bezoar-broken suction operation 3 d to 9 d before disease onset; thus, SBO may be caused by bezoar residue or debris that formed after surgery is completed.

The clinical manifestations of BI-SBO may vary according to different bezoar sizes, obstruction sites and degrees; the most common manifestations are complete mechanical intestinal obstructions, such as abdominal pain, bloating, nausea and vomiting. The diagnosis of BI-SBO based on clinical symptoms may delay surgical treatment and increase morbidity and mortality[2,22]. If BI-SBO patients revealed histories of gastrointestinal surgery or laparotomy, clinicians may initially consider adhesive intestinal obstruction and implement conservative treatments, which may adversely affect illness. Therefore, appropriate examination methods should be selected to diagnose BI-SBO in early stages and clinical treatments should be promptly administered[19,22,24].

Imaging examination is the main basis of SBO diagnosis. Abdominal X-ray, barium enema, abdominal ultrasound and endoscopy have been applied to diagnose SBO, but these examinations exhibit poor diagnostic accuracies and limitations. As such, the clinical use of these techniques is limited[9,10,19,22]. MSCT is characterized by several advantages, including fast scanning speed, non-invasive procedure and volume scanning. MSCT has become the preferred examination method to diagnose SBO. CT yields a diagnostic sensitivity for acute SBO of 73% to 95%[29] and an accuracy of 83%[30]. For BI-SBO, abdominal and pelvic CT scanning can be applied to locate bezoar causing SBO and obstructive degree, as well as co-existing multiple bezoars, intestinal ischaemia, strangulation, perforation or other potential intestinal diseases. In this procedure, acute abdominal symptoms caused by other causes are excluded; thus, right treatment options are selected and most efficient surgical approaches are determined[5,6,10,29-31].

In CT planar scanning, bezoar appears as round, oval or tubular masses with clear boundaries located inside the intestinal lumen, although densities varied and mottled gas density can be observed inside the lumen. Some bezoars may be covered with ring envelopes[5,9,31]. Altintoprak *et al*[13] reported that bezoars contain a large amount of gas and show wide intervals, as well as scattered high-density seeds characterizing hawthorn bezoars. Kim *et al*[5] suggested that gastrolith surface contains one coating layer of gastric mucosal secretions, which form a gelatinous membrane and cover bezoar surface; this membrane may be the encapsulating wall found in CT images. In CT planar scanning, air and fat can be identified by adjusting to a suitable window (WW-500HU, WL-50HU); the processed and obtained MPR image can then be used to observe intestinal bezoar, wall thickness, dilation extension, changes in intestinal perimeter and co-existence of bezoars[10,32]. Intestinal oedema and bleeding caused by bezoar incarceration can be used as "target signs". CT target signs likely prevent the passage of obstructive bezoar through the intestines. As such, conservative treatments may not be suitable or may eventually fail, and emergent surgery is thus needed[5]. In this study, 35 cases manifested typical signs, and accurate diagnosis was performed through CT planar scanning. However, 2 cases of co-existing gastrolith were misdiagnosed possibly because of radiologist's insufficient understanding of co-existing bezoars; observation was also not sufficiently comprehensive. The results also showed that 3 cases of hawthorn bezoar presented shadows of high-density seeds, whereas 1 case of diospyrobezoar did not show these high-density shadows. Furthermore, 5 cases of co-existing gastroliths were covered with an envelope, but the obstructive bezoars of the corresponding cases did not show definite capsules. This finding was explained by Kim *et al*[5]. All of the patients in our study showed no definite target signs.

Multi-slice contrast-enhanced spiral CT examination (particularly in the arterial phase) combined with post-processing technologies (MPR, CPR, MIP and

CTA) can help identify lesion segments of the small intestine, vascular anatomical and morphological changes and intestinal ischaemia or infarction; the combined technology can also be applied to observe postoperative changes, including surgical methods, anastomotic stoma and input and output loops; thus, inductive factors, such as postoperative changes, adhesions or diverticulitis, can be determined before surgery is performed[21,24]. Geffroy *et al*[33] suggested that a dilated ansa is not significantly enhanced compared with an adjacent normal intestinal ansa of patients with SBO; as such, this condition is a specific sign of intestinal ischaemia. Geffroy *et al*[33] also demonstrated that CT planar scanning results may provide a false indication that the strengthening of lesion intestinal walls is normal when contrast-enhanced images show that the density of a dilated intestinal wall is increased (sign of ischaemia). As a consequence, intestinal ischaemia is misdiagnosed or diagnosed in late stages. In this study, the CTA images of 17 enhanced examination cases showed blood supply from mesenteric arterial branches and anastomotic branches in the lesion regions. The images also accurately revealed the obstruction site, thickening and tortuosity of anastomotic blood vessels of proximal dilated intestines, mesenteric perivascular exudation, oedema and ascites of the distal end of obstructive intestines; intestinal ischaemia or necrosis signs, such as enhancement reduction, were not found.

Kim *et al*[5] considered that the thickening of the distal small intestinal wall in the obstruction site is a significant CT sign to determine the onset of basic intestinal diseases in patients with phytobezoars. However, this hypothesis should be further investigated. In our study, 11 patients with thickened distal small intestinal wall in the obstruction site did not suffer from basic intestinal diseases; this finding is not consistent with that obtained by Kim *et al*[5]. Analysing the CTA images, we found that the thickening of distal small intestinal wall in the obstruction site may be related to the blood supply of the mesenteric branches; in other words, they are formed in proximity to the obstruction site. Furthermore, intestinal swelling, mesenteric vascular tortuosity and thickening and peri-intestinal secretion become evident when the distal end of the obstruction site and the transitional segment (located in the obstruction site between the dilated intestine and the collapsed intestine) supply blood for the same artery. By contrast, the inflammation degree of the distal end of the obstructive intestine likely decreases or swelling unlikely occurs when the distal end of the obstruction site and the transitional segment separately supply blood for the arterial branch (or the transitional segment located at the junction of two blood-supplying arteries); mesenteric vascular tortuosity and thickening, as well as peri-intestinal and perivascular exudation, are also unlikely evident.

In CT diagnosis, BI-SBO should be distinguished from intestinal faeces- and gallstone-induced SBO. Bezoar and faeces related to SBO have been described; for instance, lumps should be considered as faeces if lumps inside the dilated intestines exhibit several characteristics, such as long longitudinal diameter, insufficient density in texture, no capsule, found in the proximal end of obstruction sites and floating-like properties. Lumps may be considered as bezoars if intestinal masses are located in the obstructive transitional zone, characterised by a clear edge, and bubble-like mottled behaviour and covered with an envelope[5,10,30,32]. The performance of gallstone ileus is similar to that of bezoar and can be accurately diagnosed on the basis of Rigler's image triad (SBO, pneumobilia and positive small intestinal ectopic gallstone) and biliary-enteric fistula[31,34-36]. Few bezoars may exhibit non-gas, solid soft tissue-density lumps. With CT planar scanning, small intestinal tumours or intussusceptions can be hardly identified; with enhanced CT scanning or contrast-enhanced examination, diagnosis can be confirmed.

The formation of bezoars may be related to various predisposing factors; the onset of this condition in patients is often simultaneously affected by many factors. BI-SBO exhibits regional and seasonal characteristics; thus, clinicians should understand this feature to perform efficiently. BI-SBO also shows characteristic CT signs; thus, diagnosis through CT planar scanning is relatively easy based on the observed performance. Abdominal and pelvic contrast-enhanced CT examination can also efficiently reveal intestinal lesions, peri-intestinal changes and blood-supplying arteries; thus, this technique can help clinicians administer early appropriate interventions and improve patient outcomes.

COMMENTS

Background

Small bowel obstruction (SBO) is a common clinical condition caused by various factors, including postoperative adhesions, volvulus, intussusceptions, hernia or tumours. Bezoar impaction-induced SBO (BI-SBO) is a clinically rare condition. Multi-slice spiral computed tomography (MSCT) plays an important role in the diagnosis of BI-SBO.

Research frontiers

The use of MSCT scanning can help diagnose SBO, reveal causes, obstruction site and obstruction degree and accurately determine co-existing intestinal ischaemia or potential intestinal diseases.

Innovations and breakthroughs

BI-SBO exhibits regional and seasonal characteristics. This condition is associated with various predisposing factors, such as gastric motility disorders and gastrointestinal surgery. MSCT is a valuable technology to diagnose BI-SBO. The major advantage of contrast-enhanced examination is the ability to observe vascular situations in obstructed zones, including vascular hyperaemia and arterial blood supply conditions.

Applications

Predisposing factors can trigger susceptible groups to develop BI-SBO. Contrast-enhanced MSCT examination can be applied to routinely observe

vascular conditions of patients with SBO. Further research should be conducted on SBO to promote the widespread use of MSCT.

Terminology

A bezoar refers to the coagulum formed inside the digestive tract when indigestible exogenous substances are mixed with other substances. A bezoar can be classified into different groups according to component sources: phytobezoar, trichobezoar, drug bezoar or lactic acid bacterium bezoar.

Peer-review

This study is an original research that highlights the application of MSCT to diagnose BI-SBO and simultaneously analyse predisposing factors.

REFERENCES

1 **Erzurumlu K**, Malazgirt Z, Bektas A, Dervisoglu A, Polat C, Senyurek G, Yetim I, Ozkan K. Gastrointestinal bezoars: a retrospective analysis of 34 cases. *World J Gastroenterol* 2005; **11**: 1813-1817 [PMID: 15793871]

2 **Ko S**, Lee T, Ng S. Small bowel obstruction due to phytobezoar: CT diagnosis. *Abdom Imaging* 1997; **22**: 471-473 [PMID: 9233879]

3 **Licht M**, Gold BM, Katz DS. Obstructing small-bowel bezoar: diagnosis using CT. *AJR Am J Roentgenol* 1999; **173**: 500-501 [PMID: 10430164]

4 **Kim JH**, Chang JH, Nam SM, Lee MJ, Maeng IH, Park JY, Im YS, Kim TH, Park IY, Han SW. Duodenal obstruction following acute pancreatitis caused by a large duodenal diverticular bezoar. *World J Gastroenterol* 2012; **18**: 5485-5488 [PMID: 23082068 DOI: 10.3748/wjg.v18.i38.5485]

5 **Kim JH**, Ha HK, Sohn MJ, Kim AY, Kim TK, Kim PN, Lee MG, Myung SJ, Yang SK, Jung HY, Kim JH. CT findings of phytobezoar associated with small bowel obstruction. *Eur Radiol* 2003; **13**: 299-304 [PMID: 12598994]

6 **Akcakaya A**, Sahin M, Coskun A, Demiray S. Comparison of mechanical bowel obstruction cases of intra-abdominal tumor and non-tumoral origin. *World J Surg* 2006; **30**: 1295-1299 [PMID: 16773260]

7 **Yakan S**, Sirinocak A, Telciler KE, Tekeli MT, Deneçli AG. A rare cause of acute abdomen: small bowel obstruction due to phytobezoar. *Ulus Travma Acil Cerrahi Derg* 2010; **16**: 459-463 [PMID: 21038126]

8 **Teng H**, Nawawi O, Ng K, Yik Y. Phytobezoar: an unusual cause of intestinal obstruction. *Biomed Imaging Interv J* 2005; **1**: e4 [PMID: 21625276 DOI: 10.2349/biij.1.1.e4]

9 **Yildirim T**, Yildirim S, Barutcu O, Oguzkurt L, Noyan T. Small bowel obstruction due to phytobezoar: CT diagnosis. *Eur Radiol* 2002; **12**: 2659-2661 [PMID: 12386754]

10 **Ripollés T**, García-Aguayo J, Martínez MJ, Gil P. Gastrointestinal bezoars: sonographic and CT characteristics. *AJR Am J Roentgenol* 2001; **177**: 65-69 [PMID: 11418400]

11 **Pujar K A**, Pai A S, Hiremath V B. Phytobezoar: a rare cause of small bowel obstruction. *J Clin Diagn Res* 2013; **7**: 2298-2299 [PMID: 24298509 DOI: 10.7860/JCDR/2013/7248.3504]

12 **Bedioui H**, Daghfous A, Ayadi M, Noomen R, Chebbi F, Rebai W, Makni A, Fteriche F, Ksantini R, Ammous A, Jouini M, Kacem M, Bensafta Z. A report of 15 cases of small-bowel obstruction secondary to phytobezoars: predisposing factors and diagnostic difficulties. *Gastroenterol Clin Biol* 2008; **32**: 596-600 [PMID: 18487032 DOI: 10.1016/j.gcb.2008]

13 **Altintoprak F**, Degirmenci B, Dikicier E, Cakmak G, Kivilcim T, Akbulut G, Dilek ON, Gunduz Y. CT findings of patients with small bowel obstruction due to bezoar: a descriptive study. *ScientificWorldJournal* 2013; **2013**: 298392 [PMID: 23690741 DOI: 10.1155/2013/298392]

14 **Oh SH**, Namgung H, Park MH, Park DG. Bezoar-induced Small Bowel Obstruction. *J Korean Soc Coloproctol* 2012; **28**: 89-93 [PMID: 22606648 DOI: 10.3393/jksc.2012.28.2.89]

15 **Salemis NS**, Panagiotopoulos N, Sdoukos N, Niakas E. Acute surgical abdomen due to phytobezoar-induced ileal obstruction. *J Emerg Med* 2013; **44**: e21-e23 [PMID: 22040770 DOI: 10.1016/j.jemermed.2011.06.059]

16 **Roy M**, Fendrich I, Li J, Szomstein S, Rosenthal RJ. Treatment option in patient presenting with small bowel obstruction from phytobezoar at the jejunojejunal anastomosis after Roux-en-Y gastric bypass. *Surg Laparosc Endosc Percutan Tech* 2012; **22**: e243-e245 [PMID: 22874713 DOI: 10.1097/SLE.0b013e31825d6c07]

17 **Stein CM**, Gelfand M. Gastro-intestinal phytobezoars in Zimbabwean Africans. *Trans R Soc Trop Med Hyg* 1985; **79**: 508-509 [PMID: 4082259]

18 **Ho MP**, Chou AH, Cheung WK. Small bowel obstruction secondary to a mushroom bezoar. *J Am Geriatr Soc* 2013; **61**: 1041-1043 [PMID: 23772737 DOI: 10.1111/jgs.12285]

19 **Ho TW**, Koh DC. Small-bowel obstruction secondary to bezoar impaction: a diagnostic dilemma. *World J Surg* 2007; **31**: 1072-1078; discussion 1079-1080 [PMID: 17420961]

20 **Ladas SD**, Kamberoglou D, Karamanolis G, Vlachogiannakos J, Zouboulis-Vafiadis I. Systematic review: Coca-Cola can effectively dissolve gastric phytobezoars as a first-line treatment. *Aliment Pharmacol Ther* 2013; **37**: 169-173 [PMID: 23252775 DOI: 10.1111/apt.12141]

21 **Tayeb M**, Khan FM, Rauf F, Khan MM. Phytobezoar in a jejunal diverticulum as a cause of small bowel obstruction: a case report. *J Med Case Rep* 2011; **5**: 482 [PMID: 21951579 DOI: 10.1186/1752-1947-5-482]

22 **Escamilla C**, Robles-Campos R, Parrilla-Paricio P, Lujan-Mompean J, Liron-Ruiz R, Torralba-Martinez JA. Intestinal obstruction and bezoars. *J Am Coll Surg* 1994; **179**: 285-288 [PMID: 8069423]

23 **Liou CH**, Yu CY, Lin CC, Chao YC, Liou YC, Juan CJ, Chen CY. CT diagnosis of small bowel obstruction due to phytobezoar. *J Formos Med Assoc* 2003; **102**: 620-624 [PMID: 14625606]

24 **Ulusan S**, Koç Z, Törer N. Small bowel obstructions secondary to bezoars. *Ulus Travma Acil Cerrahi Derg* 2007; **13**: 217-221 [PMID: 17978897]

25 **Sarhan M**, Shyamali B, Fakulujo A, Ahmed L. Jejunal Bezoar causing obstruction after laparoscopic Roux-en-Y gastric bypass. *JSLS* 2010; **14**: 592-595 [PMID: 21605530 DOI: 10.4293/108680810X12924466008682]

26 **de Menezes Ettinger JE**, Silva Reis JM, de Souza EL, Filho Ede M, Gãlvao do Amaral PC, Ettinger E, Fahel E. Laparoscopic management of intestinal obstruction due to phytobezoar. *JSLS* 2007; **11**: 168-171 [PMID: 17651584]

27 **de Toledo AP**, Rodrigues FH, Rodrigues MR, Sato DT, Nonose R, Nascimento EF, Martinez CA. Diospyrobezoar as a cause of small bowel obstruction. *Case Rep Gastroenterol* 2012; **6**: 596-603 [PMID: 23271989 DOI: 10.1159/000343161]

28 **Quintana JF**, Walker RN, McGeehan A. Child with small bowel obstruction and perforation secondary to ileal bezoar. *Pediatr Emerg Care* 2008; **24**: 99-101 [PMID: 18277846 DOI: 10.1097/PEC.0b013e318163dbc8]

29 **Burkill GJ**, Bell JR, Healy JC. The utility of computed tomography in acute small bowel obstruction. *Clin Radiol* 2001; **56**: 350-359 [PMID: 11384132]

30 **Zissin R**, Osadchy A, Gutman V, Rathaus V, Shapiro-Feinberg M, Gayer G. CT findings in patients with small bowel obstruction due to phytobezoar. *Emerg Radiol* 2004; **10**: 197-200 [PMID: 15290490]

31 **Billaud Y**, Pilleul F, Valette PJ. [Mechanical small bowel obstruction due to bezoars: correlation between CT and surgical findings]. *J Radiol* 2002; **83**: 641-646 [PMID: 12063427]

32 **Delabrousse E**, Lubrano J, Sailley N, Aubry S, Mantion GA, Kastler BA. Small-bowel bezoar versus small-bowel feces: CT evaluation. *AJR Am J Roentgenol* 2008; **191**: 1465-1468 [PMID: 18941086 DOI: 10.2214/AJR.07.4004]

33 **Geffroy Y**, Boulay-Coletta I, Jullès MC, Nakache S, Taourel P, Zins M. Increased unenhanced bowel-wall attenuation at multidetector CT is highly specific of ischemia complicating

small-bowel obstruction. *Radiology* 2014; **270**: 159-167 [PMID: 24029649 DOI: 10.1148/radiol.13122654]

34 **Lassandro F**, Romano S, Ragozzino A, Rossi G, Valente T, Ferrara I, Romano L, Grassi R. Role of helical CT in diagnosis of gallstone ileus and related conditions. *AJR Am J Roentgenol* 2005; **185**: 1159-1165 [PMID: 16247126]

35 **Kim Y**, Park BJ, Kim MJ, Sung DJ, Kim DS, Yu YD, Lee JH. Biliary phytobezoar resulting in intestinal obstruction. *World J Gastroenterol* 2013; **19**: 133-136 [PMID: 23326176 DOI: 10.3748/wjg.v19.i1.133]

36 **Kim TO**, Lee SH, Kim GH, Heo J, Kang DH, Song GA, Lee JW, Cho M. Common bile duct stone caused by a phytobezoar. *Gastrointest Endosc* 2006; **63**: 324; discussion 324 [PMID: 16427945]

P- Reviewer: Kasano Y, Ugezu C, Munjal K
S- Editor: Yu J **L- Editor**: Wang TQ **E- Editor**: Liu XM

World Journal of Gastroenterology

Submit a Manuscript: http://www.wjgnet.com/esps/
Help Desk: http://www.wjgnet.com/esps/helpdesk.aspx
DOI: 10.3748/wjg.v21.i33.9785

World J Gastroenterol 2015 September 7; 21(33): 9785-9792
ISSN 1007-9327 (print) ISSN 2219-2840 (online)

ORIGINAL ARTICLE

Prospective Study

Diffusion-weighted magnetic resonance imaging without bowel preparation for detection of ulcerative colitis

Li-Li Yu, Hai-Shan Yang, Bu-Tian Zhang, Zhong-Wen Lv, Fu-Rong Wang, Chun-Yu Zhang, Wei-Bo Chen, Hui-Mao Zhang

Li-Li Yu, Hai-Shan Yang, Bu-Tian Zhang, Zhong-Wen Lv, Fu-Rong Wang, Chun-Yu Zhang, Department of Radiology, The China-Japan Union Hospital of Jilin University, Changchun 130021, Jilin Province, China

Wei-Bo Chen, Philips Healthcare, Shanghai 200070, China

Hui-Mao Zhang, Department of Radiology, The First Hospital of Jilin University, Changchun 130021, Jilin Province, China

Author contributions: Yu LL conceived of the study, participated in design and coordination, acquisition of data, analysis and interpretation of data, and helped to draft the manuscript; Yang HS and Zhang HM conceived of the study and reviewed radiological images; Zhang BT performed the statistical analysis; Zhang CY communicated with patients and endoscopists; Lv ZW and Wang FR participated in the MR scan; Chen WB participated in the design of MR imaging protocol.

Informed consent statement: All study participants, or their legal guardian, provided informed written consent prior to study enrollment.

Conflict-of-interest statement: The authors declare that there are no conflicts of interest to disclose.

Data sharing statement: No additional data are available.

Correspondence to: Hui-Mao Zhang, MD, PhD, Department of Radiology, The First Hospital of Jilin University, No. 71 Xinmin Street, Changchun 130021, Jilin Province, China. yulili999@163.com
Telephone: +86-431-84995143
Fax: +86-431-88783300

Received: November 30, 2014
Peer-review started: November 30, 2014
First decision: January 8, 2015
Revised: February 6, 2015
Accepted: March 31, 2015
Article in press: March 31, 2015
Published online: September 7, 2015

Abstract

AIM: To evaluate the accuracy of diffusion-weighted imaging (DWI) without bowel preparation, the optimal *b* value and the changes in apparent diffusion coefficient (ADC) in detecting ulcerative colitis (UC).

METHODS: A total of 20 patients who underwent 3T magnetic resonance imaging (MRI) without bowel preparation and colonoscopy within 24 h were recruited. Biochemical indexes, including C-reactive protein (CRP), erythrocyte sedimentation rate, hemoglobin, leucocytes, platelets, serum iron and albumin, were determined. Biochemical examinations were then performed within 24 h before or after MR colonography was conducted. DWI was performed at various *b* values (*b* = 0, 400, 600, 800, and 1000 s/mm^2). Two radiologists independently and blindly reviewed conventional- and contrast-enhanced MR images, DWI and ADC maps; these radiologists also determined ADC in each intestinal segment (rectum, sigmoid, left colon, transverse colon, and right colon). Receiver operating characteristic (ROC) analysis was performed to assess the diagnostic performance of DWI hyperintensity from various *b* factors, ADC values and different radiological signs to detect endoscopic inflammation in the corresponding bowel segment. Optimal ADC threshold was estimated by maximizing the combination of sensitivity and specificity. MR

findings were correlated with endoscopic results and clinical markers; these findings were then estimated by ROC analysis.

RESULTS: A total of 100 segments (71 with endoscopic colonic inflammation; 29 normal) were included. The proposed total magnetic resonance score (MR-score-T) was correlated with the total modified Baron score (Baron-T; r = 0.875, P < 0.0001); the segmental MR score (MR-score-S) was correlated with the segmental modified Baron score (Baron-S; r = 0.761, P < 0.0001). MR-score-T was correlated with clinical and biological markers of disease activity (r = 0.445 to 0.831, P < 0.05). MR-score-S > 1 corresponded to endoscopic colonic inflammation with a sensitivity of 85.9%, a specificity of 82.8% and an area under the curve (AUC) of 0.929 (P < 0.0001). The accuracy of DWI hyperintensity was significantly greater at b = 800 than at b = 400, 600, or 1000 s/mm^2 (P < 0.05) when endoscopic colonic inflammation was detected. DWI hyperintensity at b = 800 s/mm^2 indicated endoscopic colonic inflammation with a sensitivity of 93.0%, a specificity of 79.3% and an AUC of 0.867 (P < 0.0001). Quantitative analysis results revealed that ADC values at b = 800 s/mm^2 differed significantly between endoscopic inflamed segment and normal intestinal segment (1.56 ± 0.58 mm^2/s *vs* 2.63 ± 0.46 mm^2/s, P < 0.001). The AUC of ADC values was 0.932 (95% confidence interval: 0.881-0.983) when endoscopic inflammation was detected. The threshold ADC value of 2.18 × 10^{-3} mm^2/s indicated that endoscopic inflammation differed from normal intestinal segment with a sensitivity of 89.7% and a specificity of 80.3%.

CONCLUSION: DWI combined with conventional MRI without bowel preparation provides a quantitative strategy to differentiate actively inflamed intestinal segments from the normal mucosa to detect UC.

Key words: Diffusion-weighted imaging; Apparent diffusion coefficient; Quantitative; Ulcerative colitis; Without bowel preparation

Core tip: Our results indicated that diffusion-weighted imaging (DWI) provides qualitative and quantitative information when this technique is combined with conventional magnetic resonance imaging without bowel preparation; the combined technique demonstrates a good diagnostic performance to detect colonic inflammation in ulcerative colitis. This technique is completely non-invasive, does not apply ionizing radiation or contrast material injection, does not require any bowel preparation and does not cause discomfort to patients. The optimal b value is 800 s/mm^2. DWI hyperintensity at b = 800 s/mm^2 detected endoscopic colonic inflammation with a sensitivity of 93.0% and a specificity of 79.3%.

Yu LL, Yang HS, Zhang BT, Lv ZW, Wang FR, Zhang CY, Chen WB, Zhang HM. Diffusion-weighted magnetic resonance imaging without bowel preparation for detection of ulcerative colitis. *World J Gastroenterol* 2015; 21(33): 9785-9792 Available from: URL: http://www.wjgnet.com/1007-9327/full/v21/i33/9785.htm DOI: http://dx.doi.org/10.3748/wjg.v21.i33.9785

INTRODUCTION

Magnetic resonance imaging (MRI) is an excellent technique to accurately detect colorectal cancer[1-3]. MRI has been applied in the diagnosis and follow-up of patients with inflammatory bowel disease[3-15]. For such examinations and certainly for endoscopy, bowel cleansing preparations are required and are often poorly tolerated by patients[16]. Consequently, the use of MRI in clinical practice may be limited.

Only a few studies have reported the use of diffusion-weighted imaging (DWI) in patients with ulcerative colitis (UC)[3,6,10-14,17]. Among these studies, only one[14] reported the value of quantitative DWI to assess inflammatory activity in UC. However, optimal b value of colon DWI to detect colonic inflammation in patients with UC has not yet been published. As such, optimal b value should be determined to produce high-quality apparent diffusion coefficient (ADC) maps that affect the accuracy of ADC measurements and visual imaging interpretations[18].

This study aimed to determine the optimal b value of colon DWI to detect colonic inflammation in patients with UC without bowel preparation at 3T, to evaluate the accuracy of DWI combined with MRI, and to investigate the changes in ADC of patients with UC.

MATERIALS AND METHODS

Patients

This prospective observational study was conducted with an approval from our institutional review board. Informed consent was also obtained from all of the patients. A total of 23 patients with known or suspected UC underwent magnetic resonance colonography, including DWI without bowel preparation followed by colonoscopy within 24 h, between January 17, 2012 and February 15, 2013. Patients who were diagnosed with UC by colonoscopy were enrolled in the study. These patients did not undergo interval treatment for UC between MRI and colonoscopy. Furthermore, patients were excluded if they were intolerant to colonoscopy or if they suffered from a toxic megacolon, revealed a history of abdominal surgery or experienced other systemic diseases.

Clinical and biological markers

The UC clinical score consisted of a modification of the four-category scoring system of the Mayo Clinic[19-22] (Mayo index), namely, rectal bleeding, stool

frequency, functional assessment by a patient and global assessment by a physician. Scores ranged from 0 (normal) to 3 (severe disease). Composite scores ranged from 0 (inactive disease) to 12 (severe disease activity). Biochemical indexes, including C-reactive protein (CRP), erythrocyte sedimentation rate (ESR), hemoglobin, leucocytes, platelets, serum iron and albumin, were obtained. Biochemical examinations were then performed within 24 h before or after MR colonography was conducted.

MRI protocol

MRI examinations were performed using a 3.0 T Philips scanner (Achieva 3.0T, YX, Best, Holland). The following sequences were obtained using an eight-channel, phased-array body coil: (1) axial and coronal balanced turbo field echo with and without fat suppression [repetition time (TR), 3.4 ms; echo time (TE), 1.4 ms; matrix, 224 × 224; flip angle, 45°; slice thickness, 6 mm; gap, 0 mm]; (2) axial and coronal T2-weighted single-shot fast spin echo with and without fat suppression (TR, 2000 ms; TE, 40 ms; matrix, 256 × 256; slice thickness, 6 mm; gap, 0 mm); (3) a 3D fast field echo (FFE) T1 sequence after intravenous administration of 0.2 mL/kg body weight of gadopentetatedimeglumine (Magnevist, Bayer, Germany) at a rate of 2 mL/s for a dynamic study of the axial plane with an arterial phase (25 s after injection) and a portal phase (70 s after injection) and a 2D FFE with fat saturation at 3 min after injection in axial and coronal planes; and (4) axial and/or coronal diffusion-weighted images (b = 0, 400, 600, 800 and 1000 s/mm^2; TR, 2357 ms; TE, 62 ms; matrix, 300 × 231; slice thickness, 5 mm; gap, 0 mm; number of signals acquired, the field of view ranged between 32 and 40 cm. Acquisition time for the DWI sequences covering the abdomen and the pelvis ranged from 3 min to 5 min.

MRI analysis

DWI was examined at b = 0, 400, 600, 800 and 1000 s/mm^2. Two experienced radiologists who were blinded to clinical and endoscopic examination results independently reviewed DWI images and evaluated the radiological signs of DWI hyperintensity. The presence and absence of DWI hyperintensity in a specific segment were rated '1' and '0', respectively. ADC maps were generated from the b factor (0 and 800 s/mm^2). To obtain ADC, we magnified the images and placed the oval regions of interest on the largest possible area covering the bowel wall. The measurements were conducted from the area of brightest signal in the bowel wall on the DWI image. The mean of the two ADCs was accepted as ADC of the segment. Based on a comprehensive review of the literature, seven radiological signs were evaluated: (1) DWI hyperintensity (b = 800 s/mm^2); (2) rapid gadolinium enhancement after intravenous contrast medium administration (20 s to 25 s after gadolinium infusion); (3) differentiation between the mucosa-submucosa complex and the muscularis; (4) bowel wall thickening (exceeding 5 mm); (5) parietal oedema; (6) the presence of ulceration(s); and (7) comb sign of engorged vasa recta that perpendicularly penetrated the bowel wall (18). These radiological signs were evaluated for each bowel segment as follows: 0 = absence and 1 = presence. The segmental MR-score (MR-score-S) was defined as the sum of the scores of the seven radiological signs for a specific segment. The total MR-score (MR-score-T) was defined as the sum of the MR-score-S for a patient, with values ranging from 0 to 35. MR-scores were independently established by two experienced radiologists who were blinded to the endoscopic data.

Colonoscopy

Colonoscopy is considered the "gold standard" to detect colonic inflammation in UC. Oral ingestion of 2000 mL to 3000 mL of polyethylene glycol electrolyte solution (Heshuang, China) was used to perform bowel preparation before colonoscopy was conducted. Colonoscopies were performed by two experienced endoscopists who had no prior knowledge of the MRI analysis results. The modified Baron score[19] represents an endoscopic lesion classification. This score ranges from 0 to 4, with 0 for normal mucosa, 1 for granular mucosa with an abnormal vascular pattern, 2 for friable mucosa, 3 for micro-ulceration with spontaneous bleeding, and 4 for gross ulceration. The colon was divided into five sections: rectum, sigmoid, left colon, transverse colon and right colon. A segmental modified Baron score (Baron-S) represents the score of each section. The total modified Baron Score (Baron-T) was defined as the sum of the segmental scores. The result was considered "positive" if Baron-S $\geqslant$ 1 and "negative" if Baron-S < 1.

Statistical analysis

Patients who underwent colonoscopy and were diagnosed with UC were recruited into the analysis. Data were performed with SPSS Statistics version 19.0 and MedCalc version 12.4. All reported P-values were two-sided and P < 0.05 was considered statistically significant.

Receiver operating characteristic (ROC) analysis was performed to assess the diagnostic performance of DWI hyperintensity from various b factors, ADC, MR-score-S and seven radiological signs to detect endoscopic inflammation in the corresponding bowel segment. Analysis was performed to calculate sensitivity, specificity and area under the ROC curve (AUROC) with the associated P-value. The Delong mode was used to compare AUROC. Youden index analysis was performed to estimate the optimal ADC threshold value by maximizing the combination of sensitivity and specificity.

Table 1 Accuracy of diffusion-weighted imaging hyperintensity from different *b* values for detecting endoscopic inflammation

	AUROC	Sens.	Spec.	*P* value
b = 400 s/mm^2	0.631	69.0	48.3	0.0410
b = 600 s/mm^2	0.732	81.7	62.1	0.0001
b = 800 s/mm^2	0.867	93.0	79.3	0.0001
b = 1000 s/mm^2	0.721	64.8	79.3	0.0010

AUROC: Area under the receiver operating characteristic curve; Sens.: Sensitivity; Spec: Specificity.

Correlative analysis was performed with Spearman's correlation coefficients as follows: (1) MR-score-S *vs* Baron-S; (2) MR-score-T *vs* Baron-T; (3) MR-score-T *vs* clinical and biological markers; and (4) Baron-T *vs* clinical and biological markers. The correlation coefficient of the MR-score was compared with that of the endoscopic scores.

The inter-observer agreement for ADC measurements was performed by two radiologists and calculated with Pearson's correlation coefficient. Inter-observer agreements between two independent radiologists for the DWI hyperintensity and MR-score were evaluated by kappa statistic.

RESULTS

Among the 23 patients with known or suspected UC, 1 failed to complete a full colonoscopy examination, and 2 were finally diagnosed with Crohn's disease. Thus, a total of 20 patients were finally recruited in the study.

Accuracy of DWI hyperintensity from various b values to detect endoscopic inflammation

Table 1 presents the sensitivity, specificity and AUROC of DWI hyperintensity at *b* = 400, 600, 800 and 1000 s/mm^2. The DWI hyperintensity at *b* = 800 s/mm^2 detected endoscopic inflammation with a sensitivity of 93.0%, a specificity of 79.3%, and an AUROC of 0.867 ($P < 0.0001$). The accuracy was significantly greater at *b* = 800 s/mm^2 than at *b* = 400, 600 or 1000 s/mm^2 ($P < 0.05$; Figure 1). No significant differences in accuracy were found for *b* = 400, 600 and 1000 s/mm^2 ($P > 0.05$).

Quantitative analysis results revealed that the mean ADC at *b* = 800 s/mm^2 of the proven endoscopic mucosal inflammation was 1.56 ± 0.58 × 10^{-3} mm^2/s (range, 0.46 × 10^{-3} mm^2/s to 2.50 × 10^{-3} mm^2/s) compared with 2.63 ± 0.46 × 10^{-3} mm^2/s (range, 1.44 × 10^{-3} mm^2/s to 4.03 × 10^{-3} mm^2/s) in normal bowel segments ($P < 0.0001$). The AUROC was 0.932 (95% confidence interval, 0.881 to 0.983). A threshold ADC value of 2.18 × 10^{-3} mm^2/s could differentiate inflamed bowel from normal bowel segments with a sensitivity of 89.7% and a specificity of 80.3%.

Correlation between MRI and endoscopic findings

MR-score-T was correlated with Baron-T ($r = 0.875$, $P < 0.0001$; Figure 2) and MR-score-S was correlated with Baron-S ($r = 0.761$, $P < 0.0001$).

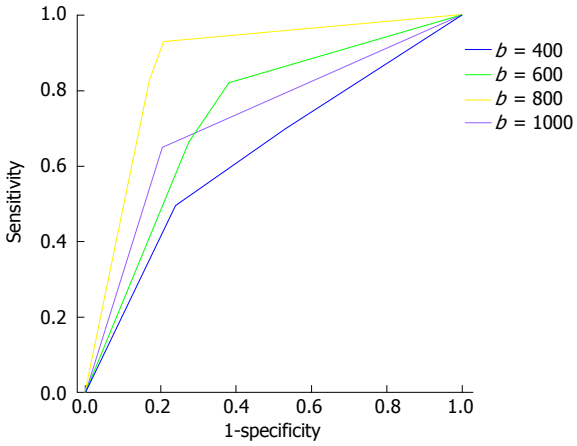

Figure 1 Accuracy of diffusion-weighted imaging hyperintensity from various *b* values to detect endoscopic inflammation.

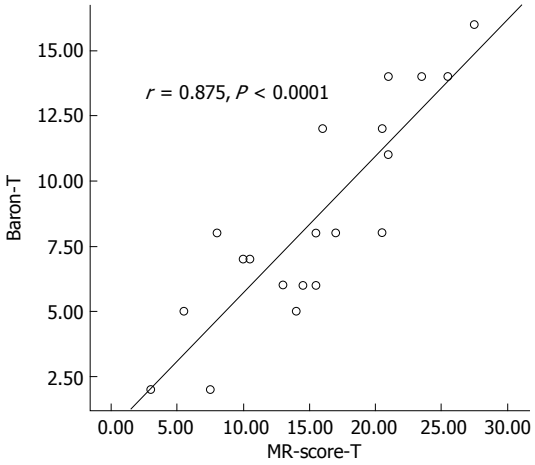

Figure 2 Correlation between total magnetic resonance score and total modified Baron score.

Diagnostic performance of MR-score-S and seven signs to detect endoscopic inflammation

Table 2 and Figure 3 present the sensitivity, specificity, AUROC and ROC of MR-score-S and the seven signs indicating endoscopic inflammation. Figure 4 shows a concrete and representative case. At MR-score-S > 1, endoscopic colonic inflammation could be detected with a sensitivity of 85.9%, a specificity of 82.8% and an AUROC of 0.929 ($P < 0.0001$). The DWI hyperintensity demonstrated a sensitivity of 93.0% and a specificity of 79.3% to detect endoscopic inflammation with an AUROC of 0.867 ($P < 0.0001$). With rapid gadolinium enhancement, endoscopic colonic inflammation was detected with a sensitivity of 73.2%, a specificity of 93.1% and an AUROC of 0.853 ($P < 0.0001$). The accuracy between DWI hyperintensity and rapid gadolinium enhancement ($P = 0.78$) was not significantly different. Differentiation between the mucosa-sub mucosa complex and the

Table 2 Accuracy of the MR-score-S and seven signs for detecting endoscopic inflammation

ROC analysis	AUROC	Sens.	Spec.	*P* value
MR-score-S > 1[1]	0.929	85.9	82.8	0.0001
DWI hyperintensity	0.867	93.0	79.3	0.0001
Rapid gadolinium enhancement after intravenous contrast medium administration	0.853	73.2	93.1	0.0001
Bowel wall thickening	0.793	66.2	89.7	0.0001
Differentiation between the mucosa-submucosa complex and the muscularis	0.842	80.3	86.2	0.0001
Parietal edema	0.684	43.7	89.7	0.0040
Ulceration	0.775	59.2	93.1	0.0001
Comb sign	0.694	43.7	93.1	0.0020

[1]Cut-offs defined by ROC analysis. AUROC: Area under the receiver operating characteristic curve; Sens.: Sensitivity; Spec: Specificity; DWI: Diffusion-weighted imaging.

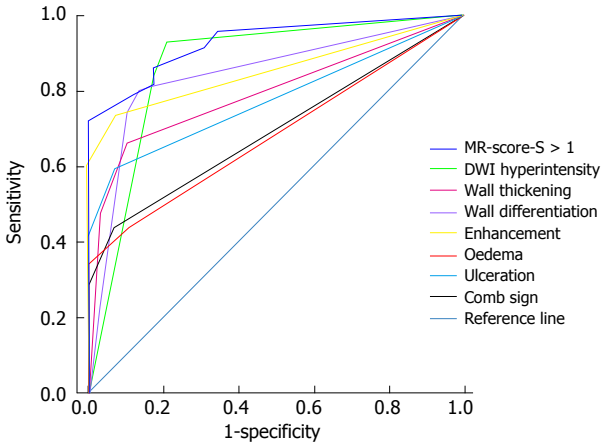

Figure 3 Accuracy of segmental magnetic resonance score and seven signs indicating endoscopic inflammation.

muscles revealed a good sensitivity (80.3%) and specificity (86.2%). The four other signs demonstrated low sensitivities (range: 43.7% to 66.2%) and excellent specificities (range: 89.7% to 93.1%). The presence of oedemas resulted in a decreased accuracy compared with the accuracy of the seven signs indicating endoscopic inflammation. No significant differences in accuracy were observed among other signs.

Correlation of MR-score-T or Baron-T with clinical and biological markers

MR-score-T was correlated with Mayo index (r = 0.831, P < 0.0001). Biological indexes included CRP, ESR, hemoglobin, leucocytes, platelets, serum iron and albumin (r = 0.445 to 0.748, P < 0.05). The correlation coefficients between MR-score-T and clinical and biological markers were similar to the corresponding correlation coefficients between Baron-T and the same disease activity markers (Table 3).

Inter-observer agreement

Inter-observer agreements in DWI hyperintensity from various *b* values were consistent with kappa values ranging from 0.719 to 0.825. The inter-observer agreements were applicable to evaluate MR-score with kappa values ranging from 0.679 to 0.897. The two radiologists' ADC measurements were compared and Pearson's correlation coefficient was 0.886 (P < 0.001), thereby indicating an excellent inter-observer agreement.

DISCUSSION

The selection of the *b* value should satisfy the following three criteria[23]: (1) clearly display and identify the tissue being examined; (2) effectively inhibit the T2 shine-through effect on DWI; and (3) use *b* values as high as possible to determine ADC of the tissue being examined for closer to the true diffusion value. A small *b* value corresponded to high signal-to-noise ratio (SNR) and contrast-to-noise ratio (CNR) of DWI images. However, the influence was more distinct on ADC with the T2 shine-through effect, perfusion effects and presence of macroscopic motion. Conversely, a large *b* value indicated that ADC was closer to the real diffusion values of the tissue. However, susceptibility artefacts and geometric deformation of images likely decreased significantly the SNR and the CNR of images. Therefore, the selection of the *b* value should weigh the two aspects of the real diffusion values of tissue and image quality. Oto *et al*[9] evaluated the value of DWI (b = 600 s/mm^2) and investigated changes in ADC values in inflamed bowels in patients with Crohn's disease at 1.5 T. Oussalah *et al*[6] also found that the *b* factor is fixed at 600 s/mm^2 with a 1.5 T scanner in UC and Crohn's disease. Kılıçkesmez *et al*[14] evaluated 28 patients with UC by DW-MRI with b = 0, 500 and 1000 s/mm^2 on a 1.5 T scanner. The current study defined the range of the *b* value from 0 and 400 s/mm^2 to 1000 s/mm^2 by referring to previous studies. In the current study, DWI hyperintensity at b = 800 s/mm^2 demonstrated the most efficient diagnostic performance to detect colonic inflammation in UC. The difference in the *b* value between the results of the current study and that described in a previous study may be related to differences in field strength and uniformity of the main magnetic field.

Oto *et al*[9] found statistically significant differences

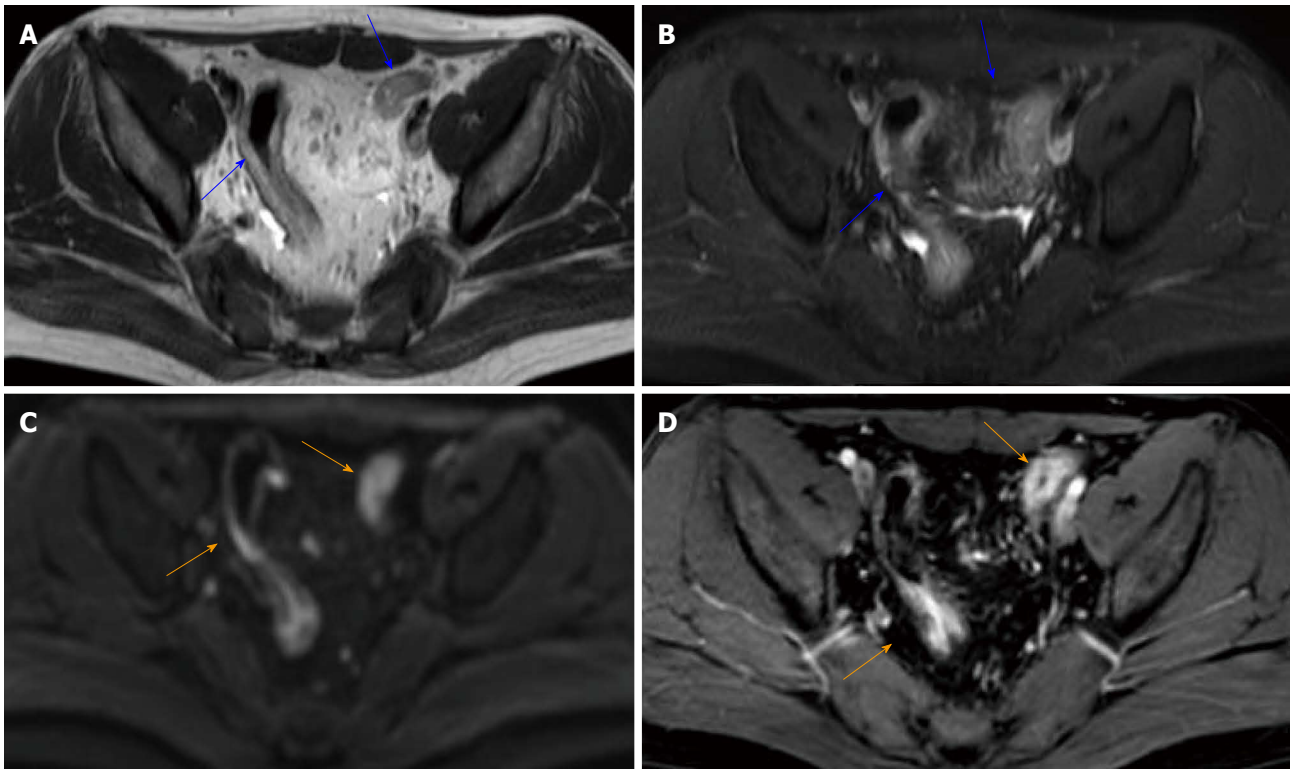

Figure 4 A 22-year-old woman with known ulcerative colitis involving the rectum and the sigmoid colon. Mayo index = 8; total modified Baron score = 12; total MR-score = 22; T2WI without fat saturation (A) and T2WI with fat saturation (B) show a mild thickening of the sigmoid colon wall (blue arrows); DWI hyperintensity (C; *b* = 800 s/mm^2; orange arrows); rapid gadolinium enhancement (D; orange arrows).

Table 3 Correlation of MR-score-T or Baron-T with clinical and biological markers

Activity markers	MR-score-T		Baron-T		MR-score-T *vs* Baron-T
	r	*P* value[1]	*r*	*P* value[1]	*P* value[2]
Mayo index	0.831	0.0001	0.926	0.0001	0.20
CRP	0.656	0.0020	0.886	0.0001	0.07
ESR	0.748	0.0001	0.810	0.0001	0.64
Hemoglobin	-0.449	0.0470	-0.580	0.0070	0.60
Leukocytes	0.481	0.0320	0.506	0.0230	0.92
Platelets	0.445	0.0490	0.534	0.0150	0.73
Serum iron	-0.497	0.0260	-0.559	0.0100	0.80
Albumin	-0.462	0.0400	-0.507	0.0220	0.86

[1]Spearman's rank correlation test; [2]Comparison of correlation coefficients.

between the ADC values of inflamed and normal bowel segments of patients with Crohn's disease (0.47 × 10^{-3} mm²/s to 2.60 × 10^{-3} mm²/s and 1.39 × 10^{-3} mm²/s to 4.03 × 10^{-3} mm²/s for inflamed and normal segments, respectively; $P < 0.05$). Kiryu *et al*[7] also found that the ADC values of the small and large bowel of patients with active disease were lower than those in patients with inactive disease (1.61 ± 0.44 × 10^{-3} mm^2/s *vs* 2.56 ± 0.51 × 10^{-3} mm²/s for the small bowel and 1.52 ± 0.43 × 10^{-3} ± 10^{-3} mm²/s *vs* 2.31 ± 0.59 × 10^{-3} mm² /s for the large bowel; $P < 0.001$). Kılıçkesmez *et al*[14] found that the ADC values of the rectum are different ($P = 0.009$) between patients in active (1.08 ± 0.14 × 10^{-3} mm^2/s) and sub-acute phases (1.13 ± 0.23 × 10^{-3} mm^2/s) of the disease and those in remission (1.29 ± 0.17 × 10^{-3} mm^2/s). In the current study, the mean ADC value of proven endoscopic inflamed bowels was 1.56 ± 0.58 × 10^{-3} mm^2/s compared with 2.63 ± 0.46 × 10^{-3} mm^2/s in normal bowel segments ($P < 0.0001$). In these studies, radiologists should be aware of possible overlaps of ADC values that may lead to misdiagnoses when only DWI is interpreted[24]. The usefulness of ADC for long-term follow-up of patients with UC warrants further investigation.

DWI is a method in which the signal required to produce MR image is determined by the "mobility of water"[25]. Diffusivity measurements are characterized by multiple components related to tissue cellularity and organisation, integrity of cell membranes, extracellular space tortuosity and perfusion[26]. Endoscopic biopsy

is considered the gold standard to detect and quantify UC; invasiveness, patient discomfort, perforation risk and poor patient acceptance of colonoscopy have prompted researchers to investigate alternatives for diagnosing and characterizing UC. In MR or endoscopy examination, oral and rectal bowel cleansing preparations are often poorly tolerated by patients[27,28]. The technique used in the current study did not require oral or rectal preparation and fasting; the duration of the procedure was relatively short (approximately 20 min for the whole examination, including patient setup, routine MR and DWI imaging). In the current study, DWI hyperintensity exhibited the same accuracy as rapid gadolinium enhancement to detect endoscopic inflammation in UC; this result suggested that the DWI sequence could replace gadolinium injection in detecting inflammatory colonic segments in UC. In other studies, DWI hyperintensity also showed a high accuracy[6-8]. DWI combined with MRI without bowel preparation represents a feasible tool. This technique is completely non-invasive, does not apply ionizing radiation[29,30] or contrast material injection, does not require any bowel preparation, and does not cause discomfort to patients. Bowel preparation has also been associated with acute exacerbation of UC. Diagnostic methods that do not require bowel preparation could avoid this potential complication. Therefore, the proposed technique can be easily combined with conventional MR examination protocol because of short duration.

Our study showed several limitations, such as small patient population. With our most efficient efforts to magnify images and use oval regions of interest to exclusively cover the bowel wall, the possibility of a partial volume effect was minimised. However, it could not be completely excluded, especially from ADC measurements of the normal bowel wall.

In conclusion, DWI combined with conventional MRI without bowel preparation yielded qualitative and quantitative information; our result demonstrated a good diagnostic performance in detecting colonic inflammation in UC.

COMMENTS

Background

Magnetic resonance imaging (MRI) is an excellent technique to accurately detect colorectal cancer. MRI has been applied to diagnose and follow patients with inflammatory bowel disease. In such examinations and endoscopy, bowel cleansing preparations are required and often poorly tolerated by patients. This procedure may limit the use of MRI in clinical practice.

Research frontiers

Only a few studies have reported the use of diffusion-weighted imaging (DWI) in patients with ulcerative colitis (UC). Among these studies, only one reported the value of quantitative diffusion-weighted MRI in the assessment of the inflammatory activity in UC. The optimal *b* value of colon DWI to detect colonic inflammation in patients with UC has not been published.

Innovations and breakthroughs

This results indicated that DWI combined with conventional MRI without bowel preparation yielded qualitative and quantitative information; this study demonstrated good diagnostic performance to detect colonic inflammation in UC.

Applications

This technique is completely non-invasive, does not apply ionizing radiation or contrast material injection, does not require any bowel preparation, and does not cause discomfort to patients. Diagnostic methods that do not require bowel preparation could avoid acute exacerbation. This procedure can be easily added to conventional MR examination protocol because of short duration.

Terminology

The segmental MR-score (MR-score-S) is defined as the sum of the scores of different radiological signs for a specific segment. The total MR-score was defined as the sum of MR-score-S for a patient.

Peer-review

DWI combined with conventional MRI without bowel preparation provided a quantitative technique to differentiate actively inflamed intestinal segments from the normal mucosa to detect UC.

REFERENCES

1 **Solak A**, Genç B, Solak I, Kalaycıoğlu S, Sahin N, Yalaz S, Sivrikoz ON. The value of diffusion-weighted magnetic resonance imaging in the differential diagnosis in diffuse bowel wall thickening. *Turk J Gastroenterol* 2013; **24**: 154-160 [PMID: 23934463]

2 **Ichikawa T**, Erturk SM, Motosugi U, Sou H, Iino H, Araki T, Fujii H. High-B-value diffusion-weighted MRI in colorectal cancer. *AJR Am J Roentgenol* 2006; **187**: 181-184 [PMID: 16794174]

3 **Kilickesmez O**, Atilla S, Soylu A, Tasdelen N, Bayramoglu S, Cimilli T, Gurmen N. Diffusion-weighted imaging of the rectosigmoid colon: preliminary findings. *J Comput Assist Tomogr* 2009; **33**: 863-866 [PMID: 19940651 DOI: 10.1097/RCT.0b013e31819a60f]

4 **Koh DM**, Miao Y, Chinn RJ, Amin Z, Zeegen R, Westaby D, Healy JC. MR imaging evaluation of the activity of Crohn's disease. *AJR Am J Roentgenol* 2001; **177**: 1325-1332 [PMID: 11717076]

5 **Maccioni F**, Patak MA, Signore A, Laghi A. New frontiers of MRI in Crohn's disease: motility imaging, diffusion-weighted imaging, perfusion MRI, MR spectroscopy, molecular imaging, and hybrid imaging (PET/MRI). *Abdom Imaging* 2012; **37**: 974-982 [PMID: 22743838 DOI: 10.1007/s00261-012-9890-6]

6 **Oussalah A**, Laurent V, Bruot O, Bressenot A, Bigard MA, Régent D, Peyrin-Biroulet L. Diffusion-weighted magnetic resonance without bowel preparation for detecting colonic inflammation in inflammatory bowel disease. *Gut* 2010; **59**: 1056-1065 [PMID: 20525970 DOI: 10.1136/gut.2009.197665]

7 **Kiryu S**, Dodanuki K, Takao H, Watanabe M, Inoue Y, Takazoe M, Sahara R, Unuma K, Ohtomo K. Free-breathing diffusion-weighted imaging for the assessment of inflammatory activity in Crohn's disease. *J Magn Reson Imaging* 2009; **29**: 880-886 [PMID: 19306416 DOI: 10.1002/jmri.21725]

8 **Oto A**, Kayhan A, Williams JT, Fan X, Yun L, Arkani S, Rubin DT. Active Crohn's disease in the small bowel: evaluation by diffusion weighted imaging and quantitative dynamic contrast enhanced MR imaging. *J Magn Reson Imaging* 2011; **33**: 615-624 [PMID: 21563245 DOI: 10.1002/jmri.22435]

9 **Oto A**, Zhu F, Kulkarni K, Karczmar GS, Turner JR, Rubin D. Evaluation of diffusion-weighted MR imaging for detection of bowel inflammation in patients with Crohn's disease. *Acad Radiol* 2009; **16**: 597-603 [PMID: 19282206 DOI: 10.1016/j.acra.2008.11.009]

10 **Langhorst J**, Kühle CA, Ajaj W, Nüfer M, Barkhausen J, Michalsen A, Dobos GJ, Lauenstein TC. MR colonography without bowel purgation for the assessment of inflammatory bowel diseases: diagnostic accuracy and patient acceptance. *Inflamm Bowel Dis* 2007; **13**: 1001-1008 [PMID: 17352384]

11 **Gandolfi L**. Comparison of magnetic resonance imaging and

endoscopy in distinguishing the type and severity of inflammatory bowel disease. *Gastrointest Endosc* 1996; **43**: 86-87 [PMID: 9026433]
12 **Madsen SM**, Thomsen HS, Munkholm P, Dorph S, Schlichting P. Active Crohn's disease and ulcerative colitis evaluated by low-field magnetic resonance imaging. *Scand J Gastroenterol* 1998; **33**: 1193-1200 [PMID: 9867099]
13 **Rimola J**, Rodríguez S, García-Bosch O, Ricart E, Pagès M, Pellisé M, Ayuso C, Panés J. Role of 3.0-T MR colonography in the evaluation of inflammatory bowel disease. *Radiographics* 2009; **29**: 701-719 [PMID: 19448111 DOI: 10.1148/rg.293085115]
14 **Kılıçkesmez O**, Soylu A, Yaşar N, Demirbaş T, Dolapçıoğlu C, Poturoğlu S, Sevindir I, Cimilli T. Is quantitative diffusion-weighted MRI a reliable method in the assessment of the inflammatory activity in ulcerative colitis? *Diagn Interv Radiol* 2010; **16**: 293-298 [PMID: 20698008 DOI: 10.4261/1305-3825.DIR.2989-09.1]
15 **Mentzel HJ**, Reinsch S, Kurzai M, Stenzel M. Magnetic resonance imaging in children and adolescents with chronic inflammatory bowel disease. *World J Gastroenterol* 2014; **20**: 1180-1191 [PMID: 24574794 DOI: 10.3748/wjg.v20.i5.1180]
16 **Achiam MP**, Løgager V, Chabanova E, Thomsen HS, Rosenberg J. Patient acceptance of MR colonography with improved fecal tagging versus conventional colonoscopy. *Eur J Radiol* 2010; **73**: 143-147 [PMID: 19041207 DOI: 10.1016/j.ejrad.2008.10.003]
17 **Aoyagi T**, Shuto K, Okazumi S, Miyauchi H, Kazama T, Matsubara H. Evaluation of ulcerative colitis using diffusion-weighted imaging. *Hepatogastroenterology* 2010; **57**: 468-471 [PMID: 20698210]
18 **Saritas EU**, Lee JH, Nishimura DG. SNR dependence of optimal parameters for apparent diffusion coefficient measurements. *IEEE Trans Med Imaging* 2011; **30**: 424-437 [PMID: 20934948 DOI: 10.1109/TMI.2010.2084583]
19 **Feagan BG**, Greenberg GR, Wild G, Fedorak RN, Paré P, McDonald JW, Dubé R, Cohen A, Steinhart AH, Landau S, Aguzzi RA, Fox IH, Vandervoort MK. Treatment of ulcerative colitis with a humanized antibody to the alpha4beta7 integrin. *N Engl J Med* 2005; **352**: 2499-2507 [PMID: 15958805]
20 **Bewtra M**. An optimized patient-reported ulcerative colitis disease activity measure derived from the Mayo Score and the Simple Clinical Colitis Activity Index. *Inflamm Bowel Dis* 2015; **21**: E1 [PMID: 25479459 DOI: 10.1097/MIB.0000000000000256]
21 **Walmsley RS**. Comment on an optimized patient-reported ulcerative colitis disease activity measure derived from the mayo score and the simple clinical colitis activity index. *Inflamm Bowel Dis* 2014; **20**: E25-E26 [PMID: 25374290 DOI: 10.1097/MIB.0000000000000248]
22 **Bewtra M**, Brensinger CM, Tomov VT, Hoang TB, Sokach CE, Siegel CA, Lewis JD. An optimized patient-reported ulcerative colitis disease activity measure derived from the Mayo score and the simple clinical colitis activity index. *Inflamm Bowel Dis* 2014; **20**: 1070-1078 [PMID: 24810138 DOI: 10.1097/MIB.0000000000000053]
23 **Li W**, Li D, Liu H, Zhou R, Feng C, Ma Y, Yu T. [3.0T MR diffusion-weighted imaging: evaluating diagnosis potency of pulmonary solid benign lesions and malignant tumors and optimizing b value]. *Zhongguo Fei Ai Za Zhi* 2011; **14**: 853-857 [PMID: 22104219 DOI: 10.3779/j.issn.1009-3419.2011.11.04]
24 **Erden A**. Are we expecting too much from the diffusion-weighted MRI? *Turk J Gastroenterol* 2013; **24**: 85-87 [PMID: 23934452]
25 **Laurent V**, Trausch G, Bruot O, Olivier P, Felblinger J, Régent D. Comparative study of two whole-body imaging techniques in the case of melanoma metastases: advantages of multi-contrast MRI examination including a diffusion-weighted sequence in comparison with PET-CT. *Eur J Radiol* 2010; **75**: 376-383 [PMID: 19497694 DOI: 10.1016/j.ejrad.2009.04.059]
26 **Qayyum A**. Diffusion-weighted imaging in the abdomen and pelvis: concepts and applications. *Radiographics* 2009; **29**: 1797-1810 [PMID: 19959522 DOI: 10.1148/rg.296095521]
27 **Belsey J**, Epstein O, Heresbach D. Systematic review: oral bowel preparation for colonoscopy. *Aliment Pharmacol Ther* 2007; **25**: 373-384 [PMID: 17269992]
28 **Florie J**, Birnie E, van Gelder RE, Jensch S, Haberkorn B, Bartelsman JF, van der Sluys Veer A, Snel P, van der Hulst VP, Bonsel GJ, Bossuyt PM, Stoker J. MR colonography with limited bowel preparation: patient acceptance compared with that of full-preparation colonoscopy. *Radiology* 2007; **245**: 150-159 [PMID: 17885188]
29 **Cakmakci E**, Erturk SM, Cakmakci S, Bayram A, Tokgoz S, Caliskan KC, Celebi I. Comparison of the results of computerized tomographic and diffusion-weighted magnetic resonance imaging techniques in inflammatory bowel diseases. *Quant Imaging Med Surg* 2013; **3**: 327-333 [PMID: 24404447 DOI: 10.3978/j.issn.2223-4292.2013.12.03]
30 **Peloquin JM**, Pardi DS, Sandborn WJ, Fletcher JG, McCollough CH, Schueler BA, Kofler JA, Enders FT, Achenbach SJ, Loftus EV. Diagnostic ionizing radiation exposure in a population-based cohort of patients with inflammatory bowel disease. *Am J Gastroenterol* 2008; **103**: 2015-2022 [PMID: 18564113 DOI: 10.1111/j.1572-0241.2008.01920.x]

P- Reviewer: Hayes MJ, Kim ES **S- Editor**: Yu J
L- Editor: Wang TQ **E- Editor**: Zhang DN

World Journal of Gastroenterology

Submit a Manuscript: http://www.wjgnet.com/esps/
Help Desk: http://www.wjgnet.com/esps/helpdesk.aspx
DOI: 10.3748/wjg.v21.i33.9793

World J Gastroenterol 2015 September 7; 21(33): 9793-9802
ISSN 1007-9327 (print) ISSN 2219-2840 (online)

CASE REPORT

Cavernous hemangioma of adult pancreas: A case report and literature review

Utpal Mondal, Nichole Henkes, David Henkes, Laura Rosenkranz

Utpal Mondal, Laura Rosenkranz, Division of Gastroenterology and Nutrition, School of Medicine, University of Texas Health Science Center at San Antonio, San Antonio, TX 78229, United States

Nichole Henkes, David Henkes, Department of Pathology and Laboratory, CHRISTUS Santa Rosa Hospital, San Antonio, TX 78240, United States

Author contributions: Mondal U designed the paper, did the acquisition, analysis and interpretation of data, reviewed literature and wrote the paper; Henkes N did literature search and proof reading; Henkes D was responsible for cytopathology and pathology; and Rosenkranz L provided clinical care including endoscopy and made critical revision of the manuscript; all authors approved the final version.

Institutional review board statement: The case study was reviewed and approved by the Office of the Institutional Review Board of the UT Health Science Center San Antonio.

Informed consent statement: Patient provided informed written consent for this publication.

Conflict-of-interest statement: None of the authors has any disclosure to make.

Correspondence to: Utpal Mondal, MD, Division of Gastroenterology and Nutrition, School of Medicine, University of Texas Health Science Center at San Antonio, 7703 Floyd Curl Drive, San Antonio, TX 78229, United States. mondalu@uthscsa.edu
Telephone: +1-210-5674880
Fax: +1-210-5671976

Received: April 5, 2015
Peer-review started: April 7, 2015
First decision: April 23, 2015
Revised: May 29, 2015
Accepted: June 26, 2015
Article in press: June 26, 2015
Published online: September 7, 2015

Abstract

Pancreatic hemangioma is a rare type of benign vascular tumor. Low clinical suspicion and inability of current cross sectional imaging techniques to differentiate it from other pancreatic lesions, contribute to the difficulty in making the correct diagnosis. Without a definitive diagnosis, and due to concern for malignancy, in many instances, surgery is performed. We report a case of pancreas cavernous hemangioma in an 18-year-old female. The patient presented with three-month history of epigastric pain. Physical examination and routine blood tests were normal. Abdominal Computed Tomography scan revealed a 5 cm × 6 cm complex non-enhancing cystic mass in the head of pancreas. Magnetic resonance imaging, endoscopic ultrasonography (EUS) and EUS guided fine needle aspiration cytology were non-diagnostic. Because of uncontrolled symptoms, the patient underwent surgical resection. Histopathology and Immunohistochemical staining confirmed the diagnosis of cavernous hemangioma of pancreas.

Key words: Hemangioma; Endoscopic ultrasound; Endoscopic ultrasonography; Fine needle aspiration; Pancreas

Core tip: Pancreas hemangioma is a very rare pathological finding in adulthood. It may mimic other more

common pancreatic lesions. Diagnosis is difficult, due to its rarity, and the absence of typical radiological findings of hemangioma. It should be considered in the differential diagnosis of cystic, mixed and solid pancreatic lesions. Surgical resection is the effective treatment in symptomatic cases, while providing a final diagnosis, however, surgery may not be necessary at all.

Mondal U, Henkes N, Henkes D, Rosenkranz L. Cavernous hemangioma of adult pancreas: A case report and literature review. *World J Gastroenterol* 2015; 21(33): 9793-9802 Available from: URL: http://www.wjgnet.com/1007-9327/full/v21/i33/9793.htm DOI: http://dx.doi.org/10.3748/wjg.v21.i33.9793

INTRODUCTION

Pancreatic cavernous hemangioma in adulthood is a very rare condition. To date, only 20 cases have been reported in the literature. Hemangioma mimics common pancreatic lesions, and modern imaging may not adequately characterize this benign condition. The following case is that of an 18-year-old female who underwent surgical resection of a large head of pancreas lesion, with a final diagnosis of cavernous hemangioma. A review of clinicopathological and radiographic features of all cases reported in the English literature to date is included.

CASE REPORT

An 18-year-old Hispanic female was referred to our Institution by her primary care physician, for the evaluation of a "pancreatic cystic lesion" found on abdominal computed tomography (CT) scan, after she presented with complaints of worsening epigastric pain for three months. The pain was described as stabbing and severe, radiating to the back, occurring postprandial. Nausea and emesis were associated with pain. Analgesia was only partially achieved with the use of prescription oral narcotics.

The patient's medical history included childhood treated pulmonary tuberculosis. There was no history of acute pancreatitis or abdominal trauma. Patient had no prior surgeries. She was on no medications, particularly has never been prescribed oral contraceptives, nor did she ever use over the counter drugs. Family history was non-contributory. Physical examination was normal. Complete blood counts, complete metabolic panel, serum amylase and lipase, coagulation panel, fasting lipid profile, serum CA 19-9 and carcinoembryonic antigen (CEA) levels were normal.

CT revealed a well-defined cystic mass with solid components in the head of pancreas. The lesion did not show contrast enhancement (Figure 1). Magnetic resonance imaging (MRI) with and without intravenous gadolinium showed a 5.3 cm × 6.2 cm, heterogeneous,

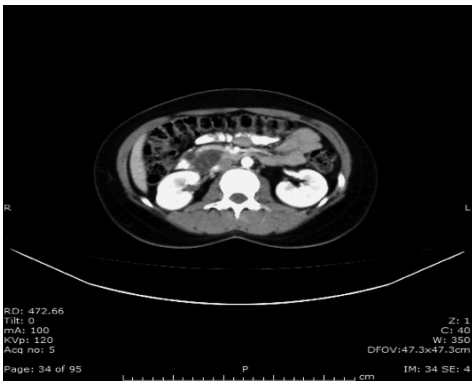

Figure 1 Contrast computed tomography scan showed a non-enhancing cystic lesion in the head of the pancreas.

multi-septated, predominantly cystic mass in the head and uncinate process of the pancreas, with variable T1 and T2 signal intensity (Figure 2). Foci of T1 hyperintensity were thought to be due to hemorrhagic or proteinaceous contents. The mass exhibited septal enhancement with maximum septal wall thickness of 2 mm. Post-contrast dynamic images showed peripheral hyperintensity with some indication of progressive centripetal enhancement. There was no ductal, vascular or nodal involvement. Magnetic resonance cholangiopancreatography (MRCP) demonstrated no ductal dilation (Figure 3).

Endoscopic ultrasonography (EUS) showed a well-circumscribed complex structure with fluid and solid components arising from the uncinate process and extending to the head of pancreas (Figure 4). The lesion was devoid of Doppler signal. The surrounding parenchyma appeared normal. There was no ductal or vascular involvement. No peri-pancreatic lymph nodes were seen. The liver, gall bladder, spleen, left adrenal and kidneys appeared normal. Fine needle aspiration (FNA) using a 22G ProCore Cook Needle (Cook Medical Inc., Winston-Salem, NC, United States) was performed, and a total of five passes with adequate sampling was obtained in the presence of a cytopathologist. No bleeding occurred during or after the procedure, and patient had an uneventful post-procedure recovery.

Microscopy of the direct smear from FNA showed abundant red blood cells and a few clusters of cells that had a cohesive nature, but no atypia (Figure 5). Some areas had increased lymphocytes, suggesting an inflammatory process. The cell block showed clusters of histiocytes, some of which had light brown material in their cytoplasm, suggestive of hemosiderin deposition. Focal fibrotic fragments of tissue were seen, without distinct vascular structures being identified. No granulomatous features were seen. Cyst fluid carcinoembryonic antigen (CEA) level was < 0.5 ng/mL, and amylase level was 13 U/L. Gram stain, acid-fast bacilli, and alpha 1 antitrypsin stains were negative. CAM 5.2 was negative. Vimentin was positive in macrophages, but no epithelioid cells were identified. Overall, the fine needle aspiration findings

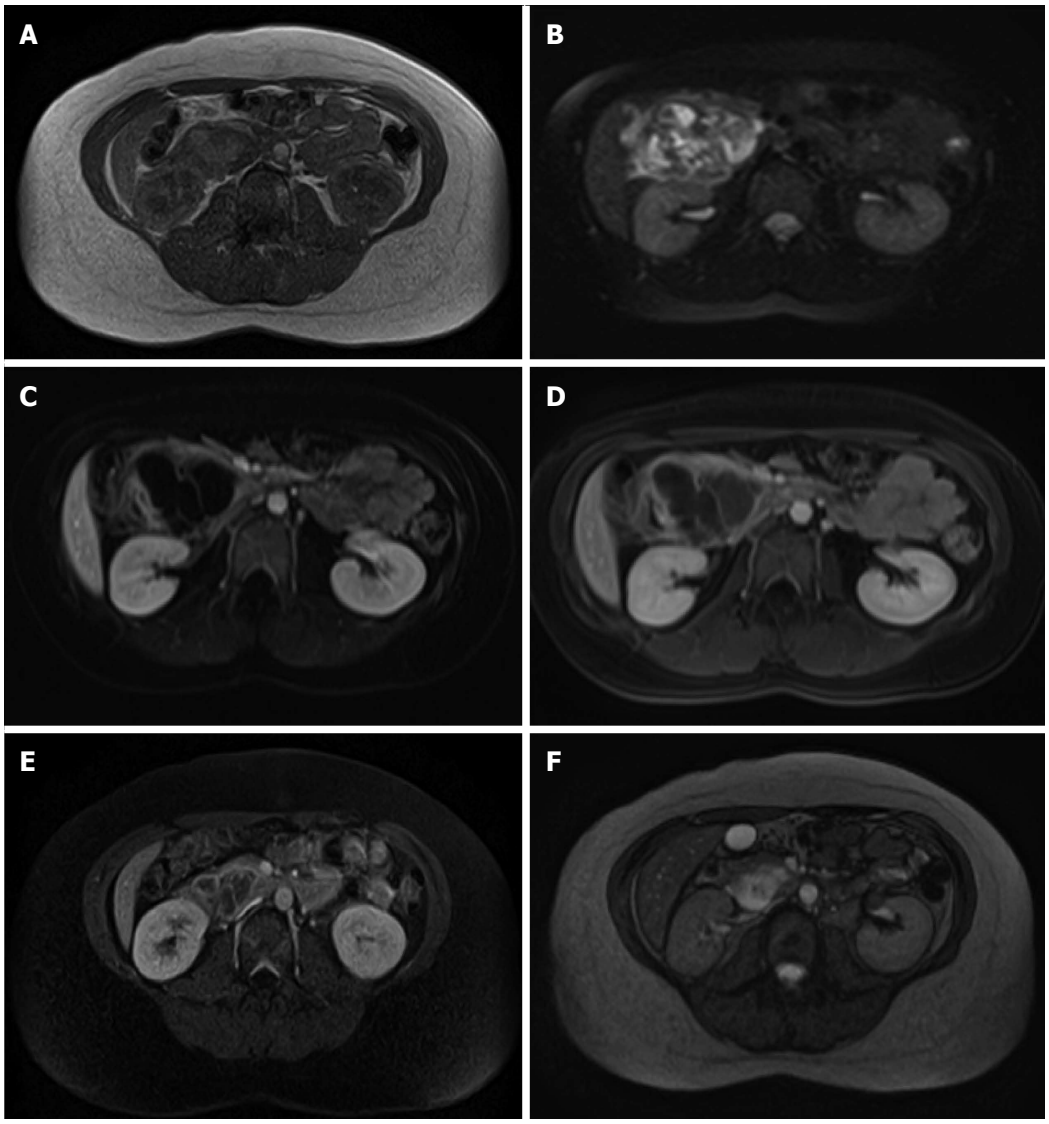

Figure 2 Magnetic resonance imaging. Variable intensity in T1 weighted (A) and T2 weighted (B) imaging. Overall, the hemangioma had hypo-intensity in T1W and hyper-intensity in T2W imaging. Peripheral enhancement after gadolinium injection with gradual centripetal filling-in (C, D: Arterial phase; E: Venous; and F: Delayed venous phase) was noticed. Intensity was parallel to that of aorta. A central cystic area remained hypo-intense.

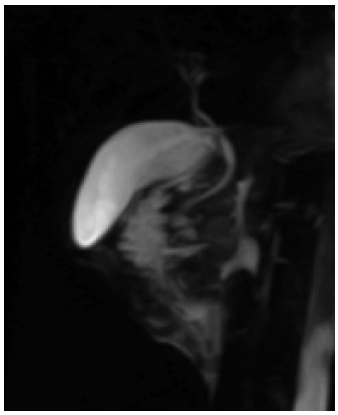

Figure 3 Magnetic resonance cholangiopancreatography demonstrated no ductal dilation.

Figure 4 Endoscopic ultrasound: Complex cyst at the head of pancreas, devoid of Doppler signals, with normal surrounding parenchyma and without any ductal or vascular abnormality.

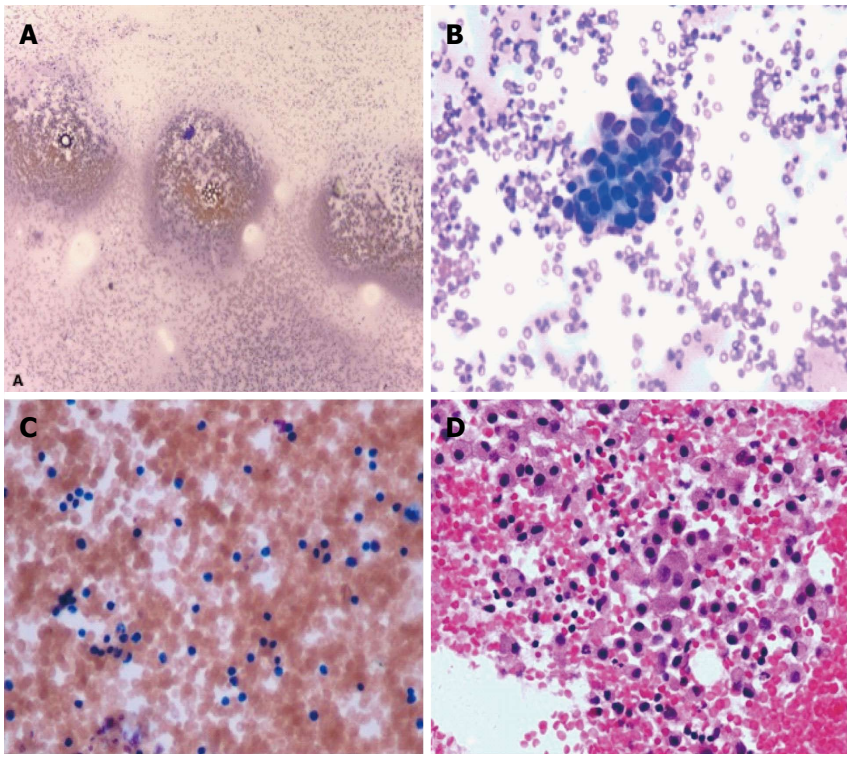

Figure 5 Fine needle aspiration cytology. Direct smear showed few clusters of cells without atypia (A, B) and increased lymphocytes (C); Cell block showed clusters of histiocytes, some of which had light brown material in their cytoplasm, suggestive of hemosiderin (D).

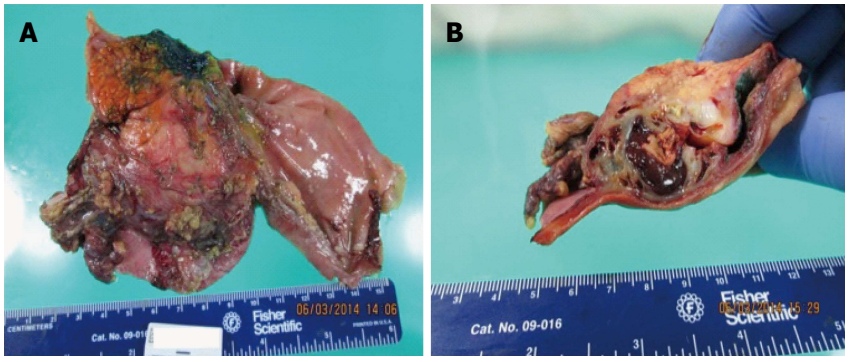

Figure 6 Gross pathology showing head of pancreas lesion (A) and cystic lesion with thick septa and recent hemorrhage evident on cross section (B).

suggested a benign process most consistent with an inflammatory benign cyst. Due to the presence of a few cohesive clusters of cells, a neoplastic cystic lesion (serous cystadenoma or solid cystic papillary tumor) could not entirely be ruled out.

The case was reviewed in the multidisciplinary Pancreatic Tumor Board. A recommendation was made to continue close clinical monitoring, and a consensus from pathologists, radiologists, gastroenterologists, and surgeons reiterated the benign etiology of the lesion. Over the next few weeks, the patient experienced worsening nausea, vomiting and abdominal pain, refractory to narcotics and antiemetics. Subsequently, the patient limited her oral intake and lost 20 pounds of body weight. The patient was eventually taken to surgery. Intra-operatively, the pancreatic lesion was found to be inseparable from the duodenum. Pylorus preserving pancreaticoduodenectomy with cholecystectomy and resection of 17 lymph nodes were performed.

The gross pathology revealed a pink-brown, partly hemorrhagic, multi-loculated cystic mass, 6 cm × 4 cm × 3.5 cm in size, with intracystic hemorrhage and no mucinous component (Figure 6). On microscopic examination (Figure 7), a single layer of flattened cells lined the blood filled cystic spaces, and had uniform nuclei and no atypia. The vessels lumina contained macrophages, some with hemosiderin within. Aggregates of chronic inflammatory cells were present in the surrounding fibrous tissue. One vessel had an organizing thrombus, also containing fibrin and foamy macrophages. On immunohistochemical

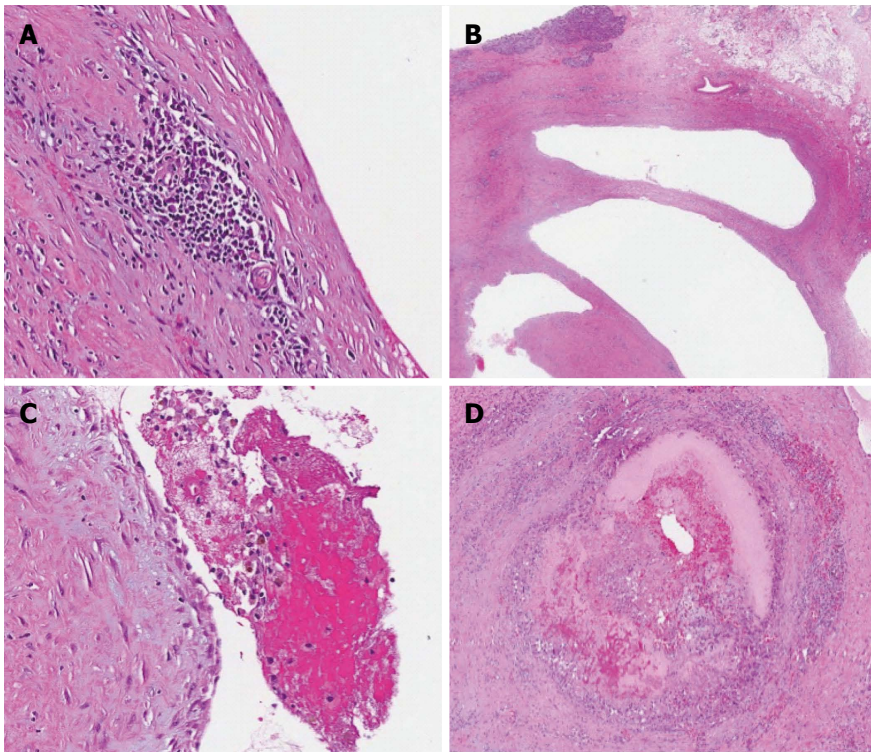

Figure 7 Histopathology. A: The hemangioma displaced the exocrine pancreas; B: It had blood filled ectatic vessels with thin endothelium lining large cavernous spaces and aggregates of chronic inflammatory cells in the surrounding fibrous tissue; C: The lumina of the vessels contained macrophages, some containing hemosiderin; D: One vessel with organizing thrombus containing fibrin and foamy macrophages.

(IHC) staining, the lining was positive for CD31, focally positive for CD34, and negative for cytokeratin (AE1/AE3) supporting the diagnosis of hemangioma. All 17 lymph nodes had normal histology.

Postoperatively, the patient was monitored in the Intensive Care unit for two days. By second day, she was tolerating oral intake of liquids. She was discharged home on the 3rd post-operative day. Six months after surgery, she remained symptom free.

DISCUSSION

Vascular tumors (hemangioma, lymphangioma, hemolymphangioma, hemangioendothelioma, hemangiopericytoma, hemangioblastoma and angiosarcoma) constitute only 0.1% of the pancreatic tumors[1]. Hemangiomas are vascular tumors composed of blood vessels lined by endothelial cells. Visceral hemangiomas can be found in various organs including the brain, parotid, thorax, liver, spleen, adrenal, retroperitoneum and gastrointestinal tract, in isolation, or with synchronous cutaneous lesions[2]. Hemangioma is the most common benign tumor of the liver, however, pancreas hemangiomas are extremely rare, both in adult and pediatric population.

A PubMed and Google Scholar search of the literature using the keywords "pancreas hemangioma" was performed, and pertinent articles and their references were reviewed. Since 1960, a total of twenty-one cases have been reported in nineteen articles (Table 1)[3-19]. Mundinger *et al*[20] in their 2009 article, stated that a number of nine cases have been described in the medical literature prior to 1939. In our review, cases of hemolymphangioma, lymphangioma and vascular malformations were excluded. Hemangiomas with retroperitoneal origin involving the pancreas were also excluded. The aim of the present review is to provide a summary of the epidemiological and clinical characteristics of this rare tumor.

The average age of the patients at diagnosis is 48.3 years (range: 18-79 years). Our patient is the youngest adult case reported. Infantile hemangiomas of pancreas are very rare, but they involute by early childhood[21]. Male to female ratio is 1:3. Other pancreatic tumors *e.g.,* mucinous cystic neoplasm (MCN), intraductal papillary mucinous neoplasm (IPMN) and solid pseudopapillary neoplasm (SPN) also show female predominance. Male to female ratio of 1:5 is reported in cavernous hemangioma of the liver. Although an association between the proliferation of hepatic cavernous hemangiomas and increased levels of estrogen (from contraceptives, pregnancy) is reported, no definite causal relationship has been proven[22].

The most common presenting symptom is epigastic pain (47%). Nausea, abdominal distention, jaundice, fever, episodic dizziness and palpitations and gastrointestinal bleeding may be associated to pain. No reported case had episodes of pancreatitis or family history of pancreas diseases. Rarely, especially in young patients, cavernous hemangiomas of the pancreas may be observed in the setting of von Hippel-Lindau disease[23]. Abnormalities of the serum

Table 1 Previously reported pancreas hemangiomas in literature

No.	Year	Country	Author	Age (yr)/ sex	Site/size (cm)	Preoperative diagnosis	Treatment	Follow up
1	1939	-	Ranstrom	61/F	Head/7	Found at autopsy	-	
2	1960	France	Ringoir	-	-	-	Surgery	
3	1961	France	Ringoir	71/F	Head/15	-	Retrocolic gastroenterostomy, vagotomy	
4	1972	France	Colardyn	42/F	Body tail/-	-	Fat free diet, anticholinergic[1]	
5	1985	France	Mangin	62/F	Head to tail/20	Multicystic heterogenous structure	Laparotomy with observation[1]	
6	1991	Japan	Kobayashi	30/M	Head/20	Cavernous hemangioma suggested on US/MRI	Pancreatoduodenectomy	
7	1991	Germany	Dageforde	79/F	Body tail/6		Observation[1]	
8	2003	Taiwan	Chang	70/F	Body tail/4	Heterogenous hypervascular solid mass. Serous/cystic adenoma/adenocarcinoma?	Subtotal pancreatectomy	Healthy at 14 mo
9	2006	Austria	Plank	36/M	Head/3	Hypervascular mass. Nonfunctioning neuroendocrine tumor	Hemangioma suspected during laparotomy, confirmed by intraoperative US. Not resected[1]	
10	2008	China	Xu	-	-	Three cases reported	-	
11	2009	United States	Mundinger	45/F	Head/5.5	Hypodensity mass in CT. Benign (duplication cyst, paraganglioma, cystic GIST) cyst	Frozen section: benign cyst. PPPD performed	
12	2010	-	Jarboui	60/F	-	-	-	
13	2011	Israel	Weidenfeld	73/F	Head/5	Cyst with solid part	Whipple's procedure	
14	2011	Malaysia	Lee	49/F	Neck/5	Non-enhancing septated cyst. Mucious cyst with malignant features	Central partial pancreatectomy and gastrostomy	Symptom free at 6 mo
15	2012	Germany	Kersting	53/M	Head/8	Non-enhancing mass. Adenocarcinoma?	Extirpation of the tumor	
16	2013	China	Zhi-hua	23/F	Head/5.4	Non enhancing multilocular cyst with fluid fluid levels	Subtotal pancreatectomy	Healthy, no recurrence at 1 yr
17	2013	United Kingdom	Malik	70/F	Head/8	Giant hemangioma suggested on CT	PPPD	Fine at 6 wk
18	2014	United Kingdom	Williamson	78/F	Head/4	Hemangioma per EUS	Observation[1]	
19	2014	Japan	Naito	40/F	Body tail/10	Multilocular septated cystic mass	Pancreatectomy	No recurrence at 6 yr
20	2015	United States	Mondal	18/F	Head/6	Benign cyst	PPPD	Fine at 6 mo

[1]Cases that were preoperatively suspected to be hemangioma and/conservatively managed. PPPD: Pylorus preserving pancreatoduodenectomy.

liver tests and thrombocytopenia may be present but no correlation between the size or of the lesions location and symptomatology was noted. In fact, these tumors can be as large as 20 cm and arising from the head of pancreas, yet they do not cause much pain or obstructive features. On the contrary, two of the smallest reported lesions, presented with obstructive jaundice (No. 8, 9). Average reported tumor size is 8.9 cm (range: 3-20 cm), with the majority (70%) involving the head of the pancreas. Hemangiomas are indolent (No. 13, 14) and do not have malignant potential. Why our patient presented with rather short duration of symptoms is unknown. Whether hemorrhage, thrombosis or necrosis within the cyst occurred and led to symptoms is not known.

Ultrasonography

Transabdominal ultrasonography (US) is reported to detect hemangiomas in 9 cases. All these lesions were more than 5 cm in size. Lesions were well demarcated, appeared overall hyper- or iso-echogenic to rest of the pancreas, and had mixed echogenicity. A 20 cm mass in the head of pancreas was diagnosed as a giant hemangioma on US (No. 6). The absence of a fine speckled internal echo pattern may suggest a vascular tumor as opposed to a mucinous cystic tumor[24]. Intra-operative US was helpful in diagnosing pancreatic hemangioma in one case and prevented pancreatectomy (No. 9). Our Endoscopic ultrasound findings were similar to those described by Lee (No. 14). We identified a cystic mass with thick septations and solid components. Doppler signal was absent within the lesion. The overall sonographic appearance was suggestive of an inflammatory or mucinous cyst. Willamson (No. 18) made a diagnosis of pancreas hemangioma based on endosonographic characteristics, which allowed a conservative approach to the management of his reported case, and surgery was avoided. Hemorrhage, thrombosis, necrosis, shunting and vascularity of the solid component

within, may account for poor Doppler signal in most pancreatic hemangiomas[9].

CT scan

Typically, hemangiomas are strongly contrast enhancing in the arterial phase of conventional contrast-enhanced CT imaging[7]. Peripheral irregular enhancement with central non-enhancement in venous phase, and progressive filling-in during the delayed phases of dynamic CT scan is typically described in hepatic hemangiomas. Based on these features, preoperative diagnosis of pancreatic giant hemangioma was suggested only in one case (No. 17). A non-enhancing three-phase contrast CT scan does not exclude hemangioma. Of the cases that reported pre-contrast CT findings, five lesions (No. 8, 9, 11, 17, 19) were heterogeneous (with both, high and low attenuation), multi-loculated cysts and five (No. 13, 14, 16, 18, 20) were hypo-attenuating "cysts" with solid components and peripheral micro- or speckled calcifications. Post-contrast CT showed poorly enhanced or unenhanced, hypo-vascular, multi-loculated, cystic tumors in some cases (No. 6, 11, 14, 15, 16, 20) and hyper-enhancement in others (No. 8, 9, 13, 17, 18, 19).

MRI

Hemangioma on MRI appears as a lobulated, hypo-intense mass in T1 -weighted images, and shows moderate hyperintensity signal in T2 -weighted images, while after intravenous gadolinium administration, there is marked enhancement[25,26]. Four articles (No. 6, 9, 16, 19) reported MRI findings of pancreas hemangiomas. Low T1W signal attenuation in (No. 6, 9, 16) and high T2W signal attenuation in (No. 16, 19) were seen on non-contrast MRI. MRI was able to diagnose a giant hemangioma of pancreas (No. 6) without further work-up. In our case, in the post-contrast dynamic imaging, there was some evidence of centripetal filling-in. No dilatation of the pancreatic and the common bile ducts was seen on MRCP in our patient.

Fine needle aspiration cytology

Since radiological imaging cannot characterize these lesions, almost all complex cystic lesions of the pancreas undergo endoscopic or per-cutaneous fine needle aspiration (FNA) to establish a diagnosis. Hemangiomas can be highly vascular. Fatality related to biopsy of hepatic hemangioma has been reported[27], therefore concern regarding FNA sampling of these lesions should rise. If the radiographic characteristics of hemangioma are absent on imaging, the risk of bleeding remains concerning following lesion sampling or during surgery. On the other hand, the article reporting 38 patients with sampled hepatic hemangiomas, along with several other small series, revealed needle biopsy to be safe[28]. FNA was performed in pancreas hemangiomas (No. 14, 17, 18), and there was no reported bleeding. We performed EUS guided FNA using a 22G ProCore Cook Needle (Cook Medical Inc., Winston-Salem, NC, United States) with 5 passes without associated bleeding.

Other imaging methods

Angiography performed in cases of pancreatic hemangiomas showed either a poorly vascular (No. 6) or a hypervascular (No. 8) tumor without encasement of surrounding vascular structures. Arteriography does not provide additional useful information beyond CT/MRI, and is not routinely performed, unless selective embolization of feeding vessels is being considered as treatment. Technetium (Tc)-99 isotope study and positron-emission tomography (PET) scan have been found useful in diagnosing hemangiomas in other organs, but none has been reported in pancreas hemangioma cases.

Differential diagnoses

As hemangiomas are essentially benign tumors, correct preoperative differentiation from other tumors could prevent surgical resection. On imaging, hemangiomas elicit characteristics that overlap with radiographic phenotypes of other common lesions of the pancreas. The list of radiological differential diagnoses for cystic-solid and cystic pancreatic lesions is broad (Table 2). Most cases proceeded to surgery without confirmatory diagnosis. The correct pre-operative or intra-operative diagnosis of hemangioma was made only in 5 out of 20 cases (No. 4, 5, 7, 9, 18), thus avoiding need for surgical resection.

Histopathology

Microscopically, hemangiomas are composed of an increased number of blood-filled ectatic capillaries lined by flat endothelium and separated by scant fibrous connective tissue stroma. Depending on the size of vascular spaces, they can be capillary or cavernous type. Vascular endothelial marker (CD31, CD34 and factor Ⅷ-related antigen) positivity, along with negative results for cytokeratin (AE1/AE3, D2-40, CAM 5.2, MNF 116) immunohistochemical staining indicates hemangioma, lymphangioma and other benign vascular tumors. Lymphangioma may be easily excluded, as they consist of lymphatics (instead of blood vessels) filled or infiltrated with lymphocytes. Using electron microscopy (EM), lymphangioma was diagnosed in a resected pancreas tumor[29], however, EM has not been described in hemangioma. A precise histopathological diagnosis of hemangioma is very important, as other vascular tumors may require wider surgical margin at resection, adjunctive therapy and closer post-resection follow up. For instance, in hemolymphangioma, 10%-27% and 50%-100% recurrences are reported after complete and partial resection, respectively[30].

Table 2 Differential diagnoses of cystic and cystic-solid lesions of pancreas

Cystic lesions	Sex/age/size/site	Imaging, cytology features
Pseudocysts	Any	Unilocular
Serous cystic neoplasms	F/60s/large/body or tail	Serous and mucinous cystadenoma similar on CT Central fibrous scar with calcification Septation Multiple cysts lined by glycogen-rich epithelial cells that are positive for periodic acid Schiff and express cytokeratins
Mucinous cystic neoplasms	F/50-60s/> 10 cm/body or tail	Single multilocular cysts that do not communicate with the ductal system Smooth shape, even wall, with or without (fine) septa with potential small nodules Peripheral egg shell calcification Cyst lined by columnar mucin-producing epithelial cells set within an ovarian-like stroma Dysplasia and malignant potential Express keratin, carcinoembryonic antigen and CA19-9, while CK20 and CDX2 (markers of intestinal differentiation) are negative
IPMN	M = F/70-80s/head	Intraductal proliferation of mucinous cells usually showing papillary projections Dysplasia, invasion and malignant potential The epithelium of IPMNs expresses keratins, CEA and CA19-9, with variable expression of MUC
Solid pseudopapillary neoplasms	Young F/> 10 cm/tail, head	Solid or cystic-solid hypervascular tumors, solid part enhances Show pseudopapillae and pseudocysts Stain for vimentin and beta catenin with partial reactivity to keratin CD56 and synaptophysin stains may be positive, chromogranin negative
Cystic change of solid tumors	PDAC is rare < 50, M = F	Recognition of adjacent solid lesion (carcinoma) is the key to correct diagnosis of ductal adenocarcinoma PDAC are fibrotic, hypo-vascular, ill defined border, early infiltration in peri-pancreatic fat, invasion of vascular structures and ducts NET and Islet cell tumors are hyper-vascular and hyper-enhancing with positive staining for chromogranin and synaptophysin
Lymphoepithelial cysts	M/50-60s/ body or tail	Lined by squamous epithelium and surrounded by dense lymphoid tissue, possibly showing germinal centers
Vascular tumors (Lymphangiomas, hemangiomas, hemolymphangioma, hemangioendothelioma, angiosarcoma	F > M/large	Cystic-solid, encapsulated, multi-loculated, micro-cystic portions appear solid and enhancing Vascular markers CD31, CD34 and factor Ⅷ are positive in endothelial cells Cytokeratins neg Lymphatic marker D2-40 neg in hemangioma, positive in lymphangioma Angiosarcomas, highly aggressive, a vascular channel lined by variably atypical endothelial cells
Metastatic from renal cell cancer		Hypervascular, invasive
Accessory splenic tissue	Tail	hypervascular
Others		Rare solid tumors of the pancreas also include: mature teratoma, hamartoma, sarcoidosis, yolk sac tumor, acinar cell carcinoma, lymphoplasmatic sclerosing pancreatitis, primary pancreatic lymphoma., duodenal tumor, duplication cysts, paraganglioma, cystic GIST, glomus tumor, *etc.*

IPMN: Intraductal papillary mucinous neoplasms; PDAC: Pancreatic ductal adenocarcinoma.

Treatment of hemangioma

Unlike pediatric hemangiomas that mostly involute, adult pancreatic hemangiomas do not. The natural history of adult pancreas hemangiomas is unknown. They appear to be very slow growing and have no malignant potential. Over a 7 years period, a hemangioma grew from 2 cm to 5 cm (No. 14). Pancreatic hemangiomas, even when large, rarely obstruct or infiltrate adjacent structures. Although the possibility of future complications (spontaneous or traumatic rupture, bleeding, pancreatitis, infection, *etc.*) is present, a conservative approach can be considered, if confident diagnosis is made preoperatively. Five cases are reported to be managed by observation strategy. However, details regarding surveillance and outcomes are not known. Propranolol, corticosteroid, interferon alpha, vincristine, cyclophosphamide and radiotherapy have been used to successfully treat infantile hemangiomas, but their role in adult hemangioma treatment is not known.

Surgical excision seems to be a reasonable strategy for large hemangiomas when diagnostic uncertainty remains, for uncontrolled symptoms with failed conservative management, or to address complications from mass effect. All resected pancreas hemangioma cases had good outcome, with resolution of symptoms and no tumor recurrence. Naito (No. 19) reported surgical removal of a giant pancreatic hemangioma without recurrence at 6-year follow up. Preoperative suspicion, use of intra-operative ultrasound and frozen sections may help in determining the best surgical method, *e.g.*, enucleation, other more conservative surgical techniques or an extensive resection.

Current imaging techniques cannot reliably diagnose pancreas hemangioma from other cystic neoplasm.

Newer techniques like contrast enhanced US, PET scan, elastography, *etc*. may be tried in future. Early suspicion by clinicians and radiologists is crucial. Although rare, pancreatic hemangioma should be considered in the differential diagnosis.

COMMENTS

Case characteristics

An 18-year-old female with nausea, vomiting and epigastric pain for 3 mo and a 5 cm x 6 cm non-enhancing cystic mass in the head of pancreas on computed tomography scan.

Clinical diagnosis

Epigastric tenderness but no mass on examination.

Differential diagnosis

Pancreatic neoplasm, pancreatic cyst

Laboratory diagnosis

Complete blood counts, complete metabolic panel, serum amylase and lipase, coagulation panel, fasting lipid profile, serum CA 19-9 and carcinoembryonic antigen levels were normal.

Imaging diagnosis

Magnetic resonance imaging showed a 5.3 cm x 6.2 cm, heterogeneous, multi-septated, predominantly cystic mass in the head of the pancreas, with variable T1W and T2W signal intensity and differential diagnoses included: serous cystadenoma, solid pseudopapillary neoplasm, inflammatory cyst and mucinous cyst.

Pathological diagnosis

Endoscopic ultrasonography guided fine needle aspiration cytology was negative for malignancy; post resection histopathology (blood-filled cavernous spaces lined by flat endothelium) and immunohistochemistry (CD31, CD34 positive and AE1/AE3, CAM 5.2 negative) confirmed the diagnosis of hemangioma.

Treatment

Pylorus preserving pancreatoduodenectomy.

Related reports

Cavernous hemangioma of pancreas is a rare condition and preoperative diagnosis is difficult. Cases reported in English literature were reviewed to identify clinicopathological and radiological characteristics of these tumors.

Experiences and lessons

Pancreas hemangiomas are rare benign tumors that mimic other more common lesions of pancreas. Confident preoperative diagnosis is challenging. Symptomatic patients need resection that also establishes the diagnosis.

Peer-review

This article describes the clinical, radiological and pathological features of a case of cavernous hemangioma of pancreas and also provides a literature review of the reported cases.

REFERENCES

1 **England RJ**, Woodley H, Cullinane C, McClean P, Walker J, Stringer MD. Pediatric pancreatic hemangioma: a case report and literature review. *JOP* 2006; **7**: 496-501 [PMID: 16998249]

2 **Schulz AS**, Urban J, Gessler P, Behnisch W, Kohne E, Heymer B. Anaemia, thrombocytopenia and coagulopathy due to occult diffuse infantile haemangiomatosis of spleen and pancreas. *Eur J Pediatr* 1999; **158**: 379-383 [PMID: 10333119]

3 **Derom F**, Ringoir S, Marlier R. [Two cases of intraabdominal hemangioma: liver and pancreas]. *Acta Chir Belg* 1960; **59**: 172-182 [PMID: 13816057]

4 **Ringoir S**, Derom F, Colle R, Mortier G. Hemangioma of the pancreas. Report of a case. *Gastroenterology* 1961; **41**: 43-45 [PMID: 13741765]

5 **Colardyn F**, Elewaut A, Van de Velde E, Barbier F. Hemangioma of the pancreas. *Tijdschr Gastroenterol* 1972; **15**: 260-267 [PMID: 4642101]

6 **Mangin P**, Perret M, Ronjon A. [Hemangioma of the pancreas]. *J Radiol* 1985; **66**: 381-384 [PMID: 4032348]

7 **Kobayashi H**, Itoh T, Murata R, Tanabe M. Pancreatic cavernous hemangioma: CT, MRI, US, and angiography characteristics. *Gastrointest Radiol* 1991; **16**: 307-310 [PMID: 1936772 DOI: 10.1007/BF01887375]

8 **Dageförde J**, Gmelin E, Otte M. [Hemangioma of the pancreas]. *Rofo* 1991; **154**: 332-333 [PMID: 1849305]

9 **Chang WT**, Lee KT, Yang SF. Cavernous hemangioma of the pancreas: report of a case. *Pancreas* 2003; **26**: 310-312 [PMID: 12657961 DOI: 10.1097/00006676-200304000-00018]

10 **Plank C**, Niederle B, Ba-Ssalamah A, Schima W. Pancreatic hemangioma: imaging features with contrast-enhanced CT and with gadolinium- and mangafodipir-enhanced MRI. *Eur J Radiol* 2006; **57**: 59-62 [DOI: 10.1016/j.ejrex.2005.11.008]

11 **Xu Q**, Wang CF, Zhao P, Shan Y, Zhao DB, Liu Q. [The diagnosis and treatment of pancreatic cavernous hemangioma]. *Zhonghua Yi Xue Za Zhi* 2008; **88**: 28-30 [PMID: 18346376]

12 **Jarboui S**, Salem A, Gherib BS, Ben Moussa M, Rajhi H, Mnif N, Zaouche A. Hemangioma of the pancreas in a 60-year-old woman: a report of a new case. *Gastroenterol Clin Biol* 2010; **34**: 569-571 [PMID: 20609542 DOI: 10.1016/j.gcb.2010.06.001]

13 **Weidenfeld J**, Zakai BB, Faermann R, Barshack I, Aviel-Ronen S. Hemangioma of pancreas: a rare tumor of adulthood. *Isr Med Assoc J* 2011; **13**: 512-514 [PMID: 21910381]

14 **Lee J**, Raman K, Sachithanandan S. Pancreatic hemangioma mimicking a malignant pancreatic cyst. *Gastrointest Endosc* 2011; **73**: 174-176 [PMID: 20932519 DOI: 10.1016/j.gie.2010.07.038]

15 **Kersting S**, Janot MS, Munding J, Suelberg D, Tannapfel A, Chromik AM, Uhl W, Bergmann U. Rare solid tumors of the pancreas as differential diagnosis of pancreatic adenocarcinoma. *JOP* 2012; **13**: 268-277 [PMID: 22572130]

16 **Lu ZH**, Wu M. Unusual features in an adult pancreatic hemangioma: CT and MRI demonstration. *Korean J Radiol* 2013; **14**: 781-785 [PMID: 24043972 DOI: 10.3348/kjr.2013.14.5.781]

17 **Malik M**, Ahmed I, Kurban L. Pancreatic Hemangioma - A case Report. *Gastroenterol Hepatol Res* 2013; **2**: 545-548 [DOI: 10.6051/j.issn.2224-3992.2013.02.236]

18 **Williamson JM**, Finch-Jones M, Pope I. Endoscopic ultrasonography allowing expectant management of pancreatic haemangioma. *Ann R Coll Surg Engl* 2014; **96**: e1-e2 [PMID: 24780776 DOI: 10.1308/003588414X13814021678231]

19 **Naito Y**, Nishida N, Nakamura Y, Torii Y, Yoshikai H, Kawano H, Akiyama T, Sakai T, Taniwaki S, Tanaka M, Kuroda H, Higaki K. Adult pancreatic hemangioma: A case report. *Oncol Lett* 2014; **8**: 642-644 [PMID: 25013478 DOI: 10.3892/ol.2014.2206]

20 **Mundinger GS**, Gust S, Micchelli ST, Fishman EK, Hruban RH, Wolfgang CL. Adult pancreatic hemangioma: case report and literature review. *Gastroenterol Res Pract* 2009; **2009**: 839730 [PMID: 19421421 DOI: 10.1155/2009/839730]

21 **Takahashi K**, Mulliken JB, Kozakewich HP, Rogers RA, Folkman J, Ezekowitz RA. Cellular markers that distinguish the phases of hemangioma during infancy and childhood. *J Clin Invest* 1994; **93**: 2357-2364 [PMID: 7911127 DOI: 10.1172/jci117241]

22 **Glinkova V**, Shevah O, Boaz M, Levine A, Shirin H. Hepatic haemangiomas: possible association with female sex hormones. *Gut* 2004; **53**: 1352-1355 [PMID: 15306599 DOI: 10.1136/gut.2003.038646]

23 **Hammel P**, Beigelman C, Chauveau D, Resche F, Bougerolles E,

Flejou JF, Bernades P, Delchier JC, Richard S. [Variety of pancreatic lesions observed in von Hippel-Lindau disease. Apropos of 8 cases]. *Gastroenterol Clin Biol* 1995; **19**: 1011-1017 [PMID: 8729413]

24 **Balderramo DC**, Di Tada C, de Ditter AB, Mondino JC. Hemolymphangioma of the pancreas: case report and review of the literature. *Pancreas* 2003; **27**: 197-199 [PMID: 12883270 DOI: 10.1097/00006676-200308000-00014]

25 **Semelka RC**, Brown ED, Ascher SM, Patt RH, Bagley AS, Li W, Edelman RR, Shoenut JP, Brown JJ. Hepatic hemangiomas: a multi-institutional study of appearance on T2-weighted and serial gadolinium-enhanced gradient-echo MR images. *Radiology* 1994; **192**: 401-406 [PMID: 8029404]

26 **Goshima S**, Kanematsu M, Kondo H, Yokoyama R, Kajita K, Tsuge Y, Shiratori Y, Onozuka M, Moriyama N. Hepatic hemangioma: correlation of enhancement types with diffusion-weighted MR findings and apparent diffusion coefficients. *Eur J Radiol* 2009; **70**: 325-330 [PMID: 18321673 DOI: 10.1016/j.ejrad.2008.01.035]

27 **Terriff BA**, Gibney RG, Scudamore CH. Fatality from fine-needle aspiration biopsy of a hepatic hemangioma. *AJR Am J Roentgenol* 1990; **154**: 203-204 [PMID: 2104717 DOI: 10.2214/ajr.154.1.2104717]

28 **Tung GA**, Cronan JJ. Percutaneous needle biopsy of hepatic cavernous hemangioma. *J Clin Gastroenterol* 1993; **16**: 117-122 [PMID: 8463614 DOI: 10.1097/00004836-199303000-00008]

29 **Murao T**, Toda K, Tomiyama Y. Lymphangioma of the pancreas. A case report with electron microscopic observations. *Acta Pathol Jpn* 1987; **37**: 503-510 [PMID: 3618222 DOI: 10.1111/j.1440-1827.1987.tb00384.x]

30 **Fang YF**, Qiu LF, Du Y, Jiang ZN, Gao M. Small intestinal hemolymphangioma with bleeding: a case report. *World J Gastroenterol* 2012; **18**: 2145-2146 [PMID: 22563205 DOI: 10.3748/wjg.v18.i17.2145]

P- Reviewer: Cosen-Binker L, Sakata N, Sumi S **S- Editor**: Ma YJ
L- Editor: A **E- Editor**: Wang CH

World Journal of Gastroenterology

Submit a Manuscript: http://www.wjgnet.com/esps/
Help Desk: http://www.wjgnet.com/esps/helpdesk.aspx
DOI: 10.3748/wjg.v21.i33.9803

World J Gastroenterol 2015 September 7; 21(33): 9803-9807
ISSN 1007-9327 (print) ISSN 2219-2840 (online)

CASE REPORT

Single skip metastasis in sentinel lymph node: In an early gastric cancer

Tivadar Jr Bara, Simona Gurzu, Ioan Jung, Zoltan Kadar, Haruhiko Sugimura, Tivadar Bara

Tivadar Jr Bara, Tivadar Bara, Department of Surgery, University of Medicine and Pharmacy, 540139 Tirgu-Mures, Romania

Simona Gurzu, Ioan Jung, Zoltan Kadar, Department of Pathology, University of Medicine and Pharmacy, 540139 Tirgu-Mures, Romania

Haruhiko Sugimura, Department of Tumor Pathology, Hamamatsu University, School of Medicine, Hamamatsu 433-8105, Japan

Author contributions: Bara T Jr wrote the manuscript and participated in the surgical intervention; Gurzu S carried out the study design and performed the histopatological assessment of surgical specimens; Jung I participated at the assessment of frozen sections and interpretation of the immunoassays; Kadar Z carried out the oncological management; Sugimura H carried out the molecular assessment and interpretation of data from the literature; Bara T carried out the surgical intervention and approved the final version of the manuscript; all authors read and approved the final manuscript.

Supported by Romanian government, the research project frame POSDRU/159/1.5/S/136893; and University of Medicine and Pharmacy of Tirgu-Mures, Romania, the team research project POS-UMFTGM-CC-13-01-V01, No. 15/16189/2013; In Japan, funds were obtained by grants from the Ministry of Health, Labour and Welfare (19-19, 10103838), and Ministry of Education, Culture, Sports, Science and Technology (MEXT) (S-001).

Informed consent statement: All study participants, or their legal guardian, provided informed written consent prior to study enrollment.

Conflict-of-interest statement: The authors declare no conflict of interest.

Correspondence to: Simona Gurzu, Professor, MD, PhD, Department of Pathology, University of Medicine and Pharmacy, 38 Ghe Marinescu Street, 540139 Tirgu-Mures, Romania. simonagurzu@yahoo.com
Telephone: +40-745673550

Received: March 3, 2015
Peer-review started: March 5, 2015
First decision: April 13, 2015
Revised: April 21, 2015
Accepted: June 10, 2015
Article in press: June 10, 2015
Published online: September 7, 2015

Abstract

Lymph node status is considered a key prognostic and predictive factor in patients with gastric cancer (GC). Although there is a practical approach to the intraoperative detection of sentinel lymph nodes (SLNs), such a procedure is not included in the European surgical protocol. In this report, we present a practical approach to SLN mapping in a representative case with early gastric cancer (EGC). A 74-year-old female was hospitalized with an endoscopically observed, superficially ulcerated tumor located in the antral region. Subtotal gastrectomy with D2 lymphadenectomy and SLN mapping was performed by injecting methylene blue dye into the peritumoral submucosal layer. An incidentally detected blue-stained lymph node located along the middle colic artery was also removed. This was detected 40 min after injection of the methylene blue. Histopathologic examination showed a pT1b-staged well-differentiated HER-2-negative adenocarcinoma. All of the 41 LNs located at the first, third, and fifth station of the regional LN compartments were found to be free of tumor cells. The only lymph node with metastasis was located along the middle colic

artery and was considered a non-regional lymph node. This incidentally identified skip metastasis indicated stage Ⅳ GC. A classic chemotherapy regimen was given, and no recurrences were observed six months after surgery. In this representative case, low-cost SLN mapping, with a longer intraoperative waiting time, totally changed the stage of the tumor in a patient with EGC.

Key words: Early gastric cancer; Sentinel lymph node; Lymph node metastasis; Skip metastasis; Middle colic artery

Core tip: The aim of this paper was to report an unusual case of early gastric cancer in which sentinel node mapping totally changed the tumor staging and therapeutic protocol.

Bara T Jr, Gurzu S, Jung I, Kadar Z, Sugimura H, Bara T. Single skip metastasis in sentinel lymph node: In an early gastric cancer. *World J Gastroenterol* 2015; 21(33): 9803-9807 Available from: URL: http://www.wjgnet.com/1007-9327/full/v21/i33/9803.htm DOI: http://dx.doi.org/10.3748/wjg.v21.i33.9803

INTRODUCTION

The term "early gastric cancer (EGC)" is used for gastric carcinomas with invasion limited to mucosa/muscularis mucosae (pT1a stage) or submucosal layer of the stomach (pT1b). Although the 5-year survival rate in EGC is reported to be about 90%, recurrences and metastases in the lymph nodes, liver, and even bones can occur[1]. For proper therapeutic management, careful preoperative evaluation of the lymph node status, tumor size and depth of infiltration is mandatory for accurate preoperative staging. Based on the international well-defined guidelines, with some national particularities, tumor resection consists of endoscopic mucosal resection (EMR), endoscopic submucosal dissection (ESD) or surgical excision[1-3]. The EMR is recommended for pT1a-staged non-ulcerated/non-metastatic differentiated carcinomas with diameter less than 2 cm. In ulcerated pT1a-differentiated carcinomas, EMR is indicated for tumors smaller than 1 cm[1-3]. ESD is recommended for non-metastatic differentiated carcinomas larger than 2 cm, with early invasion in the submucosa (pT1b), that do not involve associated angiolymphatic invasion. In larger tumors, poorly cohesive carcinomas (that are associated with a higher risk for metastases), metastatic cases (pN1-3 or M1), and advanced carcinomas (pT 2-4), gastrectomy is recommended; subtotal gastrectomy in carcinomas with at least 5 cm free margin up to the gastro-esophageal junction (8 cm in poorly cohesive carcinomas) and radical gastrectomy in the other cases[1-4].

In Eastern Europe, gastrectomy with D1/D2 lymphadenectomy is still considered the gold standard, even in EGC. Although there is a debate regarding D1 *vs* D2 lymphadenectomy, based on the duration of surgery and patient's quality of life, studies performed in dedicated centers showed that the morbidity and mortality rate was approximately 0.5% and 2%, respectively, in D2, and not significantly different from D1. Based on these facts, recent guidelines require at least 15 regional lymph nodes for accurate tumor staging, and indicate D2 dissection as the standard procedure, in surgically-removed tumors[1-4]. For the correct identification of high-risk lymph nodes, sentinel node mapping may be helpful[3].

Moreover, in EGC, patients' quality of life seems to be mainly influenced by the extent of resection and not the extent of lymphadenectomy. Independently, based on tumor stage, the morbidity and mortality of gastrectomy is high, ranging from 10% to 20%. These aspects highlight the necessity for changing therapeutic management, to reduce postoperative morbidity. The number of cases in which EMR/ESD is performed instead of surgery has increased. However, in low-income countries this change is not yet possible due to financial status, which does not allow a proper preoperative evaluation that includes endoscopic and computed tomography examinations of the thoracic and abdominal cavity, and does not facilitate proper screening programs. In these countries, gastrectomy with proper lymph node excision remains the standard, even in EGC. Taking into account the fact that the incidence of lymph node metastasis in EGC is 3%-24%[1,4], the introduction of an inexpensive and reliable system of preoperative evaluation of lymph node status is mandatory.

Although it is not universally accepted, due to the high rate of false negative results in intraoperatively examined nodes[5], the detection of sentinel lymph nodes (SLNs) is considered useful because the gastric lymphatic drainage can have aberrant flow[6] with identified sentinel nodes outside the lymphatic basin[5]. The rate of false-negative results for intraoperatively-examined lymph nodes depends on the clinical experience of the surgeon and the intraoperative method of detection (*i.e.,* blue dye, indocyanine green), but is also related to the fact that only one plane-frozen sections can be performed to examine the nodes in a short-time and to retain tissue for further paraffin-embedding; micro-metastases cannot be detected intraoperatively. Even in large centers, intraoperative false-negative results were reported in more than 40% of cases; in paraffin-embedded sections, postoperatively, the rate was 14%[5]. Postoperatively, this rate also depends heavily on the method of SLN analysis (*i.e.,* IHC, RT-qPCR), the number of intraoperatively examined lymph nodes and

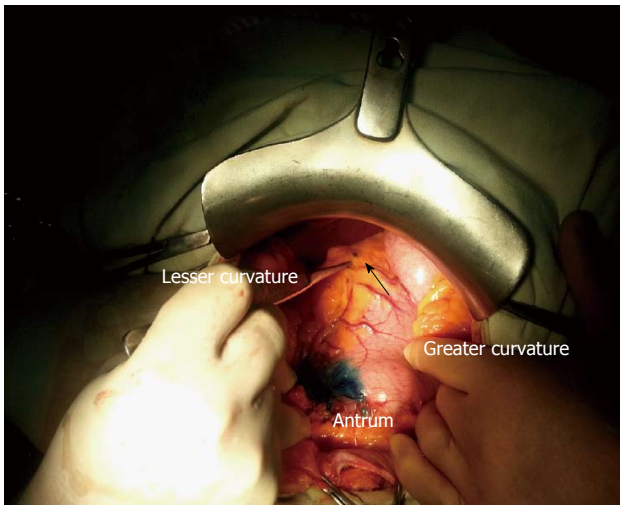

Figure 1 Intraoperative sentinel lymph node mapping with methylene blue dye injected into the submucosal layer, in a patient with gastric cancer of the antrum. The sentinel nodes are seen in the lesser curvature (arrow).

the number of sections per examined node.

In this paper, we present a representative case in which the accurate detection of SLN totally changed the postoperative therapeutic protocol in a patient with EGC.

CASE REPORT

A 74-year-old previously healthy female was hospitalized due to an episode of hematemesis. Upper endoscopy detected 3 cm × 2.5 cm ulcerated tumor located in the antrum. Histopathologic examination of the biopsy specimen showed a well-differentiated adenocarcinoma limited to the gastric submucosa; it was decided to perform subtotal gastrectomy with D2 lymphadenectomy and intraoperative SLN mapping by injecting 2 mL of methylene blue dye into the submucosal layer of the stomach, in the neighborhood of the tumor, circumferentially at four cardinal points (Figure 1). This injection was carried out before mobilization of the stomach to avoid alteration of lymphatic drainage[5]. A signed written consent for the surgical intervention was obtained from the patient.

Following submucosal injection of methylene blue (Figure 1), we waited 10 min and then removed the first two blue-stained nodes, which were located at the 5th station (lesser curvature) and considered SLNs (Figure 1); both nodes were submitted for frozen tissue section and found to be free of tumor.

Standard subtotal gastrectomy and D2 lymphadenectomy were carried out. However, during the second phase of surgery (40 min after injection of methylene blue), two blue-stained lymph nodes were incidentally detected at the level of the middle colic artery, considered the 15th lymph node station; these were removed, together with seven other non-stained neighboring nodes. Finally, lymphadenectomy which included lymph node stations 1, 3, 4, 5, and 6 (lymph node compartment Ⅰ); stations 7, 8, 9, and 12 (compartment Ⅱ); and lymph node stations 15 (compartment Ⅳ), respectively, was performed (Table 1).

Gross examination of the surgical specimen showed a 35 mm × 20 mm ulcerated tumor of the antrum and lesser curvature with a maximum thickness of 10 mm (Figure 2), which was microscopically shown to be a pT1b-staged well-differentiated adenocarcinoma. The deepest level of infiltration was the middle third of the gastric submucosa.

With regard to the lymph nodes, a total of 41 lymph nodes were identified, including those of the middle colic artery. Of the 41 nodes, with the exception of the 4 intraoperatively detected SLNs (2 from station 5 and 2 from station 15), another 8 nodes were stained blue (4 from station 3, 1 from station 6, and 3 from station 7). Of the 41 nodes, 40 were free of tumor cells. The only positive node was one of the two blue-stained nodes that were incidentally seen intraoperatively at the level of the middle colic artery; this node was considered a skip metastasis (Table 1). Because this lymph node station was far from the primary tumor, this was considered to be a distant metastasis[7], and the final tumor stage was pT1N0M1 (stage Ⅳ). There were no tumor implants in the omentum, no invasion in blood vessels, and no intraoperatively detected liver metastasis. All the resection margins were free of tumor.

The immunohistochemical and molecular examinations showed a *p53/CDH1*-wild type-tumor that displayed positivity for E-cadherin, keratin 7 and 20, and a cytoplasmic pattern of maspin; p53 and Ki67 nuclear expression was seen in over 70% of the tumor cells. HER-2 was not expressed by the tumor cells.

In terms of tumor proximity, an unusual proliferation of extremely large vessels with thick or thinner walls was noted in the mucosa and submucosa, which corresponded to Dieulafoy's lesion. Due to HER-2 negativity, trastuzumab was not included in the postoperative oncologic therapy. A classic chemotherapy regimen was recommended. The postoperative evolution was favorable; no recurrences or metastases were reported six months after surgery.

DISCUSSION

Data regarding the concept of SLN in surgical practice were first presented by Morton *et al*[8] in 1992; since then, SLN detection has become a standard of care in patients with melanoma and is used in cancers of other organs, such as the breast and colon[9,10].

With regard to gastric cancer, the application of SLN was first carried out in 2001 by Hiratsuka *et al*[11]'s team, who used indocyanine green in T1 and T2 cases, with a success rate of 99%. Later, the same team reported a high rate of false-negative results in T1 cases, using indocyanine green[5]. To increase the sensitivity, a double-marker method that used radioactive colloids

Table 1 Distribution of the identified lymph nodes

Lymph node compartment	Total number of lymph nodes	Total number of blue nodes		Total number of positive blue nodes
		Detected intraoperatively by surgeon (SLN)	Detected postoperatively by pathologist	
I	19	2	5	-
II	16	-	3	-
IV	7	2	-	1
Total	42	4	8	1

SLN: Sentinel lymph node.

Figure 2 The early gastric cancer was an ulcerated tumor of the antrum and lesser curvature.

and blue dye was recommended for EGC[6,12]. In the most recent report, non-exposed endoscopic wall-inversion surgery with sentinel node basin dissection was suggested as the standard of care in patients with EGC and a high risk of node metastases[13].

In the present case, the intraoperative examination of SLNs also revealed a preliminary false-negative result. However, in contrast to other studies, in which SLNs are removed first (10-15 min after injection of the dye) and then gastrectomy and lymphadenectomy are performed[5], we waited for the intraoperative histopathologic report before carrying out the gastrectomy. During this waiting period, the methylene blue dye migrated to the skip metastatic nodes located along the middle colic artery.

This case suggests that, due to aberrant drainage of the lymphatic fluid and a high rate of skip metastases, which is approximately 5% in EGC and 17% in advanced GC[14], SLN mapping can influence the tumor staging protocol. Increasing the period of waiting can increase the number of detected nodes and the sensitivity of SLN mapping. Although most of the skip metastases were detected in the lymph nodes located in stations 7 and 8 (compartment Ⅱ) and in the para-aortic station[4], especially in tumors located in the lesser curvature and distal stomach[15], the nodes of the middle colic artery should also be checked intraoperatively and removed if there is any suspicion of metastatic involvement. To date, no data regarding the impact of middle colic artery node removal with standard D2 lymphadenectomy have been published.

Special attention should also be paid to gastric stump cancer and cases with vascular malformations, such as Dieulafoy lesions, which can also be associated with aberrant lymphatic drainage[16]. Because most gastric vascular malformations are undiagnosed, hematemesis may be a valuable clinical sign, especially when only one episode occurs, without any other symptoms, such as in the current case.

In the case under study, which showed several indicators of node metastases risk, such as tumor size larger than 3 cm, ulceration, location in the distal stomach, involvement of the submucosa, and associated vascular malformation, the correct staging and therapeutic management were carried out as a result of a long waiting time in SLN mapping and the detection of a single skip metastasis in an extra-regional lymph node. In view of the low cost and the absence of associated side effects in GC, we suggest that all blue stained nodes, whether identified *in vivo* or *ex vivo*, should be considered as SLNs.

COMMENTS

Case characteristics

A 74-year-old female with an early gastric cancer and skip metastasis.

Clinical diagnosis

Hematemesis and ulcerated tumor of the stomach, at upper endoscopy.

Differential diagnosis

Chronic peptic ulcer, gastric metastasis.

Imaging diagnosis

Due to the diagnosis of adenocarcinoma in the gastric biopsy specimen, gastrectomy was performed without supplementary investigations.

Pathological diagnosis

Examination of the surgical specimen from the stomach revealed a well-differentiated adenocarcinoma with invasion in the middle third of the submucosal layer.

Treatment

Classic chemotherapy. HER-2 negativity did not allow therapy with trastuzumab.

Related reports

No reported cases of EGC and skip metastasis at the level of the middle colic artery.

Term explanation

Skip metastasis is a "jump" or discontinuous nodal metastasis that occurs as a result of aberrant lymphatic flow.

Experiences and lessons

This case report highlights the aberrant behavior of EGC. An inexpensive method of sentinel lymph node mapping could modify the therapeutic guideline (the type of lymphadenectomy) in patients with EGC.

Peer-review

This article showed the benefits of the proper surgeon-pathologist team work. It shows the inexpensive way of a proper diagnosis, evaluation and therapy of EGCs with aberrant behavior.

REFERENCES

1 **Kobayashi M**, Okabayashi T, Sano T, Araki K. Metastatic bone cancer as a recurrence of early gastric cancer -- characteristics and possible mechanisms. *World J Gastroenterol* 2005; **11**: 5587-5591 [PMID: 16237749]

2 **Yada T**, Yokoi C, Uemura N. The current state of diagnosis and treatment for early gastric cancer. *Diagn Ther Endosc* 2013; **2013**: 241320 [PMID: 23533320 DOI: 10.1155/2013/241320]

3 **Waddell T**, Verheij M, Allum W, Cunningham D, Cervantes A, Arnold D. Gastric cancer: ESMO-ESSO-ESTRO Clinical Practice Guidelines for diagnosis, treatment and follow-up. *Ann Oncol* 2013; **24** Suppl 6: vi57-vi63 [PMID: 24078663 DOI: 10.1093/annonc/mdt344]

4 **Gotoda T**, Yanagisawa A, Sasako M, Ono H, Nakanishi Y, Shimoda T, Kato Y. Incidence of lymph node metastasis from early gastric cancer: estimation with a large number of cases at two large centers. *Gastric Cancer* 2000; **3**: 219-225 [PMID: 11984739 DOI: 10.1007/PL00011720]

5 **Miyashiro I**, Hiratsuka M, Sasako M, Sano T, Mizusawa J, Nakamura K, Nashimoto A, Tsuburaya A, Fukushima N. High false-negative proportion of intraoperative histological examination as a serious problem for clinical application of sentinel node biopsy for early gastric cancer: final results of the Japan Clinical Oncology Group multicenter trial JCOG0302. *Gastric Cancer* 2014; **17**: 316-323 [PMID: 23933782 DOI: 10.1007/s10120-013-0285-3]

6 **Kitagawa Y**, Takeuchi H, Takagi Y, Natsugoe S, Terashima M, Murakami N, Fujimura T, Tsujimoto H, Hayashi H, Yoshimizu N, Takagane A, Mohri Y, Nabeshima K, Uenosono Y, Kinami S, Sakamoto J, Morita S, Aikou T, Miwa K, Kitajima M. Sentinel node mapping for gastric cancer: a prospective multicenter trial in Japan. *J Clin Oncol* 2013; **31**: 3704-3710 [PMID: 24019550 DOI: 10.1200/JCO.2013.50.3789]

7 **Edge SB**, Nyrd DR, Compton CC, Fritz AG, Greene FL, Trotti A, editors. Stomach. In: AJCC Cancer Staging Book. 7th ed. Berlin: Springer, 2010: 145-152

8 **Morton DL**, Wen DR, Wong JH, Economou JS, Cagle LA, Storm FK, Foshag LJ, Cochran AJ. Technical details of intraoperative lymphatic mapping for early stage melanoma. *Arch Surg* 1992; **127**: 392-399 [PMID: 1558490]

9 **Bara T**, Bara T, Bancu S, Egyed IZ, Gurzu S, Bancu L, Azamfirei L, Feher AM. [Sentinel lymph node mapping in colorectal cancer]. *Chirurgia* (Bucur) 2011; **106**: 195-198 [PMID: 21698861]

10 **Gurzu S**, Jung I, Bara T, Bara T, Szentirmay Z, Azamfirei L, Tóth E, Turcu M, Egyed-Zsigmond E. Practical value of the complex analysis of sentinel lymph nodes in colorectal carcinomas. *Rom J Morphol Embryol* 2011; **52**: 593-598 [PMID: 21655648]

11 **Hiratsuka M**, Miyashiro I, Ishikawa O, Furukawa H, Motomura K, Ohigashi H, Kameyama M, Sasaki Y, Kabuto T, Ishiguro S, Imaoka S, Koyama H. Application of sentinel node biopsy to gastric cancer surgery. *Surgery* 2001; **129**: 335-340 [PMID: 11231462 DOI: 10.1067/msy.2001.111699]

12 **Takeuchi H**, Kitagawa Y. Sentinel node navigation surgery in patients with early gastric cancer. *Dig Surg* 2013; **30**: 104-111 [PMID: 23867586 DOI: 10.1159/000350875]

13 **Goto O**, Takeuchi H, Kawakubo H, Sasaki M, Matsuda T, Matsuda S, Kigasawa Y, Kadota Y, Fujimoto A, Ochiai Y, Horii J, Uraoka T, Kitagawa Y, Yahagi N. First case of non-exposed endoscopic wall-inversion surgery with sentinel node basin dissection for early gastric cancer. *Gastric Cancer* 2015; **18**: 434-439 [PMID: 25087058 DOI: 10.1007/s10120-014-0406-7]

14 **Su Z**, Shu K, Zheng M, Sun X, Fang Z, Wang G. Sentinel lymph node and skip metastases in gastric cancer: a prospective study. *Hepatogastroenterology* 2013; **60**: 1513-1518 [PMID: 23635507]

15 **Lee JH**, Lee HJ, Kong SH, Park do J, Lee HS, Kim WH, Kim HH, Yang HK. Analysis of the lymphatic stream to predict sentinel nodes in gastric cancer patients. *Ann Surg Oncol* 2014; **21**: 1090-1098 [PMID: 24276637 DOI: 10.1245/s10434-013-3392-9]

16 **Gurzu S**, Copotoiu C, Azamfirei L, Jung I. A Caliber Persistent Artery (Dieulafoy's Lesion) which is Associated with an Early-Stage Gastric Stump Cancer Following a Distal Gastrectomy. *J Clin Diagn Res* 2013; **7**: 1717-1719 [PMID: 24086889 DOI: 10.7860/JCDR/2013/6385.3266]

P- Reviewer: Jagric T **S- Editor**: Yu J **L- Editor**: Webster JR **E- Editor**: Zhang DN

World Journal of Gastroenterology

Submit a Manuscript: http://www.wjgnet.com/esps/
Help Desk: http://www.wjgnet.com/esps/helpdesk.aspx
DOI: 10.3748/wjg.v21.i33.9808

World J Gastroenterol 2015 September 7; 21(33): 9808-9816
ISSN 1007-9327 (print) ISSN 2219-2840 (online)

CASE REPORT

IgG4-unrelated type 1 autoimmune pancreatitis

Eriko Nakano, Atsushi Kanno, Atsushi Masamune, Naoki Yoshida, Seiji Hongo, Shin Miura, Tetsuya Takikawa, Shin Hamada, Kiyoshi Kume, Kazuhiro Kikuta, Morihisa Hirota, Keisuke Nakayama, Fumiyoshi Fujishima, Tooru Shimosegawa

Eriko Nakano, Atsushi Kanno, Atsushi Masamune, Naoki Yoshida, Seiji Hongo, Shin Miura, Tetsuya Takikawa, Shin Hamada, Kiyoshi Kume, Kazuhiro Kikuta, Morihisa Hirota, Tooru Shimosegawa, Division of Gastroenterology, Tohoku University Graduate School of Medicine, Sendai 980-8574, Japan

Keisuke Nakayama, Division of Nephrology, Endocrinology and Vascular Medicine, Tohoku University Graduate School of Medicine, Sendai 980-8574, Japan

Fumiyoshi Fujishima, Department of Pathology, Tohoku University Graduate School of Medicine, Sendai 980-8574, Japan

Author contributions: Nakano E, Kanno A and Masamune A designed the study and wrote the manuscript; Yoshida N, Hongo S, Miura S, Takikawa T, Hamada S, Kume K, Kikuta K, Hirota M and Nakayama K contributed to attending physicians for the patient; Fujishima F performed pathological examination; and Shimosegawa T critically reviewed the manuscript and gave final approval for submission.

Supported by (in part) Grant-in-Aid from the Japan Society for the Promotion of Science, No. 25461020 (to Kanno A) and by the Ministry of Health, Labor, and Welfare of Japan (to Chiba T and Takeyama Y).

Institutional review board statement: This study was approved by the Institutional Review Board.

Informed consent statement: This patient provided written informed consent.

Conflict-of-interest statement: There is no conflict of interest regard to this case report.

Correspondence to: Atsushi Kanno, MD, PhD, Division of Gastroenterology, Tohoku University Graduate School of Medicine, 1-1 Seiryo-machi, Aoba-ku, Sendai 980-8574, Japan. atsushih@med.tohoku.ac.jp
Telephone: +81-22-7177171
Fax: +81-22-7177177

Received: February 14, 2015
Peer-review started: February 22, 2015
First decision: March 26, 2015
Revised: April 14, 2015
Accepted: June 26, 2015
Article in press: June 26, 2015
Published online: September 7, 2015

Abstract

A 50-year-old male was referred to our hospital for the evaluation of hyperproteinemia. Fluorodeoxyglucose positron emission tomography revealed high fluorodeoxyglucose uptake in the pancreas, bilateral lacrimal glands, submandibular glands, parotid glands, bilateral pulmonary hilar lymph nodes, and kidneys. Laboratory data showed an elevation of hepatobiliary enzymes, renal dysfunction, and remarkably high immunoglobulin (Ig) G levels, without elevated serum IgG4. Abdominal computed tomography revealed swelling of the pancreatic head and bilateral kidneys. Endoscopic retrograde cholangiopancreatography showed an irregular narrowing of the main pancreatic duct in the pancreatic head and stricture of the lower common bile duct. Histological examination by endoscopic ultrasonography-guided fine-needle aspiration revealed findings of lymphoplasmacytic sclerosing pancreatitis without IgG4-positive plasma cells. Abnormal laboratory values and the swelling of several organs were improved by the treatment with steroids. The patient was diagnosed as having type 1 autoimmune pancreatitis (AIP) based on the International Consensus Diagnostic Criteria. Therefore,

we encountered a case of compatible type 1 AIP without elevated levels of serum IgG4 or IgG4-positive plasma cells. This case suggests that AIP phenotypes are not always associated with IgG4.

Key words: IgG4-related disease; Steroid; Intestinal nephritis; Other organ involvement

Core tip: Type 1 autoimmune pancreatitis (AIP) is regarded as a pancreatic lesion of IgG4-related disease (IgG4-RD). However, the role of IgG4 in AIP or IgG4-RD phenotypes has not been established. This patient was diagnosed with compatible type 1 AIP according to the International Consensus Diagnostic Criteria without an elevation of serum IgG4 levels or IgG4-positive plasma cells. This case suggests that type 1 AIP phenotypes do not require IgG4 elevation.

Nakano E, Kanno A, Masamune A, Yoshida N, Hongo S, Miura S, Takikawa T, Hamada S, Kume K, Kikuta K, Hirota M, Nakayama K, Fujishima F, Shimosegawa T. IgG4-unrelated type 1 autoimmune pancreatitis. *World J Gastroenterol* 2015; 21(33): 9808-9816 Available from: URL: http://www.wjgnet.com/1007-9327/full/v21/i33/9808.htm DOI: http://dx.doi.org/10.3748/wjg.v21.i33.9808

INTRODUCTION

In 1995, Yoshida *et al*[1] proposed autoimmune pancreatitis (AIP) as a diagnostic entity and summarized the clinical features as follows: increased serum γ-globulin or immunoglobulin (Ig) G levels and the presence of autoantibodies; diffuse irregular narrowing of the main pancreatic duct (MPD) and enlargement of the pancreas; the occasional concurrent stenosis of the lower bile duct and other autoimmune diseases; mild symptoms, usually without attacks of acute pancreatitis; the effectiveness of steroid therapy; and histological findings of lymphoplasmacytic sclerosing pancreatitis (LPSP)[2]. With the accumulation of similar cases in Japan, the Japan Pancreas Society (JPS) proposed the world's first clinical diagnostic criteria for AIP in 2002[3]. Thereafter, diagnostic criteria for AIP have been proposed in several countries after the report of an extensive number of cases worldwide. Therefore, the International Consensus Diagnostic Criteria (ICDC) were established to form an international standard.

In 2001, Hamano *et al*[4] reported that elevated serum IgG4 levels were highly specific and sensitive for the diagnosis of AIP. IgG4 has a pivotal role in the diagnosis and pathogenesis of AIP. Recently, the concept of IgG4-related disease (IgG4-RD) was proposed[5], and the diagnostic criteria for IgG4-RD were established in 2011[6]. IgG4-RD is a specific disease that presents with high serum levels of IgG4 and the enlargement of various organs including lacrimal glands, salivary glands, thyroid glands, lungs, pancreas, kidneys, and retroperitoneum. The histopathology of IgG4-RD includes remarkable IgG4-positive cell infiltration into plasma, fibrosis, and obliterative phlebitis. Type 1 AIP is considered to be a pancreatic lesion of IgG4-RD. However, the role of IgG4 in the phenotypic expression of AIP or IgG4-RD has not been clarified.

Here, we report a case of AIP compatible with type 1 AIP but without elevated levels of serum IgG4 and IgG4-positive plasma cells. This case suggests that the phenotype of type 1 AIP does not require an elevation of IgG4.

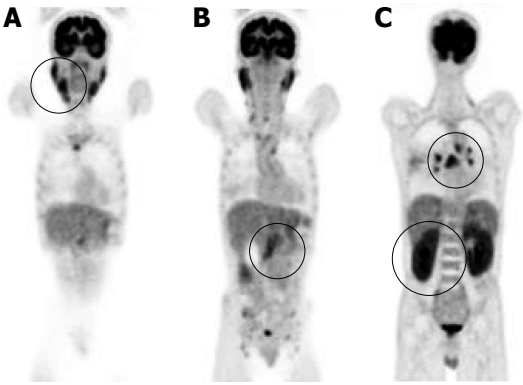

Figure 1 Findings of fluorodeoxyglucose-positron emission tomography. Positron emission tomography revealed high fluorodeoxyglucose uptake in various organs (uptake is indicated by circles). A: Submandibular glands (SUVmax 5.6) and parotid glands (SUVmax 5.8); B: Pancreas (SUVmax 4.2); C: Bilateral hilar of lymph nodes (SUVmax 7.3) and both kidneys (SUVmax 6.2).

CASE REPORT

A 50-year-old male with a history of hypertension was referred to our hospital for the evaluation of hyperproteinemia [total protein (TP), 10.0 g/da; normal range, 6.7-8.1]. He was diagnosed with hypergammaglobulinemia, and a bone marrow biopsy and fluorodeoxyglucose (FDG)-positron emission tomography (PET) were performed to rule out multiple myeloma. Multiple myeloma was excluded based on the bone marrow results; however, FDG-PET revealed high FDG uptake in several enlarged organs (Figure 1A-C). The patient was admitted to our department for further examination of the pancreas, which was swollen and exhibited high FDG uptake. A physical examination showed elastic, painless, and persistent swelling of the salivary and lacrimal glands. Laboratory data revealed elevated levels of alkaline phosphatase (ALP 386 IU/L; normal range, 115-359) and γ-glutamyl transpeptidase (γ-GTP 101 IU/L; normal range, 10-47), renal dysfunction [creatinine (Cr), 1.36 mg/dL; normal range, 0.44-1.15], and elevated levels of pancreatic enzymes (Amylase 245 IU/L; normal range, 37-125; Lipase 339 IU/L; normal range, 6-48).

Table 1 Laboratory data on admission

Test	Result	Reference range	Test	Result	Reference range	Test	Result	Reference range
WBC (10^3/μL)	6.0	4.0-9.0	TP (g/dL)	10.0	6.7-8.1	TG (mg/dL)	42	30-150
RBC (10^6/μL)	3.24	4.27-5.70	Albumin (%)	26.2	54.6-66.1	TC (mg/dL)	85	130-220
Hb (g/dL)	9.6	14.0-18.0	Alpha 1 (%)	3.0	2.7-4.3	GLU (mg/dL)	110	68-109
Ht (%)	28.4	40.0-52.0	Alpha 2 (%)	6.5	6.2-10.5	HbA1c (%)	6.4	4.6-6.2
Plt (10^3/μL)	215	150.0-350.0	Beta 1 (%)	3.7	5.0-7.5	CRP (mg/dL)	0.5	0.0-0.3
			Beta 2 (%)	n.c.	3.5-6.6			
T-Bil (IU/L)	0.4	0.2-1.0	Gamma (%)	60.6	12.3-22.8	IgG (mg/dL)	6564	870-1700
ALP (IU/L)	386	115-359	Alb (g/dL)	2.4	3.8-5.3	IgG1 (mg/dL)	4863	320-748
γ-GTP (IU/L)	101	10-47	BUN (mg/dL)	18.0	8-20	IgG2 (mg/dL)	919	208-754
AST (IU/L)	28	8-38	Cr (mg/dL)	1.36	0.44-1.15	IgG3 (mg/dL)	703	6.6-88.3
ALT (IU/L)	18	4-43	Na (mEq/L)	136.0	136-141	IgG4 (mg/dL)	78.2	4.8-105
LDH (IU/L)	187	119-229	K (mEq/L)	3.8	3.5-5.1	ANA (mg/dL)	(-)	
Lipase (IU/L)	339	6-48	Cl (mEq/L)	105.0	98-107	CEA (ng/dL)	1.1	0.0-5.0
Amylase (IU/L)	245	37-125	Ca (mg/dL)	8.0	8.6-10.1	CA19-9 (U/mL)	11.3	0.0-37.0

TP: Total protein; ALP: Alkaline phosphatase; GTP: Glutamyl transpeptidase.

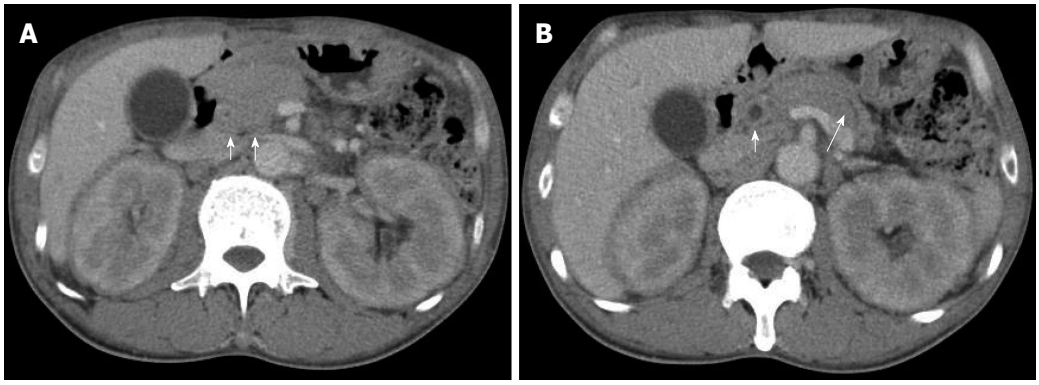

Figure 2 Findings of abdominal computed tomography. A: Localized swelling of the head of the pancreas (short arrows); B: Mild dilation of the upstream main pancreatic duct (long arrow), a thickened common bile duct wall (short arrow), and swelling of the kidneys.

The serum IgG levels were extremely high (6662 mg/dL; normal range, 870-1700); however, the serum IgG4 levels were normal (78.2 mg/dL; normal range, 4.8-105) (Table 1). Abdominal computed tomography (CT) revealed localized swelling of the head of the pancreas (Figure 2A), mild dilation of the upstream main pancreatic duct (MPD), a thickened common bile duct (CBD) wall, and swelling of the bilateral kidneys (Figure 2B). Endoscopic ultrasonography (EUS) showed hypoechoic swelling of the head of the pancreas and diffuse thickening of the CBD wall (Figure 3). Endoscopic retrograde cholangiopancreatography findings demonstrated irregular narrowing of the MPD in the head of the pancreas, dilation of the upstream MPD (Figure 4A), and a lower bile duct stricture (Figure 4B). Intraductal ultrasonography detected diffuse thickening of the bile duct wall (Figure 4C). We performed endoscopic ultrasonography-guided fine-needle aspiration (EUS-FNA) using a 19-gauge needle (Expect™; Boston-Scientific). Histological examination of the aspirate revealed marked lymphoplasmacytic infiltration (Figure 5A), storiform fibrosis, and obliterative phlebitis (Figure 5B). Immunohistochemistry showed an infiltration of CD38-positive plasma cells (Figure 5C and D); however, the infiltrating plasma cells were negative for IgG4 (Figure 5E). Furthermore, percutaneous biopsies of the swollen salivary glands and kidneys were performed to evaluate Mikulicz disease and intestinal nephritis. The results revealed remarkable lymphoplasmacytic infiltration and fibrosis. The histological diagnoses were sialadenitis and interstitial nephritis; however, the absence of IgG4-positive plasma cells was similar to the histological findings in the pancreas.

Prednisolone was orally administered at a dose of 30 mg/d to treat AIP and intestinal nephritis. After 3 wk of 30 mg/d dosing, the patient was weaned on 25 mg/d for 2 wk followed by 20 mg/d for 7 wk. Renal dysfunction and elevated hepatobiliary enzymes, pancreatic enzymes, and IgG improved with steroid treatment (Table 2). In addition, imaging modalities revealed that the enlargement of several organs, such as the pancreas, kidneys, salivary glands, and submandibular glands, was improved (Figure 6). FDG uptake in various organs was also reduced on FDG-PET (Figure 7).

The patient was diagnosed with AIP according to the ICDC, including pancreatic parenchymal imaging,

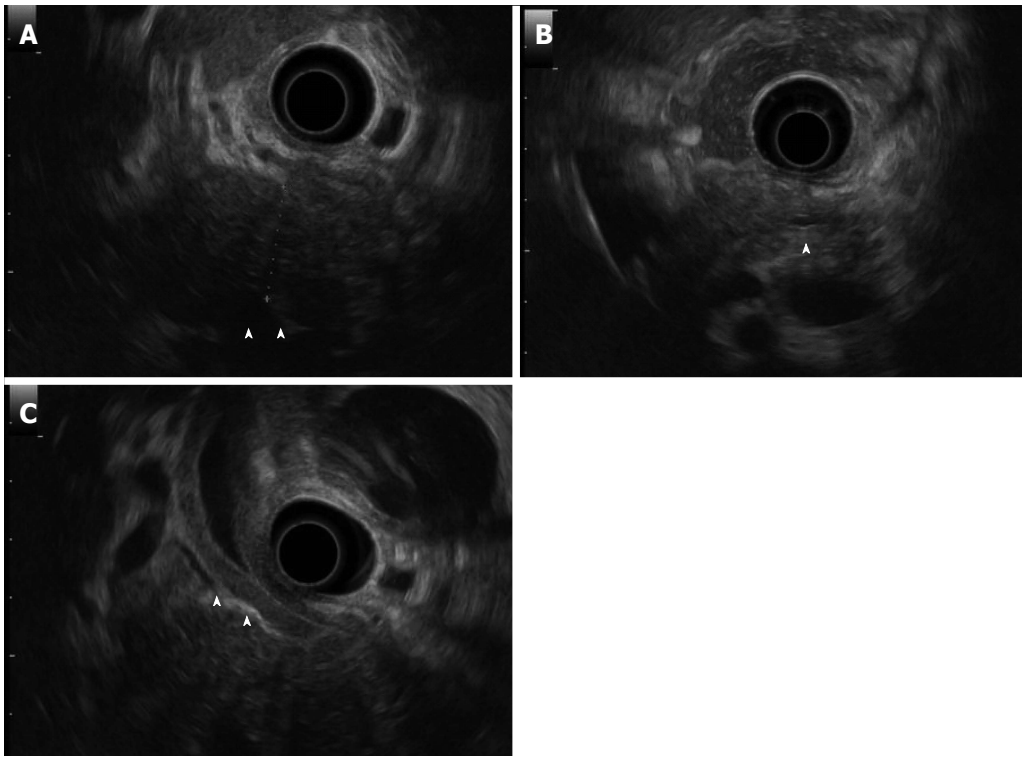

Figure 3 Findings of endoscopic ultrasonography. Endoscopic ultrasonography revealed hypoechoic swelling of the pancreatic head (A: arrowheads), mild dilation of the upstream main pancreatic duct (B: arrowheads), and diffuse thickness of the common bile duct wall (C: arrowheads).

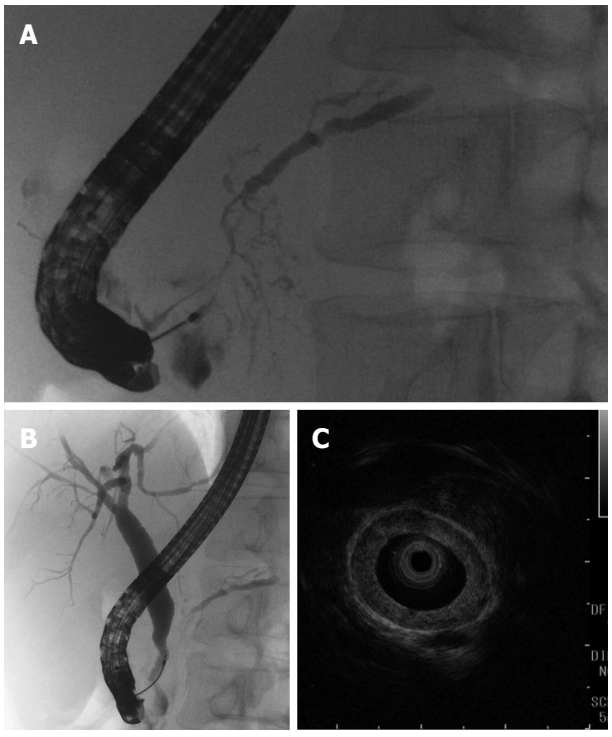

Figure 4 Findings of endoscopic retrograde cholangiopancreatography and intraductal ultrasonography. Endoscopic retrograde cholangiopancreatography revealed an irregular narrowing of the main pancreatic duct (MPD) in the pancreatic head and dilation of the upstream MPD (A); There was a lower bile duct stricture (B); and intraductal ultrasonography showed diffuse thickening of the bile duct wall (C).

irregular narrowing of MPD, other organ involvement (OOI), pancreas histology, and response to steroids; however, the serum IgG4 levels were not elevated. The patient was treated continuously with maintenance doses of prednisolone and was relapse-free after approximately 1 year.

DISCUSSION

The concept of AIP was proposed by Yoshida *et al*[1] in 1995. Recent studies suggested that there are two distinct subtypes of AIP: type 1 and type 2[7-9]. The histological descriptions of type 1 and 2 AIP are LPSP[10] and idiopathic duct-centric pancreatitis (IDCP) or granulocytic epithelial lesion (GEL)[11], respectively. The characteristic histological features of type 1 AIP are as follows: (1) marked lymphoplasmacytic infiltration with fibrosis and without granulocytic infiltration; (2) storiform fibrosis; (3) obliterative phlebitis; and (4) abundant [> 10 cells/high-power field (HPF)] IgG4-positive plasma cells. Type 1 AIP also has several specific clinical manifestations, such as increased serum levels of IgG4 and OOI and responsiveness to steroids[7]. Recently, IgG4-RD was recognized as a novel clinical entity with multiorgan involvement that is associated with the abundant infiltration of IgG4-positive plasma cells[5,6]. IgG4 may play a central role in the clinical features of IgG4-RD; however, the detailed pathophysiological mechanisms behind these

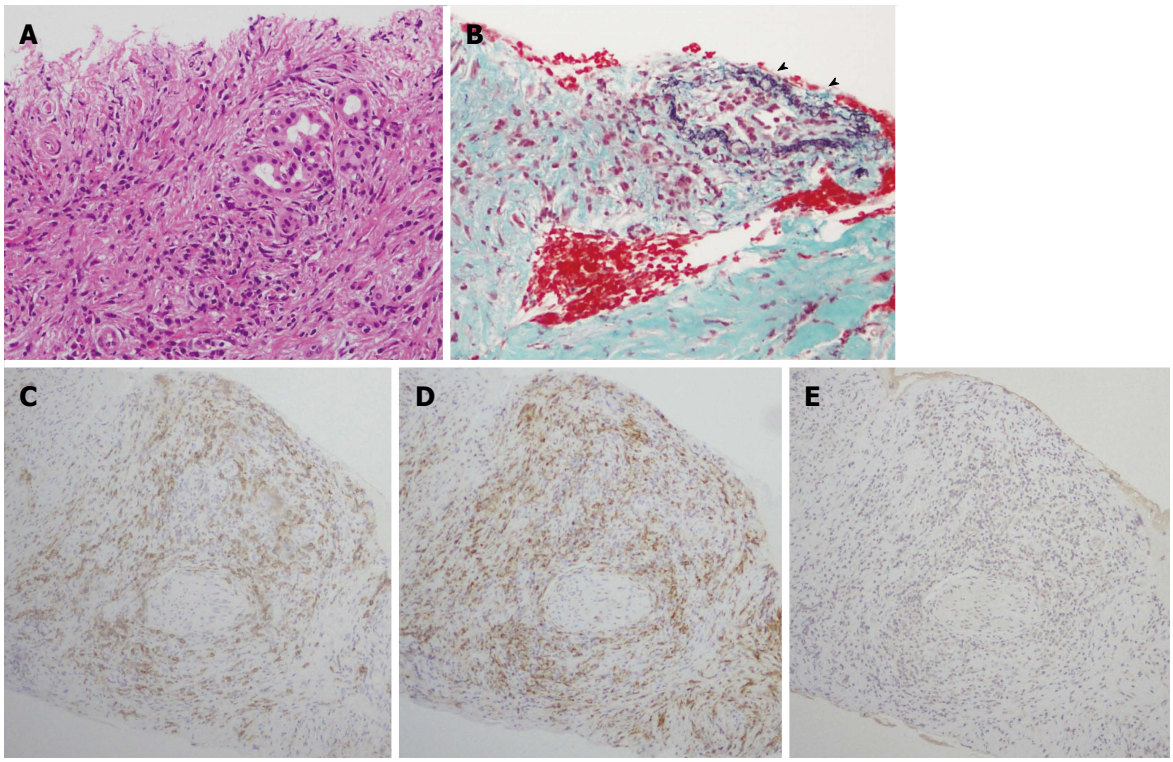

Figure 5 Histological findings of pancreas specimens. The histological examination revealed marked lymphoplasmacytic infiltration, storiform fibrosis, and obliterative phlebitis (arrowheads). Immunostaining showed CD38-positive plasma cells and CD163-positive spindle macrophage infiltration. However, no IgG4-positive plasma cells were detected. A: Hematoxylin and eosin staining (magnification × 200); B: Elastica-Masson's staining (magnification × 200); Immunohistochemical staining for CD38 (C), CD163 (D), and IgG4 (E) are also shown at magnification × 100.

Table 2 Laboratory data after steroid therapy

Test	Result	Reference range	Test	Result	Reference range	Test	Result	Reference range
WBC (10^3/μL)	9.3	4.0-9.0	TP (g/dL)	7.1	6.7-8.1	TG (mg/dL)	78	30-150
RBC (10^6/μL)	4.31	4.27-5.70	Albumin (%)	57.6	54.6-66.1	TC (mg/dL)	197	130-220
Hb (g/dL)	12.6	14.0-18.0	Alpha 1 (%)	4.7	2.7-4.3	GLU (mg/dL)	96	68-109
Ht (%)	38.4	40.0-52.0	Alpha 2 (%)	10.2	6.2-10.5	HbA1c (%)	5.8	4.6-6.2
Plt (10^3/μL)	203	150.0-350.0	Beta 1 (%)	5.7	5.0-7.5	CRP (mg/dL)	0.1	0.0-0.3
			Beta 2 (%)	3.4	3.5-6.6			
T-Bil (IU/L)	0.5	0.2-1.0	Gamma (%)	18.4	12.3-22.8	IgG (mg/dL)	1487	870-1700
ALP (IU/L)	292	115-359	Alb (g/dL)	3.9	3.8-5.3	IgG4 (mg/dL)	3.9	4.8-105
γ-GTP (IU/L)	30	10-47	BUN (mg/dL)	25.0	8-20	CEA (ng/dL)	1.3	0.0-5.0
AST (IU/L)	16	8-38	Cr (mg/dL)	0.98	0.44-1.15	CA19-9 (U/mL)	12.7	0.0-37.0
ALT (IU/L)	20	4-43	Na (mEq/L)	140	136-141			
LDH (IU/L)	203	119-229	K (mEq/L)	4.4	3.5-5.1			
Lipase (IU/L)	22	6-48	Cl (mEq/L)	104	98-107			
Amylase (IU/L)	44	37-125	Ca (mg/dL)	9.3	8.6-10.1			

effects are unclear.

This case was diagnosed with definitive type 1 AIP according to the ICDC and pancreas histology (LPSP; level 1). In this patient, parenchymal imaging, ductal imaging, and OOI were all level 2. Based on his response to steroid treatment, the only probable diagnosis was type 1 AIP. However, lymphoplasmacytic sclerosing pancreatitis without IgG4-positive plasma cells was detected in the pancreas fine needle aspirate specimens. ICDC recommends obtaining a core biopsy specimen or resection specimen for histological evaluation. However, we have previously reported that histological diagnosis of AIP is possible from an EUS-FNA specimen obtained using a 22G needle[12]. In the present case, we showed that EUS-FNA using a 19G needle provides an adequate tissue sample for histological diagnosis. Serum IgG4-negative AIP has been reported in several studies[13-16] and pediatric cases have also been reported[17]. These reports described that IgG4-negative AIP presents with weak symptoms such as abdominal pain and jaundice[13] as well as the appearance of OOI compared to IgG4-positive AIP[13,15,16]. The present case exhibited significant OOI in several organs, including the pancreas; however, there

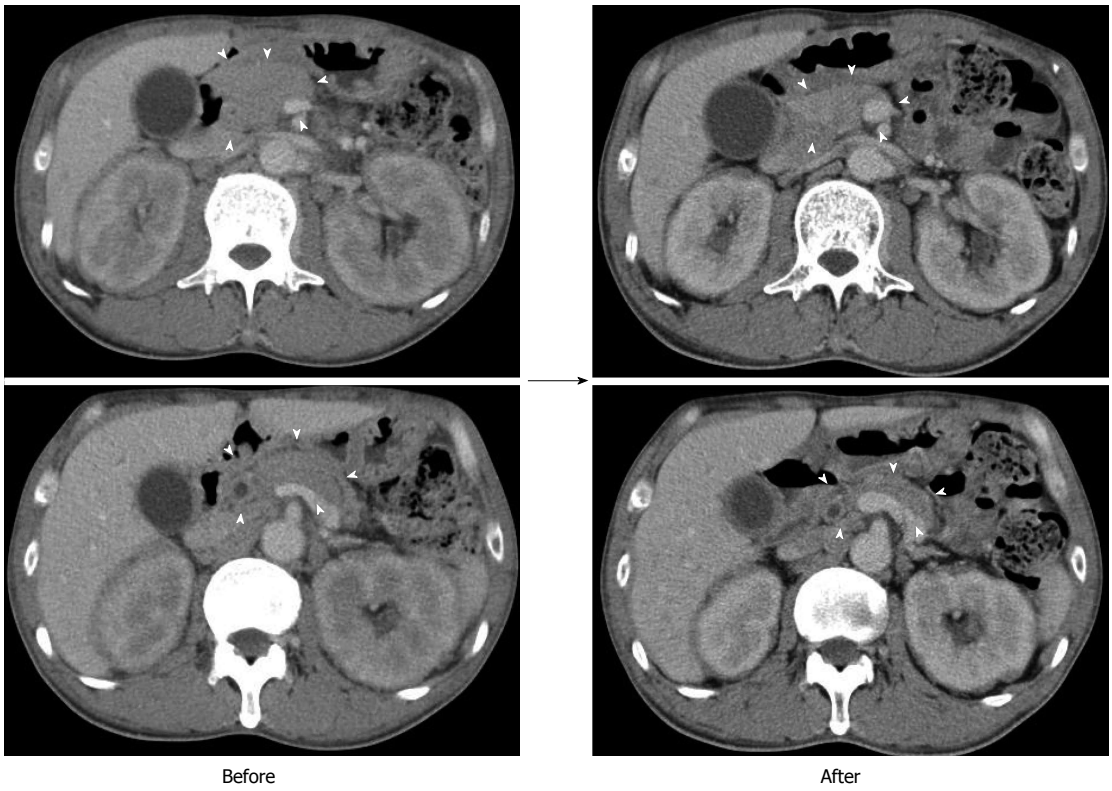

Figure 6 Findings of computed tomography after steroid therapy. Computed tomography showed improved the enlargement of the pancreas (indicated arrowheads) and kidneys.

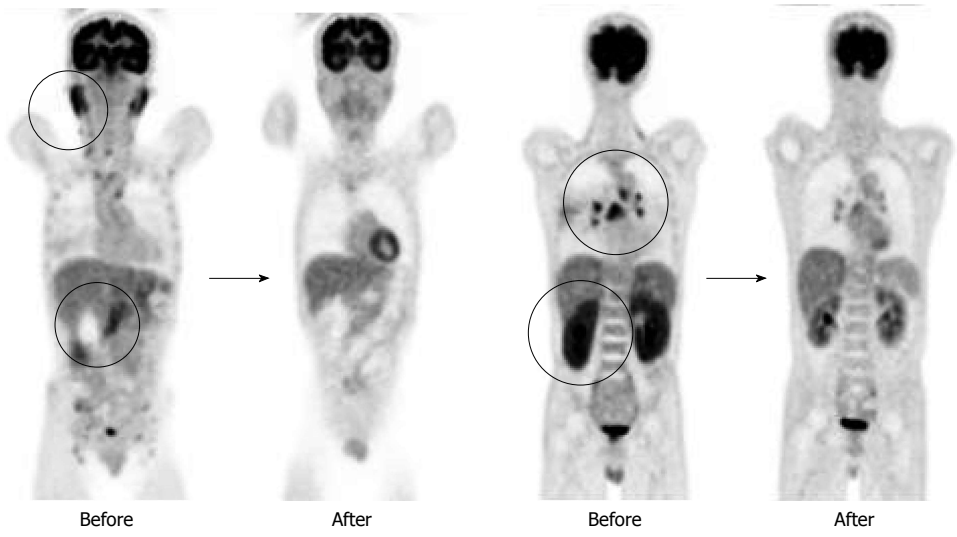

Figure 7 Findings of fluorodeoxyglucose-positron emission tomography after steroid therapy. Fluorodeoxyglucose (FDG)-positron emission tomography showed reduced FDG uptake in various organs.

was no elevation of the serum IgG4 levels or IgG4-positive plasma cell infiltration in the pancreas, salivary gland, or kidneys. In addition, the histological findings in this case revealed type I AIP without abundant IgG4-positive plasma cells. Since this case was not type 2 AIP and there was no IgG4-related type 1 AIP activity, the pathophysiological mechanism of this case may be different from the IgG4-negative AIP cases reported previously.

The mechanism by which IgG4 is produced is unclear. Several studies examining the mechanism of IgG4 production have been reported, including a T cell-dependent pathway and a T cell-independent pathway. For the T cell-dependent pathway, recent studies have described the increased production of regulatory T cell (Treg) and IL-10 in IgG4-RD tissues[18-20]. In addition, IL-10 was secreted by inducible costimulatory molecule (ICOS)-positive Tregs. The increased number of ICOS-

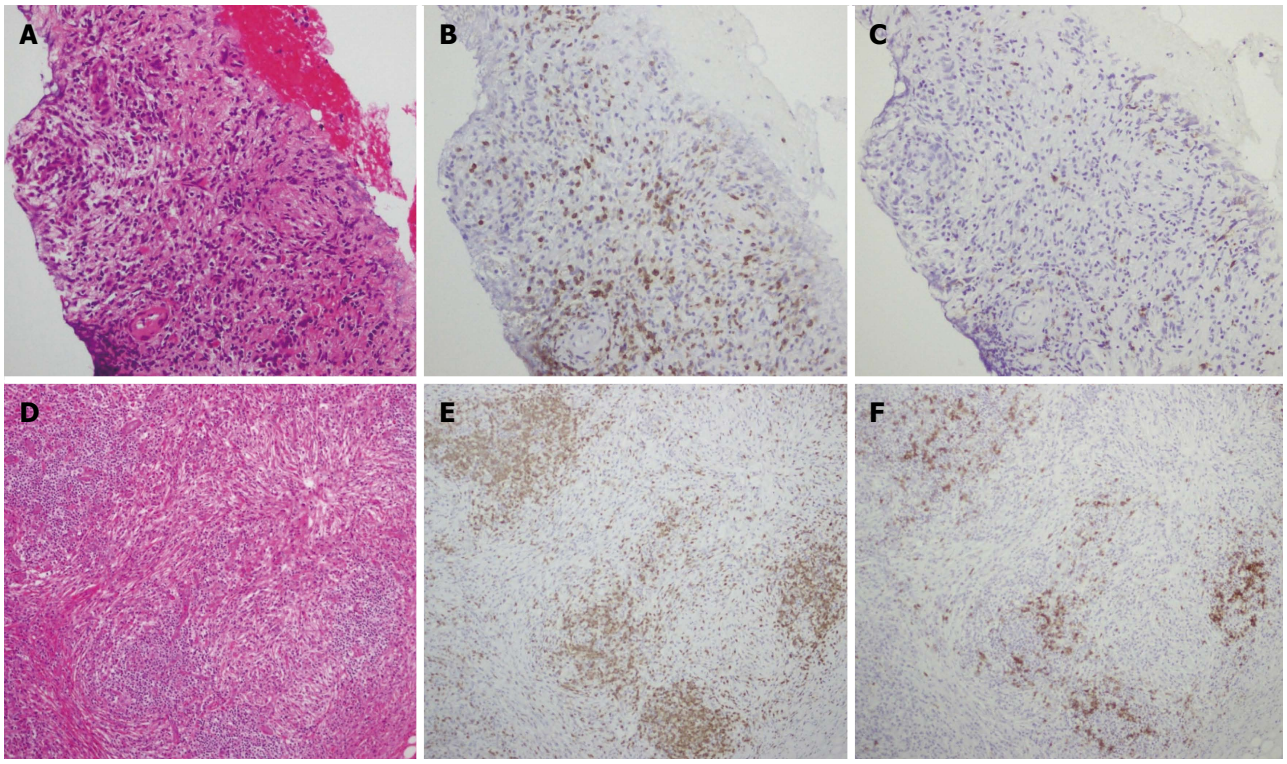

Figure 8 Histological findings of pancreas and salivary gland specimens. Pancreas and salivary gland tissues exhibited increased CD3-positive T cell infiltration compared with CD20-positive B cell infiltration. A-C: Pancreas (magnification × 100); D-F: salivary gland (magnification × 100); A, D: Hematoxylin and eosin staining; B, C, E, F: Immunohistochemical staining for CD38 (B, E) and CD20 (C, F).

positive Tregs correlated with the production of IL-10, which may influence the switching of B cells into IgG4-producing plasmacytes and the production of serum IgG4[21]. In contrast, the T cell-independent pathway involves the activation of toll-like receptors (TLRs) and nucleotide-binding oligomerization domain (NOD)-like receptors (NLRs) in monocytes by microbial antigens, which induces the production of IgG4 *via* the activation of B cell-activation factor (BAFF)-mediated signaling pathways[22,23].

There are several possible reasons for the absence of high serum IgG4 levels and IgG4-positive plasma cell infiltration in the present case. The first possible reason is an impaired class switch from IgG to IgG4. Although the elevated serum IgG concentrations in this case indicated intact IgG production, the low proportion of IgG4 suggested an impaired class switch to IgG4. In addition, immunostaining revealed a decrease in infiltrating CD20-positive B cells compared with that in CD3-positive T cells. Greater CD20-positive B cell infiltration than CD3-positive T cell infiltration is commonly observed in IgG4-negative AIP patients[13].

We evaluated pancreas aspirates with anti-CD3 and anti-CD20 antibodies to establish whether T cells or B cells were more active. In the present case, examination of the pancreas and salivary gland tissues revealed the presence of greater CD3-positive T cell infiltration than CD20-positive B cell infiltration (Figure 8). This finding was different from that in a previous report[13]. Our finding suggests that the IgG4-negative presentation is the result of a suppressed T cell-independent pathway, or of BAFF-mediated, reduced IgG4 production. The accumulation of further cases similar to the present one is required to clarify the pathogenesis of AIP.

In conclusion, we treated a patient with AIP whose symptoms were compatible with type 1 AIP but who did not show elevated serum IgG4 or IgG4-positive plasma cells in any involved organs. This finding suggests that the pathogenesis of type 1 AIP is not always associated with a mechanism involving the overproduction of IgG4.

COMMENTS

Case characteristics

A 50-year-old male was referred to our hospital for the evaluation of hyperproteinemia.

Clinical diagnosis

The physical examination showed elastic, painless, and persistent swelling of the salivary and lacrimal glands.

Differential diagnosis

Autoimmune pancreatitis, IgG4-related disease, sialadenitis, interstitial nephritis.

Laboratory diagnosis

An elevation of hepatobiliary enzymes (386 IU/L alkaline phosphatase, 101 IU/L γ-glutamyl transpeptidase) and pancreatic enzymes (245 IU/L serum amylase, 339 IU/L serum lipase), renal dysfunction (1.36 mg/dL creatinine), and the

serum levels of IgG were extremely high (6,662 mg/dL); however, serum IgG4 levels were normal (78.2 mg/dL).

Imaging diagnosis

Fluorodeoxyglucose (FDG)-positron emission tomography revealed high FDG uptake in the pancreas, both lacrimal glands, submandibular glands, parotid glands, bilateral pulmonary hilar lymph nodes, kidneys, and an abdominal computed tomography depicted localized swelling of the pancreatic head, mild dilation of the upstream main pancreatic duct, a thickened common bile duct wall, swelling of the bilateral kidneys.

Pathological diagnosis

The histological findings by endoscopic ultrasonography-guided fine-needle aspiration revealed lymphoplasmacytic sclerosing pancreatitis without IgG4-positive plasma cells, and percutaneous biopsies of the swollen salivary glands and kidneys showed remarkable lymphoplasmacytic infiltration and fibrosis.

Treatment

Prednisolone was orally administered at a dose of 30 mg/d to treat autoimmune pancreatitis (AIP) and intestinal nephritis.

Related reports

Serum IgG4-negative AIP has been reported in several studies. These reports described that IgG4-negative AIP presents with weak symptoms such as abdominal pain and jaundice as well as the appearance of other organ involvement (OOI) compared to IgG4-positive AIP. This patient exhibited significant OOI in several organs; however, there was no elevation of the serum IgG4 levels or IgG4-positive plasma cell infiltration. This case might differ from the IgG4-negative AIP cases reported previously.

Experiences and lessons

This case exhibited significant OOI in several organs including the pancreas; however, there was no elevation of the serum IgG4 levels or IgG4-positive plasma cell infiltration in the pancreas, salivary gland, or kidneys; this case suggests that the phenotype of type 1 AIP does not require IgG4 elevation.

Peer-review

The authors have provided an extensive review on the various known phenotypes of AIP and their case report offers insight into a less common phenotype. This article suggests that the pathogenesis of type 1 AIP is not always associated with a mechanism involving the overproduction of IgG4.

REFERENCES

1 **Yoshida K**, Toki F, Takeuchi T, Watanabe S, Shiratori K, Hayashi N. Chronic pancreatitis caused by an autoimmune abnormality. Proposal of the concept of autoimmune pancreatitis. *Dig Dis Sci* 1995; **40**: 1561-1568 [PMID: 7628283]

2 **Kamisawa T**, Notohara K, Shimosegawa T. Two clinicopathologic subtypes of autoimmune pancreatitis: LPSP and IDCP. *Gastroenterology* 2010; **139**: 22-25 [PMID: 20639082 DOI: 10.1053/j.gastro.2010.05.019]

3 **Members of the Criteria Committee for Autoimmune Pancreatitis of the Japan Pancreas Society**. Diagnostic criteria for autoimmune pancreatitis by the Japan Pancreas Society. *J Jpn Pancreas* (Suizou) 2002; **17**: 585-587

4 **Hamano H**, Kawa S, Horiuchi A, Unno H, Furuya N, Akamatsu T, Fukushima M, Nikaido T, Nakayama K, Usuda N, Kiyosawa K. High serum IgG4 concentrations in patients with sclerosing pancreatitis. *N Engl J Med* 2001; **344**: 732-738 [PMID: 11236777]

5 **Umehara H**, Okazaki K, Masaki Y, Kawano M, Yamamoto M, Saeki T, Matsui S, Sumida T, Mimori T, Tanaka Y, Tsubota K, Yoshino T, Kawa S, Suzuki R, Takegami T, Tomosugi N, Kurose N, Ishigaki Y, Azumi A, Kojima M, Nakamura S, Inoue D. A novel clinical entity, IgG4-related disease (IgG4RD): general concept and details. *Mod Rheumatol* 2012; **22**: 1-14 [PMID: 21881964 DOI: 10.1007/s10165-011-0508-6]

6 **Umehara H**, Okazaki K, Masaki Y, Kawano M, Yamamoto M, Saeki T, Matsui S, Yoshino T, Nakamura S, Kawa S, Hamano H, Kamisawa T, Shimosegawa T, Shimatsu A, Nakamura S, Ito T, Notohara K, Sumida T, Tanaka Y, Mimori T, Chiba T, Mishima M, Hibi T, Tsubouchi H, Inui K, Ohara H. Comprehensive diagnostic criteria for IgG4-related disease (IgG4-RD), 2011. *Mod Rheumatol* 2012; **22**: 21-30 [PMID: 22218969 DOI: 10.1007/s10165-011-0571-z]

7 **Shimosegawa T**, Chari ST, Frulloni L, Kamisawa T, Kawa S, Mino-Kenudson M, Kim MH, Klöppel G, Lerch MM, Löhr M, Notohara K, Okazaki K, Schneider A, Zhang L. International consensus diagnostic criteria for autoimmune pancreatitis: guidelines of the International Association of Pancreatology. *Pancreas* 2011; **40**: 352-358 [PMID: 21412117 DOI: 10.1097/MPA.0b013e3182142fd2]

8 **Chari ST**, Kloeppel G, Zhang L, Notohara K, Lerch MM, Shimosegawa T. Histopathologic and clinical subtypes of autoimmune pancreatitis: the Honolulu consensus document. *Pancreas* 2010; **39**: 549-554 [PMID: 20562576 DOI: 10.1097/MPA.0b013e3181e4d9e5]

9 **Chari ST**, Kloeppel G, Zhang L, Notohara K, Lerch MM, Shimosegawa T. Histopathologic and clinical subtypes of autoimmune pancreatitis: the honolulu consensus document. *Pancreatology* 2010; **10**: 664-672 [PMID: 21242705 DOI: 10.1159/000318809]

10 **Kawaguchi K**, Koike M, Tsuruta K, Okamoto A, Tabata I, Fujita N. Lymphoplasmacytic sclerosing pancreatitis with cholangitis: a variant of primary sclerosing cholangitis extensively involving pancreas. *Hum Pathol* 1991; **22**: 387-395 [PMID: 2050373]

11 **Notohara K**, Burgart LJ, Yadav D, Chari S, Smyrk TC. Idiopathic chronic pancreatitis with periductal lymphoplasmacytic infiltration: clinicopathologic features of 35 cases. *Am J Surg Pathol* 2003; **27**: 1119-1127 [PMID: 12883244]

12 **Kanno A**, Ishida K, Hamada S, Fujishima F, Unno J, Kume K, Kikuta K, Hirota M, Masamune A, Satoh K, Notohara K, Shimosegawa T. Diagnosis of autoimmune pancreatitis by EUS-FNA by using a 22-gauge needle based on the International Consensus Diagnostic Criteria. *Gastrointest Endosc* 2012; **76**: 594-602 [PMID: 22898417]

13 **Kamisawa T**, Takuma K, Tabata T, Inaba Y, Egawa N, Tsuruta K, Hishima T, Sasaki T, Itoi T. Serum IgG4-negative autoimmune pancreatitis. *J Gastroenterol* 2011; **46**: 108-116 [PMID: 20824290 DOI: 10.1007/s00535-010-0317-2]

14 **Zhang MM**, Zou DW, Wang Y, Zheng JM, Yang H, Jin ZD, Li ZS. Contrast enhanced ultrasonography in the diagnosis of IgG4-negative autoimmune pancreatitis: A case report. *J Interv Gastroenterol* 2011; **1**: 182-184 [PMID: 22586534]

15 **Paik WH**, Ryu JK, Park JM, Song BJ, Park JK, Kim YT, Lee K. Clinical and pathological differences between serum immunoglobulin G4-positive and -negative type 1 autoimmune pancreatitis. *World J Gastroenterol* 2013; **19**: 4031-4038 [PMID: 23840149 DOI: 10.3748/wjg.v19.i25.4031]

16 **Ghazale A**, Chari ST, Smyrk TC, Levy MJ, Topazian MD, Takahashi N, Clain JE, Pearson RK, Pelaez-Luna M, Petersen BT, Vege SS, Farnell MB. Value of serum IgG4 in the diagnosis of autoimmune pancreatitis and in distinguishing it from pancreatic cancer. *Am J Gastroenterol* 2007; **102**: 1646-1653 [PMID: 17555461]

17 **Friedlander J**, Quiros JA, Morgan T, Zhang Z, Tian W, Kehr E, Shackleton DV, Zigman A, Stenzel P. Diagnosis of autoimmune pancreatitis vs neoplasms in children with pancreatic mass and biliary obstruction. *Clin Gastroenterol Hepatol* 2012; **10**: 1051-1055. e1 [PMID: 22732272]

18 **Zen Y**, Fujii T, Harada K, Kawano M, Yamada K, Takahira M, Nakanuma Y. Th2 and regulatory immune reactions are increased in immunoglobin G4-related sclerosing pancreatitis and cholangitis. *Hepatology* 2007; **45**: 1538-1546 [PMID: 17518371]

19 **Tanaka A**, Moriyama M, Nakashima H, Miyake K, Hayashida JN, Maehara T, Shinozaki S, Kubo Y, Nakamura S. Th2 and regulatory immune reactions contribute to IgG4 production and the initiation of Mikulicz disease. *Arthritis Rheum* 2012; **64**: 254-263 [PMID: 21898360 DOI: 10.1002/art.33320]

20 **Akitake R**, Watanabe T, Zaima C, Uza N, Ida H, Tada S, Nishida N, Chiba T. Possible involvement of T helper type 2 responses to Toll-like receptor ligands in IgG4-related sclerosing disease. *Gut* 2010;

59: 542-545 [PMID: 20332525 DOI: 10.1136/gut.2009.200972]
21 **Kusuda T**, Uchida K, Miyoshi H, Koyabu M, Satoi S, Takaoka M, Shikata N, Uemura Y, Okazaki K. Involvement of inducible costimulator- and interleukin 10-positive regulatory T cells in the development of IgG4-related autoimmune pancreatitis. *Pancreas* 2011; **40**: 1120-1130 [PMID: 21926547 DOI: 10.1097/MPA.0b013e31821fc796]
22 **Watanabe T**, Yamashita K, Fujikawa S, Sakurai T, Kudo M, Shiokawa M, Kodama Y, Uchida K, Okazaki K, Chiba T. Involvement of activation of toll-like receptors and nucleotide-binding oligomerization domain-like receptors in enhanced IgG4 responses in autoimmune pancreatitis. *Arthritis Rheum* 2012; **64**: 914-924 [PMID: 21971969 DOI: 10.1002/art.33386]
23 **Watanabe T**, Yamashita K, Sakurai T, Kudo M, Shiokawa M, Uza N, Kodama Y, Uchida K, Okazaki K, Chiba T. Toll-like receptor activation in basophils contributes to the development of IgG4-related disease. *J Gastroenterol* 2013; **48**: 247-253 [PMID: 22744834 DOI: 10.1007/s00535-012-0626-8]

P- Reviewer: Abu-El-Haija M, Kamisawa T, Moon JH
S- Editor: Ma YJ **L- Editor**: A **E- Editor**: Wang CH

World Journal of Gastroenterology

Submit a Manuscript: http://www.wjgnet.com/esps/
Help Desk: http://www.wjgnet.com/esps/helpdesk.aspx
DOI: 10.3748/wjg.v21.i33.9817

World J Gastroenterol 2015 September 7; 21(33): 9817-9821
ISSN 1007-9327 (print) ISSN 2219-2840 (online)

CASE REPORT

Perforated appendiceal diverticulitis associated with appendiceal neurofibroma in neurofibromatosis type 1

Akihiko Ozaki, Manabu Tsukada, Kazuo Watanabe, Masaharu Tsubokura, Shigeaki Kato, Tetsuya Tanimoto, Masahiro Kami, Hiromichi Ohira, Yukio Kanazawa

Akihiko Ozaki, Manabu Tsukada, Hiromichi Ohira, Division of Surgery, Minamisoma Municipal General Hospital, Fukushima 975-0033, Japan

Kazuo Watanabe, Division of Diagnostic Pathology, Fukushima Pathology Laboratory, Fukushima 960-8164, Japan

Masaharu Tsubokura, Masahiro Kami, Division of Social Communication System for Advanced Clinical Research, Institute of Medical Science, University of Tokyo, Minato-ku, Tokyo 108-0071, Japan

Shigeaki Kato, Division of Internal Medicine, Soma Central Hospital, Fukushima 976-0016, Japan

Tetsuya Tanimoto, Jyoban Hospital of Tokiwakai Group, Fukushima 972-8322, Japan

Yukio Kanazawa, Division of Endoscopy, Minamisoma Municipal General Hospital, Fukushima 975-0033, Japan

Author contributions: Ozaki A, Tsukada M and Ohira H performed an operation, managed the patient, and wrote the paper; Watanabe K performed a pathological examination, and contributed to the conception and the design of the study; Tsubokura M, Kato K, Tanimoto T, Kami M and Kanazawa Y contributed to the conception and the design of the study.

Institutional review board statement: The study was reviewed and approved by the Minamisoma Municipal General Hospital Institutional Review Board.

Informed consent statement: The study participant provided informed written consent prior to the study enrollment.

Conflict-of-interest statement: The authors declare no conflicts of interest.

Correspondence to: Akihiko Ozaki, MD, Division of Surgery, Minamisoma Municipal General Hospital, 54-6 Takamicho 2chome, Haramachi, Minamisoma, Fukushima 975-0033, Japan. aozaki-tky@umin.ac.jp
Telephone: +81-244-223181
Fax: +81-244-228853

Received: April 4, 2015
Peer-review started: April 4, 2015
First decision: May 18, 2015
Revised: June 3, 2015
Accepted: July 8, 2015
Article in press: July 8, 2015
Published online: September 7, 2015

Abstract

An appendiceal neurofibroma (ANF) is a rare neoplasm associated with neurofibromatosis type 1(NF-1), an inheritable neurocutaneous disorder that involves multiple systems including the intraabdominal organs. Appendiceal diverticulitis occasionally ruptures in the absence of intense abdominal pain, which can lead to serious consequences. Recent reports highlight the association between appendiceal diverticulum and appendiceal neoplasms; however, there is still little information on the association between appendiceal diverticulitis and ANF in NF-1. A 51-year-old Japanese male with NF-1 was referred to the division of surgery for mild right lower quadrant pain. It was suspected he had perforated acute appendicitis with periappendiceal abscess based on clinical manifestations and findings of computed tomography. An emergency appendectomy was conducted. The pathological examination revealed diffusely proliferated tumor cells of a neurofibroma, coexistent with multiple appendiceal diverticulums, leading to the diagnosis of

perforated appendiceal diverticulitis associated with ANF. Although he developed a remnant abscess, he recovered with the conservative treatments of antibiotics and drainage. This case suggests that appendiceal diverticulitis might be a complication of appendiceal involvement of NF-1, and that it occasionally ruptures in the absence of intense abdominal pain. Clinicians should recognize that NF-1 can cause various abdominal manifestations.

Key words: Appendiceal diverticulum; Appendiceal diverticulitis; Neurofibromatosis type 1; Appendiceal neurofibroma; Appendiceal perforation

Core tip: An appendiceal neurofibroma (ANF) is a rare neoplasm associated with neurofibromatosis type 1 (NF-1), an inheritable neurocutaneous disorder that involves multiple systems including the intraabdominal organs. Appendiceal diverticulitis occasionally ruptures in the absence of intense abdominal pain, which can lead to serious consequences. There is still little information on the association between appendiceal diverticulitis and ANF in NF-1. This patient presented with NF-1 and developed an ANF, complicated with appendiceal diverticulitis, which highlights the possible association of appendiceal diverticulitis and ANF in NF-1. This case could be used to enhance clinicians' awareness of abdominal manifestations in NF-1.

Ozaki A, Tsukada M, Watanabe K, Tsubokura M, Kato S, Tanimoto T, Kami M, Ohira H, Kanazawa Y. Perforated appendiceal diverticulitis associated with appendiceal neurofibroma in neurofibromatosis type 1. *World J Gastroenterol* 2015; 21(33): 9817-9821 Available from: URL: http://www.wjgnet.com/1007-9327/full/v21/i33/9817.htm DOI: http://dx.doi.org/10.3748/wjg.v21.i33.9817

INTRODUCTION

Neurofibromatosis type 1 (NF-1) is one of the most common inheritable diseases[1]. It is a neurocutaneous disorder that possesses a high risk of multiple tumor formation[2]. It can involve intraabdominal organs as well as the nervous system and the skin[1,2].

An appendiceal neurofibroma (ANF) is a rare neoplasm associated with NF-1[3-6]. It typically presents with an appendicitis-like abdominal pain[3,4,7]. Imaging study shows an enlarged and diffusely thickened appendix[4-6]. Surgical resection is the standard treatment[4-8].

Appendiceal diverticulitis occasionally ruptures in the absence of an intense abdominal pain, and some patients develop serious consequences such as secondary peritonitis and abdominal abscesses[9-11]. In addition, it is more likely to rupture compared with acute appendicitis[9-11]. While an association between appendiceal diverticulum and appendiceal neoplasms has recently been reported[12,13], little is known about the association between appendiceal diverticulitis and ANF in NF-1. This report focuses on a patient with NF-1 who developed an ANF, complicated by appendiceal diverticulitis.

Figure 1 Enhanced computed tomography. The abdominal scan showed a periappendiceal abscess (arrow).

CASE REPORT

A fifty-one-year old Japanese male with NF-1 presented with mild right lower quadrant pain that lasted one week. He was diagnosed with NF-1 due to café-au-lait spots and cutaneous neurofibromas at age of twenty-five, thereafter his skin lesions gradually worsened.

At the initial examination, he was afebrile, but there was localized rigidity with mild tenderness in the right lower quadrant. His white blood cell count was 13580/mL with 84% neutrophils. Serum levels of C-reactive protein were 7.26 mg/dL (normal value: < 0.3 mg/dL). An emergent abdominal computed tomography showed an inflamed and diffusely thickened appendix and abdominal abscess (Figure 1). Based on the clinical diagnosis of perforated acute appendicitis with periappendiceal abscess, an emergency laparotomy was conducted. A lower midline incision was performed to successfully drain the abdominal abscess. The appendix was thickened diffusely, perforated, and surrounded by a malodorous abscess (Figure 2). The appendix was successfully resected, and the abscess was drained. During the surgery, drainage tubes were placed in the rectovesical pouch and the abscess cavity, respectively. Drainage from the rectovesical pouch was serous, and the tube was removed six days after the surgery, when the amount of drainage decreased. However, even one week after the surgery, the drainage from the abscess cavity remained purulent, leading to the diagnosis of a remnant abscess. The patient received the conservative treatments of antibiotics and drainage, and the amount of the exudates via the tube gradually decreased. The tube was removed twenty-two days

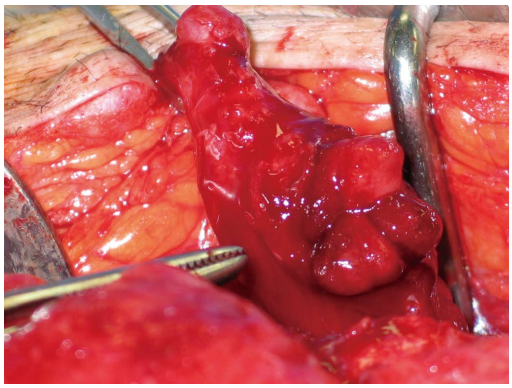

Figure 2 Surgical findings. The appendix of the patient was diffusely thickened and inflamed, with perforation.

after the surgery. He was discharged twenty-three days after the surgery.

The resected appendix was thickened diffusely and stiffened. A pathological examination showed diffuse proliferation of the tumor cells of a neurofibroma (Figure 3A), coexisting with multiple diverticulums (Figure 3B). The majority of diverticulums were small in size, causing subtle epithelial herniation. The final diagnosis was perforated appendiceal diverticulitis associated with ANF.

DISCUSSION

This case suggests that appendiceal diverticulitis may be a complication of ANF in NF-1. We cannot deny the possibility of coincidental occurrence of the two diseases since little information is available concerning the association between appendiceal diverticulitis and ANF in NF-1. However, recent studies suggest that appendiceal diverticulum might be a complication of appendiceal neoplasms[12,13]. It is speculated that tumor cells proliferating in the appendiceal wall contribute to elevation of the intraluminal pressure by obstructing the appendicular root and/or by stiffening and thickening the appendiceal wall. This process is thought to lead to the development of appendiceal diverticulum and diverticulitis[12]. The present case was compatible with these reports, considering that the appendix including its root was diffusely thickened and stiffened as a result of diffuse proliferation of the tumor cells. Evidence of elevated intraluminal pressure was not apparent because the patient presented after the development of perforation. Furthermore, the status of NF-1 was progressive in the present case. A recent study has shown that gastrointestinal neurofibromas in NF-1, including an ANF, arise during midlife or after the development of skin lesions[1]. In the present case, the majority of appendiceal diverticulums were small in size, suggesting that they were in the early phase of development[13]. Thus, it is reasonable to assume that appendiceal diverticulums and ANF concurrently developed. These findings support the possible association between appendiceal diverticulitis and ANF in NF-1.

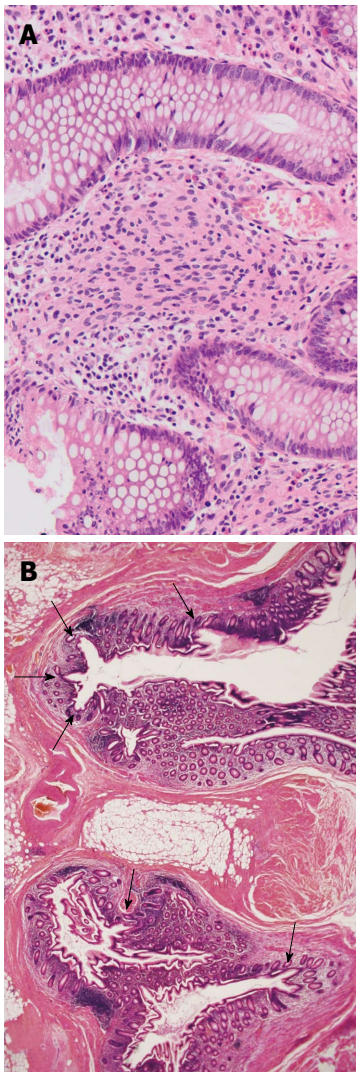

Figure 3 Pathological findings (Hematoxylin-eosin staining). A: Spindle shaped tumor cells proliferated diffusely in the interstitium between the crypts, without forming a distinct mass (magnification × 10); B: Multiple diverticulums were present in the wall of the appendix. The majority of diverticulums were small in size, causing subtle epithelial herniation (magnification × 1).

It is to be noted that the appendix ruptured in the absence of an intense abdominal pain. This finding is compatible with previous reports on appendiceal diverticulitis[9-11], while exact pathogenesis remains to be clarified. Appendiceal diverticulitis frequently presents with a mild right lower quadrant pain and more indolent clinical courses, compared with acute appendicitis[9,10]. However, it can easily rupture because the development of appendiceal diverticulum induces the epithelial herniation through the muscularis propria, which causes the thinning of appendiceal wall[10,11,14]. This case shows that perforation of the appendiceal diverticulum can cause a massive abdominal abscess. It is important to make an early diagnosis, and to initiate appropriate treatments promptly to avoid severe sequelae such

as secondary peritonitis when patients with NF-1 develop appendiceal diverticulitis[9-11]. Visualization of the appendiceal diverticulum using abdominal ultrasonography might be useful in the preoperative diagnosis of appendiceal diverticulitis[11,15,16].

NF-1 can cause various abdominal manifestations. Abdominal neurofibromas can arise from the esophagus to the anorectum, and also in the associated peritoneal and mesenteric soft tissues[1]. Other than neurofibromas, gastrointestinal stromal tumors and neuroendocrine tumors may occur[17]. An early diagnosis is important, considering the risk of malignancy and complications, such as hemorrhage, obstruction, and perforation[17,18]. However, a recent report indicates abdominal manifestations of NF-1 rarely come into the mind of clinicians due to a lack of knowledge about their frequency and wide clinicopathological spectrum[1]. Awareness of abdominal manifestations holds great importance in the management of NF-1, as it has been shown that a considerable number of patients with NF-1 develop abdominal tumors[17].

In conclusion, this case suggests that appendiceal diverticulitis might be a complication of appendiceal involvement of NF-1, and that it occasionally ruptures even in the absence of intense abdominal pain. Clinicians should recognize that NF-1 can cause various abdominal manifestations.

COMMENTS

Case characteristics

A fifty-one-year old Japanese male with neurofibromatosis type 1 presented with mild right lower quadrant pain that lasted one week.

Clinical diagnosis

The patient was afebrile, but there was localized rigidity with mild tenderness in the right lower quadrant.

Differential diagnosis

Based on the pathological findings, the diagnosis of appendiceal diverticulitis and appendiceal neurofibroma was made, although the clinical diagnosis was perforated acute appendicitis with periappendiceal abscess.

Laboratory diagnosis

The patient had elevated hematological values for white blood cell count (13580/mL) with 84% neutrophils, and C-reactive protein (7.26 mg/dL).

Imaging diagnosis

An emergent abdominal computed tomography showed an inflamed and diffusely thickened appendix and abdominal abscess.

Pathological diagnosis

The pathological examination revealed diffusely proliferated tumor cells of a neurofibroma, coexistent with multiple appendiceal diverticulums.

Treatment

An emergency appendectomy and the following conservative treatments of antibiotics and drainage were conducted.

Related reports

An appendiceal neurofibroma is a rare neoplasm associated with neurofibromatosis type 1. Appendiceal diverticulitis occasionally ruptures in the absence of intense abdominal pain. Although recent reports highlight the association between appendiceal diverticulum and appendiceal neoplasms, there is still little information on the association between appendiceal diverticulitis and appendiceal neurofibroma in neurofibromatosis type 1.

Term explanation

An appendiceal neurofibroma is a rare neoplasm associated with neurofibromatosis type 1.

Experiences and lessons

This case suggests that appendiceal diverticulitis might be a complication of appendiceal involvement of neurofibromatosis type 1, and that it occasionally ruptures in the absence of intense abdominal pain.

Peer-review

This report highlights the possible association of appendiceal diverticulitis and appendiceal neurofibroma in neurofibromatosis type 1. This case could be used to enhance clinicians' awareness of abdominal manifestations in neurofibromatosis type 1, while whether this case is just rare in clinical settings or if this case represents other patients remains to be elucidated.

REFERENCES

1 **Agaimy A**, Vassos N, Croner RS. Gastrointestinal manifestations of neurofibromatosis type 1 (Recklinghausen's disease): clinicopathological spectrum with pathogenetic considerations. *Int J Clin Exp Pathol* 2012; **5**: 852-862 [PMID: 23119102]

2 **Ferner RE**. Neurofibromatosis 1 and neurofibromatosis 2: a twenty first century perspective. *Lancet Neurol* 2007; **6**: 340-351 [PMID: 17362838 DOI: 10.1016/S1474-4422(07)70075-3]

3 **Agaimy A**, Märkl B, Kitz J, Wünsch PH, Arnholdt H, Füzesi L, Hartmann A, Chetty R. Peripheral nerve sheath tumors of the gastrointestinal tract: a multicenter study of 58 patients including NF1-associated gastric schwannoma and unusual morphologic variants. *Virchows Arch* 2010; **456**: 411-422 [PMID: 20155280 DOI: 10.1007/s00428-010-0886-8]

4 **Samuel I**, Jakate S, Ramsey MM, Saclarides TJ. Abdominal mass in a 19-year-old with neurofibromatosis. *Postgrad Med J* 1997; **73**: 325-326 [PMID: 9246326 DOI: 10.1136/pgmj.73.860.325]

5 **Guo L**, He K, Xu X, Li G, Li Z, Xia Y, Teng X, Teng L. Giant appendiceal neurofibroma in von Recklinghausen's disease: A case report and literature review. *Oncol Lett* 2014; **8**: 1957-1960 [PMID: 25295078 DOI: 10.3892/ol.2014.2498]

6 **Lockhart ME**, Smith JK, Canon CL, Morgan DE, Heslin MJ. Appendiceal ganglioneuromas and pheochromocytoma in neurofibromatosis type 1. *AJR Am J Roentgenol* 2000; **175**: 132-134 [PMID: 10882262 DOI: 10.2214/ajr.175.1.1750132]

7 **Merck C**, Kindblom LG. Neurofibromatosis of the appendix in von Recklinghausen's disease. A report of a case. *Acta Pathol Microbiol Scand A* 1975; **83**: 623-627 [PMID: 811083 DOI: 10.1111/j.1699-0463.1975.tb01389.x]

8 **Rosenberg E**, Sheiner E, Holcberg G. Neurofibromatosis type 1 and masses of the appendix: a case report. *J Reprod Med* 2006; **51**: 578-580 [PMID: 16913550]

9 **Lobo-Machín I**, Delgado-Plasencia L, Hernández-González I, Brito-García A, Burillo-Putze G, Bravo-Gutiérrez A, Martínez-Riera A, Medina-Arana V. Appendiceal diverticulitis and acute appendicitis: differences and similarities. *Rev Esp Enferm Dig* 2014; **106**: 452-458 [PMID: 25490164]

10 **Kabiri H**, Clarke LE, Tzarnas CD. Appendiceal diverticulitis. *Am Surg* 2006; **72**: 221-223 [PMID: 16553122]

11 **Yamana I**, Kawamoto S, Inada K, Nagao S, Yoshida T, Yamashita Y. Clinical characteristics of 12 cases of appendiceal diverticulitis: a comparison with 378 cases of acute appendicitis. *Surg Today* 2012; **42**: 363-367 [PMID: 22358430 DOI: 10.1007/s00595-012-0152-6]

12 **Dupre MP**, Jadavji I, Matshes E, Urbanski SJ. Diverticular disease of the vermiform appendix: a diagnostic clue to underlying appendiceal neoplasm. *Hum Pathol* 2008; **39**: 1823-1826 [PMID:

18715614 DOI: 10.1016/j.humpath.2008.06.001]
13 **Kallenbach K**, Hjorth SV, Engel U, Schlesinger NH, Holck S. Significance of acquired diverticular disease of the vermiform appendix: a marker of regional neoplasms? *J Clin Pathol* 2012; **65**: 638-642 [PMID: 22461655 DOI: 10.1136/jclinpath-2011-200647]
14 **Rabinovitch J**, Arlen M, Barnett T, Cuello R, Rabinovitch P. Diverticulosis and Diverticulitis of the Vermiform Appendix. *Ann Surg* 1962; **155**: 434-440 [PMID: 17859697 DOI: 10.1097/00000658-196203000-00012]
15 **Iki K**, Echigo M, Nogami A, Iwamoto S, Takeo T, Tsunoda T, Eto T. Preoperative diagnosis of acute appendiceal diverticulitis by ultrasonography. *Surgery* 2001; **130**: 87-89 [PMID: 11436018 DOI: 10.1067/msy.2001.110852]
16 **Kubota T**, Omori T, Yamamoto J, Nagai M, Tamaki S, Sasaki K. Sonographic findings of acute appendiceal diverticulitis. *World J Gastroenterol* 2006; **12**: 4104-4105 [PMID: 16810772]
17 **Cavallaro G**, Basile U, Polistena A, Giustini S, Arena R, Scorsi A, Zinnamosca L, Letizia C, Calvieri S, De Toma G. Surgical management of abdominal manifestations of type 1 neurofibromatosis: experience of a single center. *Am Surg* 2010; **76**: 389-396 [PMID: 20420249]
18 **Bakker JR**, Haber MM, Garcia FU. Gastrointestinal neurofibromatosis: an unusual cause of gastric outlet obstruction. *Am Surg* 2005; **71**: 100-105 [PMID: 16022006]

P- Reviewer: Glockzin G, Mayir B, Piccinni G, Ryu DH
S- Editor: Ma YJ **L- Editor**: A **E- Editor**: Ma S

World Journal of Gastroenterology

Submit a Manuscript: http://www.wjgnet.com/esps/
Help Desk: http://www.wjgnet.com/esps/helpdesk.aspx
DOI: 10.3748/wjg.v21.i33.9822

World J Gastroenterol 2015 September 7; 21(33): 9822-9826
ISSN 1007-9327 (print) ISSN 2219-2840 (online)

CASE REPORT

Cutaneous metastasis as an initial presentation of a non-functioning pancreatic neuroendocrine tumor

Woo Young Shin, Keon Young Lee, Seung Ik Ahn, Shin-Young Park, Keun-Myoung Park

Woo Young Shin, Keon Young Lee, Seung Ik Ahn, Shin-Young Park, Keun-Myoung Park, Department of Surgery, Inha University Hospital, Inha University College of Medicine, Incheon 400-711, South Korea

Author contributions: Shin WY, Lee KY, Ahn SI and Park KM participated in the study design and performance; Park SY collected the clinical data.

Institutional review board statement: This study was reviewed and approved as an exemption by the Inha University Hospital Institutional Review Board.

Informed consent statement: The study participant provided informed written consent prior to study enrollment.

Conflict-of-interest statement: There are no potential conflicts of interest in this manuscript.

Correspondence to: Woo Young Shin, MD, Assistant Professor, Department of Surgery, Inha University Hospital, Inha University College of Medicine, 27 Inhang-Ro, Jung-Gu, Incheon 400-711, South Korea. mesik@daum.net
Telephone: +82-32-8903590
Fax: +82-32-8903549

Received: April 21, 2015
Peer-review started: April 23, 2015
First decision: May 18, 2015
Revised: May 26, 2015
Accepted: July 8, 2015
Article in press: July 8, 2015
Published online: September 7, 2015

Abstract

Non-functioning pancreatic neuroendocrine tumors (NF-PNETs) are rare tumors that account for 2% of all pancreatic malignancy. About 60% of NF-PNETs present distant metastases and usually hepatic metastases. However, cutaneous metastases are very rare. Herein, we report our experience with a 60-year-old male who visited our outpatient clinic with a mass on his left hip. An abdominal computerized tomography scan demonstrated not only a left hip mass and an enlarged left inguinal lymph node, but also a huge heterogeneous enhancing mass on the pancreas. Initially, we removed the metastatic lesions, which was a small cell neuroendocrine carcinoma with 50% of the Ki-67 index in the histopathological report. After 3 wk, we performed a total pancreatectomy and a total gastrectomy. Four weeks after the 1st operation, we detected a recurrence at the operative bed on his left hip, and subsequently removed the recurring mass. The patient was receiving chemotherapy based on etoposide and cisplatin treatment.

Key words: Pancreas; Neuroendocrine tumor; Skin neoplasm; Neoplasm metastasis; Pancreatectomy

Core tip: We report the first known case of cutaneous metastasis as an initial presentation of a high grade non-functional pancreatic neuroendocrine tumor treated by surgical resection of both primary and metastatic lesions.

Shin WY, Lee KY, Ahn SI, Park SY, Park KM. Cutaneous metastasis as an initial presentation of a non-functioning pancreatic neuroendocrine tumor. *World J Gastroenterol* 2015; 21(33): 9822-9826 Available from: URL: http://www.wjgnet.

com/1007-9327/full/v21/i33/9822.htm DOI: http://dx.doi.org/10.3748/wjg.v21.i33.9822

INTRODUCTION

Non-functioning pancreatic neuroendocrine tumors (NF-PNETs) are rare. Based on the data from the Surveillance, Epidemiology, and End Results (SEER) Program, NF-PNETs account for 2% of pancreatic malignancies. The annual worldwide incidence has been gradually increasing from 1.4 per million in 1973 to 3.0 per million in 2004[1]. Clinically, PNETs are classified as either functional or non-functional tumors[2]. While functioning PNETs might secrete several peptide hormones and cause paraneoplastic symptoms, NF-PNETs do not cause paraneoplastic symptoms and present as symptoms of mass effects, distant metastases, or both. Hence, NF-PNETs are often diagnosed as late secondary due to their vague symptoms and rarity. About 60% of NF-PNETs present distant metastases, which are usually hepatic[1,3,4]. Surgical therapy for NF-PNETs has improved survival outcome of patients with localized and metastatic carcinomas[1,5]. Cytoreductive surgery is recommended for patients with advanced disease/palliation, and is known to increase survival[6,7].

Cutaneous metastasis of NF-PNET is very rare. Notably, there have been no reports in which a patient has suffered from both primary and cutaneous metastatic lesions. Herein, we present a very rare case in which high grade NF-NET with cutaneous metastasis as the first manifestation was subjected to surgical resection.

CASE REPORT

A 60-year-old male visited our outpatient clinic with a mass on his left hip. He had diabetes and alcoholic hepatitis. On physical examination, a large mass measuring 10 cm in diameter was observed on his hip and an approximate 5 cm left inguinal lymph node was palpable (Figure 1).

Serum tumor markers, including CEA and CA 19-9, were within normal limits, whereas serum amylase (227 IU/L, normal range 43-116 IU/L), lipase (378 IU/L, normal range 7-60), fasting blood sugar (144 mg/dL, normal range, 70-100 mg/dL), and liver function test levels [including aspartate aminotransferase (178 IU/L, normal range, 7-38 IU/L), alanine aminotransferase (225 IU/L; normal range, 4-43 IU/L), and serum alkaline phosphatase (370 IU/L, normal range, 103-335 IU/L)] were all above normal ranges.

An abdominal computerized tomography (CT) scan demonstrated not only a left hip mass and an enlarged left inguinal lymph node, but also a huge heterogeneous enhancing mass on the body of the pancreas (Figure 2). On a PET scan, additional metastases were not found.

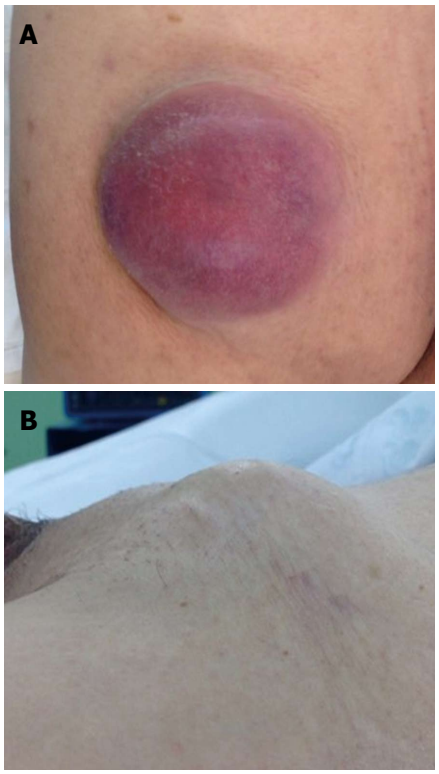

Figure 1 Gross appearance of the left hip mass (A) and the left inguinal mass (B).

We planned a staged surgery and performed a hip and inguinal mass excision on December 19, 2014. The histopathological report revealed a metastatic small cell neuroendocrine carcinoma with a maximal diameter of 10.5 cm on the buttock mass and a 7 cm growth on an inguinal lymph node. The mitotic index was over 50 mitoses per 50 HPF and the Ki-67 index measured at 50%. On January 21, 2015, we performed a total pancreatectomy and a total gastrectomy, with the findings revealing a tumor of the body of the pancreas about 9 cm × 6 cm in diameter involving the left gastric artery, splenic artery, and splenic vein. The histopathological report was the same as that of a metastatic lesion. Additionally, the tumor had spread to 8 of the 32 lymph nodes (Figure 3).

On the 7th post-operative day, the patient developed a high fever and leukocytosis. We administered an abdominal CT scan, which revealed infected fluid collection in the lesser sac and a 4.7 cm-sized recurring mass which was detected at the operative bed of the left hip (Figure 4). After infection of the abdominal cavity was treated by antibiotics, we removed the left hip recurring mass on February 3, 2015. The histopathology was the same as in the previous report; with a maximum diameter of 7.5 cm. The patient was discharged without other complications on February 9, 2015. He is currently receiving chemotherapy based on etoposide and cisplatin treatment.

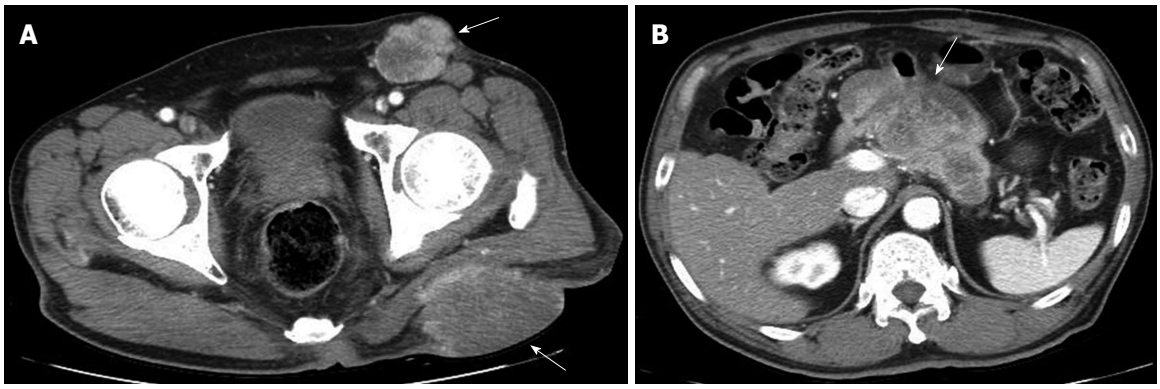

Figure 2 Abdominal computerized tomography scan revealed not only the left hip and inguinal masses (A), but also a heterogeneous enhancing mass on the body of the pancreas (B).

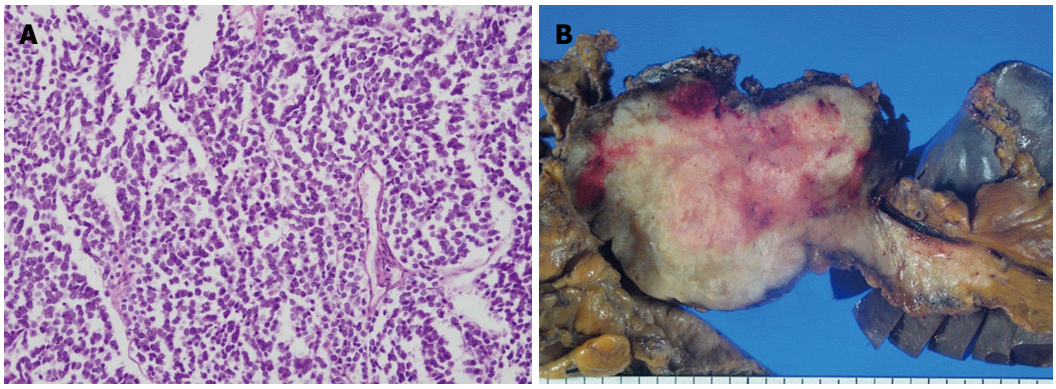

Figure 3 Hematoxylin and eosin stain demonstrated the small to medium-sized cells with scanty cytoplasm and hyperchromatic nucleoli (A, magnification × 200), and the gross appearance of the pancreatic mass (B).

Figure 4 Abdominal computerized tomography scan reveals a 4.7 cm-sized enhancing mass at the site of the previous mass excision.

DISCUSSION

Cutaneous metastasis of pancreatic cancer is rare, with only 63 reported cases in the literature. Among these, adenocarcinoma was predominant (84.1%; 53/63) and the median survival of patients was 5 mo[8]. In the case of neuroendocrine tumors, 35 cases with cutaneous or subcutaneous metastases have been reported in the literature. Of these, cutaneous metastasis of PNET comprised only 2 cases[9]. One case developed into an umbilical metastasis 2 years after distal pancreatectomy for an islet cell tumor. The survival outcome of the 1st patient was not described[10]. The other patient had a scalp metastasis of a well-differentiated PNET and died 36 mo after a skin biopsy[9]. To our knowledge, our case is the third report of a cutaneous metastasis of PNET and the first of cutaneous metastasis of pancreatic neuroendocrine carcinoma (NEC).

It might be questionable as to whether surgical resection is beneficial in our patient. Based on SEER data, the prognostic factors of NF-PNETs were: resection of the primary tumor, low tumor grade, absence of distant metastases, and a younger age. In patients with distant metastases, the survival outcome of patients where both the primary and metastatic lesions were removed has been statistically better than in patients either undergoing resection of primary or metastatic sites or not undergoing resection. High grade tumors yield very dismal outcomes. The median survival time of low, intermediate, and high grade tumors are 5 years, 4.4 years, and 7 mo, respectively ($P < 0.001$)[1]. These tumor grade results were investigated regardless of primary and/or metastatic lesion resection. According to the European Neuroendocrine Tumor Society (ENETS) consensus

guidelines, grade 3 metastatic NEC has an overall poor prognosis, regardless of whether or not they present with liver metastases[7]. ENETS suggested that resection of metastases of grade 3 NEC is generally not recommended, but may be considered in individual cases with isolated resectable metastases. It was also suggested that debulking resections with the removal of about 90% of the tumor volume can be exceptionally justified in a palliative situation[7].

Our case had a high grade of NF-PNET with distant and nodal metastases. As described, our case had recurrence within 1 mo. It took 46 d for the size of the recurrent mass to reach a 7.5 cm maximum size. The tumor grew very fast. Currently, the patient has survived for 4 mo after the 1st operation and has received 2 cycles of chemotherapy. A recent abdominal CT scan revealed an enlargement of the paraaortic lymph nodes (data not shown). Though he has undergone aggressive surgery, he has suffered from a Grade Ⅱ complication of the Clavien-Dindo classification[11]. Some authors have reported that aggressive surgery could be done with acceptable morbidity and mortality rates for patients with advanced neuroendocrine tumors[12,13]. Hence, if it could be done safely, it seemed reasonable for this case of high-grade NF-PNET to be treated by aggressive surgical resection, despite the dismal prognosis.

In summary, we report the case of a patient who had a high grade NF-PNET with cutaneous metastasis and underwent surgical resection of both primary and metastatic tumors.

COMMENTS

Case characteristics

A 60-year-old man presented with a mass on his left hip.

Clinical diagnosis

On physical examination, a mass measuring 10 cm in diameter was observed on the patient's hip and an approximately 5 cm left inguinal lymph node was palpable.

Differential diagnosis

Differential diagnosis included pancreatic adenocarcinoma with cutaneous metastasis.

Laboratory diagnosis

Serum CA 19-9 were within normal limits, whereas serum amylase (227 IU/L), lipase (378 IU/L), fasting blood sugar (144 mg/dL), and a liver function test levels [including aspartate aminotransferase (178 IU/L), alanine aminotransferase (225 IU/L), and serum alkaline phosphatase (370 IU/L)] were all above normal ranges.

Imaging diagnosis

An abdominal computerized tomography scan demonstrated not only a left hip mass and an enlarged left inguinal lymph node, but also a huge heterogeneous enhancing mass on the body of the pancreas.

Pathological diagnosis

The histopathological report revealed a metastatic small cell neuroendocrine carcinoma with 50% of the Ki-67 index.

Treatment

The patient underwent staged surgery consisting of hip and inguinal masses excision, followed by a total pancreatectomy and a total gastrectomy.

Related reports

A total of 2 cases of cutaneous metastasis of pancreatic neuroendocrine tumors (PNETs) have been reported in the literature. This is the third report of cutaneous metastasis of PNET and the first report of cutaneous metastasis of pancreatic neuroendocrine carcinoma.

Term explanation

Neuroendocrine tumors derived from the diffuse neuroendocrine system of the gastrointestinal tract and pancreas are fairly rare. They frequently have unpredictable and unusual biological behavior, and frequently present late after a delayed diagnosis.

Experiences and lessons

This is the first known case report of grade 3 non-functioning PNET (NF-PNET) with cutaneous metastasis that was surgically removed. Although the patient quickly experienced recurrence, we think that if the lesions are almost totally removed, debulking resections can be justified.

Peer-review

NF-PNETs are rare and cutaneous metastases. This is interesting case with a described long-term patient outcome.

REFERENCES

1 **Franko J**, Feng W, Yip L, Genovese E, Moser AJ. Non-functional neuroendocrine carcinoma of the pancreas: incidence, tumor biology, and outcomes in 2,158 patients. *J Gastrointest Surg* 2010; **14**: 541-548 [PMID: 19997980 DOI: 10.1007/s11605-009-1115-0]

2 **Moo-Young TA**, Prinz RA, Blumgart WRJH. Chapter 61 - Endocrine tumors of the pancreas: Clinical picture, diagnosis, and therapy. Blumgart's Surgery of the Liver, Pancreas and Biliary Tract (Fifth Edition). Philadelphia: W.B. Saunders, 2012: 934-944. e932

3 **Vagefi PA**, Razo O, Deshpande V, McGrath DJ, Lauwers GY, Thayer SP, Warshaw AL, Fernández-Del Castillo C. Evolving patterns in the detection and outcomes of pancreatic neuroendocrine neoplasms: the Massachusetts General Hospital experience from 1977 to 2005. *Arch Surg* 2007; **142**: 347-354 [PMID: 17438169 DOI: 10.1001/archsurg.142.4.347]

4 **Hill JS**, McPhee JT, McDade TP, Zhou Z, Sullivan ME, Whalen GF, Tseng JF. Pancreatic neuroendocrine tumors: the impact of surgical resection on survival. *Cancer* 2009; **115**: 741-751 [PMID: 19130464 DOI: 10.1002/cncr.24065]

5 **Dixon E**, Pasieka JL. Functioning and nonfunctioning neuroendocrine tumors of the pancreas. *Curr Opin Oncol* 2007; **19**: 30-35 [PMID: 17133109 DOI: 10.1097/CCO.0b013e328011a236]

6 **Modlin IM**, Oberg K, Chung DC, Jensen RT, de Herder WW, Thakker RV, Caplin M, Delle Fave G, Kaltsas GA, Krenning EP, Moss SF, Nilsson O, Rindi G, Salazar R, Ruszniewski P, Sundin A. Gastroenteropancreatic neuroendocrine tumours. *Lancet Oncol* 2008; **9**: 61-72 [PMID: 18177818 DOI: 10.1016/S1470-2045(07)70410-2]

7 **Pavel M**, Baudin E, Couvelard A, Krenning E, Öberg K, Steinmüller T, Anlauf M, Wiedenmann B, Salazar R; Barcelona Consensus Conference participants. ENETS Consensus Guidelines for the management of patients with liver and other distant metastases from neuroendocrine neoplasms of foregut, midgut, hindgut, and unknown primary. *Neuroendocrinology* 2012; **95**: 157-176 [PMID: 22262022 DOI: 10.1159/000335597]

8 **Zhou HY**, Wang XB, Gao F, Bu B, Zhang S, Wang Z. Cutaneous metastasis from pancreatic cancer: A case report and systematic

review of the literature. *Oncol Lett* 2014; **8**: 2654-2660 [PMID: 25364444 DOI: 10.3892/ol.2014.2610]
9 **Jedrych J**, Busam K, Klimstra DS, Pulitzer M. Cutaneous metastases as an initial manifestation of visceral well-differentiated neuroendocrine tumor: a report of four cases and a review of literature. *J Cutan Pathol* 2014; **41**: 113-122 [PMID: 24218988 DOI: 10.1111/cup.12263]
10 **Zhang Y**, Selvaggi SM. Metastatic islet cell carcinoma to the umbilicus: diagnosis by fine-needle aspiration. *Diagn Cytopathol* 2003; **29**: 91-94 [PMID: 12889048 DOI: 10.1002/dc.10305]
11 **Clavien PA**, Barkun J, de Oliveira ML, Vauthey JN, Dindo D, Schulick RD, de Santibañes E, Pekolj J, Slankamenac K, Bassi C, Graf R, Vonlanthen R, Padbury R, Cameron JL, Makuuchi M. The Clavien-Dindo classification of surgical complications: five-year experience. *Ann Surg* 2009; **250**: 187-196 [PMID: 19638912 DOI: 10.1097/SLA.0b013e3181b13ca2]
12 **Norton JA**, Kivlen M, Li M, Schneider D, Chuter T, Jensen RT. Morbidity and mortality of aggressive resection in patients with advanced neuroendocrine tumors. *Arch Surg* 2003; **138**: 859-866 [PMID: 12912744 DOI: 10.1001/archsurg.138.8.859]
13 **Phan GQ**, Yeo CJ, Hruban RH, Lillemoe KD, Pitt HA, Cameron JL. Surgical experience with pancreatic and peripancreatic neuroendocrine tumors: review of 125 patients. *J Gastrointest Surg* 1998; **2**: 472-482 [PMID: 9843608]

P- Reviewer: Chen YC **S- Editor**: Ma YJ **L- Editor**: Rutherford A
E- Editor: Ma S

World Journal of Gastroenterology

Submit a Manuscript: http://www.wjgnet.com/esps/
Help Desk: http://www.wjgnet.com/esps/helpdesk.aspx
DOI: 10.3748/wjg.v21.i33.9827

World J Gastroenterol 2015 September 7; 21(33): 9827-9832
ISSN 1007-9327 (print) ISSN 2219-2840 (online)

CASE REPORT

Giant liposarcoma of the esophagus: A case report

Zhi-Chao Lin, Xiang-Zhen Chang, Xiu-Fang Huang, Chun-Lai Zhang, Geng-Sheng Yu, Shuo-Yun Wu, Min Ye, Jian-Xing He

Zhi-Chao Lin, Department of Thoracic Surgery, Jiangmen Central Hospital, Affiliated Jiangmen Hospital of Sun Yat-sen University, Jiangmen 529030, Guangdong Province, China

Xiang-Zhen Chang, Editorial Department, Chinese Journal of Microsurgery, the First Affiliated Hospital of Sun Yat-sen University, Guangzhou 510080, Guangdong Province, China

Xiu-Fang Huang, Department of Pathology, Jiangmen Central Hospital, Affiliated Jiangmen Hospital of Sun Yat-sen University, Jiangmen 529030, Guangdong Province, China

Chun-Lai Zhang, Department of Respiratory Medicine, Jiangmen Central Hospital, Affiliated Jiangmen Hospital of Sun Yat-sen University, Jiangmen 529030, Guangdong Province, China

Geng-Sheng Yu, Department of Oncology, Jiangmen Central Hospital, Affiliated Jiangmen Hospital of Sun Yat-sen University, Jiangmen 529030, Guangdong Province, China

Shuo-Yun Wu, Min Ye, Department of Thoracic Surgery, Jiangmen Central Hospital, Affiliated Jiangmen Hospital of Sun Yat-sen University, Jiangmen 529030, Guangdong Province, China

Jian-Xing He, Department of Thoracic Surgery, the First Affiliated Hospital of Guangzhou Medical University, Guangzhou 510120, Guangdong Province, China

Author contributions: He JX designed the study; Zhang CL analyzed the data; Yu GS and Wu SY studied the relevant literature and reviewed the data; Lin ZC and Huang XF wrote the manuscript; Chang XZ and Ye M edited the manuscript and figures.

Institutional review board statement: The study was reviewed and approved by the Jiangmen Central Hospital Institutional Review Board.

Informed consent statement: All study participants, or their legal guardian, provided informed written consent prior to study enrollment.

Conflict-of-interest statement: The authors declare no conflict of interest related to the publication of this case report.

Correspondence to: Jian-Xing He, MD, PhD, Department of Thoracic Surgery, the First Affiliated Hospital of Guangzhou Medical University, 151 Yanjiang Road West, Guangzhou 510120, Guangdong Province, China. hejx@vip.163.com
Telephone: +86-20-83062114
Fax: +86-20-83395651

Received: January 18, 2015
Peer-review started: January 19, 2015
First decision: April 13, 2015
Revised: May 20, 2015
Accepted: July 3, 2015
Article in press: July 3, 2015
Published online: September 7, 2015

Abstract

Liposarcomas rarely develop in the aerodigestive tract. Here, we present a primary esophageal liposarcoma that was discovered between the T3 and T7 levels of the esophagus during right pleural exploration of a 51-year-old male patient. The patient had presented with non-specific symptoms, including progressive dysphagia over the previous 6 mo, without complaints of chest or epigastric pain, regurgitation, or weight loss. A radical three-hole esophagectomy was performed. The tumor was extremely large (14 cm × 7.0 cm × 6.5 cm), but completely encapsulated. Upon histological examination, the tumor was diagnosed as a giant, well-differentiated esophageal liposarcoma with

a dedifferentiated component. Non-specific radiological and endoscopic results during the clinical work-up delayed diagnosis until post-operative histology was performed. In this report, the clinical, radiological and endoscopic diagnostic challenges specific to the case are discussed, as well as the surgical and pathological findings.

Key words: Achalasia; Esophagectomy; Esophagus; Liposarcoma

Core tip: Primary esophageal liposarcoma is an extremely rare malignancy. In this case report, a giant, well-differentiated esophageal liposarcoma with a dedifferentiated component was removed from a 51-year-old male patient. The tumor displayed a non-specific appearance on imaging and endoscopy, which prohibited an accurate diagnosis pre-operatively. Therefore, clinical, radiological, and endoscopic aspects of the case, as well as the surgery and pathology of the tumor, are discussed in detail.

Lin ZC, Chang XZ, Huang XF, Zhang CL, Yu GS, Wu SY, Ye M, He JX. Giant liposarcoma of the esophagus: A case report. *World J Gastroenterol* 2015; 21(33): 9827-9832 Available from: URL: http://www.wjgnet.com/1007-9327/full/v21/i33/9827.htm DOI: http://dx.doi.org/10.3748/wjg.v21.i33.9827

INTRODUCTION

Liposarcoma is a rare malignant tumor that usually develops in the soft tissue of the extremities, the trunk or the retroperitoneum, and seldom in the aerodigestive tract. The first report of a primary esophageal liposarcoma was published in 1983[1], and only 30 cases have appeared in the literature since then[2]. Due to the novelty of these tumors, the clinical, radiological, endoscopic, surgical and pathological findings of a case in a Chinese patient are discussed in detail here. Briefly, a giant, well-differentiated esophageal liposarcoma with a dedifferentiated component was identified in a 51-year-old male patient. Treatment included a radical, three-hole esophagectomy to resect the disease.

CASE REPORT

A 51-year-old Chinese man presented with a 6-mo history of progressive dysphagia without complaints of chest or epigastric pain, regurgitation, or significant weight loss. In the days leading to hospitalization, the patient could not tolerate solid food and had experienced intermittent difficulties ingesting liquids. The clinical history was otherwise unremarkable, and no significant abnormalities were observed upon physical examination.

A computed tomographic (CT) scan of the chest and abdomen was performed. The esophagus was found to be extensively dilated (upper and middle thirds) from the thoracic inlet all the way to the inferior pulmonary vein level, over an area of 15 cm in length and 9.5 cm in width (Figure 1A-C). The remaining lower third of the esophagus displayed no abnormalities. An extremely dilated upper and middle esophagus was also evident on the subsequent barium swallow. The contrast passed slowly through the lower third of the esophagus but without any signs of a filling defect (Figure 1D). All radiologic results were consistent with a diagnosis of achalasia. However, further examination performed with a diagnostic flexible esophagoscope revealed a large submucosal lesion or an extrinsic compression encompassing the esophageal lumen at 20 cm to 35 cm from the incisor teeth (Figure 2). The remaining lower region of the esophagus and the gastro-esophageal junction was normal in appearance.

For exploration and radical resection of the disease, a three-hole approach - including a right thoracotomy, midline laparotomy and left cervical incision - was selected due to the gross obstruction and size and location of the lesion. During right pleural exploration, a large tumor was located between levels T3 and T7 in the upper and middle thirds of the esophagus. The tumor was 14 cm × 7.0 cm × 6.5 cm in size. It was remarkably pliable and completely encapsulated. A radical esophagectomy was subsequently performed, and the cervical esophagus was anastomosed end-to-side with a gastric conduit in the neck. The operation was successful, and the patient fully recovered without post-operative complications. The patient was discharged on post-operative day 8 with discharge orders for a soft diet.

Upon macroscopic examination, the surface of the tumor was found to be covered by normal esophageal mucosa. At one surgical margin of the specimen, a yellow lobulated transmural mass invading the esophageal wall was visible (Figure 3). The diagnosis upon histological examination was a delineated myxoid tumor in the subepithelial stroma. Spindle cells, lipoblasts, and mature fat cells were all present (Figure 4A, B and D). Immunostaining revealed a marker profile (vimentin$^+$, CD117$^-$, S-100$^+$, and CD34$^+$) consistent with a well-differentiated liposarcoma. However, a dedifferentiated component was also present as indicated by the atypia exhibited by the spindle cells in the area between the esophageal mucosa and the tumor (Figure 4C). Immunostaining also revealed strong and weak patterns of expression for CDK4 and MDM2 respectively across both well-differentiated and dedifferentiated areas (Figure 5). Finally, the resection margins and lymph nodes were all free of tumor. The patient therefore required only close follow-up without further treatment.

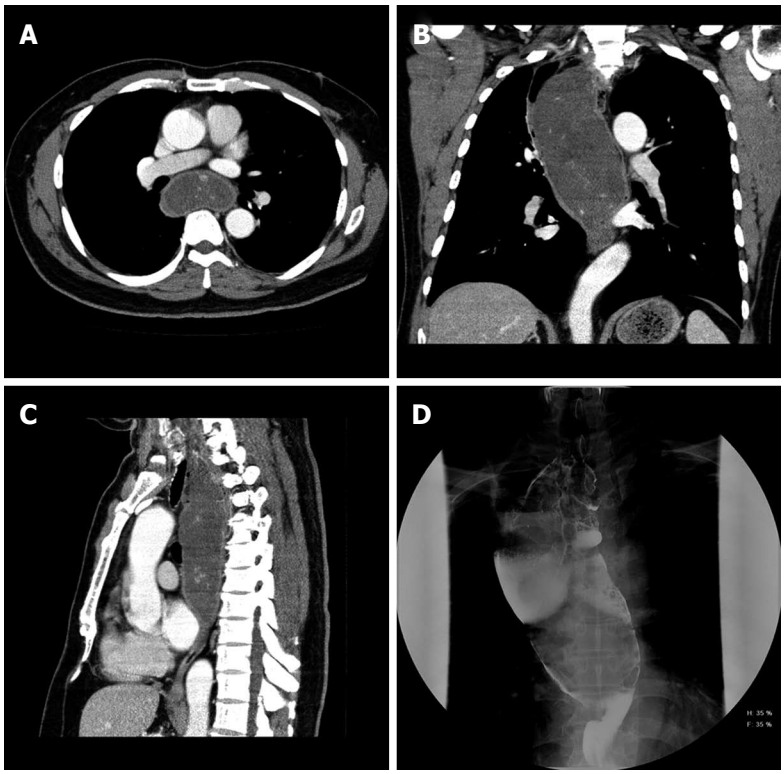

Figure 1 Radiological imaging of the esophageal liposarcoma. A-C: Computed tomographic scan; D: Barium swallow.

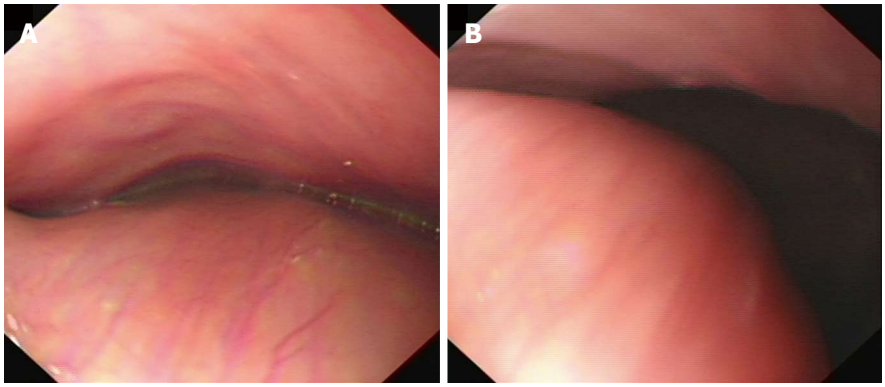

Figure 2 Endoscopic results of the esophageal liposarcoma. A large submucosal lesion or an extrinsic compression encompassing the esophageal lumen at 20 cm to 35 cm from the incisor teeth was revealed through a diagnostic flexible endoscopy. The remaining lower region of the esophagus and the gastro-esophageal junction was normal in appearance.

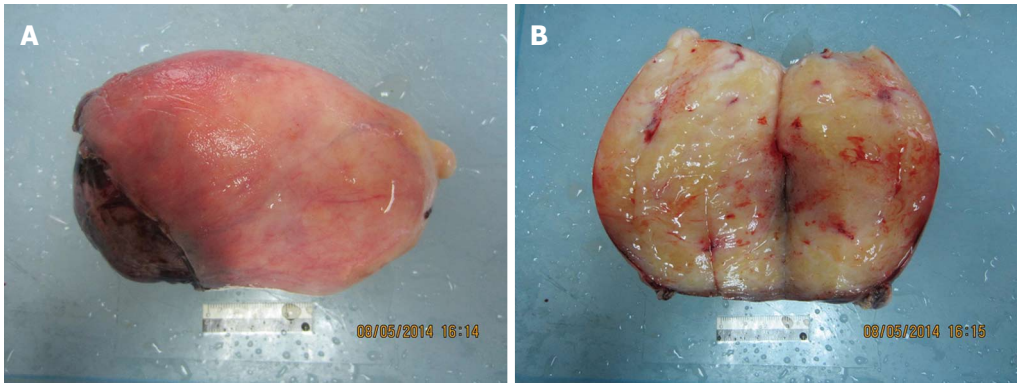

Figure 3 Surgical specimen of the esophageal liposarcoma. Normal esophageal mucosa is shown covering the surface of the tumor. A yellow lobulated transmural mass invading the esophageal wall is visible at one surgical margin of the specimen.

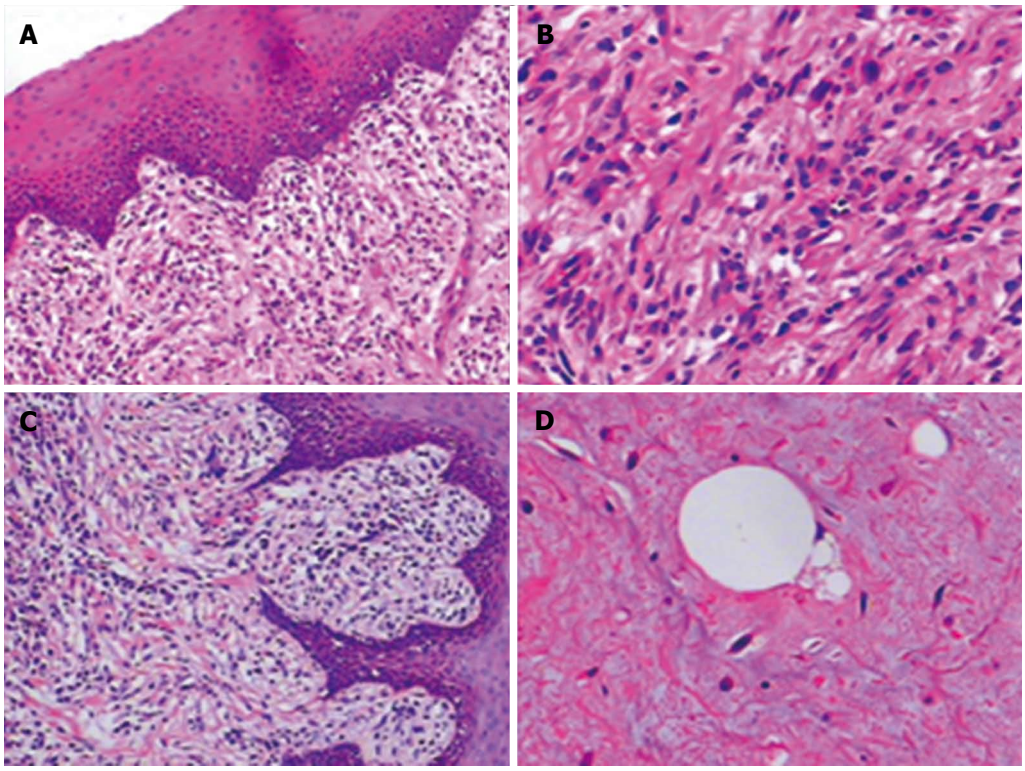

Figure 4 Histological analysis reveals a well-differentiated myxoid esophageal liposarcoma with a dedifferentiated component. Hematoxylin and eosin stain of paraffin-embedded sections highlighting histological features of the case. A: Myxoid tumor cells located just under normal squamous cell epithelia (magnification × 100); B: Spindle tumor cells (magnification × 200); C: Dedifferentiated component of the liposarcoma (magnification × 100); D: Lipoblast cells (magnification × 200).

DISCUSSION

Although liposarcoma is the most common tumor of mesenchymal origin occurring in adults, development in the esophagus is extremely rare. The incidence of gastrointestinal liposarcoma has been reported to be 0.1% to 5.8% at autopsy, with primary esophageal liposarcomas accounting for only 1.2% to 1.5% of all gastrointestinal lipomas[3,4]. Based on data from the few cases available, esophageal liposarcoma tends to occur predominantly in males (72%) at an average age of 58.4 years (range: 38-73 years) and reaching an average tumor size of 13 cm (range: 4 to 23 cm)[2]. The case in this report also presented with these general clinical features, but the diagnosis remained elusive until surgery and histological analysis had been completed.

Esophageal liposarcoma is generally considered to be a slowly growing tumor. The lesion usually grows until it reaches a considerable size and causes symptoms. The predominant clinical symptoms include progressive dysphagia, nausea, throat discomfort, retrosternal pain, odynophagia, respiratory distress, anemia, tumor regurgitation, and sudden death by asphyxia and foreign body sensation[5]. Progressive dysphagia over a 6-mo period was the main complaint of our patient. However, the symptoms of esophageal liposarcoma might be uncharacteristic making clinical diagnosis difficult. In one case report, it was significant shortness of breath, hoarseness, cough, and chest discomfort that led the patient to hospitalization[6]. In our case, the soft tissue lesion was not identified with the CT scan, and the barium swallow failed to detect any filling defect on the background of a grossly dilated esophagus. In fact, the case was misdiagnosed as achalasia until abnormalities on the esophagoscopy were observed. Thus, the final diagnosis of esophageal liposarcoma was established only after surgery.

Well-differentiated, dedifferentiated, myxoid cell, and pleomorphic are all reported histologic types of esophageal liposarcoma[7]. The most common subtype is well-differentiated esophageal liposarcoma, which comprises up to 70% of all cases[2]. The case presented was also a well-differentiated esophageal liposarcoma, but surprisingly, a small dedifferentiated component was identified in a region between esophageal mucosa and tumor. This finding confirms the existence of heterogeneity in this tumor type and is consistent with the proposal that dedifferentiated liposarcomas are biphasic malignant adipocytic tumors containing areas of well-differentiated liposarcoma with a transition to non-lipogenic sarcoma[8].

The treatment choice for esophageal liposarcoma is surgery. Surgical approaches, however, are diverse and include total or subtotal esophagectomy or minimally invasive approaches, such as endoscopic resection[7,9-11]. The prognosis of esophageal liposarcoma after radical surgery remains unknown as the number of cases published with long-term follow-up is insufficient for rigorous analysis. So far, however, tumors recurred

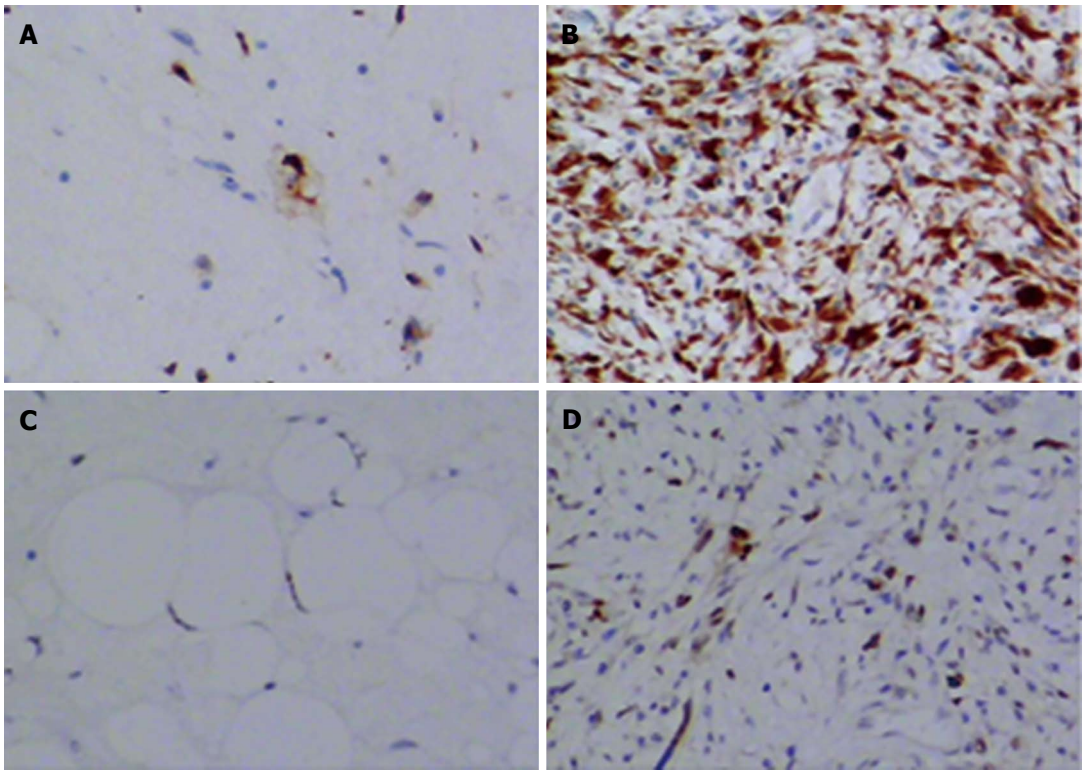

Figure 5 CDK4 and MDM2 expression in the tumor as determined by immunohistochemistry. Paraffin-embedded sections of the primary tumor are stained for A: CDK4 in a well-differentiated area (magnification × 200); B: CDK4 expression in a dedifferentiated area (magnification × 200); C: MDM2 in a well-differentiated area (magnification × 200); and D: MDM2 expression in a dedifferentiated area (magnification × 200).

in only 2/15 patients based on the medical records available[12]. Therefore, the local control rate of esophageal liposarcoma by surgery seems acceptable. For the same reason, adjuvant therapy is generally not suggested. Thus, although the exact indications for resection have not been established, total rather than incomplete resection coupled with a close surveillance program is recommended.

The case presented herein involved a well-differentiated liposarcoma of the esophagus harboring a dedifferentiated component. Atypical symptoms and radiological findings led to an initial misdiagnosis of achalasia. This rare, slowly growing tumor thus presents an important differential diagnosis for progressive dysphagia. Surgical resection is recommended as the treatment of choice for both diagnostic and therapeutic purposes.

COMMENTS

Case characteristics

A 51-year-old Chinese man presented with a 6-mo history of progressive dysphagia without complaints of chest or epigastric pain, regurgitation, or significant weight loss. The patient also experienced difficulties ingesting solid food and liquids immediately prior to consultation.

Clinical diagnosis

The patient was diagnosed with a giant, well-differentiated esophageal liposarcoma with a dedifferentiated component measuring 14 cm × 7.0 cm × 6.5 cm in size.

Differential diagnosis

All radiologic results were consistent with a diagnosis of achalasia.

Laboratory diagnosis

Laboratory tests were not reported.

Imaging diagnosis

A computed tomographic scan of the chest and abdomen was performed followed by a barium swallow. Both revealed a grossly dilated esophagus. A final flexible diagnostic esophagoscopy revealed the presence of a large lesion.

Pathological diagnosis

The diagnosis upon histological examination was a delineated myxoid tumor in the subepithelial stroma. Spindle cells, lipoblasts, and mature fat cells were all present. A dedifferentiated component was also recognized on the basis of significant atypia in the spindle cells located between the mucosa and tumor.

Treatment

Treatment included a radical, three-hole esophagectomy and close surveillance without adjuvant therapy.

Related reports

Approximately 30 cases of esophageal liposarcoma have been reported in the English literature.

Term explanation

A three-hole esophagectomy is a three-incision transthoracic approach for esophagectomy that usually involves a right thoracotomy, a midline laparotomy, and a right cervical incision for esophagogastric anastomosis. Achalasia is a primary esophageal motility disorder characterized by the absence of esophageal peristalsis and impaired relaxation of the lower esophageal sphincter in response to swallowing.

Experiences and lessons

This rare, slowly growing tumor presents an important differential diagnosis for progressive dysphagia. Furthermore, such cases are difficult to diagnose pre-operatively so that surgical resection is recommended as the treatment of choice for both diagnostic and therapeutic purposes.

Peer-review

The manuscript describing a giant esophageal well-differentiated liposarcoma with a dedifferentiated component is of clinical interest due to the rarity of its location and clinical presentation.

REFERENCES

1 **Mansour KA**, Fritz RC, Jacobs DM, Vellios F. Pedunculated liposarcoma of the esophagus: a first case report. *J Thorac Cardiovasc Surg* 1983; **86**: 447-450 [PMID: 6887958]

2 **Sui X**, Li Y, Zhao H, Wang J. Giant liposarcoma of the esophagus with Li-Fraumeni-like syndrome. *Eur J Cardiothorac Surg* 2011; **40**: 1253-1255 [PMID: 21454085]

3 **Hasanabadi MS**, Amiri M, Tajedini A, Yazdi AK, Heidarali M, Amali A, Banazadeh M, Mokhtari Z, Azizi MR. Huge myxoid liposarcoma of the esophagus: a case report. *Acta Med Iran* 2011; **49**: 118-121 [PMID: 21598223]

4 **Fernandez MJ**, Davis RP, Nora PF. Gastrointestinal lipomas. *Arch Surg* 1983; **118**: 1081-1083 [PMID: 6615219]

5 **Chung JJ**, Kim MJ, Kim JH, Lee JT, Yoo HS, Kim KW. Imaging findings of giant liposarcoma of the esophagus. *Yonsei Med J* 2003; **44**: 715-718 [PMID: 12950130]

6 **Smith MA**, Kluck E, Jagannath S, Yang SC. Giant multi-polypoid liposarcoma of the esophagus: an atypical presentation. *Ann Thorac Surg* 2010; **89**: 610-612 [PMID: 20103356]

7 **Jakowski JD**, Wakely PE. Rhabdomyomatous well-differentiated liposarcoma arising in giant fibrovascular polyp of the esophagus. *Ann Diagn Pathol* 2009; **13**: 263-268 [PMID: 19608085]

8 **Torres-Mora J**, Moyer A, Topazian M, Alexander J, Wu TT, Seys A, Fritchie K. Dedifferentiated liposarcoma arising in an esophageal polyp: a case report. *Case Rep Gastrointest Med* 2012; **2012**: 141693 [PMID: 22924136 DOI: 10.1155/2012/141693]

9 **Aloraini A**, Nahal A, Ferri LE. Transoral endoscopic resection of esophageal liposarcoma. *Ann Thorac Surg* 2012; **94**: e121-e122 [PMID: 23098986]

10 **Will U**, Lorenz P, Urban H, Meyer F. Curative endoscopic resection of a huge pedunculated esophageal liposarcoma. *Endoscopy* 2007; **39** Suppl 1: E15-E16 [PMID: 17285485 DOI: 10.1055/s-2006-944902]

11 **Temes R**, Quinn P, Davis M, Endara S, Follis F, Pett S, Wernly J. Endoscopic resection of esophageal liposarcoma. *J Thorac Cardiovasc Surg* 1998; **116**: 365-367 [PMID: 9699597]

12 **Yo I**, Chung JW, Jeong MH, Lee JJ, An J, Kwon KA, Rim MY, Hahm KB. Huge liposarcoma of esophagus resected by endoscopic submucosal dissection: case report with video. *Clin Endosc* 2013; **46**: 297-300 [PMID: 23767044 DOI: 10.5946/ce.2013.46.3.297]

P- Reviewer: Gu MJ, Ma YH **S- Editor**: Yu J **L- Editor**: A
E- Editor: Zhang DN

Published by **Baishideng Publishing Group Inc**
8226 Regency Drive, Pleasanton, CA 94588, USA
Telephone: +1-925-223-8242
Fax: +1-925-223-8243
E-mail: bpgoffice@wjgnet.com
Help Desk: http://www.wjgnet.com/esps/helpdesk.aspx
http://www.wjgnet.com

ISSN 1007-9327